

**INVESTIGATION ON SOLVATION BEHAVIOUR AND HOST
GUEST INCLUSION COMPLEXES OF SOME SIGNIFICANT
MOLECULES WITH DIVERSE CYCLIC COMPOUNDS**

A

Thesis submitted to the

UNIVERSITY OF NORTH BENGAL

For the Award of

DOCTOR OF PHILOSOPHY (Ph.D.)

In

CHEMISTRY

By

SITI BARMAN

M.Sc. in Chemistry

Guide

DR. MAHENDRA NATH ROY

PROFESSOR OF CHEMISTRY

DEPARTMENT OF CHEMISTRY
UNIVERSITY OF NORTH BENGAL
DARJEELING-734013, INDIA

July 2017





INVESTIGATION ON SOLVATION BEHAVIOUR AND HOST
GUEST INCLUSION COMPLEXES OF SOME SIGNIFICANT
MOLECULES WITH DIVERSE CYCLIC COMPOUNDS



A Thesis submitted to the

UNIVERSITY OF NORTH BENGAL

For the Award of



DOCTOR OF PHILOSOPHY (Ph.D.)

in



CHEMISTRY

by

SITI BARMAN

M.Sc. in Chemistry

Guide

DR. MAHENDRA NATH ROY

Professor of Chemistry

DEPARTMENT OF CHEMISTRY
UNIVERSITY OF NORTH BENGAL


DARJEELING 734013

INDIA





To
MY
BELOVED
PARENTS



I have never expressed in words as how much I love you
but today I want to thank you for the wonderful gifts,
your blessings and your teachings in making my life meaningful.

Grateful to you for being my life!

*"I am among those who think
that science has great beauty."
-Marie Curie*





DECLARATION



I declare that the thesis entitled "INVESTIGATION ON SOLVATION BEHAVIOUR AND HOST GUEST INCLUSION COMPLEXES OF SOME SIGNIFICANT MOLECULES WITH DIVERSE CYCLIC COMPOUNDS" has been prepared by me under the guidance of Dr. Mahendra Nath Roy, Professor of Chemistry, University of North Bengal. No part of this thesis has formed the basis for the award of any degree or fellowship previously.

Siti Barman

SITI BARMAN

Department of Chemistry,
University of North Bengal,
Darjeeling 734013,
West Bengal, India.

Date: *12/07/2017*

UNIVERSITY OF NORTH BENGAL

Accredited By NAAC with Grade "A"

PROF. (DR) M. N. ROY
UGC one time Grant Awardee (BSR)
Head, Professor and Coordinator of
UGC SAP DRS-III,
Department of Chemistry,
Email. mahendraroy2002@yahoo.co.in



Phone : 0353 2776381
Mobile: 094344 96154
Fax: +91 353 2699001
Darjeeling-734 013,
West Bengal, INDIA.
July, 2017

ENLIGHTENMENT TO PERFECTION

CERTIFICATE

I certify that **Miss Siti Barman**, M. Sc. in **Chemistry**, has prepared the thesis entitled "**INVESTIGATION ON SOLVATION BEHAVIOUR AND HOST GUEST INCLUSION COMPLEXES OF SOME SIGNIFICANT MOLECULES WITH DIVERSE CYCLIC COMPOUNDS**", for the award of *Ph. D. Degree (Doctor of Philosophy)* of the **University of North Bengal**, under my guidance. She has carried out the work at the **Department of Chemistry, University of North Bengal**.

Mahendra Nath Roy

Dr. Mahendra Nath Roy,

Professor of Chemistry,
Department of Chemistry,
University of North Bengal,
Dist: Darjeeling, Pin: 734013,
West Bengal, INDIA

DATE: 12/07/2017

Prof. (Dr.) M. N. Roy
Head of the Department of Chemistry
&
Programme Coordinator, SAP, DRS-III
University of North Bengal
Darjeeling - 734013, India

(V)





ABSTRACT



Host-guest chemistry is extremely important in pharmaceutical and drug delivery science. The knowledge of host-guest chemistry has opened the way to the formation of supramolecular (inclusion) complexes with physicochemical and spectroscopic properties. A number of host molecules have been used including crown ethers and cyclodextrins. All are capable of enclosing guest molecules such as ionic liquids and drugs.

The inclusion complexes have received considerable attention because of their increasing applications in the pharmaceutical field. For example, cyclodextrin based supramolecular complex has wide applications in medicine and single molecular devices. Due to their unique properties of polar hydrophilic outer shell and relatively hydrophobic inner cavity they can build up host-guest complexes by the inclusion of a suitable hydrophobic moiety in the guest molecule. This explains the current interest for cyclodextrins having versatile applications in pharmaceuticals, pesticides, foodstuffs, toilet articles, textile processing and other industry, supramolecular and host-guest chemistry, models for studying enzyme activity, molecular recognition and molecular encapsulation, and studying their intermolecular interactions and chemical stabilization. Of the 3 types of cyclodextrins (α , β and γ) we have taken α - β -cyclodextrin as host molecule.

Some part of our work involves the inclusion complex formation in detail based on physicochemical and spectroscopic measurements. The factors affecting the inclusion process were also discussed. Sometimes complex formation with cyclodextrin changes the properties of the guest. These changes such as enhanced fluorescence and absorption characteristics served as an aid for better understanding the inclusion mechanism, including the size/shape-fit, hydrophobicity. Detailed spatial information of the inclusion complex and related mechanisms in solution can be obtained from ^1H NMR.

Host-guest complexes provide a way to overcome inherent physicochemical difficulties with numerous chemical and medicinal agents. The future looks likely to bring many more opportunities for host-guest chemistry to play a part in our everyday lives.

Physico-chemical studies of electrolytes play a very important role in understanding the solute-solute/ion-ion, solute-solvent/ion-solvent and solvent-solvent interactions in solutions. In order to explore the strength and nature of the interactions, the investigation on thermodynamic, transport properties of electrolytes, and optical properties organic solvents exceeds the traditional boundaries of physical, inorganic, organic, analytical and electrochemistry. In one chapter we have examined the transport properties of an ionic liquids in industrially important solvents along with thermodynamic studies to characterize molecular interactions in solutions.

Solvation surrounds an ion with a cloud of loosely associated solvent molecules, it gives ions an effective size considerably bigger than their ionic radius. Solvation is the process of reorganizing solvent and solute molecules into solvation complexes (a solute molecule surrounded by solvent) until the solute is distributed evenly within the solvent. Solvation depends on factors such as hydrogen bonding and van der Waals forces. Insoluble solutes prefer to maintain interactions among solute molecules rather than break apart and become solvated by the solvent.

To estimate the extent of solvation broadly three types of approaches have been made in '*Solution Chemistry*' The first is the solvational approach involving the studies of viscosity, conductance, etc., of electrolytes and the derivation of various factors associated with ionic solvation, the second is the thermodynamic approach by measuring the free energies, enthalpies and entropies of solvation of ions from which factors associated with solvation can be elucidated, and the third is to use spectroscopic measurements where the spectral solvent shifts or the chemical shifts determine their qualitative and quantitative nature.

The mixing of different solute or solvent with another solvent/solvent mixtures gives rise to solutions that generally do not behave ideally. This deviation from ideality is expressed in terms of thermodynamic parameters, by excess properties in case of liquid-liquid mixtures and apparent molar properties in case of solid-liquid mixtures. These thermodynamic properties of solvent mixtures corresponds to the difference between the actual property and the property if the system behaves ideally and thus are useful in the study of molecular interactions and arrangements. In particular, they reflect the interaction that take place between solute-solute, solute-solvent and solvent-solvent

species. The extent of ion-solvation is dependent upon the interactions taking place between solute-solute, solute-solvent, solvent-solvent species. The assesment of ion-pairing in these systems is important because of its effect on the ionic mobility and hence on the ionic conductivity of the ions in solution. These phenomenon thus paves the path for research in solution chemistry to elucidate the nature of interaction through experimental studies involving densitometry, viscometry, interferrometry, refractometry and other suitable methods and to interpret the experimental data collected. Complete understanding of the phenomena of solution chemistry will become a reality only when solute-solute, solute-solvent and solvent-solvent interactions are elucidated and thus the present research work is intimately related to the studies of solute-solute, and solvent-solvent interactions in some industrially important liquid systems.

How substances behave in solvents is an ancient problem. Yet that understanding was in fact highly limited, mainly to ions in dilute solution. One of the causes for the workings in solution chemistry is that the structure of the solvent molecule is not known with certainty. The introduction of a solute also modifies the solvent structure to an uncertain magnitude whereas the solute molecule is also modified and the interplay of forces like solute-solute, solute-solvent and solvent-solvent interactions become predominant, though the isolated picture of any of the forces is still not known completely to the solution chemist.

A.1. CHOICE OF THE SOLUTES AND SOLVENTS USED

A.1.1 Ionic liquids, Electrolyte, Drug molecules and Cyclic compounds

The ionic liquids, Drug molecules and Cyclic compounds used in the research work are

A.1.1.1 Ionic liquids

The most noteworthy ionic liquids have been used as electrolytes during the research work are

- a. Benzyltrimethylammonium chloride
- b. Benzyltriethylammonium chloride
- c. Benzyltributylammonium chloride

- d. 1-butyl-3-methylimidazolium chloride
- e. 1-methyl-3-octylimidazolium tetrafluoroborate

A.1.1.2 Electrolytes

Tetrabutylammonium tetraphenylborate

A.1.1.3 Drug Molecules

- a. Amantadine hydrochloride
- b. Sulfanilamide
- c. Metoclopramide Hydrochloride

A.1.1.4 Cyclic compounds

- a. α - and β -cyclodextrin
- b. 18-crown-6
- c. Dibenzo-18-crown-6
- d. Dicyclo-18-crown-6

A.1.2 Solvents

The universal solvent water has been used all over the work and the non-aqueous solvent e.g., Methanol, Acetonitrile, Tetrahydrofuran, Dichloromethane.

The study about the ionic liquids, drug molecules, cyclodextrins, crown ethers and different solvents is of great importance because of their wide range of application in many industries ranging from pharmaceutical to cosmetics.

A.2. METHODS OF INVESTIGATION

Different experimental techniques have been used throughout the work to get a better approaching into the phenomena of solvation and different interactions prevailing in solution systems and to investigate the host-guest inclusion complex formation. So, we have tried to employ some important physicochemical methods, namely, *Densitometry*, *Surface chemistry (surface tension)*; transport properties viz., *Viscometric*, *Conductometric*; optical property *Refractometric* and spectroscopic properties *FTIR*, *UV-*

Visible, Fluorescence and NMR Spectroscopic method to examine, probing, exploring of various interactions occurring in the solution systems.

A.3. PHYSICO-CHEMICAL PARAMETERS AND THEIR SIGNIFICANCE

Apparent molar volume (ϕ_V^0) is estimated from experimental density values. The sign and magnitude of apparent molar volume (ϕ_V^0) provides information about the nature and magnitude of ion-solvent interaction while the experimental slope (S_V^*) provides information about ion-ion interactions.

Viscosity B -coefficients are another tool gives the useful scheme of ion-solvent interaction, estimated from experimental viscosity values.

The optical property as refractive index and spectroscopic property as FTIR spectroscopy is are used as supporting parameters to confirm the interaction occurring in the solution systems.

Limiting molar conductance (Λ_0) obtained from specific conductance as well as molar conductance gives a central idea about the ion-solvent interaction the solution. More the magnitude of conductance of the solution less is the ion-solvent interaction. Another parameter obtained from the conductance study i.e. association constant (K_A) gives an idea about the solvation of the ions by the solvent molecules.

A.4. STRUCTURE OF THE THESIS

The present thesis deals with the investigation on solvation behaviour and host-guest inclusion complex formation of some significant molecules with various cyclic compounds. Here ionic liquids, drug molecules are taken as guest molecules and cyclodextrins, crown ethers are taken as host molecules to form inclusion complexes.

In this context, the present work primarily involves (i) preparation of inclusion complex between cyclic Host and various significant Guest molecules, (ii) characterization of the complexes, (iii) determination of stability constant and thermodynamic parameters, (iv) analyzing the different type of interactions present in the inclusion complexes, (v) examination of the transport properties of ionic liquids in

industrially important solvents along with thermodynamic studies to characterize molecular interactions in solutions.

Chapter-I deals with the *objective, utility and applications of the research work*, the important electrolytes/solutes and solvents used and methods of investigation. This also occupies the summary of the works done associated with the thesis.

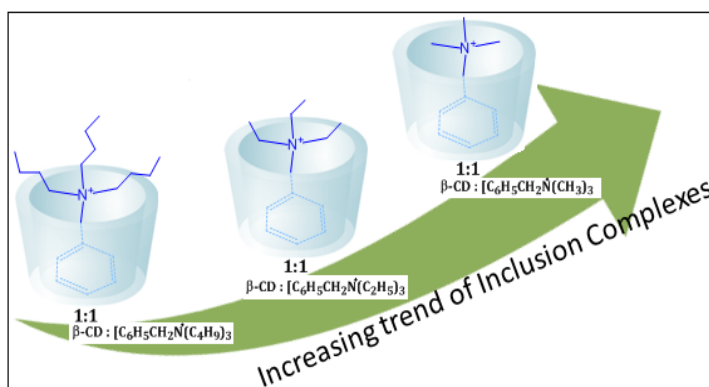


Chapter-II contains the *general introduction* of the thesis and forms the strong background of the work embodied in this thesis. A brief review of noteworthy works in the field of molecular as well as ionic interaction and host-guest chemistry have been specified. The discussion consist of what is host-guest chemistry, common example of cyclic host molecules (cyclodextrins, crown rethers) and significant guest molecules (ionic liquids, drug molecules) and it includes structure, properties of host and guest molecules and the utility of the host-guest chemistry in the field of medicine. It also discuss about the solution behaviour in terms of ion-solvent/solute-solvent, ion-ion/solute-solute and solvent-solvent interactions in binary solvent systems and of electrolytes in pure and non-aqueous solvent systems at various temperatures based on the various derived parameters, estimated from the experimentally observed physicochemical properties viz., *density, viscosity, refractive index and conductance*. Several semi-empirical models to estimate dynamic viscosity of binary liquid mixtures have been discussed. Ionic association and its dependence on ion-size parameters as well as relation between solution viscosity and limiting conductance of an ion has been discussed using Stokes' law and Walden rule. Crucial assessment of different methods on the relative merits and demerits on the basis of various assumption employed from time to time of acquiring the single ion values (viscosity *B*-coefficient and limiting equivalent conductance) and their implications have been discussed. The molecular interactions are interpreted based on various derived parameters.

Chapter-III covers the experimental section which principally involves the elementary information's such as structure, source, purification and utility of the solvent and fundamental properties of the components (ionic liquids and drug molecules) used during the entire research work. It also confines the details of the instruments, procedure, working principle and equations that are employed to understand the supramolecular host-guest chemistry and solution chemistry (physicochemical and spectroscopic properties).



In the **Chapter-IV** host-guest inclusion complexes of three sequential cationic room temperature surface active ionic liquids, benzyltrialkylammonium chloride $[(C_6H_5CH_2)N(C_nH_{2n+1})_3Cl]$; where $n=1,2,4$ with β -

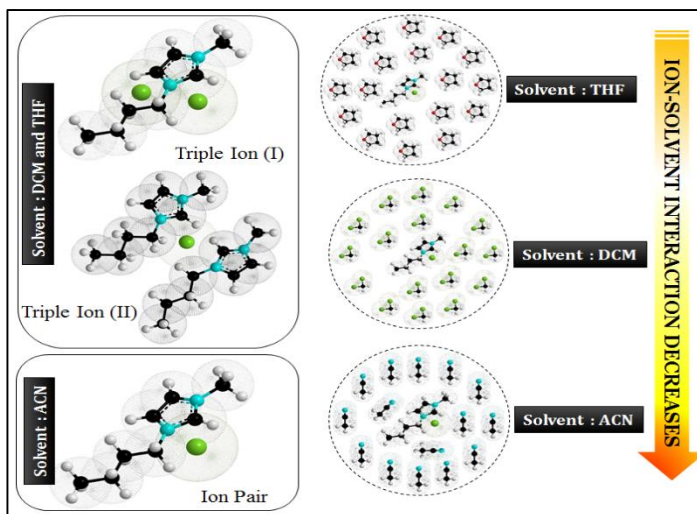


cyclodextrin in aqueous media have been studied using surface tension, conductance and NMR spectroscopy. All the studies have suggested that the hydrophobic benzyl group of ionic liquids is encapsulated inside into the cavity of β -cyclodextrin and played a crucial role in supporting the formation of inclusion complexes. The variation of the thermodynamic parameters with guest size, shape is used to draw inferences about contributions to the overall binding by means of the driving forces, viz., hydrophobic effect, steric hindrance, van der Waal force, and electrostatic force.

Chapter-V discuss about the complex formation of amantadine hydrochloride with 18-crown-6 was studied in methanol solution by surface tension, conductivity and IR study. The limiting apparent molar volume data have been used to characterize the interaction between drug molecule (amantadine hydrochloride) and 18-Crown-6 in the

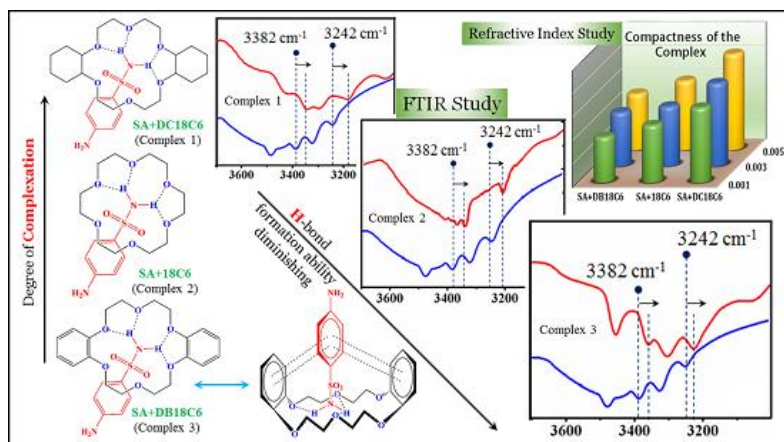
experimental ternary solution systems. A conductance study concerning the interaction between cationic organic ammonium ions amantadine with 18-crown-6 in methanol solution has been carried out at different temperatures. The formation constant ($\log K_f$) of the resulting 1:1 complex at various temperatures was determined from the conductivity study. The enthalpy (ΔH^0) entropy (ΔS^0) and free energy change (ΔG^0) of the complexation reaction was determined from the temperature dependence of the formation constant.

In **Chapter-VI** the ion-pair formation constant (K_P) and triple ion formation constant (K_T) of 1-butyl-3-methylimidazolium chloride ([bmim][Cl]) have been determined conductometrically in different solvent media in the temperature range from (298.15 to 318.15) K. The Fuoss conductance equation (1978) for



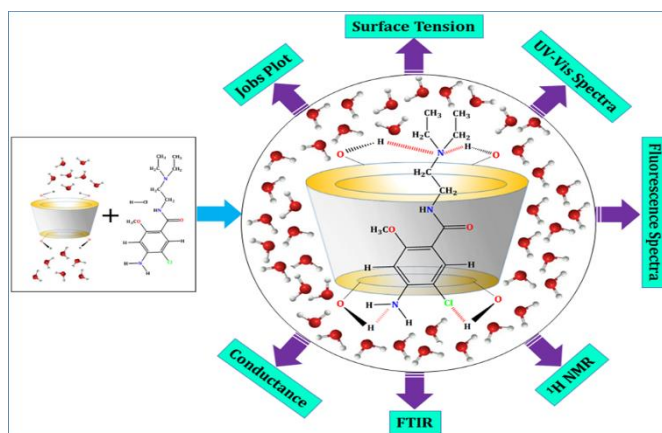
ion-pair formation and Fuoss–Kraus theory for triple-ion formations have been used for analysing the conductance data. The Walden product is obtained and discussed. However, the deviation of the conductometric curves (Λ vs \sqrt{m}) from linearity for the electrolyte in tetrahydrofuran and dichloromethane indicated/indicates triple-ion formation. Ion–solvent interactions have been studied with the help of density, viscosity and FTIR spectroscopic measurements. Apparent molar volume and viscosity B-coefficient have been calculated from experimental density and viscosity data respectively. The limiting ionic conductances (λ_o^\pm) have been estimated from the appropriate division of the limiting molar conductance of tetrabutylammonium-tetraphenylborate as “reference electrolyte” method.

Chapter-VII describe about the complexation of sulfanilamide with different crown ethers using ^1H NMR, IR and UV-visible spectra in solution state. The interactions of crown ethers with sulfanilamide have



been supported by density, viscosity, refractive index indicating higher degree of complexation in case of dicyclohexano-18-crown-6. The complexation stoichiometry was determined by Job plots and the 1:1 stoichiometry is found for all the complexes; the complex formation is confirmed by spectral shifts. The Benesi-Hildebrand method is used to calculate the binding constant of the complexes of sulfanilamide with crown ethers. The Gibbs free energy change of the inclusion complex process is calculated and the process is found to be spontaneous. Hydrogen bonding was observed to be the most important interaction for the complexation and π - π interactions also have minor contribution towards complexation of dibenzo-18-crown-6. Various factors that influence the stability of the complexes formed have been discussed for thermodynamic consideration.

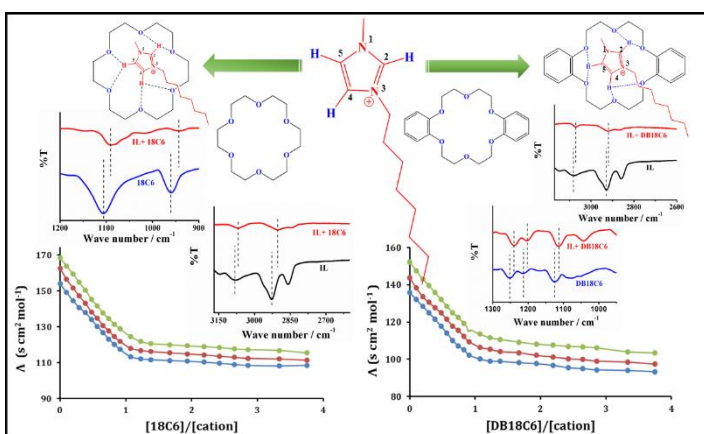
In **Chapter-VIII** the supramolecular interaction of metoclopramide hydrochloride (MP) with α -cyclodextrin (α -CD) and β -cyclodextrin (β -CD) has been inspected by ultraviolet-visible (UV-vis) light, infra-red (IR) light,



fluorescence and ^1H NMR spectroscopy. The formation of an inclusion complex greatly affects the physical-chemical properties of the guest molecules, such as solubility, chemical reactivity and the spectroscopic and electrochemical properties. Thus the changes in the spectral properties and physico-chemical properties confirm the inclusion

complex formation. Surface tension, conductivity studies and Job's plot indicate a 1 : 1 stoichiometry of the MP:CD host-guest inclusion complexes. The binding/association constants have been evaluated by both UV-Vis and fluorescence spectroscopic study indicating a higher degree of encapsulation for β -cyclodextrin (β -CD). Furthermore, the negative value of thermodynamic parameter (ΔG°) of the host guest system suggests that the inclusion process proceeded spontaneously at 298.15 K. Based on the NMR data, the plausible mode of interaction of MP: α -CD and MP: β -CD complexes were proposed, which suggested that lipophilic aromatic ring of the MP entered into the cavity of CDs from the wider side, with the amide (-CONH) and methoxy (-OMe) residues inside the CD cavity.

Chapter-IX explains the inclusion complex formation between hollow circular based compounds e.g. crown ethers and ionic liquid 1-methyl-3-octylimidazolium tetrafluoroborate in acetonitrile solvents by means of conductivity



measurements, IR spectra and NMR spectra. The results reveal the formation of 1:1 complexes between crown ethers and ionic liquid in acetonitrile. Crown ethers complexes with electron-deficient imidazolium cation which are formed by H-bond formation between the acidic protons of the imidazolium ring of the ionic liquid and lone pair of electrons of the crown oxygen atom. In case of Dibenzo-18-crown-6 complexation is caused by H-bonding but either π -stacking or charge-transfer interactions also seem to have a minor contribution towards complex formation. Thus the hydrogen bonding is mainly responsible for complexation and ion-dipole interactions also may be responsible for the complex formation between the ionic liquid molecule and crown ethers. The interactions in complexation are analyzed and discussed.

The thesis ends with **Chapter-X** where the entire work activity and final outcome described throughout the thesis has been highlighted.

PREFACE

The work in the thesis entitled "INVESTIGATION ON SOLVATION BEHAVIOUR AND HOST GUEST INCLUSION COMPLEXES OF SOME SIGNIFICANT MOLECULES WITH DIVERSE CYCLIC COMPOUNDS " was commenced on December 2012 under the supervision of Dr. Mahendra Nath Roy, Professor of Chemistry in the Department of Chemistry, University of North Bengal.

The work is an attempt to explore host guest chemistry by forming inclusion complexes of some significant molecules with diverse cyclic compounds and to investigate the solvation behaviour of the significant molecules in terms of several interactions in aqueous and non-aqueous solutions by studying their physicochemical, transport, optical, tensiometric and spectral properties.

I was blessed to participate in several meets and seminars across the country and I was highly inspired by listening and interacting with distinguished experts and scientists during the course of my research work, I was even fortunate enough to publish the works in the thesis in National and International Journals of repute.

In keeping with general practice of reporting scientific observation, due acknowledgement has been made whenever the work described was based on the finding of other investigators. I must take the responsibility of any unintentional oversights and errors, which might have sneaked in spite of precautions.

I hope that I will be given more challenges in my life so that the knowledge that I have gained during my work can be invest in action in the future.

ACKNOWLEDGEMENT

Throughout the journey of my research period at the University of North Bengal, the company of great and wise people has always enriched me and made me a better person. Although a little thank you seems to be powerless to express my deep gratitude, but no other opportunity could be better than this to express how overwhelmed I am by your generosity. I express my heart felt gratitude to all those who kept their faith on me & did contribute in different ways to achieve my goal.

First and foremost I would like to express my humble gratitude to my supervisor Prof. (Dr.) Mahendra Nath Roy, the Honourable Head of the Department, for his encouragement & providing me healthy atmosphere for pursuing research. I would not have been travelled so far without his excellent guidance and flexibility as an academic advisor. It is a pleasure to learn from him and he will always be an inspiration. I am grateful to him for never giving up hopes, in spite of my failures and mistakes during my research work. I thank him for his unconditional faith and trust in me and also for his liberty that he gave me throughout the tenure of my work. Without his motivation and priceless inputs, this dissertation would not have seen daylight. I feel blessed and privileged to work under his superlative guidance.

I express my sincere thanks to present and former faculties of our department for their constant inspiration and encouragement to carry out my research work. Also, I would like to thank all non-teaching staff of our department who extended their affirmative support and help.

I would also like to thank all past and present members of our lab whom I worked with. In particular Dr. Deepak Ekka, Biraj Kumar Barman, Dr. Milan Chandra Roy, Subhadeep Saha, Mitali Kundu, Biswajit Dutta, Kanak Roy, Koyeli Das, Aditi Roy, Ananya Yasmin, Raja Ghosh, Biplab Rajbanshi and Sayanta Roy for their help, encouragement and making a friendly atmosphere in lab. I feel honoured to have company like them in my life.

I would like to express my deepest gratitude to the headmistress, colleagues and friends of my school (Chopra Girls High School) where I have been serving as an Assistant Teacher in Chemistry. I am grateful to them for their invaluable suggestions and friendly cooperation to proceed my research work.

I take this opportunity to sincerely acknowledge the University of North Bengal for providing a second home away from home & a mesmerizing environment. I am also grateful to Departmental Special Assistance Scheme under University Grants Commission, New Delhi (No. F540/27/DRS/2007, SAP-1) for providing financial support & instrumental assistance to give a shape to my research work.

Finally, I would like to express deepest gratitude and affection to my parents for their unconditional love and continuous encouragement throughout my PhD degree to pursue my interest. All of them are like my silent partners who propel me to greater heights with their unrelenting support. The aforesaid list is neither complete in names, nor in deeds of all the people whom I met across my path of progress towards achieving my PhD degree. Thank you all for never letting me down, this dissertation would not have got a complete shape without their blessings.

Once again I am glad to have this chance to pursue my PhD because it has truly been a wonderful experience.

Siti Barman
12/07/2017

Siti Barman

Research Scholar

Department of Chemistry

University of North Bengal

Dist.: Darjeeling, Pin: 734013

West Bengal, INDIA

TABLE OF CONTENTS

[Page No.]

Declaration	(iv)
Certificate	(v)
Abstract	(vi-xv)
Preface	(xvi)
Acknowledgements	(xvii-xviii)
List of Tables	1-6
List of Figures	7-11
List of Schemes	13-14
List of Appendices	
• Appendix A: List of Publications/Communications.....	15-18
• Appendix B: List of Seminars / Symposiums / Conferences Attended.....	19
• Appendix C: List of abbreviation and symbol.....	21-22

CHAPTER: I

Necessity of the Research Work	25-33
I.1. Aims and Objectives	
I.1.1. Importance of Physicochemical Parameters	
I.1.2. The main objectives of our work	
I.2. Chemicals Used	
I.3. Methods of Investigation	
I.4. Scope of the Work	

CHAPTER: II

General Introduction (Review of the Earlier Works)	35-104
II.1. Host-guest chemistry	
II.2. Cyclodextrins	
II.2.1. Discovery of Cyclodextrin	

II.2.2. Structural features and properties of Cyclodextrins

II.2.3. Inclusion complex formation

II.2.4. Equilibrium

II.2.5. Higher order complexes

II.2.6. Binding constants

II.2.7. Applications of Cyclodextrins

II.3. Macrocyclic Polyethers

II.3.1. Discovery of Crown Ethers

II.3.2. Structure of Crown Ethers

II.3.3. Factors Governing Complexation and Selectivity of crown ethers

II.3.4. Applications of Crown Ethers

II.4. Methods of detecting the inclusion process

II.4.1. NMR Spectroscopy

II.4.2. FT-IR Spectra of solid inclusion complexes

II.4.3. Optical Spectroscopy

II.4.3.1. UV-visible Spectroscopy

II.4.3.2. Fluorescence Spectroscopy

II.4.4. Surface Tension

II.4.5. Conductance Study

II.5. Significant Molecules

II.5.1. Drug molecules

II.5.2. Ionic Liquids

II.6. Solvation Behaviour

II.6.1. Interactions in solution systems

II.6.2. Investigation on different kind of Interactions

II.6.2.1. Ion-solvent Interaction

II.6.2.2. Ion-Ion Interactions

II.6.3. Density

II.6.4. Viscosity

II.6.5. Conductance

II.6.6. Refractive index

II.6.7. FTIR Spectroscopy

CHAPTER: III

Experimental Section.....105-136

III.1. Name, Structure, Physical and Chemical Properties, Purification and Applications of the Chemicals used in the Research Work

III.1.1. Ionic Liquids

III.1.2. Drug molecules

III.1.3. Macrocyclic Compounds

III.1.4. Solvents

III.2. Experimental Methods

III.2.1. Preperation of Solutions

III.2.2. Preperation of Multicomponent liquid mixtures

III.2.3. Measurements of Experimental Properties

III.2.3.1. Mass Measurement

III.2.3.2. Conductivity Measurement

III.2.3.3. Density Measurement

III.2.3.4. Viscosity Measurement

III.2.3.5. Refractive Index Measurement

III.2.3.6. Surface Tension Measurement

III.2.3.7. FTIR Spectroscopy

III.2.3.8. UV-VIS Spectra Measurement

III.2.3.9. Quanta Master 40 spectrofluorometer

III.2.3.10. NMR Spectra Measurement

III.2.3.11. Water Distiller

III.2.3.12. Thermostat Water Bath (Science India, Kolkata)

CHAPTER: IV

NMR, Surface Tension and Conductance Study to Investigate Host-Guest Inclusion Complexes of Three Sequential Ionic Liquids with β -Cyclodextrin in Aqueous Media.....137-152

[Published in Chemical Physics Letters. 658 (2016) 43-50]

IV.1. Introduction

IV.2. Experimental Section

- IV.2.1. Reagents
- IV.2.2. Instrumentation
- IV.3. Results and discussion**
 - IV.3.1. Critical Micellization Concentration (CMC)
 - IV.3.2. Surface Tension
 - IV.3.3. Conductance
 - IV.3.4. ¹H NMR
 - IV.3.5. Association Constant and Other thermodynamic properties
- IV.4. Conclusion**

CHAPTER: V

Probing Inclusion Complex Formation of Amantadine

Hydrochloride with 18-Crown-6 in Methanol by Physicochemical

Approach.....153-169

[Published in Zeitschrift für Physikalische Chemie 231(2016) 1111-1126]

- V.1. Introduction**
- V.2. Experimental Section**
 - V.2.1. Reagents
 - V.2.2. Instrumentations
- V.3. Results and discussion**
 - V.3.1. Conductance
 - V.3.2. Association constant and Thermodynamic parameter
 - V.3.3. Surface tension
 - V.3.4. IR Study
 - V.3.5. Apparent molar volume
 - V.3.6 Temperature dependent limiting apparent molar volume
- V.4. Conclusion**

CHAPTER: VI

Investigation on Solvation Behavior of an Ionic Liquid (1-butyl-3-methylimidazolium chloride) with the Manifestation of Ion

Association Prevailing in Different Pure Solvent Systems.....171-196

[Published in Indian Journal of Advances in Chemical Science 5 (2017) 1-16]

VI.1. Introduction

VI.2. Experimental Section

VI.2.1. Reagents

VI.2.2. Instrumentations

VI.3. Results and discussion

VI.3.1. Electrical Conductance

VI.3.1.1. Ion-pair formation

VI.3.1.2. Thermodynamic Parameters

VI.3.1.3. Triple-ion formation

VI.3.2. Volumetric Properties

VI.3.3. Temperature dependent limiting apparent molal volume

VI.3.4. Viscosity B Coefficients

VI.3.5. Infrared Spectroscopy

VI.4. Conclusion

CHAPTER: VII

Interactions of an Antifungal Sulfa Drug with Diverse Macrocyclic Polyethers Explaining Mechanism, Performance and Physiognomies Leading to Formation of Stable Complexes.....197-228

[Communicated]

VII.1. Introduction

VII.2. Experimental Section

VII.2.1. Reagents

VII.2.2. Instrumentations

VII.3. Results and discussion

VII.3.1. Job plot demonstrate the Stoichiometry

VII.3.2. FTIR spectral analysis

VII.3.3. NMR Study

VII.3.4. Apparent molar volume

VII.3.5. Temperature dependent limiting apparent molar volume

VII.3.6. Viscosity B Coefficients

VII.3.7. Refractive index calculation

VII.3.8. Typical Features of Specific Interactions involved in the Complexation

VII.3.9. Association constant and Thermodynamic parameters

VII.4. Conclusion

CHAPTER: VIII

Subsistence of Host-Guest Inclusion Complexes of Metoclopramide Hydrochloride with α - and β -Cyclodextrin Molecules Probed by Physicochemical Investigation.....229-254

[Communicated]

VIII.1. Introduction

VIII.2. Experimental Section

VIII.2.1. Reagents

VIII.2.2. Instrumentations

VIII.2.3. Preparation of MP: α -CD and MP: β -CD inclusion complexes

VIII.3. Results and discussion

VIII.3.1. Job plot demonstrate the Stoichiometry

VIII.3.2. Surface tension study

VIII.3.3. Conductivity study

VIII.3.4. Association constants from UV-Vis spectroscopy

VIII.3.5. Association constant from fluorescence spectroscopy

VIII.3.6. The thermodynamics of inclusion process

VIII.3.7. $^1\text{H-NMR}$ analysis of inclusion complexes

VIII.3.8. FT-IR Spectra of solid inclusion complexes

VIII.3.9. Driving force of the inclusion complex formation

VIII.4. Conclusions

CHAPTER: IX

Hollow Circular Compound-Based Inclusion Complexes of an Ionic liquid.....255-272

[Published in RSC Advances 2016 (6) 76381-76389]

IX.1. Introduction

IX.2. Experimental Section

IX.2.1 Reagents

IX.2.2 Instrumentations

IX.3. Results and discussion

IX.3.1. Conductance

IX.3.2. Association constant and Thermodynamic parameter

IX.3.3. IR Study

IX.3.4. NMR Study

IX.3.5. Typical Features of Specific Interactions involved in the
Complexation

IX.4. Conclusion

CHAPTER: X

Concluding Remarks.....273-277

BIBLIOGRAPHY.....279-310

INDEX.....311-315

ENCLOSURES

Reprint of the Published Papers

LIST OF TABLES

<u>CHAPTERS</u>	<u>TABLE CAPTIONS</u>	<u>PAGE NO.</u>
Chapter-II	Table II.1: Characteristics of Cyclodextrin.	39
Chapter-IV	Table IV.1: Molar Conductance (Λ) and Surface tension (γ) values with corresponding concentration at the CMC and saturation point of inclusion; and concentration ratio (ratio of inclusion IL: β -CD) at the break point of the surfactants solution (0.01 M) in aqueous β -CD	141
	Table IV.2: Free energy of micellization (ΔG_{mic}) and free energy of change (ΔG) obtained from degree of micelle ionization (α) and association constant (K_a) of the solution (β -CD+ionic liquid) at 25°C evaluated from the conductance and surface tension measurement respectively	142
Chapter-V	Table V.1: Values of observed molar conductivities (Λ) at various mole ratios for the system Amantadine-18C6 at different temperature	157-158
	Table V.2: Values of formation constant, enthalpy, entropy and free energy change of amantadine-18C6 complex in methanol solution	160
	Table V.3: Experimental values of surface tension (γ) corresponding to concentration of 18C6 in methanolic solution	161
	Table V.4: Values of surface tension (γ) at the break point with corresponding to concentration of 18C6 in methanolic solution at 298.15 K	163
	Table V.5: Experimental values of density (ρ) in different mass fraction of methanolic solution of 18C6	164
	Table V.6: Experimental values of densities (ρ) corresponding to concentration in different mass fractions of methanolic solution of 18C6 at different temperature	165

	Table V.7: Limiting apparent molar volume ($\phi_{v^{\circ}}$) and experimental slope (S_{v^*}) in different mass fractions of methanolic solution of 18-crown-6	165-166
	Table V.8: Limiting apparent molar expansibilities (ϕ_E^0) for amantadine hydrochloride in different mass fraction of 18C6 in methanol solution (w_1) at 298.15K to 308.15K respectively	168
Chapter VI	Table VI.1: Density (ρ), viscosity (η) and relative permittivity (ϵ) of the different solvents Acetonitrile, Tetrahydrofuran and Dichloromethane	174
	Table VI.2: The concentration (m) and molal conductance (Λ) of [bmim][Cl] in Acetonitrile, Dichloromethane and Tetrahydrofuran at 298.15 K, 303.15K and 308.15K respectively	175-176
	Table VI.3: Limiting molar conductance (Λ_0), association constant (K_A), co-sphere diameter (R) and standard deviations of experimental Λ (δ) obtained from Fuoss conductance equation of [bmim][Cl] in Acetonitrile at 298.15 K, 303.15 K and 308.15 K respectively	178
	Table VI.4: Walden product ($\Lambda_0 \cdot \eta$) and Gibb's energy change (ΔG°) of [bmim][Cl] in Acetonitrile at 298.15 K, 303.15 K and 308.15 K respectively	179
	Table VI.5: Limiting Ionic Conductance (λ_{o^\pm}), Ionic Walden Product ($\lambda_{o^\pm} \eta$), Stokes' Radii (r_s), and Crystallographic Radii (r_c) of [bmim][Cl] in Acetonitrile at 298.15 K, 303.15 K and 308.15 K respectively	179
	Table VI.6: Thermodynamic parameters for [bmim][Cl] in ACN	180
	Table VI.7: The calculated limiting molar conductance of ion-pair (Λ_0), limiting molar conductances of triple ion Λ_0^T , experimental slope and intercept obtained from Fuoss-Kraus Equation for [bmim][Cl] in DCM and THF at 298.15 K, 303.15 K and 308.15 K respectively	183

	<p>Table VI.8: Salt concentration at the minimum conductivity (C_{min}) along with the ion-pair formation constant (K_P), triple ion formation constant (K_T) for [bmim][Cl] in DCM and THF at 298.15 K, 303.15 K and 308.15 K respectively</p>	184
	<p>Table VI.9: Salt concentration at the minimum conductivity (C_{min}), the ion pair fraction (α), triple ion fraction (α_T), ion pair concentration (C_P) and triple-ion concentration (C_T) for [bmim][Cl] in DCM and THF at 298.15 K, 303.15 K and 308.15 K respectively</p>	186
	<p>Table VI.10: Density (ρ) and viscosity (η) of 1-butyl-3-methylimidazolium chloride in different mass fraction of Acetonitrile, Dichloromethane and Tetrahydrofuran at different temperatures</p>	187-188
	<p>Table VI.11: Apparent molal volume (ϕ_V) and $\frac{(\eta_r - 1)}{\sqrt{m}}$ for 1-butyl-3-methylimidazolium Chloride ([bmim][Cl]) in different mass fraction of Acetonitrile, Dichloromethane and Tetrahydrofuran at different temperatures</p>	189
	<p>Table VI.12: Limiting apparent molar volume (ϕ_V^0), experimental slope (S_V^*), viscosity B-and viscosity A- coefficient for [bmim][Cl] in ACN, DCM and THF at T= (298.15 to 308.15) K respectively</p>	190
	<p>Table VI.13: Values of empirical coefficients (a_0, a_1, and a_2) of Equation 26 of the [bmim][Cl] in ACN, DCM and THF</p>	192
	<p>Table VI.14: Limiting apparent molal expansibilities (ϕ_E^0) of [bmim][Cl] in ACN, DCM and THF at T= (298.15 to 308.15) K</p>	193
	<p>Table VI.15: Stretching frequencies of the functional groups present in the pure solvent and change of frequency after addition of [bmim][Cl] in the solvents</p>	195

Chapter VII	Table VII.1: Data for the Job plot performed by UV-Vis spectroscopy for SA-DC18C6 system	201
	Table VII.2: Data for the Job plot performed by UV-Vis spectroscopy for SA-18C6 system	201
	Table VII.3: Data for the Job plot performed by UV-Vis spectroscopy for SA-DB18C6 system	202
	Table VII.4: Comparison between the Frequencies change (cm^{-1}) of different functional group of free compound and their complexes	205
	Table VII.5: Experimental values of density (ρ) and viscosity (η) of sulfa drug in different mass fraction of DC18C6 (w_1), 18C6 (w_2) and DB18C6 (w_3) in ACN at T= (293.15 to 308.15) K	209-211
	Table VII.6: Limiting apparent molar volume (ϕ_V^0) and viscosity B-coefficient of sulfa drug in different mass fraction of different crown ethers in ACN at T= (293.15 to 308.15) K	213-214
	Table VII.7: Values of empirical coefficients (a_0 , a_1 , and a_2) of Equation 14 of sulfa drug in different mass fraction of DC18C6 (w_1), 18C6 (w_2) and DB18C6 (w_3) in ACN at T= (293.15 to 308.15) K	215
	Table VII.8: Limiting apparent molal expansibilities (ϕ_E^0) of sulfa drug in different mass fraction of DC18C6 (w_1), 18C6 (w_2) and DB18C6 (w_3) in ACN at T= (293.15 to 308.15) K	216
	Table VII.9: Values of dB/dT of sulfa drug in different mass fraction of DC18C6 (w_1), 18C6 (w_2) and DB18C6 (w_3) in ACN at T= (293.15 to 308.15) K respectively	219

	Table VII.10: Values of Refractive Index (n_D) and Molar Refraction (R_M) of sulfa drug in different mass fraction of DC18C6 (w_1), 18C6 (w_2) and DB18C6 (w_3) in ACN at $T=298.15$ K respectively	221-222
	Table VII.11: Limiting molar refractions (R_M^0) values of sulfa drug in different mass fraction of DC18C6 (w_1), 18C6 (w_2) and DB18C6 (w_3) in ACN at $T=298.15$ K respectively	223
	Table VII.12: Values of Association constant (K_a) and free energy change (ΔG^0) of the three SA-CEs complexes	225
	Table VII.13: Data for the Benesi-Hildebrand double reciprocal plot performed by UV-Vis spectroscopy for SA-DC18C6 system	227
	Table VII.14: Data for the Benesi-Hildebrand double reciprocal plot performed by UV-Vis spectroscopy for SA-18C6 system	227
	Table VII.15: Data for the Benesi-Hildebrand double reciprocal plot performed by UV-Vis spectroscopy for SA-DB18C6 system	227
Chapter VIII	Table VIII.1: Data for the Job plot performed by UV-Vis spectroscopy for aqueous MP: α -CD system at $298.15K^a$	234
	Table VIII.2: Data for the Job plot performed by UV-Vis spectroscopy for aqueous MP: β -CD system at $298.15K^a$	235
	Table VIII.3: Data for surface tension and conductivity study of aqueous MP: α -CD system at $298.15K^a$	237
	Table VIII.4: Data for surface tension and conductivity study of aqueous MP: β -CD system at $298.15K^a$	238
	Table VIII.5: Values of surface tension (γ) at the break point with corresponding concentrations of MP and CD at $298.15K^a$	239
	Table VIII.6: Values of conductivity (κ) at the break point with corresponding concentrations of MP and CD at $298.15K^a$	240

	Table VIII.7: Data for the Benesi-Hildebrand double reciprocal plot performed by UV-Vis spectroscopy for MP: α -CD system	241
	Table VIII.8: Data for the Benesi-Hildebrand double reciprocal plot performed by UV-Vis spectroscopy for MP: β -CD system	243
	Table VIII.9: Data for the Benesi-Hildebrand double reciprocal plot performed by fluorescence spectroscopy for MP: α -CD system	244
	Table VIII.10: Data for the Benesi-Hildebrand double reciprocal plot performed by fluorescence spectroscopy for MP: β -CD system	245
	Table VIII.11: Values of Association constants (K_a) obtained by Benesi-Hildebrand method both from UV-vis spectroscopy and Fluorescence spectroscopy and corresponding free energy change (ΔG^0) of the MP:CD inclusion complexes at 298.15K ^a	246
	Table VIII.12: Comparison between the Frequencies change (cm^{-1}) of different functional group of free compound and their solid complexes	252-253
Chapter IX	Table IX.1: Values of observed molar conductivities, Λ , at various mole ratios for the system IL-18C6 (complex 1) and IL-DB186 (complex 2) at different temperature	258
	Table IX.2: Values of formation constant, enthalpy, entropy and free energy change of different crown ethers complexes in ACN solution	260
	Table IX.3: Comparison between the Frequencies change (cm^{-1}) of different functional group of free compound and their complexes	266

LIST OF FIGURES

<u>CHAPTERS</u>	<u>FIGURE CAPTIONS</u>	<u>PAGE NO.</u>
Chapter-II	Figure II.1: Schematic representation for host-guest complexation by Cyclodextrin	35
	Figure II. 2: Schematic representation of various interactions involved in host-guest chemistry	36
	Figure II. 3: From molecular to supramolecular chemistry	36
	Figure II. 4: Structures of the α -, β - and γ -cyclodextrin	38
	Figure II. 5: General structure of cyclodextrin molecule with interior and exterior protons ($n = 6, 7$ for α -CD and β -CD respectively)	39
	Figure II.6: Different stoichiometries of host-guest inclusion complexes	41
	Figure II.7: Schematic drawing of cation- π interactions showing the contact of K^+ ion and benzene	43
	Figure II.8: Several example of crown ethers	44
	Figure II.9: Pedersen's reaction	45
	Figure II.10: Growth rate of ionic liquid publications, 1986-2006	54
	Figure II.11: Annual growth of ionic liquid patents, 1996-2006	55
	Figure II.12: A diagram for the explanation of molal volume.	64
Chapter-IV	Figure IV.1: Plot of surface tension (γ) with corresponding conc. (M) of ionic liquids	140
	Figure IV.2: Plot of molar conductance (Λ) with corresponding conc. (M) of ionic liquids	142
	Figure IV.3: Plot of surface tension (γ) of ionic liquids (0.01M) with corresponding conc.(M) of β -CD	143
	Figure IV.4: Plot of molar conductance (Λ) of ionic liquids (0.01M) with corresponding conc. (M) of β -CD	144
	Figure IV.5: Plot of surface tension (γ) with corresponding conc. of ionic liquids in absence (solid fill) and in presence (no fill) of β -CD	145

	Figure IV.6: (a) Stereo-chemical configuration, (b) truncated conical structure of β -cyclodextrin with interior and exterior protons	148
	Figure IV.7: ^1H NMR spectra of (a) β -CD, (b) $[(\text{C}_6\text{H}_5\text{CH}_2)\text{N}(\text{CH}_3)_3]\text{Cl}$, and (c) inclusion complex	148
	Figure IV.8: ^1H NMR spectra of (a) β -CD, (b) $[(\text{C}_6\text{H}_5\text{CH}_2)\text{N}(\text{C}_2\text{H}_5)_3]\text{Cl}$, and (c) inclusion complex	149
	Figure IV.9: ^1H NMR spectra of (a) β -CD, (b) $[(\text{C}_6\text{H}_5\text{CH}_2)\text{N}(\text{C}_4\text{H}_9)_3]\text{Cl}$, and (c) inclusion complex.	149
	Figure IV.10: Relationship between (S_o-S) and $(S_o/S)-1$ for solution of ionic liquids along and mixed with β -CD	150
Chapter-V	Figure V.1: A space filling model of 18-crown-6 showing the open space at the center of the crown and electron pairs present on the exposed oxygen atoms (in pink)	155
	Figure V.2: Molar conductance vs $[18\text{C}6]/[\text{amantadine ion}]$ at 298.15 K (\blacktriangle), 303.15 K (\boxtimes), 308.15 K (\bullet)	157
	Figure V.3: The linear relationship of $\log K_f$ vs $1/T$ for the interaction between amantadine hydrochloride with 18C6	159
	Figure V.4: Variation of surface tension of amantadine with increasing concentration of 18C6 at 298.15 K	162
	Figure V.5: FTIR spectra of pure amantadine hydrochloride (black), 18-crown-6 (blue) and complex (red)	163
	Figure V.6: Plot of limiting apparent molar volume (φ_v°) of amantadine against different temperature (298.15 K, 303.15 K, 308.15 K) in mass fractions $w_1=0.001$ (\blacksquare), $w_1=0.004$ (\blacksquare), $w_1=0.007$ (\blacksquare) mass fractions of 18C6 in methanol solution	166
Chapter VI	Figure VI.1: Plot of molar conductance (Λ) versus \sqrt{m} of $[\text{bmim}][\text{Cl}]$ in ACN at 298.15 K (\blacklozenge), 303.15 K (\bullet) and 308.15 K (\blacktriangle)	175
	Figure VI.2: The linear relationships of $\ln K_a$ vs. $1/T$ for the ion pair formation in ACN	181

	Figure VI.3: Plot of molar conductance (Λ) versus \sqrt{m} for [bmim][Cl] in DCM at 298.15 K (\blacklozenge), 303.15 K (\bullet) and 308.15 K (\blacktriangle) and in THF at 298.15 K (\blacklozenge), 303.15 K (\circ) and 308.15 K (\blacktriangle)	182
	Figure VI.4: Plot of limiting apparent molal volume (ϕ_V^0) versus temperature for [bmim][Cl] in ACN (yellow), DCM (green) and THF (blue)	191
	Figure VI.5: Plot of viscosity B-coefficient versus temperature for [bmim][Cl] in ACN (blue), DCM (red) and THF (green)	194
Chapter VII	Figure VII.1: Job plot of (a) SA-DC18C6 system, (b) SA-18C6 system, (c) SA-DB18C6 system at T= 298.15 K	200
	Figure VII.2: FTIR spectra of free DC18C6 (Black), SA (Blue) and complex 1 (Red)	203
	Figure VII.3: FTIR spectra of free 18C6 (Black), SA (Blue) and complex 2 (Red)	203
	Figure VII.4: FTIR spectra of free DB18C6 (Black), SA (Blue) and complex 3 (Red)	204
	Figure VII.5: The ^1H NMR spectra of complex 1 (SA-DC18C6) (upper), uncomplexed SA and DC18C6 (lower) recorded at 300 MHz in CD_3CN at 298.15 K	206
	Figure VII.6: The ^1H NMR spectra of complex 2 (SA-18C6) (upper), uncomplexed SA and 18C6 (lower) recorded at 300 MHz in CD_3CN at 298.15 K	207
	Figure VII.7: The ^1H NMR spectra of complex 3 (SA-DB18C6) (upper), uncomplexed SA and DB18C6 (lower) recorded at 300 MHz in CD_3CN at 298.15 K	207
	Figure VII.8: Plot of limiting apparent molar volume (ϕ_V^0) of SA in mass fractions (a) 0.001, (b) 0.003, (c) 0.005 (w) of different CEs in ACN at T= (293.15 to 308.15)K respectively	212

	Figure VII.9: Plot of viscosity B-coefficient of SA in mass fractions (a) 0.001, (b) 0.003, (c) 0.005 (w) of different CEs in ACN at T= (293.15 to 308.15)K respectively	218
	Figure VII.10: Plot of limiting molar refraction (R_M^0) of SA in different mass fractions (w) of different CEs in ACN at T= 298.15 K respectively	220
	Figure VII.11: Benesi-Hildebrand double reciprocal plot for the effect of (a) DC18C6, (b) 18C6, (c) DB18C6 on the absorbance of Sulfa drug	226
Chapter VIII	Figure VIII.1: Job plots of (a) MP: α -CD system and (b) MP: β -CD system at $\lambda_{max} = 272$ nm at 298.15 K. $R = [SS]/([MP] + [CD])$, $\Delta A =$ absorbance difference of MP with and without CD	234
	Figure VIII.2: Variation of surface tension of aqueous MP with increasing concentration of (a) α -CD and (b) β -CD solution respectively at 298.15 K.	236
	Figure VIII.3: Variation of surface tension of aqueous MP with increasing concentration of (a) α -CD and (b) β -CD solution respectively at 298.15 K.	239
	Figure VIII.4: (a) Absorption spectra of MP (50 μ M) in different α -CD concentrations (μ M): 1) without α -CD, 2) 30 μ M, 3) 40 μ M, 4) 50 μ M, 5) 60 μ M, 6) 70 μ M. (b) Benesi-Hildebrand plot of $1/A - A_0$ vs. $1/[\alpha\text{-CD}]$ for 1:1 complexation of MP with α -CD	241
	Figure VIII.5: (a) Absorption spectra of MP (50 μ M) in different β -CD concentrations (μ M): 1) without β -CD, 2) 30 μ M, 3) 40 μ M, 4) 50 μ M, 5) 60 μ M, 6) 70 μ M. (b) Benesi-Hildebrand plot of $1/A - A_0$ vs. $1/[\beta\text{-CD}]$ for 1:1 complexation of MP with β -CD.	242
	Figure VIII.6: (a) Fluorescence emission spectra of MP (5 μ M) in different α -CD concentrations (μ M): 1) without α -CD, 2) 10 μ M, 3) 20 μ M, 4) 30 μ M, 5) 40 μ M, 6) 50 μ M. (b) Benesi-Hildebrand plot of $1/I - I_0$ vs. $1/[\alpha\text{-CD}]$ for 1:1 complexation of MP with α -CD.	244

	Figure VIII.7: (a) Fluorescence emission spectra of MP (5 μM) in different $\beta\text{-CD}$ concentrations (μM): 1) without $\beta\text{-CD}$, 2) 10 μM , 3) 20 μM , 4) 30 μM , 5) 40 μM , 6) 50 μM . (b) Benesi–Hildebrand plot of $1/I - I_0$ vs. $1/[\beta\text{-CD}]$ for 1:1 complexation of MP with $\beta\text{-CD}$	245
	Figure VIII.8: ^1H NMR spectra of (a) $\alpha\text{-CD}$, (b) MP and (c) 1:1 M ratio of $\alpha\text{-CD}$ & MP in D_2O at 298.15 K.	247
	Figure VIII.9: ^1H NMR spectra of (a) $\beta\text{-CD}$, (b) MP and (c) 1:1 M ratio of $\beta\text{-CD}$ & MP in D_2O at 298.15 K	247
	Figure VIII.10: FTIR spectra of free $\alpha\text{-CD}$, MP and their 1:1 inclusion complex (MP: $\alpha\text{-CD}$)	251
	Figure VIII.11: FTIR spectra of free $\beta\text{-CD}$, MP and their 1:1 inclusion complex (MP: $\beta\text{-CD}$)	251
Chapter IX	Figure IX.1: Molar conductance vs $[\text{18C6}]/[\text{cation}]$ at 298.15 K (\blacktriangle), 303.15 K (\blacksquare), 308.15 K (\bullet)	261
	Figure IX.2: Molar conductance vs $[\text{DB18C6}]/[\text{cation}]$ at 298.15 K (Δ), 303.15 K (\square), 308.15 K (\circ)	261
	Figure IX.3: The linear relationship of $\log K_f$ vs. $1/T$ for the interaction of IL with 18C6 (\bullet) and DB18C6 (\blacksquare).	263
	Figure IX.4: FTIR spectra of free IL (Black), 18-crown-6 (Blue) and complex (Red)	265
	Figure IX.5: FTIR spectra of free IL (Black), Dibenzo-18-crown-6 (Blue) and complex (Red).	265
	Figure IX.6: The ^1H NMR spectra of complex 1 (18C6.IL) (upper) and uncomplexed imidazolium cation (lower) recorded at 300 MHz in CD_3CN at 298.15 K	268
	Figure IX.7: The ^1H NMR spectra of complex 2 (DB18C6.IL) (upper) and uncomplexed imidazolium cation (lower) recorded at 300 MHz in CD_3CN at 298.15 K	268

LIST OF SCHEMES

<u>CHAPTERS</u>	<u>SCHEME CAPTIONS</u>	<u>PAGE NO.</u>
Chapter-IV	Scheme IV.1: <i>Molecular structure of cationic surfactant and β-cyclodextrin</i>	138
	Scheme IV.2: <i>Schematic illustration of plausible micelle (2a), distraction of micelle (2b) and plausible inclusion formation (2c).</i>	145
	Scheme IV.3: <i>Schematic representation of mechanism of formation of inclusion complexes of cationic ionic liquids with β-cyclodextrin</i>	146
	Scheme IV.4: <i>Schematic representation of inclusion complexes of cationic ionic liquids with β-cyclodextrin</i>	147
Chapter-V	Scheme V.1: <i>Molecular structure of Amantadine hydrochloride and 18C6</i>	154
	Scheme V.2: <i>Schematic presentation of complexation between amantadine ion and 18C6 and corresponding energy minimized structure of the complex</i>	162
Chapter-VI	Scheme VI.1: <i>Molecular structures of the IL and the solvents</i>	172
	Scheme VI.2: <i>Pictorial representation of ion-pair and triple-ion formation for the electrolyte in diverse solvent systems</i>	185
	Scheme VI.3: <i>Extent of ion-solvent interaction of IL in various solvent systems</i>	191
Chapter-VII	Scheme VII.1: <i>Molecular structure of crown ethers and SA</i>	198
	Scheme VII.2a: <i>Schematic presentation of complex formation between SA and DC18C6 and corresponding energy minimized structure of the complex</i>	223-224
	Scheme VII.2b: <i>Schematic presentation of complex formation between SA and 18C6 and corresponding energy minimized structure of the complex</i>	
	Scheme VII.2c: <i>Schematic presentation of complex formation between SA and DB18C6 and corresponding energy minimized structure of the complex</i>	

<u>CHAPTERS</u>	<u>SCHEME CAPTIONS</u>	<u>PAGE NO.</u>
Chapter-VIII	<i>Scheme VIII.1:</i> Molecular structures of (a) metoclopramide hydrochloride and (b) cyclodextrin molecule with interior and exterior protons ($n = 6, 7$ for α -CD and β -CD respectively)	231
	<i>Scheme VIII.2:</i> Plausible schematic presentation of mechanism for formation of 1:1 inclusion complex between metoclopramide hydrochloride and cyclodextrin	248
Chapter-IX	<i>Scheme IX.1:</i> Molecular structure of crown ethers and IL	256
	<i>Scheme IX.2:</i> Plausible schematic presentation of complex formation between imidazolium cation and crown ethers	259

LIST OF APPENDICES

- ✓ **Appendix A:** List of Publications/Communications
- ✓ **Appendix B:** List of Seminars / Symposiums/
Conferences Attended
- ✓ **Appendix C:** List of abbreviation and symbol

APPENDIX-A

LIST OF RESEARCH PUBLICATION(S)

- [1] NMR, Surface tension and Conductance Study to Investigate Host-guest Inclusion Complexes of Three Sequential Ionic Liquids with β -cyclodextrin in Aqueous Media



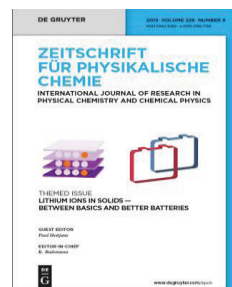
Chemical Physics Letters

658 (2016) 43–50.

(Included in the Thesis)



- [2] Investigation Probing Inclusion Complex Formation of Amantadine Hydrochloride with 18-Crown-6 in Methanol by Physicochemical Approach



Zeitschrift für Physikalische Chemie

231 (2016) 1111–1126.

(Included in the Thesis)



- [3] Investigation on Solvation Behavior of an Ionic Liquid (1-butyl-3-methylimidazolium chloride) with the Manifestation of Ion Association Prevailing in Different Pure Solvent Systems



*Indian Journal of Advances in
Chemical Science*
5 (2017) 1-16.

(Included in the Thesis)



- [4] Interactions of an Antifungal Sulfa Drug with Diverse Macrocyclic Polyethers Explaining Mechanism, Performance and Physiognomies Leading to Formation of Stable Complexes

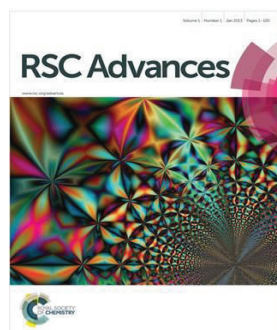
Communicated

(Included in the Thesis)

- [5] Subsistence of Host-Guest Inclusion Complexes of Metoclopramide Hydrochloride with α - and β -Cyclodextrin Molecules Probed by Physicochemical Investigation

Communicated

(Included in the Thesis)

[6] Hollow Circular Compound-Based Inclusion Complexes of an Ionic Liquid

RSC Advances
6 (2016) 76381-76389.

(Included in the Thesis)

**[7]** Self Assembly Inclusion of Ionic Liquid into Hollow Cylinder Oligosaccharides

Journal of Molecular Liquids
214 (2016), 264-269.



- [8] Study on Diverse Interactions of Vitamin Molecules Insight into H₂O + [Epy]BF₄ Systems by Physicochemical Contrivance



*Indian Journal of Advances
in Chemical Science*
3 (2015) 204-218.



- [9] Exploration of Inclusion Complexes of Neurotransmitters with β -Cyclodextrin by Physicochemical Techniques



Chemical Physics Letters
655-656 (2016), 43-50.



- [10] Host-guest Inclusion Complexes of RNA Nucleosides inside aqueous Cyclodextrins Explored by Physicochemical and Spectroscopic Methods



RSC Advances
6 (2016) 8881-8891.



APPENDIX-B

LIST OF SEMINARS/ SYMPOSIUMS/ CONFERENCES ATTENDED

1. **National Seminar on Frontiers in Chemistry - 2014** Sponsored by University Grants Commission (SAP-DRS-III), New Delhi, organized by Department of Chemistry, University of North Bengal on March 11th & 12th, 2014.
2. **Science Academies' Lecture Workshop on "Spectroscopy of Emerging Materials"** organised by the Department of Chemistry, University of North Bengal on November 26th & 27th, 2014.
3. **National Seminar on Frontiers in Chemistry - 2015** Funded by University Grants Commission and SAP (DRS-III) New Delhi, organized by the Department of Chemistry, University of North Bengal on February 17th & 18th, 2015.
4. **22nd West Bengal State Science & Technology Congress-2015** Organized by Department of Science and Technology, Govt. of West Bengal, West Bengal State Council of Science and Technology and University of North Bengal, Raja Rammohanpur, Darjeeling-734013 on February 28th & March 1st, 2015.
5. **Recent Trends on Chemistry and Biology Interface-2015** Organized by Chemical Research Society of India, NBU-Local Chapter, Department of Chemistry, University of North Bengal (Darjeeling) on August 28, 2015.
6. **19th CRSI National Symposium in Chemistry-2016** Organized by Department of Chemistry, University of North Bengal, Raja Rammohanpur, Darjeeling-734013 on July 14th to 16th, 2016.
7. **20th CRSI National Symposium in Chemistry-2017** Organized by Department of Chemistry, Gauhati University, Guwahati on February 3rd to 5th, 2017.
8. **Current Trends in University- Industries Linkages-2017** Funded by University Grants Commission and Organized by Department of Chemistry, University of North Bengal, Darjeeling-734013, W.B, India on 24th March, 2017.

APPENDIX: C

LIST OF ABBREVIATION

ACN	Acetonitrile
ADH	Amantadine Hydrochloride
[bmim][Cl]	1-butyl-3-methylimidazolium Chloride
CMC	Critical Micellar Concentration
CH ₃ OH	Methanol
CD	Cyclodextrin
α -CD	α -cyclodextrin
β -CD	β -cyclodextrin
CEs	Crown Ethers
18C6	18-crown-6
DB18C6	Dibenzo-18-crown-6
DC18C6	Dicyclohexyl-18-crown-6
°C	Degree Celcius
DCM	Dichloromethane
FTIR	Fourier Transform Infra-red Spectroscopy
ILs	Ionic liquids
M	Molarity
mL	Milli Litre
mM	Milli Molar
mPa	Milli Pascal
MP	Metoclopramide hydrochloride
¹ H-NMR	Proton-Nuclear Magnetic Resonance
RI	Refractive Index
Str.	Stretching
SA	Sulfanilamide
THF	Tetrahydrofuran
UV	Ultra Violet

LIST OF SYMBOL

ρ	Density
ϕ_V	Apparent molar volume
ϕ_V^0	Limiting apparent molar volume
S_V^*	Experimental slopes
ϕ_E^0	Limiting apparent molar expansibilities
η	Viscosity of the solution
η_0	Viscosity of the solvent
$\eta_r = \eta / \eta_0$	Relative viscosity
Λ	Molar conductance
Λ_0	Limiting molar conductance
ϵ	Relative permittivity of the solvent
$\Lambda_0 \eta$	Walden product
λ_0^\pm	Ionic limiting molar conductances
$\lambda_0^\pm \eta$	Limiting ionic Walden product
r_s	Stokes' radii
r_c	Crystallographic Radii
K_A	Association constant
R	Distance of closest approach
$a = (r_+ + r_-)$	Sum of the crystallographic radii of the cation (r_+) and anion (r_-)
d	Average distance corresponding to the side of a cell occupied by a solvent molecule
$\lambda_0^\pm \eta$	The limiting ionic Walden product
E_a	Activation energy
T	Absolute temperature
K_p	Ion-pair formation constant
K_T	Triple-ion formation constant
C_p	Ion-pair concentrations
C_T	Triple-ion concentrations
α	Fraction of ion-pairs present in the solutions
α_T	Fraction of triple-ions present in the solutions.

Thesis Overview Schematic

Chapter I

Necessity of the Research Work

Chapter II

General Introduction
(Review of the Earlier Works)

Chapter III

Experimental Section

Chapter IV

NMR, Surface Tension and Conductance Study to Investigate Host-Guest Inclusion Complexes of Three Sequential Ionic Liquids with β -Cyclodextrin in Aqueous Media

Investigation on solvation behaviour and host guest inclusion complexes of some significant molecules with diverse cyclic compounds

Chapter V

Probing Inclusion Complex Formation of Amantadine Hydrochloride with 18-Crown-6 in Methanol by Physicochemical Approach

Chapter VI

Investigation on Solvation Behaviour of an Ionic Liquid (1-butyl-3-methylimidazolium chloride) with the Manifestation of Ion Association Prevailing in Different Pure Solvent Systems

Interactions of an Antifungal Sulfa Drug with Diverse Macrocyclic Polyethers Explaining Mechanism, Performance and Physiognomies leading to Formation of Stable Complexes

Chapter VIII

Subsistence of Host Guest Inclusion Complexes of Metoclopramide Hydrochloride with α - and β -Cyclodextrin Molecules Probed by Physicochemical Investigation

Chapter IX

Hollow Circular Compound-Based on Inclusion Complexes of an Ionic Liquid

Chapter X

Concluding Remarks

CHAPTER: I

NECESSITY OF THE RESEARCH WORK

I.1. AIMS AND OBJECTIVES

Scientific research work motivated by discovery of unknown. It is especially pleasing when the work offers the promise of new knowledge, as well as imminent applications.

Supramolecular chemistry is often defined as “the chemistry beyond the molecule” or “the chemistry of the noncovalent bond”. One of the forefront contributions of supramolecular chemistry is in designing and synthesizing macrocycles that can selectively bind a particular guest. This is extremely important especially in our pursuit of knowledge in biological systems. Where it is difficult to study the humongous molecules such as enzyme, it is much easier to simulate the studies in smaller molecules that have the same properties. This is where supramolecules come in useful; where it can mimic the features of biosystems.

Majority of drug products available in market suffer from solubility problems. Because of poor solubility, good numbers of new molecules are not reaching the market. The solubility can be enhanced by several techniques. One of the prominent approaches to enhance solubility is the complexation with cyclodextrin (CD) and formation of solid inclusion complex [1]. Cyclodextrins are employed as complex forming agents thereby enhancing the aqueous solubility of poorly soluble drugs [2,3]. Thus they improve the bioavailability and stability of drugs, reduce gastrointestinal drug irritation, prevent drug–excipient and drug–drug interactions. To overcome gastrointestinal tract irritant effects caused by many of nonsteroidal anti-inflammatory drugs, it becomes necessary to formulate the drug in an appropriate dosage form which can be administered through skin. Due to the major advantage of CDs to act as drug delivery vehicles, it is proposed to study CD complexation of various significant molecules, an important constituent of numerous pharmaceutical products, by using

analytical techniques. The proposed studies employ cyclodextrins as potential drug delivery vehicles [4-6] as they can change the physical, chemical and biological activities of guest molecules by forming inclusion complexes. The principal advantages of natural cyclodextrins as drug carriers are the following: (1) well-defined chemical structure (2) availability of cyclodextrins having appropriate cavity size (3) low toxicity and low pharmacological activity (4) certain water solubility (5) they can protect included drugs from biodegradation.

The Host-guest complex formation based on the macrocyclic molecules is a facile and reversible process, which organise for the feasibilities to design stimuli-responsive supramolecular systems and these macrocyclic molecules are basically friendly to the biological environment and exhibit good biocompatibilities [7-9]. Crown ether-based host-guest interactions, which show good selectivity, high efficiency, and reversibility, have been structurally characterized and the underlying supramolecular chemistry has been presented in our work. Supramolecular chemistry i.e. host-guest complex formation through noncovalent interactions offer the basis for novel approaches in medicine and also helps in understanding the interactions present in living systems. It was also found that host-guest complexation with crown ethers resembles an established principle i.e. the hydrogen bonding acceptance as well as the donation propensity of crown ethers.

To understand the binding behavior of the different unique host system, "Inclusion complex", will be prepared and it is proposed to characterize them by various analytical tools such as IR, UV, fluorescence, NMR, conductance and surface tension studies. This will throw light not only on the role of host molecule in offering protection against degradations but also on stabilising potential conformers *via* various interactions such as hydrogen bonding *etc.*

When one substance dissolves in another the properties of the substances changes. Solution chemistry is the branch of physical chemistry where this type of changes are studied. In '**Solution Chemistry**' broadly three types of approaches have been made to estimate the extent of solvation. The first is the ionic solvation of the electrolytes involving the studies of viscosity, conductance [10], the second is the thermodynamic approach by measuring the free energies, enthalpies and entropies of

solvation of ions from which factors associated with solvation can be elucidated [11], and the third is to use spectroscopic measurements where the spectral solvent shifts or the chemical shifts determine their qualitative and quantitative nature [12]. Interactions taking place between solute-solute, solute-solvent, solvent-solvent species govern the strength of ion-solvation [13,14]. The interpretation of solute-solute, solute-solvent and solvent-solvent interactions gives a complete information about the phenomena of solution chemistry. Hence we have concentrated on the studies of solute-solute, and solvent-solvent interactions in some industrially important liquid systems.

The molecular interaction in liquids explored by physicochemical methods has paying attention, as thermodynamic parameters are appropriate to interpret intermolecular interaction patterns in non-electrolytic solvent mixtures [15]. The different sequence of solubility, difference in solvating power and possibilities of chemical or electrochemical reactions unaware in aqueous chemistry have open vistas for chemists and interest in the organic solvents transcends the traditional boundaries of physical, inorganic, organic, analytical and electrochemistry.

Solvation behaviour is one of the most essential properties of any liquid as it regulates more complex processes such as solvation and reaction dynamics. The physico chemical properties of a solution (liquid) is a outcome of the strength of their intermolecular forces. The molecules are acquired partial charges through the *intermolecular forces*, e.g., dipole-dipole forces, dipole-induced dipole forces, hydrogen bonding, Van der Waal forces and electrostatic interaction etc. *Intermolecular forces* in a solution control their thermodynamic properties and the understanding of the solvation thermodynamics is essential to the characterization and interpretation of any process performed in the liquid systems. Therefore, the studies on the thermodynamic along with the transport and spectral properties of solutions would provide a clear idea about the nature of the forces, interacting manner existing between the constituents of solution. This type of study thus opens a path for research in solution chemistry to discover the nature of interaction through experimental studies involving density, viscosity, refractive index, conductometry, spectroscopy study and to interpret the experimental data collected.

Due to significant physicochemical properties such as negligible vapour pressure, high thermal and electrochemical stability, high solvating power, etc. the ionic liquids (ILs) are advantageous in various fields. The choice of the cation and the anion constituting an ionic liquid has a profound effect on the physicochemical properties such as density, viscosity, conductivity and polarity. This variety opens wide opportunities in the tailoring of ILs suitable for practical applications. The understanding of the behaviour of ILs and their properties is crucial for any practical application. But the available chemical and physical data are unfortunately inadequate in comparison to the amount of already commercially available ILs. Moreover, the existing data are often inconsistent. In this perspective, we focused on the reliable determination of physicochemical, transport and spectral properties of ILs in various solvent systems to explore and to understand the molecular as well as ionic level of interfaces of ILs prevailing in solvent systems by studying their thermodynamic properties based on various physicochemical approach.

1.1.1 Importance of Physicochemical Parameters

The nature of intermolecular interactions present in the studied system can be understood in terms of derived parameters based on the physicochemical approach.

Apparent molar volumes obtained from density measurements, are usually expedient parameters for interpreting ion-solvent/solute-solvent and ion-ion/solute-solute interactions in solution. Ionic apparent molar volume for the individual ions has been obtained with the help of “*reference electrolyte*” method. The compressibility, a second derivative to Gibbs energy, is also a sensitive indicator of molecular interactions, which provide useful information in such cases where partial molar volume data alone cannot provide an unequivocal interpretation of these interactions.

The change in viscosity of solutions by the addition of electrolyte is attributed to inter-ionic and ion-solvent effects. The viscosity *B*-coefficients are also separated into ionic components by the ‘*reference electrolyte*’ method and from the temperature dependence of ionic values, a satisfactory interpretation of ion-solvent interactions such as the effects of solvation, structure-breaking or structure-making, polarization, etc. has been given.

The transport properties in most cases are studied using the conductance data, especially the conductance at infinite dilution. Conductance data obtained as a function of concentration can be used to study the ion-association with the help of appropriate equations. The limiting ionic conductance of the each ion has been calculated from the same method “*reference electrolyte*” using tetrabutylammonium tetraphenylborate. The ionic conductances also play the crucial role to the interpretation of the ionic level of interaction, association or ion-solvent interactions of ions as well as molecules.

The spectroscopic study has been established by the investigation of FTIR spectroscopy. The study has been taking into account to qualitative interpreting the molecular as well as ionic association of the electrolytes in the solutions.

1.1.2 The main objectives of our work

My research work is:

- ✓ To investigate the host-guest inclusion complex formation between cyclic Host and various significant Guest molecules by suitable technique.
- ✓ To perform stability studies on guest and its complex with cyclodextrin.
- ✓ To find out solvation behaviour of some significant molecules.
- ✓ To understand the different type of interactions present in the inclusion complexes.
- ✓ To collect detailed information about the nature and strength of various interactions.
- ✓ To employ Host-Guest complexes in various field of science.
- ✓ To examine the transport properties of ionic liquids in industrially important solvents along with thermodynamic studies to characterize molecular interactions in solutions.

I.2. CHEMICALS USED

The name of the significant molecules which have been used throughout the research work are ionic liquids (Benzyltrimethylammonium chloride, Benzyltriethylammonium chloride, Benzyltributylammonium chloride, 1-ethyl-3-

methylimidazolium chloride, 1-methyl-3-octylimidazolium tetrafluoroborate), drug molecules (Amantadine hydrochloride, Sulfanilamide, Metoclopramide Hydrochloride), cyclic compounds (α -cyclodextrin, β -cyclodextrin, 18-crown-6, Dibenzo-18-crown-6, Dicyclo-18-crown-6)

The solvents which have been used during the research work are Water, Methanol, Acetonitrile, Dichloromethane, Tetrahydrofuran. The detailed description has been given in **Chapter III**.

I.3. METHODS OF INVESTIGATION

Existence of free ions, solvated ions, ion-pairs and triple-ions of the electrolytes/non-electrolytes in aqueous and non-aqueous media depends upon the concentrations of the solution, size of ions, and *intermolecular forces*, e.g., electronegativity of the atom, dipole-dipole forces, dipole-induced dipole forces, H-bonding, Van der Waal forces, columbic forces and electrostriction, +I, -I effect, side chain effect etc. Hence, the study of assorted interfaces and equilibrium of ions in diverse concentration regions are of immense importance to the technologist, theoretician, industrialist, researchers as most of the chemical processes take place in these systems.

Interestingly the different experimental techniques have been employed to find out a better understanding the occurrence of solvation and different interactions prevailing in solution. Therefore, we have employed the five significant physicochemical methods, viz., conductometry, volumetry, viscometry, and refractometry to explore the solvation phenomena and NMR, FT-IR, UV-vis and Fluorescence spectroscopy to characterize the inclusion complex.

I.4. SCOPE OF THE PRESENT WORK

Among the macrocycles constituting the great class of 'hosts' in supramolecular chemistry, cyclodextrins are the most attractive as they possess a unique molecular architecture, with a hydrophilic exterior and a hydrophobic interior. Though there are many cavitand host molecules such as calixarenes, crown ethers, cucurbiturils *etc.*,

cyclodextrins are very special as they can complex with a broad spectrum of guest molecules of appropriate size, shape and polarity. The physicochemical characteristics of guest molecules are beneficially modified after inclusion into these elegant 'organized' assemblies. Among all potential hosts, cyclodextrins have been extensively utilized as confined media to modify organic reactions, to achieve selectivity to a greater extent and this plays a key role in organic syntheses.

Cyclodextrin can form inclusion complexes with various biologically active guest molecules, among them drug-CD formulations are very significant and important because of the enhanced solubility, bioavailability and stability of drug molecules after complexation with CD. Structural characterization is of particular significance for these supramolecular host-guest complexes, which are the basis of most CD applications in medicine, catalysis or in food chemistry, separation and sensor technology. Pharmaceutical uses of CDs for drug protection or targeting now legally require structural characterization of the administered compounds. To gain insight of reactivity and selectivity in organic reactions and also to understand the binding behavior of this unique host system, the present work "Inclusion complex formation", is carried out by physicochemical characterization of CD complexes with various analytical techniques.

Supramolecular chemistry i.e. host-guest complex formation through noncovalent interactions offer the basis for novel approaches in medicine and also helps in understanding the interactions present in living systems. Hence in **Chapter IV** size, shape, structural effect of ionic liquids in the formation of the inclusion complexes have been studied quantitatively and qualitatively to find the nature of host-guest inclusion complexes of consecutive cationic surface active ionic liquids, benzyltrialkylammonium chloride with β -cyclodextrin in aqueous media using surface tension, conductance and NMR study. It is expected to provide important conclusions and results on binding behavior, importance of hydrogen bonding and the role of hydrophobic group in complex formation.

Crown ether-ammonium complexes are of fundamental interest as prototypical systems involving multiple hydrogen bonds. Study of these simple multiply-bound complexes is a promising means of gaining insight into much more complex macromolecular systems, such as those involved in protein folding or in the pairing of

nucleo bases in polynuclear nucleic acids. In **Chapter V** conductance study, surface tension study and density study of the complex formed between amantadine hydrochloride (ADH) and 18-crown-6 (18C6) in methanol solution was reported and discuss the influence of several structural and medium parameters on the complexation reaction. The study (carried out for the first time) is expected to provide information on the potential utility of this substrate for optoelectronic applications. It was also found that host-guest complexation with crown ethers resembles an established principle i.e. the hydrogen bonding acceptance as well as the donation propensity of crown ethers.

In **Chapter VI**, we have investigated on conductometric properties of the ionic liquid 1-butyl-3-methylimidazolium chloride in polar aprotic solvents acetonitrile (ACN), tetrahydrofuran (THF), dichloromethane (DCM) at different temperatures. The experimental data was analysed using Fuoss conductance equation and Fuoss-Kraus theory to calculate the ion pair formation constant K_p and triple ion formation constants K_T . The main purpose of this study is to obtain experimental and quantitative information for the interactions between the ions. Here the ion pair formation constants are expected to reflect strongly the direct interactions between the ions.

Crown ethers have proved to be unique cyclic molecules for molecular recognition of suitable substrates by hydrogen bonds, ionic interactions and hydrophobic interactions. The study of interactions involved in the complex formation is important for a better understanding of the mechanism of biological transport, molecular recognition, and other analytical applications. In this **Chapter (VII)**, we have studied the complexation of Sulfanilamide with three different crown ethers (1) Dicyclohexano-18-crown-6 (DC18C6) (2) 18-crown-6 (18C6) and (3) Dibenzo-18-crown-6 (DB18C6) in acetonitrile (ACN). The complexes were characterized by ^1H NMR, IR and UV-visible spectra.

Metoclopramide hydrochloride is used as an anti-emetic in the treatment of some forms of nausea and vomiting and to treat heartburn caused by gastroesophageal reflux in people who have used other medications without relief of symptoms. Metoclopramide hydrochloride have a greater impact on the treatment of disorders of the gastrointestinal tract. Since metoclopramide has been confirmed as an effective drug in treating and preventing various types of disease hence the stabilization and

regulatory release of this drug is of great concern in pharmacology. Thus to protect these drugs from external effects and to reduce side effects for their regulatory release, it is crucial to investigate whether they can be encapsulated into the cyclodextrin molecule. Hence in **Chapter VIII**, the inclusion complex formation of metoclopramide hydrochloride with both α and β -cyclodextrins (CDs) was studied in detail based on physicochemical and spectroscopic measurements. The factors affecting the inclusion process were discussed. Enhanced fluorescence and absorption characteristics served as an aid for better understanding the inclusion mechanism, including the size/shape-fit, hydrophobicity. Especially, detailed spatial information in solution has been studied by ^1H NMR.

CHAPTER-II

GENERAL INTRODUCTION

(REVIEW OF THE EARLIER WORKS)

II.1. HOST-GUEST CHEMISTRY

Supramolecular host-guest chemistry emphasizes on the interaction between molecules rather than within molecules and on the study of intermolecular bond rather than covalent bond [1]. Supramolecular chemistry is often defined as “the chemistry beyond the molecule” or “the chemistry of the noncovalent bond”. In host-guest chemistry host molecule encapsulate the guest molecule into the inner cavity of the host (**Figure II.1**). All the compounds exhibit supramolecular properties such as molecular recognition, self-assembly, self-organization, and kinetic and thermodynamic complementarity. A great deal of effort in supramolecular chemistry has been used in attempts to model or mimic biological processes [2]. Enzyme mimicking is one of the most attractive studies in recent years. The principles, perspectives and recent developments in the field of supramolecular chemistry have grown exponentially in the last few decades [3-10].

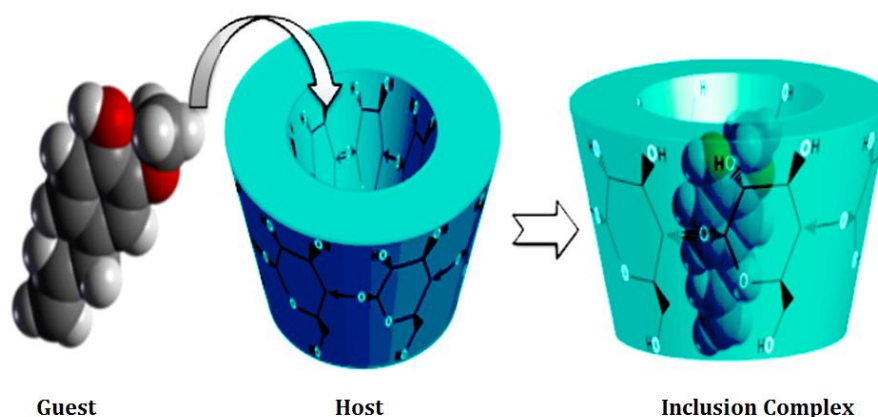


Figure II.1: Schematic representation for host-guest complexation by Cyclodextrin.

The emergence of supramolecular host-guest chemistry has had a profound effect on how efficiently chemists prepare structures using spontaneous secondary interactions such as hydrogen bonding, dipole-dipole, charge transfer, van der Waals and

π - π stacking interactions (**Figure II.2**)[11-15]. The supramolecular field was and is the basis for most of the essential biochemical process of life. The diagrammatic outline from molecular to supramolecular chemistry is shown in **Figure II.3** [16]. The example of some supramolecular host systems are such as Cyclodextrins, Crown ethers, Calixarenes, Cucurbit etc. with large cavities capable of accommodating small guest molecules and ions [17]. Macrocyclic host molecules are of great importance in inclusion complexes as the cyclized and constrained conformation provide the advantages of molecular selectivity [18]. Here we have discussed mainly about the cyclodextrins and crown ethers (as host) in details.

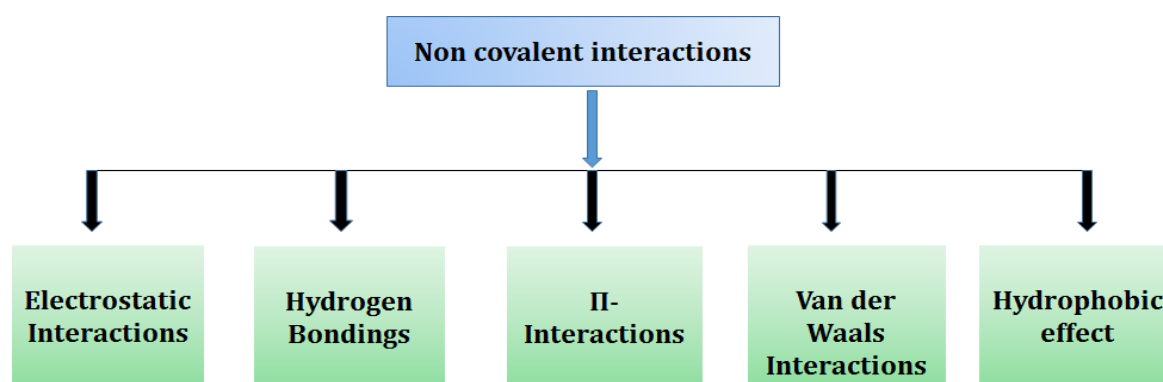


Figure II.2: Schematic representation of various interactions involved in host-guest chemistry.

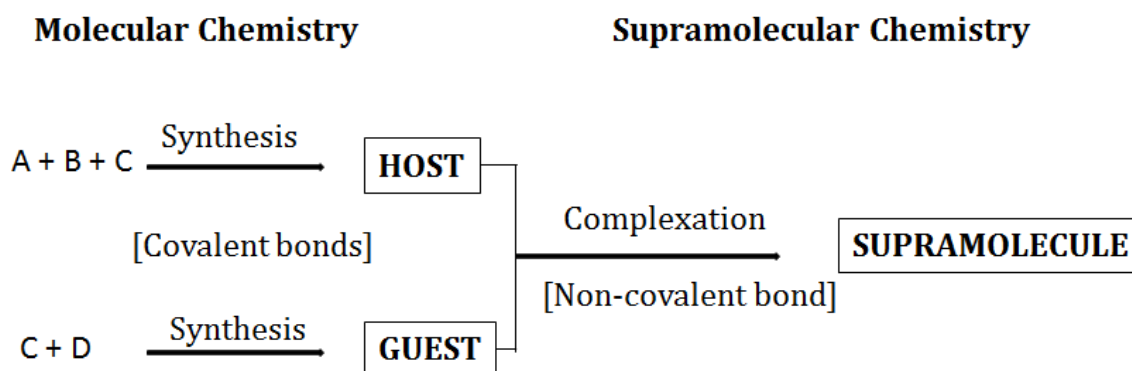


Figure II.3: From molecular to supramolecular chemistry.

II.2. CYCLODEXTRINS

Cyclodextrins (CDs) are useful molecular chelating agents. They possess a cage-like supramolecular structure, which is the same as the structures formed from cryptands, calixarenes, cyclophanes, spherands and crown ethers. Compared to all the supramolecular hosts mentioned above, cyclodextrins are most important. Through their inclusion complex forming ability, important properties of the complexed substrates can be modified significantly. As a result of molecular complexation phenomena CDs are widely used in many industrial products, technologies and analytical methods. The negligible cytotoxic effects of CDs are an important attribute in applications such as drug carrier, food and flavours, cosmetics, packing, textiles, separation processes, environment protection, fermentation and catalysis.

II.2.1 Discovery of Cyclodextrin

The oligosaccharide cyclodextrin were first isolated and discovered by Villers in 1891 by enzymatic cleavage of starch [19]. Schardinger confirms his result in 1904 by further identification of cyclic structure of glucose oligomers and enzymes responsible for the synthesis of cyclodextrins [20]. Because of his pioneering work the name Schardinger dextrans was often used for cyclodextrins in early literature. In the early literature, cyclodextrins are also sometimes called cycloamyloses or cyclomaltooligosaccharides. The next major contributor to cyclodextrin chemistry was Karl Freudenberg [21], who developed a method for obtaining of pure α -CD and β -CD and in the process also isolated another crystalline dextrin, which he named γ -CD. It was Freudenberg, who characterized these as cyclic structures composed of α - 1, 4 linked glucose unit [22]. However, the molecular weights of the most common CDs were not determined until much later [23]. The foundations of cyclodextrin chemistry were laid down in the first part of the 20th century. Cramer and French [24] were the first, who recognized and studied possible applications by forming complexes of CDs. Because of their research, the way was opened for the use of cyclodextrins as enzyme models. However, until 1970 only small amounts of cyclodextrins could be produced and high production costs prevented their wide spread usage. Today the cost of cyclodextrins is

reduced dramatically and as a result, the group of scientists interested in cyclodextrins is continually growing.

II.2.2 Structural features and Properties of cyclodextrins

Cyclodextrin (CD) are cyclic oligosaccharides consisting of glucopyranosyl units linked by α -(1,4) bonds. The widely used natural cyclodextrins are α -, β - and γ -cyclodextrin consisting of 6, 7 and 8 glucopyranose units, respectively (**Figure II.4**). Owing to lack of free rotation about the bonds connecting the glucopyranose units, the cyclodextrins are not perfectly cylindrical molecules but the torroidal or cone shaped with a hydrophobic cavity and a hydrophilic surface [**Figure II.5**] [25]. Based on this architecture the primary hydroxyl groups are located on the narrow side of the cone shape, while the secondary hydroxyl groups are located on the wider edge. The primary and secondary hydroxyls on the outside of the cyclodextrins make cyclodextrins water-soluble. Cyclodextrins are insoluble in most organic solvents. The hydrophobic cavity of the cyclodextrin is capable of trapping the hydrophobic parts present in the molecules [26-28]. From the crystal structure, it is shown that they have a truncated cone shape with a height of approximately 8Å and an inner cavity diameter varying between ≈ 5 (α -CD) and 8.30 nm (γ -CD). **Figure II.5** indicates the general structure of the native cyclodextrins. **Table II.1** indicate the common parameters reported by Szejtli [2]. Each D-glucose unit in the cyclodextrin structure contains five chiral carbon atoms and which make CD as a chiral macrocycle.

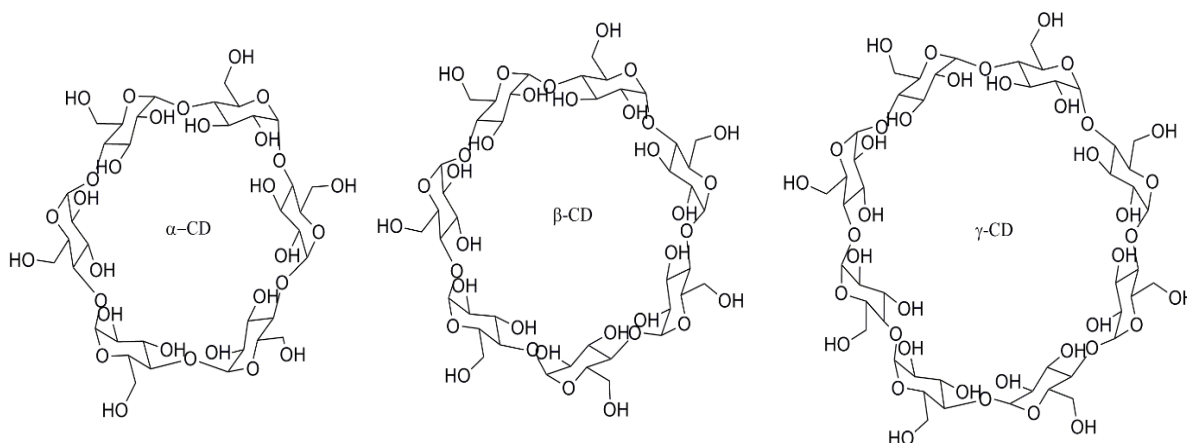


Figure II.4: Structures of the α -, β - and γ -cyclodextrin

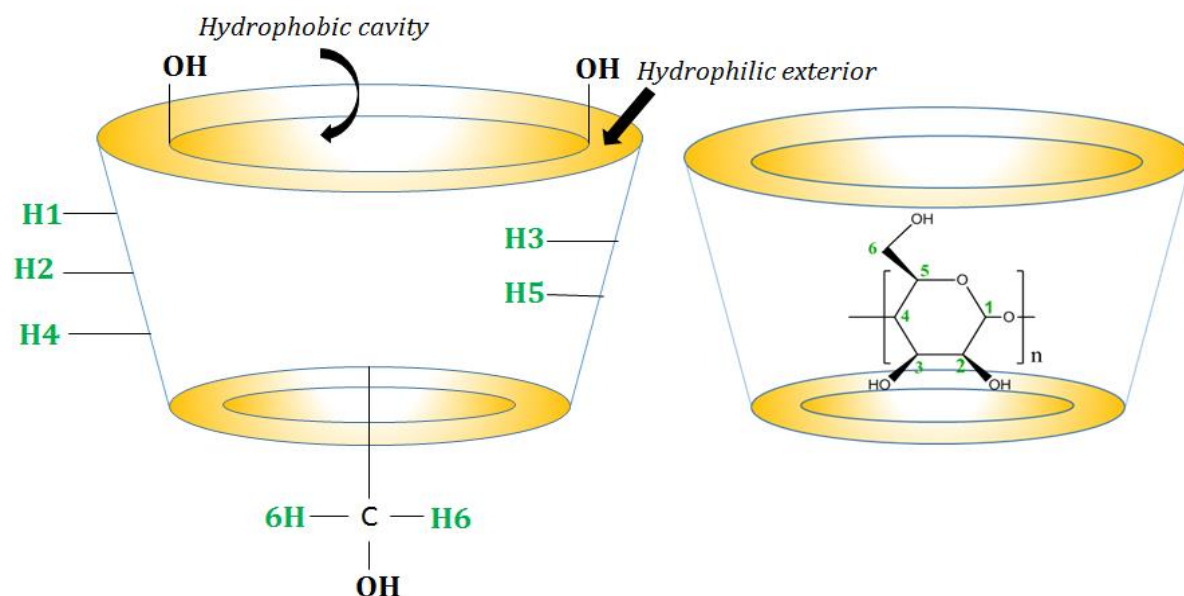


Figure II.5: General structure of cyclodextrin molecule with interior and exterior protons ($n = 6, 7$ for α -CD and β -CD respectively).

Table II.1: Characteristics of Cyclodextrin.

Property	α -CD	β -CD	γ -CD
No. of glucose units	6	7	8
Empirical formula (anhydrous)	$C_{38}H_{60}O_{30}$	$C_{42}H_{70}O_{35}$	$C_{48}H_{80}O_{40}$
Mol. Wt. (anhydrous)	972	1135	1297
H ₂ O solubility (g/100 mL) at 25°C	14.5	1.85	23.2
Cavity diameter [Å]	4.7-5.3	6.0-6.5	7.5-8.3
Cavity length [Å]	7.9 ± 0.1	7.9 ± 0.1	7.9 ± 0.1
Approx Cavity Volume (Å ³)	174	262	427

The low solubility of β -CD is attributed to the interruption by aggregated β -CD with its 7-fold symmetry units [29]. Szejtli [30] proposes that the intramolecular hydrogen bonds of the β -CD rim are responsible for its low solubility. Alkylation of β -CD hydroxyls leads to an increase in solubility and this phenomenon has constituted a motivation for carrying out such chemical modifications [27].

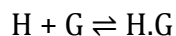
II.2.3 Inclusion Complex formation

Complex formation is a dimensional fit between the host cavity and the guest molecule [31]. The hydrophobic cavity of CD molecules arrange for a microenvironment into which appropriately sized non-polar moieties can enter to form inclusion complexes [32]. No covalent bonds are formed during the formation of the inclusion complex [33]. The main driving force of complex formation is the release of enthalpy-rich water molecules from the cavity resulting in a more stable lower energy state. The host-guest complexes can be prepared by various methods like co-precipitation method, paste method, dry mixing method, slurry method and analyzed by varieties of technique like FTIR, UV-visible and NMR spectroscopy, Powder XRD, DSC, TGA, Circular Dichroism spectroscopy, etc. [34]. The formation of inclusion complex of β -CD and a guest substance is accompanied by changes in their IR spectra as compared with the individual components [35, 36].

The binding of the guest molecules within the host CD is a dynamic equilibrium. Inclusion into CDs exerts a profound effect on the physicochemical properties of guest molecules giving rise to beneficial modification of guest molecules, which are not achieved otherwise [37]. The ability of a cyclodextrin to form an inclusion complex with a guest molecule is a function of two key factors. The first is steric and depends on the relative size of the CD to the guest molecule or certain key functional groups within the guest. The second critical factor is the thermodynamic interactions between the different components of the system (CD, guest and solvent). For a complex to form there must be a favorable net energetic driving force that pulls the guest into the CD.

II.2.4 Equilibrium

In an aqueous solution, the slightly apolar cyclodextrin cavity is occupied by water molecules which are energetically unfavored (polar-apolar interaction), and therefore can be readily substituted by appropriate 'guest molecules' which are less polar than water. One, two or three cyclodextrin molecules contain one or more entrapped 'guest' molecules. Most frequently the host: guest ratio is 1:1. The association of the host CD and guest (G) molecules, and the dissociation of the formed CD/guest complex are governed by a thermodynamic equilibrium,



$$K = \frac{[H.G]}{[H][G]}$$

II.2.5 Higher order complexes

The complexation depends upon the cavity diameter of CD as well as the size of organic compound or guest molecule. Usually complexation occurs between one cyclodextrin and one guest (1:1 ratio) molecule. However, 1:2, 2:1, 2:2 and higher order complex equilibria also exist in the system [Figure II.6] [38-46].

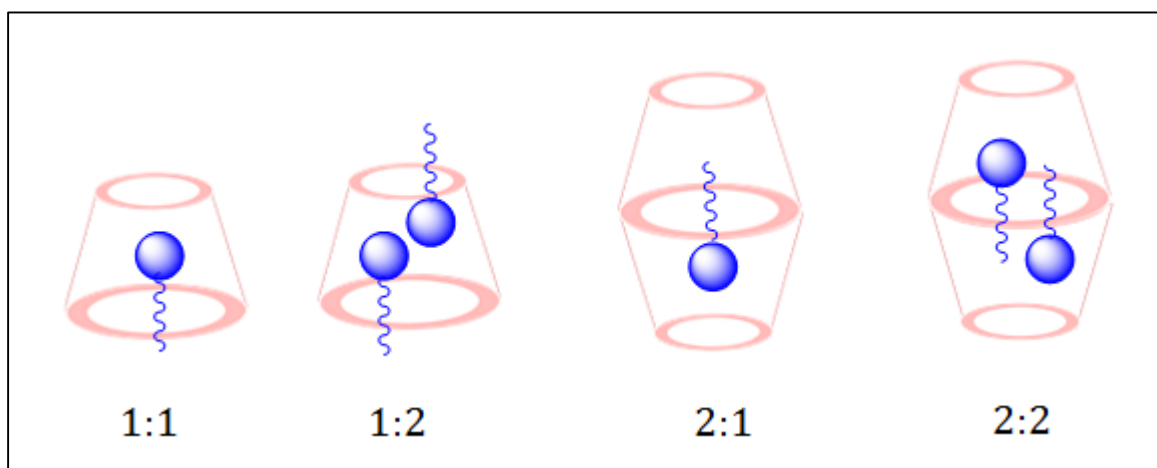


Figure II.6: Different stoichiometries of host-guest inclusion complexes.

II.2.6 Binding constants

Equilibrium constants for molecular association (binding constants/association constants/formation constants) have been measured using a variety of chemical approaches, including UV-visible, fluorescence and NMR spectroscopy and gas and liquid chromatography [47]. Benesi-Hildebrand method [48] is often used to calculate the binding constant values for 1:1 association. For UV studies, B.H equation is

$$\frac{1}{A - A_0} = \frac{1}{\Delta\epsilon[G]K_a} \cdot \frac{1}{[CD]} + \frac{1}{\Delta\epsilon[G]}$$

and for Fluorescence studies, the equation is

$$\frac{1}{I-I_0} = \frac{1}{[I'-I_0]K_a} \cdot \frac{1}{[CD]} + \frac{1}{I'-I_0}$$

II.2.7 Applications of cyclodextrins

Upon inclusion in cyclodextrins and modified CDs, the guest molecules undergo beneficial modifications. Cyclodextrins find versatile applications in innumerable fields ranging from agriculture to pharmaceuticals.

Cyclodextrins are extensively used in separations due to their ability to discriminate between positional isomers, functional groups, homologues and enantiomers. Cyclodextrins are used as chiral stationary phases bonded to solid support or as mobile phase additives in high performance liquid chromatography (HPLC) and in capillary electrophoresis for the separation of chiral compounds [49].

Cyclodextrins are potential candidates to play the role of drug delivery vehicles [50]. The majority of pharmaceutical active agents do not have sufficient solubility in water. The solubility of such drugs enhances by the formation of inclusion complex with cyclodextrin hence used in drug delivery system [51]. Drug solubility and dissolution, bioavailability, safety and stability are the main features in pharmaceutical applications of CDs [52]. Cyclodextrins stabilize penicillin from amylase degradation through complex formation [53]. The CDs also increase drug efficacy by sustained release of the drug [54]. The CD complexation enables enhanced absorption in different delivery routes such as oral, ocular, nasal, dermal, retinal etc. [55]

Cyclodextrins do not damage the microbial cells or enzymes. Cyclodextrins act as excellent 'enzyme models'. They catalyze biomimetic reactions of enzymes. Since CDs bind substrates, they are considered as artificial enzymes. They show substrate specificity and stereospecificity [56]. Quinine- β -CD complex provides an excellent model for mimicking enzyme-substrate interactions [57].

CDs are used in the food industry to protect active ingredients against light, heat and fermentation. Long-lasting perfumes are possible by slow release of fragrance through CD complexation. Unpleasant odors and bitter taste can be masked through complexation with CDs [58]. CD inclusion complex containing oily antimicrobial and

volatile agents are coated on a water absorbing sheet with a natural resin binder used for wrapping fresh products [59]. CDs find applications in waste water treatment. Also highly toxic materials from industrial effluents, organic pollutants and heavy metals from soil are solubilised in cyclodextrins and hence are removed [59]. Polymers in paints interact with each other resulting in thickening of paints and increase the coefficient of viscosity. β -cyclodextrin formulations prevent this undesirable effect [60]. A supramolecular chemosensor for aromatic compounds has been devised using β - cyclodextrin [61].

II.3. MACROCYCLIC POLYETHERS

Crown ethers, as originally defined are those compounds with multiple ether oxygen atoms incorporated in a monocyclic backbone. The term “crown” was used because the cavity shape of the macrocycle resembled a crown [62]. Crown ethers have proved to be unique cyclic molecules for molecular recognition of suitable substrates by hydrogen bonds, ionic interactions, cation- π or π - π interactions. Cation- π interactions are well described by a schematic drawing such as **Figure II.7** showing a K^+ ion interacting with the negatively charged π -electron cloud of benzene. The study of interactions involved in complexation of different cations with crown ethers in mixtures of solvents is important for a better understanding of the mechanism of biological transport, molecular recognition, and other analytical applications. **Figure II.8** shows some of the more common crown ethers.

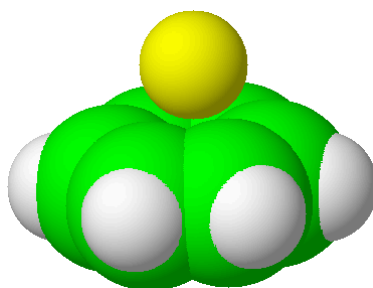


Fig. II.7: Schematic drawing of cation- π interactions showing the contact of K^+ ion and benzene.

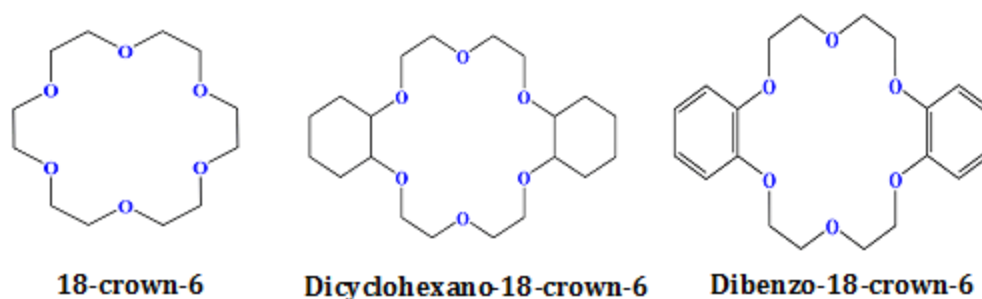


Figure II.8: Several example of crown ethers.

We chose 18-crown-6, Dicyclohexano-18-crown-6 (DC18C6) and Dibenzo-18-crown-6 (DB18C6) three crown ethers in our study. DB18C6 and DC18C6 were used to find out the effect of cyclohexyl group (electron donating group) and benzene group (electron withdrawing group) on the association constant.

Crown ethers are well known for their binding strengths and selectivities towards alkali and alkaline earth metal cations [63]. Their complexation with organic ammonium [64,65], arenediazonium [66-68], guanidinium [69-72], tropylium [73,74] and pyridinium [75] cations has also been studied.

II.3.1 Discovery of Crown Ethers

In 1987, Charles J. Pedersen, Jean-Marie Lehn and Donald J. Cram were jointly awarded the Nobel Prize in chemistry for their contributions to the development and use of supramolecular chemistry [76]. Pedersen serendipitously discovered dibenzo 18-crown-6 as a byproduct of a reaction in which he had sought to obtain bis[2-(*o*-hydroxyphenoxy) ethyl] ether, **1**. (**Figure II.9**). While trying to purify his product, he isolated a small amount of a white crystalline solid. Further analysis showed no alcohol groups to be present, and more interestingly, its UV spectrum changed significantly in the presence of sodium hydroxide. The unknown byproduct was identified as dibenzo-18-crown-6, **2**. Although this was not the first cyclic polyether to be reported in the literature, Pedersen was the first to recognize the unique properties of this type of compound, thereby opening up a whole new field of host-guest chemistry [77].

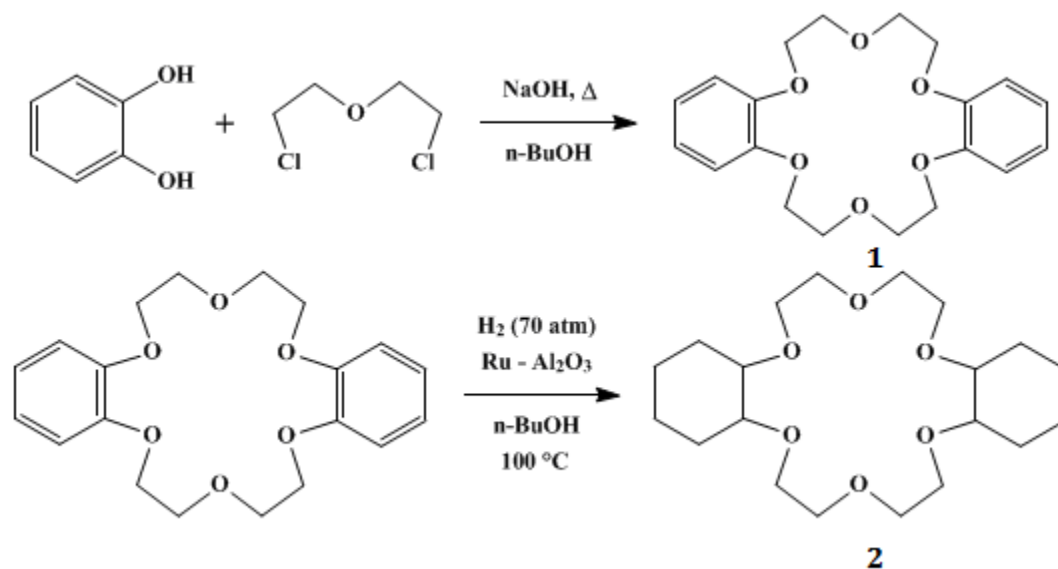


Figure II.9: Pedersen's reaction⁷⁸

Actually long before Pedersen discovered crown ether by accident, there were others like Luttringhaus (Luttringhaus, 1937) who had preceded Pedersen in synthesizing macrocyclic polyethers. However, those researchers did not understand the unique cation-ligating properties of the cyclic polyethers. So Pedersen is widely regarded as the father of these important compounds. Since Pedersen's discovery in 1967, many scientists and research groups have synthesized crown ethers and have investigated the properties of many more examples of this class of compounds that serve as hosts for cations [79], anions [80, 81] and some neutral molecules [81].

II.3.2 Structure of Crown Ethers

Cyclic polyethers such as the one discovered by Pedersen consist of polyethylene glycol derivatives in a cyclic array wherein the heteroatom, most commonly oxygen, is directed toward the center of the cavity. The hydrocarbon backbone is located on the periphery of the ring, thereby rendering the cyclic polyether 'hydrophobic' on the outside and 'hydrophilic' on the inside. The heteroatoms, through their lone electron pairs are able to complex cationic guest molecules. Pedersen envisioned that the cyclic polyethers "crown" the cations; hence, the origin of the common name for these types of compounds: *crown ethers*.

II.3.3 Factors Governing Complexation and Selectivity of Crown Ethers

The factors responsible for the stability of cation-crown complexes can be classified as (a) relative size of a cation and crown compound cavity, (b) cation charge, (c) cation type, (d) counter anion, (e) number of donor atoms, (f) type of donor atom, (g) electron density of crown cavity, (h) crown substituents, (i) crown ether-ring flexibility, and (j) physical properties of a solvent. The major contributing factor towards binding and selectivity is attributed to size compatibility of the cation and the crown ether cavity. The cations that match the cavity size of the macrocycle are located in its center and optimize the interactions with the oxygen heteroatoms.

Functional groups also have been incorporated into host compounds in an effort to modify their complexation properties. Benzo substituent groups reduce the binding strength and selectivity of coronands and cryptands [82]. There are a number of reasons thought to be responsible for this:

(i) The O-O distance is smaller between the two oxygens joined by the benzene ring than those connected by an ethylene unit, thereby resulting in reduced cavity size.

(ii) The benzene ring also is electron withdrawing, thereby reducing the electron density and basicity of the adjacent oxygen atoms.

(iii) Benzo groups provide a rigid component that reduces the overall flexibility of the crown ether.

II.3.4 Applications of Crown ethers

Crown ethers have appreciable binding strengths and selectivities toward alkali and alkaline earth metal cations [77]. These special properties make crown ethers the first synthetic compounds that mimic many of the naturally occurring cyclic antibiotics. Due to the importance of alkali and alkaline earth metals (sodium, potassium, magnesium, calcium) in biological systems, in high -power batteries (lithium) and in isotope chemistry and radiochemistry, crown ethers are important ligands in the study of the chemistry of these metal ions [83].

Crown ethers are used in a wide range of areas such as analyses; separations, recovery or removal of specific species, ion selective electrodes, biological mimics and

reaction catalysts. Derivatives of crown ethers used as potential powerful anti tumor agents which is a very important step in fighting deadly diseases such as AIDS.

The studies of crown ethers and their derivatives have led to important advances in the area of molecular recognition and to the emergence of new concepts such as supramolecular chemistry [83]. The rapid development and the importance of molecular recognition as applied to macrocyclic compounds can be seen in the awarding of the Nobel Prize in chemistry in 1987 to three of its pioneers, namely Pedersen, Cram and Lehn.

II.4. METHODS OF DETECTING THE INCLUSION PROCESS

Structural characterization is of particular significance for supramolecular host-guest complexes, which are the basis of most CD applications in medicine, catalysis or in food chemistry, separation and sensor technology. NMR spectroscopy has become the most important method for structural elucidation of inclusion complexes. There are a few alternatives to NMR in the study of inclusion complexes such as fluorescence, UV-visible spectroscopy studies play a major role in measuring complexation energetics. IR, MASS methods are used in characterizing solid inclusion complexes.

II.4.1 NMR Spectroscopy

NMR spectroscopy has proved to be an efficient technique for the determination of the interactions between macrocyclic hosts and organic guests [84-89]. The study of cyclodextrin complexes by NMR was initiated by Demarco and Thakkar, [90] who observed ^1H chemical shift variations of CD protons (H3 and H5) in the presence of various substrates and inferred that inclusion in the CD cavity had taken place. The spectacular advance of NMR techniques during the last few years has led to a much more detailed structural elucidation of inclusion complexes of macrocyclic hosts. NMR spectroscopy has been used from the very beginning to identify the hydrogen-bonding network in CDs. Inoue [91] and Schneider *et al.* [92] have reviewed NMR studies of the CD complexes. A typical structural inference is that if only H3 undergoes a shift in the presence of the substrate, then the cavity penetration is shallow, whereas if H5 also shifts,

the penetration is deep [27]. Structural information about the crown ether complexes can also be obtained from NMR spectra [75,93,94].

II.4.2 FT-IR Spectra of solid inclusion complexes

The solid inclusion complex formation is analyzed by FT-IR spectroscopy. FT-IR spectrum is used to confirm the formation of the solid inclusion complex by considering the deviation of peak shape position and intensity [88, 95-98].

II.4.3 Optical Spectroscopy

II.4.3.1 UV-visible spectroscopy

UV-vis spectroscopy is a convenient and widely used method for the study of binding phenomena [48,99-102]. Complexation between the macrocyclic hosts such as cyclodextrin and crown ethers and either completely or partially included guest molecules results in a number of interesting spectroscopic effects. Spectrophotometric determinations of inclusion complexes rely on the difference in the absorptivities of free and complexed substrate. Since the host molecule may in principle modify both photochemical and photophysical properties of their guest molecules, both absorbance and fluorescence signals can be used to gain insight into the characteristics of the complexes formed [103]. On adding host to the substrate solution in a suitable solvent, there is a hike in the absorbance in most cases, followed by a red/blue shift in absorbance maximum in a few cases.

II.4.3.2 Fluorescence spectroscopy

The supramolecular interaction of guest molecules with CDs can be investigated by spectrofluorimetry [104-108]. With an increase in the CDs (α -CD and β -CD) concentration, however, the fluorescence intensity of the guest molecules enhanced accompanied by a slight hypsochromic shift of the emission peak. These findings indicates the formation of host-guest inclusion complexes. Cramer *et al.* first noticed that 8-(phenylamino)-1-naphthalenesulfonate exhibited a more intense emission in the presence of β -cyclodextrin and presumed a 1:1 complex was formed. Since then other

authors have reported enhancement of fluorescence of benzene and its derivatives in cyclodextrin [109]. The development of fluorescence methods for quantitative analysis is particularly important due to their sensitivity, selectivity and instrumental simplicity.

II.4.4 Surface Tension

Surface tension (γ) is another valuable parameter which also suggests the formation of inclusion complex of a guest molecule into cavity of host molecule. The addition of CD to pure water does not show any considerable change to the surface tension of water which is an indication that both cyclodextrins are almost surface inactive compounds. With the successive addition of aqueous cyclodextrin solution the surface tension values substantially increased for the surface active guest molecules probably due to the removal of surface active guest molecules from the surface of the solution, i.e., the hydrophobic part enter the hydrophobic cavity of the cyclodextrin forming the host guest inclusion complexes [110]. If we get a single break point in the surface tension curve and after that point if the γ value becomes approximately steady which confirms the formation of a 1 : 1 inclusion complex. More break points in the surface tension curve is the indication of the formation of inclusion complexes with complex stoichiometry such as 1 : 2, 2 : 1, 2 : 2 etc. [111,112].

II.4.5 Conductance Study

The conductivity (k) study not only confirms the formation of a host-guest inclusion complex but also gives the stoichiometry of the assembly [113,114]. With the successive addition of cyclodextrin in the solution of guest molecule, the conductivity of the guest molecules decreases on a regular basis. This type of observation is in good agreement with the formation of inclusion complexes. The insertion of the guest molecule inside the cavity of the CD molecule decreases the number of free guest molecule, resulting in the reduction in conductivity of the solution. The curves having a noticeable break suggests the formation of host-guest inclusion with a stoichiometry of 1 : 1.

II.5. SIGNIFICANT MOLECULES

Significant molecules are those molecules which are very much imperative and essential to our environment systems and which can be used in medical applications. Such molecules are ionic liquids, vitamins, drug molecules and amino acids etc. Here we have discussed about ionic liquids and drug molecules.

II.5.1 Drug molecules

➤ *Drugs: Definition*

By definition, drugs are chemical substances that affect/alter the physiology when taken into a living system. They can be natural or synthetic. Chemically, they are low molecular mass structures. When a drug is therapeutically active and is used for the diagnosis, treatment or prevention of a disease, it is called medicine (legal drugs). They target the macromolecules inside the body and generate a biological response. Most of them interrupt the nervous system (especially brain) for the generation of a proper biological response. However, they can be toxic in higher doses called lethal dose.



➤ *Classification of Drugs*

Classification of drugs can be done on the basis of different criteria. Some of the criteria for the classification of drugs are given below.

❖ *On the basis of pharmacological effect:*

How a drug or medicine affects or influences the cells of an organism is referred to as the pharmacological effect. Drugs have different pharmacological effects on an organism; say, for example, an analgesic reduces the pain while an anti-inflammatory drug reduces the inflammation of the body. Thus, drugs can be classified based on the pharmacological effect.

❖ **On the basis of drug action:**

Different drugs act differently i.e., each drug has its own way of generating response called drug action. Drug action is more specified according to how it generates a response. For example, there are lots of medicines to treat hypertension but each type of drug has different drug action. All the hypertension medicines reduce the blood pressure but in a different pathway.

❖ **On the basis of chemical structure:**

This is a common classification of drugs. Generally, drugs which have same drug action and pharmacological effect have a basic skeletal structure and a minute variation in the branching. This is why some drugs have more potential than the other. For example, all sulphonamides have the same skeletal structure.

❖ **On the basis of molecular targets:**

Drugs target the macromolecules inside the body to generate a biological response. Such macromolecules are called target molecules or drug targets. Drugs which have the same mechanism of action will have the same target. This basis for classification of drugs is more helpful during clinical trials.

➤ **Discovery of drug**

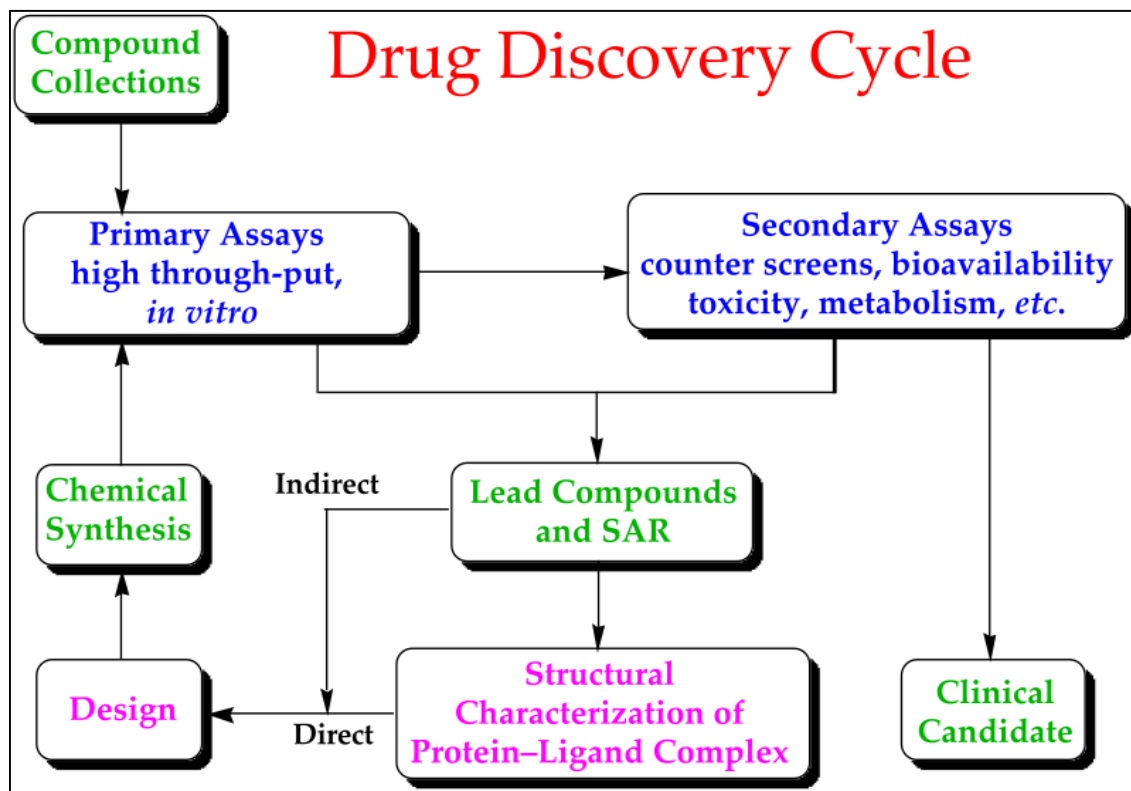
Drug discovery is the process of finding new drugs. It has evolved from early serendipitous discovery from natural sources, such as morphine from poppy seeds, to today's industrial-scale screening projects [115,116]. Modern drug discovery starts with the identification of a biological target that can be

modulated to induce the desired therapeutic effect. To search for potential drugs, compounds are tested for their ability to modulate the target.

Technologies such as high-throughput screening (HTS) and combinatorial chemistry facilitate screening of libraries of millions of compounds. However, even though screening capacity reaches millions of compounds and continues to grow, the number of possible molecules that could be synthesized and tested is infinitely larger. This notion



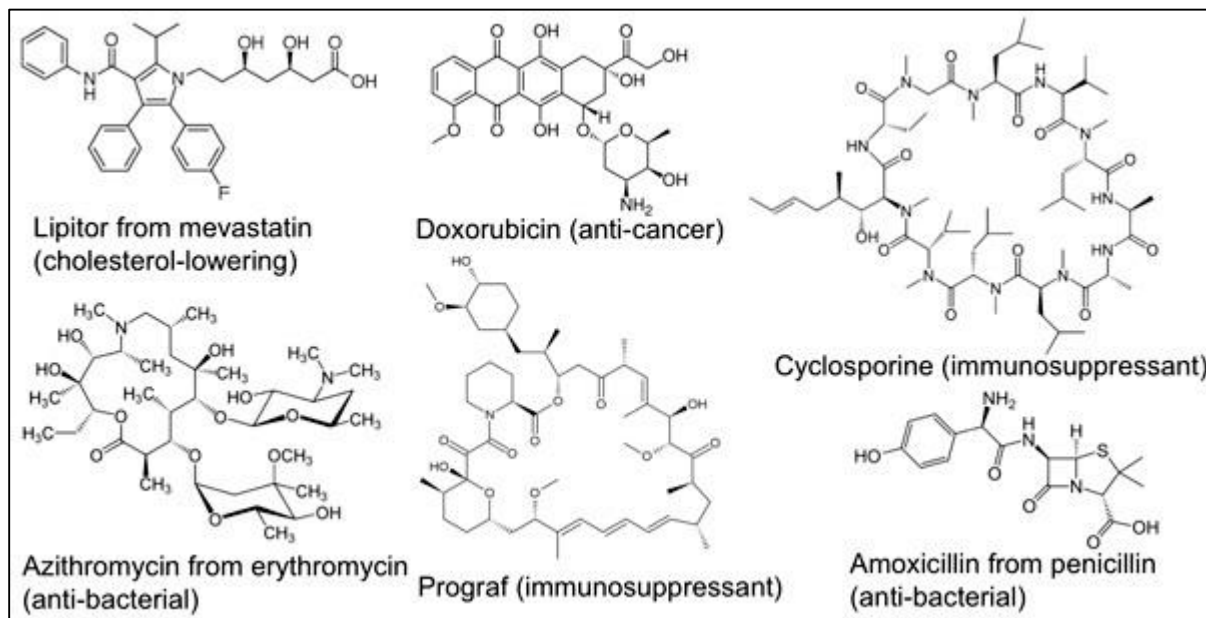
has important consequences; apparently, we can only test a tiny sample of what is virtually available.



It includes pre-clinical research (microorganisms/animals) and clinical trials (on humans) and may include the step of obtaining regulatory approval to market the drug.

The development of every drug begins with the search for a target on which the drug can act. To find one, scientists need to have very precise knowledge of the biochemical processes that take place in the body and how these are changed by a disease. They must be able to bind well to the target protein; i.e. they must fit into the target like a key into a lock.

❖ Some Examples of Drug Molecules



II.5.2 Ionic Liquids

In the last decades a new class of compounds came into the focus of many research groups around the world: ionic liquids (IL). The count of publications with the topic “*ionic liquids*” grew steadily over the last ten years. But what are ionic liquids and why are they so interesting? The following section gives a short overview over this wide field. A much more exhaustive overview about the possible applications and properties of ionic liquids can be found in the recent book “*Ionic Liquids in Syntheses*”, edited by Peter Wasserscheid and Tom Welton [117]. The commonly accepted definition of ionic liquids is that they are “*ionic materials that are liquid below 373 K*”. Ionic liquids have gained a lot of attention as emerging environmentally benign solvents. They can replace conventional organic solvents in several applications due to their unique features. Ionic liquids are salts with melting points below 373 K. They consist of an organic cation combined with an organic or inorganic anion. Ionic liquids show, in general, a very interesting set of properties to be used for different applications in chemical industry. The melting points of these organic salts are frequently found below 150 °C [118] and occasionally as low as -96 °C. Some ionic liquids are stable up to 500 K. At room temperature they have no

measurable vapor pressure due to their ionic nature. They normally have high solvency power for polar and non-polar compounds. Billions of ionic liquids can be designed and synthesized by selecting different ion pair combinations, which enable them to possess specific properties. Furthermore, the ability to tune the solvent properties of the ionic liquids is one of their outstanding features, which makes them unique solvents for various reactions and separations. Moreover ionic liquids are almost nonflammable, highly thermally and (electro) chemically stable and present a large liquid range.

Interest in ionic liquids has now been grown dramatically in the scientific community (both in academia and industry) with over 8000 papers having been published in the last decade [119]. This growth can be observed in **Figure II.10**. (number of publications per year) and **Figure II.11**. (number of patents per year), where the number of publications and patents are increasing exponentially. There are about one million (10^6) simple ionic liquids that can be easily prepared in the laboratory by combination of different cations and anions and this total are just for simple primary systems. If there are one million possible simple IL systems, then there are one billion (10^{12}) possible binary combinations of these, and one trillion (10^{18}) ternary possible IL systems that can be prepared from the combination of anions, cations, and substituents. Hence in this field many mores to discover.

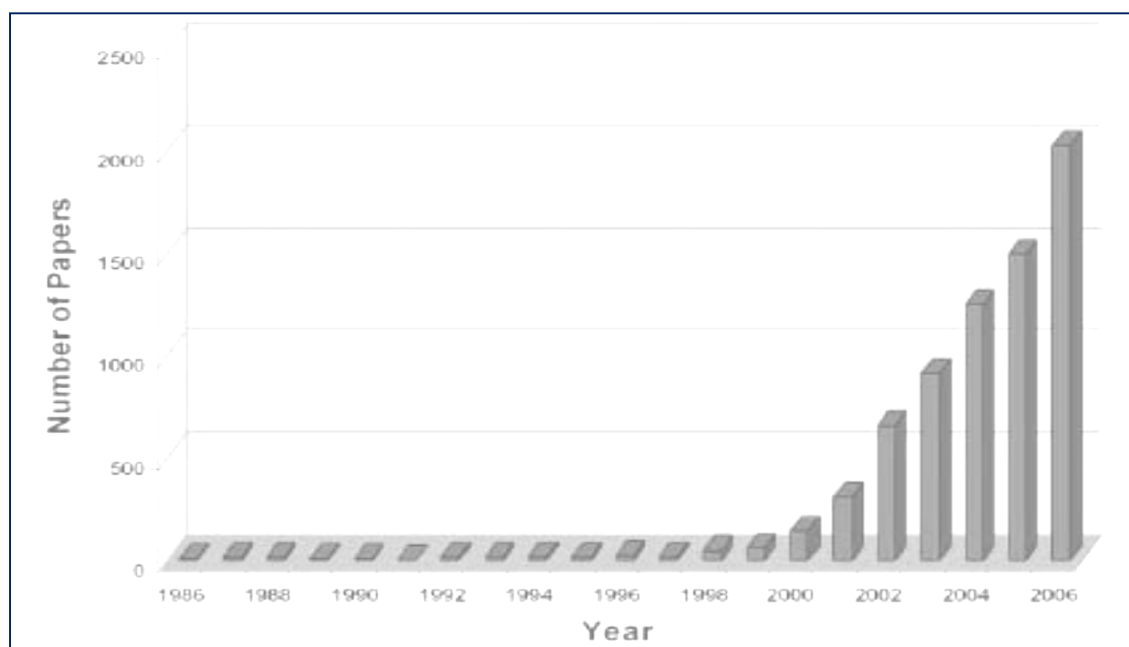


Figure II.10: Growth rate of ionic liquid publications, 1986-2006.

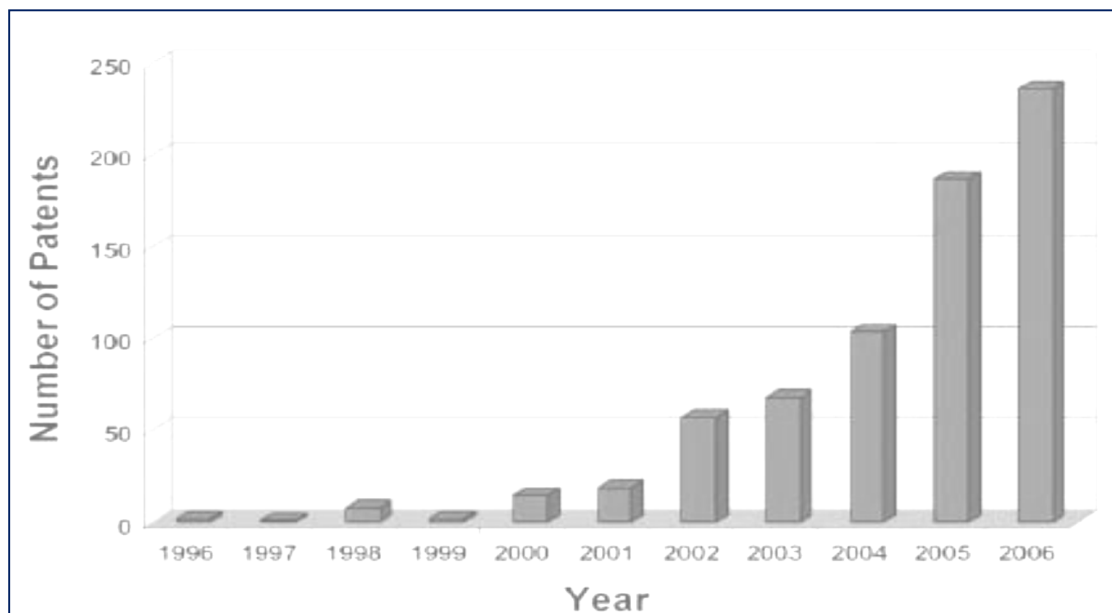


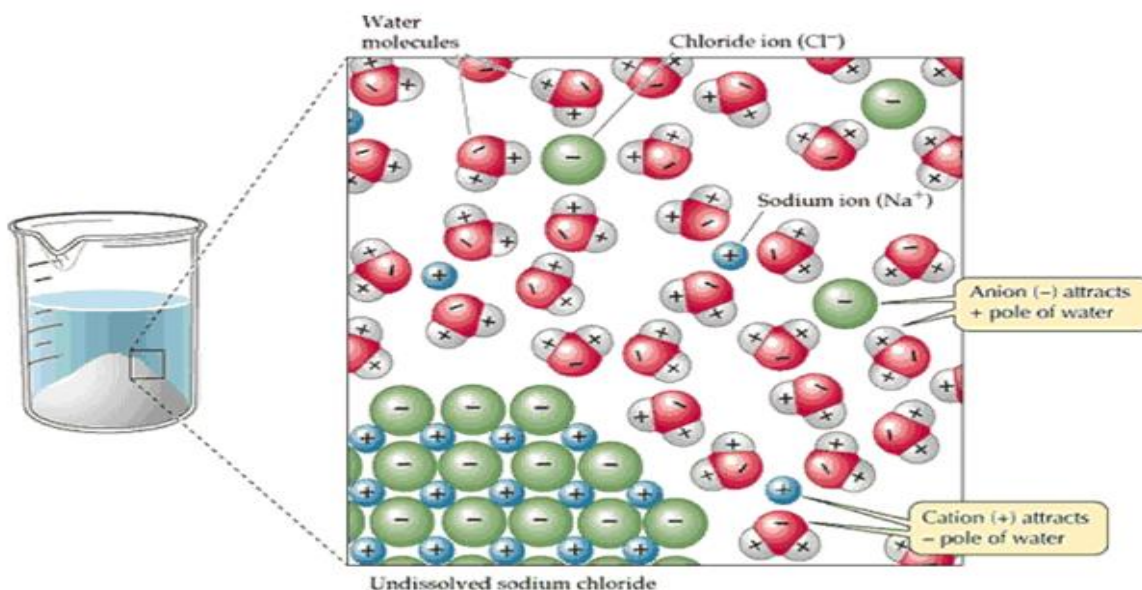
Figure II.11: Annual growth of ionic liquid patents, 1996-2006.

Until 1998, the number of entries with the terms “*ionic liquid*” or “*ionic liquids*” in the Chemical Abstracts was below or around twenty per year, but this number is increasing from 45 per year in 1999 to 1255 per year in 2005 and 1717 in 2006 with their different use in various field.

II.6. SOLVATION BEHAVIOUR

The term “Solvation Behaviour” which is connected with dissolved state of matter has drawn the interest of physical chemists for quite a long time. This chemistry in fact forms the origin of careful investigations to understand the physicochemical properties of solution and to know the mechanistic paths of solvation of different solutes like ionic liquids and drug molecules [120-125]. In fact, lot of chemistry relates to and is conducted in liquid solutions and involves ionic and non-ionic species. The vast bodies of multi-component aqueous salt solutions of oceans, nature of physiological fluids, dissolution of proteins, nutrients, enzymes, sugars, etc., in body fluids, oxygen in blood, various industrial processes, use of different solvents in the fields of chemical, analytical, electrochemical, food, pharmaceuticals, ecological and photochemical chemistry all are

the general subject of interest of solution chemists. In earlier experiments the chemists were attracted [122-129] about the role of different solutes on various physicochemical properties and processes in aqueous, non-aqueous and mixed solvents. The role of solvents was assumed to offer an inert and homogeneous medium for the chemical reactions. But later, it has been duly recognized that solvent molecules play a significant role in dictating various aspects of physico-chemical properties, equilibrium, and kinetic behavior of reactions in solution phase.



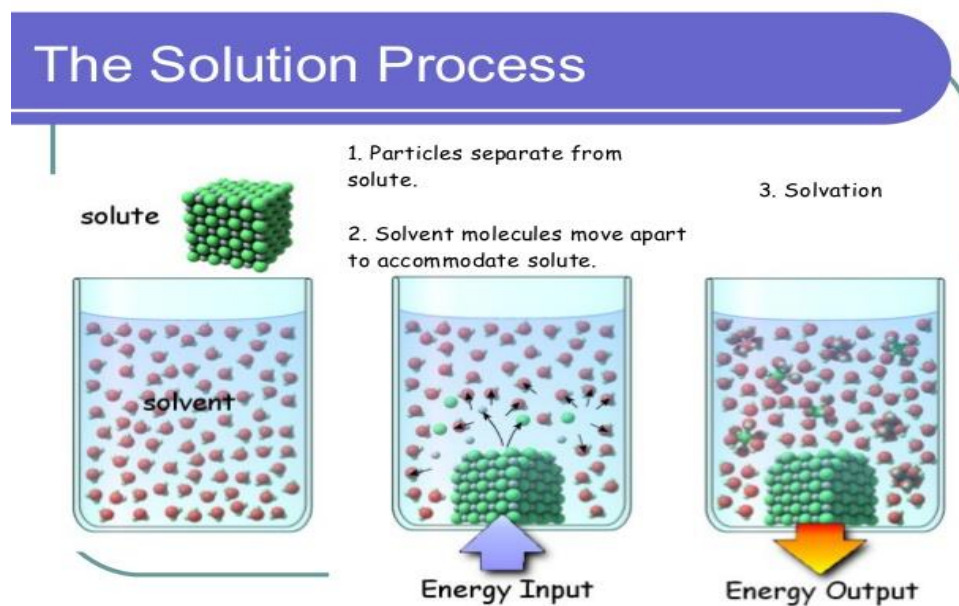
Solvation behaviour have been studied in a wide range of aqueous, non-aqueous, electrolytes and mixed solvents based on the various properties viz. lowering of vapor pressure by solutes [129], order of ionic mobilities [125,129,130], viscosity B-coefficients [129-132], partial molar volume of ionic and non-ionic solutes, dielectric decrement produced by ions [133], solubility of substances [134], effect of ionic and non-ionic solutes on solvent spectra [133,135,136], etc. Several investigations [122,124,130,135,137,138-144] were carried out by the use of spectroscopic methods such as UV-VIS, IR, NMR and considering thermodynamic, kinetic, transport and electrochemical properties at infinite dilution. All these studies provide an idea about the solute/ion-solvent interactions [129, 130,145]. Last few decades have witnessed an exponential growth on the fundamental research involving solute-solute, solute-solvent, and solvent-solvent interactions in aqueous and aquo-organic mixtures in particular but

in pure or mixed organic solvents the research was not established to that extent. In this context, much attention has been given also to determine the various thermodynamic parameters such as enthalpy, entropy and Gibbs free energy change of solutions [146-149]. The purposes of such studies were to gain the ideas about various mechanisms of some significant molecules during solvation. The exploration of molecular interaction existing in solution is always an interest to the chemists. Molecular interaction can be studied in solution phase by studying its thermodynamic and transport properties. Results of such proposed studies will have enormous fundamental and physical consequences in the land of solution chemistry, biophysical chemistry, and pharmaceutical sciences.

Solvation (specifically, hydration) is important for many biological structures and processes. For instance, protein folding occurs spontaneously because of a favourable change in the interactions between the protein and the surrounding water molecules. Proteins are stabilized by 5-10 kcal/mol when folded due to a combination of solvent and hydrogen bonding effects. Minimizing the number of hydrophobic side-chains exposed to water by burying them in the centre of a folded protein is a driving force related to solvation. Solvation can also drive host-guest complexation. Host molecules having hydrophobic cavity can encapsulate a hydrophobic guest within its cavity. These interactions can be used in applications such as drug delivery, such that a hydrophobic drug molecule can be delivered in a biological system without needing to covalently modify the drug in order to solubilize it. Polarity of the solvent affects the binding constants for host-guest complexes.

Our work is concerned mainly with solvation of solutes (ionic liquids) and their thermodynamic aspects. The term 'solvation' can be defined as the more or less specific interaction between a solute molecule and one or more solvent molecules with a force intermediate between weak physical interaction and strong covalent bonding [151]. As we know solutes are generally two types; one is electrolytes and another is nonelectrolytes. Electrolytes when dissolved in suitable solvent, called the ionizing medium, produce ions. The basic difference between electrolytes and non-electrolytes then lies in the ability of the former to generate ions, which are distinguished by their integral charge, and the intense electric field associated with it. In fact, solute-solvent

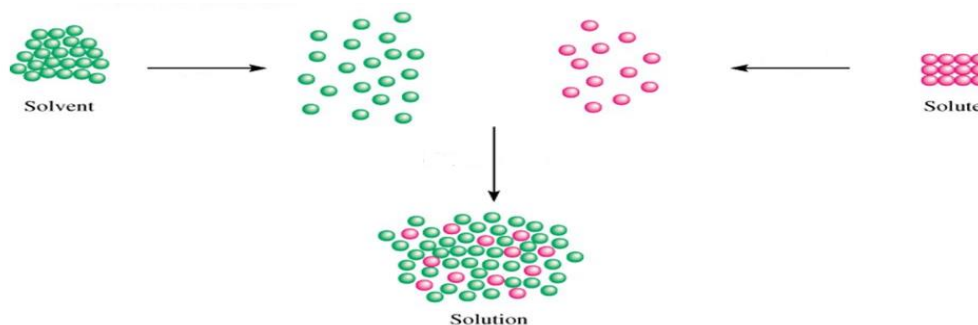
interactions guide all the properties of solutions. Solvation phenomena have been studied in a wide range of aqueous, non-aqueous and mixed solvents from various properties. Remarkable advancements have been made by a number of researchers providing answer to a wide range of relevant problems, concerning solute-solvent interactions from both experimental and theoretical stand points also.



II.6.1 Interactions in Solution Systems

Three types of interactions are mainly observed the solution systems:

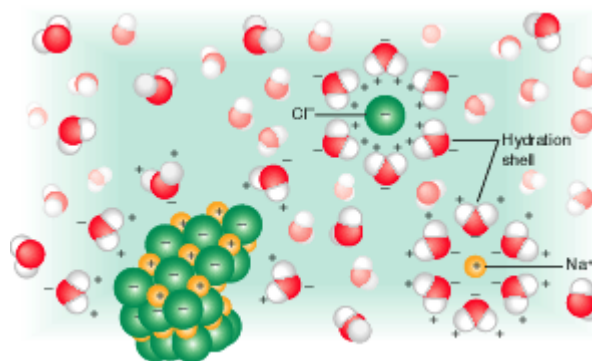
- (a) Solvent-solvent interactions:** energy required to break weak bonds between solvent molecules.
- (b) Solute-solute interactions:** energy required to break intermolecular bonds between the solute molecules.
- (c) Solute-solvent interactions:** ΔH is negative since bonds are formed between them.



For liquid systems, the macroscopic properties are usually quite well known, whereas the microscopic structure is often much less studied. The liquid phase is characterized by local order and long-range disorder, and to study processes in liquids, it is therefore valuable to use methods that probe the local surrounding of the constituent particles. The same is also true for solvation processes: a local probe is important to obtain insight into the physical and chemical processes going on.

II.6.2 Investigation on Different Kind of Interactions

When salt is dissolved in water, the ions of the salt dissociate from each other and associate with the dipole of the water molecules. This result in a solution is called 'solvation'.



This means that the forces of interaction (attraction or repulsion) depending on whether like or unlike charges are closer together. On average, dipoles in a liquid orient themselves to form attractive interactions with their neighbours, but thermal motion makes some instantaneous configurations unfavourable.

The investigation on thermodynamic, transport and optical properties of different electrolytes in various solvents would thus offer an important step in this direction. Naturally, in the development of theories, dealing with electrolyte solutions, much attention has been devoted to 'ion-solvent interactions' which are the controlling forces in infinitely dilute solutions where ion-ion interactions are absent. The contributions due to cations and anions in the solute-solvent interactions can be obtained by separating these functions into ionic contributions. Thus ion-solvent interactions play a crucial role to understand the thermodynamic and physicochemical properties of solutions.

One of the causes for the intricacies in solution chemistry is that the structure of the solvent molecule is not known with certainty. The introduction of a solute also modifies the solvent structure to an uncertain magnitude whereas the solute molecule is also modified and the solute-solute, solute-solvent and solvent-solvent interactions become prominent, though the isolated picture of any of the forces is still not known completely to the solution chemist.

The ion-solvent interactions can be studied from the physicochemical, and thermodynamic point of view, where the changes of free energy, enthalpy and entropy, etc. associated with a particular reaction. Qualitatively and quantitatively evaluated various physicochemical parameters, from which concluded regarding the factors associated with the ion-solvent interactions occurred in the studied solutions.

Similarly, the ion-solvent interactions can be studied using solvational approaches involving the studies of different properties such as, density, viscosity, ultrasonic speed, refractive index and conductance of electrolytes and various derived parameters, factors associated with ionic solvation.

We shall particularly dwell upon the different aspects of these physicochemical, thermodynamic, transports, acoustic and optical properties as the present research work is warmly allied to the studies of ion-ion, ion-solvent and solvent-solvent interactions.

II.6.2.1 Ion-Solvent Interaction

Ion-solvation is a phenomenon of primary interest in many milieu of chemistry because solvated ions are omnipresent on Earth. Hydrated ions occur in aqueous solution in many chemical and biological systems [152]. Solvated ions appear in high

concentrations in living organisms, where their presence or absence can fundamentally alter the functions of life. Ions solvation in organic solvents, mixtures with water and other organic solvents are awfully common [153]. The exchange of solvent molecules around ions in solutions is fundamental clue to the understanding of the reactivity of ions in solution [154]. Solvated ions also play a key role in electrochemical applications, where for instance the conductivity of electrolytes depends on ion-solvent interactions [155]. The significance of ion-solvent interactions was realized after extensive studies in aqueous, non-aqueous and mixed solvents [156-165].

Most chemical processes of individual and biological importance occur in solution. The role of solvent is so great that million fold rate changes take place in some reactions simply by changing the reaction medium. As water is the most abundant solvent in nature and its major importance to chemistry, biology, agriculture, geology, etc., water has been extensively used in kinetic and equilibrium studies. But still our knowledge of molecular interactions in water is extremely limited. Moreover, the uniqueness of water as a solvent has been questioned [166,167] and it has been realized that the studies of other solvent media like non aqueous and mixed solvents would be of great help in understanding different molecular interactions. The organic solvents have been classified on the basis of dielectric constants, organic group types, acid base properties, or association through hydrogen bonding donor-acceptor properties [168,169] hard and soft acid-base principles [170] etc. As a result, the different solvents show a wide change in properties, ultimately influencing their physicochemical, thermodynamic, transport and acoustic properties qualitatively and quantitatively, in presence of electrolytes and non-electrolytes in these solvents.

II.6.2.2 Ion-Ion Interaction

Ion-solvent interactions are only a part of the story of an ion related to its environment. The surrounding of an ion sees only other ions, no solvent molecules. The mutual interactions between these ions represent the essential part '*ion-ion interactions*'. The properties of solution is affected by the degree of ion-ion interactions. Solution chemistry will become understandable only when solute-solute/ion-ion, solute-solvent/ion-solvent and solvent-solvent interactions are elucidated. And thus the work on

solvation of ionic liquid is related to the studies of solute-solute/ion-ion, solute-solvent/ion-solvent and solvent-solvent interactions in some liquid systems.

II.6.3 Density

The physicochemical properties of liquid mixtures have attracted much attention from both theoretical and engineering applications points of view. Many engineering applications require quantitative data on the density of liquid systems. They also provide information about the nature and molecular interactions between electrolyte or non-electrolyte and liquid components.

The volumetric property '*Density*' is a function of weight, volume and mole fraction and excess volumes of mixing. One of the well-recognized approaches to the study of molecular interactions in fluids is the use of physicochemical, thermodynamic methods. Physicochemical properties are generally convenient parameters for interpreting solute-solvent/ion-solvent and ion-ion/solute-solute interactions occurring in the solution phase. Fundamental properties such as enthalpy, entropy and Gibbs energy represent the macroscopic state of the system as an average of numerous microscopic states at a given temperature and pressure. Molecular phenomena is generally difficult to understand in terms of density value hence higher derivatives of these properties employed. The volumetric information may be of immense importance in this regard. Various concepts regarding molecular interaction in solutions is electrostriction [171], hydrophobic hydration [172], micellization [173], and co-sphere overlap during ion-solvent/solute-solvent interactions [174] have been derived and interpreted from the partial molar volume data for electrolytes and non-electrolytes.

❖ Apparent and Partial Molar Volumes

Density data can be used for the calculation of molar volume of a pure substance. In complex multi-component systems such as solutions, it is easier to describe a system in terms of the intrinsic or molal properties rather than the extensive properties. Any extensive property of a system can be calculated as the sum of the respective partial molal properties if all components have a known concentration. Although the additive

definition of partial molal properties is convenient, direct measurement of these solution properties are difficult, because interactions with other species contribute to partial molal properties. When dealing with solutions it is more common to measure the apparent molal quantities, ϕ_Y , which can be defined as the change in property, Y , due to a known amount of solute in a known amount of solvent, assuming the contribution by the solvent is the same as that of the pure species. In other words, all changes in the state properties can be attributed to the presence of the solute, even if these changes contribute to a change in partial molal property of the solvent. The apparent molal property of any solute, $\phi_{2,Y}$, can be defined as

$$\phi_{2,Y} = \frac{Y - n_1 \bar{\phi}_Y^0}{n_2} \quad (\text{II. 1a})$$

Where, n_1 and n_2 represent the mole of the solvent and solute respectively, in the system. $\bar{\phi}_Y^0$, denotes the partial molal property of the pure solvent. Because the solvent is assumed to contribute a definite, constant quantity for all solute concentrations at fixed temperature and pressure, the partial derivative of the extensive property with respect to the number of moles of solute can be defined in terms of the apparent molal quantity:

$$\left(\frac{\partial Y}{\partial n_2} \right)_{n_1, T, P} = \left(\frac{\partial \phi_{2,Y}}{\partial n_2} \right)_{n_1} + \phi_{2,Y} \quad (\text{II. 1b})$$

Eqs (II.1a) and (II.1b) shows that if the apparent molal property and its derivative with respect to moles of solute is known, the partial molal property can be calculated. In other words, if any appropriate Eq. for the apparent molal property with respect to any concentration scale, which is in good agreement with experimental data is known, the apparent molal property at infinite dilution can also be found out. Theoretically, as the concentration approaches zero, the apparent molal property approaches the partial molal property of the solute at infinite dilution, because by definition the solvent is already assumed to be in its pure form. If the apparent molal property is assumed to reflect the apparent molal property of the solute only and not the solute-solvent complex, then the apparent molal property at infinite dilution, $\phi_{2,Y}^\infty$, would be equal to the standard state molal property of the solute, as defined by Henry's law. Ignoring the previous

equality, equation of state developed for standard state partial molal variables have been used successfully to describe partial molal quantities at infinite dilution.

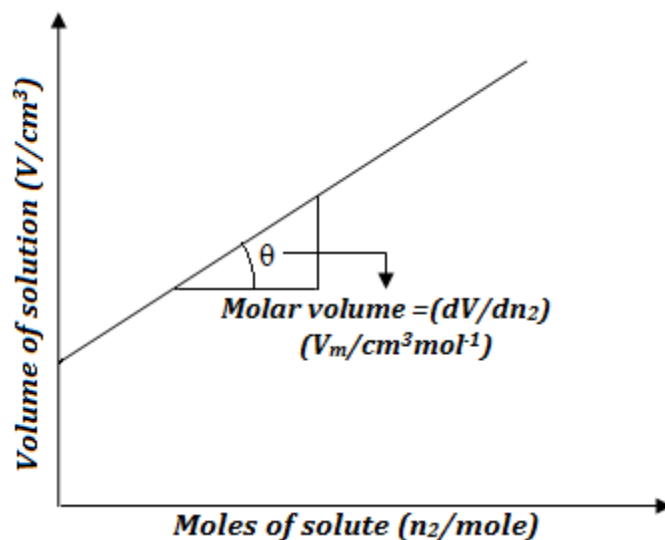


Figure II.12: A diagram for the explanation of molal volume.

The easiest way to explain this is in terms of the molal volume, V_m , shown in the **Figure II.12**, where the volume increases with respect to the amount of solute added. A dissolved solute has its own property, referred to as partial molal property.

Therefore for a two component system, where one component is the solvent and the other is solute, the total volume of the system can be represented as the sum of the partial molal volumes of the solvent, \bar{V}_1 , and the solute, \bar{V}_2 :

$$V = n_1 \bar{V}_1 + n_2 \bar{V}_2 \quad (\text{II. 1c})$$

Dividing Eq. (II. 1c) by $n_1 + n_2$, the molal volume of the solution is obtained as:

$$V_m = x_1 \bar{V}_1 + x_2 \bar{V}_2 \quad (\text{II. 1d})$$

where, x_1 and x_2 represent the mole fraction of the solvent and the solute, respectively. The partial molal property of a solute is defined as the change in the total property of the system with respect to the change in the number of moles of solute added, with all other variables (T , P , and the amount of the solvent) are held constant. An alternative, widely used property of the solute is the apparent molal property. The apparent molal volume

is the volume that should be attributed to the solute in solution if it is assumed that the solvent contributes the exact volume it would if it was in its pure state.

Under this assumption, the apparent molal volume of the solute, $\phi_{2,v}$, as defined by Harned and Owen, is the difference between the total volume (or the total molal volume) and the partial molal volume of the pure solvent (\bar{V}_1^0) divided by the number of moles (or the mole fraction) of the solute present:

$$\phi_{2,v} = \frac{V - n_1 \bar{V}_1^0}{n_2} \quad (\text{II. 1e})$$

$$\phi_{2,v} = \frac{V_m - x_1 \bar{V}_1^0}{x_2} \quad (\text{II. 1f})$$

In experimentation, \bar{V}_1^0 is generally considered to be constant over the range of solute concentration at constant temperature and pressure. Hence, $\phi_{2,v}$, can be easily calculated using Eq. (II. 1e) or (II. 1f) when the total volume or molal volume is known. Eq. (II. 1e) can be modified in order to find out the apparent molal volume of a solute using density of the solution containing the solute and the density of the pure solvent, ρ and ρ_0 , respectively. Assuming there is 1 kilogram (kg) of solvent:

$$n_1 = \frac{1}{M_1}, \quad \text{therefore,} \quad V = \frac{\bar{V}_1^0}{M_1} + m_2 \cdot \phi_{2,v} \quad (\text{II. 1g})$$

where, M_1 is the molal mass of the solvent.

Since, $\rho_1 = \frac{\bar{V}_1^0}{M_1}$, Eq. (II. 1g) becomes:

$$V = \frac{1}{\rho_1} + m_2 \cdot \phi_{2,v} \quad (\text{II. 1h})$$

where, m_2 is the molality of the solute (which is equivalent to n_1 if 1kg of solvent is present). The entire mass of the solution will be composed of the mass of the solvent (1kg) and the mass of the solute ($m_2 \cdot M_2$). Since volume is the ratio of mass to density, the equation for V becomes:

$$\frac{1 + m_2 \cdot M_2}{\rho_1} = \frac{1}{\rho_1} + m_2 \cdot \phi_{2,v} \quad (\text{II. 1i})$$

By rearranging this Eq. (II. 1h) and solving for $\phi_{2,v}$, an equation for apparent molal volume for 1 kg of the solute is obtained:

$$\phi_{2,v} = \frac{\rho_2 - \rho_1}{m_2 \rho_1 \rho_2} + \frac{M_2}{\rho_2} \quad (\text{II. 1j})$$

However, the volume contributed to a solvent by the addition of one mole of an ion is difficult to determine. This is so because, upon entry into the solvent, the ions change the volume of the solution due to a breakup of the solvent structure near the ions and the compression of the solvent under the influence of the ion's electric field, *i.e.*, *electrostriction*. Electrostriction is a general phenomenon and whenever there are electric fields of the order of 10^9 - 10^{10} V·m⁻¹, the compression of ions and molecules is likely to be significant. The effective volume of an ion in solution, the partial molar volume, can be determined from a directly obtainable quantity apparent molar volume (ϕ_v). Thus the apparent molar volumes of the solutes can be calculated by using the following relation [175];

$$\phi_v = \frac{M}{\rho_0} - \frac{1000(\rho - \rho_0)}{c\rho_0} \quad (\text{II.1k})$$

or

$$\phi_v = \frac{M}{\rho} - \frac{1000(\rho - \rho_0)}{m\rho\rho_0} \quad (\text{II.1l})$$

Where M is the molar mass of the solute, c is the molarity, m is the molality of the solution; ρ_0 and ρ are the densities of the solvent and the solution respectively. The partial molar volumes, ϕ_{2v} can be obtained from the equation [176];

$$\phi_{2v} = \phi_v + \frac{(1000 - c\phi_v)}{2000 + c^{3/2} \left(\frac{\partial \phi_v}{\partial \sqrt{c}} \right)} c^{1/2} \left(\frac{\partial \phi_v}{\partial \sqrt{c}} \right) \quad (\text{II. 2})$$

The extrapolation of the apparent molar volume of electrolyte to infinite dilution and the expression of the concentration dependence of the apparent molar volume have been made by four major equations over a period of years – the Masson equation [177], the

Redlich-Meyer equation [178], the Owen-Brinkley equation [179], and the Pitzer equation [180]. According to Masson

$$\phi_V = \phi_V^0 + S_V^* \sqrt{c} \quad (\text{II. 3a})$$

$$\phi_V = \phi_V^0 + S_V^* \sqrt{m} \quad (\text{II. 3b})$$

Where, ϕ_V^0 is the apparent molar volume (equal to the partial molar volume) at infinite dilution and S_V^* the experimental slope. The majority of ϕ_V data in water [181] and nearly all ϕ_V data in non-aqueous [182-186] solvents have been extrapolated to infinite dilution through the use of equation (II. 3a) or (II.3b).

The temperature dependence of ϕ_V^0 in various solvents can be expressed by the general equation as follows:

$$\phi_V^0 = a_0 + a_1 T + a_2 T^2 + \dots \quad (\text{II. 4})$$

where a_0 , a_1 , a_2 are the coefficients of a particular electrolyte and T is the temperature in Kelvin.

The limiting apparent molar expansibilities (ϕ_E^0) can be obtained by the following equation:

$$\phi_E^0 = \left(\delta \phi_V^0 / \delta T \right)_p = a_1 + 2a_2 T \quad (\text{II. 5})$$

The limiting apparent molar expansibilities (ϕ_E^0) change in magnitude with the change of temperature. During the past few years it has been emphasized by a number of workers that S_V^* is not the sole criterion for determining the structure-making or breaking tendency of any solute. Helper [187] developed a technique of examining the sign of $\left(\delta \phi_E^0 / \delta T \right)_p$ for the solute in terms of long-range structure-making and breaking capacity of the electrolytes in the mixed solvent systems. The general thermodynamic expression used is as follows:

$$\left(\delta \phi_E^0 / \delta T \right)_p = \left(\delta^2 \phi_V^0 / \delta T^2 \right)_p = 2a_2 \quad (\text{II. 6})$$

If the sign of $(\delta\phi_E^0/\delta T)_P$ is positive or small negative the electrolyte is act as structure maker and when the sign of $(\delta\phi_E^0/\delta T)_P$ is negative, it is a structure breaker. Redlich and Meyer [178] have shown that an equation (II. 3a) or (II. 3b) cannot be any more than a limiting law where for a given solvent and temperature, the slope S_v^* should depend only upon the valence type. They suggested the equation:

$$\phi_v = \phi_v^0 + S_v \sqrt{c} + b_v c \quad (\text{II. 7})$$

$$\text{Where } S_v = Kw^{3/2} \quad (\text{II. 8})$$

S_v is the theoretical slope, based on molar concentration, including the valence factor where

$$w = 0.5 \sum_i^j Y_i Z_i^2 \quad (\text{II. 9})$$

$$\text{And } K = N^2 e^2 \left(\frac{8\pi}{1000 \epsilon^3 RT} \right)^{1/2} \left[\left(\frac{\partial \ln \epsilon}{\partial p} \right)_T - \frac{\beta}{3} \right] \quad (\text{II. 10})$$

In equation (II. 10), K is the compressibility of the solvent and the other terms have their usual significance.

❖ **Limiting Ionic Partial Molar Volumes**

The individual partial ionic volumes provide information relevant to the general question of the structure near the ion, i.e., its solvation. The calculation of the ionic limiting partial molar volumes in organic solvents is, however, a difficult one. At present, however, most of the existing ionic limiting partial molar volumes in organic solvents were obtained by the application of methods originally developed for aqueous solutions to non-aqueous electrolyte solutions. In the last few years, the method suggested by Conway *et al.*[188] has been used more frequently. The authors used the method to determine the limiting partial molar volumes of the anion for a series of homologous tetra-alkyl ammonium chlorides, bromides and iodides in aqueous solution. They plotted the limiting partial molar volume $\phi_{vR_4NX}^0$, for a series of these salts with a halide ion in

common as a function of the formula weight of the cation, $M_{R_4N^+}$ and obtained straight-lines for each series. Therefore, they suggested the following equation:

$$\phi_{V_{R_4NX}}^0 = bM_{R_4N^+} + \phi_{V_{X^-}}^0 \quad (\text{II. 11})$$

The extrapolation to zero cationic formula weight gave the limiting partial molar volumes of the halide ions $\phi_{V_{X^-}}^0$. Uosaki *et al.* [189] used this method for the separation of some literature values and of their own $\phi_{V_{R_4NX}}^0$ values into ionic contributions in organic electrolyte solutions.

II.6.4 Viscosity

As fundamental and significant property of liquids is **viscosity**, provide a lot of information on the structures and molecular interactions in liquid systems. Viscosity and volume are different types of properties of one liquid, and there is a certain relationship between them. So by measuring and studying them together, relatively more realistic and comprehensive information could be expected to be gained. Viscosity, one of the most important transport properties is used for the determination of ion-solvent interactions and studied extensively [190,191]. It is not a thermodynamic quantity, but of an electrolytic solution along with the physicochemical property, the partial molar volume $\phi_{v,2}^0$, gives a lot of information and insight regarding ion-solvent interactions and the nature of structures in the electrolytic solutions.

❖ **Viscosity of Pure Liquids and Liquid Mixtures**

Since the molecular motion in liquids is controlled by the influence of the neighboring molecules, the transport of momentum in liquids takes place, in sharp contrast with gases at ordinary pressures, not by the actual movement of molecules but by the intense influence of intermolecular force fields. It is this aspect of the mechanism of momentum transfer which forms the basis of the procedures for predicting the variations in the viscosity of liquids and liquid systems.

❖ *Viscosity of Electrolytic Solutions*

The viscosity relationships of electrolytic solutions are highly complicated. Because ion-ion and ion-solvent interactions are occurring in the solution and separation of the related forces is a difficult task. But, from careful analysis, vivid and valid conclusions can be drawn regarding the structure and the nature of the solvation of the particular system. As viscosity is a measure of the friction between adjacent, relatively moving parallel planes of the liquid, anything that increases or decreases the interaction between the planes will raise or lower the friction and thus, increase or decrease the viscosity. If large spheres are placed in the liquid, the planes will be keyed together in increasing the viscosity. Similarly, increase in the average degree of hydrogen bonding between the planes will increase the friction between the planes, thereby viscosity. An ion with a large rigid co-sphere for a structure-promoting ion will behave as a rigid sphere placed in the liquid and increase the inter-planar friction. Similarly, an ion increasing the degree of hydrogen bonding or the degree of correlation among the adjacent solvent molecules will increase the viscosity. Conversely, ions destroying correlation would decrease the viscosity. In 1905, Grüneisen [192] performed the first systematic measurement of viscosities of a number of electrolytic solutions over a wide range of concentrations. He noted non-linearity and negative curvature in the viscosity concentration curves irrespective of low or high concentrations. In 1929, Jones and Dole [193] suggested an empirical equation quantitatively correlating the relative viscosities of the electrolytes with molar concentrations (c):

$$\frac{\eta}{\eta_o} = \eta_r = 1 + A\sqrt{c} + Bc \quad (\text{II. 12})$$

The above equation can be rearranged as:

$$\frac{\eta_r - 1}{\sqrt{c}} = A + B\sqrt{c} \quad (\text{II. 13})$$

Where A and B are constants specific to ion-ion and ion-solvent interactions. The equation is applicable equally to aqueous and non-aqueous solvent systems where there is no ionic association and has been used extensively. The term $A\sqrt{c}$, originally ascribed to Grüneisen effect, arose from the long-range coulombic forces between the ions. The significance of the term had since then been realized due to the development Debye-

Hückel Theory [194] of inter-ionic attractions in 1923. The A -coefficient depends on the ion-ion interactions and can be calculated from interionic attraction theory [195-197] and is given by the Falkenhagen Vernon [197] equation:

$$A_{Theo} = \frac{0.2577A_o}{\eta_o(\epsilon T)^{0.5} \lambda_+^o \lambda_-^o} \left[1 - 0.6863 \left(\frac{\lambda_+^o \lambda_-^o}{A_o} \right)^2 \right] \quad (II. 14)$$

Where the symbols have their usual significance. In very accurate work on aqueous solutions [131, 198], A -coefficient has been obtained by fitting η_r to equation (II. 13) and compared with the values calculated from equation (II. 14), the agreement was excellent. The accuracy achieved with partially aqueous solutions was however poorer [199]. A -coefficient suggesting that should be calculated from conductivity measurements. Crudden *etal.* [200] suggested that if association of the ions occurs to form an ion pair, the viscosity should be changed and thus analyzed by the equation:

$$\frac{\eta_r - 1 - A\sqrt{\alpha c}}{\alpha c} = B_i + B_p \left(\frac{1 - \alpha}{\alpha} \right) \quad (II. 15)$$

Where A , B_i and B_p are characteristic constants and α is the degree of dissociation of ion-pair. Thus, a plot of $\frac{\eta_r - 1 - A\sqrt{\alpha c}}{\alpha c}$ vs $\left(\frac{1 - \alpha}{\alpha} \right)$, when extrapolated to $\left(\frac{1 - \alpha}{\alpha} \right) = 0$ give the intercept B_i . However, for the most of the electrolytic solutions both aqueous and non-aqueous, the equation (II. 13) is valid up to 0.1 (M) [201,202] within experimental errors. At higher concentrations the extended Jones-Dole equation (II. 16), involving an additional coefficient D , originally used by Kaminsky [203], has been used by several workers [204,205] and is given below:

$$\frac{\eta}{\eta_o} = \eta_r = 1 + A\sqrt{c} + Bc + Dc^2 \quad (II. 16)$$

The coefficient D cannot be evaluated properly and the significance of the constant is also not always meaningful and therefore, equation (II. 13) is used by the most of the workers.

The plots of $\frac{(\eta / \eta_o - 1)}{\sqrt{c}}$ against \sqrt{c} for the electrolytes should give the value of A -coefficient. But sometimes, the values come out to be negative or considerably scatter

and also deviation from linearity occur [206-211]. Thus, instead of determining A -coefficient from the plots or by the least square method, the A -coefficient are generally calculated using Falkenhagen-Vernon equation (II. 14). A -coefficient should be zero for non-electrolytes. According to Jones and Dole, the A -coefficient probably represents the stiffening effect on the solution of the electric forces between the ions, which tend to maintain a space-lattice structure [193]. The sign of the B -coefficient may be either positive or negative which depends on the ions and the solvent. The B -coefficients are obtained as slopes of the straight lines using the least square method and intercepts equal to the A -coefficient.

The factors influencing B -coefficients are [208,209]:

- (a) The destruction of the three dimensional structure of solvent molecules (i.e., structure breaking effect or depolymeriation effect) decreases η values.
- (b) The solvent having high molal volume and low dielectric constant yield high B -values.
- (c) Reduced B -values are obtained when the primary solution of ions is sterically hindered in high molal volume solvents or if either ion of a binary electrolyte cannot be specifically solvated.

❖ *Viscosities at Higher Concentration*

It had been found that the viscosity at high concentrations (1 M to saturation) can be represented by the empirical formula suggested by Andrade:

$$\eta = A \exp^{\frac{b}{T}} \quad (\text{II. 17})$$

The several alternative formulations have been proposed for representing the results of viscosity measurements in the high concentration range [209-215] and the equation suggested by Angell [216,217] based on an extension of the free volume theory of transport phenomena in liquids and fused salts to ionic solutions is particularly noteworthy. The equation is:

$$\frac{1}{\eta} = A \exp \left[-\frac{K_1}{N_o - N} \right] \quad (\text{II. 18})$$

Where N represents the concentration of the salt in $\text{eq}\cdot\text{litre}^{-1}$, A and K_1 are constants supposed to be independent of the salt composition and N_o is the hypothetical concentration at which the system becomes glass.

❖ *Division of B-Coefficient into Ionic Values*

The viscosity B -coefficients have been determined by a large number of workers in aqueous, mixed and non-aqueous solvents [218-248]. However, the B -coefficients as determined experimentally using the Jones-Dole equation, does not give any impression regarding ion-solvent interactions unless there is some way to identify the separate contribution of cations and anions to the total solute-solvent interaction. The division of B -values into ionic components is quite arbitrary and based on some assumptions, the validity of which may be questioned. The following methods have been used for the division of B -values in the ionic components:

- [1]. Cox and Wolfenden [249] carried out the division on the assumption that B_{ion} values of Li^+ and IO_3^- in LiIO_3 are proportional to the ionic volumes which are proportional to the third power of the ionic mobilities. The method of Gurney [250] and also of Kaminsky [203] is based on:

$$B_{K^+} = B_{Cl^-} \text{ (in water)} \quad (\text{II. 19})$$

The argument in favor of this assignment is based on the fact that the B -coefficients for KCl is very small and that the motilities' of K^+ and Cl^- are very similar over the temperature range 288.15–318.15K. The assignment is supported from other thermodynamic properties. Nightingale [251], however preferred RbCl or CsCl to KCl from mobility considerations.

- [2]. The method suggested by Desnoyers and Perron [204] is based on the assumption that the Et_4N^+ ion in water is probably closest to be neither structure breaker nor a structure maker. Thus, they suggest that it is possible to apply with a high degree of accuracy of the Einstein's equation [252],

$$B = 0.0025\bar{V}_o \quad (\text{II. 20})$$

and by having an accurate value of the partial molar volume of the ion, V_o , it is possible to calculate the value of 0.359 for $B_{Et_4N^+}$ in water at 298.15 K. Recently, Sacco *et al.* proposed the “reference electrolytic” method for the division of B -values.

Thus, for tetraphenylphosphonium tetraphenylborate in water, we have:

$$B_{BPh_4^-} = B_{PPh_4^+} = B_{BPh_4PPh_4} / 2 \quad (II. 21)$$

$B_{BPh_4PPh_4}$ (Scarcely soluble in water) has been obtained by the following method:

$$B_{BPh_4PPh_4} = B_{NaBPh_4} + B_{PPh_4Br} - B_{NaBr} \quad (II. 22)$$

The values obtained are in good agreement with those obtained by other methods. The criteria adopted for the separation of B -coefficients in non-aqueous solvents differ from those generally used in water. However, the methods are based on the equality of equivalent conductances of counter ions at infinite dilutions.

(a) Criss and Mastroianni assumed $B_{K^+} = B_{Cl^-}$ in ethanol based on equal mobilities of ions [253]. They also adopted $B_{Me_4N^+}^{25} = 0.25$ as the initial value for acetonitrile solutions.

(b) For acetonitrile solutions, Tuan and Fuoss [254] proposed the equality, as they thought that these ions have similar mobilities. However, according to Springer *et al.* [255] $\lambda_{25}^o(Bu_4N^+) = 61.4$ and $\lambda_{25}^o(Ph_4B^-) = 58.3$ in acetonitrile.

$$B_{Bu_4N^+} = B_{Ph_4B^-} \quad (II. 23)$$

(c) Gopal and Rastogi [219] resolved the B -coefficient in N-methyl propionamide solutions assuming that $B_{Et_4N^+} = B_{I^-}$ at all temperatures.

(d) In dimethyl sulphoxide, the division of B -coefficients were carried out by Yao and Bennion [207] assuming:

$$B_{[(i-pe)_3Bu_4N^+]} = B_{Ph_4B^-} = \frac{1}{2} B_{[(i-pe)_3BuNPh_4B]} \quad (II. 24)$$

at all temperatures.

It is apparent that almost all these methods are based on certain approximations and anomalous results may arise unless proper mathematical theory is developed to calculate B -values.

❖ **Thermodynamics of Viscous Flow**

Assuming viscous flow as a rate process, the viscosity (η) can be represented from Eyring's [256] approaches as:

$$\eta = A e^{\frac{E_{vis}}{RT}} = \left(\frac{hN_A}{V} \right) e^{\frac{\Delta G^*}{RT}} = \left(\frac{hN_A}{V} \right) e^{\left(\frac{\Delta H^*}{RT} - \frac{\Delta S^*}{R} \right)} \quad (\text{II. 25})$$

Where E_{vis} = the experimental entropy of activation determined from a plot of $\ln \eta$ against $1/T$. ΔG^* , ΔH^* and ΔS^* are the free energy, enthalpy and entropy of activation, respectively.

Nightingale and Benck [257] dealt in the problem in a different way and calculated the thermodynamics of viscous flow of salts in aqueous solution with the help of the Jones-Dole equation (neglecting the $A c$ term). Thus, we have:

$$R \left[\frac{d \ln \eta}{d \left(\frac{1}{T} \right)} \right] = r \left[\frac{d \ln \eta_o}{d \left(\frac{1}{T} \right)} \right] + \frac{R}{1+Bc} \frac{d(1+Bc)}{d \left(\frac{1}{T} \right)} \quad (\text{II. 26})$$

$$\Delta E_{\eta(Soln)}^{\ddagger} = \Delta E_{\eta(Solv)}^{\ddagger} + \Delta E_V^{\ddagger} \quad (\text{II. 27})$$

ΔE_V^{\ddagger} can be interpreted as the increase or decrease of the activation energies for viscous flow of the pure solvents due to the presence of ions, *i.e.*, the effective influence of the ions upon the viscous flow of the solvent molecules. Feakins *et al.* [258] have suggested an alternative formulation based on the transition state treatment of the relative viscosity of electrolytic solution. They suggested the following expression:

$$B = \frac{(\phi_{V,2}^0 - \phi_{V,1}^0)}{1000} + \phi_{V,2}^0 \frac{(\Delta \mu_2^{0\ddagger} - \Delta \mu_1^{0\ddagger})}{1000RT} \quad (\text{II. 28})$$

Where $\phi_{v,1}^0$ and $\phi_{v,2}^0$ are the partial molar volumes of the solvent and solute respectively and $\Delta \mu_2^{0\ddagger}$ is the contribution per mole of solute to the free energy of activation for viscous

flow of solution. $\Delta\mu_1^{0\neq}$ is the free energy of activation for viscous flow per mole of the solvent which is given by:

$$\Delta\mu_1^{0\neq} = \Delta G_1^{0\neq} = RT \ln(\eta_0 \phi_{v,1}^0 / hN_A) \quad (\text{II. 29})$$

Further, if B is known at various temperatures, we can calculate the entropy and enthalpy of activation of viscous flow respectively from the following equations as given below:

$$\frac{d(\Delta\mu_2^{0\neq})}{dT} = -\Delta S_2^{0\neq} \quad (\text{II. 30})$$

$$\Delta H_2^{0\neq} = \Delta\mu_2^{0\neq} + T \Delta S_2^{0\neq} \quad (\text{II. 31})$$

❖ *Effects of Shape and Size*

Stokes and Mills have dealt in the aspect of shape and size extensively. The ions in solution can be regarded to be rigid spheres suspended in continuum. The hydrodynamic treatment presented by Einstein [252] leads to the equation:

$$\frac{\eta}{\eta_0} = 1 + 2.5\phi \quad (\text{II. 32})$$

Where ϕ is the volume fraction occupied by the particles. Modifications of the equation have been proposed by (i) Sinha [259] on the basis of departures from spherical shape and (ii) Vand on the basis of dependence of the flow patterns around the neighboring particles at higher concentrations. However, considering the different aspects of the problem, spherical shapes have been assumed for electrolytes having hydrated ions of large effective size (particularly polyvalent monatomic cations). Thus, we have from equation (II. 32):

$$2.5\phi = A\sqrt{c} + Bc \quad (\text{II. 33})$$

Since $A\sqrt{c}$ term can be neglected in comparison with Bc and $\phi = c\phi_{v,1}^0$ where $\phi_{v,1}^0$ is the partial molar volume of the ion, we get:

$$2.5\phi_{v,1}^0 = B \quad (\text{II. 34})$$

In the ideal case, the B -coefficient is a linear function of partial molar volume of the solute, $\phi_{v,1}^0$ with slope to 2.5. Thus, B_{\pm} can be equated to:

$$B_{\pm} = 2.5\phi_{\pm}^0 = \frac{2.5 \times 4}{3} \frac{(\pi R_{\pm}^3 N)}{1000} \quad (\text{II. 35})$$

assuming that the ions behave like rigid spheres with an effective radii, R_{\pm} moving in a continuum. R_{\pm} , calculated using the equation (II. 35) should be close to crystallographic radii or corrected Stoke's radii if the ions are scarcely solvated and behave as spherical entities. But, in general, R_{\pm} values of the ions are higher than the crystallographic radii indicating appreciable solvation.

The solvation number (n_b) can be easily calculated by comparing the Jones-Dole equation with the Einstein's equation:

$$B_{\pm} = \frac{2.5}{1000(\phi_i + n_b\phi_s)} \quad (\text{II. 36})$$

Where ϕ_i is the molar volume of the base ion and ϕ_s , the molar volume of the solvent. The equation (II. 36) has been used by a number of workers to study the nature of solvation and solvation number.

❖ *Viscosity of Non-Electrolytic Solutions*

The equations of Vand [260], Thomas [261], and Moulik [262-264] proposed mainly to account for the viscosity of the concentrated solutions of bigger spherical particles have been also found to correlate the mixture viscosities of the usual nonelectrolytes. These equations are:

$$\text{Vand equation:} \quad \ln \eta_r = \frac{\alpha}{1-Q} = \frac{2.5V_h c}{1-QV_h c} \quad (\text{II. 37})$$

$$\text{Thomas equation:} \quad \eta_r = 1 + 2.5V_h c + 10.05cV_h^2 c \quad (\text{II. 38})$$

$$\text{Moulik equation:} \quad \eta^2 = I + Mc^2 \quad (\text{II. 39})$$

Where η_r is the relative viscosity, α is constant depending on axial ratios of the particles, Q is the interaction constant, V_h is the molar volume of the solute including rigidly held

solvent molecules due to hydration, c is the molar concentration of the solutes; l and M are constants. The viscosity equation proposed by Eyring and coworkers for pure liquids on the basis of pure significant liquid structures theory, can be extended to predict the viscosity of mixed liquids also. The final expression for the liquid mixtures takes the following form:

$$\eta_m = \frac{6N_A h}{\sqrt{2}r_m(V_m - V_{Sm})} \left[\sum_i^n \left\{ 1 - \exp\left(\frac{-\theta_i}{T}\right) \right\}^{-x_i} \right] \exp\left[\frac{a_m E_{Sm} V_{Sm}}{RT(V_m - V_{Sm})} \right] + \frac{V_m - V_{Sm}}{V_m} \left[\sum_i^n \frac{2}{3d_i^2} \left(\frac{m_i kT}{\pi^3} \right)^{\frac{1}{2}} x_i \right] \quad (\text{II. 40})$$

Where n is 2 for binary and 3 for ternary liquid mixtures. The mixture parameters, r_m , E_{Sm} , V_m , V_{Sm} and a_m were calculated from the corresponding pure component parameters by using the following relations:

$$r_m = \sum_i^n x_i^2 r_i + \sum_{i \neq j} 2x_i x_j x_{ij} \quad (\text{II. 41})$$

$$E_{Sm} = \sum_i^n x_i^2 E_{Si} + \sum_{i \neq j} 2x_i x_j E_{Sij} \quad (\text{II. 42})$$

$$V_m = \sum_i^n x_i V_i \quad V_{Sm} = \sum_i^n x_i V_{Si} \quad a_m = \sum_i^n x_i a_i \quad (\text{II. 43})$$

$$r_{ij} = (r_i r_j)^{\frac{1}{2}} \text{ and } E_{Sij} = (E_{Si} E_{Sj})^{\frac{1}{2}} \quad (\text{II. 44})$$

$$\theta = \frac{h}{\kappa 2\pi} \left(\frac{b}{m} \right)^{\frac{1}{2}} \quad (\text{II. 45})$$

$$b = 2Z\varepsilon \left[22.106 \left(\frac{N_A \sigma^2}{V_s} \right)^4 - 10.559 \left(\frac{N_A \sigma^3}{V_s} \right)^2 \right] \frac{1}{\sqrt{2}\sigma^2} \left(\frac{N_A \sigma^3}{V_s} \right)^{\frac{2}{3}} \quad (\text{II. 46})$$

Where σ and ε_r are Lennard-Jones potential parameters and the other symbols have their usual significance.

❖ **Viscosity Deviation**

Viscosity of liquid mixtures can also provide information for the elucidation of the fundamental behavior of liquid mixtures, aid in the correlation of mixture viscosities with those of pure components, and may provide a basis for the selection of physico-chemical methods of analysis. Quantitatively, as per the absolute reaction rates theory [265], the deviations in viscosities ($\Delta\eta$) from the ideal mixture values can be calculated as:

$$\Delta\eta = \eta - \sum_{i=1}^j (x_i \eta_i) \quad (47)$$

Where η is the dynamic viscosities of the mixture and $x_i \eta_i$ are the mole fraction and viscosity of i^{th} component in the mixture, respectively.

❖ **Gibbs Excess Energy of Activation for Viscous Flow**

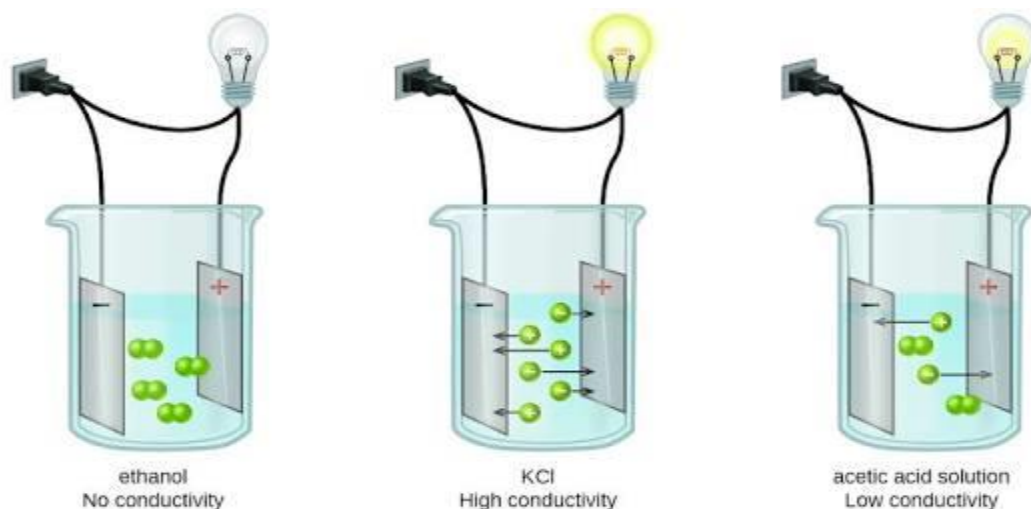
Quantitatively, the Gibbs excess energy of activation for viscous flow ΔG^* can be calculated as [266]:

$$\Delta G^E = RT \left[\ln \eta V - \sum_{i=1}^j (x_i \ln \eta_i V_i) \right] \quad (\text{II. 48})$$

Where η and V are the viscosity and molar volume of the mixture; η_i and V_i are the viscosity and molar volume of i^{th} pure component, respectively.

II.6.5 Conductance

One of the most precise and direct technique available to determine the extent of the dissociation constants of electrolytes in aqueous, mixed and non-aqueous solvents is the “*conductimetric method.*” Conductance data in conjunction with viscosity measurements, gives much information regarding ion-ion and ion-solvent interaction.



Dissolved Ions Conduct Electricity

The studies of conductance measurements were pursued vigorously during the last five decades, both theoretically and experimentally and a number of important theoretical equations have been derived. We shall dwell briefly on some of these aspects in relation to the studies in aqueous, non-aqueous, pure and mixed solvents. The successful application of the Debye-Hückel theory of interionic attraction was made by Onsager [267], to derive the Kohlrausch's equation representing the molar conductance of an electrolyte. For solutions of a single symmetrical electrolyte the equation is given by:

$$\Lambda = \Lambda_o - S\sqrt{c} \quad (\text{II. 49})$$

Where,

$$S = \alpha\Lambda_o + \beta \quad (\text{II. 50})$$

$$\alpha = \frac{(z^2)k}{3(2 + \sqrt{2})\epsilon_r kT\sqrt{c}} = \frac{82.406 \times 10^4 z^3}{(\epsilon_r T)^{\frac{3}{2}}} \quad (\text{II. 51a})$$

$$\beta = \frac{z^2 e F k}{3\pi\eta\sqrt{c}} = \frac{82.487 z^3}{\eta\sqrt{\epsilon_r T}} \quad (\text{II. 51b})$$

The equation has no explanation for the short-range interactions and also of shape or size of the ions in solution. The ions were regarded as rigid charged spheres in an electrostatic and hydrodynamic continuum, i.e., the solvent [268]. In the subsequent years, Pitts (1953) [269] and Fuoss and Onsager (1957) [270] individually worked out the solution of the problem of electrolytic conductance accounting for both long-range

and short-range interactions. The conductance values at infinite dilution (Λ_o) are different for two different theory (Fuoss-Onsager theory and Pitt's theory) and the derivation of the Fuoss-Onsager equation was questioned [271,272]. Fuoss and Hsia [273,274] further modified the original Fuoss-Onsager equation who recalculated the relaxation field, retaining the terms which had previously been neglected.

The results of conductance theories can be expressed in a general form:

$$\Lambda = \frac{\Lambda_o - \alpha\Lambda_o\sqrt{c}}{(1 + \kappa\alpha)} \left(\frac{1 + \kappa\alpha}{\sqrt{2}} \right) - \frac{\beta\sqrt{c}}{(1 + \kappa\alpha)} + G(\kappa\alpha) \quad (\text{II. 52})$$

Where $G(\kappa\alpha)$ is a complicated function of the variable. The simplified form:

$$\Lambda = \Lambda_o - S\sqrt{c} + Ec \ln c + J_1c + J_2\sqrt[3]{c} \quad (\text{II. 53})$$

However, it has been found that these equations have certain limitations, in some cases it fails to fit experimental data. Some of these results have been discussed elaborately by Fernandez-Prini [275]. Further correction of the equation (II. 53) was made by Fuoss and Accascin. They took into consideration the change in the viscosity of the solutions and assumed the validity of Walden's rule. The new equation becomes:

$$\Lambda = \Lambda_o - S\sqrt{c} + Ec \ln c + J_1c + J_2\sqrt[3]{c} - FAc \quad (\text{II. 54})$$

Where,

$$Fc = \frac{4\pi R^3 N_A}{3} \quad (\text{II. 55})$$

In most cases, however, J_2 is made zero but this leads to a systematic deviation of the experimental data from the theoretical equations. It has been observed that Pitt's equation gives better fit to the experimental data in aqueous solutions [276].

❖ Ionic Association

The equation (II. 54) successfully represents the behavior of completely dissociated electrolytes. The plot of Λ against \sqrt{c} (limiting Onsager equation) is used to assign the dissociation or association of electrolytes. The electrolyte may be regarded as completely dissociated when positive deviation occurs ($\Lambda_{o\text{exp}} > \Lambda_{o\text{theo}}$) but if negative deviation ($\Lambda_{o\text{exp}} < \Lambda_{o\text{theo}}$) or positive deviation from the Onsager limiting tangent

$(\alpha\lambda_o + \beta)$ occurs, the electrolyte may be regarded to be associated. Here the electrostatic interactions are large so as to cause association between cations and anions. The difference in $\lambda_{o, \text{exp}}$ and $\lambda_{o, \text{theo}}$ would be considerable with increasing association [277].

Conductance measurements help us to determine the values of the ion-pair association constant, K_A for the process:



$$K_A = \frac{(1-\alpha)}{\alpha^2 c \gamma_{\pm}^2} \quad (\text{II. 57})$$

$$\alpha = 1 - \alpha^2 K_A c \gamma_{\pm}^2 \quad (\text{II. 58})$$

Where γ_{\pm} is the mean activity coefficient of the free ions at concentration αc .

For strongly associated electrolytes, the constant K_A and λ_o have been determined using Fuoss-Kraus equation [278] or Shedlovsky's equation [279].

$$\frac{T(z)}{\Lambda} = \frac{1}{\lambda_o} + \frac{K_A}{\lambda_o^2} \cdot \frac{c \gamma_{\pm}^2 \Lambda}{T(z)} \quad (\text{II. 59})$$

Where $T(z) = F(z)$ (Fuoss-Kraus method) and $1/T(z) = S(z)$ (Shedlovsky's method).

$$F(z) = 1 - z(1 - z(1 - \dots))^{\frac{1}{2}} \quad (\text{II. 96a})$$

$$\text{and} \quad \frac{1}{T(z)} = S(z) = 1 + z + \frac{z^2}{2} + \frac{z^3}{8} + \dots \quad (\text{II. 96b})$$

A plot of $T(z)/\Lambda$ against $c \gamma_{\pm}^2 \Lambda / T(z)$ should be a straight line having $1/\lambda_o$ for its intercept and K_A/λ_o^2 for its slope. The values of λ_o and K_A obtained from equation (II. 95) show uncertainty when K_A is large.

The Fuoss-Hsia [273] conductance equation for associated electrolytes is given by:

$$\Lambda = \lambda_o - S\sqrt{\alpha c} + E(\alpha c) \ln(\alpha c) + J_1(\alpha c) - J_2(\alpha c)^{\frac{3}{2}} - K_A \Lambda \gamma_{\pm}^2(\alpha c) \quad (\text{II. 60})$$

The equation was modified by Justice [280]. The conductance of symmetrical electrolytes in dilute solutions can be represented by the equations:

$$\Lambda = \alpha(\lambda_o - S\sqrt{\alpha c} + E(\alpha c) \ln(\alpha c) + J_1 R(\alpha c) - J_2 R(\alpha c)^{\frac{3}{2}}) \quad (\text{II. 61})$$

$$\frac{(1-\alpha)}{\alpha^2 c \gamma_{\pm}^2} = K_A \quad (\text{II. 62})$$

$$\ln \gamma_{\pm} = \frac{-k\sqrt{q}}{(1+kR\sqrt{\alpha c})} \quad (\text{II. 63})$$

The conductance parameters are obtained from a least square treatment after setting, $R = q = \frac{e^2}{2\varepsilon kT}$ (Bjerrum's critical distance).

According to Justice the method of fixing the J -coefficient by setting, $R = q$ clearly permits a better value of K_A to be obtained. Since the equation (II. 61) is a series expansion truncated at the $c^{3/2}$ term, it would be preferable that the resulting errors be absorbed as much as possible by J_2 rather than by K_A , whose theoretical interest is greater as it contains the information concerning short-range cation-anion interaction. From the experimental values of the association constant K_A , one can use two methods in order to determine the distance of closest approach, 'a', of two free ions to form an ion-pair. The following equation has been proposed by Fuoss [281];

$$K_A = \frac{4\pi N_A \alpha^3}{3000} \exp\left(\frac{e^2}{\alpha \varepsilon kT}\right) \quad (\text{II. 64})$$

In some cases, the magnitude of K_A was too small to permit a calculation of a . The distance parameter was finally determined from the more general equation due to Bjerrum [282].

$$K_A = \frac{4\pi N_A \alpha}{1000} \int_{r=a}^{r=q} r^2 \exp\left(\frac{z^2 e^2}{r \varepsilon kT}\right) dr \quad (\text{II. 65})$$

❖ Ion Size Parameter and Ionic Association

For plotting, equation (II. 54) can be rearranged to the 'A' function as:

$$A_1 = A + S\sqrt{c} - Ec \ln c = A_0 + J_1 c + J_2 \sqrt[3]{c} = A_0 + J_1 c \quad (\text{II. 66})$$

with J_2 term omitted.

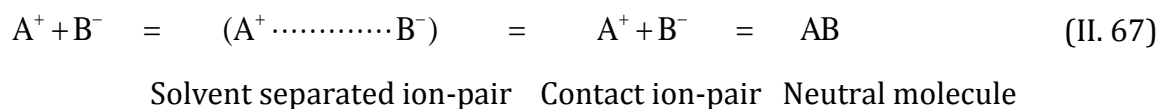
Thus, a plot of A_0 vs. c gives a straight line with A_0 as intercept and J_1 as slope and 'a' values can be calculated from J_1 values. The 'a' values obtained by this method for

DMSO were much smaller than would be expected from sums of crystallographic radii. One of the reasons attributed to it is that ion-solvent interactions are not included in the continuum theory on which the conductance equations are based. The inclusion of dielectric saturation results in an increase in 'a' values (much in conformity with the crystallographic radii) of alkali metal salts (having ions of high surface charge density) in sulpholane. The viscosity correction leads to a larger value of 'a' [283] but the agreement is still poor. However, little of real physical significance may be attached to the distance of closest approach derived from J_1 [284]. Fuoss [285] in 1975 proposed a new conductance equation. Latter he subsequently put forward another conductance equation in 1978 replacing the old one as suggested by Fuoss and co-workers.

He classified the ions of electrolytic solutions in one of the three categories.

- (i) Ions finding an ion of opposite charge in the first shell of nearest neighbours (contact pairs) with $r_{ij} = a$. The nearest neighbours to a contact pair are the solvent molecules forming a cage around the pairs.
- (ii) Ions with overlapping Gurney's co-spheres (solvent separated pairs). For them $r_{ij} = a + ns$, where n is generally 1 but may be 2, 3 etc.; 's' is the diameter of sphere corresponding to the average volume (actual plus free) per solvent molecule.
- (iii) Ions finding no other unpaired ion in a surrounding sphere of radius R , the diameter of the co-sphere (unpaired ions).

Thermal motions and interionic forces establish a steady state, represented by the following equilibria:



Contact pairs of ionogens may rearrange to neutral molecules $A^+B^- = AB$, e.g., H_3O^+ and CH_3COO^- . Let γ be the fraction of solute present as unpaired ($r > R$) ions. If $c\gamma$ is the concentration of unpaired ion and α is the fraction of paired ions ($r \leq R$), then the concentration of unpaired ion and $c(1-\alpha)(1-\gamma)$ and that of contact pair is $\alpha c(1-\gamma)$.

The equation constants for Eq. (II. 67) are:

$$K_R = \frac{(1-\alpha)(1-\gamma)}{c\gamma^2 f^2} \quad (\text{II. 68})$$

$$K_S = \frac{\alpha}{1-\alpha} = \exp\left(\frac{-E_S}{kT}\right) = e^{-\varepsilon} \quad (\text{II. 69})$$

Where K_R refer to the formation and separation of solvent separated pairs by diffusion in and out of spheres of diameter R around cations and can be calculated by continuum theory; K_S is the constant describing the specific short-range ion-solvent and ion-ion interactions by which contact pairs form and dissociate. E_S is the difference in energy between a pair in the states ($r = R$) and ($r = a$); ε is E_S measured in units of kT .

Now,

$$(1-\alpha) = \frac{1}{1+K_S} \quad (\text{II. 70})$$

and the conductometric pairing constant is given by:

$$K_A = \frac{(1-\alpha)}{c\gamma^2 f^2} = \frac{K_R}{1-\alpha} = K_R(1+K_S) \quad (\text{II. 71})$$

The equation determines the concentration, $c\gamma$ of active ions that produce long-range interionic effects.

The various patterns can be reproduced by theoretical fractions in the form:

$$A = p \left[A_o \left(\frac{1+\Delta X}{X} \right) + \Delta A_e \right] = p \left[A_o (1+R_X) + E_L \right] \quad (\text{II. 72})$$

Which is a three parameter equation $A = A(c, A_o, R, E_S), \Delta X / X$ (the relaxation field) and ΔA_e (the electrophoretic counter current) are long range effects due to electrostatic interionic forces and p is the fraction of Gurney co-sphere.

The parameters K_R (or E_S) is a catch-all for all short range effects:

$$p = 1 - \alpha(1 - \gamma) \quad (\text{II. 73})$$

In case of ionogens or for ionophores in solvents of low dielectric constant, α is very near to unity ($-E_S/kT \gg 1$) and the equation becomes:

$$A = \gamma \left[A_o \left(\frac{1+\Delta X}{X} \right) \right] + \Delta A_e \quad (\text{II. 74})$$

The equilibrium constant for the effective reaction, $A^+ + B^- + AB$, is then

$$K_A = \frac{(1-\gamma)}{c\gamma^2 f^2} \approx K_R K_S \quad (\text{II. 75})$$

as $K_S \gg 1$. The parameters and the variables are related by the set of equations:

$$\gamma = 1 - \frac{K_R c \gamma^2 f^2}{(1-\alpha)} \quad (\text{II. 76})$$

$$K_R = \left(\frac{4\pi N_A R^3}{3000} \right) \exp\left(\frac{\beta}{R} \right) \quad (\text{II. 77})$$

$$-\ln f = \frac{\beta\kappa}{2(1+\kappa R)}, \quad \beta = \frac{e^2}{\epsilon\kappa T} \quad (\text{II. 78})$$

$$\kappa^2 = 8\pi\beta\gamma\eta = \frac{\pi\beta N_A \gamma c}{125} \quad (\text{II. 79})$$

$$-\varepsilon = \ln \left[\frac{\alpha}{1-\alpha} \right] \quad (\text{II. 80})$$

The details of the calculations are presented in the 1978 paper [285]. The shortcomings of the previous equations have been rectified in the present equation that is also more general than the previous equations and can be used for higher concentrations (0.1 N in aqueous solutions).

❖ *Extension of Fuoss Conductance Equation*

As Fuoss 1978 conductance equation contained a boundary condition error [286,287], Fuoss introduced a slight modification to his model [288,289]. According to him, the ion pairs (ion approaching with their Gurney co-sphere) are divided into two categories- contact pairs (with no contribution to conductance) and solvent separated ion pairs (which can only contribute to the net transfer of charge). To rectify the boundary errors contained in Fuoss 1978 conductance equation, Lee-Wheaton [290(a)] in the same year described in the derivation of a new conductance equation, based on the Gurney co-sphere model and henceforth the new equation is referred to as the Lee-Wheaton equation [290(b)]. The conductance data were analyzed by means of the Lee-Wheaton conductance equation [291] in the form:

$$\Lambda = \alpha_i \left[\Lambda_o \left\{ 1 + C_1 \beta \kappa + C_2 (\beta \kappa)^2 + C_3 (\beta \kappa)^3 \right\} - \frac{\rho \kappa}{1 + \kappa R} \left\{ 1 + C_4 \beta \kappa + C_5 (\beta \kappa)^2 + \frac{\kappa R}{12} \right\} \right] \quad (\text{II. 81})$$

The mass action law association [292] is

$$K_{A,c} = \frac{(1 - \alpha_i) \gamma_A}{\alpha_i^2 c_i \gamma_{\pm}^2} \quad (\text{II. 82})$$

and the equation for the mean ionic activity coefficient:

$$\gamma_{\pm} = \exp \left[- \frac{q \kappa}{1 + \kappa R} \right] \quad (\text{II. 83})$$

Where C_1 to C_5 are least square fitting coefficients as described by Pethybridge and Taba [293], Λ_o is the limiting molar conductivity, $K_{A,c}$, is the association constant, α_i is the dissociation degree, q is the Bjerrum parameter and γ the activity coefficient and $\beta = 2q$. The distance parameter R is the least distance that two free ions can approach before they merge into ion pair. The Debye parameter κ , the Bjerrum parameter q and ρ are defined by the expressions [293]:

$$\kappa = 16000 \pi N_A q c_i \alpha_i \quad (\text{II. 84})$$

$$q = \frac{e^2}{8 \epsilon_o \epsilon_r \kappa T} \quad (\text{II. 85})$$

$$\rho = \frac{F e}{299.79 \times 3 \pi \eta} \quad (\text{II. 86})$$

Where the symbols have their usual significance [294].

The equation (II. 78) was resolved by an iterative procedure. For a definite R value the initial value of Λ_o and $K_{A,c}$, were obtained by the Kraus-Bray method [295]. The parameter Λ_o and $K_{A,c}$, were made to approach gradually their best values by a sequence of alternating linearization and least squares optimizations by the Gauss-Siedel method [296] until satisfying the criterion for convergence. The best value of a parameter is the one when equation (II. 78) is best fitted to the experimental data corresponding to

minimum standard deviation (σ_A) for a sequence of predetermined R value and standard deviation (σ_A) was calculated by the following equation:

$$\sigma_A^2 = \sum_{i=1}^n \frac{[A_{i(calc)} - A_{i(obs)}]^2}{n - m} \quad (\text{II. 87})$$

Where n is the number of experimental points and m is the number of fitting parameters. The conductance data were analyzed by fixing the distance of closest approach R with two parameter fit ($m=2$). For the electrolytes with no significant minima observed in the σ_A versus R curves, the R values were arbitrarily preset at the centre to centre distance of solvent-separated pair:

$$R = a + d \quad (\text{II. 88})$$

where $a = r_c^+ + r_c^-$, i.e., the sum of the crystallographic radii of the cation and anion and d is the average distance corresponding to the side of a cell occupied by a solvent molecule. The definitions of d and related terms are described in the literature [297]. R was generally varied by a step 0.1 Å and the iterative process was continued with equation (78).

❖ Limiting Ionic Conductance

The limiting ionic conductance of an electrolyte can be easily determined from the theoretical equations and experimental observations. At infinite dilutions, the motion of an ion is limited solely by the interactions with the surroundings solvent molecules as the ions are infinitely apart. Under these conditions, the validity of Kohlrausch's law of independent migration of ions is almost axiomatic. Thus:

$$\Lambda_0 = \lambda_o^+ + \lambda_o^- \quad (\text{II. 89a})$$

At present, limiting ionic conductance is the only function which can be divided into ionic components using experimentally determined transport number of ions, i.e.

$$\lambda_o^+ = t_+ \Lambda_0 \quad \text{and} \quad \lambda_o^- = t_- \Lambda_0 \quad (\text{II. 89b})$$

Thus, from accurate value of λ_o of ions it is possible to separate the contributions due to cations and anions in the solute-solvent interactions. However, accurate transference number determinations are limited to few solvents only.

In the absence of experimentally measured transference numbers it would be useful to develop indirect methods to obtain the ionic limiting equivalent conductances in solvents for which experimental transference numbers are not yet available.

The method has been summarized by Krumgalz [298] and some important points are mentioned as follows:

(i) Walden equation [299]

$$(\lambda_o^\pm)^{25}_{\text{water}} \cdot \eta_{o,\text{water}} = (\lambda_o^\pm)^{25}_{\text{acetone}} \cdot \eta_{o,\text{acetone}} \quad (\text{II. 90})$$

(ii) $(\lambda_{o,\text{pic}} \cdot \eta_o) = 0.267$, $\lambda_{o,\text{Et}_4\text{N}^+} \cdot \eta_o = 0.269$ [299,300] (II.91)

$$\text{based on } \Lambda_{o,\text{Et}_4\text{N}_{\text{pic}}} = 0.563$$

Walden considered the products to be independent of temperature and solvent. However, the $\Lambda_{o,\text{Et}_4\text{N}_{\text{pic}}}$ values used by Walden were found to differ considerably from the data of subsequent more precise studies and the values of (ii) are considerably different for different solvents.

(iii) $\lambda_o^{25}(\text{Bu}_4\text{N}^+) = \lambda_o^{25}(\text{Ph}_4\text{B}^-)$ (II. 92)

The equality holds good in nitrobenzene and in mixture with CCl_4 but not realized in methanol, acetonitrile and nitromethane.

(iv) $\lambda_o^{25}(\text{Bu}_4\text{N}^+) = \lambda_o^{25}(\text{Bu}_4\text{B}^-)$ [301] (II. 93)

The method appears to be sound as the negative charge on boron in the Bu_4B^- ion is completely shielded by four inert butyl groups as in the Bu_4N^+ ion while this phenomenon was not observed in case of Ph_4B^- .

(v) The equation suggested by Gill [302] is:

$$\lambda_o^{25}(R_4N^+) = \frac{zF^2}{6\pi N_A \eta_o [r_i - (0.0103\epsilon_o + r_y)]} \quad (\text{II. 94})$$

Where Z and r_i are the charge and crystallographic radius of proper ion, respectively; η_o and ϵ_o are solvent viscosity and dielectric constant of the medium, respectively; r_y = adjustable parameter taken equal to 0.85 Å and 1.13 Å for dipolar non-associated solvents and for hydrogen bonded and other associated solvents respectively.

However, large discrepancies were observed between the experimental and calculated values [298(a)]. In a paper [298(b)], Krumgalz examined the Gill's approach more critically using conductance data in many solvents and found the method reliable in three solvents e.g. butan-1-ol, acetonitrile and nitromethane.

$$(vi) \quad \lambda_o^{25} [(i-Am)_3 BuN^+] = \lambda_o^{25} (Ph_4B^-) \quad (II. 95)$$

It has been found from transference number measurements that the $\lambda_o^{25} [(i-Am)_3 BuN^+]$ and $\lambda_o^{25} (Ph_4B^-)$ values differ from one another by 1%.

$$(vii) \quad \lambda_o^{25} (Ph_4B^-) = 1.01 \lambda_o^{25} [(i-Am)_4 B^-] \quad (II. 96)$$

Krumgalz suggested a method for determining the limiting ion conductance in organic solvents. Large tetraalkyl (aryl) onium ions are not solvated in organic solvents as there is extremely weak electrostatic interactions between solvent molecules and the large ions having low surface charge density and this phenomenon can be utilized as a suitable model for distributing Λ_o values into ionic components for non-aqueous electrolytic solutions.

Considering the motion of solvated ion in an electrostatic field as a whole, it is possible to calculate the radius of the moving particle by the Stokes equation:

$$r_s = \frac{|z|F^2}{A\pi\eta_o\lambda_o^\pm} \quad (II. 97)$$

Where A is a coefficient varying from 6 (in the case of perfect sticking) to 4 (in case of perfect slipping). Since the r_s values, the real dimension of the non-solvated tetraalkyl (aryl) onium ions must be constant, we have:

$$\lambda_o^\pm \eta_o = \text{constant} \quad (II. 98)$$

This relation has been verified using λ_o^\pm values determined with precise transference numbers. The relationship can be well utilized to determine λ_o^\pm of ions in other organic solvents from the determined Λ_o values

❖ *Solvation*

Several types of interactions exist between the ions in solutions. Due to this types of interactions solvent molecules orient themselves towards the ion. The number of solvent molecules that are involved in the solvation of the ion is called *solvation number*. If the solvent is water, this is called *hydration number*. Solvation region can be classified as primary and secondary solvation regions. Here we are concerned with the primary solvation region. The primary solvation number is defined as the number of solvent molecules which surrender their own translational freedom and remain with the ion, tightly bound, as it moves around, or the number of solvent molecules which are aligned in the force field of the ion.

If the limiting conductance of the ion i of charge Z_i is known, the effective radius of the solvated ion can be determined from Stokes' law. The volume of the solvation shell is given by the equation.

$$V_s = \left(\frac{4\pi}{3}\right)(r_s^3 - r_c^3) \quad (\text{II. 99})$$

Where r_c is the crystallographic radius of the ion. The solvation number n_s would then be obtained from

$$n_s = \frac{V_s}{V_o} \quad (\text{II. 100})$$

Assuming Stokes' relation to hold well, the ionic solvated volume can be obtained, because of the packing effects [303], from

$$V_s^o = 4.35r_s^3 \quad (\text{II. 101})$$

Where V_s° is expressed in mol·lit⁻¹ and r_s in angstroms. However, this method is not applicable to ions of medium size though a number of empirical and theoretical corrections [304-307] have been suggested in order to apply it to most of the ions.

❖ *Stokes' Law and Walden's Rule*

According to Stokes' law the limiting ionic Walden product (the product of the limiting ionic conductance and solvent viscosity) for any singly charged, spherical ion is as function only of the ionic radius and thus, under normal conditions, is constant. For of a spherical ion having radius R_i with movements in a solvent of dielectric field, the limiting conductances λ_o^i can be written, according to Stokes' hydrodynamics, as

$$\lambda_o^i = \frac{|z_i e| e F}{6\pi\eta_o R_i} = \frac{0.819|z_i|}{\eta_o R_i} \quad (\text{II. 102})$$

Where η_o = macroscopic viscosity by the solvent in poise, R_i is in angstroms. If the radius R_i is assumed to be the same in every organic solvent, as would be the case, in case of bulky organic ions, we get:

$$\lambda_o^i \eta_o = \frac{0.819 z_i}{R_i} = \text{constant} \quad (\text{II. 103})$$

This is known as the Walden rule [308]. The effective radii obtained using this equation can be used to estimate the solvation numbers. However, Stokes' radii failed to give the effective size of the solvated ions for small ions.

Robinson and Stokes [309], Nightingale [251] and others [310-312] have suggested a method of correcting the radii. The tetraalkylammonium ions were assumed to be not solvated and by plotting the Stokes' radii against the crystal radii of those large ions, a calibration curve was obtained for each solvent. However, the experimental results indicate that the method is incorrect as the method is based on the wrong assumption of the invariance of Walden's product with temperature. The idea of microscopic viscosity [313] was invoked without much success [314,315] but it has been found that:

$$\lambda_o^i \eta_o = \text{constant} \quad (\text{II. 104})$$

where i is usually 0.7 for alkali metal or halide ions and $i = 1$ for the large ions [316,317] Gill [302] has pointed out the inapplicability of the Zwanzig theory [318] of dielectric friction for some ions in non-aqueous and mixed solvents and has proposed an empirical modification of Stokes' Law accounting for the dielectric friction effect quantitatively and predicts actual solvated radii of ions in solution. This equation can be written as:

$$r_i = \frac{|z|F^2}{6\pi N_A \eta_o \lambda_o^i} + 0.0103D + r_y \quad (\text{II. 105})$$

Where r_i is the actual solvated radius of the ion in solution and r_y is an empirical constant dependent on the nature of the solvent [302,318].

The dependence of Walden product on the dielectric constant led Fuoss to consider the effect of the electrostatic forces on the hydrodynamics of the system. Considering the excess frictional resistance caused by the dielectric relaxation in the solvent caused by ionic motion, Fuoss proposed the relation:

$$\lambda_o^i = \frac{Fe|z_i|}{6\pi R_\infty} \left(\frac{1+A}{\epsilon R_\infty^2} \right) \quad (\text{II. 106})$$

$$\text{or,} \quad R_i = R_\infty + \frac{R}{\infty} \quad (\text{II. 107})$$

Where R_∞ is the hydrodynamic radius of the ion in a hypothetical medium of dielectric constant where all electrostatic forces vanish and A is an empirical constant.

Boyd [305] gave the expression:

$$\lambda_o^i = \frac{Fe|z_i|}{6\pi\eta_o r_i \left[\left(1 + \frac{2}{27} \pi\eta_o \right) \cdot \left(\frac{z_i^2 e^2 \tau}{r_i^4 \epsilon_o} \right) \right]} \quad (\text{II. 108})$$

By considering the effect of dielectric relaxation in ionic motion; τ is the Debye relaxation time for the solvent dipoles. Zwanzig [306] treated the ion as a rigid sphere of radius r_i moving with a steady state viscosity, V_i through a viscous incompressible dielectric continuum. The conductance equation suggested by Zwanzig is:

$$\lambda_o^i = \frac{z_i^2 eF}{\left[A_v \pi \eta_o r_i + A_D \left\{ \frac{z_i^2 e^2 (\epsilon_r^o - \epsilon_r^\infty) \tau}{\epsilon_r^o (2\epsilon_r^o + 1) r_i^3} \right\} \right]} \quad (\text{II. 109})$$

Where ε_r^o and ε_r^∞ are the static and limiting high frequency (optical) dielectric constants. $A_v = 6$ and $A_D = 3/8$ for perfect sticking and $A_v = 4$ and $A_D = 3/4$ for perfect slipping. It has been found that Born's and Zwanzig's equations are very similar and both may be written in the form:

$$\lambda_o^i = \frac{Ar_i^3}{r_i^4 + B} \quad (\text{II. 110})$$

The theory predicts [319] that λ_o^i passes through a maximum of $27^{\frac{1}{4}}A/4B^{\frac{1}{4}}$ at $r_i = (3B)^{1/4}$. The phenomenon of maximum conductance is well known. The relationship holds good to a reasonable extent for cations in aprotic solvents but fails in case of anions. The conductance, however, falls off rather more rapidly than predicted with increasing radius. For comparison with results in different solvents, the equation (II. 109) can be rearranged as [320]:

$$\frac{z_i^2 eF}{\lambda_o^i \eta_o} = \frac{A_v \pi r_i + A_D z_i^2}{r_i^3} \cdot \frac{e^2 (\varepsilon_r^o - \varepsilon_r^\infty)}{\varepsilon_r^o (2\varepsilon_r^o + 1)} \left(\frac{\tau}{\eta_o} \right) \quad (\text{II. 111})$$

$$L^* = A_v \pi r_i + \frac{A_D z_i^2}{r_i^3 P^*} \quad (\text{II. 112})$$

In order to test Zwanzig's theory, the equation (II. 111) was applied for Me_4N^+ and Et_4N^+ in pure aprotic solvents like methanol, ethanol, acetonitrile, butanol and pentanol [319-324]. Plots of L^* against the solvent function P^* were found to be straight line. It is noted that relaxation effect is not the predominant factor affecting ionic mobility and these mobility differences could be explained quantitatively if the microscopic properties of the solvent, dipole moment and free electron pairs were considered the predominant factors in the deviation from the Stokes' law.

The Zwanzig's theory is found to be successful for bulky organic cations in aprotic media where solvation is seems to be minimum and the viscous friction predominates over that caused by dielectric relaxation. The theory breaks down whenever the dielectric relaxation term becomes large, i.e., for solvents of high P^* and for ions of small r_i . Like any continuum theory Zwanzig has the inherent weakness of its inability to account for the structural features [325], e.g.,

(i) It does not allow for any correlation in the orientation of the solvent molecules as the ion passes by and this may be the reason why the equation is not applicable to the hydrogen-bonded solvents [321].

(ii) The theory does not distinguish between positively and negatively charged ions and therefore, cannot explain why certain anions in dipolar aprotic media possess considerably higher molar concentrations than the fastest cations.

❖ **Thermodynamics of Ion-Pair Formation**

The standard Gibbs energy changes (ΔG°) for the ion- association process can be calculated from the equation

$$\Delta G^\circ = -RT \ln K_A \quad (\text{II. 113})$$

The values of the standard enthalpy change, ΔH° and the standard entropy change, ΔS° , can be evaluated from the temperature dependence of values as follows;

$$\Delta H^\circ = -T^2 \left[\frac{d(\Delta G^\circ / T)}{dT} \right]_P \quad (\text{II. 114})$$

$$\Delta S^\circ = -T^2 \left[\frac{d(\Delta G^\circ)}{dT} \right]_P \quad (\text{II. 115})$$

The values can be fitted with the help of a polynomial of the type:

$$\Delta G^\circ = c_0 + c_1(298.15 - T) + c_2(298.15 - T)^2 \quad (\text{II. 116})$$

And the coefficients of the fits can be compiled together with the σ % values of the fits. The standard values at 298.15 K are then:

$$\Delta G_{298.15}^\circ = c_0 \quad (\text{II. 117})$$

$$\Delta S_{298.15}^\circ = c_1 \quad (\text{II. 118})$$

$$\Delta H_{298.15}^\circ = c_0 + 298.15c_1 \quad (\text{II. 119})$$

The standard entropy of ion-association of electrolytes depends on

- (i) the size and shape of the ions,
- (ii) charge density on the ions,
- (iii) electrostriction of the solvent molecules around the ions,

- (iv) penetration of the solvent molecules inside the space of the ions, and the influence of these factors are discussed later.

The non-columbic part of the Gibbs energy ΔG° can also be calculated using the following equation:

$$\Delta G^\circ = N_A W_\pm \quad (\text{II. 120})$$

$$K_A = \left(\frac{4\pi N_A}{1000} \right) \int_a^R r^2 \exp\left(\frac{2q}{r} - \frac{W_\pm}{kT} \right) dr \quad (\text{II. 121})$$

Where the symbols have their usual significance. The quantity $2q/r$ is Columbic part of the interionic mean force potential and W_\pm is its non-columbic part.

❖ *Triple-Ion Formations from Electrical Conductance*

While solutions of electrolytes in solvents of high and of intermediate dielectric constant have been studied extensively, similar solutions in solvents of very low dielectric constant have not been investigated systematically. We know only that such solutions generally are poor conductors and that the equivalent conductance falls rapidly with decreasing concentration. In addition to a number of isolated observations on the conductance of solutions in benzene [326] and several series of measurements relating to the conductance of complex compounds in various solvents at relatively high concentrations [327], the literature includes two important papers by Walden and his co-workers [328], who investigated the conductance of a variety of *salts* in benzene, ether, carbon tetrachloride and similar solvents. In solvents of somewhat higher dielectric constant, the conductance passes through a minimum at moderate concentration and thereafter increases.

The influence of the dielectric constant on conductance is satisfactorily accounted for by the interionic attraction theory in solvents of high dielectric constant, it is not known to what extent interionic forces are primarily concerned in solvents of low dielectric constant. Due to the deviation of the conductometric curves from linearity in case of low dielectric constant solvents, the conductance data have been analyzed by the classical Fuoss-Kraus theory of triple-ion formation [329,330] in the form

$$\Lambda g(c)\sqrt{c} = \frac{\Lambda_0}{\sqrt{K_p}} + \frac{\Lambda_0^T K_T}{\sqrt{K_p}} \left(1 - \frac{\Lambda}{\Lambda_0}\right) c \quad (\text{II.122})$$

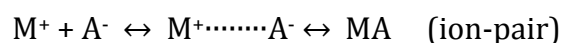
where $g(c)$ is a factor that lumps together all the intrinsic interaction terms and is defined by

$$g(c) = \frac{\exp\{-2.303 \beta' (c\Lambda)^{0.5} / \Lambda_0^{0.5}\}}{\{1 - S(c\Lambda)^{0.5} / \Lambda_0^{1.5}\} (1 - \Lambda / \Lambda_0)^{0.5}} \quad (\text{II.123})$$

$$\beta' = 1.8247 \times 10^6 / (\epsilon_r T)^{1.5} \quad (\text{II.124})$$

$$S = \alpha \Lambda_0 + \beta = \frac{0.8204 \times 10^6}{(\epsilon_r T)^{1.5}} \Lambda_0 + \frac{82.501}{\eta(\epsilon_r T)^{0.5}} \quad (\text{II.125})$$

In all the above usable equations, the Λ_0 term signify the sum of the molar conductance of the simple ions at infinite dilution, the Λ_0^T is the sum of the conductance value of the two possible formation of triple-ions. Where the constants as K_P and K_T are implies that the ion-pair and triple-ion formation constants respectively and S is the limiting Onsager coefficient. If K_P is greater than K_T , indicates the electrolytes are exists as ion-pair with a major portion and as triple-ion with a minor portion. We know that the electrostatic ionic interactions are very large due to the higher force field effect, for very low relative permittivity solvents, i.e., $\epsilon_r < 10$. Therefore the formed ion-pairs were attracted by the free movable cations or anions present in the solution medium; as the distance of the closest approach of the ions becomes minimum, these results in the formation of triple-ions, which acquires the charge of the respective ions, attracted from the solution bulk [330,331] i.e.;



Where the symbols M^+ and A^- are implies for the cation and anions respectively. The effect of ternary association [332] thus clearly explained the non-linearity of the conductometric curve. According to the consequence of this ternary association, some formative non-conducting species MA, removed from solution and replaces by triple-ions which increase the conductance values evident by non-linearity observed in conductance curves.

Additionally, the ion-pair and triple-ion concentrations, C_P and C_T , respectively, at the minimum molar concentration of the salt solution have also been calculated using the K_P and K_T value by following set of equations [330]

$$\alpha = 1 / (K_P^{1/2} \cdot C^{1/2}) \quad (\text{II.126})$$

$$\alpha_T = (K_T / K_P^{1/2}) C^{1/2} \quad (\text{II.127})$$

$$C_P = C(1 - \alpha - 3\alpha_T) \quad (\text{II.128})$$

$$C_T = (K_T / K_P^{1/2}) C^{3/2} \quad (\text{II.129})$$

At this point, the fraction of ion-pairs (α) and triple-ions (α_T), present in the salt-solutions. From the appraisal of comparison of the C_P and C_T values, if C_P is higher with respect to C_T ; indicates the major portion of ions are present as ion-pair even at high concentration and a small fraction exist as triple-ion.

Using the K_P values, the interionic distance parameter a_{IP} has been calculated with the aid of the Bjerrum's theory of ionic association [332] in the form

$$K_P = \frac{4\pi N_A}{1000} \left[\frac{e^2}{\epsilon_r KT} \right]^3 Q(b) \quad (\text{II.130})$$

$$Q(b) = \int_2^b y^{-4} \exp(y) dy \quad (\text{II.131})$$

$$b = \frac{e^2}{a_{IP} \epsilon_r KT} \quad (\text{II.132})$$

The $Q(b)$ and b values have been calculated by the literature procedure [329].

The interionic distance a_{TI} for the triple ion can be calculated using the expressions [331]

$$K_T = \frac{2\pi N_A a_{IP}^3}{1000} I(b_3) \quad (\text{II.133})$$

$$b_3 = \frac{e^2}{a_{TI} \epsilon_r KT} \quad (\text{II.134})$$

$I(b_3)$ is a double integral tabulated in the literature [330] for a range of values of b_3 . Since $I(b_3)$ is a function of a_{TI} , the a_{TI} values have been calculated by an iterative computer program. These values also suggested the small fraction exist as triple-ion formation compared to the ion-pair.

❖ *Solvation Models (Some Recent Trends)*

The interactions between particles in chemistry have been based upon empirical laws- principally on Coulomb's law. This is also the basis of the attractive part of the potential energy used in the Schrödinger equation. Quantum mechanical approach for ion-water interactions was begun by Clementi in 1970. A quantum mechanical approach to solvation can provide information on the energy of the individual ion-water interactions provided it is relevant to solution chemistry, because it concerns potential energy rather than the entropic aspect of solvation. Another problem in quantum approach is the mobility of ions in solution affecting solvation number and coordination number. However, the Clementi calculations concerned stationary models and cannot have much to do with the dynamic solvation numbers. Covalent bond formation enters little into the aqueous calculations; however, with organic solvents the quantum mechanical approaches to bonding may be essential. The trend pointing to the future is thus the molecular dynamics technique. In molecular dynamic approach, a limited number of ions and molecules and Newtonian mechanics of movement of all particles in solution is concerned. The basis of such an approach is the knowledge of the intermolecular energy of interactions between a pair of particles. Computer simulation approaches may be useful in this regard and the last decade (1990-2000) witnessed some interesting trends in the development of solvation models and computer software. C.J. Cramer, D.G. Truhlar and co-workers from the University of Minnesota, U.S.A. constructed a series of solvation models (SM1-SM5 series) based on a collection of experimental free energy of solvation data, to predict and calculate the free energy of

solvation of a chemical compound [333-337]. These models are applicable to virtually any substance composed of H, C, N, O, F, P, S, Cl, Br and/or I. The only input data required are, molecular formula, geometry, refractive index, surface tension, Abraham's a (acidity parameter) and b (basicity parameter) values, and, in the latest models, the dielectric constants. The advantage of models like SM5 series is that they can be used to predict the free energy of self-solvation to better than 1 KJ/mole. These are especially useful when other methods are not available. One can also analyze factors like electrostatics, dispersion, hydrogen bonding, etc. using these tools. They are also relatively inexpensive and available in easy to use computer codes.

A. Galindo *et al.* [338,339] have developed Statistical Associating Fluid Theory for Variable Range (SAFT-VR) to model the thermodynamics and phase equilibrium of electrolytic aqueous solutions. The water molecules are modeled as hard spheres with four short-range attractive sites to account for the hydrogen-bond interactions. The electrolyte is modeled as two hard spheres of different diameter to describe the anion and cation. The Debye-Hückel and mean spherical approximations are used to describe the interactions. The relative permittivity becomes very close to unity, especially when the mean spherical approximation is used, indicating a good description of the solvent. E. Bosch *et al.* [340] of the University of Barcelona, Spain, have compared several "Preferential Solvation Models" specially for describing the polarity of dipolar hydrogen bond acceptor-cosolvent mixture.

II.6.6 Refractive Index

Optical data (refractive index, n_D) provide interesting information related to molecular interactions and structure of the solutions, as well as complementary data on practical procedures, such as concentration measurement or estimation of the extent of solvation of electrolytes/non-electrolytes in liquid systems.

The light bending property is a result of variation of the velocity with which light is transmitted. Refractive index (n_D) of liquid, changes not only with the wave length of light used but also with the temperature. Molar refractions are influenced by the arrangement of atoms in the molecule or by factors like unsaturation, ring closure etc. linear optical properties of liquids and liquid mixtures have been widely studied to obtain

information on their physical, chemical, and molecular properties. Fialkov et. al. [341,342] stated that the refractive index is an additive properties of pure components when composition is expressed in terms of volume fraction. Several researchers have estimated the refractivity of liquid systems using the well known mixing rules viz. Arago-Biot, Newton, Heller, Gladstone-Dale, Eyring-John, Eykman, Lorentz-Lorenz, Weiner and Oster relations [343-346]. These empirical approaches for calculating the excess properties attempt to explain the non-ideality in terms of specific and non-specific intermolecular interactions. Refractive index or refractivity is a property of intrinsic interest in the fields of pharmaceutical research such as formulation of eye preparations, in optoelectronic and photonic applications.

The ratio of the speed of light in a vacuum to the speed of light in another substance is defined as the index of refraction (n_D) for the substance.

$$\text{Refractive Index } (n_D) = \frac{\text{Speed of light in vacuum}}{\text{Speed of light in solution systems}}$$

Due to the change in speed of light its direction of travel also changes as it crosses a boundary from one medium into another, i.e., it is refracted. The relationship between light's speed in the two mediums (V_A and V_B), the angles of incidence ($\sin \theta_A$) and refraction ($\sin \theta_B$) and the refractive indexes of the two mediums (n_A and n_B) is shown below:

$$\frac{V_A}{V_B} = \frac{\sin \theta_A}{\sin \theta_B} = \frac{n_B}{n_A} \quad (\text{II. 135})$$

It is possible to determine the refractive index of the sample quite accurately by measuring the angle of refraction, and knowing the index of refraction of the layer that is in contact with the sample, instead of measuring speed of light.

The refractive index of mixing can be correlated by the application of a composition-dependent polynomial equation. Molar refractivity, was obtained from the Lorentz-Lorenz relation [347,348] by using, n_D experimental data according to the following expression

$$R_M = \frac{(n_D^2 - 1)}{(n_D^2 + 2)} \left(\frac{M}{\rho} \right) \quad (\text{II. 136})$$

Where M is the mean molecular weight of the mixture and ρ is the mixture density. n_D can be expressed as the following:

$$n_D = \sqrt{\frac{(2A+1)}{(1-A)}} \quad (\text{II. 137})$$

Where A is given by:

$$A = \left[\left\{ \frac{(n_1^2 - 1)}{(n_1^2 + 2)} (1/\rho_1) \right\} - \left\{ \frac{(n_1^2 - 1)}{(n_1^2 + 2)} (w_2/\rho_1) \right\} + \left\{ \frac{(n_2^2 - 1)}{(n_2^2 + 2)} (w_2/\rho_2) \right\} \rho \right] \quad (\text{II. 138})$$

Where n_1 and n_2 are the pure component refractive indices, w_j the weight fraction, ρ the mixture density, and ρ_1 and ρ_2 the pure component densities.

The molar refractivity deviation is calculated by the following expression:

$$\Delta R = R - \phi_1 R_1 - \phi_2 R_2 \quad (\text{II. 139})$$

Where ϕ_1 and ϕ_2 are volume fractions and R , R_1 , and R_2 the molar refractivity of the mixture and of the pure components, respectively.

The deviations of refractive index were used for the correlation of the binary solvent mixtures:

$$\Delta n_D = n_D - x_1 n_{D1} - x_2 n_{D2} \quad (\text{II. 140})$$

Where Δn_D is the deviation of the refractive index for this binary system and n_D , n_{D1} , and n_{D2} are the refractive index of the binary mixture, refractive index of component-1, and refractive index of component-2, respectively, 'x' is the mole fractions.

The computed deviations of refractive indices of the binary mixtures are fitted using the following Redlich-Kister expression [349].

$$\Delta n_{Dew} = w_e w_w \sum_{P=0}^S B_p (w_e w_w)^P \quad (\text{II. 141})$$

Where B_p are the adjustable parameters obtained by a least squares fitting method, w is the mass fraction, and S is the number of terms in the polynomial.

The molar refractivity is isomorphic to a volume for which the ideal behavior may be expressed in terms of mole fraction: in this case smaller deviations occur but data are more scattered because of the higher sensitivity of the expression to rounding errors in the mole fraction. For the sake of completeness, both calculations of refractivity deviation function, molar refractivity deviation was fitted to a Redlich and Kister-type expression [349] and the adjustable parameters and the relevant standard deviation σ are calculated for the expression in terms of volume fractions and in terms of mole fractions, respectively.

II.6.7 FTIR Spectroscopy

The spectroscopic study has been established by the investigation of FTIR spectroscopy. The study has been taking into account to qualitative interpreting the molecular as well as ionic association of the electrolytes in the solutions. FTIR spectroscopy is one of the most appropriate optical properties which qualitatively interpreted the nature, mode, manner of the electrolytes and non-electrolytes in the solution system, eventually it also is able to give information about the configurational structure of the solute or solvents present in the solutions.

Infrared (IR) spectroscopy is is the absorption measurement of different IR frequencies by a sample positioned in the path of an IR beam. The chemical functional groups present in the sample can be analysed by IR spectroscopy. IR spectrometers can be applicable for wide range of sample types such as gases, liquids, and solids. Hence, IR spectroscopy is found to be an important analytical technique for structural elucidation and compound identification.

Infrared radiation spans a section of the electromagnetic spectrum having wave numbers from roughly 13,000 to 10 cm^{-1} , or wavelengths from 0.78 to 1000 μm . It is bound by the red end of the visible region at high frequencies and the microwave region at low frequencies.

IR absorption positions are generally presented as either wave numbers (ν) or wavelengths (λ). Wave number defines the number of waves per unit length i.e. wave numbers are directly proportional to frequency, as well as the energy of the IR absorption. The unit of the wave number is cm^{-1} (reciprocal centimeter) in modern IR

instruments that are linear in the cm^{-1} scale. In the contrast, wavelengths are inversely proportional to frequencies and their associated energy. At present, the recommended unit of wavelength is μm (micrometers), but μ (micron) is used in some older literature. Wave numbers and wavelengths can be interconverted using the following equation:

$$\nu (\text{cm}^{-1}) = \frac{1}{\lambda (\mu\text{m})} \times 10^4 \quad (\text{II.142})$$

In the IR spectrum, wavelength or wavenumber taken as the x-axis and absorption intensity or percent transmittance as the y-axis.

Transmittance, T , is the ratio of radiant power transmitted by the sample (I) to the radiant power incident on the sample (I_0). Absorbance (A) is the logarithm to the base 10 of the reciprocal of the transmittance (T).

$$A = \log_{10}(1/T) = -\log_{10}(T) = -\log_{10}\left(\frac{I}{I_0}\right) \quad (\text{II.143})$$

The transmittance spectra offer better contrast between intensities of strong and weak bands as transmittance ranges from 0 to 100% T whereas absorbance ranges from infinity to zero.

CHAPTER-III

EXPERIMENTAL SECTION

III.1. NAME, STRUCTURE, PHYSICAL AND CHEMICAL PROPERTIES, PURIFICATION AND APPLICATIONS OF THE CHEMICALS USED IN THE RESEARCH WORK

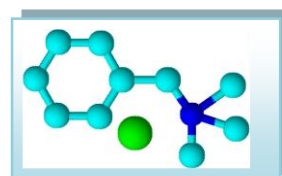
III.1.1 Ionic Liquids

➤ **Benzyltrimethylammonium chloride:**

Benzyltrimethylammonium chloride is a light yellow solid with a mild almond odor, exists as a molten solid phase (white crystalline) with the melting point 243°C.

- ❖ **Source:** Sigma Aldrich, Germany
- ❖ **Purification:** Used as purchased. The purity of the chemical is >99.0%
- ❖ **Application:**

Benzyltrimethylammonium chloride used as plating agents and surface treating agents, processing aids, not otherwise listed, surface active agents, Electrical and Electronic Products, Fabric, Textile, and Leather Products not covered elsewhere, Paints and Coatings



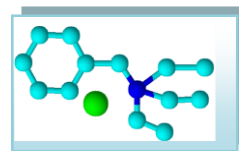
<i>Benzyltrimethylammonium chloride</i>	
<i>Appearance</i>	: White Crystalline
<i>Molecular Formula</i>	: $C_{10}H_{16}ClN$
<i>Molecular Weight</i>	: $185.695g \cdot mol^{-1}$
<i>Melting Point</i>	: $243^{\circ}C$
<i>Relative Density</i>	: 1.07

➤ **Benzyltriethylammonium chloride:**

Benzyltrimethylammonium chloride, is a quaternary ammonium salt that functions as an organic base. It is usually handled as a solution in water or methanol. The compound is colourless though the solutions often appear slightly yellowish. Commercial samples often have a distinctive fish-like odor, presumably due to the presence of trimethylamine via hydrolysis.

- ❖ **Source:** Sigma Aldrich, Germany
- ❖ **Purification:** Used as purchased. The purity of the chemical is >99.0%
- ❖ **Application:**

Benzyltriethylammonium chloride is perhaps used as phase transfer catalyst. The ionic liquid may be used in organic synthesis and bio-catalysis, dye sensitized-cells, batteries, electrochemical application and phase transfer catalyst, etc.



***Benzyltriethylammonium
chloride***

<i>Appearance</i>	: <i>White Crystalline</i>
<i>Molecular Formula</i>	: $C_{13}H_{22}ClN$
<i>Molecular Weight</i>	: $227.776 \text{ g}\cdot\text{mol}^{-1}$
<i>Relative Density</i>	: <i>No data available</i>

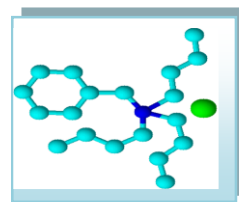
➤ ***Benzyltributylammonium chloride:***

Benzyltributylammonium chlorides are quaternary ammonium compounds. They have a central nitrogen atom which is joined to four organic radicals and one acid radical. They are prepared by treatment of an amine with an alkylating agent. They show a variety of physical, chemical, and biological properties and most compounds are soluble in water and strong electrolytes.

- ❖ **Source:** Sigma Aldrich, Germany
- ❖ **Purification:** Used as purchased. The purity of the chemical is >98.0%

❖ **Application:**

The ionic liquid *Benzyltributylammonium chloride* used for synthesis, antistatic Agent, detergent sanitisers, softner for textiles and paper products, phase transfer catalyst, antimicrobials, disinfection agents And sanitizers, Slimicidal Agents, Algaecide, Emulsifying Agents, Pigment Dispersers



***Benzyltributylammonium
chloride***

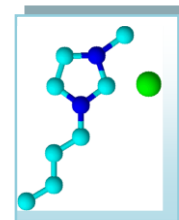
<i>Appearance</i>	: <i>White Crystalline</i>
<i>Molecular Formula</i>	: $C_{19}H_{34}ClN$
<i>Molecular Weight</i>	: $311.938 \text{ g}\cdot\text{mol}^{-1}$
<i>Melting point</i>	: $152-159 \text{ C}$

➤ **1-butyl-3-methylimidazolium chloride:**

1-butyl-3-methylimidazolium chloride anionic liquid based on imidazole chemistry.

- ❖ **Source:** Sigma Aldrich, Germany
- ❖ **Purification:** Used as purchased. The purity of the chemical is >99.0%
- ❖ **Application:**

1-butyl-3-methylimidazolium chloride is currently of interest in industry due to their ability to be infinitely recycled and their amenability to solvation at room temperature, making them excellent green solvents.



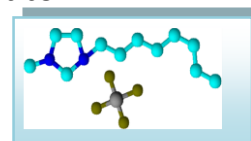
1-butyl-3-methylimidazolium chloride	
<i>Appearance</i>	: White Crystalline
<i>Molecular Formula</i>	: $C_8H_{15}ClN_2$
<i>Molecular Weight</i>	: $174.67 \text{ g}\cdot\text{mol}^{-1}$
<i>Relative Density</i>	: No data available

➤ **1-methyl-3-octylimidazolium tetrafluoroborate:**

1-methyl-3-octylimidazolium tetrafluoroborate is an imidazolium based ionic liquid, of molecular formula $C_{12}H_{23}BF_4N_2$, containing methyl, octyl group with two active nitrogen atoms in the imidazole or five member ring, exist as a molten liquid phase.

- ❖ **Source:** Sigma Aldrich, Germany
- ❖ **Purification:** Used as purchased. The purity of the chemical is >99.0%
- ❖ **Application:**

1-methyl-3-octylimidazolium tetrafluoroborate is used as solvents for polymer chemistry. The ionic liquid are good examples of neoteric solvents, new types of solvents, or older materials that are finding new applications as solvents, which is environmentally friendly (or eco-friendly) because they are less hazardous for human body as well as less toxic for living organisms, used as recyclable solvents for organic reactions and



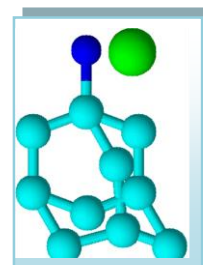
1-methyl-3-octylimidazolium tetrafluoroborate	
<i>Appearance</i>	: liquid
<i>Molecular Formula</i>	: $C_{12}H_{23}BF_4N_2$
<i>Molecular Weight</i>	: $282.13 \text{ g}\cdot\text{mol}^{-1}$
<i>Relative Density</i>	: $1.1070 \text{ g}\cdot\text{cm}^{-3}$

separation processes, lubricating fluids, heat transfer fluids for processing biomass and electrically conductive liquids as electrochemical device in the field of electrochemistry (batteries and solar cells) and so forth. In the modern technology, industry, and also in academic research field, the vast application is frequently increases.

III.1. 2 Drug Molecules

➤ **Amantadine Hydrochloride:**

Amantadine is an antiviral and an antiparkinsonian drug. This drug has U.S. Food and Drug Administration approval. 1-adamantylamine or 1-aminoadamantane contains an adamantane backbone that has an amino group which is substituted at one of the four methyne positions. One derivative of adamantane is rimantadine which has parallel biological properties.



Amantadine Hydrochloride	
<i>Appearance</i>	: white crystalline solid
<i>Molecular Formula</i>	: $C_{10}H_{18}NCl$
<i>Molecular Weight</i>	: $151.249 \text{ g}\cdot\text{mol}^{-1}$
<i>Melting Point</i>	: 273.15 K
<i>Relative Density</i>	: $1.247 \text{ g}\cdot\text{cm}^{-3}$

❖ **Source:** Sigma Aldrich, Germany

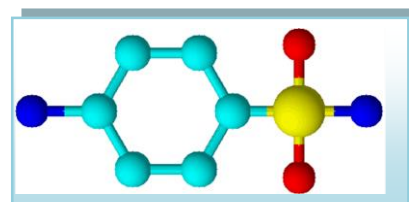
❖ **Purification:** Used as purchased. The chemical more than 95.0% pure.

❖ **Application:**

Apart from medical uses, this compound is useful as a building block in organic synthesis, allowing the insertion of an adamantyl group.

➤ **Sulphanilamide:**

Sulphanilamide (also spelled sulphanilamide) is a sulfonamide antibacterial. Chemically, it is an organic compound consisting of an aniline derivatized with a sulfonamide group.



Sulphanilamide	
<i>Appearance</i>	: Crystalline
<i>Molecular Formula</i>	: $C_6H_8N_2O_2S$
<i>Molecular Weight</i>	: $172.80 \text{ g}\cdot\text{mol}^{-1}$
<i>Melting Point</i>	: 165 C
<i>Relative Density</i>	: $1.08 \text{ g}\cdot\text{cm}^{-3}$

❖ **Source:** Sigma Aldrich, Germany

❖ **Purification:** Used as purchased. The purity of the chemical is >98.0%

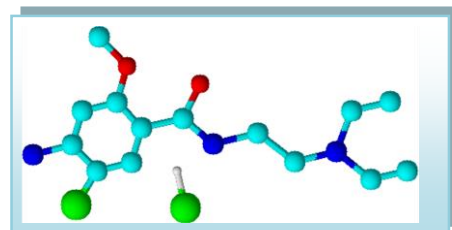
❖ **Application:**

In the World War II to Powdered sulfanilamide was used to reduce infection rates, which helped widely to reduce the mortality rate than earlier wars. Modern antibiotics are associated with supplanted sulfanilamide; however, sulfanilamide remains in use for treatment of vaginal yeast infections.

➤ **Metoclopramide Hydrochloride:**

Metoclopramide hydrochloride (MP) is a white crystalline, odorless substance, freely soluble in water. Chemically, it is 4-amino-5-chloro-N-[2-(diethylamino) ethyl]-2-methoxy benzamide monohydrochloride.

- ❖ **Source:** Sigma Aldrich, Germany
- ❖ **Purification:** Used as purchased. The purity of the chemical is >98.0%
- ❖ **Application:**



Metoclopramide Hydrochloride	
<i>Appearance</i>	:Crystalline
<i>Molecular Formula</i>	:C ₁₄ H ₂₃ Cl ₂ N ₃ O ₂
<i>Molecular Weight</i>	:299.80 g·mol ⁻¹
<i>Melting Point</i>	: 147.3 C
<i>Relative Density</i>	:1.08 g·cm ⁻³

Metoclopramide hydrochloride (MP) is used as an anti-emetic in the treatment of some forms of nausea and vomiting and to treat heartburn caused by gastroesophageal reflux in people who have used other medications without relief of symptoms. MP have a greater impact on the treatment of disorders of the gastrointestinal tract. MP is prokinetic agents in gastroenterology. Prokinetic drugs enhances the response to acetylcholine of tissue in upper gastrointestinal tract causing enhanced motility and accelerated gastric emptying without stimulating gastric, biliary, or pancreatic secretions; increases lower oesophageal sphincter tone.

III.1.3 Macrocyclic Compounds

➤ **α-Cyclodextrin (α-CD) :**

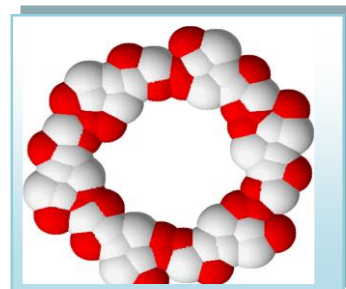
α-Cyclodextrin is a cyclic oligosaccharide composed of 6 glucose groups. This is white amorphous solid having a cylinder like molecular structure. The structural

arrangement makes it versatile in different fields. The properties are widely used in industry for various purpose.

- ❖ **Source:** Sigma Aldrich, Germany.
- ❖ **Purification:** Used as purchased. The purity is 99.98%.

❖ **Application:**

α -Cyclodextrin is a new substance which can be widely applied in production and modification of medicine, food, amino acids, vitamins and many essential substrates for animals. It can be applied widely in improving stability, solubility and good odour. In the production of medicine, it can strengthen the stability of medicine without being oxidized and resolving. On the other hand, it can improve the solubility incorporating the drug molecule inside into it. Due to its proper cavity size it is very useful in Host-Guest chemistry. It can also be used to lower the toxicity and side-effect of medicine and cover the strange and bad smell. It again improves the stability of perfume and condiment and keeps food dry or wet at will. β -CD with a cavity diameter of 4.7-5.3 Å, is of great interest because its cavity size allows for a number of substrates to fit inside it. Like other host molecules e.g., γ -cyclodextrin, calixarin, cucarbit etc. it can accommodate small molecules as guest molecules. For this reason, α -cyclodextrin is widely used as a complexing agent with hormones, vitamins, and many compounds and these are frequently used in tissue and cell culture applications. Thus α -cyclodextrin plays a vital role in the host-guest chemistry and its low cost production helps it to be versatile.

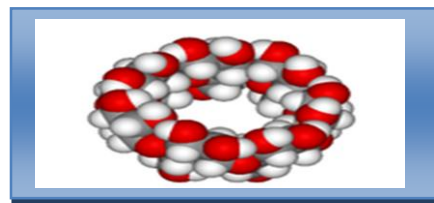


α -Cyclodextrin

<i>Appearance</i>	:Crystalline Powder
<i>Molecular Formula</i>	: $C_{42}H_{70}O_{35}$
<i>Molecular Weight</i>	:1134.98 $g \cdot mol^{-1}$
<i>Melting Point</i>	:563.15-573.15 K
<i>Boiling Point</i>	:1814.33 K
<i>Relative Density</i>	:1.44 $g \cdot cm^{-3}$ at 20°C
<i>Refractive Index</i>	:1.59 (n_D^{20})

➤ **β -Cyclodextrin (β -CD):**

β -Cyclodextrin is white amorphous solid compound composed of 7 glucose groups having a cylinder like molecular structure. The function of β -Cyclodextrin depends on its molecular structure which can be easy to integrate other materials. That feature is applied widely in industry.



- ❖ **Source:** Sigma Aldrich, Germany.
- ❖ **Purification:** Used as purchased. The purity is 99.98%.
- ❖ **Application:**

β-Cyclodextrin	
<i>Appearance</i>	:Crystalline Powder
<i>Molecular Formula</i>	: $C_{42}H_{70}O_{35}$
<i>Molecular Weight</i>	:1134.98 $g \cdot mol^{-1}$
<i>Melting Point</i>	:563.15-573.15 K
<i>Boiling Point</i>	:1814.33 K
<i>Relative Density</i>	:1.44 $g \cdot cm^{-3}$ at 20°C
<i>Refractive Index</i>	:1.59 (n_D^{20})

β -Cyclodextrin is a new stuff which can be widely applied in production of medicine and food. It can be applied widely in production of medicine, food and cosmetics, whose function is improved stability, solubility and good smelled. In the production of medicine, it can strengthen the stability of medicine without being oxidized and resolving. On the other hand, it can improve the solubility. And the effect on living of medicine, lower the toxic and side-effect of medicine and cover the strange and bad smell. In the production of food, it can mainly cover strange and bad smell of food, improve the stability of perfume and condiment and keep food dry or wet at will. β -CD with a cavity diameter of 6.4-7.5 Å, is the most interest because its cavity size allows for the best special fit for many common guest moieties. For this reason, β -cyclodextrin is most commonly used as a complexing agent in hormones, vitamins, and many compounds frequently used in tissue and cell culture applications. This capability has also been of assistance for different applications in medicines, cosmetics, food technology, pharmaceutical, and chemical industries as well as in agriculture and environmental engineering as an encapsulating agent to protect sensitive molecules in hostile environment.

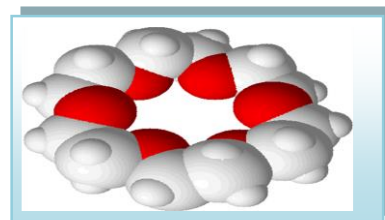
➤ **18-crown-6:**

1,4,7,10,13,16-hexaoxacyclooctadecane in short 18-Crown-6 has a molecular structure $[C_{12}H_{24}O_6]$. It is a white, hygroscopic crystalline solid with a low melting point.

- ❖ **Source:** Sigma Aldrich, Germany
- ❖ **Purification:** Used as purchased. The purity of the chemical is >98.0%
- ❖ **Application:**

18-Crown-6 binds to a variety of small cations, using all six oxygens as donor atoms.

Crown ethers are often used as phase transfer catalysts. For example, potassium permanganate dissolves in benzene In the presence of 18-crown-6, giving the so-called "purple benzene", which can be used to oxidize diverse organic compounds.



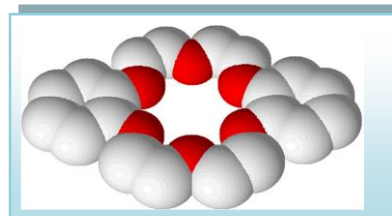
18-crown-6	
<i>Appearance</i>	:Crystalline
<i>Molecular Formula</i>	: $C_{12}H_{24}O_6$
<i>Molecular Weight</i>	: $264.315 \text{ g}\cdot\text{mol}^{-1}$
<i>Melting Point</i>	: 37 to 40 C
<i>Relative Density</i>	: $1.237 \text{ g}\cdot\text{cm}^{-3}$

➤ **Dibenzo-18-crown-6:**

Dibenzo-18-Crown-6 has strong complexing abilities and has high affinity for alkali metal cations.

- ❖ **Source:** Sigma Aldrich, Germany
- ❖ **Purification:** Used as purchased. The purity of the chemical is >98.0%
- ❖ **Application:**

Dibenzo-18-Crown-6 can be used as phase transfer catalysts for monoazaporphyrin syntheses and also used for ion transfer across membranes and as a synthon for preparation of liquid crystal polyesters.



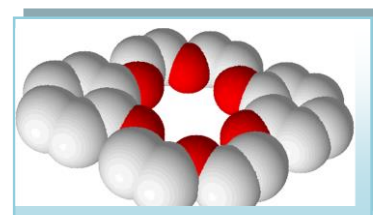
Dibenzo-18-crown-6	
<i>Appearance</i>	:hygroscopic crystalline solid
<i>Molecular Formula</i>	: $C_{20}H_{24}O_6$
<i>Molecular Weight</i>	: $360.41 \text{ g}\cdot\text{mol}^{-1}$

➤ **Dicyclo-18-crown-6:**

Dicyclo-18-Crown-6 has strong complexing abilities and has high affinity for alkali metal cations.

- ❖ **Source:** Sigma Aldrich, Germany
- ❖ **Purification:** Used as purchased. The purity of the chemical is >98.0%
- ❖ **Application:**

Dicyclo-18-Crown-6 can be used as phase transfer catalysts and also used for ion transfer across membranes.



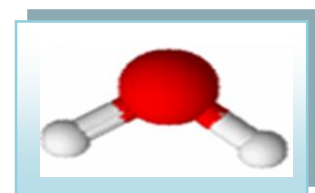
Dicyclo-18-crown-6	
<i>Appearance</i>	:hygroscopic crystalline solid
<i>Molecular Formula</i>	: $C_{20}H_{36}O_6$
<i>Molecular Weight</i>	:372.496 $g \cdot mol^{-1}$

III.1.4 Solvents

The details of the aqueous and non-aqueous solvents used in the research work are given below:

➤ **Water (H_2O):**

Water is an omnipresent chemical substance is composed of hydrogen and oxygen and is essential for all known forms of life. In typical usage, water refers only to its liquid form or state, but the substance also exists as solid state, ice, and a gaseous state, water vapour or steam. Water is a good solvent and is often referred to as the universal solvent.



- ❖ **Source:** Distilled water, distilled from fractional distillation method in Lab.

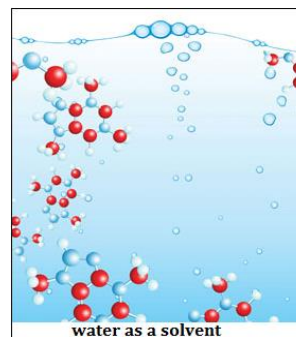
❖ **Purification:** Water was first deionised and then distilled in an all glass distilling set along with alkaline $KMnO_4$ solution to remove any organic matter therein. The doubly distilled water was finally distilled using an all glass distilling

WATER	
<i>Appearance</i>	:Liquid
<i>Molecular Formula</i>	: H_2O
<i>Molecular Weight</i>	:18.02 $g \cdot mol^{-1}$
<i>Density</i>	:0.99713 $g \cdot cm^3$
<i>Viscosity</i>	:0.891 $mP \cdot s$
<i>Refractive Index</i>	:1.3333
<i>Ultrasonic Speed</i>	:1500.0 $m \cdot s^{-1}$
<i>Dielectric Constant</i>	:78.35 at 298.15K

set. Precautions were taken to prevent contamination from CO₂ and other impurities. The triply distilled water had specific conductance less than $1 \times 10^{-6} \text{ S}\cdot\text{cm}^{-1}$.

❖ **Application:**

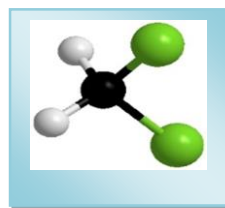
Water is widely used in chemical reactions as a solvent or reactant and less commonly as a solute or catalyst. In inorganic reactions, water is a common solvent, dissolving many ionic compounds. Supercritical water has recently been a topic of research. Oxygen saturated supercritical water combusts organic pollutants efficiently. It is also use in various industries.



It is an excellent solvent, generally called the universal solvent, due to the marked polarity and its tendency of forming hydrogen bonds with other molecules. Water is the main component of life in this earth. Not only a high percentage of living bodies, both plants and animals are found in water, all life on earth is thought to have arisen from water and the bodies of all living organisms are composed mostly of water. About 70 to 90 percent of all organic substance is water. The chemical reactions in all plants and animals that support life take place in water medium. Water not only provides the medium to make these life sustaining reactions possible, but water itself is often an important reactant or product of all these reactions. In short, the chemistry of life is nothing but the “water chemistry.”

➤ **Dichloromethane (DCM):**

Dichloromethane (DCM, or methylene chloride) is an organic compound with the formula CH₂Cl₂. This is colorless, volatile liquid with a moderately sweet smelling. This is widely used as a solvent. Although it is not miscible with water, it is miscible with many organic solvents.[10] One of the most well-known applications of dichloromethane is in the drinking bird heat engine.



Dichloromethane	
<i>Appearance</i>	: Colourless Liquid
<i>Molecular Formula</i>	: CH ₂ Cl ₂
<i>Molecular Weight</i>	: 84.93 g·mol ⁻¹
<i>Density</i>	: 1.3266g·cm ³
<i>Viscosity</i>	: 0.43mP·s
<i>Refractive Index</i>	: 1.4244
<i>Dielectric Constant</i>	: 8.93 at 298.15 K

❖ **Source:** Merck, India.

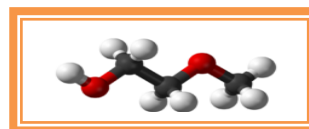
❖ **Purification:** Dichloromethane (DCM) obtained from Merck, India was used after further purification. It was distilled from P_2O_5 and then from CaH_2 in an all-glass distillation apparatus [1].

❖ **Application:**

Dichloromethane is used as a solvent for many different purposes such as DCM's volatility and ability to dissolve a wide range of organic compounds makes it a useful solvent for many chemical processes. It is widely used as a paint stripper and a degreaser. In the food industry, it has been used to decaffeinate coffee and tea as well as to prepare extracts of hops and other flavorings. Its volatility has led to its use as an aerosol spray propellant and as a blowing agent for polyurethane foams.

➤ **Acetonitrile (ACN):**

Acetonitrile is the colourless liquid and of the simplest organic nitrile. It is produced mainly as a byproduct of acrylonitrile manufacture.



❖ **Source:** Merck, India.

❖ **Purification:** Acetonitrile (ACN) obtained from Merck, India was used after further purification. It was distilled from P_2O_5 and then from CaH_2 in an all-glass distillation apparatus [1]. The middle fraction was collected. About 99% purified acetonitrile with specific conductivity $0.8 - 1.0 \times 10^{-8} \text{ S cm}^{-3}$ was obtained. The purity of the liquid was checked by measuring its density and viscosity which were in good agreement with the literature values [1,2]

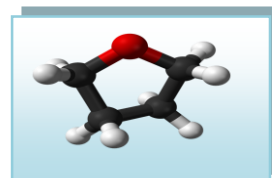
Acetonitrile	
<i>Appearance</i>	: Colourless Liquid
<i>Molecular Formula</i>	: CH_3CN
<i>Molecular Weight</i>	: $41.05 \text{ g} \cdot \text{mol}^{-1}$
<i>Density</i>	: $0.786 \text{ g} \cdot \text{cm}^3$
<i>Viscosity</i>	: $0.346 \text{ mP} \cdot \text{s}$
<i>Refractive Index</i>	: 1.3441
<i>Ultrasonic Speed</i>	: $1282.6 \text{ m} \cdot \text{s}^{-1}$
<i>Dielectric Constant</i>	: 35.95 at 298.15 K

❖ **Application:**

It is widely used in electrochemical cells industry as it has relatively high dielectric constant and the ability to dissolve electrolytes more efficiently. For similar reasons it is a popular solvent in cyclic voltammetry. Its low viscosity and low chemical reactivity make it a popular choice for liquid chromatography. Acetonitrile plays a considerable role as a solvent for manufacturing DNA oligonucleotides from its monomers. Industrially, it is used as a solvent in the purification of butadiene and in the manufacture of pharmaceuticals and photographic film. Acetonitrile is a common two-carbon building block in organic synthesis as in the production of pesticides to perfumes.

➤ **Tetrahydrofuran (THF):**

Tetrahydrofuran (THF) is an organic compound with the formula $(\text{CH}_2)_4\text{O}$. The compound is classified as heterocyclic compound, specifically a cyclic ether. It is a colorless, water-miscible organic liquid with low viscosity. THF has an odor similar to acetone. It is mainly used as a precursor to polymers. Being polar and having a wide liquid range, THF is a versatile solvent.



❖ **Source:** Merck, Indian.

❖ **Purification:** Tetrahydrofuran (THF), Merck, Indian was kept several days over potassium hydroxide (KOH), refluxed for 24 h and distilled over lithium aluminium hydride (LiAlH_4) described earlier [3]. The purified solvent had a boiling point of 339 K and a specific conductance of $0.81 \times 10^{-6} \text{ S cm}^{-3}$. The density and viscosity of the purified solvent were in good agreement with the literature data [4,5] as shown in Table IV.1. The purity of the solvent was $\geq 98.9\%$.

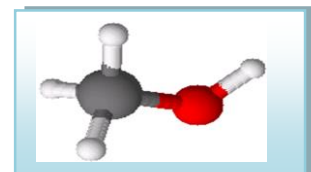
Tetrahydrofuran	
<i>Appearance</i>	: Colourless Liquid
<i>Molecular Formula</i>	: $\text{C}_4\text{H}_8\text{O}$
<i>Molecular Weight</i>	: $72.11 \text{ g}\cdot\text{mol}^{-1}$
<i>Density</i>	: $0.88074 \text{ g}\cdot\text{cm}^3$
<i>Viscosity</i>	: $0.48 \text{ mP}\cdot\text{s}$
<i>Refractive Index</i>	: 1.4072
<i>Ultrasonic Speed</i>	: $1279.0 \text{ m}\cdot\text{s}^{-1}$
<i>Dielectric Constant</i>	: 7.58 at 298.15 K

❖ **Application:**

The main application of THF is as an industrial solvent for PVC and in varnishes. It is an aprotic solvent with a moderately polar solvent and can dissolve a wide range of non-polar and polar chemical compounds. THF is a popular solvent in the laboratory when a moderately higher-boiling ethereal solvent is required and its water miscibility is not an issue. THF is often used in polymer science as dissolve polymers prior to determining their molecular mass using gel permeation chromatography, to PVC as well and thus it is the main ingredient in PVC adhesives. For liquefying old PVC cement this is widely used and often to degrease metal parts it is used industrially. THF is also used as a component in mobile phases for reversed-phase liquid chromatography.

➤ **Methanol (MeOH):**

Methanol, also known as methyl alcohol, wood alcohol, wood naphtha or wood spirits, is the simplest alcohol, and is a light, volatile, colourless, flammable, liquid with a distinctive odour that is very similar to but slightly sweeter than ethanol (drinking alcohol).



❖ **Source:** Merck, India.

❖ **Purification:** It was passed through Linde Å molecular sieves and then distilled [6].

❖ **Application:**

The largest use of methyl alcohol by far is in making other chemicals. Methanol is a traditional denaturant for ethanol, thus giving the term methylated spirit. Methanol is also used as a solvent, and as an antifreeze in pipelines. In some waste water treatment plants, a small amount of methanol is added to waste water to provide a food source of

Methanol	
<i>Appearance</i>	: Colourless Liquid
<i>Molecular Formula</i>	: CH ₄ O
<i>Molecular Weight</i>	: 32.04 g·mol ⁻¹
<i>Density</i>	: 0.7866 g·cm ³
<i>Viscosity</i>	: 0.5445 mP·s
<i>Refractive Index</i>	: 1.3284
<i>Ultrasonic Speed</i>	: 1103.0 m·s ⁻¹
<i>Dielectric Constant</i>	: 32.6 at 298.15 K

carbon for the denitrifying bacteria, which converts nitrates to nitrogen to reduce the denitrification of sensitive aquifers. Methanol is used on a limited basis to fuel internal combustion engines. Methanol is also useful as an energy carrier. It is easier to store than hydrogen, burns cleaner than fossil fuels, and is biodegradable.

III.2. EXPERIMENTAL METHODS

III.2.1 Preparation of Solutions

A stock solution for each salt was prepared by mass (digital electronic analytical balance, Mettler Toledo, AG 285, Switzerland), and the working solutions were obtained by mass dilution of the stock solution. The uncertainty of concentration (molarity or molality) of different working solutions was evaluated to be ± 0.0002 .

III.2.2 Preparation of Multicomponent Liquid Mixtures

The binary and multicomponent liquid mixtures can be prepared by any one of the methods discussed below:

(a) **Mole fraction**

(b) **Weight fraction**

(c) **Volume fraction**

(a) Mole fraction: The mole fraction (x_i) of the multicomponent liquid mixtures can be prepared using the following relation:

$$x_i = \frac{(w_i / M_i)}{\sum_{i=1}^n (w_i / M_i)}$$

Where w_i , and M_i are weight and molecular weight of i^{th} component, respectively.

The values of i depends on the number of components involved in the formation of a mixture.

(b) Weight fraction: The mole fraction (w_i) of the multicomponent liquid mixtures can be prepared using the following relation:

$$w_i = \frac{(x_i / M_i)}{\sum_{i=1}^n (x_i M_i)}$$

(c) Volume fraction: The volume fraction (ϕ_i) of the multicomponent liquid mixtures can be prepared by following employing three methods:

i. Using volume: The volume fraction (ϕ_i) of the multicomponent liquid mixtures can be prepared by following relation

$$\phi_i = \frac{V_i}{\sum_{i=1}^n V_i}$$

Where V_i , is the volume of pure liquid i .

ii. Using molar volume: The volume fraction (ϕ_i^l) of the multicomponent liquid mixtures can be prepared by following relation

$$\phi_i^l = \frac{x_i V_{mi}}{\sum_{i=1}^n (x_i V_{mi})}$$

Where V_{mi} is the molar volume of pure liquid i .

iii. Using excess volume: The volume fraction (ϕ_i^{ex}) of the multicomponent liquid mixtures can be prepared by following relation

$$\phi_i^{ex} = \frac{x_i V_i}{\sum_{i=1}^n (x_i V_i) + V^E}$$

Where V^E is the excess volume of the liquid mixture.

III.2.3 Measurements of Experimental Properties

III.2.3.1 Mass Measurement

Using digital electronic analytical balance Mettler Toledo, AG 285, Switzerland mass in different cases were measured.

It can measure mass to a very high precision and accuracy. The weighing pan of a high precision (0.0001g) is inside a transparent enclosure with doors so that

dust does not collect and so any air currents in the room do not affect the balance's operation.



Instrument Specification:

Readability	: 0.1 mg/ 0.01mg
Maximum capacity	: 210 g/81g/41g
Taring range	: 0... 210 g
Repeatability	: 0.1 mg/ 0.05 mg
Linearity	: ± 0.2 mg/ ± 0.1 mg
Stabilization time	: 3 s/ 15 s
Adjustment with external weights	: 200 g
Sensitivity	: $\pm 0.003\%$
Display	: LCD
Interface	: Local CAN universal interface
Weighing	: Φ 85 mm, stainless steel
Effective height above pan	: 240 mm
Dimensions(w/d/h)	: 205 \times 330 \times 310 mm
Net wt/with packaging	: 4.9 kg/7.25 kg

III.2.3.2 Conductivity Measurement

Conductivity measurement was done using Systronics Conductivity TDS meter-308. It is a microprocessor based instrument used for measuring specific conductivity of solutions. It can provide both automatic and manual temperature compensation.



Systronic-308 Conductivity Bridge

The conductance measurements were carried out on this conductivity bridge of accuracy $\pm 0.01\%$, using a dip-type immersion conductivity cell, CD-10 having a cell constant of approximately $(0.1 \pm 0.001) \text{ cm}^{-1}$. Measurements were made in a thermostate water bath maintained at $T = (298.15 \pm 0.01) \text{ K}$. The cell was calibrated by the method proposed by Lind et al. [7] and cell constant was measured based on 0.01 M aqueous KCl solution [8]. During the conductance measurements, cell constant was maintained within the range $1.10\text{--}1.12 \text{ cm}^{-1}$. The conductance data were reported at a frequency of 1 kHz with the accuracy of $\pm 0.3\%$. The conductivity cell was sealed to the side of a 500 cm^3 conical flask closed by a ground glass fitted with a side arm through which dry and pure nitrogen gas was passed to stop admittance of air into the cell during the addition of solvent or solution. The measurements were made in a thermostatic water bath maintained at the required temperature with an accuracy of $\pm 0.01 \text{ K}$ by means of mercury in glass thermos-regulator[9].

Instrument Specifications:

Frequency	: 100 Hz or 1 KHz Automatic
Conductivity	
Range	: 0.1 μ S to 100 mS. (6 decadic range)
Accuracy	: $\pm 1\%$ of F.S. ± 1 digit
Resolution	: 0.001 μ S
TDS	
Range	: 0.1 ppm to 100 ppt. (6 decadic range)
Accuracy	: $\pm 1\%$ of F.S. ± 1 digit
Temperature	
Range	: 0°C to 100°C (Auto/Manual)
Accuracy	: ± 0.2 °C ± 1 digit
Resolution	: 0.1 °C
Cell Constant	: Acceptable from 0.1 to 5.0
Auto Temp. Compensation	: 0°C to 100°C with PT 100 sensor
Manual Temp. Compensation	: 0°C to 60°C user selectable
Conductivity temp. Co-efficient	: 0.0% to 9.9% user selectable
Display	: 7 digits, 7 segment LEDs (3 digits for TEMP/TEMPCO 4 digits for Conductivity/TDS) With automatic decimal point selection
TDS-factor	: 0.00 to 9.99 user selectable
Printer Port	: Epson compatible 80 Column Dot Matrix
Power	: 230V AC, $\pm 10\%$, 50 Hz
Dimensions	: 250(W) \times 205(D) \times 75(H)
Weight	: 1.25 Kg (Approx.)
Accessories	: i) Conductivity cell, cell constant 0.1 ii) Conductivity cell, cell constant 1.0 iii) Temp. Probe (PT-100 sensor) iv) Stand & Clamp

Solutions were prepared by weight precise to $\pm 0.02\%$. The weights were taken on a Mettler electronic analytical balance (AG 285, Switzerland). The molarity being converted to molality as required. Several independent solutions were prepared and runs were performed to ensure the reproducibility of the results. Due correction was made for the specific conductance of the solvents at desired temperatures.

III.2.3.3 Density Measurement

The density measurement was performed with the help of Anton Paar DMA 4500M digital density-meter with a precision of $\pm 0.0005 \text{ g}\cdot\text{cm}^{-3}$.



Anton Paar DMA 4500M digital density-meter

In the digital density meter, the mechanic oscillation of the U-tube is e.g. electromagnetically transformed into an alternating voltage of the same frequency. The period τ can be measured with high resolution and stands in simple relation to the density ρ of the sample in the oscillator:

$$\rho = A \cdot \tau^2 - B \quad (\text{III.1})$$

A and B are the respective instrument constants of each oscillator. The values of A and B are determined by the calibration with the solutions of two different substances of known densities ρ_1 and ρ_2 . Modern instruments calculate and store the constants A and B after the two calibration measurements, which are mostly performed with air and water. They produce suitable values to balance various influences during the measurement, e.g., the influence of the sample's viscosity and the non-linearity caused by the measuring instrument's finite mass. The instrument was calibrated by triply-distilled water and dry air.

Instrument Specification:

Density	: 0 to 1.5 g.cm ⁻³
Temperature	: 15°C to 25°C
Pressure	: 0 to 6 bar
Repeatability Standard Deviation	
Density	: 0.00001 g.cm ⁻³
Temperature	: 0.01 °C
Additional information	
Minimum sample volume	: approx. 2 ml
Dimensions (L×W×H)	: 400×225×231 mm
Weight	: approx. 15 kg
Automatic bubble detection	: yes
Interfaces	: 2×CAN
Power	: Supplied by the master instrument

III.2.3.4 Viscosity Measurement

By Brookfield DV-III Ultra Programmable Rheometer: The viscosities (η) were measured using a Brookfield DV-III Ultra Programmable Rheometer with fitted spindle size-42. The viscosities were obtained using the following equation

$$\eta = (100 / RPM) \times TK \times \text{torque} \times SMC$$

Where, *RPM*, *TK* (0.09373) and *SMC* (0.327) are the speed, viscometer torque constant and spindle multiplier constant, respectively. The calibration of the instrument was done using the standard viscosity sample solutions supplied with the instrument, water and aqueous CaCl₂ solutions [10]. The temperature was maintained to within $\pm 0.01^\circ\text{C}$ using Brookfield Digital TC-500 thermostat bath. This instrument provides viscosity values with an accuracy of $\pm 1\%$. Each measurement was reported as an average of three separate reading with a precision of 0.3 %.



Instrument Specifications:

<i>Speed Range</i>	<i>: 0-250 RPM, 0.1 RPM increments</i>
<i>Viscosity Accuracy</i>	<i>: ±1.0% of full scale range for a specific spindle running at a specific speed.</i>
<i>Temperature sensing range</i>	<i>: -100°C to 300°C (-148°F to 572°F)</i>
<i>Temperature accuracy</i>	<i>: ±1.0°C from -100°C to 150°C ±2.0°C from +150°C to 300°C</i>
<i>Analog Torque Output</i>	<i>: 0 - 1 Volt DC (0 - 100% torque)</i>
<i>Analog Temperature Output</i>	<i>: 0 - 4 Volts DC (10mv / °C)</i>

III.2.3.5 Refractive Index Measurement

Refractive index was be measure with the help of Digital Refractometer (Mettler Toledo 30GS).

The instrument was calibrated using double-distilled water, toluene, cyclohexane, and carbon tetrachloride at defined temperature. The accuracy of the instrument is ± 0.0005 . A few drops of the sample solution were placed onto the measurement cell and the value of refractive index was taken. As refractive index is dependent on temperature, refractometer is designed to determine the temperature to produce the exact value.



Specifications-Refracto 30GS- extended RI measuring range

<i>Model</i>	: <i>Refracto 30GS</i>
<i>Measurement range</i>	: <i>1.32 -1.65</i>
<i>Resolution</i>	: <i>0.0001</i>
<i>Accuracy</i>	: <i>+/- 0.0005</i>
<i>Measurement range BRIX</i>	: <i>0 - 85 Brix%</i>
<i>Resolution</i>	: <i>0.1 Brix%</i>
<i>Accuracy</i>	: <i>+/- 0.2 Brix%</i>
<i>Temperature range</i>	: <i>10 - 40°</i>
<i>Resolution of temperature</i>	: <i>0.1°</i>
<i>display</i>	: <i>°C or °F</i>
<i>Trade Name</i>	: <i>51324660</i>

The ratio of the speed of light in a vacuum to the speed of light in another substance is defined as the index of refraction (aka refractive index or n_D) for the substance.

$$\text{Refractive index of the substance } (n_D) = \frac{\text{Speed of light in vacuum}}{\text{Speed of light in substance}} \quad (\text{III.5})$$

$$\frac{V_A}{V_B} = \frac{\sin \theta_A}{\sin \theta_B} = \frac{n_B}{n_A} \quad (\text{III.6})$$

Hence, without measuring the speed of light in a sample its index of refraction can easily be determined. Measuring the angle of refraction and refraction index of layer in contact with the sample it determines the refractive index of the sample accurately [11]. Nearly all refractometers utilize this principle, but may differ in their optical design.

Whenever light changes speed as it crosses a boundary from one medium into another its direction of travel also changes, i.e., it is refracted (Figure 1). (In the special case of the light traveling perpendicular to the boundary there is no change in direction upon entering the new medium.) The relationship between light's speed in the two mediums (v_A and v_B), the angles of incidence (θ_A) and refraction (θ_B) and the refractive indexes of the two mediums (n_A and n_B) is shown below:

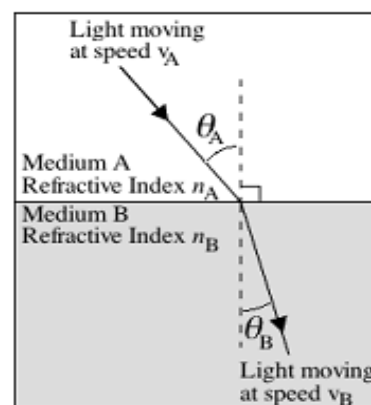


Figure 1. Light crossing from any transparent medium into another in which it has a different speed, is refracted, i.e., bent from its original path (except when the direction of travel is perpendicular to the boundary). In the case shown, the speed of light in medium A is greater than the speed of light in medium B

A light from its source is projected towards the illuminating prism with ground bottom surface that means roughened like a ground-glass joint so that each point on this surface can be regarded as producing light rays to be travelled in all directions. As in figure2 light propagating from point A to point B with largest angle of incidence (q_i) and consequently the largest possible angle of refraction (q_r) for a particular sample. Rest of the rays of light which go into the refracting prism with q_r and consequently get revealed to the left of point C. Thus, the detector positioned on the back side of the refracting prism would show a light region to the left and a dark region to the right.

III.2.3.6 Surface Tension Measurement

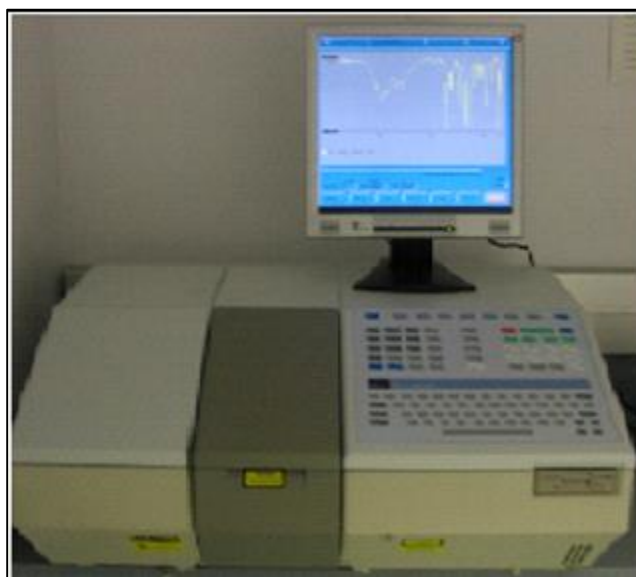
Surface tension were measured by using Digital Tensiometer KRUSS K9 (Germany). The tensiometer is a precision instrument which will only perform reliably on a solid and vibration-free base. It places the same demands on its surroundings as a laboratory balance with a resolution of 0.1 mg. In addition surface tension measurements require a clean and dust-free atmosphere as atmospheric pollutants could directly falsify the results.



III.2.4.7 FTIR Measurement

Infrared spectra were recorded in 8300 FTIR spectrometer (Shimadzu, Japan). It measures the intensity of light passing through the blank (I_0) and measures the intensity of light (I) passing through the sample.

The blank solution is identical to the sample solution only differing in the case that it does not contain the substrate which absorbs light. (In practice, instrument



measures the power rather than the intensity of the light. The power is the energy per second, which is the product of the intensity (photons per second) and the energy per photon. The experimental data is used to analyse two quantities: the transmittance (T) and the absorbance (A).

$$T = \frac{I}{I_0}; \quad A = -\log_{10} T \quad (\text{III.7})$$

The fraction of light in the original beam passing through the sample and reaches the detector is the transmittance.

III.2.4.8 UV-VIS Spectra Measurement

Compounds that absorb Ultraviolet and/or visible light have characteristic absorbance curves as a function of wavelength. Absorbance of different wavelengths of light occurs as the molecules move to higher energy states.



The UV-VIS spectrophotometer uses two light sources, a deuterium (D₂) lamp for ultraviolet light and a tungsten (W) lamp for visible light. After bouncing off a mirror, the light beam passes through a slit and hits a diffraction grating. The grating can be rotated allowing for a specific wavelength to be selected. At any specific orientation of the grating, only monochromatic (single wavelength) successfully passes through a slit. A filter is used to remove unwanted higher orders of diffraction. There is a half mirror where half of the light is reflected and the other half passes through. Before the half mirror the light beam hits a second mirror to avoid the splitting. One of the beams is allowed to pass through a reference cuvette (which contains the solvent only), the other passes through the sample cuvette. The intensities of the light beams are then measured at the end. Regarding this the Beer-Lambert law has been stated below.

Beer-Lambert Law

The change in intensity of light (dI) after passing through a sample should be proportional to the following:

- (i) Path length (b), the longer the path, more photons should be absorbed
- (ii) Concentration (c) of sample, more molecules absorbing means more photons absorbed
- (iii) Intensity of the incident light (I), more photons means more opportunity for a molecule to see a photon. Thus, dI is proportional to bcl or $dI/I = -kbc$ (where k is a proportionality constant, the negative sign is shown because this is a decrease in intensity of the light, this makes b , c and I always positive. Integration of the above equation leads to Beer-Lambert's law [12]:

$$- \ln I/I_0 = kbc \quad (\text{III.8})$$

$$- \log I/I_0 = 2.303kbc \quad (\text{III.9})$$

$$\epsilon = 2.303k \quad (\text{III.10})$$

$$A = - \log I/I_0 \quad (\text{III.11})$$

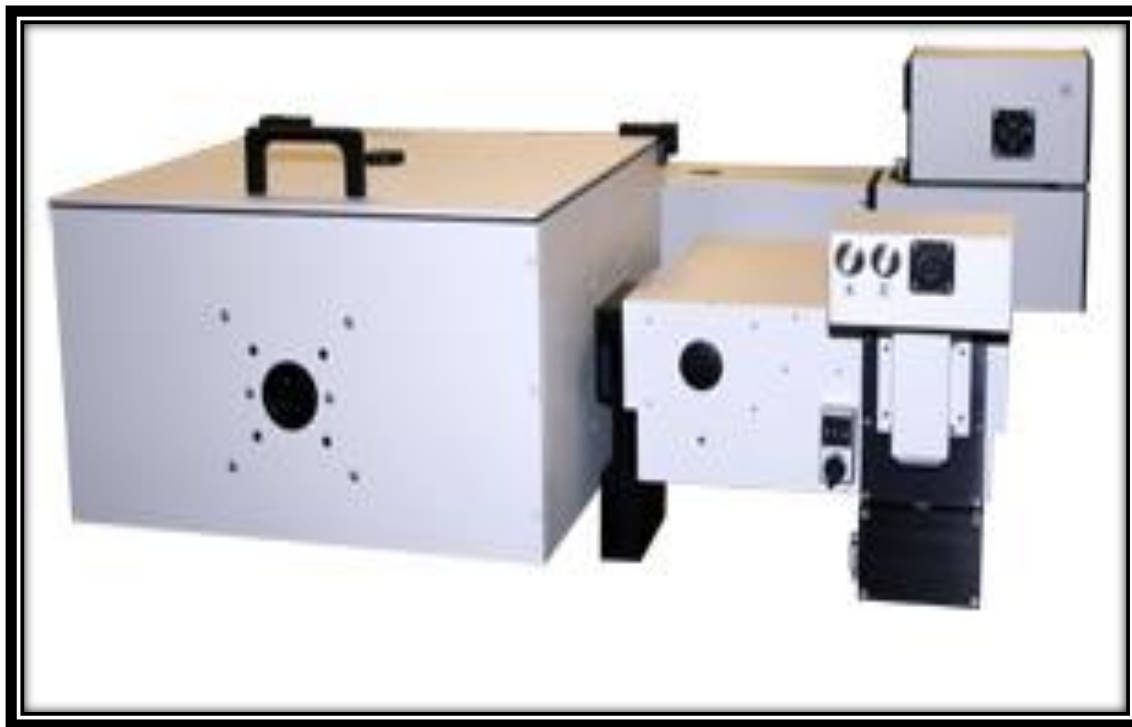
$$A = \epsilon bc \quad (\text{III.12})$$

A is defined as absorbance and it is found to be directly proportional to the path length, b and the concentration of the sample, c . The extinction coefficient is characteristic of the substance under study and of course is a function of the wavelength.

III.2.3.9 Quanta Master 40 spectrofluorometer

Fluorescence is the emission of light from a molecule resulting from a transition from one electronic state to a lower electronic state of the same multiplicity.

Detection Limit	460 attomolar fluorescein in 0.1 M NaOH
Signal to Noise Ratio	10,000:1 or better (350 nm excitation, 5 nm spectral bandpass, 1 s integration time)
Data Acquisition Rate	50,000 points/sec. to 1 point/100 sec
Inputs	4 analog (+/- 10 volts)
	2 photon counting (TTL)
	1 analog reference channel (+/- 10 volts)
	2 TTL
Outputs	2 analog (+/- 10 volts)
	2 TTL
Emission Range	185 nm to 680 nm (optional to 900 nm)
Light Source	High efficiency continuous Xenon arc lamp
Monochromators	Czerny-Turner design
Focal Length	200 mm
Excitation Grating	1200 line/mm 300 nm blaze
Emission Grating	1200 line/mm 400 nm blaze
Optional Grating	75 to 2400 line/mm and holographic models available
Bandpass	0 to 24 nm, continuously adjustable (computer control available)
Wavelength Accuracy	+/- 0.5 nm
Wavelength Resolution	0.06 nm
Detection	Photon counting/analog
System Control	Computer interface with spectroscopy software
Dimensions	38 x 30 inches



The most commonly observed fluorescence from organic molecules is caused by a transition from an excited singlet state to the ground singlet state.

Molecules have various states referred to as energy levels. Fluorescence spectroscopy is associated with electronic and vibrational states in principal. Generally, the molecules of a particular species consist of ground electronic state and an excited electronic state and a number of vibrational states within these two electronic states.

The fluorescence spectroscopy consist a number of steps. First of all the species is excited from its ground electronic state to one of the different vibrational states of higher energy. The excited molecules may collide with other molecules and lose vibrational energy until it reaches the lowest vibrational state of the ground electronic state. This process is described with a Jablonski diagram. The molecule then emits a photon to fall down to one of the various vibrational levels of the ground electronic state again. As a number of vibrational levels in the ground state are available, the emitted photons will

have frequencies. Thus the analysing of different frequencies, along with their relative intensities, the structure of the various vibrational levels can be determined.

In a typical experiment, the different wavelengths of fluorescent light emitted by a sample are measured using a monochromator, holding the excitation light at a constant wavelength. This is called an *emission spectrum*. An emission map is measured by recording the emission spectra resulting from a range of excitation wavelengths and combining them all together. This is a three dimensional surface data set: emission intensity as a function of excitation and emission wavelengths, and is typically depicted as a contour map.

The QuantaMaster 40 spectrofluorometer has widespread applications. Below are some examples:

- Protein folding/unfolding
- Anisotropy
- FRET
- Chemiluminescence
- Bioluminescence
- Semiconductor Research
- Electroluminescence Measurements
- Photovoltaic Measurements

III.2.4.10 NMR Spectra Measurement

As on the strength of the magnetic field the resolution is mainly dependent, the NMR spectrometers are designed with very strong, big and liquid helium-cooled superconducting magnet. Less expensive machines where permanent magnets are used are also available, which still give sufficient performance for certain application such as reaction monitoring and quick checking of samples but resolution is quite low.



The protons of the solvents, as most regular solvents are hydrocarbons, are NMR active. Thus, deuterium (hydrogen-2) is substituted (99+ %). Generally deuteriochloroform (CDCl_3) is used as a solvent. Apart from deuteriochloroform deuterium oxide (D_2O) and deuterated DMSO (DMSO-d_6) are also used where applicable. While recording the NMR spectra often known solvent residual proton peak was taken as the internal standard where applicable instead of adding tetramethylsilane.

NMR spectra were recorded in D_2O unless otherwise stated. ^1H NMR spectra were recorded at 300 MHz and 400 MHz using Bruker ADVANCE 300 MHz and Bruker ADVANCE 400 MHz instruments respectively at 298.15K. Signals are quoted as δ values in ppm using residual protonated solvent signals as internal standard (D_2O : δ 4.79 ppm). Data are reported as chemical shift.

➤ **Other Instruments Used:**

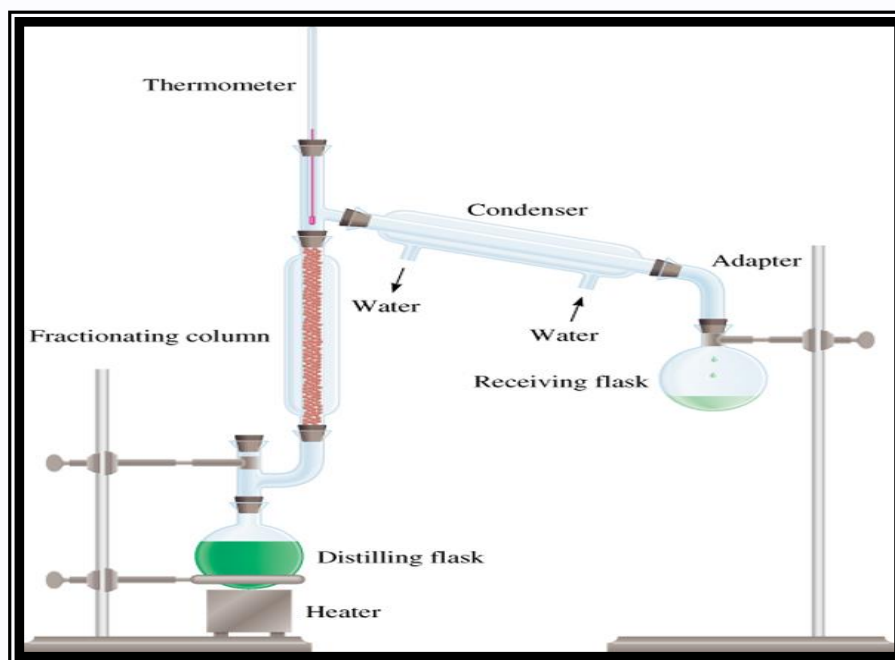
III.2.4.11 Water Distiller

Water from the natural sources is manually or automatically fed into steaming chamber of the distiller unit's. The steam arises from the steaming chamber is passed through a built-in vent to condenser where the steam gets converted into water which

then passes through and store into a container. Minerals and salts due to high boiling point remains in the boiling chamber as hard deposits or scale. The distilled water is then collected in a storage tank. If the unit is an automatic model, it is set to operate to fill the storage tank. The distillation apparatus contains a flask with heating elements embedded in glass and fused in spiral type coil internally of the bottom and tapered round glass, joints at the top double walled condenser with B-40/B-50 ground glass joints, suitable to work on 220 volts, 50 cycles AC supply.



Water distillation units produce highly treated and disinfected water for laboratory usage. The distillation process removes minerals and microbiological contaminants and can reduce levels of chemical contaminants.



Fractional Distillation Apparatus

III.2.4.12 Thermostat Water Bath (Science India, Kolkata):

Temperature was controlled using thermostatic water bath and in which the experiments were also carried out. The temperature was maintained with an accuracy of ± 0.01 K of the desired temperature.



Thermostat water bath

Laboratory water bath is a system in which a vessel containing the material to be heated is placed into or over the one containing water and to quickly heat it. These laboratory equipment supplies are available in different volumes and construction with both digital and analogue controls and greater temperature uniformity, durability, heat retention and recovery. The chambers of water bath lab products are manufactured using rugged, leak proof and highly resistant stainless steel and other lab supplies.

CHAPTER-IV

NMR, SURFACE TENSION AND CONDUCTANCE STUDY TO INVESTIGATE HOST-GUEST INCLUSION COMPLEXES OF THREE SEQUENTIAL IONIC LIQUIDS WITH β -CYCLODEXTRIN IN AQUEOUS MEDIA

IV.1. INTRODUCTION

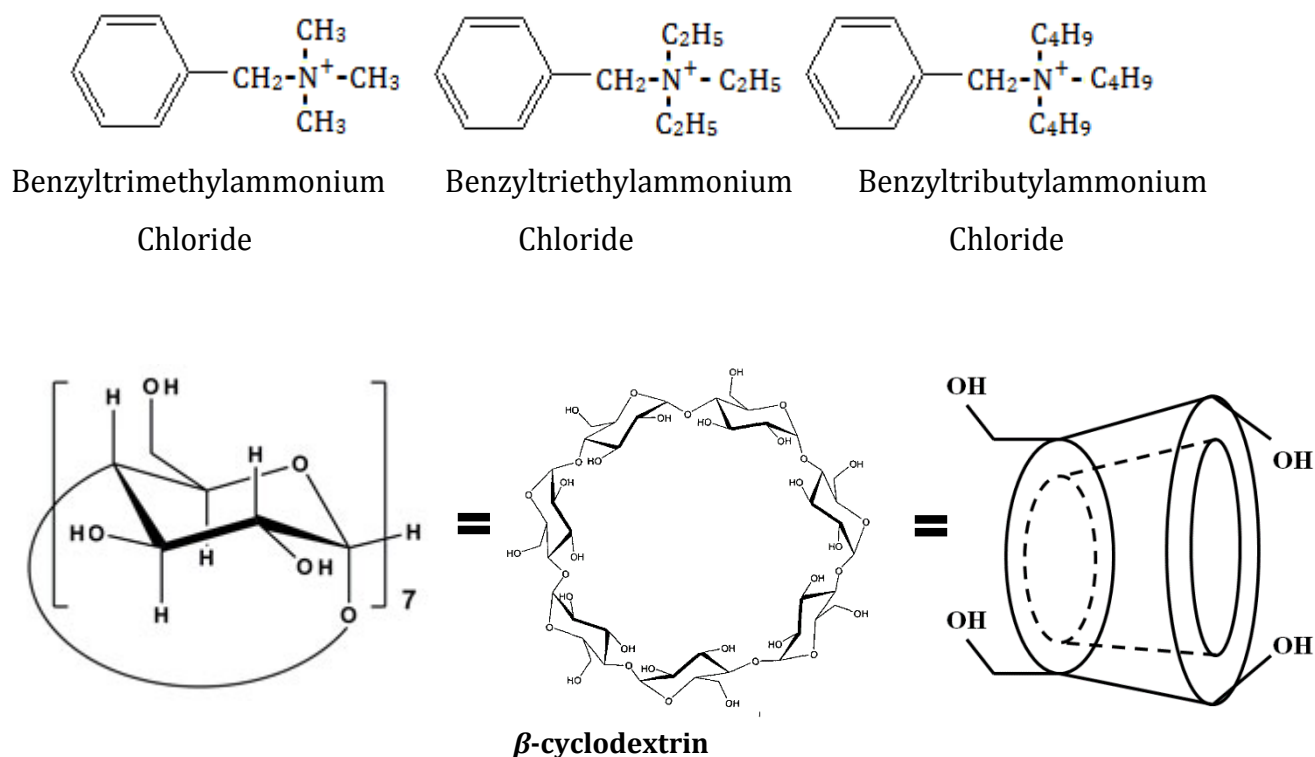
Supramolecular assembly is the association of guest molecules into the inner cavity of a host molecule by noncovalent bonds under equilibrium conditions [1]. Cyclodextrin seems to be the most promising host molecule to form inclusion complexes [2]. β -Cyclodextrin (β -CD) is a cyclic oligosaccharide (consists of seven α -D-glucopyranose units, linked by glycosidic bonds α -1,4 obtained as the main product from the enzymatic conversion of the starch [3-6]. Due to lack of free rotation about the glycosidic bond, β -CD (as the α - and γ -CDs) has a unique spatial configuration, showing a cylindrical hollow truncated cone shape; cavity with 6.0Å of width and 7.9Å of height, has a hydrophobic character, while the rims are hydrophilic: the wider one, with fourteen primary hydroxyl groups (-OH), and a narrower one with, the seven secondary OH groups (-CH₂OH) (Scheme IV.1). These structural features give all the fitting and encapsulating properties to β -CD, for forming inclusion complexes with molecules that fit into the hydrophobic cavity.

Cationic ionic liquids are the prominent surface active agents with positively charged hydrophilic head group and a hydrophobic tail group, have attracted immense interest in the development of methods for separation, purification, extraction of DNA; and also been tested for gene delivery and gene transfection that involve in current clinical trials based on gene therapy [7, 8].

The driving force of inclusion complex formation is the displacement of water molecules by more hydrophobic guest molecules present in the solution to attain an apolar-apolar association [2]. The surface active ionic liquids are form inclusion complex

with β -CD; may be applied in industries, agriculture, textile, detergent, food, cosmetics and the drug or pharmaceutical [9, 10], as antibacterial, antistatic, corrosion inhibitory, dispersants, emulsifying, wetting and solubilizing agent's etc [9, 11, 12]. In addition to these industrial applications, CDs are related to many interesting topics, such as molecular recognition and self-assembly, molecular encapsulation, chemical stabilization, and intermolecular interactions [13, 14].

However, to the best of our knowledge, no work has yet been done in as our chosen system. In this paper, size, shape, structural effect of ionic liquids in the formation of the inclusion complexes have been studied quantitatively and qualitatively to find the nature of ionic host-guest inclusion complexes of sequential cationic room temperature surface active ionic liquids, benzyltrialkylammonium chloride $[(C_6H_5CH_2)N(C_nH_{2n+1})_3]Cl$; where $n=1,2,4$] (**Scheme IV.1**) with β -cyclodextrin in aqueous media using surface tension, conductance and NMR study.



Scheme IV.1: Molecular structure of cationic surfactant and β -cyclodextrin.

IV.2. EXPERIMENTAL SECTION

IV.2.1 Reagents

The cationic surfactants benzyltrimethylammonium chloride (97%), benzyltriethylammonium chloride (99%), benzyltributylammonium chloride (98%) and β -cyclodextrin (97%) were bought from Sigma-Aldrich, Germany and used as purchased.

IV.2.2 Instrumentations

Prior to the start of the experimental work solubility of the chosen cyclodextrins in triply distilled and degassed water (with a specific conductance of $1 \times 10^{-6} \text{ S} \cdot \text{cm}^{-1}$) and title compounds *viz.*, cationic surfactant in aqueous β -cyclodextrin have been precisely checked and it was observed that the selected cationic surfactant freely soluble in all proportion of aq. β -cyclodextrins. All the stock solutions of the cationic surfactant were prepared by mass (weighed by Mettler Toledo AG-285 with uncertainty 0.0003g), and then the working solutions were obtained by mass dilution at 298.15 K .

The surface tension experiments were done by platinum ring detachment method using a Tensiometer (K9, KRÚSS; Germany) at 298.15 K . The accuracy of the measurement was within $\pm 0.1 \text{ mN} \cdot \text{m}^{-1}$. Temperature of the system has been maintained by circulating auto-thermostated water through a double-wall glass vessel containing the solution.

The conductance measurements were carried out in a Systronics-308 conductivity bridge of accuracy $\pm 0.01\%$, using a dip-type immersion conductivity cell, CD-10 having a cell constant of approximately $(0.1 \pm 0.001) \text{ cm}^{-1}$ [15]. The measurements were made in an auto-thermostated water bath maintaining the temperature at 298.15 K and using the HPLC grade water with specific conductance of $6.0 \mu\text{S m}^{-1}$. The cell was calibrated using a 0.01M aqueous KCl solution. The uncertainty in temperature was 0.01K .

NMR spectra were recorded in D_2O unless otherwise stated. ^1H NMR spectra were recorded at 400 MHz using Bruker ADVANCE 400 MHz instrument at 298.15K . Signals are quoted as δ values in ppm using residual protonated solvent signals as internal standard (D_2O : δ 4.79 ppm). Data are reported as chemical shift.

IV.3. RESULTS AND DISCUSSION

IV.3.1. Critical Micellization Concentration (CMC)

The micelle forming concentration of the three cationic room temperature ionic liquids was measured by surface tension, (γ) and molar conductivity (Λ) in aqueous media.

In **Figure IV.1** the surface tension (γ) values obtained for the cationic based ionic liquid solution is plotted as a function of the ionic liquid concentration at 298 K. Surface tension decreases with the increase of ionic liquid concentration, reach a minima (called critical micellization concentration, CMC) and the slight increase or taken as almost constant variation with further addition of ionic liquids, have disclosed no effective variation in the surface tension as expected very seriously [16]. The break point in Figure IV.1 demonstrates that the micelle starts to form at the critical micellization concentration (CMC) of $3.0 \cdot 10^{-3}$, $2.6 \cdot 10^{-3}$, and $2.0 \cdot 10^{-3}$ M (**Table IV.1**) for $[(C_6H_5CH_2)N(CH_3)_3]Cl$, $[(C_6H_5CH_2)N(C_2H_5)_3]Cl$ and $[(C_6H_5CH_2)N(C_4H_9)_3]Cl$ respectively.

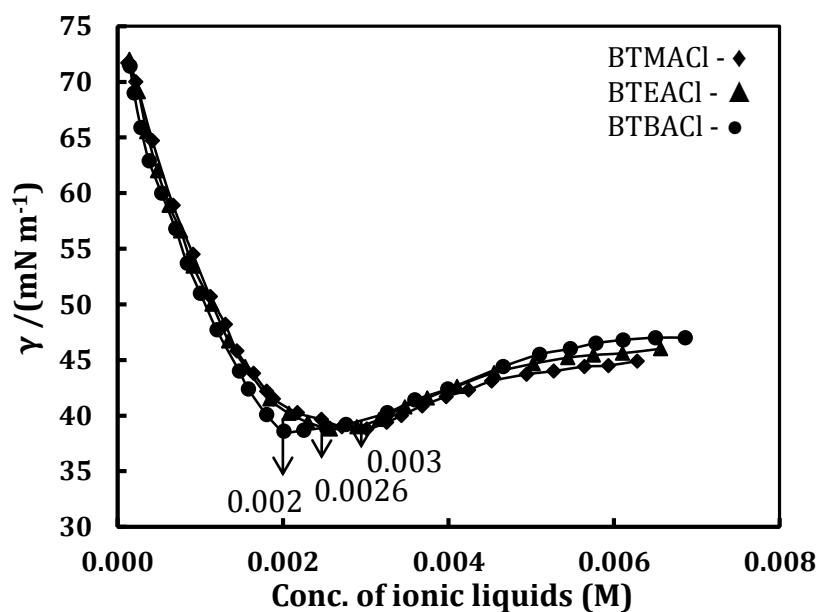


Figure IV.1: Plot of surface tension (γ) with corresponding conc. (M) of ionic liquids.

Table IV.1: Molar Conductance (Λ) and Surface tension (γ) values with corresponding concentration at the CMC and saturation point of inclusion; and concentration ratio (ratio of inclusion IL: β -CD) at the break point of the surfactants solution (0.01 M) in aqueous β -CD.

Ionic liquids	CMC (M)	Λ_{CMC} (S cm ² mol ⁻¹)	Conc. (M)	Λ (S cm ² mol ⁻¹) at break point	Conc. ratio (IL: β -CD)
[(C ₆ H ₅ CH ₂)N(CH ₃) ₃ Cl	0.0031	40.31	0.0101	11.90	1 : 1.01
[(C ₆ H ₅ CH ₂)N(C ₂ H ₅) ₃ Cl	0.0029	32.50	0.0103	11.71	1 : 1.03
[(C ₆ H ₅ CH ₂)N(C ₄ H ₉) ₃ Cl	0.0019	18.72	0.0105	12.30	1 : 1.05
Ionic liquids	CMC (M)	γ_{CMC} (mN m ⁻¹)	Conc. (M)	γ (mN m ⁻¹) at break point	Conc. ratio (IL: β -CD)
[(C ₆ H ₅ CH ₂)N(CH ₃) ₃ Cl	0.0030	39.1	0.0101	68.0	1 : 1.01
[(C ₆ H ₅ CH ₂)N(C ₂ H ₅) ₃ Cl	0.0026	38.9	0.0102	65.5	1 : 1.02
[(C ₆ H ₅ CH ₂)N(C ₄ H ₉) ₃ Cl	0.0020	38.6	0.0105	63.8	1 : 1.05

The conductance values (Λ) obtained for the cationic ionic liquid solution is also plotted as a function of the ionic liquid concentration. Conductivity increases monotonically with the increase of the ionic liquid concentration, but after a certain point (called break point) the conductance data have not vary effectively even further addition of ionic liquid. The break point (**Figure IV.2**) at the concentration of 3.1×10^{-3} , 2.9×10^{-3} , and 1.9×10^{-3} M for [(C₆H₅CH₂)N(CH₃)₃]Cl, [(C₆H₅CH₂)N(C₂H₅)₃]Cl and [(C₆H₅CH₂)N(C₄H₉)₃]Cl respectively (**Table IV.1**), demonstrates the critical micellization concentration (CMC), where, the micelles starts to form. The point is confirmed by conductance result in **Figure IV.2** where break point is also seen in good agreement with surface tension (**Figure IV.1**).

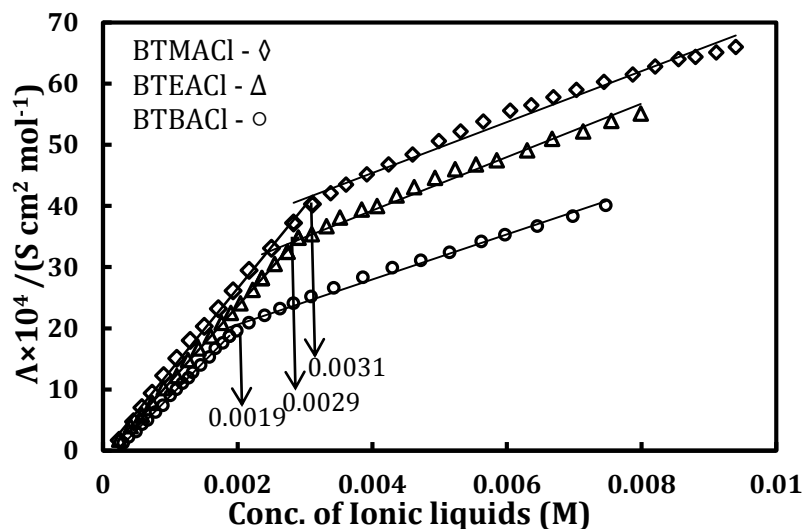


Figure IV.2: Plot of molar conductance (Λ) with corresponding conc. (M) of ionic liquids.

Table IV.2: Free energy of micellization (ΔG_{mic}) and free energy of change (ΔG) obtained from degree of micelle ionization (α) and association constant (K_a) of the solution (β -CD+ionic liquid) at 25°C evaluated from the conductance and surface tension measurement respectively.

Salt	α	ΔG_{mic} (kJ/mol)	K_a	ΔG (kJ/mol)	β	$10^6 \Gamma_{max}$ (mol m ⁻²)	A_{min} (Å ²)
$[(C_6H_5CH_2)N(CH_3)_3Cl]$	0.57	-16.29	252.25 ± 19	19.14	0.43	2.37	70.19
$[(C_6H_5CH_2)N(C_2H_5)_3Cl]$	0.54	-16.56	524.39 ± 22	18.17	0.46	2.28	72.67
$[(C_6H_5CH_2)N(C_4H_9)_3Cl]$	0.51	-16.83	136.36 ± 13	17.44	0.49	2.13	77.88

IV.3.2. Surface Tension

Surface tension (γ) measurement gives significant indication about the formation of inclusion complex as well as stoichiometry of the host-guest assembly [17-20].

Figure IV.3 illustrates the variations of surface tension (γ) of 0.01M chosen three aforesaid ionic liquids with β -CD concentration at 298 K. The surface tension curves vary linearly with an addition of β -CD concentration to a maximum, and after then surface tension data not vary effectively with further adding of β -CD into the solutions. The linear

rising surface tension data demonstrates the decreasing tendency of the surface activity of the surface active ionic liquids. This is due to the fact that ionic liquids are encapsulated insight into the cavity of the β -CD and form the inclusion complexes (ICs) and loss their surface activity. The constant variation of surface tension after saturation point, make clear that the rest surface tension is only for the aqueous solutions of β -CD or pure water; because the inclusion complexes and aqueous solution of β -CD do not possess any surface activity [21]. The stoichiometry of the inclusion complexes has been obtained from concentration ratio of the ionic liquid and β -CD (IL: β -CD) at the break point or the saturation point of the inclusion. From **Table IV.1** it has been seen that the concentration ratio of IL: β -CD is 1:1.01, 1:1.02, and 1:1.05 for $[(C_6H_5CH_2)N(CH_3)_3]Cl$, $[(C_6H_5CH_2)N(C_2H_5)_3]$ and $[(C_6H_5CH_2)N(C_4H_9)_3]Cl$ respectively, shows the 1:1 stoichiometric ratio of inclusion complex. From **Figure IV.4** it is found that the surface tension curves of the three selected ionic liquids in the presence of fixed amount (0.005M) of β -CD are higher than those in the absence of β -CD.

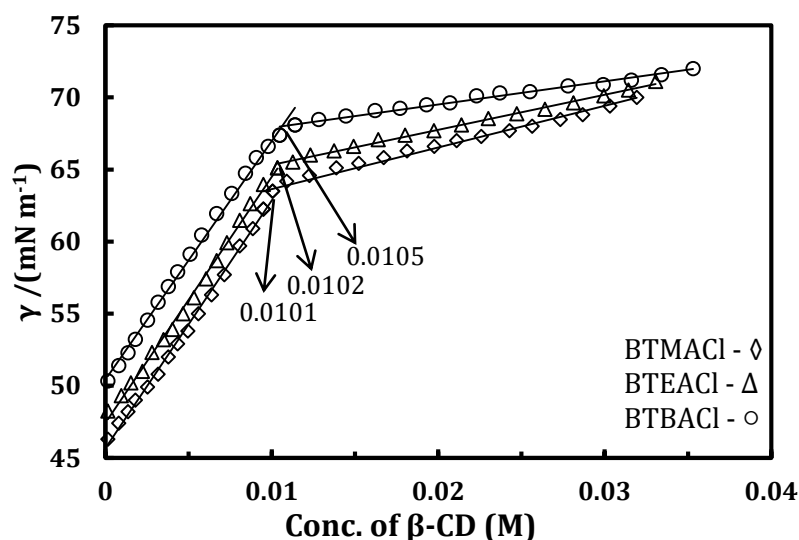


Figure IV.3: Plot of surface tension (γ) of ionic liquids (0.01M) with corresponding conc. (M) of β -CD.

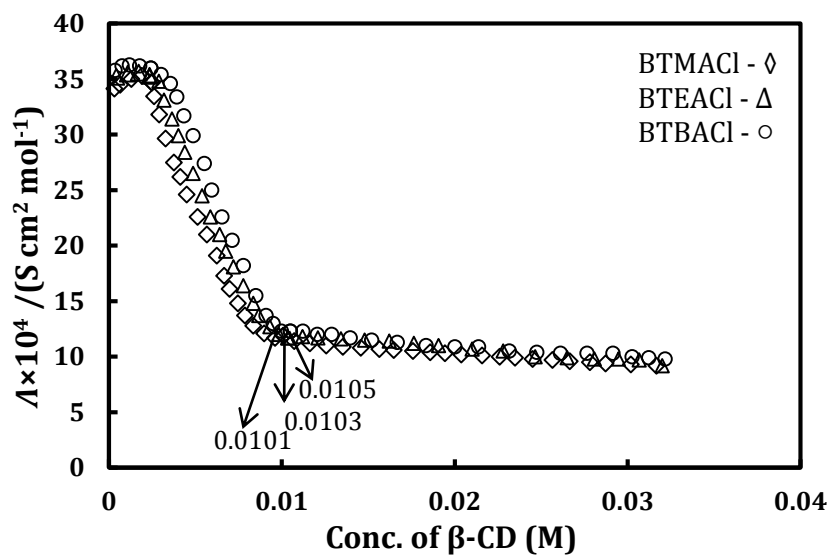


Figure IV.4: Plot of molar conductance (Λ) of ionic liquids (0.01M) with corresponding conc. (M) of β -CD.

The concentration at which surface tension of ionic liquids (for fixed 0.005M β -CD) is almost constant is called as apparent critical micelle concentrations (CMC*). The CMC* 0.00499, 0.00503, and 0.00505 for $[(C_6H_5CH_2)N(CH_3)_3Cl]$, $[(C_6H_5CH_2)N(C_2H_5)_3Cl]$ and $[(C_6H_5CH_2)N(C_4H_9)_3Cl]$ respectively, also suggested the 1:1 stoichiometric ratio of inclusion. Higher the CMC* values caused by the presence of β -CD indicates that the formation of β -CD-ionic liquid inclusion complexes decreases the micelle formation ability of the ionic liquids. The surface tension values of each ionic liquid after the CMC in the presence of β -CD remain constant as that of the absence of β -CD. This also indicates that the inclusion complexes have no surface activity and that there is little interaction between the inclusion complexes and the micelles or the free surfactants.

IV.3.3. Conductance

The shape of the curve (**Figure IV 5**) is quite similar to those generally obtained for an aqueous mixtures of ionic liquids and monomers of β -CD [22] as the concentration in β -CD cavities rises, the conductance of the mixture slightly increases, passes through a maximum, then decreases gradually, reach a minima, up to the saturation point (existence of a break in the curve) and then the change is constant even further addition

of β -CD into the solution systems. Such a behaviour denotes the formation of inclusion complexes between the ionic liquid molecules with the β -CD cavities.

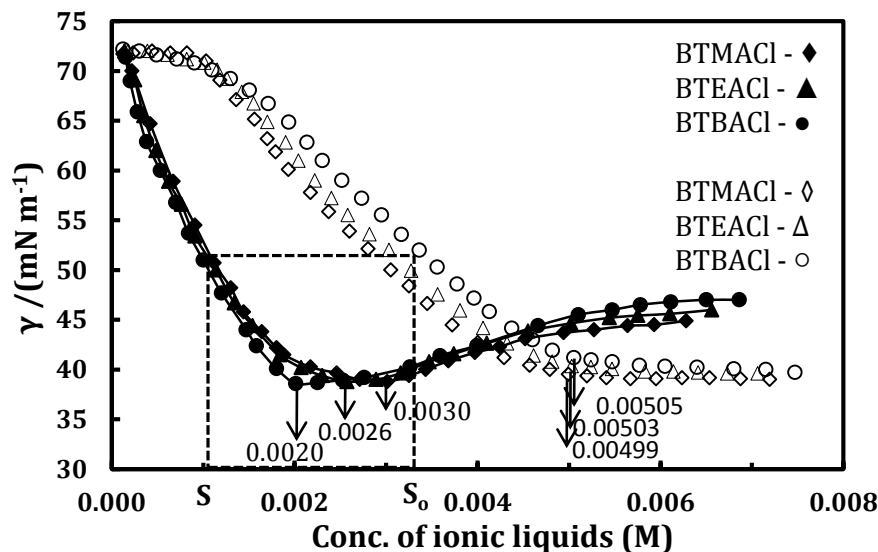
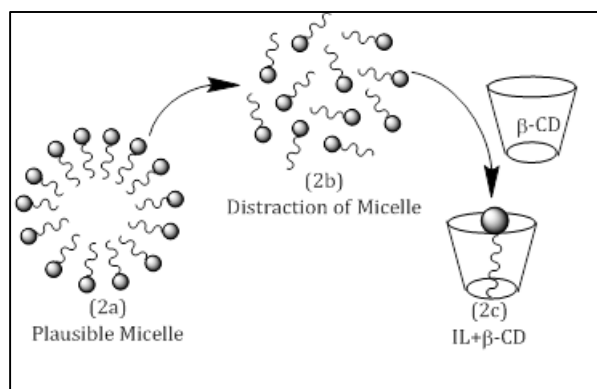


Figure IV.5: Plot of surface tension (γ) with corresponding conc. of ionic liquids in absence (solid fill) and in presence (no fill) of β -CD.

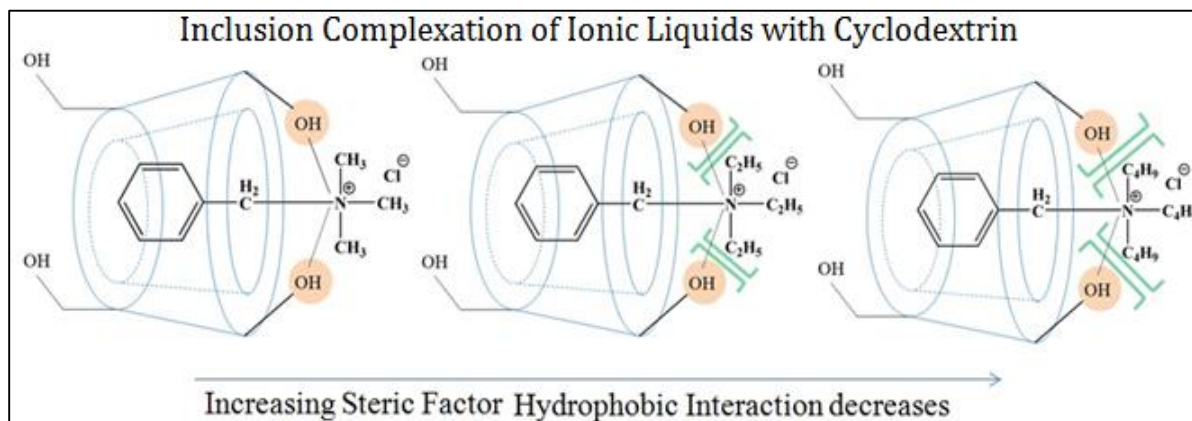
The initial increase of conductance at very low conc. of β -CD is ascribed to the progressive destruction of the micelles (**Scheme IV.2a**) of ionic liquids by inclusion of the benzyl group of ionic liquid into the β -CD cavities (i.e., the β -CD-ionic liquid interactions are stronger than those of the ionic liquid-ionic liquid interactions [23]). The destruction of the micelles is accompanied by a release of surfactant monomers and a release of counter ions initially linked to the surface of the micelles, which increases the conductance values.



Scheme IV.2: Schematic illustration of plausible micelle (2a), distraction of micelle (2b) and plausible inclusion formation (2c).

At the maximum of the conductance, micelles are supposed to have completely disappeared (**Scheme IV.2b**) and an excess of β -CD cavities reduces the quantity of free ionic liquids by formation of inclusion complexes (**Scheme IV.2c**), leading to a decrease of the conductance values. When most of the ionic liquid molecules are incorporated insight into the cyclodextrin cavities, a plateau of conductance is observed and its value is ascribed only to the charged inclusion complexes and to the counter ion Cl⁻.

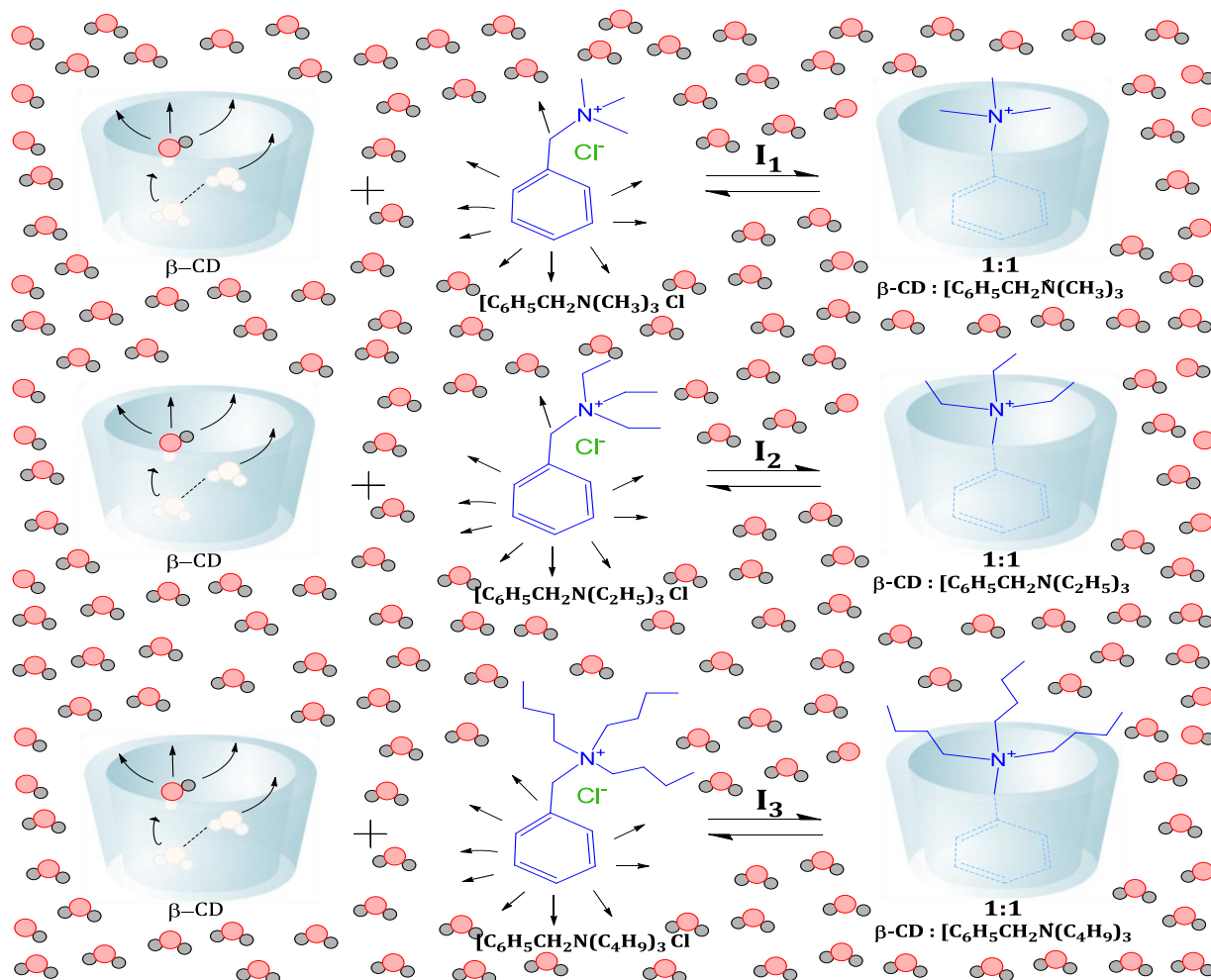
From output of the **Figure IV.5** and **Table IV.1**, the ratio of the β -CD concentration to the ionic liquid concentration at the saturation point or break point is equal to the 1.01, 1.03, and 1.05 for $[(C_6H_5CH_2)N(CH_3)_3]Cl$, $[(C_6H_5CH_2)N(C_2H_5)_3]Cl$ and $[(C_6H_5CH_2)N(C_4H_9)_3]Cl$ respectively, has showed that β -CD-ionic liquid complexes are mainly formed with a 1:1 stoichiometry, i.e., only one molecule of ionic liquid encapsulated per β -CD cavity (**Scheme IV.3**).



Scheme IV.3: Schematic representation of mechanism of formation of inclusion complexes of cationic ionic liquids with β -cyclodextrin.

In the surface tension (γ) study for the aforesaid three ionic liquids with β -CD shows single break point (**Figure IV.3**) in each γ vs. conc. curve, which clearly indicates β -CD can form 1:1 inclusion complexes with the hydrophobic benzyl moiety. The hydrophilic ammonium moiety or positive charge on the nitrogen atom remains hydrated at the outside of the cyclodextrin cavity and stabilized with oxygen atom of the

-OH group present in the rim of cyclodextrin (only in case of benzyltrimethylammonium chloride) (**Scheme IV.4**).



Scheme IV.4: Schematic representation of inclusion complexes of cationic ionic liquids with β -cyclodextrin.

IV.3.4. ^1H NMR

Inclusion of a guest molecule into the cavity of β -cyclodextrin has been studied by the upfield chemical shift of the protons of cyclodextrin molecule in ^1H NMR spectra. According to the ^1H NMR study in the molecular structure of β -cyclodextrin the H3 and H5 hydrogen's are situated inside the conical cavity, mainly, the H3 are placed near the wider rim whereas H5 are placed near the narrower rim, the other H1, H2 and H4

hydrogens are situated at the exterior of the cyclodextrin molecule (**Figure IV.6**). Since the H3 is located near the wider rim of CD, through which the guest enters, the shift is higher for it than the H5 proton [24].

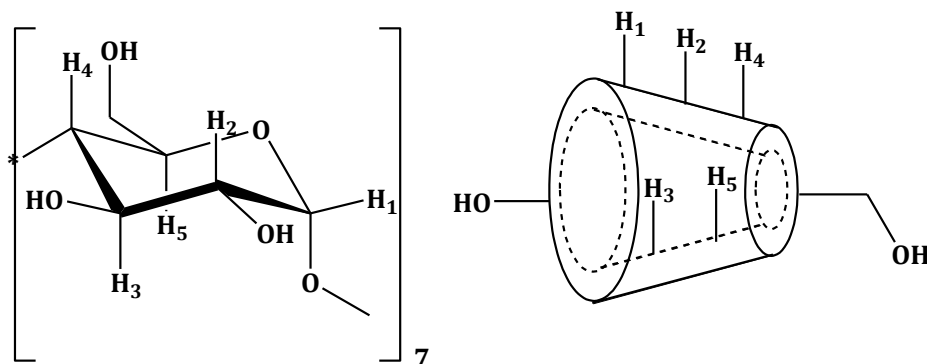


Figure IV.6: (a) Stereo-chemical configuration, (b) truncated conical structure of β -cyclodextrin with interior and exterior protons.

The other H1, H2 and H4 hydrogen's also show reasonable upfield chemical shift, but it is less compared to that of the interior protons [25-27]. Here, the inclusion phenomenon of chosen benzyltrialkylammonium chloride $[(C_6H_5CH_2)N(C_nH_{2n+1})_3]Cl$; where $n=1,2,4$] with β -CD have been studied by 1H NMR spectra by taking 1:1 molar ratio in D_2O (**Figure IV.7-9**).

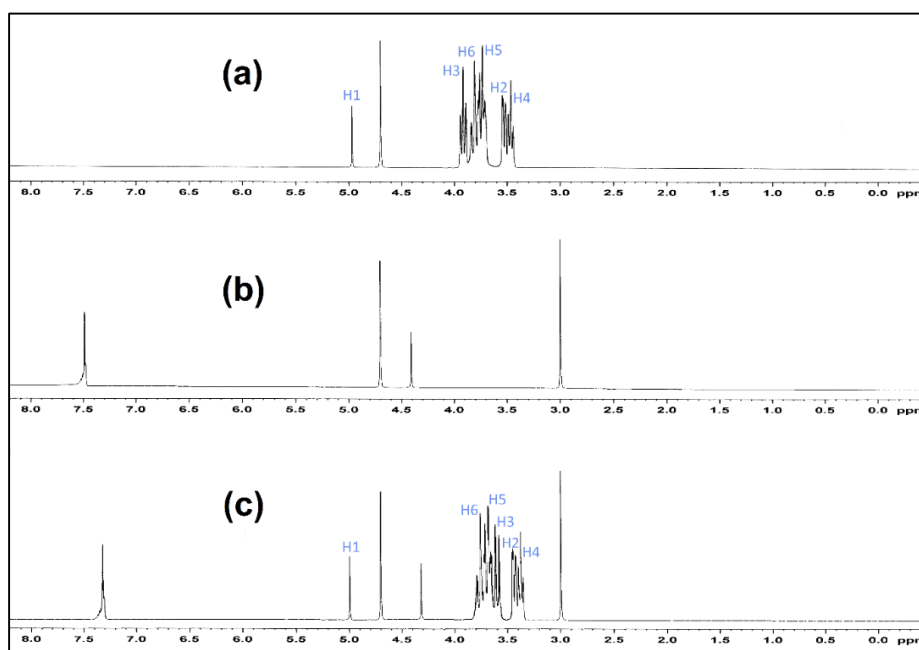


Figure IV.7: 1H NMR spectra of (a) β -CD, (b) $[(C_6H_5CH_2)N(CH_3)_3]Cl$, and (c) inclusion complex.

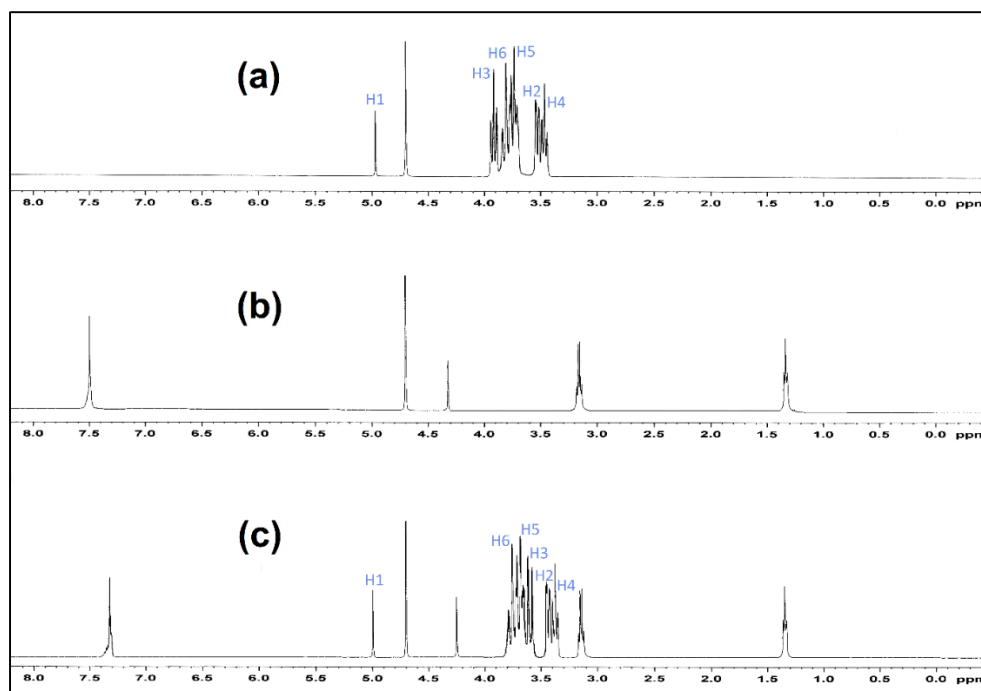


Figure IV.8: ^1H NMR spectra of (a) β -CD, (b) $[(\text{C}_6\text{H}_5\text{CH}_2)\text{N}(\text{C}_2\text{H}_5)_3]\text{Cl}$, and (c) inclusion complex.

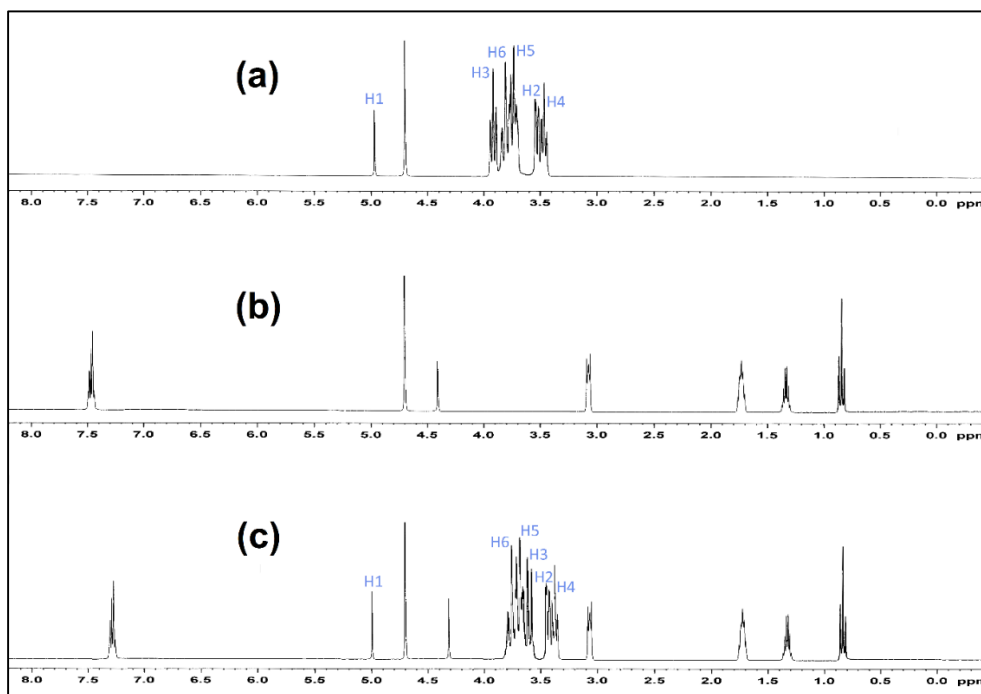


Figure IV.9: ^1H NMR spectra of (a) β -CD, (b) $[(\text{C}_6\text{H}_5\text{CH}_2)\text{N}(\text{C}_4\text{H}_9)_3]\text{Cl}$, and (c) inclusion complex.

It has been found that there are considerable upfield shifts of interior H3 and H5 protons, as well as that of the interacting protons i.e., aromatic and methylene protons of the benzyl group of benzyltrialkylammonium cations [28]. This establishes that inclusion phenomenon has occurred between the chosen ionic liquid with cavity of the β -CD molecule [29, 30].

IV.3.5. Association Constant and Other thermodynamic properties

The association constants for 1:1 inclusion complexes of β -CD and ionic liquid was determined from the surface tension measurements by using the numerical method developed by Lu et al. [21]. We have used two surface tension curves in **Figure IV.5** (with and without β -CD) to determine the value of association constant, which allows justification of the assumption made. The plot of $S_0 - [S]$ vs $\left(\frac{S_0}{[S]} - 1\right)$ shown in **Figure IV.10** gives the slope $\left(-\frac{1}{K_a}\right)$, and thus the association constants (K_a) for the inclusion complexes of β -CD-ionic liquids¹⁶ and free energy change (ΔG) are determined, and listed in **Table IV.2**.

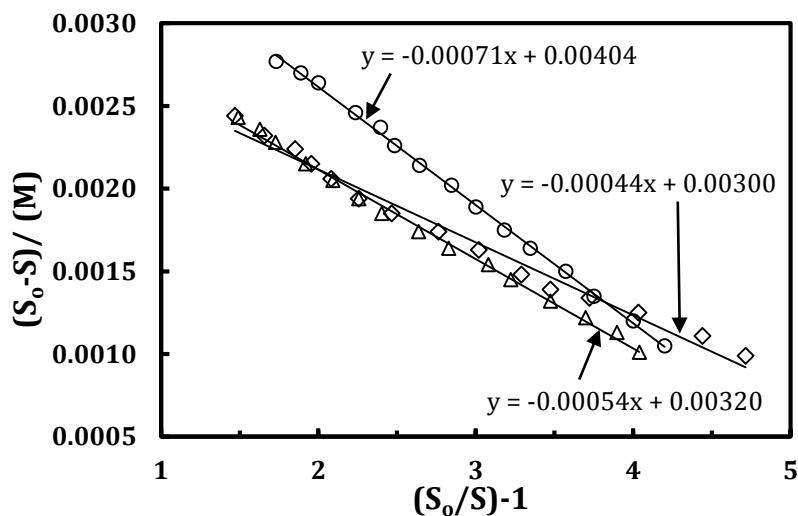


Figure IV.10: Relationship between $(S_0 - S)$ and $(S_0/S) - 1$ for solution of ionic liquids along and mixed with β -CD.

Free energy of micellization (ΔG_{mic}), degree of micellization (θ) and degree of counterion binding (ϕ) evaluated from the conductance; association constant (K_a), free energy of change (ΔG), Γ_{max} , and A_{min} obtained from surface tension of the solution (β -

CD+ionic liquid) at 25°C respectively (**Table IV.2**). The degree of micelle ionization (θ) was calculated by taking the ratio between the slopes of the linear portions above and below the break point in the conductivity profiles. The larger value of θ for the complex micelles is indication of an increased degree of ionic dissociation (**Table IV.2**) as a result of the interaction of ionic liquids with β -CD. The free energy of micellization (ΔG_{mic}) can be calculated using the equation of [31]

$$\Delta G_{mic} = RT(2-\theta)\ln CMC$$

The negative ΔG_{mic} values (**Table IV.2**) indicates that the presence of β -CD makes the process feasible and can be explained on the basis that more β -CD will be able to encapsulate more monomers and the amount of ionic liquids needed to form the micelle will obviously disappeared. The degree of counter ions binding (ϕ) onto the self-aggregated assemblies was obtained from the slopes of the Λ vs $[(C_6H_5CH_2)N(C_nH_{2n+1})_3]Cl$ isotherm in the pre-micellar region (S_1) and the post-micellar region (S_2) using the following relationship:

$$\phi = 1 - \frac{S_2}{S_1}$$

The ϕ factor includes the fraction of free energy required to condense the counter ions on the aggregate to reduce the repulsion between the adjacent monomer head groups [32].

From the perusal of **Table IV.2** it is clear that the association constants (K_a) for benzyltrimethylammonium chloride is higher compared to the other two ionic liquids; is obviously due to the fact of steric factor of the side chain group of cationic part of the chosen ionic liquids. The higher the side chain group increases the steric hindrance effect, i.e., butyl group in $[(C_6H_5CH_2)N(C_4H_9)_3]Cl$ is more steric effect than ethyl group in $[(C_6H_5CH_2)N(C_2H_5)_3]Cl$, which is in turn more than methyl group in $[(C_6H_5CH_2)N(CH_3)_3]Cl$ (**Scheme IV.4**); which clearly state the benzyl group of benzyltrimethylammonium cationic part of the ionic liquid is more associated/encapsulated with β -CD (**Scheme IV.4**). On other hand more negative ΔG for $[(C_6H_5CH_2)N(CH_3)_3]Cl$ than the rest two is also undoubtedly speak out that benzyltrimethylammonium charge or cationic part of the ionic liquid is more feasibly associated.

The maximum surface excess concentration (Γ_{\max}), and the minimum area of exclusion per molecule at the air-solution interface (A_{\min}) were estimated for the three surface active ionic liquids to the slope of the tensiometric profile near the CMC, is quantified by applying the Gibbs adsorption isotherm [33]. The values of Γ_{\max} and A_{\min} are also listed in **Table IV.2**. The increase in the A_{\min} values with temperature may be ascribed to the greater kinetic motion of the monomers populating the air-solution interface. It was noticed from **Table IV.2** that the values of Γ_{\max} decrease and those of A_{\min} increase, with the increase of alkyl chain length; which means the ionic liquid molecules with the short alkyl chain (i.e., trimethyl group) can make packing more closely or arrange more tightly than longer one.

IV.4. CONCLUSIONS

The surface tension, conductance and NMR study gives the clear indication of 1:1 host-guest inclusion complex formation of a series of surface active ionic liquids, benzyltrialkylammonium chloride $[(C_6H_5CH_2)N(C_nH_{2n+1})_3Cl]$; where $n=1,2,4$] with aq. β -cyclodextrin. The study also expose that benzyl, the hydrophobic group of ionic liquids encapsulated insight into the cavity of β -cyclodextrin and form the inclusion complex. This study also demonstrated that hydrophobic interactions and hydrogen bonding contribute to the inclusion of ionic liquids in CDs. It was found that addition of β -CD causes the shifting of micellization of the ionic liquids towards the higher concentration. This indicates the inclusion complex formation between the ionic liquids and β -CD.

CHAPTER-V

PROBING INCLUSION COMPLEX FORMATION OF AMANTADINE HYDROCHLORIDE WITH 18-CROWN-6 IN METHANOL BY PHYSICOCHEMICAL APPROACH

V.1. INTRODUCTION

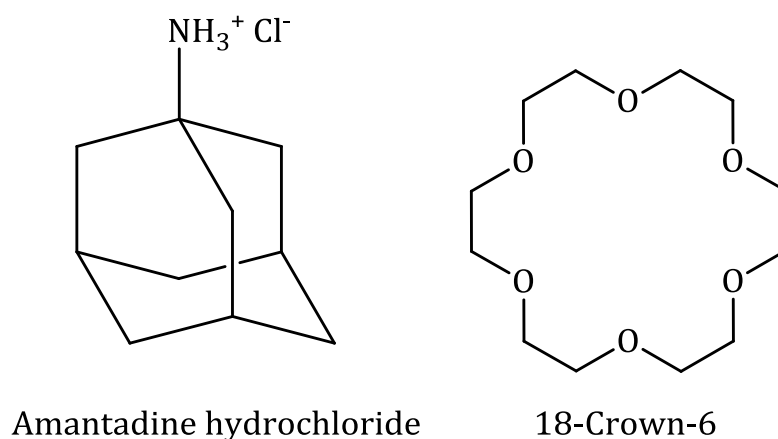
Host-guest interaction has been termed 'a complementary stereo-electronic arrangement of binding sites in host and guest' [1]. In the chemical sense the host is usually an organic molecule containing specific receptor sites while the guest is normally a metal or organic cation. Host-guest interactions have recognized importance in many biological processes, including enzyme catalysis and inhibition, antibody-antigen interactions, and membrane transport. A particularly fruitful field of organic synthesis during the past several years has been the design and preparation of macrocyclic molecules of the cyclic polyether type with the intent to mimic certain biological host-guest interactions [1-4]. Several workers have reported the attachment of organic ammonium [5] groups to hosts which are analogues of 18-crown-6 with the subsequent enhancement of a reaction between host and guest components away from the site of primary binding.

The crown ethers were of a great interest since their discovery had been reported by Pedersen in 1967 [6]. The ability of these macrocycles to form non-covalent, H-bonding complexes with ammonium cations has been actively investigated with an eye toward biological applications [7,8], molecular recognition [9,10], self-assembly [11,12], crystal engineering [13,14], and catalysis [15]. The stoichiometry and stability of these host-guest complexes depend both on the size of the crown ether and on the nature of the ammonium cation (NH_4^+ , RNH_3^+ etc) [16,17]. The numerous studies of 18-crown-6 (18C6) and its derivatives, which have the highest affinity for ammonium cations, invariably showed a 1:1 stoichiometry with both NH_4^+ and RNH_3^+ cations in solution [18] and in the solid state [19,20].

Crown ether-ammonium complexes are of fundamental interest as prototypical systems involving multiple hydrogen bonds. Study of these simple multiply-bound complexes is a promising means of gaining insight into much more complex

macromolecular systems, such as those involved in protein folding or in the pairing of nucleobases in polynucleic acids [21]. Host parameters of importance in binding both metals and organic ammonium cations include cavity size, donor atom number and type, ring number and type, ring substituents, and ring conformation. Guest parameters for organic ammonium cations differ from those of metal cations because of the different binding mechanisms involved for the two types of guest. Metal cations are sequestered within the macrocyclic ring, whereas ammonium cations hydrogen bond to the ring donor atoms. Thus, guest parameters significant to organic ammonium cation binding include number of hydrogen atoms available for hydrogen bonding.

Amantadine (**Scheme V.1**) is tricyclic aminohydrocarbons with antiviral activity directed uniquely against influenza A virus. The compounds have a potential to inhibit the early phases of viral replication by preventing uncoating of the viral genome and virus-mediated membrane fusion. The drug is used in the prevention and treatment of influenza A infections [22, 23].



Scheme V.1: Molecular structure of Amantadine hydrochloride and 18C6.

On the other hand, macrocyclic [24] and macrobicyclic polyethers [25] have been extensively used as interesting model compounds for the study of molecular effect on membrane permeability [26,27], due to their many similarities to cyclic antibiotics and biological transport agents. Considerable attention has been focused on the interactions between different protonated amines and macrocyclic ligands in order to study the molecular effect on membrane permeability [28-30].

One interesting property of crown ethers is that the electron pairs present in the ring heteroatoms provide the molecule with the ability to complex a wide range of cations in the empty cavity present in the centre of the ring [31]. A space filling model of 18-crown-6 is shown in **Figure V.1** illustrating the central cavity in which K^+ ions bind by coordinating to the six surrounding ether oxygen atoms. In the case of 18-crown-6, the diameter of the interior hole is about 4.0 Å [31]. That structural feature allows for crown ethers to form a number of complexes with cationic species [32].

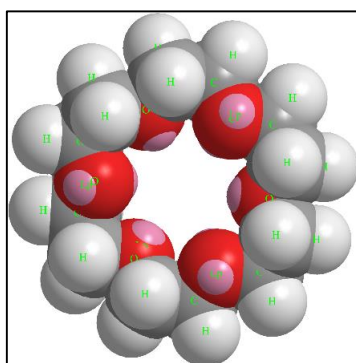


Figure V.1: A space filling model of 18-crown-6 showing the open space at the center of the crown and electron pairs present on the exposed oxygen atoms (in pink).

Conductance measurements as a sensitive and powerful technique to study the complexation of macrocyclic ligands with different cations in a variety of non-aqueous and mixed solvents [33,34]. The thermodynamics of complexation of amantadine ion with different crown ethers and cryptands in acetonitrile solvents have been reported in the literature [35]. In this paper a conductance study, surface tension study and density study of the complex formed between amantadine hydrochloride (ADH) and 18-crown-6 (18C6) in methanol solution was reported and discuss the influence of several structural and medium parameters on the complexation reaction. The structure of the crown ether is shown in **Scheme V.1**.

V.2. EXPERIMENTAL SECTION

V.2.1 Reagents

The Amantadine hydrochloride (ADH) and 18-crown-6(18C6) of puriss grade were bought from Sigma-Aldrich, Germany and used as purchased. The mass fraction purity of ADH and 18C6 were ≥ 0.99 and 0.98 respectively.

V.2. 2. Instrumentations

Prior to the start of the experimental work solubility of the chosen crown ether in methanol and ADH in methanolic solution of 18C6 have been precisely checked and observed that the drug molecule ADH freely soluble in all proportion of methanolic 18C6 solution. All the stock solutions of the drug molecule were prepared by mass (weighed by Mettler Toledo AG-285 with uncertainty 0.0003g), and then the working solutions were obtained by mass dilution at 298.15 K. The conversions of molarity into molality have been done [36] using density values. Adequate precautions were made to reduce evaporation losses during mixing.

The surface tension experiments were done by platinum ring detachment method using a Tensiometer (K9, KRÜSS; Germany) at the experimental temperature. The accuracy of the measurement was within $\pm 0.1 \text{ mN}\cdot\text{m}^{-1}$. Temperature of the system was maintained at 298.15 K by using Omniset thermostat having uncertainty in temperature $\pm 0.01 \text{ K}$.

The conductance values were obtained by using Systronics-308 [37]. The study was carried out using Brookfield TC-550 water bath with thermostat maintaining at the experimental temperatures having uncertainty of $\pm 0.01 \text{ K}$.

The densities (ρ) of the solvents were measured by means of vibrating *U*-tube Anton Paar digital density meter (DMA 4500M) with a precision of $\pm 0.00005 \text{ gcm}^{-3}$ maintained at $\pm 0.01 \text{ K}$ of the desired temperature. It was calibrated by passing triply distilled, degassed water and dry air.

Infrared spectra were recorded in 8300 FT-IR spectrometer (Shimadzu, Japan). The details of the instrument have formerly been described [38].

V.3. RESULTS AND DISCUSSION

V.3.1. Conductance

The molar conductance (Λ) of ADH ($5 \times 10^{-4} \text{ M}$) in methanol solution was monitored as a function of crown ether to amantadine ion mole ratio at various temperatures [Table V.1]. The resulting molar conductance vs. crown/cation mole ratio plots at 298.15, 303.15, and 308.15 K are shown in Figure V.2. In every case, there is a gradual decrease in the molar conductance with an increase in the crown ether concentration. This behavior indicates that the complexed amantadine ion is less mobile than the corresponding amantadine ion in methanol. As can be seen from

Figures V.2, the complexation of amantadine ion with 18C6, addition of the crown solution to the amantadine solution causes a continuous decrease in the molar conductance, which begins to level off at a mole ratio greater than one, indicating the formation of a stable 1:1 complex [39, 40]. By comparison of the molar conductance-mole ratio plot for amantadine ion -18C6 systems obtained at different temperatures (**Figure V.2**), it can be observed, that the corresponding molar conductance increased rapidly with temperature, due to the decreased viscosity of the solvent and, consequently, the enhanced mobility of the charged species present.

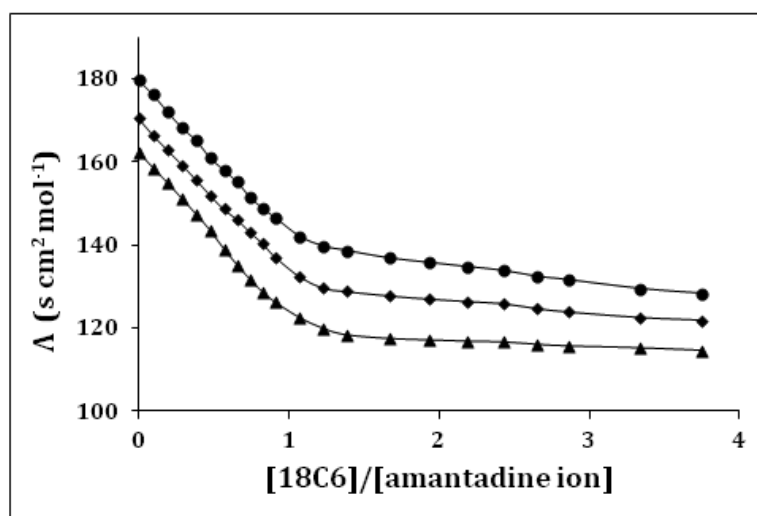


Figure V.2: Molar conductance vs $[18C6]/[amantadine\ ion]$ at 298.15 K (▲), 303.15 K (◆), 308.15 K (●).

Table V.1: Values of observed molar conductivities (Λ) at various mole ratios for the system Amantadine-18C6 at different temperature.

Mole Ratio	Conductance (Λ) ($S. cm^2. mol^{-1}$)		
	293.15 K	298.15 K	303.15 K
0	162.40	170.60	179.74
0.099	158.46	166.42	176.18
0.196	154.84	162.80	172.00
0.291	151.06	159.32	168.20
0.385	147.32	155.68	165.16
0.476	143.50	152.02	161.00
0.566	139.12	148.68	158.16

0.654	135.24	146.20	155.24
0.740	131.68	143.12	151.56
0.825	128.58	140.34	148.82
0.909	126.20	137.10	146.60
1.071	122.46	132.38	142.12
1.228	119.88	129.60	139.76
1.379	118.34	128.82	138.72
1.667	117.44	127.76	136.88
1.935	117.10	127.00	135.80
2.187	116.80	126.42	134.80
2.424	116.62	125.90	133.90
2.647	116.04	124.72	132.48
2.857	115.66	123.92	131.64
3.333	115.20	122.60	129.52
3.750	114.58	121.94	128.34

V.3.2. Association constant and Thermodynamic parameter

The 1: 1 complexation of amantadine ion with 18C6 crown ether can be expressed by the following equilibrium



The corresponding equilibrium constant, K_f is given by

$$K_f = \frac{[MC^+]}{[M^+][C]} \times \frac{f(MC^+)}{f(M^+)f(C)} \quad (2)$$

where $[MC^+]$, $[M^+]$, $[C]$ and f represent the equilibrium molar concentrations of the complex, free cation, free ligand and the activity coefficients of the species indicated, respectively. Under the dilute conditions used, the activity coefficient of uncharged macrocycle, $f(C)$, can be reasonably assumed as unity [41]. The use of the Debye-Hückel limiting law [42], leads to the conclusion that $f(M^+) \sim f(MC^+)$, so the activity coefficients in Equation (2) cancel. The complex formation constant can be expressed in terms of the molar conductances, Λ , by the following equations [39, 41].

$$K_f = \frac{[MC^+]}{[M^+][C]} = \frac{(\Lambda_M - \Lambda_{obs})}{(\Lambda_{obs} - \Lambda_{MC})[C]} \quad (3)$$

$$\text{Where } [C] = C_C - \frac{C_M(\Lambda_M - \Lambda_{obs})}{(\Lambda_M - \Lambda_{MC})} \quad (4)$$

Here, Λ_M is the molar conductance of the metal ion before addition of ligand, Λ_{MC} the molar conductance of the complexed ion, Λ_{obs} the molar conductance of the solution during titration, C_C the analytical concentration of the macrocycle added and C_M the analytical concentration of the salt. The complex formation constant, K_f , and the molar conductance of the complex, Λ_{MC} , were evaluated by using Equations (3) and (4).

In order to have a better understanding of the thermodynamics of the complexation reactions of amantadine ion with the 18C6 crown ether it is useful to consider the enthalpic and entropic contributions to these reactions. The ΔH° and ΔS° values for the complexation reactions were evaluated from the corresponding $\log K_f$ and temperature data by applying a linear least-squares analysis according to the equation:

$$2.303 \log K_f = -\frac{\Delta H^\circ}{RT} + \frac{\Delta S^\circ}{R} \quad (5)$$

Plots of $\log K_f$ vs. $\frac{1}{T}$ for Amantadine -18C6 complex is linear (**Figure V.3**).

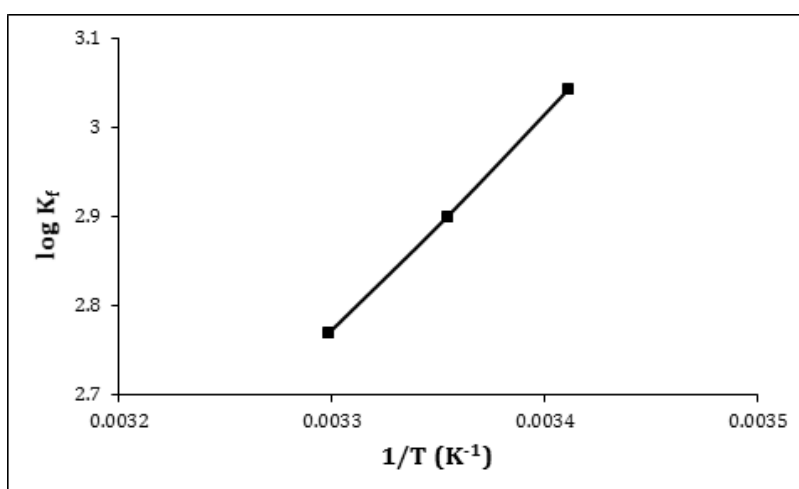


Figure V.3: The linear relationship of $\log K_f$ vs $1/T$ for the interaction between amantadine hydrochloride with 18C6.

The enthalpy (ΔH°) and entropy (ΔS°) of complexation were determined in the usual manner from the slopes and intercepts of the plots and the results are also included in **Table V.2**. Both of these two parameters have negative values. The negative values of enthalpy confirm that when ADH interact with the crown ether molecules the overall energy of the system is decreased, i.e., there is some stabilization interaction in the system, whereas negative values of entropy factor indicate that there is an ordered arrangement, i.e., complex formation takes place between the ADH and the 18C6 molecule. The negative value of entropy is unfavourable for the spontaneity of the complex formation, but this effect is overcome by higher negative value of ΔH° . The values of ΔG° (**Table V.2**) for the complex formation was found negative suggesting that the complex formation process proceeds spontaneously. The data shown in table indicates that formation constant $\log K_f$ for amantadine ion with 18C6 is highest at 298.15 K and decreases with increase in temperature i.e. amantadine ion form stable complex with 18C6 at 298.15K.

Table V.2: Values of formation constant, enthalpy, entropy and free energy change of amantadine-18C6 complex in methanol solution.

Cation	Crown	Log K_f			ΔH° (kJ mol ⁻¹)	ΔS° (J mol ⁻¹ K ⁻¹)	ΔG° (kJ mol ⁻¹)
		298.15K	303.15K	308.15K			
Amantadine	18C6	3.04	2.90	2.77	-46.56	-100.58	-16.57

V.3.3. Surface tension

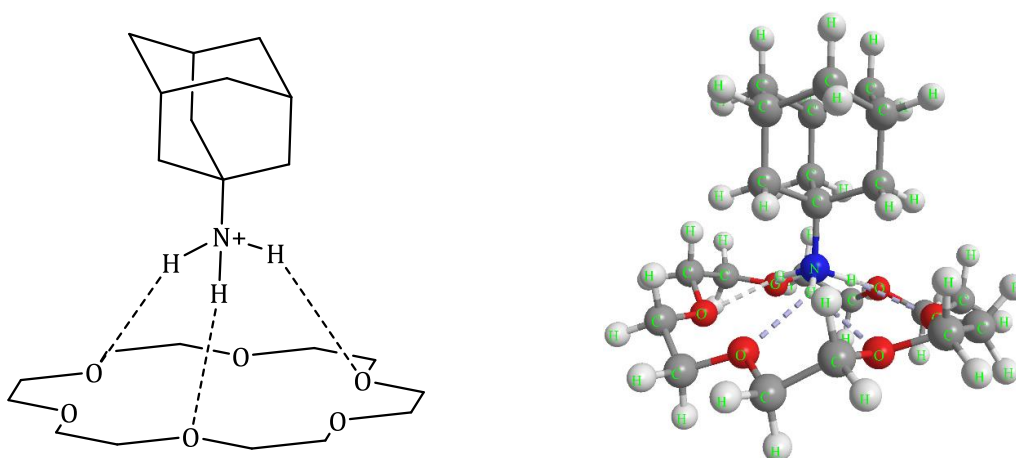
Surface tension (γ) measurement provides significant indication about formation of inclusion complex as well as stoichiometry of the host-guest assembly [43-45]. The values of surface tension at different concentration of 18C6 are listed in **Table V.3**.

Table V.3: Experimental values of surface tension (γ) corresponding to concentration of 18C6 in methanolic solution.

Conc. of 18C6 (mM)	Surface tension (γ) (mN.m ⁻¹)
0.00	26.5
0.91	25.8
1.67	25.2
2.31	24.7
2.86	24.1
3.33	23.7
3.75	23.3
4.12	22.9
4.44	22.5
4.74	22.2
5.00	21.9
5.24	21.8
5.45	21.7
5.65	21.7
5.83	21.6
6.00	21.6
6.15	21.5
6.30	21.5
6.43	21.4
6.55	21.4
6.67	21.4

In the present work ADH have a hydrophobic group and a terminal $-\text{NH}_3^+$ group (**Scheme V.1**) due to which ADH shows surfactant like activities, thus γ of the ADH solution shows decreasing trend. In this work when 18C6 was added in ADH solution the proton of the $-\text{NH}_3^+$ group binds to the alternate three oxygen atom of the crown ether and the formation of three H-bonds occurs (**Scheme V.2**). As a result charged portion of the amantadine ion form complex with 18C6 and due to the formation of complex effect of hydrophobic portion increases i.e. surface tension of the solution

again decreases slowly. At a certain conc. of ADH and crown ether, a single break was observed in the surface tension curve (**Figure V.4**).



Scheme V.2: Schematic presentation of complexation between amantadine ion and 18C6 and corresponding energy minimized structure of the complex.

The break point in surface tension curve not only indicates the formation of complex between amantadine ion and 18C6 but also about its stoichiometry, i.e., appearance of single break point in the plot indicates 1:1 stoichiometry of the complex. The value of γ at the break point and corresponding concentration of crown ether have been listed in **Table V.4**. Hence the plausibility of formation of complex can be predicted from surface tension study.

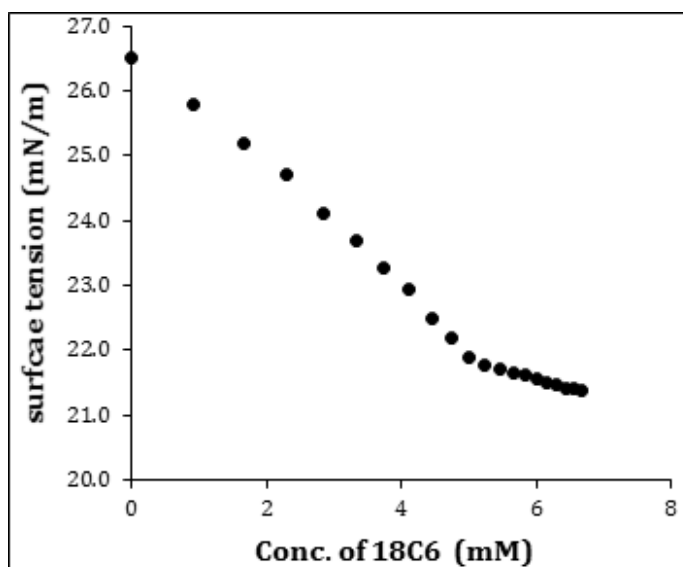


Figure V.4: Variation of surface tension of amantadine with increasing concentration of 18C6 at 298.15 K.

Table V.4: Values of surface tension (γ) at the break point with corresponding to concentration of 18C6 in methanolic solution at 298.15 K.

Conc. (mM)	γ (mN.m ⁻¹)
5.07	21.99

V.3.4. IR Study

FTIR spectra of the complex, 18C6 and that of pure ADH were obtained in the region 400-4000 cm⁻¹. If the FTIR spectrum of 18C6 was compared with that of complex, it was noticed that the peaks observed in pure 18C6 (**Figure V.5**) at 1120 cm⁻¹ correspond to COC group shift to 1106 cm⁻¹ in the complex (**Figure V.5**). The frequency of the C-O-C asymmetric stretching vibrations of a polyether, ν_{as} (COC), decreases upon interaction of the O atoms with the protons of the ammonium group via hydrogen H bonds. The N-H stretching band of the ammonium group expected for amantadine ion in the region 2961 to 3087 cm⁻¹ by Pierre D. Harvey [46] was observed in pure ADH at 3047 cm⁻¹. This peak shifts to 3027 cm⁻¹ revealed that the N-H bonds were involved in the complex formation. The characteristic peak of ADH at 2927 cm⁻¹ was shifted to 2909 cm⁻¹ in the complex. The peak at 1086 cm⁻¹ corresponding to C-N bend of the C-N bond of ADH shifts to higher frequencies [47]. Thus it may be concluded that amantadine was strongly bound to 18C6 through H-bonds of the ammonium group.

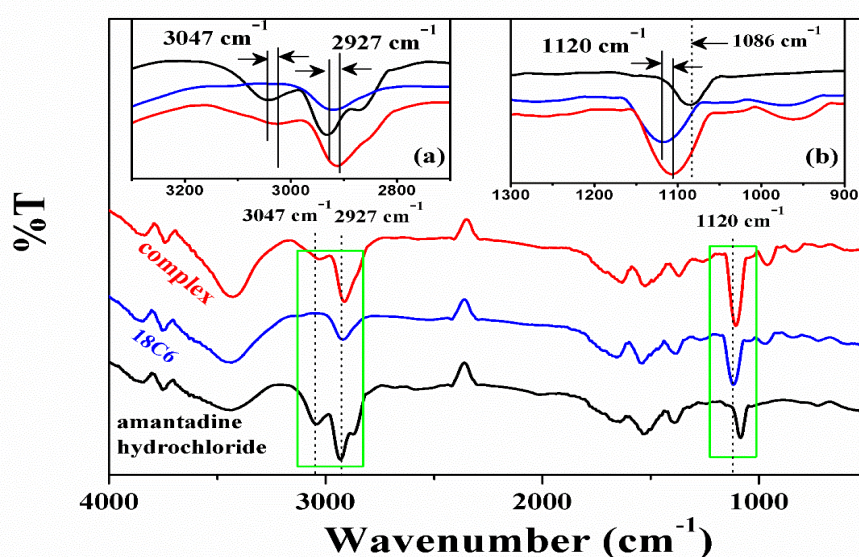


Figure V.5: FTIR spectra of pure amantadine hydrochloride (black), 18-crown-6 (blue) and complex (red).

V.3.5. Apparent molar volume

The characteristic behavior of interaction present in complex of solute has also been obtained from apparent molar volume. The sum of the geometric volume of the central solute molecule and changes in the solvent volume due to its interaction with the solute around the co-sphere is the measure of apparent molar volume. The physical properties of binary mixtures in different mass fractions ($w_1=0.001, 0.004, 0.007$) of methanolic 18C6 solutions at 298.15, 303.15, 308.15 K are reported in **Table V.5**. Here ϕ_v has been determined from the measured density of the solutions at 298.15 K, 303.15 K, 308.15 K (**Table V.6**) and by using the suitable equation. ϕ_v varies linearly with the square root of molal concentration and is fitted to the Masson equation, from where the limiting apparent molar volume (ϕ_v^0) has been determined (**Table V.7**) [48]. The limiting molar volume (ϕ_v^0) signify the solute-solvent interactions in the amantadine + 18C6 ternary solution systems. The magnitude of which is found to be positive for all the systems under study, indicating strong solute-solvent interactions [44,49].

Table V.5: Experimental values of density (ρ) in different mass fraction of methanolic solution of 18C6.

Solvent mixture	Temp (K)	$\rho \cdot 10^{-3}$ ($\text{kg} \cdot \text{m}^{-3}$)
$w_1=0.001$	298.15	0.79378
	303.15	0.79141
	308.15	0.78899
$w_1=0.004$	298.15	0.79540
	303.15	0.79207
	308.15	0.78962
$w_1=0.007$	298.15	0.79627
	303.15	0.79336
	308.15	0.78107

Table V.6: Experimental values of densities (ρ) corresponding to concentration in different mass fractions of methanolic solution of 18C6 at different temperature.

Concentration (M)	$\rho \cdot 10^{-3}$ ($\text{kg} \cdot \text{m}^{-3}$)		
	298.15 K	303.15 K	308.15 K
W₁ = 0.001			
0.002	0.79392	0.79156	0.78914
0.004	0.79407	0.79172	0.78930
0.006	0.79423	0.79188	0.78947
0.008	0.79440	0.79205	0.78965
W₁ = 0.004			
0.002	0.79552	0.79221	0.78977
0.004	0.79566	0.79236	0.78994
0.006	0.79581	0.79252	0.79012
0.008	0.79597	0.79270	0.79029
W₁ = 0.007			
0.002	0.79638	0.79348	0.79121
0.004	0.79651	0.79362	0.79137
0.006	0.79666	0.79377	0.79154
0.008	0.79681	0.79394	0.79172

Table V.7: Limiting apparent molar volume (ϕ_v^0) and experimental slope (S_v^*) in different mass fractions of methanolic solution of 18-crown-6.

Temp.(K)	$\phi_v^0 \times 10^6$ ($\text{m}^3 \cdot \text{mol}^{-1}$)	$S_v^* \times 10^6$ ($\text{m}^3 \cdot \text{mol}^{-3/2} \cdot \text{kg}^{1/2}$)
W₁=0.001		
298.15	156.91	-174.98
303.15	152.32	-162.19
308.15	148.11	-139.57
W₁=0.004		
298.15	174.48	-280.76
303.15	164.06	-254.20
308.15	153.75	226.20

	$W_1=0.007$	
298.15	181.95	-311.69
303.15	175.74	-294.20
308.15	163.04	-284.41

The plot of ϕ_v° values against different temperature at different mass fractions are represented in **Figure V.6**, which suggests that ϕ_v° values increases with increase of mass fraction at same temperature and decreases with increasing the temperature. The values of ϕ_v° increases with the increase of mass fractions of 18C6 in methanol indicating that the ion-hydrophilic group interactions are stronger than the ion-hydrophobic group interactions. In the present ternary system interactions are taking place between the positive charge of ammonium groups and the alternative oxygen atom of the crown ether. The decreasing trend with increasing temperature suggests that the interactions between the drug molecule and crown molecules are decreased with increasing temperature. The facts support the data and the results observed from surface tension and conductivity study discussed earlier also support the facts.

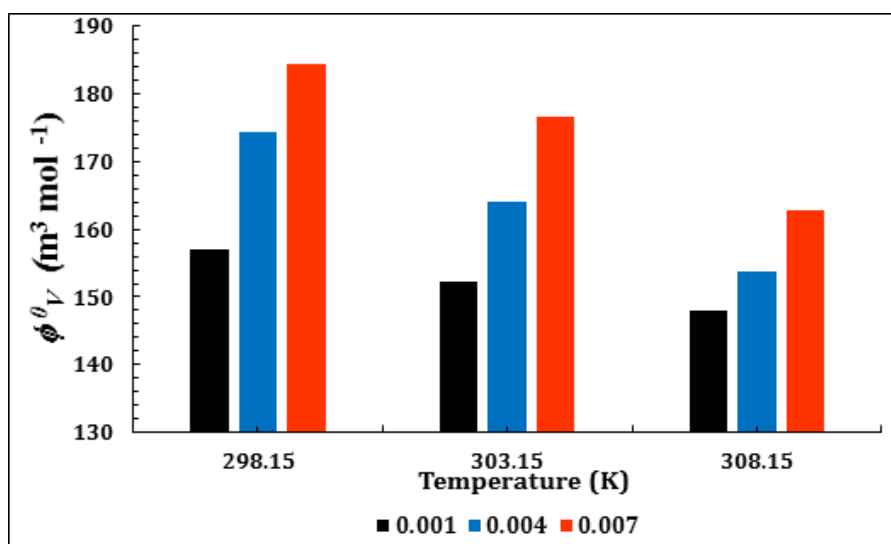


Figure V.6: Plot of limiting apparent molar volume (ϕ_v°) of amantadine against different temperature (298.15 K, 303.15 K, 308.15 K) in mass fractions $w_1=0.001$ (■), $w_1=0.004$ (■), $w_1=0.007$ (■) mass fractions of 18C6 in methanol solution.

The parameter S_V^* is the volumetric virial coefficient, and it characterizes the pair wise interaction of solute species in solution [50,51]. S_V^* is found to be negative under investigations, which suggest that the pair wise interaction is restricted by the interaction of the charged functional group of ADH with crown. From **Table V.7**, a quantitative comparison between ϕ_V^0 and S_V^* values show that, the magnitude of ϕ_V^0 values is higher than S_V^* , suggesting that the solute-solvent interactions dominate over the solute-solute interactions in all solutions at the investigated temperatures.

V.3.6. Temperature dependent limiting apparent molar volume:

The variation of ϕ_V^0 with the temperature of the ADH in methanolic solution of 18C6 can be expressed by the general polynomial equation as follows,

$$\phi_V^0 = a_0 + a_1T + a_2T^2 \quad (6)$$

where a_0 , a_1 , a_2 are the empirical coefficients depending on the solute, mass fraction (w_1) of the co-solute Crown, and T is the temperature range under study in Kelvin.

The limiting apparent molar expansibilities, ϕ_E^0 , can be obtained by the following equation,

$$\phi_E^0 = \left(\delta\phi_V^0 / \delta T \right)_p = a_1 + 2a_2T \quad (7)$$

The limiting apparent molar expansibilities, ϕ_E^0 , change in magnitude of limiting apparent molar volume with the change of temperature. The values of ϕ_E^0 for different solutions of the studied ADH at 298.15, 303.15, and 308.15 K are reported in **Table V.8**. The table reveals that ϕ_E^0 is small negative in all studied temperature. This fact can ascribed to the presence of small caging or packing effect [52] for ADH in solutions.

Table V.8: Limiting apparent molar expansibilities (ϕ_E^0) for amantadine hydrochloride in different mass fraction of 18C6 in methanol solution (w_1) at 298.15K to 308.15K respectively.

solvent mixture	$\phi_E^0 \cdot 10^6 (\text{m}^3 \cdot \text{mol}^{-1} \cdot \text{K}^{-1})$		
	Amandine + 18C6		
	298.15 K	303.15 K	308.15 K
$w_1 = 0.001$	-0.956	-0.880	-0.804
$w_1 = 0.004$	-2.095	-2.073	-2.051
$w_1 = 0.007$	-1.034	-2.170	-2.906

V.4. CONCLUSION

The present study shows that amantadine ion can bind nicely to three of the six available oxygen atoms in the 18C6 ring to form a stable complex (**Scheme V.2**) with 1:1 stoichiometry. The N-H...O hydrogen bridges between the ammonium functionalities and the oxygen acceptor heteroatoms of the crown ethers play a significant role in packing the host-guest complexes. The stable complex formation is established by physicochemical methods surface tension measurements, conductivity and IR study and the density data also support the interaction between amantadine ion and 18C6 systems. The inclusion complex formation has been explained qualitatively as well as quantitatively so as to make it dependable in its field of application.

The Host-guest complex formation based on the macrocyclic molecules is a facile and reversible process, which provides the feasibilities to design stimuli-responsive supramolecular systems and these macrocyclic molecules are basically friendly to the biological environment and exhibit good biocompatibilities. Crown ether-based host-guest interactions, which show good selectivity, high efficiency, and reversibility, have been structurally characterized and the underlying supramolecular chemistry has been presented in this work. Supramolecular chemistry i.e host-guest complex formation through noncovalent interactions offer the basis for novel approaches in medicine and also helps in understanding the interactions present in living systems. It was also found that host-guest complexation with crown ethers

resembles an established principle i.e. the hydrogen bonding acceptance as well as the donation propensity of crown ethers.

Amantadine is an antiviral agent that specifically inhibits influenza A virus replication at micromolar concentration. This drug is also very effective in the treatment of human Parkinson's disease. The host-guest complex is capable of protecting the drug molecule from chemical reactions and photochemical/thermal degradation in biological environment and the encapsulated drug can also be released sustainably from the cavity of macrocyclic molecule, achieving prolonged therapeutic effect.

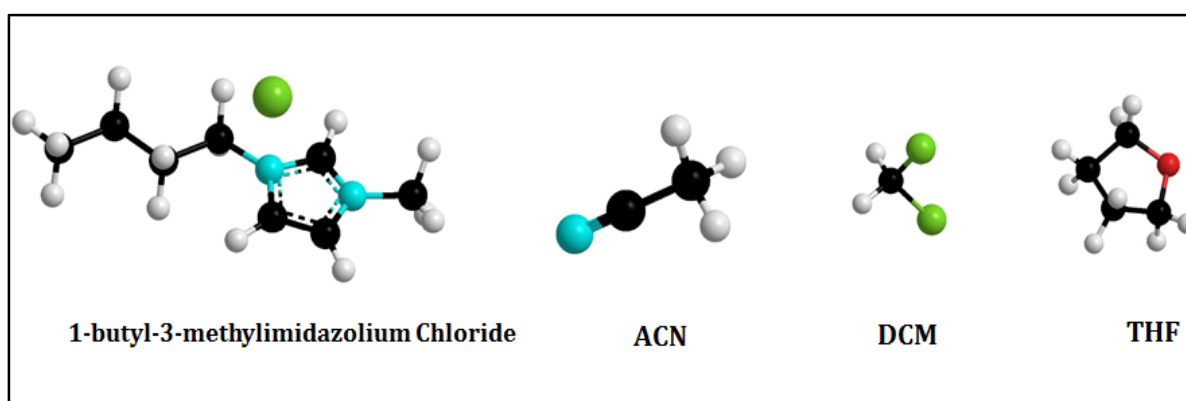
CHAPTER-VI

INVESTIGATION ON SOLVATION BEHAVIOR OF AN IONIC LIQUID (1-BUTYL-3-METHYLIMIDAZOLIUM CHLORIDE) WITH THE MANIFESTATION OF ION ASSOCIATION PREVAILING IN DIFFERENT PURE SOLVENT SYSTEMS

VI.1. INTRODUCTION

Ionic liquids (IL) presently experience important consideration in many areas of chemistry. There is competition to find a proper niche for these materials, and also more insight is needed. The most attractive property is the “tunability” of the physical and chemical properties of ILs by varying structure. There are several reviews available on different aspects of ILs [1]. Ionic liquids (ILs) have attracted significant attention over the last two decades, as many of them have a negligible vapour pressure, exceptional thermal and electrochemical stability, favorable dissolution properties with many organic/inorganic compounds, and low flammability [2, 3]. ILs, which may consist of a diverse variety of cations and anions, have been widely investigated for a variety of applications including biphasic systems for separation, solvents for synthetic and catalytic applications [4], lubricants [5, 6], lithium batteries [7-9], supercapacitors [10–12], actuators [13,14], reaction media [15] replacement of conventional solvents [3], and active pharmaceutical ingredients [15]. Importantly, IL properties can be tailored for specific chemical or electrochemical applications by tuning the combination of cations and anions to achieve the desired thermodynamic, solvating, and transport properties, as well as safety. In the modern technology, the application of the ionic liquid is well understood by studying the ionic solvation or ion association. Ionic association of electrolytes in solution depends upon the mode of solvation of its ions [16-19] which in turn depends on the solvent properties such as viscosity and the relative permittivity. These properties support in determining the extent of ion association and the solvent-solvent interactions. The non-aqueous arrangement has been of enormous prominence [20, 21] to the technologist and theoretician as numerous chemical processes ensue in these systems.

In this study, we have investigated on conductometric properties of the ionic liquid [IL] 1-butyl-3-methylimidazolium chloride [bmim][Cl] in polar aprotic solvents acetonitrile (ACN), tetrahydrofuran (THF), dichloromethane (DCM) at different temperatures 298.15 K, 303.15 K and 308.15 K. The experimental data was analyzed using Fuoss conductance equation and Fuoss–Kraus theory to calculate the ion pair formation constant K_p and triple ion formation constants K_T . The main purpose of this study is to obtain experimental and quantitative information for the interactions between the ions. Here the ion pair formation constants are expected to reflect strongly the direct interactions between the ions. The structure of the IL and solvents are presented in **Scheme VI.1**.



Scheme VI.1: Molecular structures of the IL and the solvents.

VI.2. EXPERIMENTAL SECTION

VI.2.1 Reagents

The IL [bmim][Cl] (purity $\geq 98\%$) was obtained from Sigma-Aldrich, Germany and the IL was preserved in vacuum desiccator containing anhydrous P_2O_5 and any water content of the solvents was removed by using molecular sieves.

The solvents ACN, THF, and DCM were procured from Merck, India. The solvents were further purified by standard methods [22]. The purity of the solvents were checked by measuring its density and viscosity which were in good agreement with the literature values [23, 24] as shown in **Table VI.1**. The purities of the solvents were $\geq 99.5\%$.

VI.2.2 Instrumentations

All the stock solutions of the IL in considered solvents were prepared by mass (weighed by Mettler Toledo AG-285 with uncertainty 0.0003 g). In case of conductometric study the working solutions were achieved by mass dilution of the stock solutions.

Temperature of the solution was maintained to within ± 0.01 K using Brookfield Digital TC-500 temperature thermostat bath. The viscosities were measured with an accuracy of $\pm 1\%$. Each quantity reported herein is an average of triplicate reading with a precision of 0.3%.

The conductance values were obtained by using Systronics-308. Measurements were made in a thermostat water bath maintained at $T = (298.15 \pm 0.01)$ K. The cell was calibrated by the method proposed by Lind et al. [25] and cell constant was calculated based on 0.01 (M) aqueous KCl solution. During the conductance measurements, cell constant was maintained within the range 1.10–1.12 cm^{-1} . The conductance data were reported at a frequency of 1 kHz and the accuracy was $\pm 0.3\%$. During all the measurements, uncertainty of temperatures were ± 0.01 K.

The density values of the solvents and experimental solutions (ρ) were measured using vibrating u-tube Anton Paar digital density meter (DMA 4500M) with a precision of ± 0.00005 g cm^{-3} maintained at ± 0.01 K of the desired temperature. It was calibrated by triply-distilled water and passing dry air.

Brookfield DV-III Ultra Programmable Rheometer with fitted spindle size-42 fitted to a Brookfield digital bath TC-500 helps in measuring the viscosity values. The viscosities were obtained using the following equation

$$\eta = (100/\text{RPM}) \times \text{TK} \times \text{torque} \times \text{SMC}$$

Where RPM= speed, TK (0.09373)= viscometer torque constant and SMC (0.327)= spindle multiplier constant, respectively. The instrument was standardized against the standard viscosity samples provided with the instrument, water and aqueous CaCl_2 solutions [26]. The viscosities were measured with an accuracy of $\pm 1\%$.

Fourier transform infrared spectra (FT-IR) were recorded in a Perkin Elmer FT-IR spectrometer. The spectra were acquired in the frequency range 4000–400 cm^{-1} at a resolution of 4 cm^{-1} with a total of 10 scans. The concentration of the studied solutions used in the IR study was 0.05 M.

VI.3. RESULTS AND DISCUSSION

VI.3.1 Electrical Conductance

VI.3.1.1 Ion-pair formation:

The formation of ion pair in ACN have been explored from the conductivity studies of [bmim][Cl] by using the Fuoss conductance equation [27]. The physical properties solvent are given in **Table VI.1**. The molar conductance (Λ) for all studied system was calculated using suitable equation [28].

Table VI.1: Density (ρ), viscosity (η) and relative permittivity (ϵ) of the different solvents Acetonitrile, Tetrahydrofuran and Dichloromethane.

Temp./K	$\rho^a \cdot 10^{-3}/\text{kg m}^{-3}$	$\eta^b/\text{mPa s}$	ϵ
Acetonitrile			
298.15	0.78597	0.36	35.94
303.15	0.78278	0.35	35.01
308.15	0.77996	0.34	34.30
Tetrahydrofuran			
298.15	0.88599	0.48	7.58
303.15	0.88591	0.45	7.24
308.15	0.88586	0.41	7.09
Dichloromethane			
298.15	1.32571	0.43	8.93
303.15	1.31852	0.41	8.84
308.15	1.30955	0.39	8.73

^a Uncertainty in the density values: $\pm 0.00001 \text{ g cm}^{-3}$

^b Uncertainty in the viscosity values: $\pm 0.03 \text{ mPa s}$

The plot of molal conductivity, Λ , versus the square root of the molal concentration, \sqrt{m} , gives a linear conductance curves for the solvent with higher to moderate relative permittivity ($\epsilon_r = 35.95$ to 14.47), shown in **Figure VI.1** and the values are listed in the **Table VI.2**. Extrapolation of $\sqrt{m} = 0$ evaluated the starting limiting molar conductances for the electrolyte [29].

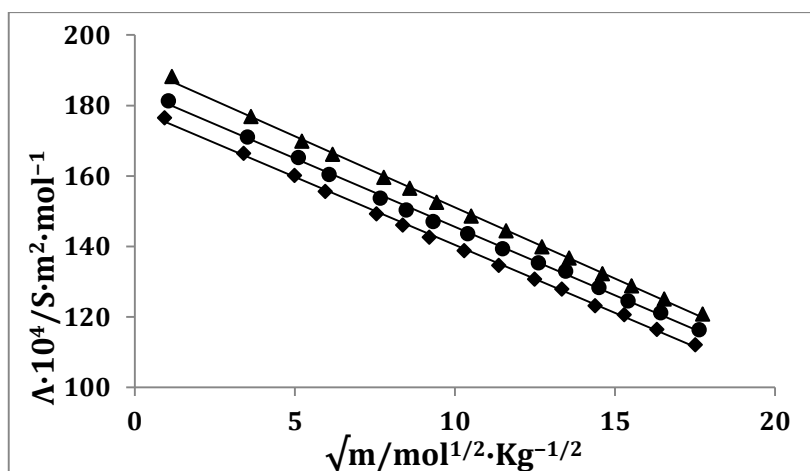


Figure VI.1: Plot of molar conductance (Λ) versus \sqrt{m} of [bmim][Cl] in ACN at 298.15 K (◆), 303.15 K (●) and 308.15 K (▲).

Table VI.2: The concentration (m) and molal conductance (Λ) of [bmim][Cl] in Acetonitrile, Dichloromethane and Tetrahydrofuran at 298.15 K, 303.15K and 308.15K respectively.

$m \cdot 10^4 /$ $\text{mol} \cdot \text{dm}^{-3}$	$\Lambda \cdot 10^4 /$ $\text{S} \cdot \text{m}^2 \cdot \text{mol}^{-1}$	$m \cdot 10^4 /$ $\text{mol} \cdot \text{dm}^{-3}$	$\Lambda \cdot 10^4 /$ $\text{S} \cdot \text{m}^2 \cdot \text{mol}^{-1}$	$m \cdot 10^4 /$ $\text{mol} \cdot \text{dm}^{-3}$	$\Lambda \cdot 10^4 /$ $\text{S} \cdot \text{m}^2 \cdot \text{mol}^{-1}$
Acetonitrile		Dichloromethane		Tetrahydrofuran	
298.15 K					
0.87	176.54	8.97	41.77	0.95	40.11
11.58	166.42	10.74	39.95	1.60	38.48
24.95	160.14	13.06	37.68	2.83	37.13
35.44	155.66	15.15	36.2	4.07	36.10
57.00	149.3	17.64	34.67	6.22	34.76
70.02	146.04	19.85	33.29	7.79	33.96
84.63	142.6	22.85	31.8	10.19	32.86
105.80	138.81	25.01	30.88	13.55	31.66
129.30	134.62	27.70	29.91	15.79	31.36
156.12	130.7	33.74	27.98	17.81	30.76
177.99	127.9	39.25	26.79	20.05	30.36
206.72	123.23	46.61	26.17	22.80	30.36
233.73	120.68	53.92	26.99	25.68	30.16
266.02	116.52	60.72	28.57	29.66	31.06

306.52	112.13	66.97	31.18	34.29	33.87
303.15K					
1.10	181.36	4.63	50.59	1.06	43.96
12.40	171.07	6.28	48.32	2.18	41.26
26.14	165.28	8.13	46.13	3.59	39.46
36.86	160.46	10.43	44.22	4.97	38.06
58.79	153.67	13.22	42.31	7.33	36.41
72.00	150.37	15.94	41.03	9.03	35.51
86.81	147.06	19.51	39.12	11.59	34.77
108.23	143.67	22.45	37.61	14.19	33.89
131.99	139.38	26.01	36.52	17.04	33.3
159.07	135.36	29.35	35.72	19.66	32.66
181.15	132.99	32.26	35.03	22.00	32.52
210.12	128.42	34.70	33.99	25.05	32.2
237.34	124.58	42.13	34.22	27.89	33.06
269.87	121.16	46.64	35.91	30.55	34.96
310.65	116.36	53.03	38.92	33.42	36.46
308.15 K					
1.34	188.20	9.09	52.14	1.43	49.66
13.18	176.91	11.09	50.22	2.70	47.56
27.27	169.90	13.94	48.54	4.25	45.86
38.20	166.20	17.04	46.62	6.34	44.06
60.49	159.61	21.29	44.93	8.26	42.67
73.87	156.51	23.94	43.84	10.06	41.69
88.87	152.51	28.20	42.53	12.75	40.61
110.53	148.64	31.74	41.37	16.49	39.38
134.52	144.42	35.92	40.73	18.95	38.4
161.85	139.90	39.74	40.06	22.09	37.96
184.12	136.73	45.02	39.26	23.59	37.56
213.32	132.26	47.84	38.88	25.72	37.66
240.74	128.82	54.21	38.56	29.68	37.96
273.49	125.10	60.05	39.74	32.43	39.46
314.53	120.82	64.25	42.32	35.37	41.36

The limiting molar conductance (Λ_0), the association constant (K_A) and the distance of closest approach of ions (R) these three adaptable parameters are derived from the following set of equations (Fuoss equation) using a given set of conductivity values ($c_j, \Lambda_j, j=1, \dots, n$) :

$$\Lambda = P\Lambda_0[(1+R_X) + E_L] \quad (1)$$

$$P = 1 - \alpha(1 - \gamma) \quad (2)$$

$$\gamma = 1 - K_A m \gamma^2 f^2 \quad (3)$$

$$-\ln f = \beta \kappa / 2(1 + \kappa R) \quad (4)$$

$$\beta = e^2 / (\epsilon_r k_B T) \quad (5)$$

$$K_A = K_R / (1 - \alpha) = K_R / (1 + K_S) \quad (6)$$

Where R_X is the relaxation field effect, E_L is the electrophoretic counter current, α is the fraction of contact pairs, γ is the fraction of solute present as unpaired ion, K_A is the overall pairing constant, f is the activity coefficient, m is the molality of the solution, β is twice the Bjerrum distance, κ is the radius of the ion atmosphere, e is the electron charge, ϵ_r is the relative permittivity of the solvent mixture, k_B is the Boltzmann constant, T is the absolute temperature, K_R is the association constant of the solvent-separated pairs and K_S is the association constant of the contact-pairs.

The computations were performed using a program suggested by Fuoss [27]. The initial Λ_0 values for the iteration procedure were obtained from Shedlovsky extrapolation of the data [30]. Input for the program is the set ($m_j, \Lambda_j, j=1, \dots, n$), n, ϵ, η, T , initial Λ_0 value, and an instruction to cover a pre-selected range of R values. The best values of a parameter is the one when equations is best fitted to the experimental data corresponding to minimum standard deviation δ for a sequence of predetermined R values, and standard deviation δ was calculated by the following equation:

$$\delta^2 = \sum [A_j(cal) - A_j(obs)]^2 / (n - m) \quad (7)$$

Where n is the number of experimental points and m is the number of fitting parameters. The conductance data were examined by fixing the distance of closest approach (R) of ions with two fitting parameter ($m = 2$). No significant minima were detected in the δ vs. R curves, whereas the R values were arbitrarily preset at the center to center distance of solvent-separated ion pair [26, 29]. Thus, R values are

assumed to be $R = (a + d)$; where $a = (r_+ + r_-)$ is the sum of the crystallographic radii of the cation (r_+) and anion (r_-) and d is the average distance corresponding to the side of a cell occupied by a solvent molecule. The distance, d is given by Fuoss and Accascina [31].

$$d (\text{\AA}) = 1.183 (M / \rho)^{1/3} \quad (8)$$

Where M is the molar mass of the solvent and ρ is its density. The values of Λ_o , K_A and R obtained by using Fuoss conductance equation for [bmim][Cl] in ACN at 298.15 K, 303.15 K and 308.15 K are represented in **Table VI.3**. The values in table shows that the limiting molar conductances (Λ_o) of [bmim][Cl] is highest in ACN (**Table VI.3**) and lowest in case of THF (Table VI.7). Thus the observed trend of the Λ_o values is ACN > DCM > THF. The observed trend of solvent Λ_o is found to be the opposite of the viscosity trend. As expected, limiting molar conductance values decrease when the viscosity of the solvents increases because ionic mobility is diminished in viscous media.

Table VI.3: Limiting molar conductance (Λ_o), association constant (K_A), co-sphere diameter (R) and standard deviations of experimental Λ (δ) obtained from Fuoss conductance equation of [bmim][Cl] in Acetonitrile at 298.15 K, 303.15 K and 308.15 K respectively.

T/K	$\Lambda_o \cdot 10^4 / \text{S} \cdot \text{m}^2 \cdot \text{mol}^{-1}$	$K_A / \text{dm}^3 \cdot \text{mol}^{-1}$	$R / \text{\AA}$	δ
298.15	178.45	725.21	8.98	3.43
303.15	191.43	641.23	8.82	3.54
308.15	199.56	571.34	8.73	3.92

Ion-solvation can also be explained with the help of another characteristic property called the Walden product ($\Lambda_o \eta$) (**Table VI.4**) [32]. Λ_o increases for the IL in ACN with increasing temperature and the $\Lambda_o \eta$ also increases even though the viscosity of the solvent decreases. This fact indicates the prevalence of Λ_o over η .

Table VI.4: Walden product ($\Lambda_0 \cdot \eta$) and Gibb's energy change (ΔG°) of [bmim][Cl] in Acetonitrile at 298.15 K, 303.15 K and 308.15 K respectively.

T/K	$\Lambda_0 \cdot \eta \cdot 10^4 /$ $S \cdot m^2 \cdot mol^{-1} mPa$	$\Delta G^\circ /$ $kJ \cdot mol^{-1}$
298.15	64.24	-16.33
303.15	67.00	-16.29
308.15	67.85	-16.26

To investigate the role of the individual IL ions in ion-solvation, we have to split the limiting molar conductance values into their ionic contributions. The ionic conductances λ_0^\pm for the [bmim]⁺ cation and Cl⁻ anion in different solvents were calculated using tetrabutylammonium tetraphenylborate (Bu₄NBPh₄) as a 'reference electrolyte' by the method of Das et al. [33]. The ionic limiting molar conductances λ_0^\pm values for [bmim]⁺ cation and [Cl]⁻ anion has been determined in ACN solvents by interpolating conductance data from the literature [34] using cubic spline fitting and the values are given in **Table VI.5**.

Table VI.5: Limiting Ionic Conductance (λ_0^\pm), Ionic Walden Product ($\lambda_0^\pm \eta$, Stokes' Radii (r_s), and Crystallographic Radii (r_c) of [bmim][Cl] in Acetonitrile at 298.15 K, 303.15 K and 308.15 K respectively.

T/K	ion	λ_0^\pm $/S \cdot m^2 \cdot mol^{-1}$	$\lambda_0^\pm \eta$ $/S \cdot m^2 \cdot mol^{-1} mPa$	$r_s / \text{\AA}$	$r_c / \text{\AA}$
298.15	bmim ⁺	87.41	31.47	3.15	2.25
	Cl ⁻	99.42	35.78	2.19	1.95
303.15	bmim ⁺	89.42	31.28	3.14	2.27
	Cl ⁻	103.31	36.15	2.16	1.98
308.15	bmim ⁺	93.24	31.70	3.12	2.28
	Cl ⁻	105.84	35.99	2.12	2.03

It is observed from **Table VI.5** that a smaller limiting molar conductivity value of the [bmim]⁺ than Cl⁻ in a solvent suggests enhanced solvation of the cation in that specific medium i.e., the [bmim]⁺ cation is responsible for a greater portion of ionic

association with the solvents. Estimation of the ionic contributions to conductance is based mostly on Stokes' law, which provides valuable insight for the limiting ionic Walden product. The law states that the limiting ionic Walden product ($\lambda_{o^{\pm}}\eta$); the product of the limiting ionic conductance and solvent viscosity) for any singly charged, spherical ion is a function of the ionic radius (crystallographic radius), and thus, is a constant under normal conditions. The values of ionic conductance $\lambda_{o^{\pm}}$ and the product of ionic conductance and viscosity of the solvent named ionic Walden product ($\lambda_{o^{\pm}}\eta$) along with Stokes' radii (r_s) and Crystallographic Radii (r_c) of [bmim][Cl] in ACN at different temperatures are given in **Table VI.5**.

VI.3.1.2. Thermodynamic Parameters:

The Gibbs free energy change ΔG^0 is given by the following relationship [35] and is given in **Table VI.4**.

$$\Delta G^0 = -RT \ln K_A \quad (9)$$

The negative values of ΔG^0 can be explained by considering the participation of specific covalent interaction in the ion-association process.

The variation of conductance of an ion with temperature can be treated as similar to the variation of the rate constant with temperature which is given by the Arrhenius equation [27]:

$$\Lambda_0 = A e^{E_a/RT} \quad (10)$$

$$\log \Lambda_0 = \log A - \frac{E_a}{2.303RT} \quad (11)$$

Where A is an Arrhenius constant, E_a is the activation energy of the rate process which determines the rate of movement of ions in solution. The slope of the linear plot of $\log \Lambda_0$ versus $1/T$ gives the value of E_a (**Table VI.6**).

Table VI.6: Thermodynamic parameters for [bmim][Cl] in ACN.

$\Delta G_a^0 / \text{kJ}\cdot\text{mol}^{-1}$	$\Delta H_a^0 / \text{kJ}\cdot\text{mol}^{-1}$	$\Delta S_a^0 / \text{J K}^{-1}\text{mol}^{-1}$	$E_a / \text{kJ}\cdot\text{mol}^{-1}$
-16.33	-18.22	-6.35	8.55

To have a better understanding of the thermodynamics of the ion-association process, it is beneficial to consider the contributions obtained from the thermodynamic parameters. The ΔH_a^0 and ΔS_a^0 values for the ion-association process

were evaluated by applying the linear least-squares analysis according to the equation:

$$\ln K_a = -\frac{\Delta H_a^\circ}{RT} + \frac{\Delta S_a^\circ}{R} \quad (12)$$

From the slopes and intercepts of linear Plots of $\ln K_a$ vs. $\frac{1}{T}$ (**Figure VI.2**) the values of enthalpy (ΔH_a°) and entropy (ΔS_a°) of ion association process were determined and the results are also included in **Table VI.6**. Both of these two parameters have negative values. The negative values of enthalpy confirm that when ion association occurs the overall energy of the system is decreased, i.e., there is some stabilization interaction in the system, whereas negative values of entropy factor indicate that there is an ordered arrangement, i.e., ion pair formation takes place. The negative value of entropy is unfavorable for the spontaneity of the system, but this effect is overcome by higher negative value of ΔH° . The value of ΔG_a° was calculated by using equation $\Delta G_a^\circ = \Delta H_a^\circ - T \Delta S_a^\circ$. The negative values of ΔG_a° (**Table VI.6**) suggests that the ion pair formation process proceeds spontaneously.

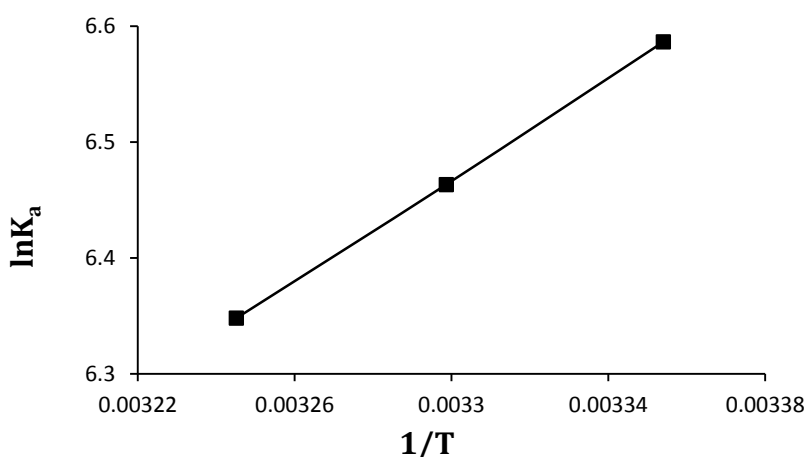


Figure VI.2: The linear relationships of $\ln K_a$ vs. $1/T$ for the ion pair formation in ACN.

VI.3.1.3 Triple-ion formation:

Figure VI.3 shows the deviations in the conductance curves from linearity which indicates the triple ion formation. The curves shows a decrease in conductance values with increasing concentration, reaches a minimum and then increases.

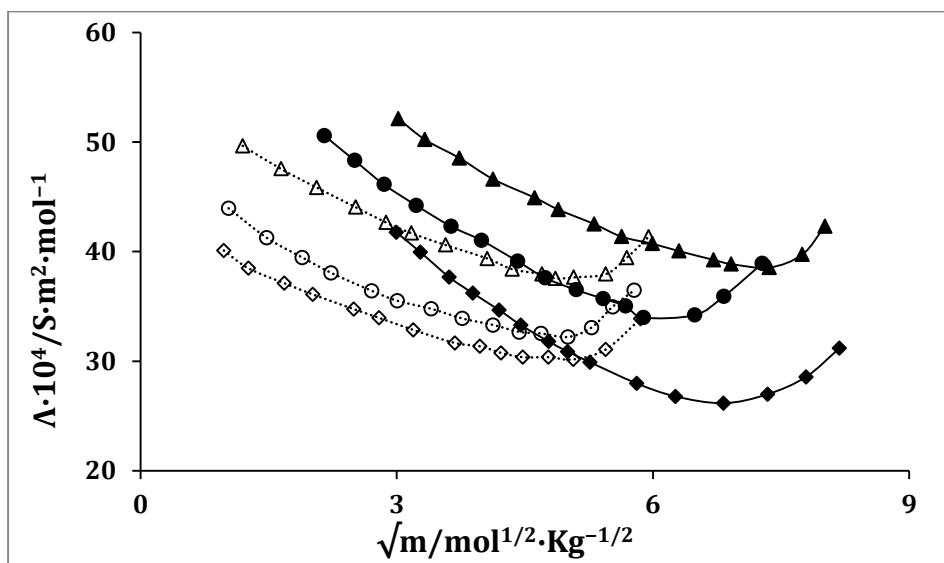


Figure VI.3: Plot of molar conductance (Λ) versus \sqrt{m} for [bmim][Cl] in DCM at 298.15 K (\blacklozenge), 303.15 K (\bullet) and 308.15 K (\blacktriangle) and in THF at 298.15 K (\diamond), 303.15 K (\circ) and 308.15 K (Δ).

The conductance data for the IL in THF and DCM have been analyzed by the classical Fuoss-Kraus theory of triple-ion formation in the form [31, 35]:

$$\Lambda g(c)\sqrt{c} = \frac{\Lambda_0}{\sqrt{K_p}} + \frac{\Lambda_0^T K_T}{\sqrt{K_p}} \left(1 - \frac{\Lambda}{\Lambda_0}\right) c \quad (13)$$

Where $g(c)$ is a factor that lumps together all the intrinsic interaction terms and is defined by:

$$g(c) = \frac{\exp\{-2.303 \beta' (c\Lambda)^{0.5} / \Lambda_0^{0.5}\}}{\{1 - S(c\Lambda)^{0.5} / \Lambda_0^{1.5}\} (1 - \Lambda / \Lambda_0)^{0.5}} \quad (14)$$

$$\beta' = 1.8247 \times 10^6 / (\epsilon T)^{1.5} \quad (15)$$

$$S = \alpha \Lambda_0 + \beta = \frac{0.8204 \times 10^6}{(\epsilon T)^{1.5}} \Lambda_0 + \frac{82.501}{\eta (\epsilon T)^{0.5}} \quad (16)$$

In the above equations, Λ_0 is the sum of the molar conductance of the simple ions at infinite dilution, Λ_0^T is the sum of the conductance value of the two triple-ions [bmim⁺]₂Cl⁻ and bmim⁺[Cl⁻]₂. $K_P \approx K_A$ and K_T are the ion-pair and triple-ion formation constants respectively and S is the limiting Onsager coefficient. To make equation (13) applicable, the symmetrical approximation of the two possible formation constants of triple-ions, $K_{T1} = \frac{[(\text{bmim}^+)_2][\text{Cl}^-]}{[\text{bmim}^+][\text{bmim}][\text{Cl}^-]}$ and $K_{T2} = \frac{[\text{bmim}][(\text{Cl}^-)_2]}{[\text{Cl}^-]}$

[[bmim][Cl]] equal to each other has been adopted, i.e. $K_{T1} = K_{T2} = K_T$ [36] and values for the studied electrolyte have been calculated following the scheme as suggested by Krumgalz [37]. Λ_0^T has been calculated by setting the triple-ion conductance equal to $\frac{2}{3} \frac{\Lambda_0^T}{\Lambda_0}$ [38].

Thus, the ratio $\frac{\Lambda_0^T}{\Lambda_0}$ was set equal to 0.667 during linear regression analysis of equation (13). The linear regression analysis of equation (13) for the electrolytes with an average regression constant, $R^2 = 0.9436$, gives intercepts and slopes. The calculated limiting molal conductance of simple ion (Λ_0), limiting molal conductance of triple ion (Λ_0^T), slope and intercept of equation (13) for [bmim][Cl] in DCM, THF at different temperature are given in **Table VI.7**.

Table VI.7: The calculated limiting molar conductance of ion-pair (Λ_0), limiting molar conductances of triple ion Λ_0^T , experimental slope and intercept obtained from Fuoss-Kraus Equation for [bmim][Cl] in DCM and THF at 298.15 K, 303.15 K and 308.15 K respectively.

Solvents	$\Lambda_0 \cdot 10^4$ /S·m ² ·mol ⁻¹	$\Lambda_0^T \cdot 10^4$ /S·m ² ·mol ⁻¹	Slope × 10 ⁻²	Intercept × 10 ⁻²
298.15 K				
DCM	42.71	28.83	0.19	-5.21
THF	35.59	23.61	0.14	-6.83
303.15 K				
DCM	47.53	31.35	0.34	-5.27
THF	39.33	25.15	0.27	-6.91
308.15 K				
DCM	52.43	35.59	0.46	-5.53
THF	43.93	27.98	0.47	-7.83

We obtain K_P and K_T by applying the Fuoss-Kraus equation, the values are presented in **Table VI.8**.

Table VI.8: Salt concentration at the minimum conductivity (C_{\min}) along with the ion-pair formation constant (K_P), triple ion formation constant (K_T) for [bmim][Cl] in DCM and THF at 298.15 K, 303.15 K and 308.15 K respectively.

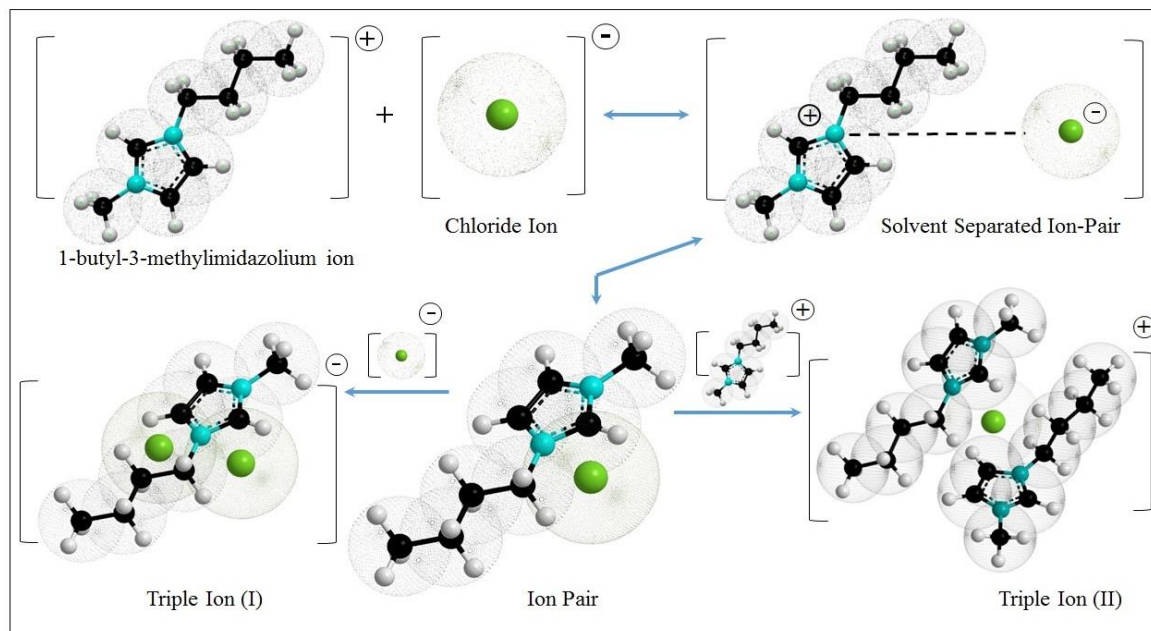
Solvents	$c_{\min} \cdot 10^4 /$ $\text{mol} \cdot \text{dm}^{-3}$	$\log c_{\min}$	$K_P \cdot 10^2 /$ $(\text{mol} \cdot \text{dm}^{-3})^{-1}$	$K_T \cdot 10^3 /$ $(\text{mol} \cdot \text{dm}^{-3})^{-1}$	$K_T / K_P \cdot 10^5$	$\log K_T / K_P$
298.15 K						
DCM	5.31	0.7298	5.62	57.63	10.25	1.011
THF	5.25	0.7158	5.25	62.54	11.91	1.076
303.15 K						
DCM	6.36	0.8655	5.18	64.21	12.39	1.093
THF	5.38	0.7291	5.03	67.59	13.44	1.128
308.15 K						
DCM	7.12	0.8675	5.03	66.97	13.31	1.124
THF	5.51	0.7381	4.98	69.95	14.05	1.148

These values permit the calculation of other derived parameters such as K_P and K_T listed in **Table VI.8**. The values of K_P and K_T predicts that a major portion of the electrolytes exists as ion-pairs with a minor portion as triple ions. The tendency of triple ion formation can be judged from the K_T/K_P ratios and $\log (K_T/K_P)$, which are highest in THF. These ratios suggest that strong association between the ions is due to the coulombic interactions as well as covalent forces present in the solution. These results are in good agreement with those of Hazra et al. [39]. At very low permittivity of the solvent, i.e., $\epsilon < 10$, electrostatic ionic interactions are very large. So the ion-pairs attract the free cations (+ve) or anions (-ve) present in the solution medium as the distance of the closest approach of the ions becomes minimum resulting in the formation of triple-ions, which acquires the charge of the respective ions, attracted from the solution bulk [34, 35], i.e.,



Where M^+ is [bmim⁺] and A^- is [Cl⁻]. The effect of ternary association [40] thus removes some non-conducting species, MA, from solution, and replaces them with triple-ions which increase the conductance manifested by non-linearity observed in conductance

curves for the electrolyte in DCM, THF [Figure VI.3]. The pictorial representation of triple-ion formation for the selected ionic liquid ([bmim⁺][Cl⁻]) in DCM and THF solvents is depicted in Scheme VI.2.



Scheme VI.2: Pictorial representation of ion-pair and triple-ion formation for the electrolyte in diverse solvent systems.

The ion-pair and triple-ion concentrations, C_P and C_T , respectively of the IL in DCM, THF have also been calculated using the following set of equations [41]

$$\alpha = 1 / (K_P^{1/2} \cdot C^{1/2}) \quad (20)$$

$$\alpha_T = (K_T / K_P^{1/2}) C^{1/2} \quad (21)$$

$$C_P = C(1 - \alpha - 3\alpha_T) \quad (22)$$

$$C_T = (K_T / K_P^{1/2}) C^{3/2} \quad (23)$$

The fraction of ion-pairs (α) and triple-ions (α_T) present in the salt-solutions are given in **Table VI.9**. The calculated values of C_P and C_T are also presented in **Table VI.9**. Comparison of the C_P and C_T values shows that the C_P is higher than C_T , indicating that the major portion of ions are present as ion-pairs even at high concentrations, and a small fraction exist as triple-ions. The conductance value decreases with increasing concentration and reach a minimum called Λ_{\min} . The concentration at

which the conductance value reaches a minimum is termed C_{\min} (**Table VI.9**); after that the fraction of triple-ions in the solution increases with the increasing concentration in the studied solution medium.

Table VI.9: Salt concentration at the minimum conductivity (c_{\min}), the ion pair fraction (α), triple ion fraction (α_T), ion pair concentration (c_P) and triple-ion concentration (c_T) for [bmim][Cl] in DCM and THF at 298.15 K, 303.15 K and 308.15 K respectively.

Solvents	$c_{\min} \cdot 10^4 / \text{mol} \cdot \text{dm}^{-3}$	$\alpha \cdot 10^{-2}$	$\alpha_T \cdot 10^2$	$c_P \cdot 10^{-3} / \text{mol} \cdot \text{dm}^{-3}$	$c_T \cdot 10^{-2} / \text{mol} \cdot \text{dm}^{-3}$
298.15 K					
DCM	6.89	14.98	57.34	0.96	3.43
THF	5.19	17.67	59.23	0.94	3.12
303.15 K					
DCM	6.86	15.21	65.24	1.56	5.45
THF	5.11	16.14	67.81	1.04	3.46
308.15 K					
DCM	6.84	18.34	71.26	1.61	5.97
THF	5.04	15.93	68.92	1.21	3.62

VI.3.2. Volumetric Properties:

The apparent molar volume (ϕ_V) and limiting apparent molar volume (ϕ_V^0) provide information regarding the solute-solvent interactions present in our systems. [42]. The apparent molal volume of the IL can be considered to be the sum of the geometric volume of the solute molecule [bmim][Cl] and changes in the solvent volume due to its interaction with the solute [43]. The values of ϕ_V of the IL (**Table VI.10**) at different concentrations were calculated using density data (**Table VI.11**) through the following equation:

$$\phi_V = M / \rho - (\rho - \rho_0) / m \rho_0 \rho \quad (24)$$

Where M is the molar mass of the solute, m is the molality of the solution, ρ and ρ_0 are the densities of the solution and solvent, respectively.

Table VI.10: Density (ρ) and viscosity (η) of 1-butyl-3-methylimidazolium chloride in different mass fraction of Acetonitrile, Dichloromethane and Tetrahydrofuran at different temperatures.

molality/mol·kg ⁻¹	$\rho \cdot 10^{-3}/\text{kg m}^{-3}$		$\eta/\text{mPa s}$
	ACN	298.15 K	
0.0127		0.78713	0.38
0.0319		0.78893	0.40
0.0510		0.79078	0.42
0.0702		0.79267	0.43
0.0895		0.79460	0.45
0.1087		0.79656	0.46
303.15 K			
0.0128		0.78389	0.36
0.0320		0.78563	0.38
0.0513		0.78742	0.39
0.0705		0.78925	0.40
0.0899		0.79112	0.42
0.1092		0.79303	0.43
308.15 K			
0.0128		0.78101	0.35
0.0321		0.78266	0.36
0.0515		0.78437	0.38
0.0708		0.78613	0.39
0.0902		0.78792	0.40
0.1097		0.78975	0.42
DCM		298.15 K	
0.0076		1.32586	0.45
0.0189		1.32618	0.47
0.0303		1.32658	0.49
0.0417		1.32704	0.51
0.0532		1.32756	0.53
0.0647		1.32814	0.55

303.15 K		
0.0076	1.31863	0.42
0.0190	1.31890	0.44
0.0305	1.31924	0.46
0.0420	1.31965	0.47
0.0535	1.32012	0.49
0.0651	1.32074	0.51
308.15 K		
0.0076	1.30963	0.40
0.0192	1.30985	0.42
0.0307	1.31016	0.44
0.0423	1.31055	0.46
0.0539	1.31099	0.47
0.0655	1.31158	0.49
THF 298.15 K		
0.0113	0.88627	0.49
0.0283	0.88676	0.51
0.0454	0.88733	0.53
0.0626	0.88796	0.55
0.0799	0.88864	0.57
0.0972	0.88934	0.59
303.15 K		
0.0113	0.88616	0.47
0.0283	0.88662	0.50
0.0454	0.88715	0.52
0.0626	0.88774	0.55
0.0799	0.88839	0.57
0.0972	0.88907	0.59
308.15 K		
0.0113	0.88607	0.42
0.0283	0.88648	0.44
0.0455	0.88697	0.46
0.0627	0.88750	0.48
0.0799	0.88810	0.50
0.0973	0.88874	0.53

Table VI.11: Apparent molal volume (ϕ_V) and $\frac{(\eta_r - 1)}{\sqrt{m}}$ for 1-butyl-3-methylimidazolium Chloride ([bmim][Cl]) in different mass fraction of Acetonitrile, Dichloromethane and Tetrahydrofuran at different temperatures.

Molality /mol·kg ⁻¹	$\phi_V \cdot 10^6$ /m ³ ·mol ⁻¹	$\frac{(\eta_r - 1)}{\sqrt{m}}$	Molality /mol·kg ⁻¹	$\phi_V \cdot 10^6$ /m ³ ·mol ⁻¹	$\frac{(\eta_r - 1)}{\sqrt{m}}$	Molality /mol·kg ⁻¹	$\phi_V \cdot 10^6$ /m ³ ·mol ⁻¹	$\frac{(\eta_r - 1)}{\sqrt{m}}$
ACN			298.15 K			303.15 K		
0.0127	74.66	0.556	0.0128	81.35	0.286	0.0128	89.34	0.235
0.0319	71.61	0.703	0.0320	77.52	0.488	0.0321	85.49	0.409
0.0510	69.25	0.778	0.0513	74.96	0.571	0.0515	82.61	0.529
0.0702	67.26	0.829	0.0705	72.87	0.658	0.0708	80.13	0.627
0.0895	65.39	0.924	0.0899	70.95	0.756	0.0902	78.17	0.700
0.1087	63.73	0.953	0.1092	69.10	0.804	0.1097	76.29	0.807
DCM			298.15 K			303.15 K		
0.0076	120.45	0.465	0.0076	124.14	0.244	0.0076	127.28	0.256
0.0189	117.58	0.588	0.0190	120.95	0.463	0.0192	124.23	0.487
0.0303	115.36	0.698	0.0305	118.83	0.610	0.0307	121.74	0.641
0.0417	113.52	0.793	0.0420	116.90	0.666	0.0423	119.51	0.754
0.0532	111.83	0.879	0.0535	115.15	0.737	0.0539	117.68	0.804
0.0647	110.20	0.957	0.0651	113.65	0.837	0.0655	115.86	0.879
THF			298.15 K			303.15 K		
0.0113	165.55	0.208	0.0113	168.96	0.444	0.0113	173.48	0.244
0.0283	162.39	0.395	0.0283	165.12	0.675	0.0283	169.19	0.463
0.0454	159.35	0.521	0.0454	162.18	0.811	0.0455	165.86	0.610
0.0626	156.73	0.622	0.0626	159.62	0.919	0.0627	163.53	0.728
0.0799	154.43	0.709	0.0799	157.18	1.016	0.0799	161.06	0.830
0.0972	152.67	0.786	0.0972	155.21	1.075	0.0973	158.94	0.934

The values of the the apparent molar volume at infinite dilution (ϕ_V^0) and the experimental slopes (S_V^*) were determined by using leastsquares fitting of the linear plots of ϕ_V against the square root of the molar concentrations ($m^{1/2}$) using the Masson equation [44].

$$\phi_V = \phi_V^0 + S_V^* \cdot \sqrt{m} \quad (25)$$

The calculated values of ϕ_V^0 and S_V^* are reported in **Table VI.12**.

Table VI.12: Limiting apparent molar volume (ϕ_V^0), experimental slope (S_V^*), viscosity *B*-and viscosity *A*- coefficient for [bmim[Cl] in ACN, DCM and THF at T= (298.15 to 308.15) K respectively.

Solvents	$\phi_V^0 \cdot 10^6$ /m ³ ·mol ⁻¹	$S_V^* \cdot 10^6$ /m ³ ·mol ^{-3/2} ·kg ^{1/2}	<i>B</i> /kg ^{1/2} ·mol ^{-1/2}	<i>A</i> /kg ^{-1/2} ·mol ^{-1/2}
298.15 K				
ACN	80.511	-50.44	2.0710	+0.3593
DCM	125.89	-61.04	2.5905	+0.1910
THF	172.77	-64.16	3.0063	-0.0855
303.15 K				
ACN	87.607	-55.78	2.6746	+0.0371
DCM	129.6	-62.31	2.9687	-0.0252
THF	176.32	-67.25	3.3026	+0.1360
308.15 K				
ACN	96.189	-60.06	2.9162	-0.0555
DCM	133.46	-67.99	3.2438	-0.0381
THF	181.02	-70.56	3.5642	-0.1072

The plot of ϕ_V^0 values for the studied IL in different solvent systems at different temperatures has shown in **Figure VI.4**. The values of ϕ_V^0 are positive for all the systems and is highest in THF, suggesting presence of strong solute-solvent interactions in case of THF than in DCM than in ACN shown in the **Scheme VI.3**.

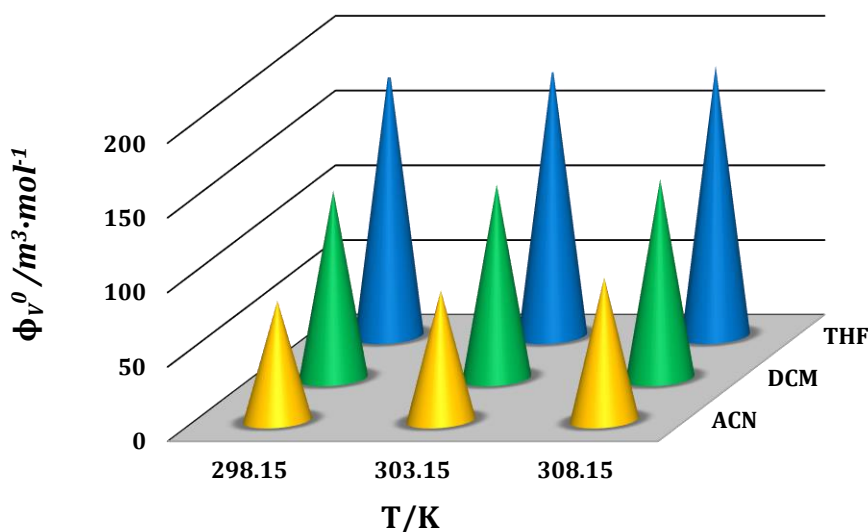
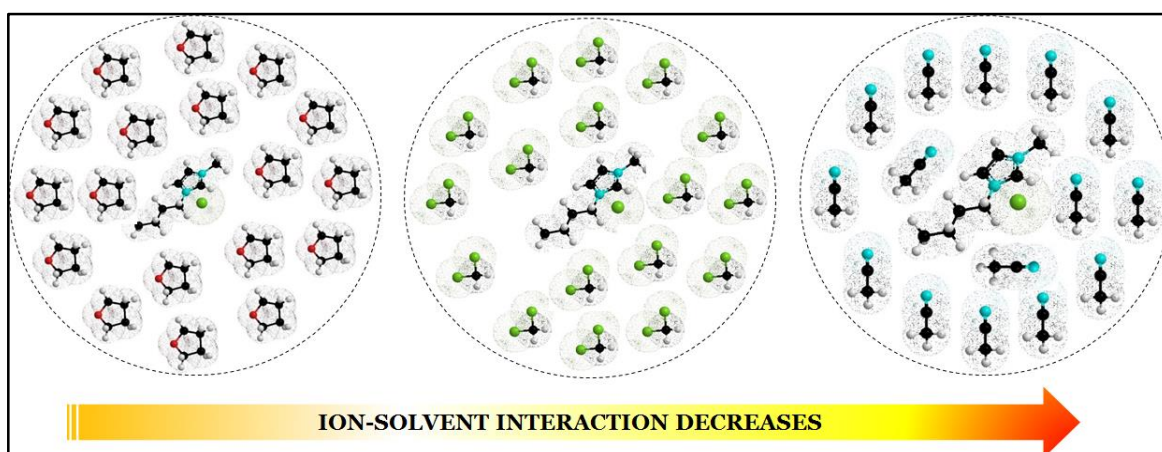


Figure VI.4: Plot of limiting apparent molal volume (ϕ_V^0) versus temperature for [bmim][Cl] in ACN (yellow), DCM (green) and THF (blue).

The values of ϕ_V^0 increases with an increase in temperature which indicates that stronger interaction occur between the IL and solvent at higher temperatures [45, 46]. Because of the release of some of the solvent molecules from loose solvation layers during the solute solvent interactions, the value of ϕ_V^0 increases with the increase in temperature.



Scheme VI.3: Extent of ion-solvent interaction of IL in various solvent systems.

The highest values of ϕ_V^0 in THF leads to lower conductance of [bmim][Cl] than in DCM and ACN as discussed in above section. The S_V^* values designate the extent of ion-ion interaction and the small values indicates the presence of less ion-ion interaction

in the medium. The degree of ion-ion interactions are highest in case of ACN and are lowest in THF. A quantitative comparison shows that the magnitude of ϕ_V^0 values is much greater than the magnitude of S_V^* values suggests that the ion-solvent interactions dominant over ion-ion interactions.

VI.3.3. Temperature dependent limiting apparent molal volume

The variation of ϕ_V^0 values with temperature can be expressed by the general polynomial equation as follows,

$$\phi_V^0 = a_0 + a_1T + a_2T^2 \quad (26)$$

Where T is the temperature in degree kelvin and a_0 , a_1 , a_2 are the empirical coefficients and the values of these coefficients have been calculated by the least-squares fitting of apparent molar volume at different temperatures [Table VI.13].

Table VI.13: Values of empirical coefficients (a_0 , a_1 , and a_2) of Equation 26 of the [bmim][Cl] in ACN, DCM and THF.

Solvents	$a_0 \cdot 10^6$	$a_1 \cdot 10^6$	$a_2 \cdot 10^6$
	/m ³ ·mol ⁻¹	/m ³ ·mol ⁻¹ ·K ⁻¹	/m ³ ·mol ⁻¹ ·K ⁻²
ACN	2343.6	-16.451	0.0297
DCM	175.82	-1.062	0.0030
THF	2039.9	-13.12	0.0230

The limiting apparent molar expansibilities, ϕ_E^0 , can be obtained by the following equation,

$$\phi_E^0 = \left(\delta \phi_V^0 / \delta T \right)_P = a_1 + 2a_2T \quad (27)$$

Differentiation of equation 26 with respect to temperature gives the values of the limiting apparent molar expansibilities (ϕ_E^0) [Table VI.14]. These values are also employed in interpreting of the structure-making or breaking properties of various solutes. Positive expansivity i.e increasing volume with increasing temperature is a characteristic property of nonaqueous solutions of hydrophobic solvation [47].

Table VI.14: Limiting apparent molal expansibilities (ϕ_E^0) of [bmim][Cl] in ACN, DCM and THF at T= (298.15 to 308.15) K.

T/ K ^a	$\phi_E^0 \cdot 10^6$ /m ³ ·mol ⁻¹ ·K ⁻¹	$(\partial\phi_E^0/\partial T)_P \cdot 10^6$ /m ³ ·mol ⁻¹ ·K ⁻²
[bmim][Cl]+ ACN		
298.15	0.595	
303.15	0.825	0.046
308.15	1.055	
[bmim][Cl]+ DCM		
298.15	0.727	
303.15	0.757	0.006
308.15	0.787	
[bmim][Cl]+ THF		
298.15	1.259	
303.15	1.556	0.059
308.15	1.853	

^aStandard uncertainties in temperature (T) = ±0.01 K.

Hepler [48] developed a method of investigative the sign of $(\delta\phi_E^0/\delta T)_P$ for the solute in terms of long-range structure-making and -breaking capacity of the solute in the solution using the general thermodynamic expression,

$$(\delta\phi_E^0/\delta T)_P = (\delta^2\phi_V^0/\delta T^2)_P = 2a_2 \quad (28)$$

If the sign of the second derivatives of the limiting apparent molal volume with respect to the temperature $(\delta\phi_E^0/\delta T)_P$ is positive or a small negative, the molecule is a structure maker; otherwise, it is a structure breaker [49]. It is evident from **Table VI.14** that the values for all the complexes are positive i.e. [bmim][Cl] is predominantly structure makers in all the solvent systems studied here.

VI.3.4. Viscosity B Coefficients

The experimental values of viscosity (η) measured at different temperatures for the studied systems under investigation are listed in **Table VI.11**. The relative viscosity (η_r) has been analyzed applying the Jones-Dole equation [50]

$$(\eta/\eta_0 - 1)/\sqrt{m} = (\eta_r - 1)/\sqrt{m} = A + B\sqrt{m} \quad (29)$$

Where relative viscosity $\eta_r = \eta/\eta_0$, η_0 and η are the viscosities of the solvent and solution respectively, and m is the molality of the IL in the solutions. A and B are experimental constants known as viscosity A - and B -coefficients, which are specific to ion-ion and ion-solvent interactions, respectively. The values of A and B coefficients are obtained from the slope of linear plot of $(\frac{\eta}{\eta_0} - 1)/\sqrt{m}$ against \sqrt{m} (**Table VI.10**)

by least-squares method, and reported in **Table VI.12**.

The viscosity B coefficient is a measure of the effective solvodynamic volume of solvated species and depends on shape, size, and ion-ion interactions [51]. Positive values of the B -coefficient indicates the presence of strong ion-solvent interaction of the IL in the studied solvent system. This type of ion-solvent interaction arises mainly due to the hydrogen bonding of the solvent with the IL molecule and resulting in an increase in viscosity of the solution due to the large size of the moving molecules. The higher values of the B -coefficient are due to the solvated solutes molecule associated by the solvent molecules all round to the formation of associated molecule by ion-solvent interaction, would present greater resistance, and this type of interactions are strengthened with a rise in temperature and follow the trend THF > DCM > ACN [**Figure VI.5**]. These observations are in excellent agreement with the conclusions drawn from the analysis of apparent molal volume, ϕ_V^0 discussed earlier.

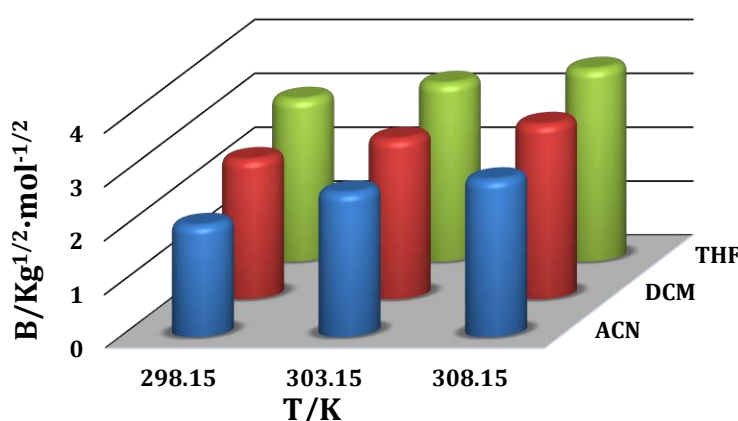


Figure VI.5: Plot of viscosity B -coefficient versus temperature for [bmim][Cl] in ACN (blue), DCM (red) and THF (green).

Thus, the volumetric and viscometric properties of the sulfa drug in the present work provide useful information in medicinal and pharmaceutical chemistry for the prediction of absorption and permeability of drug through membranes.

VI.3.5. Infrared Spectroscopy

Solvation is caused by specific interactions of functional groups. The FT-IR spectroscopy provide the supportive evidence for such type of ion-solvent interactions present in the studied solvent system. The IR spectra of the pure solvents as well as the solutions of {[bmim][Cl] + solvents} were investigated in the wave number range 400–4000 cm^{-1} and the stretching frequencies of the functional groups are given in **Table VI.15**.

Table VI.15: Stretching frequencies of the functional groups present in the pure solvent and change of frequency after addition of [bmim][Cl] in the solvents.

Solvents	Functional Group	Stretching frequencies (cm^{-1})	
		Pure Solvents	Solvent + [bmim][Cl]
ACN	$\text{C}\equiv\text{N}$	2253.66	2290.64
DCM	C-Cl	746.54	736.00
THF	C-O	1069.30	1086.00

The $\nu(\text{C}\equiv\text{N})$ stretching vibrations of ACN is observed at 2253.66 cm^{-1} and this peak is shifted to 2290.64 cm^{-1} when the IL is added to ACN solvent. The shifts of the IR spectra occurs due to the disruption of the dipole–dipole interaction of acetonitrile [52] leading to the formation of ion–dipole interaction between the [bmim]⁺ ions and $\text{C}\equiv\text{N}$ bond. A sharp peak for C-O is obtained at 1069.30 cm^{-1} in case of THF and a peak for C-Cl is obtained at 746.54 cm^{-1} in DCM. After addition of IL to THF and DCM solvent these peaks are shifted to 1086 cm^{-1} and 736 cm^{-1} respectively. The observed shifts in the bands are due to the disruption of weak H-bonding interaction between the solvent molecules and formation of ion–dipole interaction between IL and solvent molecules [26].

VI.4. CONCLUSION

An extensive study was done on the ion-solvation behavioural aspect of the IL 1-butyl-3-methylimidazolium chloride in industrially-important non-aqueous polar solvents acetonitrile (CH_3CN), dichloromethane (CH_2Cl_2) and tetrahydrofuran ($\text{C}_4\text{H}_8\text{O}$) with the help of conductometric, FTIR, density and viscosity measurements. From the conductometric measurements it becomes clear that the IL exists as ion-pairs in acetonitrile and as triple ions in tetrahydrofuran, dichloromethane solvents. The tendency of the ion-pair and triple-ion formation of $[\text{bmim}][\text{Cl}]$ depends on the dielectric constant of the medium. The present study revealed that this type of experimental study is being accompanied for a better understanding of the interionic interactions of ionic liquids. The evaluated values of thermodynamic functions of association suggest the spontaneity of the association process.

CHAPTER-VII

INTERACTIONS BETWEEN AN ANTIFUNGAL SULFA DRUG AND DIVERSE MACROCYCLIC POLYETHERS EXPLAINING MECHANISM, PERFORMANCE AND PHYSIOGNOMIES LEADING TO FORMATION OF STABLE COMPLEXES

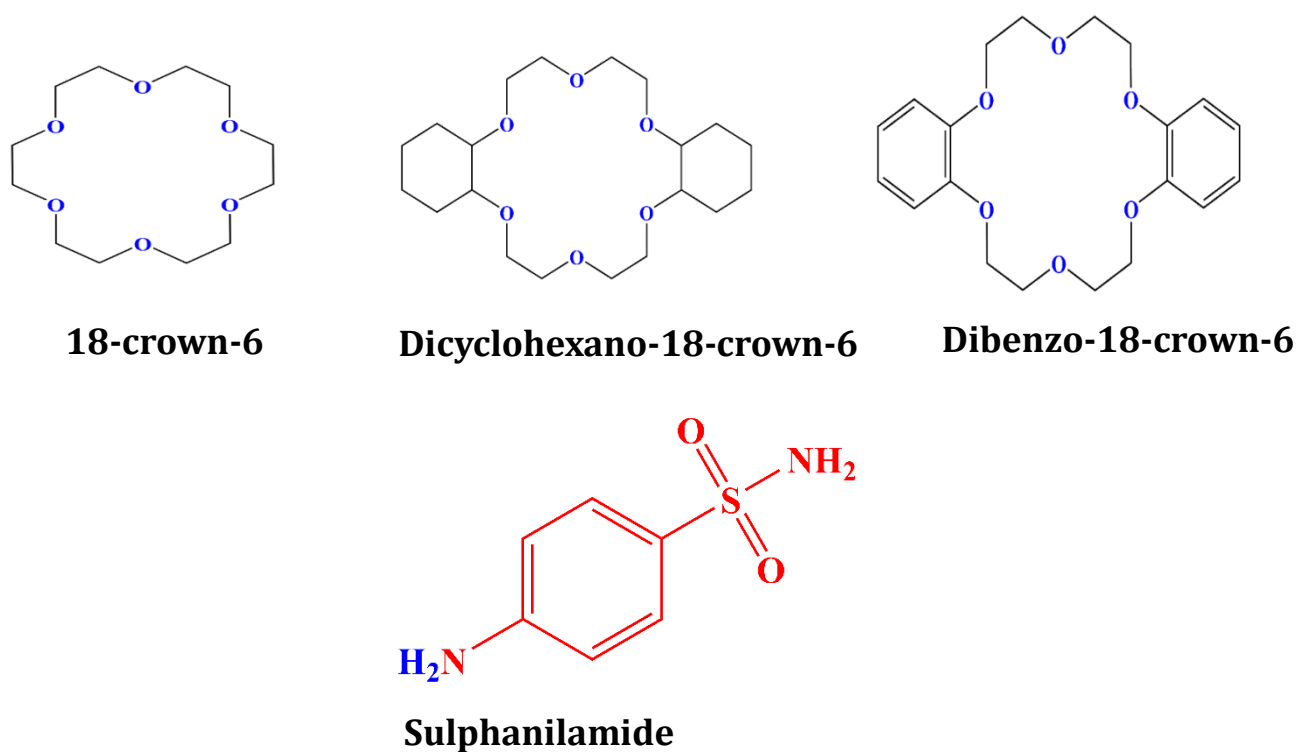
VII.1. INTRODUCTION

Crown ethers are macrocyclic ligands discovered by Pedersen 1967 [1-3]. Crown ethers are one of the most widely studied family of host compounds in the field of supramolecular chemistry, involving non-covalent interactions. The important characteristics of crown ethers are the number and type of donor atoms, the dimension of the macrocyclic cavity and the preorganization of the host molecule for most effective coordination. Macrocyclic compounds can form complexes with inorganic cations, organic cations and organic neutral molecules in their cavity via different types of interactions with multiple oxygen atoms [4, 5]. Applications of CEs as drug carriers [6] has been in progress on the basis of their inclusion ability. Crown ethers have proved to be unique cyclic molecules for molecular recognition of suitable substrates by hydrogen bonds, ionic interactions and hydrophobic interactions. The study of interactions involved in the complex formation is important for a better understanding of the mechanism of biological transport, molecular recognition, and other analytical applications [7]. They also have medical applications as diagnostic or therapeutic agents [8, 9].

Sulfonamides are considered as an important group of drugs which are used widely as antimicrobial, high ceiling diuretics, anti-thyroid and anti-inflammatory agents [10]. Sulfanilamide, 4-aminobenzenesulfonamide, is the simplest representative in the group of sulfonamide drugs [11]. This compound is an antibacterial and antimicrobial agent used in the treatment of both topical and internal infections. It can be found in

medications for vaginal and urinary tract infections as well as in medications for pneumonia, bowel diseases and other infections. It works by stopping the growth of yeast (fungus) that causes the infection. Further research may identify additional product or industrial usages of this chemical. Powdered sulfanilamide was used by the Allies in WWII to reduce infection rates.

In this work, we have studied the complexation of Sulfanilamide (SA) with three different crown ethers (CEs) (1) Dicyclohexano-18-crown-6 (DC18C6) [complex 1], (2) 18-crown-6 (18C6) [complex 2] and (3) Dibenzo-18-crown-6 (DB18C6) [complex 3] in acetonitrile (ACN). The complexes were characterized by ^1H NMR, IR and UV-visible spectra. The structure of the SA and all crown ethers are shown in **Scheme VII.1**.



Scheme VII.1: Molecular structure of crown ethers and SA.

VII.2. EXPERIMENTAL SECTION

VII.2.1 Reagents

The sulfa drug (99%) and crown ethers [18C6 (99%), DB18C6 (98%), DC18C6 (98%)] were bought from Sigma-Aldrich, Germany and used as purchased.

VII.2.2 Instrumentations

Prior to the start of the experimental work solubility of the chosen CEs and SA in ACN have been precisely checked and it was observed that the selected sulfa drug freely soluble in all proportion of CEs solution.

Infrared spectra were recorded in 8300 FT-IR spectrometer (Shimadzu, Japan). The details of the instrument have formerly been described [12]. The FTIR measurements were performed in the scanning range of 4000–400 cm^{-1} at room temperature.

^1H NMR spectra were recorded in CD_3CN at 300 MHz using Bruker ADVANCE 300 MHz instrument. Signals are quoted as δ values in ppm using residual protonated solvent signals as internal standard (CD_3CN : δ 1.97 ppm). Data are reported as chemical shift.

UV-visible spectra were recorded by JASCO V-530 UV/VIS Spectrophotometer, with an uncertainty of wavelength resolution of ± 2 nm. All the absorption spectra were recorded at $25^\circ\text{C} \pm 1^\circ\text{C}$. The measuring temperature was held constant by an automated digital thermostat.

The densities (ρ) of the solutions were calculated by using vibrating *U*-tube Anton Paar digital density meter (DMA 4500M) having precision ± 0.00005 g cm^{-3} and uncertainty in temperature was $\pm 0.01\text{K}$. The density meter was calibrated by standard method [13].

Viscosities (η) were determined by Brookfield DV-III Ultra Programmable Rheometer with spindle size 42. The detail has already been depicted before [13].

Refractive indexes of the solutions were studied with a Digital Refractometer from Mettler Toledo having uncertainty ± 0.0002 units. The detail has already been described before [13].

VII.3. RESULT AND DISCUSSION

VII.3.1 Job plot demonstrate the Stoichiometry

The continuous variation method (Job's plot) was used to determine the stoichiometry of SA-CEs complexes [14, 15]. The plot of $\Delta A \times R$ against R represents the job plot where ΔA is the differences in absorbance of sulfa drug with and without CEs and $R = [SA] / ([CEs] + [SA])$ and is presented in **Figure VII.1**. Absorbance values were measured at respective λ_{\max} for a series of solutions at 298.15 K.

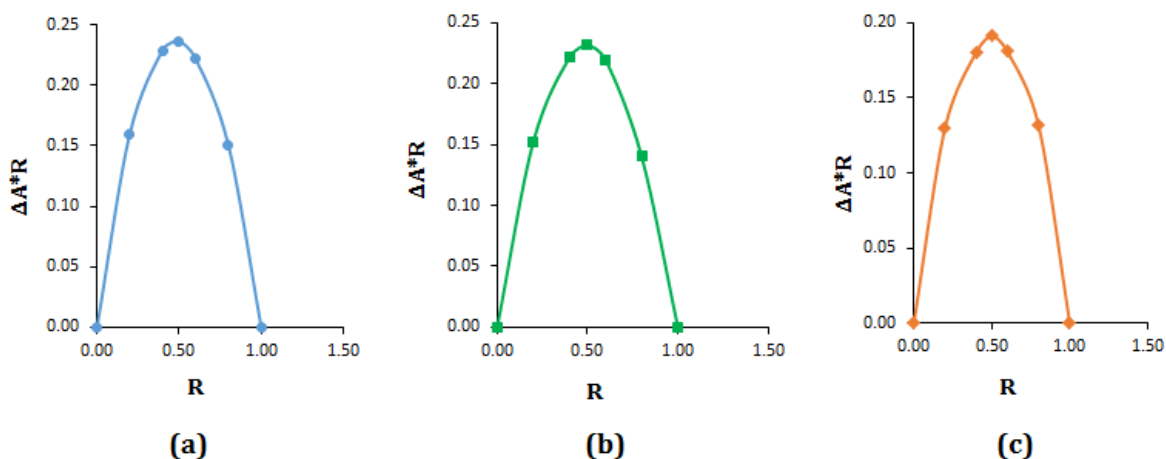


Figure VII.1: Job plot of (a) SA-DC18C6 system, (b) SA-18C6 system, (c) SA-DB18C6 system at $T = 298.15$ K.

In this method, the total molar concentration of the two binding partners ($[SA] + [CEs]$) is kept constant at $100\mu\text{M}$ but their mole fraction are varied so that the mole fractions of SA complete the range of 0-1 (**Table VII.1**, **Table VII.2** and **Table VII.3**) [16, 17].

Table VII.1: Data for the Job plot performed by UV-Vis spectroscopy for SA-DC18C6 system.

SA (mL)	DC18C6 (mL)	SA (μM)	DC18C6 (μM)	$R = \frac{[\text{SA}]}{[\text{SA}] + [\text{DC18C6}]}$	Absorbance (A)	ΔA	$\Delta A * R$
0	3	0	100	0.0	0.0	1.01185	0.0
0.6	2.4	20	80	0.2	0.21129	0.80056	0.16011
1.2	1.8	40	60	0.4	0.43896	0.57289	0.22915
1.5	1.5	50	50	0.5	0.53905	0.47280	0.23640
1.8	1.2	60	40	0.6	0.64153	0.37032	0.22219
2.4	0.6	80	20	0.8	0.82361	0.18824	0.15059
3	0	100	0	1	1.01185	0.0	0.0

Table VII.2: Data for the Job plot performed by UV-Vis spectroscopy for SA-18C6 system.

SA (mL)	18C6 (mL)	SA (μM)	18C6 (μM)	$R = \frac{[\text{SA}]}{[\text{SA}] + [\text{18C6}]}$	Absorbance (A)	ΔA	$\Delta A * R$
0	3	0	100	0.0	0.01981	0.99204	0.0
0.6	2.4	20	80	0.2	0.25067	0.76118	0.15224
1.2	1.8	40	60	0.4	0.45858	0.55327	0.22131
1.5	1.5	50	50	0.5	0.54919	0.46266	0.23133
1.8	1.2	60	40	0.6	0.64606	0.36579	0.21947
2.4	0.6	80	20	0.8	0.83681	0.17504	0.14003
3	0	100	0	1	1.01185	0.0	0.0

Table VII.3: Data for the Job plot performed by UV-Vis spectroscopy for SA-DB18C6 system.

SA (mL)	DB18C6 (mL)	SA (μ M)	DB18C6 (μ M)	$R = \frac{[SA]}{[SA] + [DB18C6]}$	Absorbance (A)	ΔA	ΔA^*R
0	3	0	100	0.0	0.25859	0.75326	0.0
0.6	2.4	20	80	0.2	0.36268	0.64917	0.12983
1.2	1.8	40	60	0.4	0.56147	0.45038	0.18015
1.5	1.5	50	50	0.5	0.62905	0.38280	0.19140
1.8	1.2	60	40	0.6	0.72059	0.29126	0.17475
2.4	0.6	80	20	0.8	0.84731	0.16454	0.13163
3	0	100	0	1	1.01185	0.0	0.0

According to this method, maximum point of the molar ratio (R) corresponds to the complexation stoichiometry. The each of the three plots in **Figure VII.1** shows the maximum at a molar ratio of about 0.5, indicating that the complexes were formed with 1:1 stoichiometry.

VII.3.2 FTIR spectral analysis

The complexation between the sulfa drug (SA) and CEs was investigated using FTIR spectroscopy. **Figure VII.2, VII.3** and **VII.4** depict the FTIR spectra of free SA, 18C6, DC18C6, DB18C6 and their corresponding complexes in the 4000–500 cm^{-1} region. The investigation of the inclusion complexes was complicated due to the strong stretching frequency of CEs overlapping with the bands of the drugs. The IR spectrum of SA drug (**Figure VII.2, Figure VII.3** and **Figure VII.4**) was characterised by principal absorption peaks at 3382 and 3242 cm^{-1} (for NH stretching and antistretching in $\text{SO}_2\text{-NH}$ group), 1310 cm^{-1} (for SO_2 asymmetric stretching), 1149 cm^{-1} (for SO_2 symmetric stretching) [18, 19]. The IR spectral features of the pure drug has changed in the complexes. The band assigned to the NH stretching and antistretching in $\text{SO}_2\text{-NH}$ group were shifted in all the complexes (**Figure VII.2, VII.3** and **VII.4**). The symmetric and asymmetric vibrations of

SO₂ group at 1149 and 1310 cm⁻¹ are shifted to 1124 cm⁻¹ and 1290 cm⁻¹ in complex 1, 1131 and 1296 cm⁻¹ in complex 2 and 1130 and 1291 cm⁻¹ in complex 3 respectively.

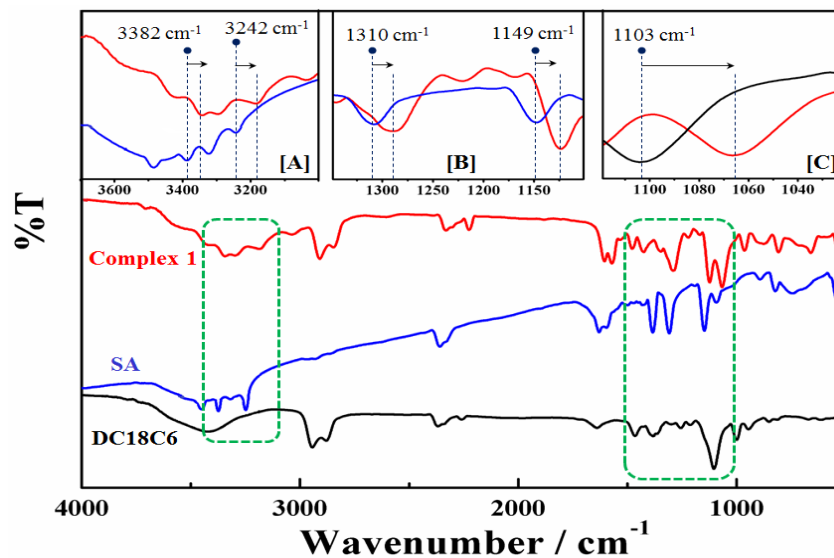


Figure VII.2: FTIR spectra of free DC18C6 (Black), SA (Blue) and complex 1 (Red).

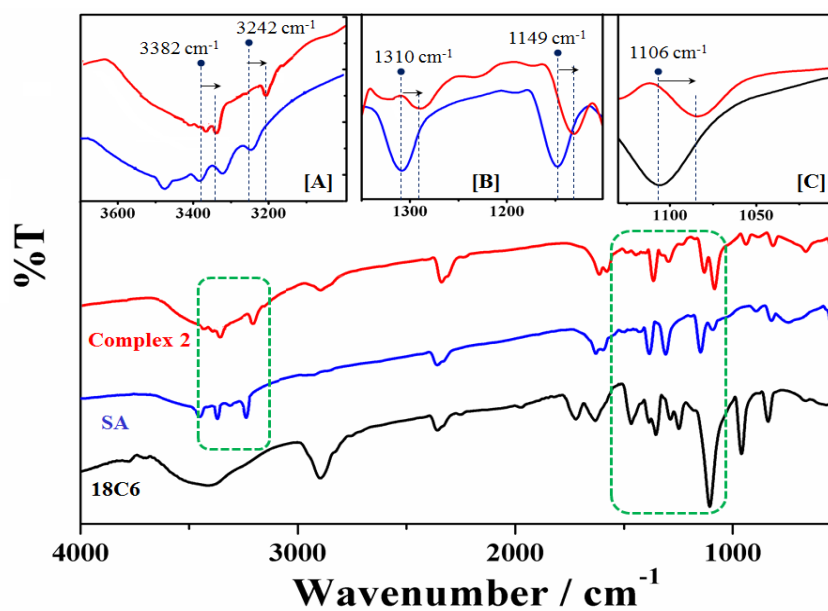


Figure VII.3: FTIR spectra of free 18C6 (Black), SA (Blue) and complex 2 (Red).

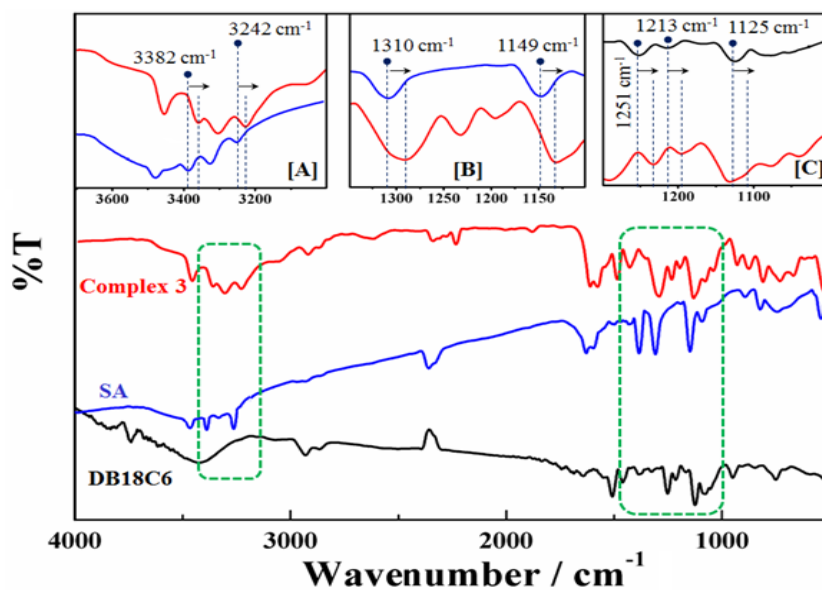


Figure VII.4: FTIR spectra of free DB18C6 (Black), SA (Blue) and complex 3 (Red).

In our investigation, the the NH stretching and anti-stretching in $\text{SO}_2\text{-NH}$ group were shifted to 3346 and 3187 cm^{-1} in complex 1 (**Figure VII.2**), 3349 and 3203 cm^{-1} in complex 2 (**Figure VII.3**) and 3357 and 3220 in complex 3 (**Figure VII.4**). The above changes can be due to the formation of SA-CEs inclusion complex formation. According to the above FTIR analysis of all the three complexes, we might suggest that the sulfonamide ring of the SA was involved in the complexation. The bands positioned at 1103 cm^{-1} corresponding to the $\nu(\text{C} - \text{O} - \text{C})$ of DC18C6 shifted to 1066 cm^{-1} in the complex 1 (**Figure VII.2**). The stretching frequencies of $\nu(\text{C} - \text{O} - \text{C})_{\text{aliph}}$ of 18C6 at 1106 cm^{-1} shifted to 1083 cm^{-1} in the complex 2 (**Figure VII.3**). The shift of IR spectra of crown ethers in ACN solution indicates that the specific interactions observed in the crown ether complexes are in fact due to the hydrogen bonds of SA with the donor atoms of the crown ether. Comparing with the spectrum of the free crown ethers, most of these bands are shifted to lower energy presumably due to less restriction on the coupling of some vibrational modes caused by bonding of oxygen atoms of the polyether ring with the in both the complexes. The $\nu(\text{C} - \text{O} - \text{C})_{\text{arom}}$ stretching vibrations of DB18C6 are observed at 1125 cm^{-1} and these peak is also shifted to lower frequency 1108 cm^{-1} in the complex

3 (**Figure VII.4**). The anisole oxygens of DB18C6 are also involved in H-bond formation in the complex 2, as indicated by the shifts of the $\nu_{as}(\text{Ph-O-C})$ and $\nu_s(\text{Ph-O-C})$ bands from 1213 and 1251 cm^{-1} to 1194 and 1231 cm^{-1} , respectively [20]. In the IR spectra, the bands in the 2800–3000 cm^{-1} region correspond to the CH stretching vibrations of the methylene groups of crown ethers. Selected IR data for the free compounds and their complexes and corresponding changes in frequencies are listed in **Table VII.4**.

Table VII.4: Comparison between the Frequencies change (cm^{-1}) of different functional group of free compound and their complexes.

Functional Group	Wavenumber (cm^{-1})		Changes (cm^{-1})
	DC18C6	Complex 1	
$\nu(\text{C} - \text{O} - \text{C})$	1103	1066	37
	18C6	Complex 2	
$\nu(\text{C} - \text{O} - \text{C})_{\text{aliph.}}$	1106	1083	23
	DB18C6	Complex 3	
$\nu(\text{C} - \text{O} - \text{C})_{\text{arom}}$	1125	1108	27
$\nu_{as}(\text{Ph-O-C})$	1213	1194	19
$\nu_s(\text{Ph-O-C})$	1251	1231	20
	SA	Complex 1	
$\nu_{as}(\text{NH}_2)_{\text{sulfonamide}}$	3382	3346	36
$\nu_s(\text{NH}_2)_{\text{sulfonamide}}$	3242	3187	55
$\nu_{as}(\text{SO}_2)$	1310	1290	20
$\nu_s(\text{SO}_2)$	1149	1124	25
	SA	Complex 2	
$\nu_{as}(\text{NH}_2)_{\text{sulfonamide}}$	3382	3349	33
$\nu_s(\text{NH}_2)_{\text{sulfonamide}}$	3242	3203	39
$\nu_{as}(\text{SO}_2)$	1310	1296	14
$\nu_s(\text{SO}_2)$	1149	1131	18
	SA	Complex 3	
$\nu_{as}(\text{NH}_2)_{\text{sulfonamide}}$	3382	3357	25
$\nu_s(\text{NH}_2)_{\text{sulfonamide}}$	3242	3220	22
$\nu_{as}(\text{SO}_2)$	1310	1291	19
$\nu_s(\text{SO}_2)$	1149	1130	19

VII.3.3 NMR Study

NMR spectroscopy has proved to be an efficient technique for the determination of the interactions between macrocyclic hosts and organic guests [21, 22]. A comparison of the ^1H NMR spectra revealed that the most significant change in the chemical shift of SA was observed in the move of the signal for $-\text{NH}_2$ protons (H2) of $-\text{SO}_2\text{NH}_2$ group towards higher field for complex 1 and complex 2 and lower field for complex 3 (**Figure VII.5-VII.7**) which suggests H-bonding via the protons of the sulfonyl group rather than amine group as the hydrogen atoms on the sulfonyl group are relatively acidic.

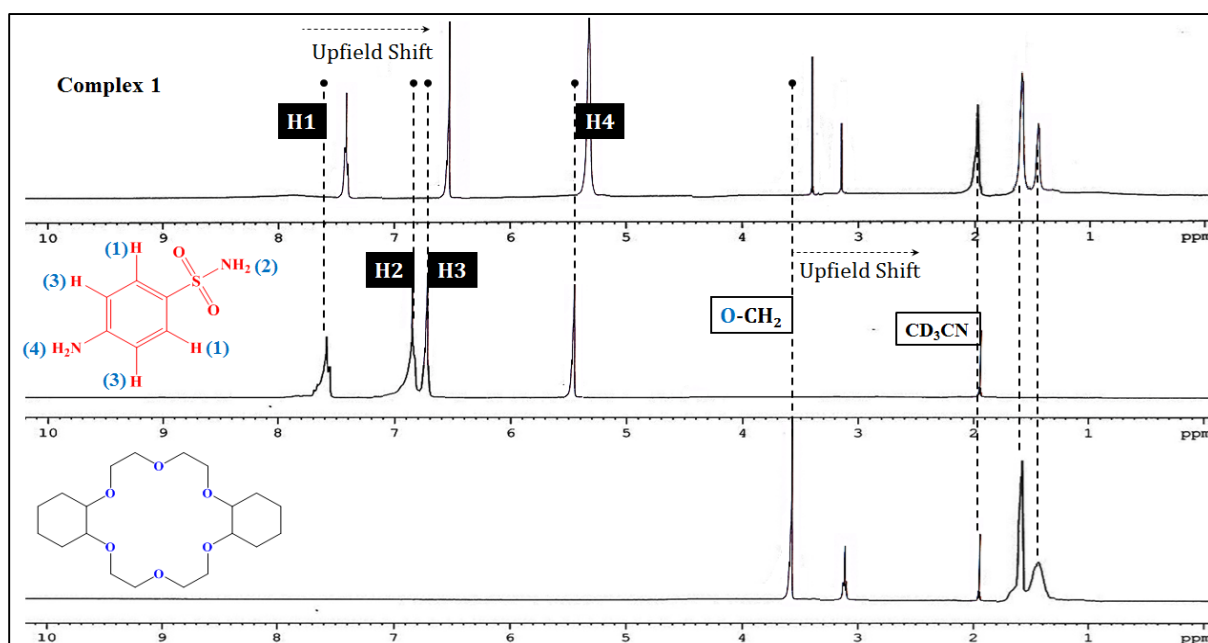


Figure VII.5: The ^1H NMR spectra of complex 1 (SA-DC18C6) (upper), uncomplexed SA and DC18C6 (lower) recorded at 300 MHz in CD_3CN at 298.15 K.

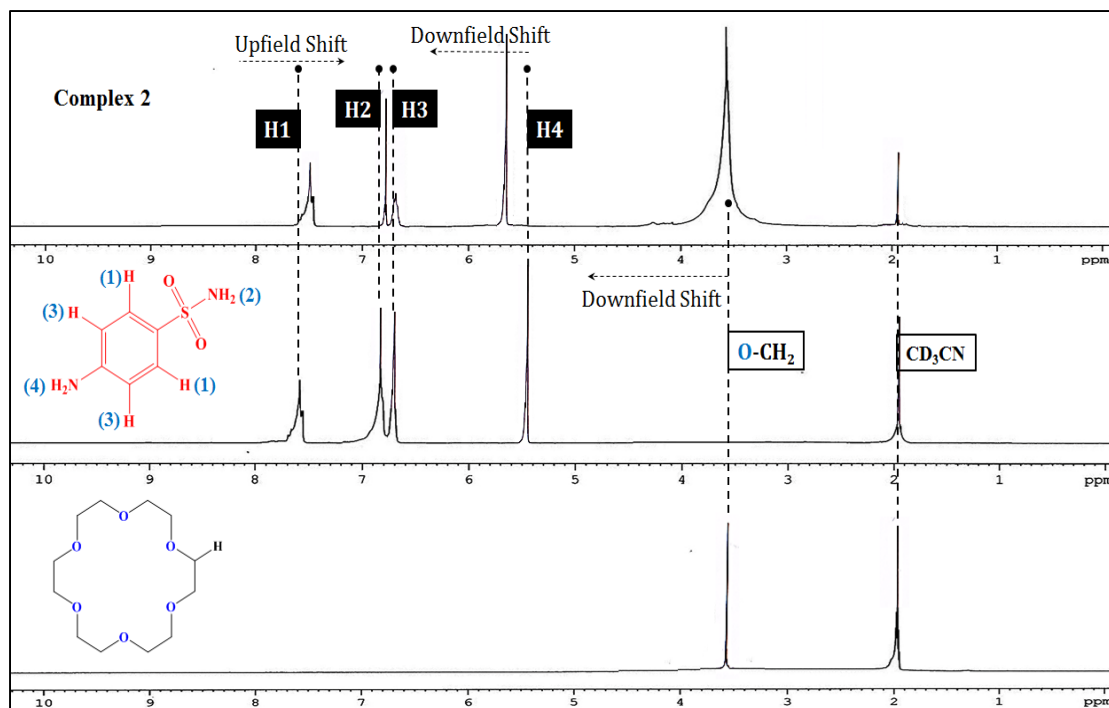


Figure VII.6: The ^1H NMR spectra of complex 2 (SA-18C6) (upper), uncomplexed SA and 18C6 (lower) recorded at 300 MHz in CD_3CN at 298.15 K.

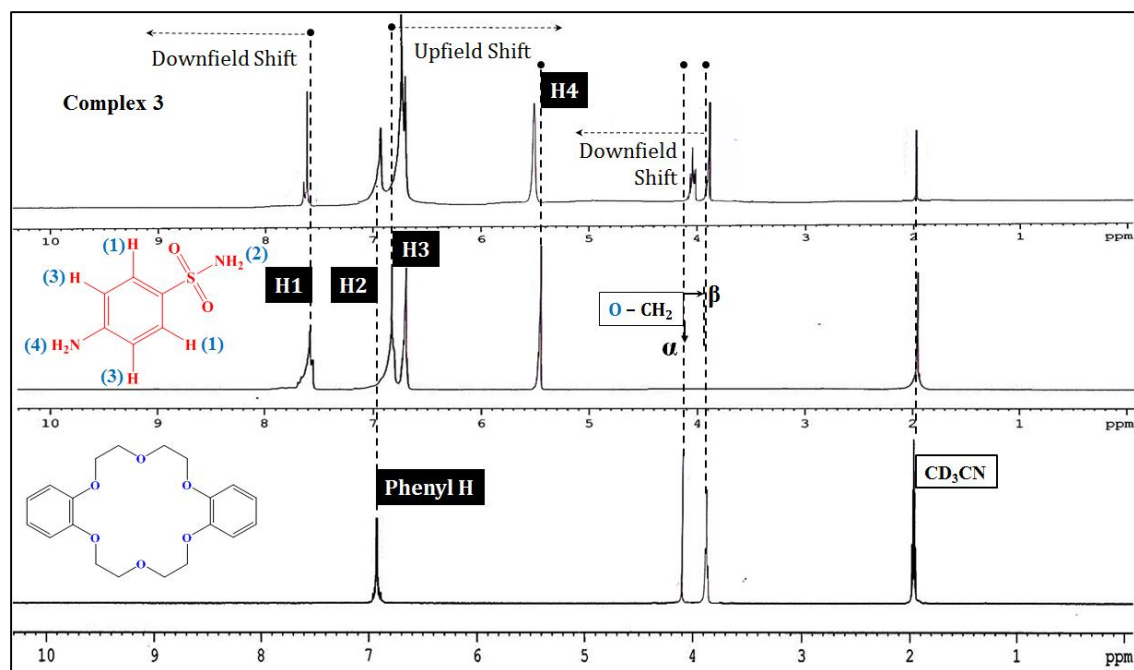


Figure VII.7: The ^1H NMR spectra of complex 3 (SA-DB18C6) (upper), uncomplexed SA and DB18C6 (lower) recorded at 300 MHz in CD_3CN at 298.15 K.

These changes in chemical shifts confirm the host-guest complexation of SA with all the studied crown ethers and gives the more accurate information about the conformations of host-guest complexes in solution which allows for a better understanding of molecular recognition [23-25]. Signals for the $-OCH_2$ protons of the crown ethers for complex 1 and complex 3 were found to be little upfield shifted relative to those signals for the free individual component (**Figure VII.5** and **Figure VII.7**). The observed upfield shift in **Figure VII.5** and **VII.7** represent, of course, the difference in the environment of the crown ether's $-OCH_2$ groups in the free and complexed ligand. In case of complex 2 $-OCH_2$ protons of the crown ether show downfield shift (**Figure VII.6**). The magnitude of the shift reflects the tightness of the crown-SA complex i.e., the overlap of the lone pair orbitals of the donating oxygen atoms of the macrocyclic ring and the outer orbitals of protons involved in H-bonding, which in turn induces a rather large change in the electronic environment of the $-OCH_2$ groups.

Selected 1H NMR data

Sulfanilamide (SA): 1H NMR (CD_3CN , 298.15 K): δ 7.56-7.71 (aryl, 2H), 6.81-6.84 ($-SO_2NH_2$, 2H), 6.69-6.72 (aryl, 2H), 5.47-5.51 (aniline $-NH_2$, 2H).

18-crown-6(18C6): 1H NMR (CD_3CN , 298.15 K): δ 3.52-3.59 (OCH_2 , 24H).

Dicyclohexano-18-crown-6(DC18C6): 1H NMR (CD_3CN , 298.15 K): δ 3.54-3.59 (OCH_2 , 16H), 3.11-3.13 (cyclohexane, 4H), 1.56-1.59 (cyclohexane, 8H), 1.39-1.50 (cyclohexane, 8H).

Dibenzo-18-crown-6(DB18C6): 1H NMR (CD_3CN , 298.15 K): δ 6.89-6.96 (aryl, 8H), 4.10-4.13 (OCH_2 , 8H), 3.85-3.88 (OCH_2 , 8H).

DC18C6-SA (complex 1): 1H NMR (CD_3CN , 298.15 K): δ 7.37-7.46 (aryl, 2H), 6.55-6.59 ($-SO_2NH_2$, 2H), 6.49-6.52 (aryl, 2H), 5.34-5.41 (aniline $-NH_2$, 2H), 3.34-3.38 (OCH_2 , 16H).

18C6-SA (complex 1): 1H NMR (CD_3CN , 298.15 K): δ 7.55-7.66 (aryl, 2H), 6.79-6.80 ($-SO_2NH_2$, 2H), 6.68-6.72 (aryl, 2H), 5.62-5.63 (aniline $-NH_2$, 2H), 3.46-3.69 (m, OCH_2 , 24H).

DB18C6-SA (complex 3): 1H NMR (CD_3CN , 298.15 K): δ 7.57-7.79 (aryl, 2H), 6.90-6.95 ($-SO_2NH_2$, 2H), 5.48-5.49 (aniline $-NH_2$, 2H), 6.90-6.95 (aryl, 8H), 4.03-4.12 (OCH_2 , 8H), 3.83-3.85 (OCH_2 , 8H).

VII.3.4 Apparent molar volume

The interactions between SA and cyclic CEs can be studied from the apparent molar volume (ϕ_V) and limiting apparent molar volume (ϕ_V^0) [26]. The apparent molar volume can be considered to be the sum of the geometric volume of the solute molecule and changes in the solvent volume due to its interaction with the solute [27]. For this purpose, the apparent molar volumes ϕ_V were determined from the solutions densities (Table VII.5) using the following equation

$$\phi_V = M / \rho - (m - m_0) / m_0 \rho_0 \quad (1)$$

where M is the molar mass of the solute, m is the molality of the solution, ρ and ρ_0 are the densities of the solution and reference solvent [crown ether + ACN], respectively.

Table VII.5: Experimental values of density (ρ) and viscosity (η) of sulfa drug in different mass fraction of DC18C6 (w_1), 18C6 (w_2) and DB18C6 (w_3) in ACN at T= (293.15 to 308.15) K.

m /mol kg ⁻¹	$\rho \cdot 10^{-3}$ /kg·m ⁻³	η /mPa·s	$\rho \cdot 10^{-3}$ /kg·m ⁻³	H /mPa·s	$\rho \cdot 10^{-3}$ /kg·m ⁻³	η /mPa·s	$\rho \cdot 10^{-3}$ /kg·m ⁻³	η /mPa·s
Sulfa+DC186								
w₁=0.001^b								
293.15 K ^a			298.15 K ^a		303.5 K ^a		308.15 K ^a	
0.001	0.78249	0.38	0.77710	0.37	0.77165	0.36	0.76619	0.35
0.003	0.78263	0.38	0.77724	0.37	0.77179	0.36	0.76633	0.35
0.005	0.78277	0.38	0.77738	0.38	0.77193	0.36	0.76647	0.35
0.007	0.78292	0.39	0.77753	0.38	0.77208	0.36	0.76661	0.36
0.009	0.78308	0.39	0.77768	0.39	0.77223	0.37	0.76676	0.36
w₁=0.003^b								
0.001	0.78290	0.40	0.77753	0.39	0.77209	0.37	0.76663	0.36
0.003	0.78302	0.40	0.77765	0.39	0.77221	0.37	0.76675	0.36
0.005	0.78316	0.40	0.77778	0.39	0.77234	0.38	0.76688	0.36
0.007	0.78329	0.41	0.77792	0.40	0.77248	0.38	0.76702	0.37
0.009	0.78344	0.41	0.77806	0.40	0.77262	0.38	0.76716	0.37

w₁=0.005^b								
0.001	0.78316	0.42	0.77777	0.41	0.77236	0.38	0.76690	0.36
0.003	0.78327	0.42	0.77788	0.41	0.77247	0.38	0.76701	0.36
0.005	0.78339	0.43	0.77800	0.41	0.77258	0.39	0.76712	0.37
0.007	0.78351	0.43	0.77812	0.42	0.77270	0.39	0.76724	0.37
0.009	0.78364	0.43	0.77824	0.42	0.77283	0.39	0.76736	0.37
Sulfa+18C6								
w₂=0.001^b								
0.001	0.78241	0.37	0.77702	0.36	0.77161	0.35	0.76615	0.34
0.003	0.78257	0.37	0.77718	0.36	0.77176	0.35	0.76630	0.34
0.005	0.78273	0.37	0.77734	0.37	0.77192	0.35	0.76645	0.34
0.007	0.78290	0.38	0.77750	0.37	0.77208	0.36	0.76661	0.35
0.009	0.78307	0.38	0.77767	0.37	0.77224	0.36	0.76677	0.35
w₂=0.003^b								
0.001	0.78283	0.37	0.77745	0.37	0.77201	0.36	0.76655	0.35
0.003	0.78296	0.38	0.77758	0.37	0.77215	0.36	0.76669	0.35
0.005	0.78311	0.38	0.77773	0.37	0.77229	0.36	0.76683	0.35
0.007	0.78326	0.38	0.77787	0.38	0.77243	0.37	0.76697	0.36
0.009	0.78341	0.38	0.77803	0.38	0.77258	0.37	0.76712	0.36
w₂=0.005^b								
0.001	0.78311	0.40	0.77772	0.38	0.77230	0.36	0.76684	0.35
0.003	0.78323	0.40	0.77784	0.38	0.77242	0.37	0.76696	0.35
0.005	0.78336	0.40	0.77797	0.38	0.77255	0.37	0.76709	0.35
0.007	0.78350	0.41	0.77811	0.39	0.77268	0.37	0.76722	0.35
0.009	0.78364	0.41	0.77825	0.39	0.77282	0.38	0.76736	0.36
Sulfa+DB186								
w₃=0.001^b								
0.001	0.78237	0.34	0.77698	0.32	0.77157	0.31	0.76609	0.29
0.003	0.78252	0.35	0.77713	0.33	0.77173	0.32	0.76625	0.30
0.005	0.78268	0.35	0.77729	0.33	0.77188	0.32	0.76640	0.30
0.007	0.78284	0.35	0.77745	0.33	0.77204	0.32	0.76656	0.30
0.009	0.78301	0.35	0.77761	0.33	0.77220	0.32	0.76672	0.31

w₃=0.003^b								
0.001	0.78269	0.36	0.77730	0.35	0.77189	0.32	0.76643	0.32
0.003	0.78282	0.36	0.77743	0.35	0.77202	0.33	0.76656	0.32
0.005	0.78296	0.36	0.77757	0.35	0.77215	0.33	0.76669	0.32
0.007	0.78310	0.37	0.77771	0.36	0.77229	0.33	0.76683	0.33
0.009	0.78325	0.37	0.77785	0.36	0.77243	0.34	0.76697	0.33
w₃=0.005^b								
0.001	0.78292	0.37	0.77753	0.35	0.77211	0.32	0.76664	0.32
0.003	0.78304	0.37	0.77765	0.35	0.77223	0.33	0.76676	0.32
0.005	0.78317	0.37	0.77778	0.35	0.77236	0.33	0.76689	0.32
0.007	0.78330	0.38	0.77791	0.36	0.77249	0.33	0.76701	0.33
0.009	0.78344	0.38	0.77804	0.36	0.77262	0.33	0.76714	0.33

^aStandard uncertainties in temperature (T) = ±0.01 K.

^bw₁, w₂ and w₃ are the mass fraction of the solvent (ACN+DC18C6), (ACN+18C6), (ACN+DB18C6) respectively.

The values of ϕ_V are large and positive for all the systems, suggesting strong solute-solvent interactions. The values of the the apparent molar volume at infinite dilution (ϕ_V^0) and the experimental slopes (S_V^*) were determined by using least squares fitting of the linear plots of ϕ_V against the square root of the molar concentrations ($m^{1/2}$) in accordance with the Masson equation [28].

$$\phi_V = \phi_V^0 + S_V^* \cdot \sqrt{m} \quad (2)$$

The calculated values of ϕ_V^0 and S_V^* are reported in **Table VII.6**. This table shows that positive values of ϕ_V^0 for all the three complexes increases with an increase in mass fraction of the respective crown and temperature (**Figure VII.8**) which indicates that stronger interaction occur between SA and CEs in ACN solvent at higher mass fraction of crown ether and high temperature [29, 30]. Since S_V^* values for large organic molecules are not of much significance, they have not been discussed here [31]. The observed ϕ_V^0 positive values (**Table VII.6**) are mainly due to the interactions between acidic protons

of $-\text{SO}_2\text{NH}_2$ group and lone pair of electrons of O_{crown} . From **Figure VII.6** it can be observed that ϕ_V^0 values for SA in complex 1 is highest, then complex 1 and then complex 3. This can be explained on the basis of the strength of the interacting groups present in the crown ethers molecules. In complex 1 i.e. complex of DC18C6, electron pumping of cyclohexyl groups of DC18C6 is a major reason that its complex is more stable than those with 18C6, most possibly due to the increased basicity of the oxygen atoms of the ring, as H-bond acceptors. In the case of complex 3 i.e. complex of DB18C6, the electron-withdrawing power of the benzo group(s) which weaken the electron-donor ability of the oxygen atoms resulting in a weaker interaction. Thus from this study, we can say that the trend in the solute-solvent interaction is

Complex 3 < complex 2 < complex 1

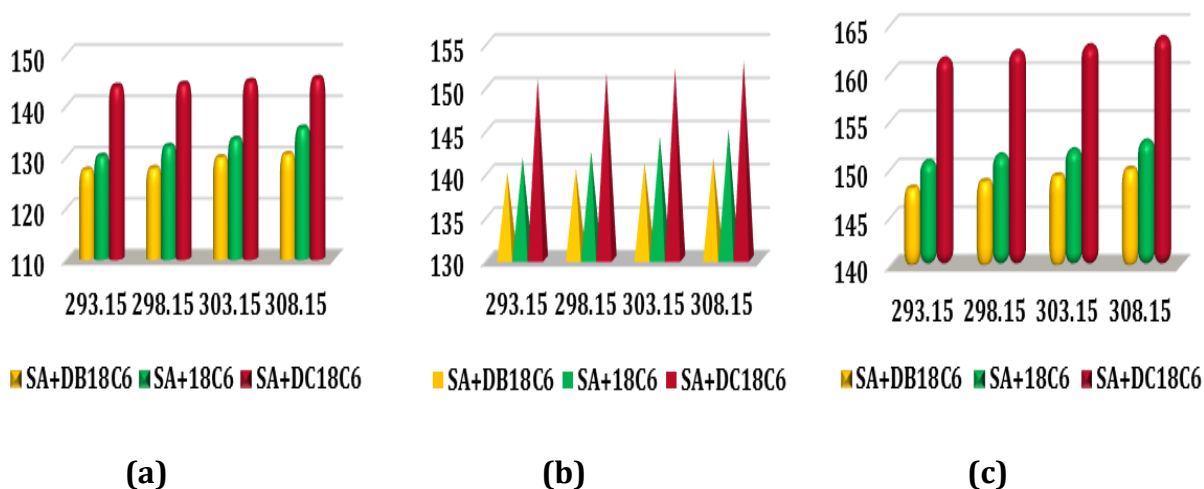


Figure VII.8: Plot of limiting apparent molar volume (ϕ_V^0) of SA in mass fractions (a) 0.001, (b) 0.003, (c) 0.005 (w) of different CEs in ACN at T= (293.15 to 308.15)K respectively.

Table VII.6: Limiting apparent molar volume (ϕ_V^0) and viscosity B -coefficient of sulfa drug in different mass fraction of different crown ethers in ACN at T= (293.15 to 308.15) K.

Temp/K ^a	$\phi_V^0 \cdot 10^6$ /m ³ ·mol ⁻¹	$S_V^* \cdot 10^6$ /m ³ ·mol ^{-3/2} ·kg ^{1/2}	B /kg ^{1/2} ·mol ^{-1/2}
SA+DC18C6		w₁ = 0.001^b	
293.15	143.75±0.01	-146.86	0.5357±0.0080
298.15	144.16±0.00	-135.29	0.5475±0.0147
303.15	144.71±0.01	-126.16	0.5556±0.0219
308.15	145.29±0.01	-112.42	0.5674±0.0259
SA+18C6		w₂ = 0.001^b	
293.15	130.12±0.01	-129.53	0.3639±0.0257
298.15	132.04±0.01	-119.47	0.4090±0.0297
303.15	133.42±0.02	-102.75	0.4281±0.0219
308.15	135.62±0.00	-97.90	0.4631±0.0271
SA+DB18C6		w₃ = 0.001^b	
293.15	127.43±0.01	-86.41	0.2948±0.0380
298.15	127.73±0.01	-74.63	0.3648±0.0268
303.15	129.85±0.01	-70.02	0.3859±0.0174
308.15	130.47±0.01	-63.48	0.4597±0.0133
SA+DC18C6		w₁ = 0.003^b	
293.15	151.05±0.01	-149.01	0.6482±0.0165
298.15	151.97±0.01	-139.49	0.6553±0.0266
303.15	152.66±0.00	-131.80	0.6745±0.0157
308.15	153.73±0.02	-126.72	0.6912±0.0254
SA+18C6		w₂ = 0.003^b	
293.15	141.72±0.01	-137.14	0.4951±0.0049
298.15	142.43±0.01	-123.67	0.5506±0.0080
303.15	144.17±0.01	-108.21	0.6054±0.0167
308.15	144.97±0.01	-103.23	0.6904±0.0126

SA+DB18C6		w₃ = 0.003^b	
293.15	140.05±0.01	-88.73	0.3930±0.0211
298.15	140.46±0.01	-73.19	0.4437±0.0098
303.15	141.10±0.02	-58.04	0.5221±0.0160
308.15	141.72±0.01	-50.03	0.6012±0.0170
SA+DC18C6		w₁ = 0.005^b	
293.15	161.51±0.01	-155.69	0.7414±0.0157
298.15	162.28±0.00	-144.31	0.7930±0.0000
303.15	162.88±0.01	-133.79	0.8243±0.0290
308.15	163.73±0.01	-124.02	0.8704±0.0290
SA+18C6		w₂ = 0.005^b	
293.15	150.87±0.01	-137.59	0.5921±0.0117
298.15	151.53±0.01	-129.91	0.6407±0.0181
303.15	152.06±0.00	-115.89	0.6810±0.0150
308.15	152.97±0.01	-108.57	0.7268±0.0123
SA+DB18C6		w₃ = 0.005^b	
293.15	148.03±0.01	-95.43	0.4796±0.0204
298.15	148.72±0.01	-85.25	0.5399±0.0080
303.15	149.31±0.01	-72.50	0.6141±0.0106
308.15	149.99±0.01	-61.08	0.6977±0.0202

^aStandard uncertainties in temperature (T) = ±0.01 K.

^bw₁, w₂ and w₃ are the mass fraction of the solvent (ACN+DC18C6), (ACN+18C6), (ACN+DB18C6) respectively.

VII.3.5 Temperature dependent limiting apparent molar volume

The temperature dependence of ϕ_V^0 values can be expressed by the general polynomial equation as follows,

$$\phi_V^0 = a_0 + a_1T + a_2T^2 \quad (3)$$

where a_0 , a_1 , a_2 are the empirical coefficients and the values of these coefficients have been evaluated by the least-squares fitting of apparent molar volume at different temperatures [Table VII.7].

Table VII.7: Values of empirical coefficients (a_0 , a_1 , and a_2) of Equation 14 of sulfa drug in different mass fraction of DC18C6 (w_1), 18C6 (w_2) and DB18C6 (w_3) in ACN at T= (293.15 to 308.15) K.

Mass fraction	$a_0 \cdot 10^6$ /m ³ ·mol ⁻¹	$a_1 \cdot 10^6$ /m ³ ·mol ⁻¹ ·K ⁻¹	$a_2 \cdot 10^6$ /m ³ ·mol ⁻¹ ·K ⁻²
SA + DC18C6			
$w_1 = 0.001^b$	267.00	-0.919	0.0017
$w_1 = 0.003^b$	235.40	-0.727	0.0015
$w_1 = 0.005^b$	191.23	-0.336	0.0008
SA + 18C6			
$w_1 = 0.001^b$	278.29	-1.326	0.0028
$w_1 = 0.003^b$	155.56	-0.311	0.0009
$w_1 = 0.005^b$	336.69	-1.367	0.0025
SA + DB18C6			
$w_1 = 0.001^b$	350.43	-1.699	0.0032
$w_1 = 0.003^b$	296.61	-1.150	0.0021
$w_1 = 0.005^b$	171.94	-0.287	0.0007

^b w_1 , w_2 and w_3 are the mass fraction of the solvent (ACN+DC18C6), (ACN+18C6), (ACN+DB18C6) respectively.

The limiting apparent molar expansibilities, ϕ_E^0 , can be obtained by the following equation,

$$\phi_E^0 = \left(\delta \phi_V^0 / \delta T \right)_P = a_1 + 2a_2 T \quad (4)$$

Differentiation of eq. 4 with respect to temperature gives the values of the limiting apparent molar expansibilities (ϕ_E^0) [Table VII.8]. These values are also employed in

interpreting of the structure-making or breaking properties of various solutes. Positive expansivity i.e increasing volume with increasing temperature is a characteristic property of nonaqueous solutions of hydrophobic solvation [32].

Table VII.8: Limiting apparent molal expansibilities (ϕ_E^0) of sulfa drug in different mass fraction of DC18C6 (w_1), 18C6 (w_2) and DB18C6 (w_3) in ACN at T= (293.15 to 308.15) K.

Mass fraction	$\phi_E^0 \cdot 10^6$ /m ³ ·mol ⁻¹ ·K ⁻¹				$(\partial\phi_E^0/\partial T)_P \cdot 10^6$ /m ³ ·mol ⁻¹ ·K ⁻²
SA + DC18C6					
T/K ^a	293.15	298.15	303.15	308.15	
$w_1 = 0.001^b$	0.078	0.095	0.112	0.129	0.003
$w_1 = 0.003^b$	0.152	0.167	0.182	0.197	0.003
$w_1 = 0.005^b$	0.133	0.141	0.149	0.157	0.002
SA + 18C6					
T/K ^a	293.15	298.15	303.15	308.15	
$w_2 = 0.001^b$	0.316	0.344	0.372	0.400	0.006
$w_2 = 0.003^b$	0.216	0.225	0.234	0.243	0.002
$w_2 = 0.005^b$	0.099	0.124	0.149	0.174	0.005
SA + DB18C6					
T/K ^a	293.15	298.15	303.15	308.15	
$w_3 = 0.001^b$	0.177	0.209	0.241	0.273	0.006
$w_3 = 0.003^b$	0.081	0.103	0.124	0.145	0.004
$w_3 = 0.005^b$	0.124	0.131	0.138	0.145	0.001

^aStandard uncertainties in temperature (T) = ±0.01 K.

^b w_1 , w_2 and w_3 are the mass fraction of the solvent (ACN+DC18C6), (ACN+18C6), (ACN+DB18C6) respectively.

Hepler [33] developed a technique of examining the sign of $(\delta\phi_E^0/\delta T)_p$ for the solute in terms of long-range structure-making and -breaking capacity of the solute in the solution using the general thermodynamic expression,

$$(\delta\phi_E^0/\delta T)_p = (\delta^2\phi_V^0/\delta T^2)_p = 2a_2 \quad (5)$$

If the sign of the second derivatives of the limiting apparent molar volume with respect to the temperature $(\delta\phi_E^0/\delta T)_p$ is positive or a small negative, the molecule is a structure maker; otherwise, it is a structure breaker [34]. As is evident from **Table VII.8**, the $(\delta\phi_E^0/\delta T)_p$ values for all the complexes are positive i.e. SA is predominantly structure makers in all of the complexes of crown ethers and this tendency is enhanced with increasing crown concentration.

VII.3.6 Viscosity B Coefficients

The experimental viscosity (η) data measured at different temperatures for the studied systems are tabulated in **Table VII.5**. The relative viscosity (η_r) has been analyzed using the Jones-Dole equation [35]

$$(\eta/\eta_0 - 1)/\sqrt{m} = (\eta_r - 1)/\sqrt{m} = A + B\sqrt{m} \quad (6)$$

Where relative viscosity $\eta_r = \eta/\eta_0$, η and η_0 are the viscosities of the ternary solutions (SA + crown ether + ACN) and binary reference solvent (crown ether + ACN), respectively, and m is the molality of the SA in the ternary solutions. A and B are experimental constants known as viscosity A - and B -coefficients, which are specific to solute-solute and solute-solvent interactions, respectively. The values of B coefficients are obtained from the slope of linear plot of $(\eta_r - 1)/\sqrt{m}$ against \sqrt{m} by least-squares method, and reported in **Table VII.6**.

B -Coefficients are known to provide information regarding the solvation of the solutes and their effects on the structure of the solvent in the near environment of the solute molecules [36,37]. The values of B -coefficient for SA in complex 1 are highest of the three complexes and the smallest for complex 3 in ACN [**Table VII.6**]. Positive values of the B -coefficient suggest hydrogen bonding of the solvent with the drug molecule and

indicate an increase in viscosity of the solution due to the large size of the moving molecules. The solvated solutes molecule associated by the solvent molecules all round to the formation of associated molecule by solute-solvent interaction are responsible for the higher values of the B -coefficient, would present greater resistance, and this type of interactions are strengthened with a rise in temperature and also increase with an increase of mass fraction of CEs in the solvent mixtures [Figure VII.9].

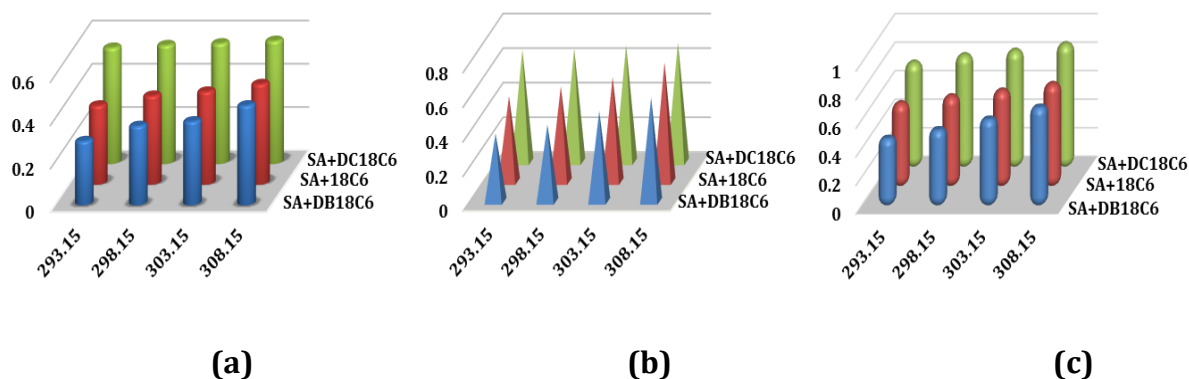


Figure VII.9: Plot of viscosity B-coefficient of SA in mass fractions (a) 0.001, (b) 0.003, (c) 0.005 (w) of different CEs in ACN at T= (293.15 to 308.15)K respectively.

These observations are in excellent agreement with the conclusions drawn from the analysis of apparent molar volume, ϕ_v^0 discussed earlier. The calculated values of dB/dT are small positive shown in **Table VII.9** reflects the structure-maker behaviors of the sulfa drug [27].

Table VII.9: Values of dB/dT of sulfa drug in different mass fraction of DC18C6 (w_1), 18C6 (w_2) and DB18C6 (w_3) in ACN at T= (293.15 to 308.15) K respectively.

Mass fraction	$\frac{dB}{dT}$ /kg ^{1/2} ·mol ^{1/2} ·K ⁻¹				
	SA + DC18C6		SA + 18C6		SA + DB18C6
$w_1 = 0.001^b$	0.006	$w_2 = 0.001^b$	0.002	$w_3 = 0.001^b$	0.010
$w_1 = 0.003^b$	0.012	$w_2 = 0.003^b$	0.003	$w_3 = 0.003^b$	0.014
$w_1 = 0.005^b$	0.008	$w_2 = 0.005^b$	0.008	$w_3 = 0.005^b$	0.014

^b w_1 , w_2 and w_3 are the mass fraction of the solvent (ACN+DC18C6), (ACN+18C6), (ACN+DB18C6) respectively.

Thus, the volumetric and viscometric properties of the sulfa drug in the present work provide useful information in medicinal and pharmaceutical chemistry for the prediction of absorption and permeability of drug through membranes.

VII.3.7 Refractive index calculation

Experimental refractive index data n_D for (SA + crown ether + ACN) ternary solutions were measured as a function of the molarities of several crown ethers at T =298.15 K. The values of measured n_D are tabulated in **Table VII.10**. The molar refraction R_M can be evaluated from the Lorentz-Lorenz relation [38].

$$R_M = \left\{ \frac{(n_D^2 - 1)}{(n_D^2 + 2)} \right\} (M/\rho) \quad (7)$$

Where R_M , n_D , M and ρ are the molar refraction, the refractive index, the molar mass and the density of solution respectively. Because the R_M value is directly proportional to molecular polarizability [39], this quantity is a measure of the ability of the molecular orbitals to be impaired under an electrical field [40].

Table VII.10 indicates that the R_M values increase with an increasing amount of crown in the ternary solutions studied because its electron cloud becomes more decentralized, indicating high polarizability in the presence of crown ethers. The

refractive index, molar refraction (R_M) and consequently the limiting molar refraction (R_M^0) (Table VII.11) values of a substance is higher when its molecules are more tightly packed or in general when the compound is denser. In the present ternary solution system, the interactions occurring between the SA and three different crown ether are explored. It is evident from Figure VII.10 that DC18C6 interacts more strongly with SA than with 18C6 and DB18C6 which is probably due to stable complex formation of DC18C6 through the H-bond formation between acidic protons of sulfonyl group ($-SO_2NH_2$) and O_{crown} i.e. DC18C6 form compact structure which is reflected in their high R_M^0 values; moreover, the strength of the interactions are increases with increasing molarity of crown.

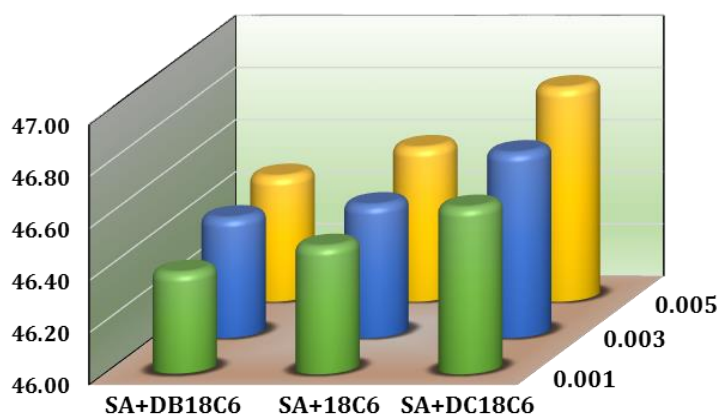


Figure VII.10: Plot of limiting molar refraction (R_M^0) of SA in different mass fractions (w) of different CEs in ACN at $T= 298.15$ K respectively.

Table VII.10: Values of Refractive Index (n_D) and Molar Refraction (R_M) of sulfa drug in different mass fraction of DC18C6 (w_1), 18C6 (w_2) and DB18C6 (w_3) in ACN at T= 298.15 K respectively.

Conc. (m)		n_D	$R_M / \text{m}^3 \cdot \text{mol}^{-1}$
$w_1 = 0.001^b$			
SA + DC18C6	0.001	1.3428	46.79
	0.003	1.3436	46.88
	0.005	1.3442	46.95
	0.007	1.3447	47.00
	0.009	1.3452	47.06
$w_2 = 0.001^b$			
SA + 18C6	0.001	1.3415	46.64
	0.003	1.3422	46.72
	0.005	1.3429	46.79
	0.007	1.3435	46.86
	0.009	1.3440	46.91
$w_3 = 0.001^b$			
SA + DB18C6	0.001	1.3409	46.57
	0.003	1.3417	46.66
	0.005	1.3423	46.72
	0.007	1.3429	46.79
	0.009	1.3435	46.85
$w_1 = 0.003^b$			
SA + DC18C6	0.001	1.3436	46.87
	0.003	1.3443	46.95
	0.005	1.3449	47.01
	0.007	1.3454	47.07
	0.009	1.3459	47.12

$w_2 = 0.003^b$			
SA + 18C6	0.001	1.3423	46.71
	0.003	1.3431	46.80
	0.005	1.3438	46.88
	0.007	1.3445	46.96
	0.009	1.3451	47.02
$w_3 = 0.003^b$			
SA + DB18C6	0.001	1.3416	46.63
	0.003	1.3423	46.71
	0.005	1.3429	46.78
	0.007	1.3436	46.86
	0.009	1.3440	46.90
$w_1 = 0.005^b$			
SA + DC18C6	0.001	1.3450	47.03
	0.003	1.3459	47.13
	0.005	1.3465	47.21
	0.007	1.3473	47.29
	0.009	1.3479	47.35
$w_2 = 0.005^b$			
SA + 18C6	0.001	1.3428	46.76
	0.003	1.3436	46.85
	0.005	1.3442	46.91
	0.007	1.3448	46.98
	0.009	1.3453	47.03
$w_3 = 0.005^b$			
SA + DB18C6	0.001	1.3421	46.68
	0.003	1.3430	46.79
	0.005	1.3437	46.86
	0.007	1.3444	46.94
	0.009	1.3450	47.01

^b w_1 , w_2 and w_3 are the mass fraction of the solvent (ACN+DC18C6), (ACN+18C6), (ACN+DB18C6) respectively.

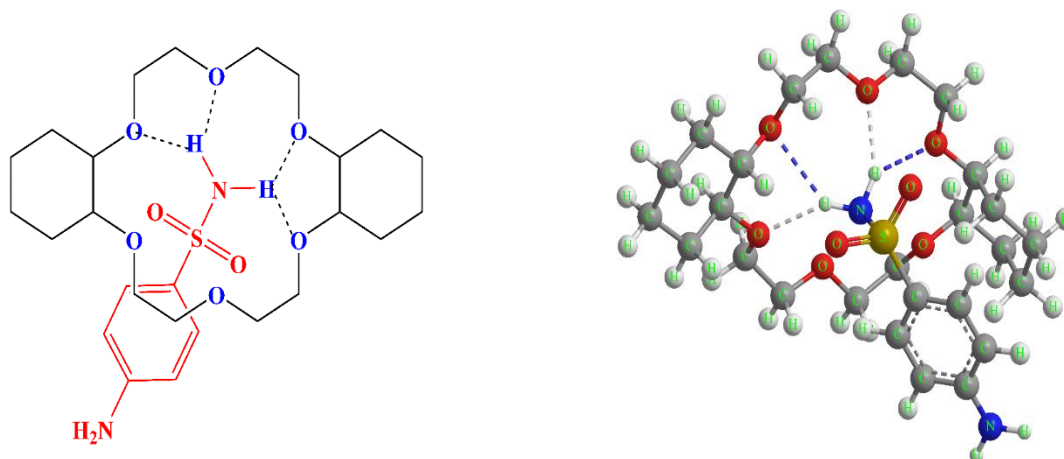
Table VII.11: Limiting molar refractions (R_M^0) values of sulfa drug in different mass fraction of DC18C6 (w_1), 18C6 (w_2) and DB18C6 (w_3) in ACN at T= 298.15 K respectively.

Mass fraction	$R_M^0 / \text{m}^3 \cdot \text{mol}^{-1}$		
	SA + DC18C6	SA + 18C6	SA + DB18C6
$w_1 = 0.001^b$	46.64	46.49	46.64
$w_1 = 0.003^b$	46.71	46.51	46.71
$w_1 = 0.005^b$	46.82	46.59	46.82

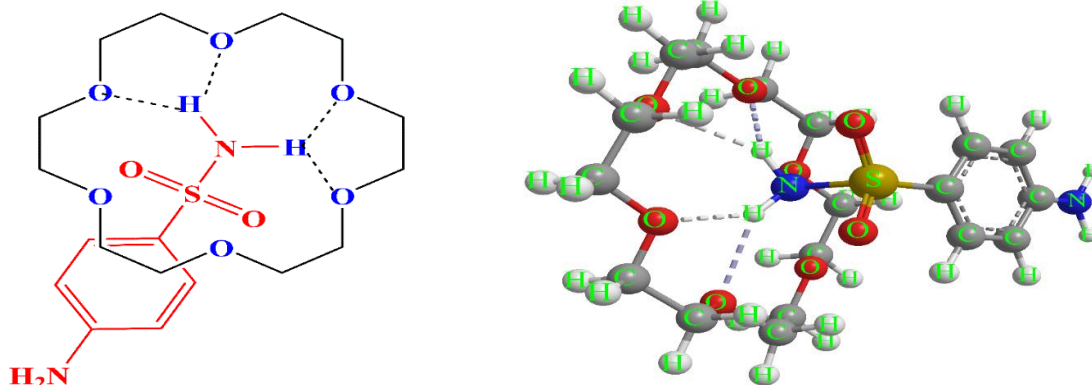
^b w_1 , w_2 and w_3 are the mass fraction of the solvent (ACN+DC18C6), (ACN+18C6), (ACN+DB18C6) respectively.

VII.3.8 Typical Features of Specific Interactions involved in the Complexation

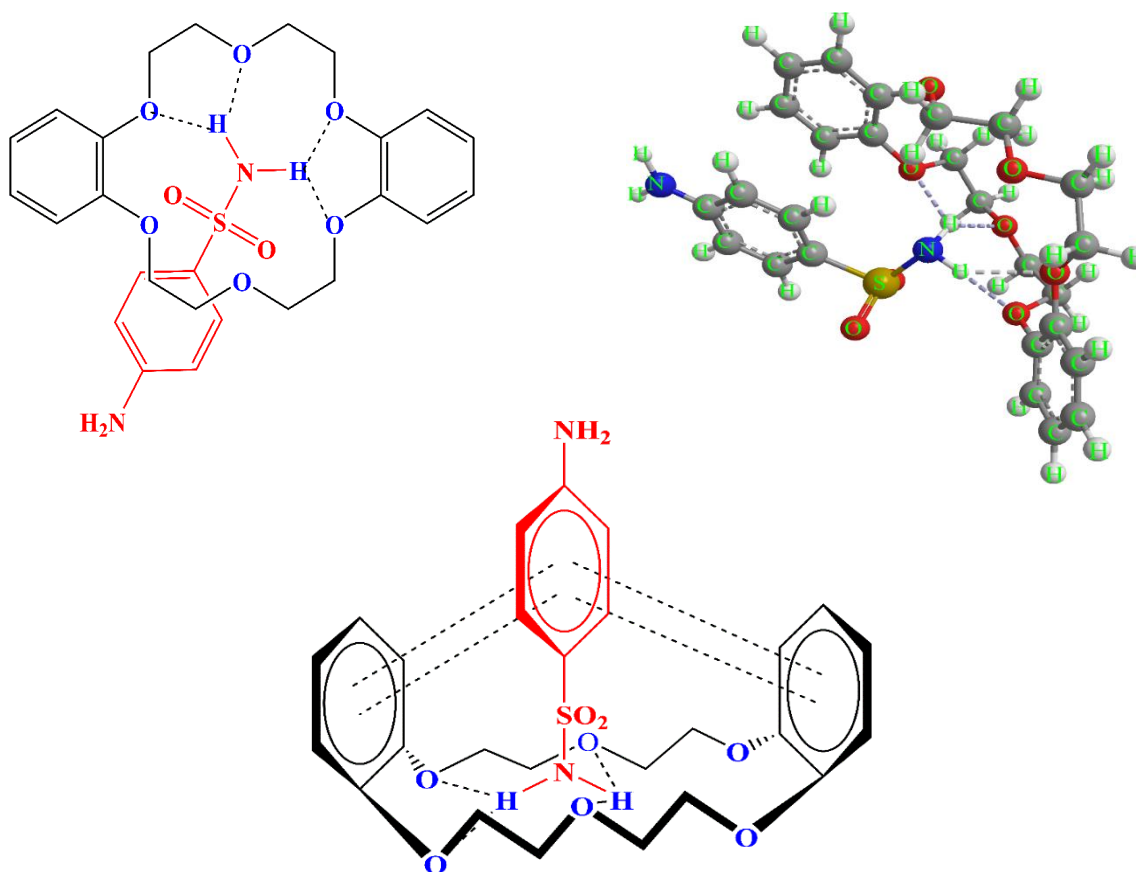
The all three complexes of CEs (**Scheme VII.2**) are stabilized mainly by hydrogen bonds formed between acidic protons of $-\text{NH}_2$ group and ether oxygen atoms. This can be shown by the suitable plausible mechanism (**Scheme VII.2**). But in case of complex 3 i.e. complex of DB18C6, hydrogen bonding seems to play a secondary role because the benzene rings of the DB18C6 decrease the negative charge of the oxygen atoms and hence their ability to undergo hydrogen bonding. The π - π interaction is present only in this complex which also slightly stabilized the complex (**Scheme VII.2**) [41-43].



Scheme VII.2a: Schematic presentation of complex formation between SA and DC18C6 and corresponding energy minimized structure of the complex.



Scheme VII.2b: Schematic presentation of complex formation between SA and 18C6 and corresponding energy minimized structure of the complex.



Scheme VII.2c: Schematic presentation of complex formation between SA and DB18C6 and corresponding energy minimized structure of the complex.

VII.3.9 Association constant and Thermodynamic parameters

The stability constants (K_a) for 1:1 complexation were measured in ACN solution by UV-visible spectroscopy and are presented in **Table VII.12**.

Table VII.12: Values of Association constant (K_a) and free energy change (ΔG^0) of the three SA-CEs complexes.

	T/K ^a	K_a/ M^{-1}	$\Delta G^0/KJ mol^{-1}$
Complex 1		541.88	-15.60
Complex 2	298.15	412.27	-14.94
Complex 3		372.80	-14.67

^a Standard uncertainties in temperature are: (T) = ± 0.01 K.

UV-vis spectroscopy is a convenient and widely used method for the study of binding phenomena [44]. The sulfa drug absorbs light at different wavelengths in free and complexed states and the differences in the UV-vis spectra may suffice for the estimation of molecular recognition thermodynamics. In UV spectroscopic titration experiments, the addition of varying concentration of host molecules results in a gradual increase or decrease of characteristic absorptions of the guest molecules. The association constants of the supramolecular systems formed were calculated according to the modified Benesi-Hildebrand equation, Eq. (8) [45], (**Figure VII.11**)

$$\frac{1}{\Delta A} = \frac{1}{\Delta \epsilon [SA] K_a} \cdot \frac{1}{[CE]} + \frac{1}{\Delta \epsilon [SA]} \quad (8)$$

Where [CE] and [SA] refer to the total concentration of crown ether and SA respectively, $\Delta \epsilon$ is the change in molar extinction coefficient between the free and complexed crown ether and ΔA denotes the absorption changes of SA on the addition of CEs. The values of K_a for each of the complexes were evaluated by dividing the intercept by the slope (**Table VII.13-VII.15**) of the straight line of the double reciprocal plot. The free energy change (ΔG), has been easily estimated from association constant by using following equation [46, 47]

$$\Delta G = -RT \ln K \quad (9)$$

The ΔG values (**Table VII.12**) for all the three complexes are negative which indicates that the Complex formation process proceeds spontaneously at 298.15K. In all the complexes, H-bonding to the ether oxygen atoms is obviously responsible for complexation but either π -stacking or charge-transfer interactions (**Scheme VII.2**) also seem to have a minor contribution towards complexation. The stability constants for complex 3 is slightly lower than the corresponding value of complex 1 and complex 2 (**Table VII.12**) as the aromatic rings of the crown ether decrease the electron density of the adjacent oxygen atoms, and this seems to decrease the strength of any H-bonding in complex 3. Although complex 3 has the potential for π -stacking or charge transfer interactions which is absent in the complex 1 and complex 2 indicates that H-bonding bonding to the ether oxygen atoms is dominant here for the complexation.

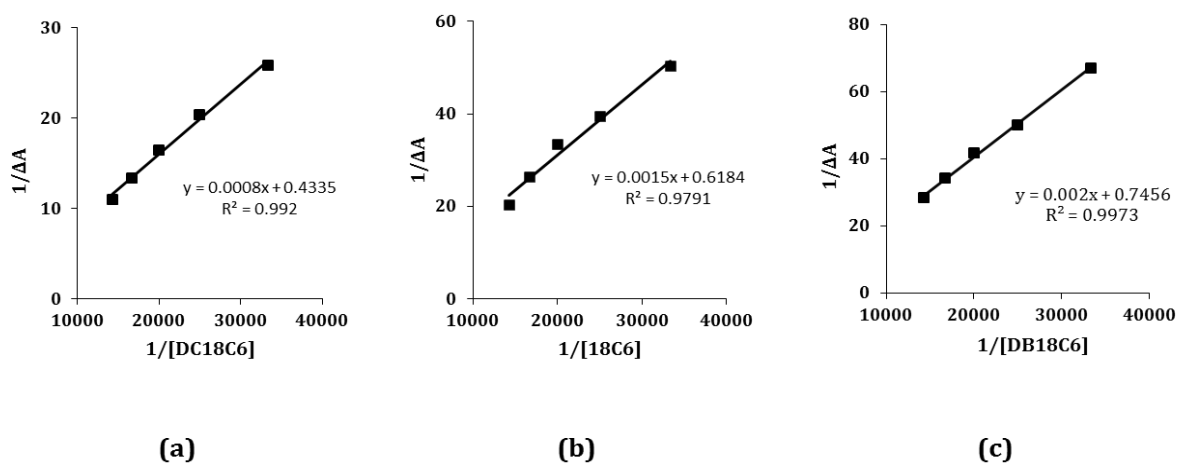


Figure VII.11: Benesi-Hildebrand double reciprocal plot for the effect of (a) DC18C6, (b) 18C6, (c) DB18C6 on the absorbance of Sulfa drug.

Table VII.13: Data for the Benesi-Hildebrand double reciprocal plot performed by UV-Vis spectroscopy for SA-DC18C6 system at T=298.15K.

[SA] / μM	[18C6] / μM	A_0	A	ΔA	$1/[\text{DC18C6}]$ / M^{-1}	$1/\Delta A$	Intercept	Slope	K_a / M^{-1}
50	30		1.10102	0.03868	33333	25.8531			
50	40		1.09072	0.04898	25000	20.4165			
50	50	1.13970	1.07887	0.06083	20000	16.4392	0.4335	0.0008	541.88
50	60		1.06496	0.07474	16667	13.3797			
50	70		1.04830	0.09140	14286	10.9409			

^a Standard uncertainties in temperature are: (T) = ± 0.01 K.

Table VII.14: Data for the Benesi-Hildebrand double reciprocal plot performed by UV-Vis spectroscopy for SA-18C6 system at T=298.15K.

[SA] / μM	[18C6] / μM	A_0	A	ΔA	$1/[\text{18C6}]$ / M^{-1}	$1/\Delta A$	Intercept	Slope	K_a / M^{-1}
50	30		1.11983	0.01987	33333	50.3271			
50	40		1.11434	0.02536	25000	39.4322			
50	50	1.13970	1.10973	0.02997	20000	33.3667	0.6184	0.0015	412.27
50	60		1.10165	0.03805	16667	26.2812			
50	70		1.09040	0.04930	14286	20.2840			

^a Standard uncertainties in temperature are: (T) = ± 0.01 K.

Table VII.15: Data for the Benesi-Hildebrand double reciprocal plot performed by UV-Vis spectroscopy for SA-DB18C6 system at T=298.15K.

[SA] / μM	[18C6] / μM	A_0	A	ΔA	$1/[\text{DB18C6}]$ / M^{-1}	$1/\Delta A$	Intercept	Slope	K_a / M^{-1}
50	30		1.15464	0.01494	33333	66.9344			
50	40		1.15971	0.02001	25000	49.9750			
50	50	1.13970	1.16372	0.02402	20000	41.6319	0.7456	0.0020	372.80
50	60		1.16887	0.02917	16667	34.2818			
50	70		1.17509	0.03539	14286	28.2565			

^a Standard uncertainties in temperature are: (T) = ± 0.01 K.

VII.4. CONCLUSION

The formation of three complexes of sulfa drug with several crown ethers in ACN have been investigated with the help of above mentioned spectroscopic and physicochemical studies. ^1H NMR data confirms the complex formation and the Job plot suggests the formation of complexes with 1:1 stoichiometry. The interaction of sulfa drug with crown ethers in the solution have been interpreted by density, viscosity, refractive index measurements. These measurements provide valuable information on ion-solvent and ion-ion interactions of the complexes in solutions. The formation constants are found highest for complex 2, then complex 1 and then complex 3 which indicates that SA form most stable complex with DC18C6 compared to other complexes. The probable structures of the three complexes of sulfa drug with crown ethers have been proposed by the above mentioned studies.

In this work we have found that the studied complexes are mainly stabilised by hydrogen bonds, and π -stacking play only a secondary role in case of complex 3 i.e complex of benzene substituted crown ether. The 1:1 complexation of the sulfa drug by different crown ethers proceeds spontaneously ($\Delta G^\circ < 0$). The roles of guest SA has been established in directing the formation of supramolecular architectures between crown ether and $-\text{NH}_2$ group of $-\text{SO}_2\text{NH}_2$ in SA by host-guest hydrogen-bonding interactions. Here the present work helps to understand the vital role of $-\text{NH}_2$ group in the design and construction of supramolecular host-guest materials. These results are also significant for other host-guest systems. However, with the knowledge acquired from the solution chemistry of SA-Crown complexes, we believe that the scope and future prospect of this type of studies with other supramolecules are also a promising preposition.

CHAPTER- VIII

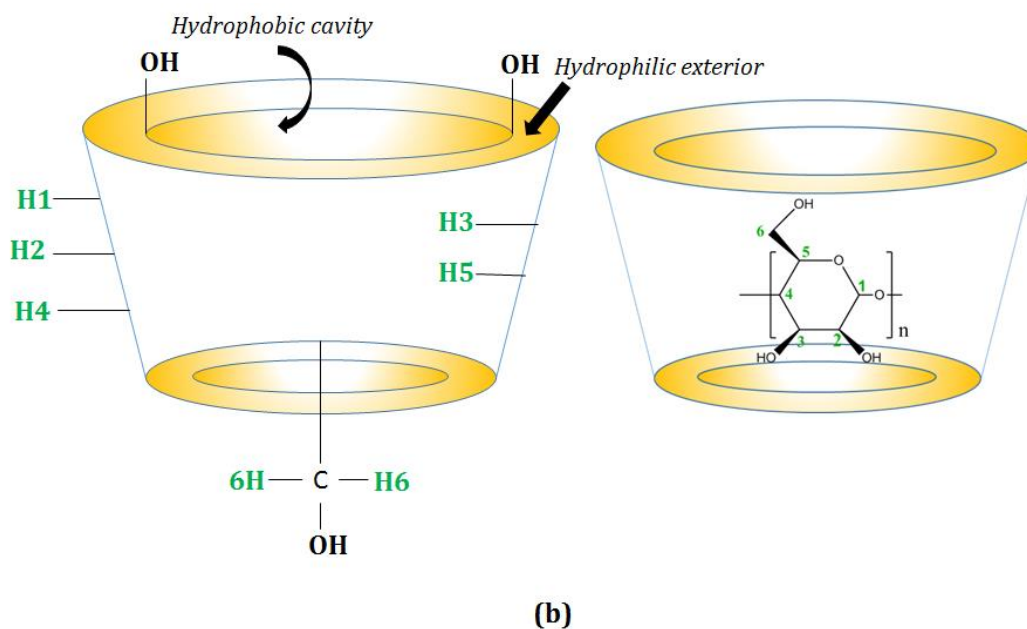
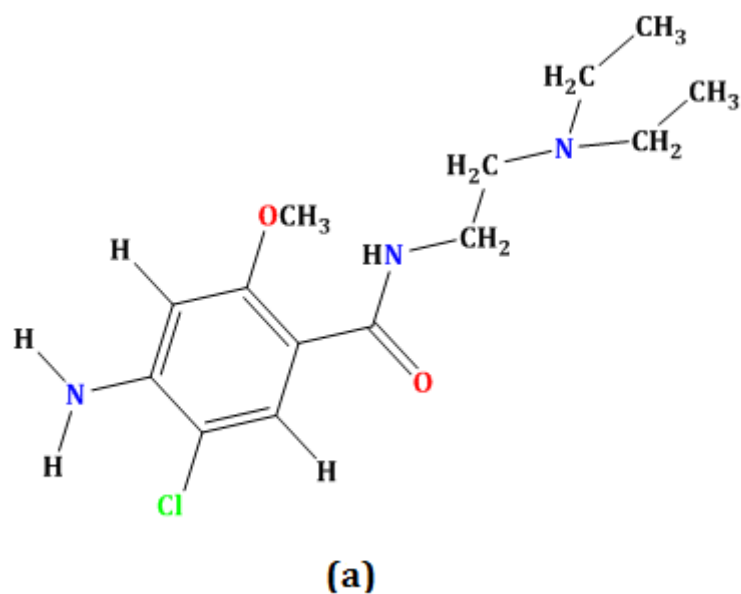
SUBSISTENCE OF HOST-GUEST INCLUSION COMPLEXES OF METOCLOPRAMIDE HYDROCHLORIDE WITH α - AND β -CYCLODEXTRIN MOLECULES PROBED BY PHYSICO-CHEMICAL INVESTIGATION

VII.1. INTRODUCTION

Enhancement of drug-delivery performance using formulations based on cyclodextrin (CD)-drug inclusion complexes is well known because of the enhanced solubility, bioavailability and stability of drug molecules after complexation with CD. Cyclodextrins (CDs) are cyclic oligosaccharides containing six (α -CD), seven (β -CD) and eight (γ -CD) glucopyranose units which are bound together by α -(1-4) linkages forming a truncated conical structure, which allows CDs to form host-guest ICs with different sized guest molecules. Owing to lack of free rotation about the bonds connecting the glucopyranose units, the cyclodextrins are not perfectly cylindrical molecules but the torroidal or cone shaped with a hydrophobic cavity and a hydrophilic surface [**Scheme VIII.1**] [1]. The primary hydroxyl groups are located on the narrow side of the cone shape, while the secondary hydroxyl groups are located on the wider edge due to the presence of specific architecture of the cyclodextrin. The hydrophobic cavity of the cyclodextrin is capable of trapping the hydrophobic parts present in the molecules within to produce stable host-guest inclusion complexes through various interactions, such as hydrogen-bonding, van der Waals, and hydrophobic interactions [2-8]. As a result, the solubility of the hydrophobic and amphiphilic compounds increases. Many advantages of drug- complexation with Cyclodextrins have been reported in scientific literature which includes increased solubility, enhanced bioavailability, improved stability, masking of bad test or odour, reduced volatility, transformation of liquid or gas into solid form reduced side effect and the possibility of a drug release system, etc [9]. Due to these abilities, cyclodextrins are of great interests in pharmaceutical chemistry [10-13], agriculture [14], cosmetics [15, 16], food [17], drug delivery [18-21] and industries [22-24].

Metoclopramide hydrochloride (MP) is a white crystalline, odorless substance, freely soluble in water. Chemically, it is 4-amino-5-chloro-N-[2-(diethylamino) ethyl]-2-methoxy benzamide monohydrochloride, and is used as an anti-emetic in the treatment of some forms of nausea and vomiting and to treat heartburn caused by gastroesophageal reflux in people who have used other medications without relief of symptoms. MP have a greater impact on the treatment of disorders of the gastrointestinal tract. MP is prokinetic agents in gastroenterology. Prokinetic drugs enhances the response to acetylcholine of tissue in upper gastrointestinal tract causing enhanced motility and accelerated gastric emptying without stimulating gastric, biliary, or pancreatic secretions; increases lower oesophageal sphincter tone [25]. It is also used to treat slow gastric emptying in people with diabetes, also called diabetic gastroparesis which can cause nausea, vomiting, heartburn, loss of appetite, and a feeling of fullness after meals. Metoclopramide Hydrochloride blocks dopamine receptors and (when given in higher doses) also blocks serotonin receptors in chemoreceptor trigger zone of the Central Nervous System. Since metoclopramide has been confirmed as an effective drug in treating and preventing various types of disease hence the stabilization and regulatory release of this drug is of great concern in pharmacology. Thus to protect these drugs from external effects and to reduce side effects for their regulatory release, it is crucial to investigate whether they can be encapsulated into the CD molecule.

In this work, the inclusion complex (IC) formation of metoclopramide hydrochloride (MP) with both α and β -cyclodextrins (CDs) was studied in detail based on physicochemical and spectroscopic measurements. The factors affecting the inclusion process were discussed. Enhanced fluorescence and absorption characteristics served as an aid for better understanding the inclusion mechanism, including the size/shape-fit, hydrophobicity. Especially, detailed spatial information in solution has been studied by ^1H NMR. The related mechanisms proposed to explain the inclusion process.



Scheme VIII.1: Molecular structures of (a) metoclopramide hydrochloride and (b) cyclodextrin molecule with interior and exterior protons ($n = 6, 7$ for α -CD and β -CD respectively).

VII.2. EXPERIMENTAL SECTION

VIII.2.1 Reagents

Metoclopramide Hydrochloride, α -cyclodextrin and β -cyclodextrin of high purity grade were purchased from Sigma-Aldrich and used as received. Purity of Metoclopramide Hydrochloride, α -cyclodextrin and β -cyclodextrin were $\geq 98.0\%$, $\geq 98.0\%$ and $\geq 97.0\%$ respectively.

VIII.2.2 Instrumentations

UV-visible spectra were recorded by JASCO V-530 UV/VIS Spectrophotometer, with an uncertainty of wavelength resolution of ± 2 nm. All the absorption spectra were recorded at $25^\circ\text{C} \pm 1^\circ\text{C}$. The measuring temperature was held constant by an automated digital thermostat.

The surface tension experiments were accomplished by platinum ring detachment technique using digital tensiometer K9, KRÜSS, Germany at the experimental temperature. Accuracy in the measurement was ± 0.1 mNm⁻¹. Temperature was maintained at 298.15 K by circulating auto-thermostat water through a double-wall glass vessel containing the solution.

Specific conductivities of the experimental solutions were measured by Mettler Toledo Seven Multi conductivity meter with uncertainty ± 1.0 $\mu\text{S m}^{-1}$. The experiments were carried out in an auto-thermostat water bath maintaining the temperature at 298.15 K and using the HPLC grade water with specific conductance of 6.0 $\mu\text{S m}^{-1}$. The cell was calibrated using a 0.01M aqueous KCl solution.

Steady state fluorescence emission study was carried out in bench top spectrofluorimeter from Photon Technologies International (Quantmaster-40, USA) with excitation and emission slit widths fixed at 3.0 nm and 2.0 nm respectively. Samples were taken in Hellma quartz cuvette of optical length 1.0 cm.

¹H NMR spectra were recorded in D₂O at 300 MHz in Bruker Avance 300 MHz instrument at 298 K. Signals are cited as δ values in ppm using residual protonated solvent signal as internal standard (HDO: δ 4.79 ppm). Data are reported as chemical shift.

Fourier transform infrared spectra were recorded in a Perkin Elmer FT-IR spectrometer according to the KBr disk method. KBr disks were made in 1:100 ratios of sample and KBr. FTIR studies were carried out in the scanning range of 4000–400 cm^{-1} at room temperature.

VIII.2.3 Preparation of MP: α -CD and MP: β -CD inclusion complexes

Prior to the start of the experimental work solubility of the chosen CDs and MP have been precisely checked and it was observed that the selected drug freely soluble in all proportion of CD solution. The two solid ICs (MP+ α -CD and MP + β -CD) have been prepared in 1:1 molar ratio of MP and CD. For each complex, 1.0 millimole MP and 1.0 millimole CD were dissolved in 30 mL water separately and stirred for 2 hours. Then the aqueous solution of MP was added drop wise to the aqueous solution of CD. The resulting mixture was stirred for an additional 24 h at room temperature and filtered. The filtrate was concentrated by evaporating, and the resulting precipitate was collected and dried at 50°C for 12 h. The white inclusion complexes were used to characterize by different physical and spectroscopic methods.

VII.3. RESULTS AND DISCUSSION

VIII.3.1 Job plot demonstrate the Stoichiometry

To establish the stoichiometry of the complex, the continuous variation method (Job's plot) was used to follow the changes in absorbance [26-28]. The absorbance of a set of solutions of MP with α and β -CD was/were measured by using UV-visible spectroscopy. The plot of $\Delta A \times R$ against R represents the job plot where ΔA is the differences in absorbance of MP with and without CDs and $R = \frac{[MP]}{[MP] + [CD]}$ and is presented in **Figure VIII.1a** and **VIII.1b**. Absorbance values were calculated at $\lambda_{\text{max}}=272$ nm for all the solutions at 298.15 K. In this method, the total molar concentration of the two binding partners ($[MP] + [CD]$) is kept constant but their mole fraction are varied in the range of 0-1 (**Table VIII.1 and VIII.2**) [29, 30].

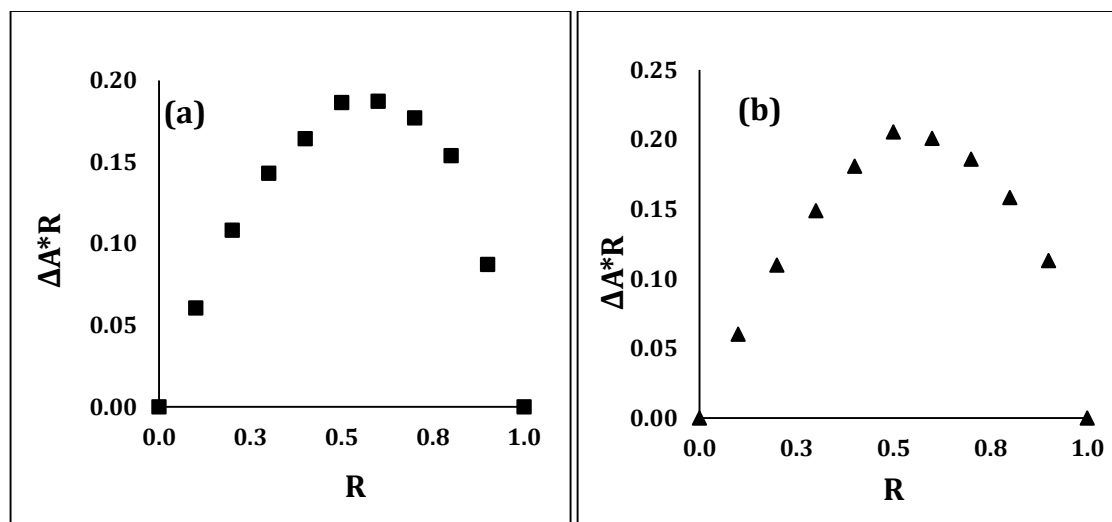


Figure VIII.1: Job plots of (a) MP:α-CD system and (b) MP:β-CD system at $\lambda_{\max} = 272$ nm at 298.15 K. $R = [SS]/([MP] + [CD])$, ΔA = absorbance difference of MP with and without CD.

According to this method, the value of R at the maxima on the curve provides the stoichiometry of IC, thus, the ratio of guest and host is 1:2 if $R \approx 0.33$; 1:1 if $R \approx 0.5$; 2:1 if $R \approx 0.66$ etc. The maxima for each of the two plots in **Figure VIII.1a** and **VIII.1b** were the found at $R \approx 0.5$, which indicate 1:1 stoichiometry of the host-guest inclusion complexes.

Table VIII.1: Data for the Job plot performed by UV-Vis spectroscopy for aqueous MP:α-CD system at 298.15K^a

MP (mL)	α-CD (mL)	MP (μM)	α-CD (μM)	$R = \frac{[MP]}{[MP] + [\alpha-CD]}$	Absorbance (A)	ΔA	ΔA*R
0	3	0	50	0.0	0.00000	0.7114	0.0000
0.3	2.7	05	45	0.1	0.10455	0.6068	0.0607
0.6	2.4	10	40	0.2	0.16964	0.5417	0.1083
0.9	2.1	15	35	0.3	0.23445	0.4769	0.1431
1.2	1.8	20	30	0.4	0.30051	0.4109	0.1643
1.5	1.5	25	25	0.5	0.33845	0.3729	0.1865
1.8	1.2	30	20	0.6	0.39919	0.3122	0.1873
2.1	0.9	35	15	0.7	0.45848	0.2529	0.1770
2.4	0.6	40	10	0.8	0.51901	0.1924	0.1539
2.7	0.3	45	05	0.9	0.61435	0.0970	0.0873
3.0	0	50	0	1.0	0.71136	0.0000	0.0000

^a Standard uncertainties in temperature u are: $u(T) = \pm 0.01$ K.

Table VIII.2: Data for the Job plot performed by UV-Vis spectroscopy for aqueous MP: β -CD system at 298.15K^a

MP (mL)	β - CD (mL)	MP (μ M)	β - CD (μ M)	$R = \frac{[MP]}{[MP] + [\beta-CD]}$	Absorbance (A)	ΔA	$\Delta A * R$
0	3	0	50	0.0	0.0000	0.7114	0.0000
0.3	2.7	05	45	0.1	0.1086	0.6028	0.0603
0.6	2.4	10	40	0.2	0.1624	0.5490	0.1098
0.9	2.1	15	35	0.3	0.2151	0.4963	0.1489
1.2	1.8	20	30	0.4	0.2590	0.4523	0.1809
1.5	1.5	25	25	0.5	0.3007	0.4107	0.2054
1.8	1.2	30	20	0.6	0.3766	0.3348	0.2009
2.1	0.9	35	15	0.7	0.4457	0.2657	0.1860
2.4	0.6	40	10	0.8	0.5133	0.1981	0.1584
2.7	0.3	45	05	0.9	0.5856	0.1257	0.1131
3.0	0	50	0	1.0	0.7114	0.0000	0.0000

^a Standard uncertainties in temperature u are: $u(T) = \pm 0.01$ K.

VIII.3.2 Surface tension study

Surface tension (γ) study provides significant evidence regarding the formation and the stoichiometry of the host-guest inclusion complex [31-33]. MP behaves like surfactant molecule, which is reflected in the lower γ value of its aqueous solution compared to pure aqueous media [34,35]. CDs in contrast, because of having hydrophobic outer surface and hydrophilic rims, hardly show any change in γ while dissolved in aqueous medium for a wide range of concentration [36,37]. In the present study γ of aqueous MP was measured with increasing concentration of α and β -CD at 298.15K (**Table VIII.3** and **VIII.4**). In both cases there were progressively rising trend of γ with increasing concentration of α and β -CD (**Figure VIII.2a** and **VIII.2b**), may be as a result of encapsulation of the MP molecule from the surface of the solution into the

hydrophobic cavity of CDs forming host-guest ICs (**Scheme VIII.2**) [30]. Both the plots also demonstrate that there are single noticeable breaks in each curve (**Figure VIII.2a** and **VIII.2b**), which not only reveal the formation of IC but also specify the 1:1 stoichiometric ratio for each of the ICs formed [31,32].

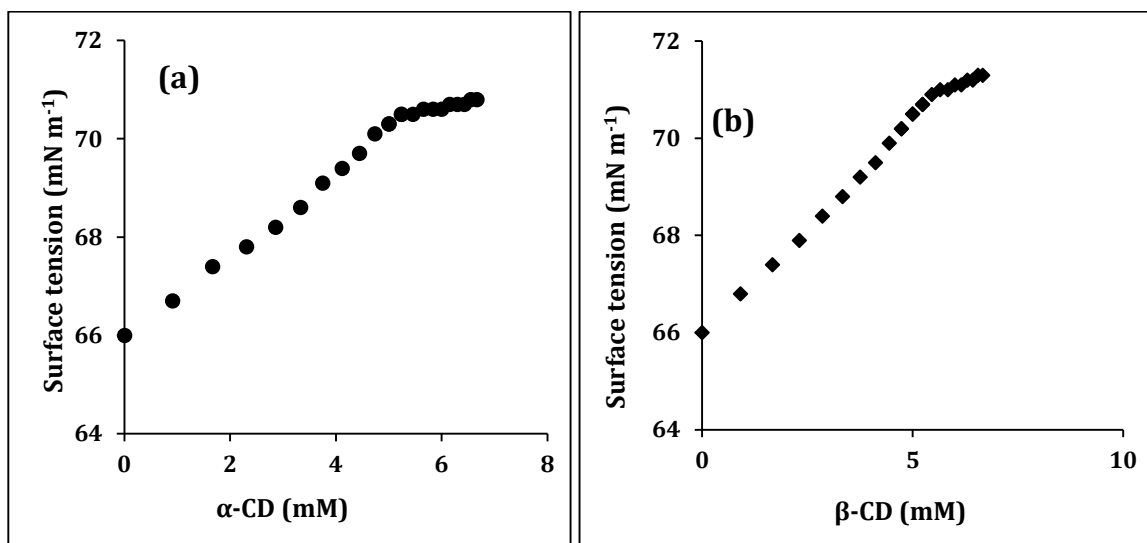


Figure VIII.2: Variation of surface tension of aqueous MP with increasing concentration of (a) α -CD and (b) β -CD solution respectively at 298.15 K.

Table VIII.3: Data for surface tension and conductivity study of aqueous MP: α -CD system at 298.15K^a

Conc. of MP (mM)	Conc. of α -CD (mM)	Surface tension (mN m ⁻¹)	Conductivity (mS m ⁻¹)
10	0	66	1.280
9.091	0.909	66.7	1.163
8.333	1.667	67.4	1.075
7.692	2.308	67.8	0.997
7.143	2.857	68.2	0.929
6.667	3.333	68.6	0.870
6.250	3.750	69.1	0.812
5.882	4.118	69.4	0.761
5.556	4.444	69.7	0.719
5.263	4.737	70.1	0.684
5.000	5.000	70.3	0.652
4.762	5.238	70.5	0.643
4.545	5.455	70.5	0.635
4.348	5.652	70.6	0.628
4.167	5.833	70.6	0.621
4.000	6.000	70.6	0.615
3.846	6.154	70.7	0.610
3.704	6.296	70.7	0.605
3.571	6.429	70.7	0.599
3.448	6.552	70.8	0.595
3.333	6.667	70.8	0.591

^a Standard uncertainties in temperature u are: $u(T) = \pm 0.01$ K.

Table VIII.4: Data for surface tension and conductivity study of aqueous MP: β -CD system at 298.15K^a

Conc. of MP (mM)	Conc. of β -CD (mM)	Surface tension (mN m ⁻¹)	Conductivity (mS m ⁻¹)
10	0	66	1.280
9.091	0.909	66.8	1.160
8.333	1.667	67.4	1.070
7.692	2.308	67.9	0.988
7.143	2.857	68.4	0.917
6.667	3.333	68.8	0.856
6.250	3.750	69.2	0.799
5.882	4.118	69.5	0.750
5.556	4.444	69.9	0.708
5.263	4.737	70.2	0.675
5.000	5.000	70.5	0.640
4.762	5.238	70.7	0.630
4.545	5.455	70.9	0.621
4.348	5.652	71.0	0.613
4.167	5.833	71.0	0.604
4.000	6.000	71.1	0.598
3.846	6.154	71.1	0.586
3.704	6.296	71.2	0.579
3.571	6.429	71.2	0.572
3.448	6.552	71.3	0.565
3.333	6.667	71.3	0.560

^a Standard uncertainties in temperature u are: $u(T) = \pm 0.01$ K.

The values of γ and corresponding concentrations of MP and CDs at each break have been listed in **Table VIII.5**, which also point out that at each break point the concentration ratio of host and guest is about 1:1, establishing the formation of 1:1 ICs between MP and CDs [30, 35].

Table VIII.5: Values of surface tension (γ) at the break point with corresponding concentrations of MP and CD at 298.15 K^a

	Conc. of MP/mM	Conc. of CD/mM	$\gamma^a/\text{mN}\cdot\text{m}^{-1}$
α -CD	4.80	5.20	70.4
β -CD	4.46	5.36	70.7

^a Standard uncertainties (u): temperature: $u(T) = \pm 0.01$ K, surface tension: $u(\gamma) = \pm 0.1$ $\text{mN}\cdot\text{m}^{-1}$

VIII.3.3 Conductivity study

Conductivity (κ) study is an essential tool to elucidate the inclusion phenomenon in solution phase [38,39]. It identifies the formation as well as the stoichiometry of the ICs [34,36]. In the present study the conductivity of aqueous solution of MP was measured with continuous addition of α and β -CD (**Table VIII.3** and **VIII.4**).

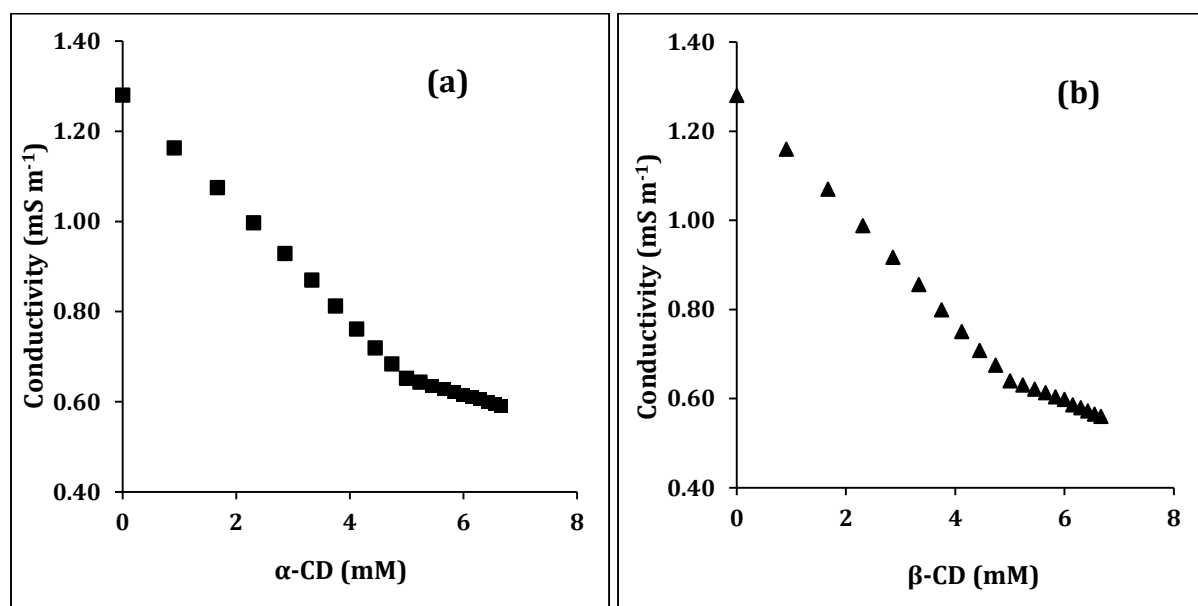


Figure VIII.3: Variation of surface tension of aqueous MP with increasing concentration of (a) α -CD and (b) β -CD solution respectively at 298.15 K.

In aqueous solution MP has substantial conductance value which show gradually decreasing trend of κ (**Figure VIII.3a** and **VIII.3b**) with the successive addition of aqueous solution of CDs, may be because of less number of free MP molecules in the medium due to encapsulation into the cavity of CDs [40,41]. Thus, the conductivities of the solutions are noticeably affected by the inclusion phenomenon (Scheme VIII.2) [39]. At certain concentrations of α and β -CD single breaks were found in each conductivity curve signifying the formation of 1:1 IC (**Figure VIII.3a** and **VIII.3b**) [30,34]. The values of κ and corresponding concentrations of MP and CDs at each break have been listed in **Table VIII.6**, which inform that the ratio of the concentrations of MP and each CD at the break point is roughly 1:1, suggesting that MP-CD IC is equimolar, *i.e.*, the host-guest ratio is 1:1 [36,39]. There always exists a dynamic equilibrium between the host and guest molecule. At the break point most of the guest molecules are inserted in the cavity of CD *i.e.*, at this point maximum inclusion takes place than before. After this point the concentration of CD is more than the drug molecule and the equilibrium is shifted toward the ICs.

Table VIII.6: Values of conductivity (κ) at the break point with corresponding concentrations of MP and CD at 298.15 K^a

	Conc. of MP/mM	Conc. of CD/mM	κ^a /mS.m ⁻¹
α -CD	5.05	4.95	0.651
β -CD	5.01	4.99	0.659

^a Standard uncertainties (*u*): temperature: $u(T) = \pm 0.01$ K, conductivity: $u(\kappa) = \pm 0.001$ mS.m⁻¹

VIII.3.4 Association constants from UV-vis spectroscopy

Spectrophotometric titration is carried out to determine the molecular encapsulation behavior of MP with CDs in aqueous solution [42-45]. The absorption spectral data of MP with various concentrations of CD are given in **Table VIII.7** and **VIII.8**. The absorption intensity of MP gradually increased with the stepwise addition of

CDs [Figure VIII.4a and VIII.5a][30]. This change might be partly attributed to the shielding of chromophore groups of MP in the CD cavity [28].

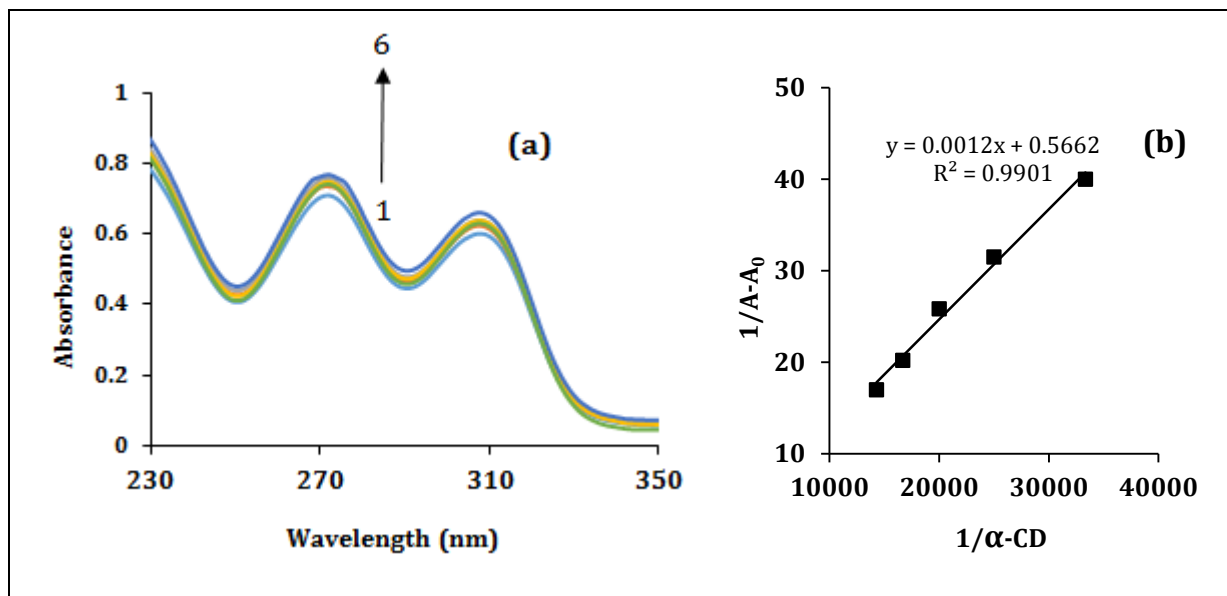


Figure VIII.4: (a) Absorption spectra of MP (50 μM) in different $\alpha\text{-CD}$ concentrations (μM): 1) without $\alpha\text{-CD}$, 2) 30 μM , 3) 40 μM , 4) 50 μM , 5) 60 μM , 6) 70 μM . (b) Benesi-Hildebrand plot of $1/A-A_0$ vs. $1/[\alpha\text{-CD}]$ for 1:1 complexation of MP with $\alpha\text{-CD}$.

Table VIII.7: Data for the Benesi-Hildebrand double reciprocal plot performed by UV-Vis spectroscopy for MP: $\alpha\text{-CD}$ system

[MP] / μM	$[\alpha\text{-CD}]$ / μM	A_0	A	$A - A_0$	$1/[\alpha\text{-CD}]$ / M^{-1}	$1/A - A_0$	Intercept	Slope	K_a / M^{-1}
50	30		0.73636	0.02500	33333	40.00000			
50	40		0.74309	0.03173	25000	31.51592			
50	50	0.71136	0.75008	0.03872	20000	25.82645	0.5662	0.0012	472
50	60		0.76079	0.04943	16667	20.23063			
50	70		0.77018	0.05882	14286	17.00102			

^a Standard uncertainties in temperature are: (T) = ± 0.01 K.

In this case, the association constant for the formation of MP: CD complexes are determined by analyzing the changes in the absorbance of MP with the CDs concentration. The association constant K_a and stoichiometry of the inclusion complex of MP with both CDs can be determined by the Benesi-Hildebrand equation [Figure VIII.4b and VIII.5b][46]:

$$\frac{1}{A - A_0} = \frac{1}{\Delta\epsilon[MP]K_a} \cdot \frac{1}{[CD]} + \frac{1}{\Delta\epsilon[MP]}$$

where [CD] and [MP] refer to the total concentration of cyclodextrin and metoclopramide drug respectively, $\Delta\epsilon$ is the change in molar extinction coefficient of the chromophore MP as the MP molecules go from the polar aqueous environment to the apolar cavity of α or β -CD making the ICs [36]. $A - A_0$ denotes the absorption changes of MP on the addition of CDs. The values of K_a for each of the complexes were evaluated by dividing the intercept by the slope of the straight line of the double reciprocal plot (Table VIII.7 and VIII.8). The change of absorbance ($A - A_0$) was measured as a function of concentration of α and β -CD molecule to find out the association constant (K_a). The good linearity of the plot shows the formation of a 1:1 complex between MP and CDs.

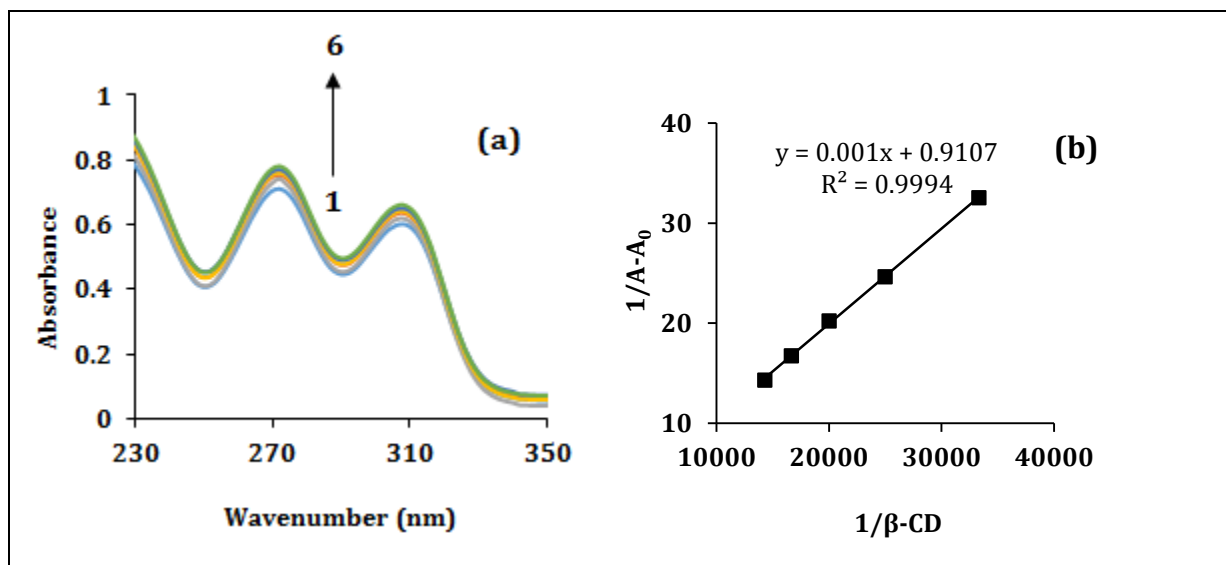


Figure VIII.5: (a) Absorption spectra of MP (50 μM) in different β-CD concentrations (μM): 1) without β-CD, 2) 30 μM, 3) 40 μM, 4) 50 μM, 5) 60 μM, 6) 70 μM. (b) Benesi-Hildebrand plot of $1/A - A_0$ vs. $1/[\beta\text{-CD}]$ for 1:1 complexation of MP with β-CD

Table VIII.8: Data for the Benesi-Hildebrand double reciprocal plot performed by UV-Vis spectroscopy for MP:β-CD system at 298.15K

[MP] /μM	[β-CD] /μM	A ₀	A	A - A ₀	1/[β-CD] /M ⁻¹	1/A - A ₀	Intercept	Slope	K _a /M ⁻¹
50	30		0.74208	0.03072	33333	32.55208			
50	40		0.75195	0.04059	25000	24.63661			
50	50	0.71136	0.76078	0.04942	20000	20.23472	0.9107	0.001	911
50	60		0.77105	0.05969	16667	16.75322			
50	70		0.78121	0.06985	14286	14.31639			

^a Standard uncertainties in temperature u are: $u(T) = \pm 0.01$ K.

VIII.3.5 Association constant from fluorescence spectroscopy

The supramolecular interaction of MP with CDs was been investigated by spectrofluorimetry [47-49]. As shown in **Figure VIII.6a** and **VIII.7a**, with an increase in the CDs (α -CD and β -CD) concentration, however, the fluorescence intensity of MP was enhanced accompanied by a slight hypsochromic shift of the emission peak [**Table VIII.9** and **VIII.10**]. These findings indicated the formation of MP-CDs inclusion complexes. Molecules partially or fully encapsulated in the CD cavity often exhibit an enhancement in their fluorescence intensity. This is because the cyclodextrin's cavity offers a protective microenvironment which can shield the excited singlet species from quenching and nonradiative decay process occurring in the bulk aqueous solution [50,51].

The association constants (K_a) of both the complexes were calculated from fluorescence data using the modified Benesi-Hildebrand equation [46]:

$$\frac{1}{I - I_0} = \frac{1}{[I' - I_0]K_a} \cdot \frac{1}{[CD]} + \frac{1}{I' - I_0}$$

Where I and I_0 represent the fluorescence intensities of MP in the presence and absence of CDs, respectively; $[CD]$ represent the concentrations of both CDs; K_a is the association constant of the complexes and I' denotes the fluorescence intensity when all MP

molecules are essentially complexed with CDs. The double reciprocal plots $1/(I-I_0)$ vs. $1/[CD]$ for MP complexed with α -CD and β -CD (shown in **Figure 6b** and **7b**) exhibit good linearity, implying that the inclusion complexes have a stoichiometric ratio of 1:1.

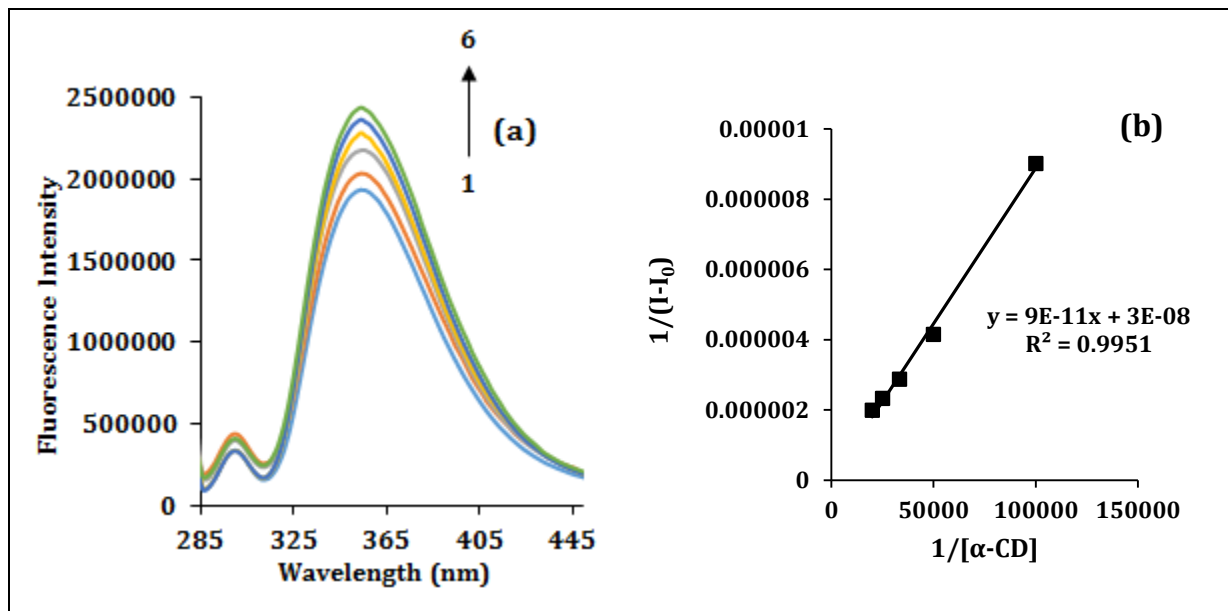


Figure VIII.6: (a) Fluorescence emission spectra of MP (5 μ M) in different α -CD concentrations (μ M): 1) without α -CD, 2) 10 μ M, 3) 20 μ M, 4) 30 μ M, 5) 40 μ M, 6) 50 μ M. (b) Benesi-Hildebrand plot of $1/I-I_0$ vs. $1/[\alpha\text{-CD}]$ for 1:1 complexation of MP with α -CD.

Table VIII.9: Data for the Benesi-Hildebrand double reciprocal plot performed by fluorescence spectroscopy for MP: α -CD system at 298.15K^a

[MP] / μ M	[α -CD] / μ M	I_0	I	$I - I_0$	$1/[\alpha\text{-CD}]$ / M^{-1}	$1/I - I_0$	Intercept	Slope	K_a / M^{-1}
5	10		2042391	110928	100000	9.01×10^{-6}			
5	20		2172112	240649	50000	4.16×10^{-6}			
5	30	1931463	2278802	347339	33333	2.88×10^{-6}	3×10^{-6}	9×10^{-6}	333
5	40		2360301	428838	25000	2.33×10^{-6}			
5	50		2433963	502499	20000	1.99×10^{-6}			

^a Standard uncertainties in temperature u are: $u(T) = \pm 0.01$ K.

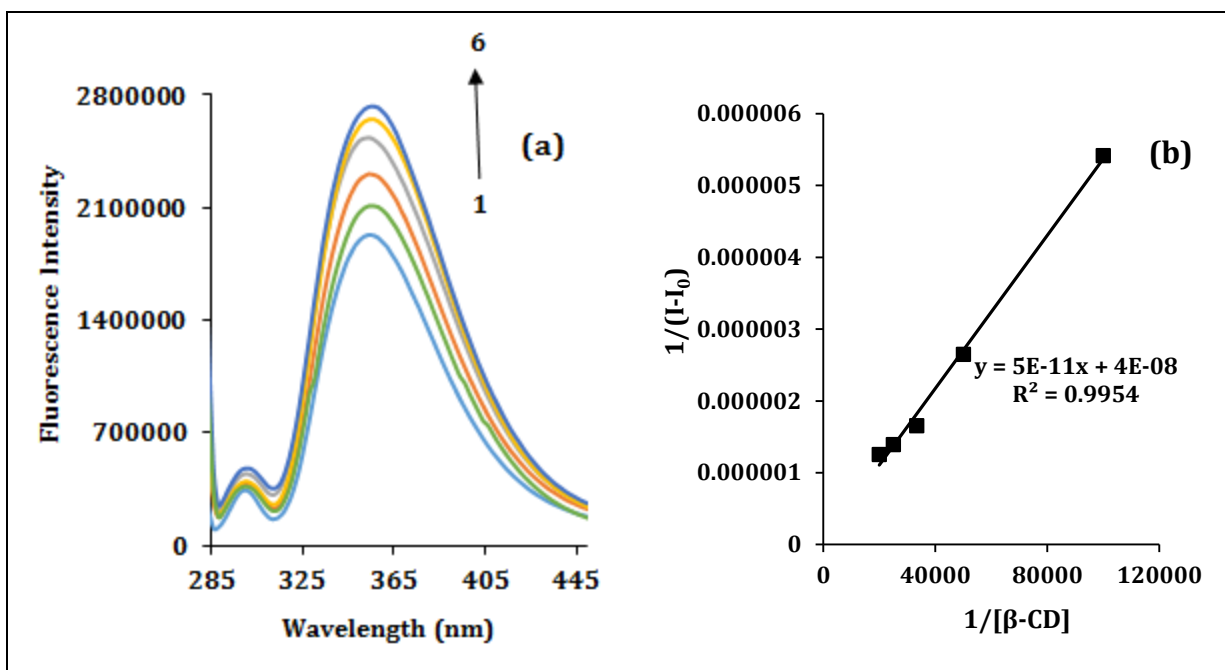


Figure VIII.7: (a) Fluorescence emission spectra of MP (5 μM) in different $\beta\text{-CD}$ concentrations (μM): 1) without $\beta\text{-CD}$, 2) 10 μM , 3) 20 μM , 4) 30 μM , 5) 40 μM , 6) 50 μM . (b) Benesi-Hildebrand plot of $1/(I-I_0)$ vs. $1/[\beta\text{-CD}]$ for 1:1 complexation of MP with $\beta\text{-CD}$.

Table VIII.10: Data for the Benesi-Hildebrand double reciprocal plot performed by fluorescence spectroscopy for MP: $\beta\text{-CD}$ system at 298.15K^a

[MP] / μM	[$\beta\text{-CD}$] / μM	I_0	I	$I - I_0$	$1/[\beta\text{-CD}]$ / M^{-1}	$1/(I - I_0)$	Intercept	Slope	K_a / M^{-1}
5	30	2116069	184606	100000	5.42×10^{-4}				
5	40	2309301	377838	50000	2.65×10^{-4}				
5	50	1931463	2535769	604306	33333	1.65×10^{-4}	4×10^{-8}	5×10^{-11}	800
5	60	2648717	717254	25000	1.39×10^{-4}				
5	70	2727701	796238	20000	1.26×10^{-4}				

^a Standard uncertainties in temperature u are: $u(T) = \pm 0.01$ K.

The association constant of MP: $\beta\text{-CD}$ complex is higher than MP: $\alpha\text{-CD}$ complex [Table VIII.11] which indicates that the capability of $\beta\text{-CD}$ to form an inclusion complex

with MP is higher than probably due to its larger cavity size than that of α -CD i.e the size of its cavity is more appropriate to encapsulate the drug molecules.

Table VIII.11: Values of Association constants (K_a) obtained by Benesi–Hildebrand method both from UV-vis spectroscopy and Fluorescence spectroscopy and corresponding free energy change (ΔG^0) of the MP:CD inclusion complexes at 298.15K^a

	$K_a \times 10^{-2} / M^{-1b}$	$\Delta G^0 / KJ \text{ mol}^{-1b}$	$K_a \times 10^{-2} / M^{-1b}$	$\Delta G^0 / KJ \text{ mol}^{-1b}$
	UV-vis spectroscopy		Fluorescence spectroscopy	
MP: α -CD	4.72	-3.85	3.33	-2.98
MP: β -CD	9.11	-5.48	8.00	-5.15

^aStandard uncertainties in temperature u are: $u(T) = \pm 0.01$ K.

^bMean errors in $K_a = \pm 0.02 \times 10^{-3} M^{-1}$; $\Delta G^0 = \pm 0.01$ kJ mol⁻¹.

VIII.3.6 The thermodynamics of inclusion process

The thermodynamic parameters ΔG for the binding of guest molecule to cyclodextrin cavity can be calculated from the association constant 'K' by using the following equation

$$\Delta G = - RT \ln K_a$$

The thermodynamic parameters ΔG for the binding of guest molecules (MP) to CD cavity are given in **Table VIII.11**. The negative value of ΔG suggests that the inclusion process proceeded spontaneously at 298.15 K.

VII.3.7 ¹H-NMR analysis of inclusion complexes

NMR study is the most important tool which ascertains the inclusion phenomena of the guest drug molecule inside the host CD molecule. Hence, further investigations of inclusion complexes were performed by ¹H-NMR analysis. Chemical shifts and the changes of the chemical shifts of protons in MP: CD complex compared with the pure compounds of MP and CDs (**Figure VIII.8** and **VIII.9**).

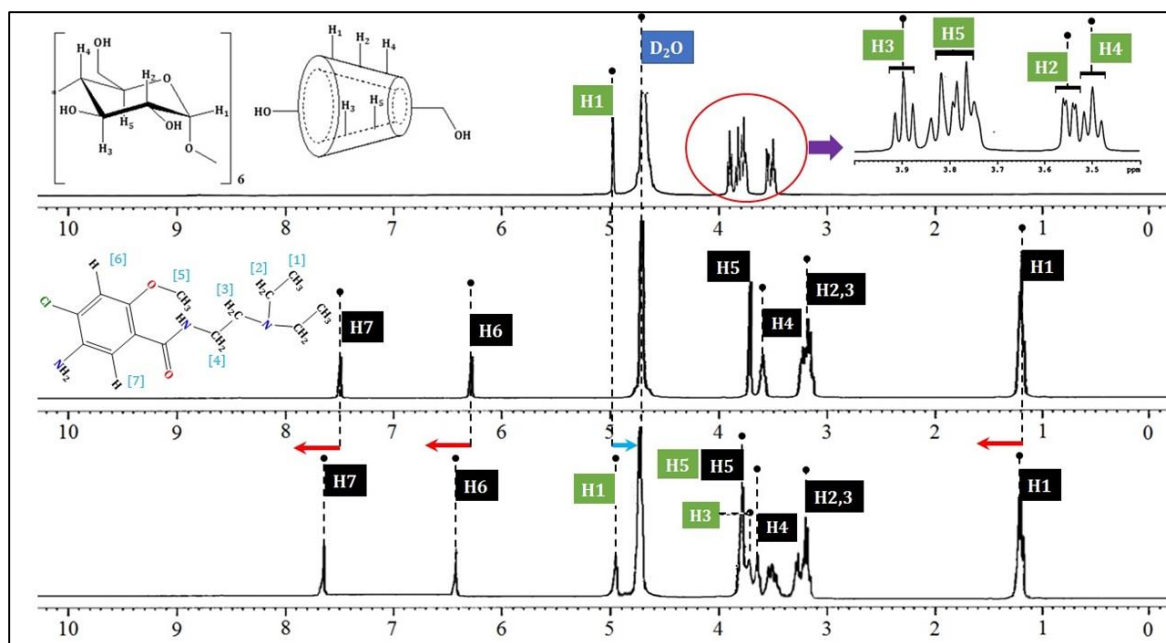


Figure VIII.8: ^1H NMR spectra of (a) α -CD, (b) MP and (c) 1:1 M ratio of α -CD & MP in D_2O at 298.15 K.

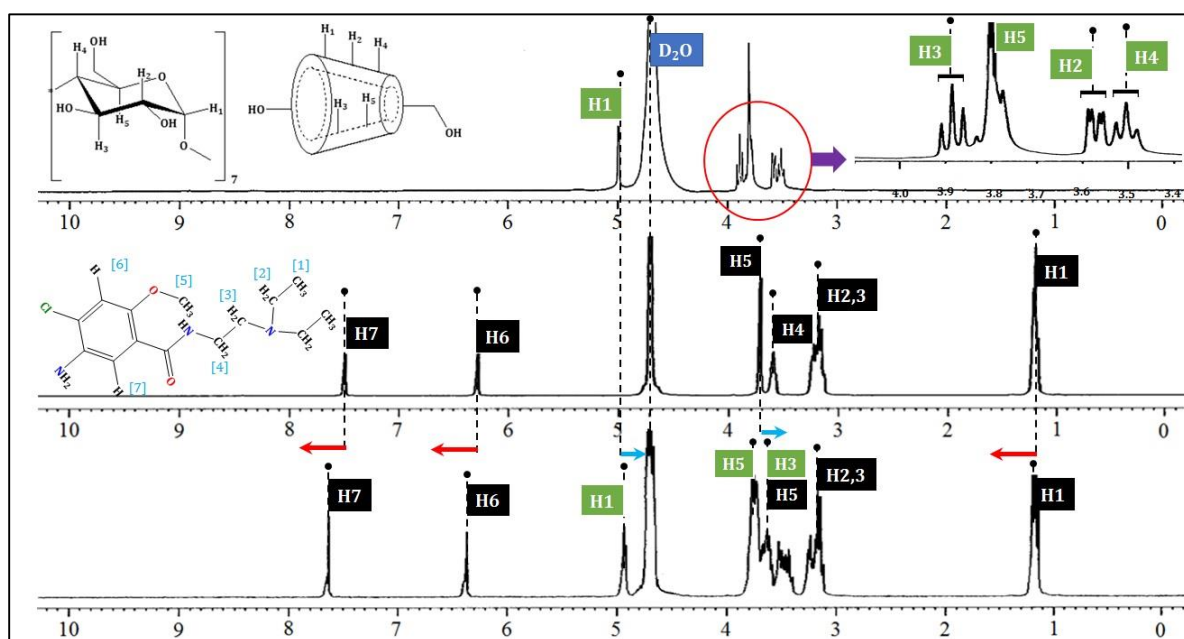
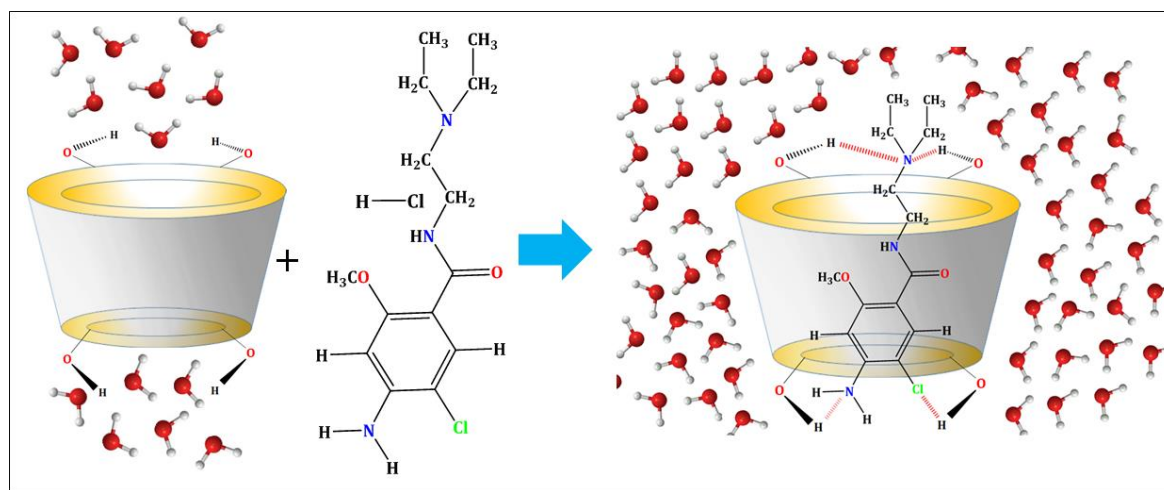


Figure VIII.9: ^1H NMR spectra of (a) β -CD, (b) MP and (c) 1:1 M ratio of β -CD & MP in D_2O at 298.15 K.

In the structure of CD it may be observed that the H3 and H5 hydrogens are located inside the conical cavity, particularly, the H3 are placed near the wider rim while H5 are placed near the narrower rim and the other H1, H2 and H4 hydrogens are located at the exterior of the CD molecule (**Scheme VIII.1**) [28,52]. The observable changes in the chemical shifts of CD protons were detected for H3, H5 and H6 protons which is in accordance with the involvement of these protons in the formation of inclusion complex [20,31,53,54]. The highest proton shifts of CD in the complex have been observed for the H3 protons, and slightly lower for the H5 and H6 protons. The signals of the included MP are shifted by complexation to a variable extent. The spectral changes that can be observed in case of encapsulation of aromatic guest molecules are due to the interactions of interacting protons of CD by the aromatic moiety of the guest [54]. The chemical shift difference for the protons belonging to the phenyl ring are higher than that for the other group protons i.e. the H6 and H7 protons of the aromatic ring were more involved in the interaction with CD. Conversely, the protons of three ethyl group bonded with N atom experience very little perturbation. Thus from the above discussion we can say that the changes in chemical shifts of protons H-5, H-3, and H-6 of both CD (**Figure VIII.8** and **VIII.9**) and protons H6, H7 and H5 of the MP (Fig. 5), which show the most marked variations. Upfield chemical shift is also observed for the exterior protons of the CD but to lesser extent. The shifts of the interacting protons illustrates the mechanism of insertion as depicted in **Scheme VIII.2**.



Scheme VIII.2: Plausible schematic presentation of mechanism for formation of 1:1 inclusion complex between metoclopramide hydrochloride and cyclodextrin.

Based on the NMR data, the plausible mode of interaction of MP- α -CD and MP- β -CD complexes were proposed, which suggested that lipophilic aromatic ring of the MP entered into the cavity of CDs from the wider side, with the amide (-CONH) and methoxy (-OMe) residues inside the CD cavity, and the -N(CH₂CH₃)₂ group was close to the wider rim and exposed outside the cavity. Also the -NH₂ and -Cl moieties exposed outside the cavity near the narrower rim.

Selected ¹H NMR data

Metoclopramide Hydrochloride: ¹H NMR (D₂O, 298.15 K): δ /ppm 1.154-1.202 (6H, m), 3.144-3.237 (6H, m), 3.584-3.602 (2H, m), 3.697-3.706(3H, m), 6.262-6.271 (1H, s), 7.474-7.484 (1H, s).

α - Cyclodextrin (α -CD): ¹H NMR (D₂O, 298.15 K): δ /ppm 3.480-3.517 (6H, t, J = 9.00 Hz), 3.534-3.560 (6H, dd, J = 10.00, 3.00 Hz), 3.749-3.839 (18H, m), 3.877-3.914 (6H, t, J = 9 Hz), 4.965-4.971 (6H, d, J = 3 Hz).

β - Cyclodextrin (β -CD): ¹H NMR (D₂O, 298.15 K): δ /ppm 3.497-3.543 (7H, t, J = 9.2 Hz), 3.570-3.603 (7H, dd, J = 9.6, 3.2 Hz), 3.790-3.848 (21H, m), 3.878-3.925 (7H, t, J = 9.2 Hz), 5.003-5.012 (7H, d, J = 3.6 Hz)

MP- α -CD (1:1 molar ratio): ¹H NMR (D₂O, 298.15 K): δ /ppm 1.162-1.212 (6H, m), 3.149-3.245 (6H, m), 3.427-3.531 (12H, m), 3.607-3.646 (2H, m), 6.404 (1H, s), 7.617 (1H, s), 3.717-3.760 (6H, m), 3.805 (21H, m), 4.923-4.934 (6H, m).

MP- β -CD (1:1 molar ratio) ¹H NMR (D₂O, 298.15 K): δ /ppm 1.157-1.208 (6H, m), 3.180-3.281 (6H, m), 3.428-3.553 (12H, m), 3.612-3.696 (2H+6H, m), 6.392-6.406 (1H, s), 7.622-7.667 (1H, s), 3.747-3.819 (21H+3H, m), 4.936-4.947 (6H, m).

VIII.3.8 FT-IR Spectra of solid inclusion complexes

The solid inclusion complex formation is analyzed by FT-IR spectroscopy. FT-IR spectrum is used to confirm the formation of the solid inclusion complex by considering the deviation of peak shape position and intensity [55-58]. The characteristic IR frequencies of MP, α -CD, β -CD and their solid ICs are listed in **Table VIII.12** with the chemical bonds responsible for the corresponding stretching frequencies and the spectra

are shown in **Figure VIII.10** and **VIII.11**. In the IR spectra, symmetric stretching of vibrations of amine N-H is observed at 3316 cm^{-1} [59]. Owing to the result of inclusion the stretching of N-H vibration got slightly shifted. The peaks observed at 3369 cm^{-1} and 3201 cm^{-1} were assigned to amide group N-H asymmetric and symmetric stretching vibrations. The carbonyl stretching vibration of C=O group is appeared at 1640 cm^{-1} for amides [60]. The IR spectrum of the MP (**Figure VIII.10** and **VIII.11**) is also characterized by absorption peaks at 2939 cm^{-1} (for C-H stretching vibration in aromatic ring), 1590 cm^{-1} (for N-H bending vibration), 1213 cm^{-1} and 1026 cm^{-1} (for asymmetric and symmetric C-O stretching vibration of $-\text{OCH}_3$ group), 1309 cm^{-1} (for aromatic -C-N stretching vibration), 593.41 cm^{-1} (for C-Cl stretching vibration).

However, several peaks of the MP are either absent or shifted which is due to the change in environment of the guest molecule after inclusion in the cavity of CDs. The $(\text{N-H})_{\text{amide}}$ and $(\text{C-H})_{\text{aromatic}}$ band of the MP are almost completely masked by very intense and broad CDs bands. The $(>\text{C}=\text{O})_{\text{amide}}$ stretching signal was at 1640.81 cm^{-1} for MP, which was shifted at 1624 cm^{-1} in case of α -CD and at 1619 cm^{-1} in case of β -CD IC may be as a result of encapsulation into the CD cavity.

Broad characteristic peaks of $-\text{OH}$ at about 3363 cm^{-1} and 3372 cm^{-1} are present in the spectrum for α and β -CD. However, the peaks are shifted at 3398.66 cm^{-1} and 3397 cm^{-1} respectively in the solid inclusion complex. The $-\text{O-H}$ stretching of both α and β -CD is shifted in the spectrum of both ICs possibly due to involvement of the $-\text{O-H}$ groups of the host molecules in hydrogen bonding with the guest molecules. The stretching frequencies of the other characteristic peaks, which are shifted in solid inclusion complex due to various interactions, are given in the table 9. According to the above FT-IR analysis of inclusion complexes, we might recommend that the aromatic ring of the guest molecule is encapsulated in the hydrophobic cavity of α and β -CD. Hence, the FT-IR study provides significant indications of formation of ICs in the solid form, supporting the outcomes of the other above studies.

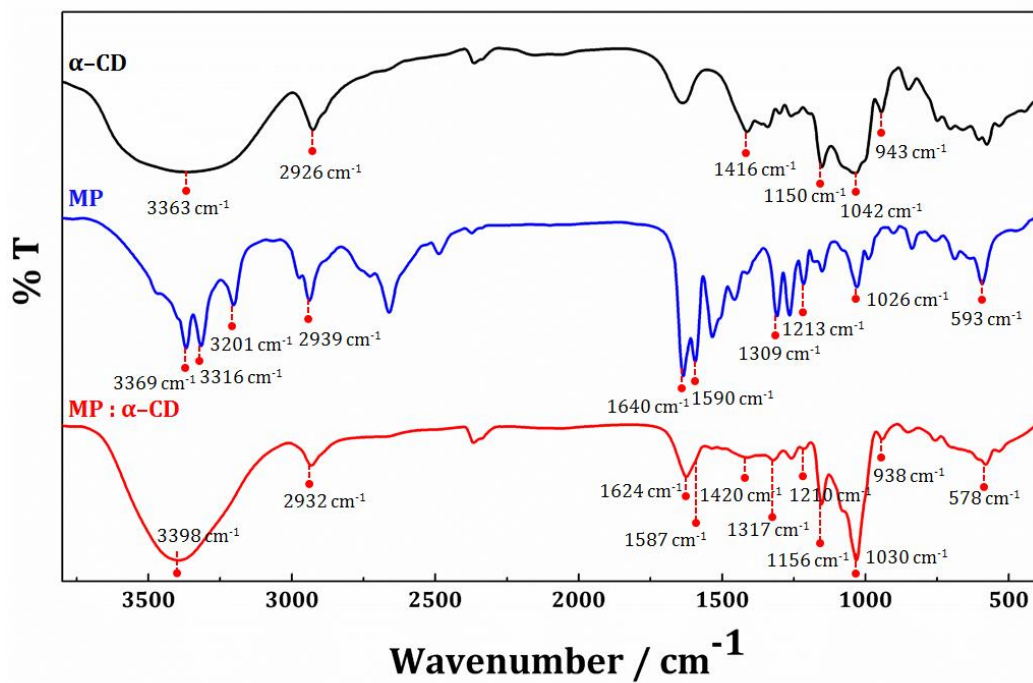


Figure VIII.10: FTIR spectra of free α -CD, MP and their 1:1 inclusion complex (MP: α -CD).

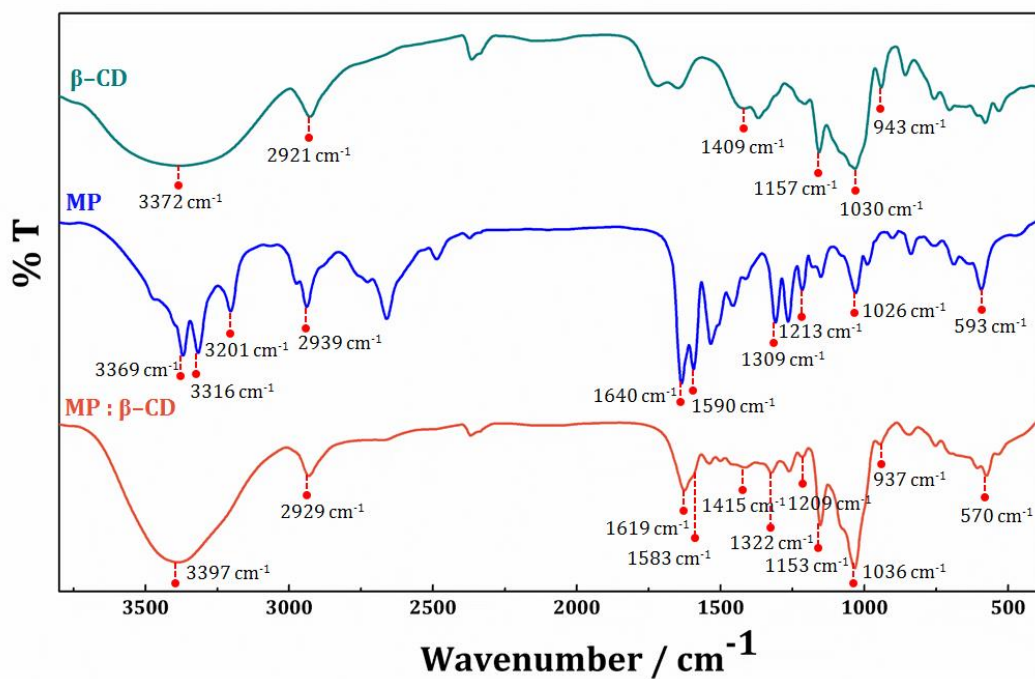


Figure VIII.11: FTIR spectra of free β -CD, MP and their 1:1 inclusion complex (MP: β -CD).

Table VIII.12: Comparison between the Frequencies change (cm^{-1}) of different functional group of free compound and their solid complexes

MP			
Functional Group	Wavenumber (cm^{-1})	Functional Group	Wavenumber (cm^{-1})
N-H asymmetric stretching of amide	3369	N-H bending	1590
N-H symmetric stretching of amide	3201	(aromatic)-C-N stretching	1309
N-H stretching of amine	3316	-C-O asymmetric stretching of -OCH ₃	1213
>C=O stretching of amide	1640	-C-O symmetric stretching of -OCH ₃	1026
Aromatic -C-H stretching	2939	-C-Cl stretching	593
α-Cyclodextrin		β-Cyclodextrin	
Functional Group	wave number/ cm^{-1}	Functional Group	wave number/ cm^{-1}
stretching of O-H	3363	stretching of O-H	3372
stretching of -C-H from -CH ₂	2926	stretching of -C-H from -CH ₂	2921
bending of -C-H from -CH ₂ and bending of O-H	1416	bending of -C-H from -CH ₂ and bending of O-H	1409
bending of C-O-C	1150	bending of C-O-C	1157
stretching of C-C-O Skeletal vibration	1042	stretching of C-C-O skeletal vibration	1030
involving α -1,4 linkage	943	involving α -1,4 linkage	943

MP- α -CD inclusion complex		MP- β -CD inclusion complex	
Functional Group	wave number/ cm^{-1}	Functional Group	wave number/ cm^{-1}
stretching of O-H of α -CD	3398	stretching of O-H of β -CD	3397
stretching of -C-H from -CH ₂ of α -CD	2932	stretching of -C-H from -CH ₂ of β -CD	2929
bending of -C-H from -CH ₂ and bending of O-H of α -CD	1420	bending of -C-H from -CH ₂ and bending of O-H of β -CD	1415
bending of C-O-C of α -CD	1156	bending of C-O-C β -CD	1153
Stretching C-C-O skeletal vibration involving α -1,4 linkage	1030	Stretching C-C-O skeletal vibration involving β -1,4 linkage	1036
>C=O stretching of amide (aromatic)-C-N stretching	938	>C=O stretching of amide (aromatic)-C-N stretching	937
-C-Cl stretching	1624	-C-Cl stretching	1619
N-H bending	1317	N-H bending	1322
-C-O asymmetric stretching of -OCH ₃	578	-C-O asymmetric stretching of -OCH ₃	570
	1587		1583
	1210		1209

VIII.3.9 Driving force of the inclusion complex formation

The formation of host-guest ICs between the MP drug and CDs not only depends upon the size of the guest molecules but also on the cavity diameter of host. The cavity diameter of α and β -CD are 4.7-5.3 Å and 6.0-6.5Å respectively. Considering the size of MP, it is found that β -CD is more suitable for forming ICs due to the size of its cavity is more appropriate to encapsulate MP molecules which is in agreement with spectroscopic and physicochemical observations. Another structural suitability of the CD molecule for the hydrophobic guest molecule has been explained by Shekaari and his co-worker [61] where, polar water molecules inside into the hydrophobic CD molecule are bound by polar-apolar interaction which is however not so strong and as a consequence the relatively more hydrophobic drug molecules form inclusion complex with relatively stronger apolar-apolar interaction removing the water molecules from the cavity. It results in a more stable lower energy state of the system and also reduces the ring strain of CD moiety. The stoichiometry of the host guest IC is 1:1 probably because of difficulty for the second molecule of MP to be trapped by the cavity after inclusion of one. The N atoms of the MP form H-bonds with the -OH groups at the rim of CD, thus stabilizing the whole IC.

VIII.4. CONCLUSION

The results obtained from UV-Visible, Fluorescence, NMR, FT-IR spectra and Mass analysis serve as a proof for the formation of inclusion complex of MP with both α and β -CD and MP. Taking all the parameters and results in account the plausible mechanism of the inclusion was depicted. The association constants of the complexes, calculated from uv and fluorescence data, discovered that the capability of β -CD to form an inclusion complex with MP is higher than that of α -CD, probably due to its larger cavity size. ^1H NMR data demonstrated that the hydrophobic aromatic ring with the amide (-CONH) and methoxy (-OMe) residues of MP were embedded inside the cavity of CDs, leaving the other residue exposed outside the cavity, while surface tension, conductivity and Job's measurement suggest 1:1 stoichiometry. Therefore, complexes of MP with CDs would certainly show advantage over the free drug usage in the field of medicine. As the CDs are prepared from starch by enzymic conversion, their safety profile is also assured and this formulation would open new vistas in the field of drug delivery.

CHAPTER-IX

HOLLOW CIRCULAR COMPOUND-BASED INCLUSION COMPLEXES OF AN IONIC LIQUID

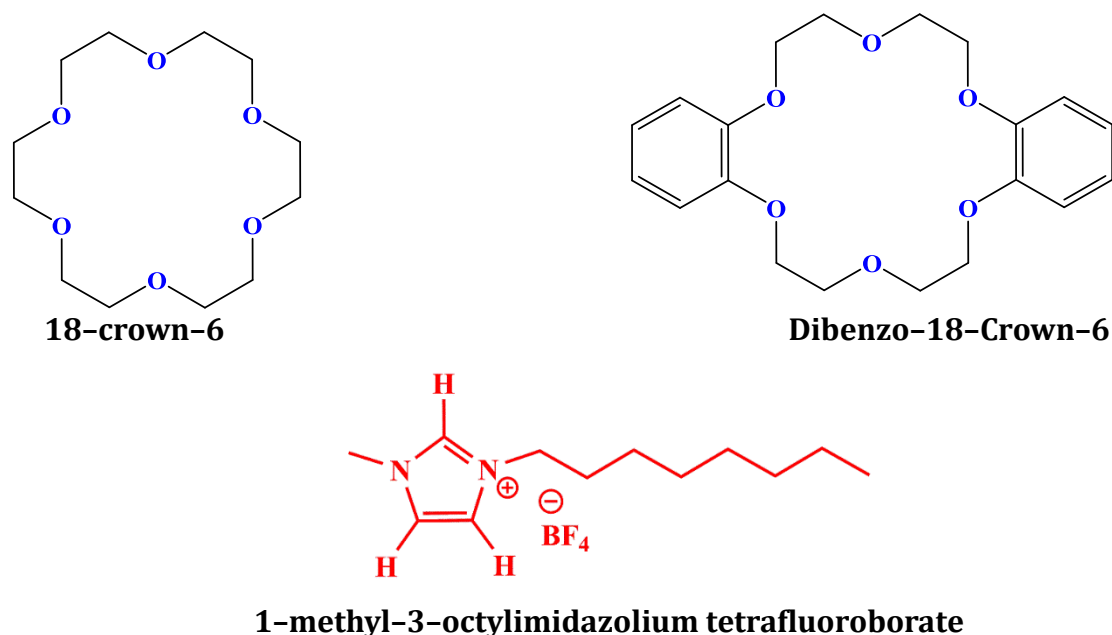
IX.1. INTRODUCTION

The crown ether (CE) family of macrocyclic compounds has attracted a huge amount of interest since their discovery in 1967 [1,2], especially in the fields of host-guest and coordination Chemistry. They can form complexes with a variety of guest species, such as metal cations, protonated species and neutral molecules, in their cavity via different types of interactions with multiple oxygen atoms [3,4]. Applications of CEs, such as phase transfer catalyst [5,6], photo-switching devices [7], and drug carriers [8], have been in progress on the basis of the inclusion ability. Crown ethers have proved to be unique cyclic molecules for molecular recognition of suitable substrates by hydrogen bonds, ionic interactions and hydrophobic interactions. The study of interactions involved in complexation of different cations with crown ethers in mixtures of solvents is important for a better understanding of the mechanism of biological transport, molecular recognition, and other analytical applications [9].

It is already known that the imidazolium cation can form inclusion complexes with large crown-ether-type hosts via H-bonding [10]. 1, 3-disubstituted imidazolium salts are known to form an inclusion complex with DB24C8 or its derivatives through intermolecular hydrogen-bond formation as demonstrated by different research groups [11-14]. In 1,3-disubstituted imidazolium salts, all protons on the imidazolium ring are quite acidic, as the positive charge is delocalized over the entire imidazolium ring [15]. The acidic protons are attractive in supramolecular chemistry, since the acidic protons participate in stronger hydrogen-bond formation with the lone pair of electrons of the oxygen this accounts for the stability of the adduct formed. Biologically important heterocyclic bases, like imidazole, form planar cations, act as an effective structural unit

at the active sites of various proteins and nucleic acids. However, during enzymatic reactions imidazole can also exist as a protonated cation, and may then interact with the substrate by direct electrostatic or π - π interactions. Imidazolium salts have been and are going to be significant not only in organometallic chemistry as precursors of N-heterocyclic carbenes [16, 17], but also in organic chemistry and material science areas as ionic liquids due to their unique chemical, physical, and electrical properties [18-21].

In this work, we have studied the inclusion complex formation of ionic liquid (IL) 1-methyl-3-octylimidazolium tetrafluoroborate with hollow circular based host 18-crown-6 (18C6) [complex 1] and dibenzo-18-crown-6 (DB18C6) [complex 2] in acetonitrile (ACN). The complexes were characterized by Conductance and IR study. The formation constant and thermodynamic parameters of the above specific interactions in solutions are discussed here. The structure of the IL 1-methyl-3-octylimidazolium tetrafluoroborate and both crown ethers are shown in **Scheme IX.1**.



Scheme IX.1: Molecular structure of crown ethers and IL.

IX.2. EXPERIMENTAL SECTION

IX.2.1 Reagents

The ionic liquid (97%) and crown ethers [18C6 (99%), DB18C6 (98%)] were bought from Sigma-Aldrich, Germany and used as purchased.

IX.2.2 Instrumentations

Prior to the start of the experimental work solubility of the chosen CEs and IL in ACN have been precisely checked and it was observed that the selected IL salt freely soluble in all proportion of CEs solution.

The conductance measurements were carried out in a Systronics-308 conductivity bridge of accuracy $\pm 0.01\%$, using a dip-type immersion conductivity cell, CD-10 having a cell constant of approximately $(0.1 \pm 0.001) \text{ cm}^{-1}$ [22]. The measurements were made in an auto-thermostated water bath maintaining the experimental temperature. The cell was calibrated using a 0.01M aqueous KCl solution. The uncertainty in temperature was 0.01 K.

Infrared spectra were recorded in 8300 FT-IR spectrometer (Shimadzu, Japan). The details of the instrument have formerly been described [23].

^1H NMR spectra were recorded in CD_3CN at 300 MHz using Bruker ADVANCE 300 MHz instrument. Signals are quoted as δ values in ppm using residual protonated solvent signals as internal standard (CD_3CN : δ 1.98 ppm). Data are reported as chemical shift.

IX.3. RESULTS AND DISCUSSION

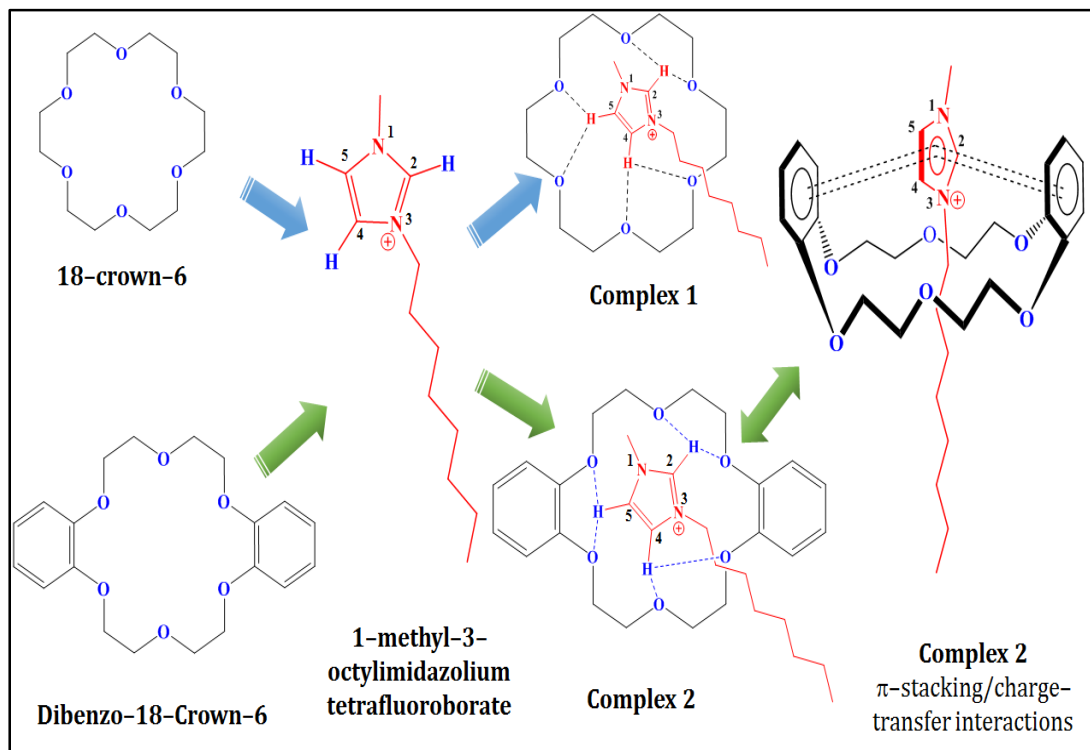
IX.3.1 Conductance

The benefit of the conductometric study is that the measurements can be carried out with high precision at very low concentration in solution systems. Conductance measurements of a solution of IL in presence of a crown ether provide information about the stability and transport phenomena of the cation-crown ether complex in the solution. Also, it is one of the most reliable methods for obtaining the formation constants of cation-macrocyclic complexes (Takeda et al., 1991) [24].

A conductance study of the interaction between imidazolium cation of the IL with 18C6 and DB18C6 in ACN solutions is reported at different temperatures and the values are presented in the **Table IX.1**. The stability of these complexes depends mainly on the strength of the bonds between acidic protons of the imidazolium ring and crown ethers oxygen atoms (**Scheme IX.2**).

Table IX.1: Values of observed molar conductivities, Λ , at various mole ratios for the system IL-18C6 (complex 1) and IL-DB186 (complex 2) at different temperature

Mole Ratio	Λ (S. cm ² . Mol ⁻¹)					
	DB18C6			18C6		
	293.15 K	298.15 K	303.15 K	293.15 K	298.15 K	303.15 K
0	135.80	143.72	152.21	154.00	162.58	168.36
0.099	132.10	138.34	147.60	149.10	156.50	163.84
0.196	128.50	133.80	143.12	144.60	151.68	159.56
0.291	125.07	130.60	139.72	140.76	147.20	154.72
0.385	121.61	127.82	135.80	137.88	143.12	150.50
0.476	117.82	124.92	132.24	134.10	138.34	145.42
0.566	114.24	121.52	128.56	130.18	134.80	141.64
0.654	110.12	117.92	125.14	126.84	130.60	137.68
0.740	107.30	115.60	122.46	123.18	127.82	134.54
0.825	105.20	112.32	119.32	120.24	124.50	131.50
0.909	102.30	109.50	116.22	117.46	121.92	128.96
1.071	100.14	106.44	113.6	113.38	118.06	124.58
1.228	99.06	105.46	111.52	112.14	116.82	121.80
1.379	98.90	104.14	110.72	111.70	116.22	120.62
1.667	98.20	103.56	109.28	111.22	115.54	120.04
1.935	97.70	102.12	108.14	110.82	114.92	119.38
2.187	96.80	101.30	107.58	110.34	114.34	118.92
2.424	95.50	100.28	107.02	109.68	113.62	118.46
2.647	95.00	99.88	106.66	109.06	113.02	117.70
2.857	94.40	99.08	106.16	108.52	112.44	117.32
3.333	94.02	98.52	104.08	108.24	112.06	116.84
3.750	93.36	97.44	103.42	108.58	111.42	115.46



Scheme IX.2: Plausible schematic presentation of complex formation between imidazolium cation and crown ethers.

The molar conductance (Λ) of imidazolium salt (5×10^{-4} M) in ACN solution was monitored as a function of crown ether to imidazolium cation mole ratio at various temperatures. The resulting molar conductance vs. crown/cation mole ratio plots at 298.15, 303.15, and 308.15 K are shown in **Figure IX.1** and **IX.2**. In both case, there is a gradual decrease in the molar conductance with an increase in the crown ether concentration. This behavior indicates that the complexed imidazolium cation is less mobile than the corresponding free imidazolium cation in ACN and since the imidazolium salt is strong electrolyte in acetonitrile the changes are not due to ion pairing, unless the complexation of the cation causes the imidazolium salt to associate. Both **Figure IX.1** and **Figure IX.2** shows that the complexation of imidazolium cation with both crown ethers, addition of the crown solution to the imidazolium salt solution causes a continuous decrease in the molar conductance, which begins to level off at a mole ratio greater than one, indicating the formation of a stable 1:1 complex [25,26]. By comparison of the molar

conductance-mole ratio plot for imidazolium cation–crown ether systems obtained at different temperatures (**Figure IX.1** and **Figure IX.2**), it can be observed, that the corresponding molar conductance increased rapidly with temperature, due to the decreased viscosity of the solvent and, consequently, the enhanced mobility of the charged species present.

The stability of these complexes depends mainly on the strength of the bonds between acidic protons of the imidazolium ring and crown ethers oxygen atoms (**Scheme IX.2**). The formation constants determined by the conductivity study and thermodynamic values for the complex formation between crown ethers and imidazolium cation in acetonitrile solution are summarized in **Table IX.2**. The formation constants ($\log K_f$) of the 1:1 complexes at different temperatures varied in the order 18C6 > DB18C6 for the IL. Thus, a decrease in the net charge on oxygen atoms during the introduction of two benzo group into the macrocycle makes the obtained complex less stable.

Table IX.2: Values of formation constant, enthalpy, entropy and free energy change of different crown ethers complexes in ACN solution

Crown	$\log K_f$ (M^{-1})			ΔH° ($kJ\ mol^{-1}$)	ΔS° ($J\ mol^{-1}K^{-1}$)	ΔG° ($kJ\ mol^{-1}$)
	298.15 K	303.15 K	308.15K			
18C6	3.35	3.14	2.97	-65.02	-157.67	-18.01
DB18C6	3.05	2.96	2.87	-29.90	-43.57	-16.91

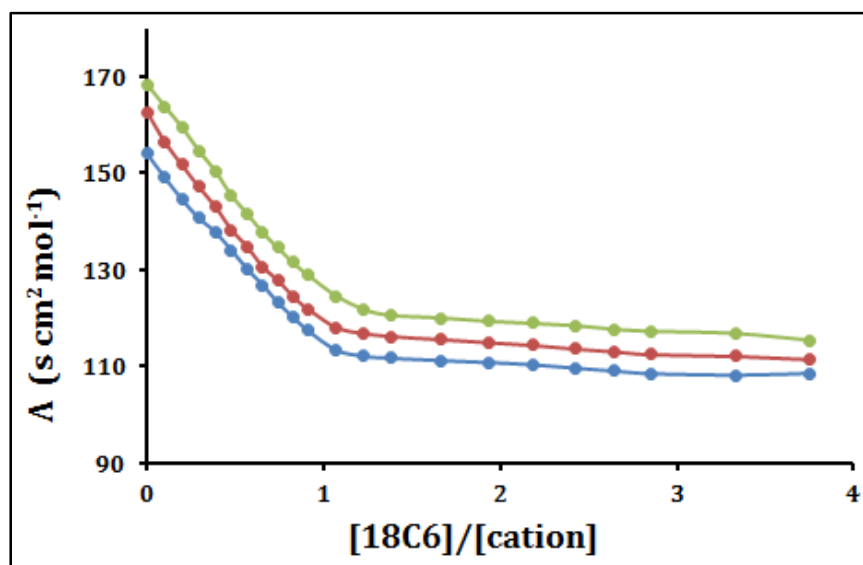


Figure IX.1: Molar conductance vs $[\text{18C6}]/[\text{cation}]$ at 298.15 K (\blacktriangle), 303.15 K (\blacksquare), 308.15 K (\bullet).

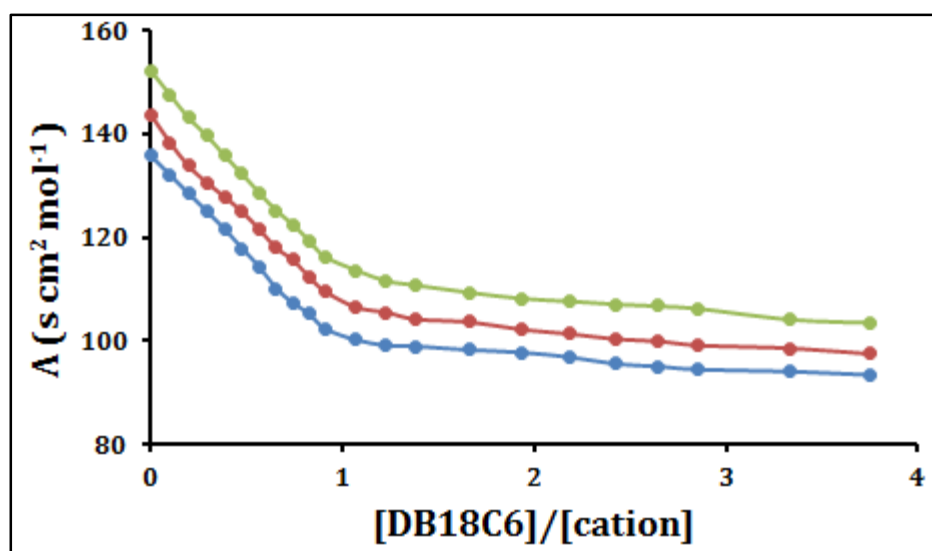


Figure IX.2: Molar conductance vs $[\text{DB18C6}]/[\text{cation}]$ at 298.15 K (Δ), 303.15 K (\square), 308.15 K (\circ).

IX.3.2 Association constant and Thermodynamic parameter

The following mathematical treatment to calculate the formation constant is based on Evans et al. (1972) [27]

The 1:1 complexation of IL with 18C6 crown ether can be expressed by the following equilibrium



The corresponding equilibrium constant, K_f is given by

$$K_f = \frac{[MC^+]}{[M^+][C]} \times \frac{f(MC^+)}{f(M^+)f(C)} \quad (2)$$

where $[MC^+]$, $[M^+]$, $[C]$ and f symbolize the equilibrium molar concentrations of the complex, free cation, free ligand (crown ethers) and the activity coefficients of the species indicated, respectively. Under the dilute conditions used, the activity coefficient of uncharged macrocycle, $f(C)$, can be reasonably assumed as unity [28]. The use of the Debye-Hückel limiting law [29], leads to the conclusion that $f(M^+) \sim f(MC^+)$, so the activity coefficients in Equation (2) cancel. The complex formation constant in terms of the molar conductances, Λ , can be expressed as [25,28].

$$K_f = \frac{[MC^+]}{[M^+][C]} = \frac{(\Lambda_M - \Lambda_{obs})}{(\Lambda_{obs} - \Lambda_{MC})[C]} \quad (3)$$

$$\text{Where } [C] = C_C - \frac{C_M(\Lambda_M - \Lambda_{obs})}{(\Lambda_M - \Lambda_{MC})} \quad (4)$$

Here, Λ_M is the molar conductance of the metal ion before addition of ligand, Λ_{MC} the molar conductance of the complexed ion, Λ_{obs} the molar conductance of the solution during titration, C_C the analytical concentration of the macrocycle added and C_M the analytical concentration of the salt. The complex formation constant, K_f , and the molar conductance of the complex, Λ_{MC} , were evaluated by using Equations (3) and (4).

Complexation enthalpy changes are mainly related to: (i) cation-crown interactions, (ii) solvation energies of the species in solvent systems involved in the complexation reactions (iii) repulsion between neighboring donor atoms, and (iv) steric deformation of the crown (v) number of H-bond present for H-bonding. Entropy changes

are linked to: (i) change in the number of particles involved in the complexation process, and (ii) conformational changes of the crown ether accompanying the complexation.

In order to have a better understanding of the thermodynamics of the complexation reactions of imidazolium cation with crown ethers is useful to consider the enthalpic and entropic contributions to these reactions. The ΔH° and ΔS° values for the complexation reactions were evaluated from the corresponding $\log K_f$ and temperature data by applying a linear least-squares analysis according to the equation:

$$2.303 \log K_f = -\frac{\Delta H^\circ}{RT} + \frac{\Delta S^\circ}{R} \quad (5)$$

Plots of $\log K_f$ vs. $\frac{1}{T}$ for both complex (complex 1 and complex 2) is linear (**Figure IX.3**).

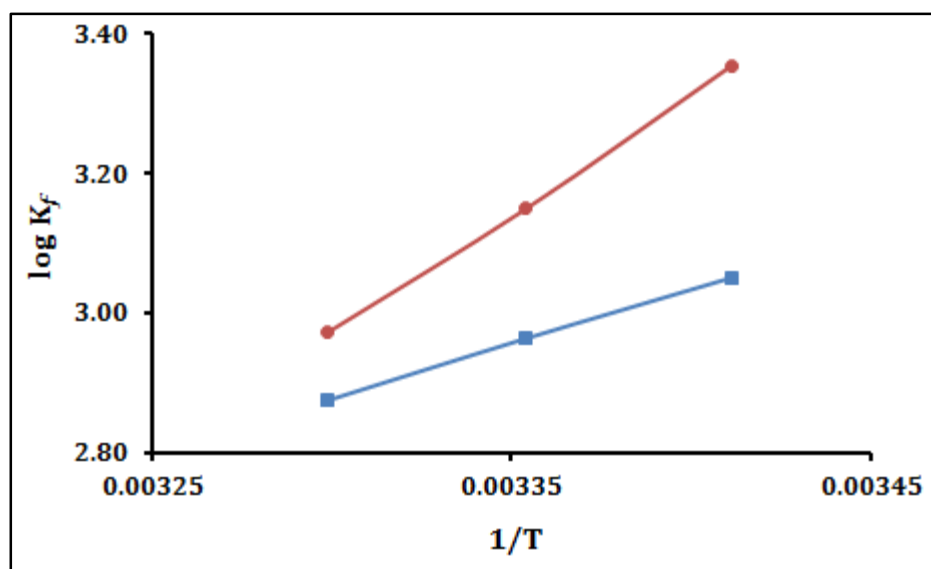


Figure IX.3: The linear relationship of $\log K_f$ vs. $1/T$ for the interaction of IL with 18C6 (●) and DB18C6 (■).

The enthalpy (ΔH°) and entropy (ΔS°) of complexation were determined from the slopes and intercepts of the plots and the results are also listed in **Table IX.2**. Both of these two parameters have negative values. True molecular recognition and a physical

attraction between host and guest should result in a favorable enthalpy change (ΔH) on complexation. The negative values of enthalpy confirm that when imidazolium cation interact with the crown ether molecules the overall energy of the system is decreased, i.e., there is some stabilization interaction in the system, whereas negative values of entropy factor indicate that there is an ordered arrangement, i.e., complex formation takes place between the imidazolium and the crown molecules. Other investigators [30-32] established that the binding of the free amino acids with 18C6 has negative enthalpy and negative entropy which indicates that the process is driven by a favorable enthalpy change only.

The two fundamental equations $\Delta G = -RT \ln K$ and $\Delta G = \Delta H - T\Delta S$ are useful in comparing the contributions of enthalpy and entropy towards the stability of different complexes. The negative value of entropy is unfavorable for the spontaneity of the complex formation, but this effect is overcome by higher negative value of ΔH^0 . The values of ΔG^0 (**Table IX.2**) for the complex formation was found negative suggesting that the complex formation process proceeds spontaneously.

The data shown in **Table IX.2** indicates that formation constant $\log K_f$ for imidazolium cation with both crown is highest at 298.15K and decreases with increase in temperature i.e. imidazolium cation form stable complex with crown at 298.15K.

IX.3.3 IR Study

The IR spectra of 18C6, IL and complex 1 are shown in **Figure IX.4** and the spectra of DB18C6, IL and complex 2 are shown in the **Figure IX.5** in the 4000–500 cm^{-1} region. The shift of IR spectra of crown ethers in ACN solution indicates that the specific interactions observed in the crown ether complexes are in fact typical hydrogen bonds of the imidazolium ring with the donor atoms of the crown ether. Comparing with the spectrum of the free crown ethers, most of these bands are shifted to lower energy presumably due to less restriction on the coupling of some vibrational modes caused by bonding of oxygen atoms of the polyether ring with the C-H protons of the imidazolium ring in both the complexes.

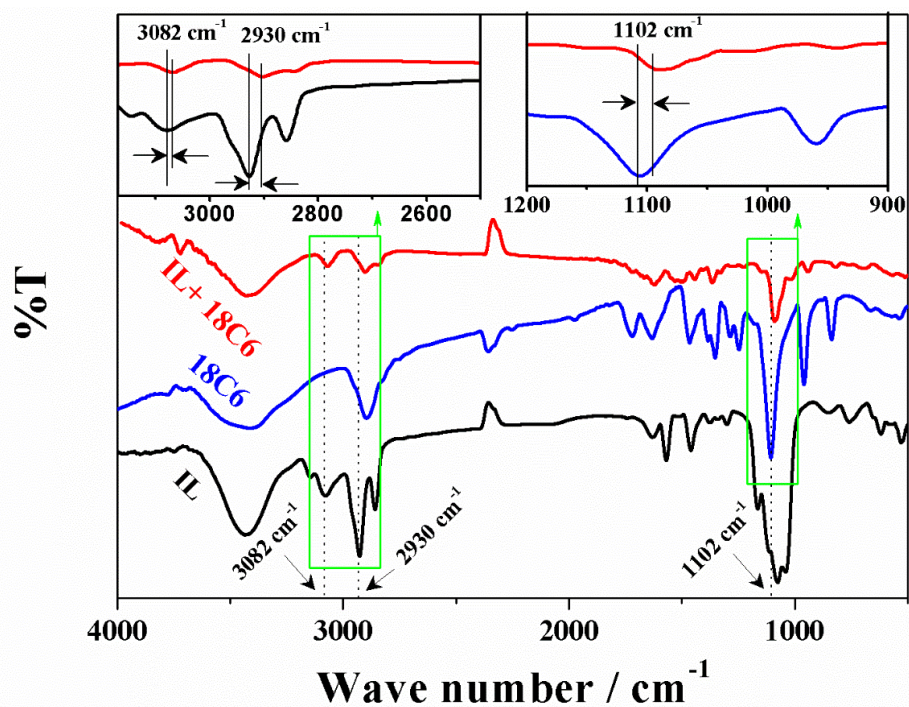


Figure IX.4: FTIR spectra of free IL (Black), 18-crown-6 (Blue) and complex (Red).

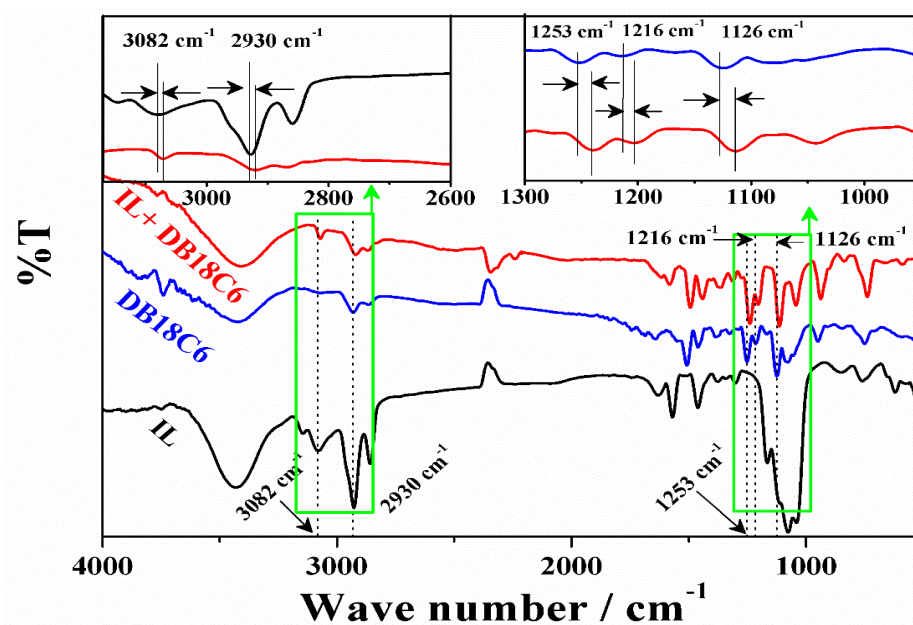


Figure IX.5: FTIR spectra of free IL (Black), Dibenzo-18-crown-6 (Blue) and complex (Red).

In the case of 18C6 a very strong and sharp IR band centered at 1102 cm^{-1} is assigned to the characteristic absorption due to the C-O-C asymmetric stretching vibrational motion [$\nu(\text{C}-\text{O}-\text{C})_{\text{aliph.}}$]. This sharp peak is shifted to lower frequency 1082 cm^{-1} in the complex 1 (**Figure IX.4**). The $\nu(\text{C}-\text{O}-\text{C})_{\text{arom}}$ stretching vibrations of DB18C6 are observed at 1126 cm^{-1} and these peak is also shifted to lower frequency 1108 cm^{-1} in the complex 2 (**Figure IV.5**). The presence of benzene rings in the DB18C6 make the IR spectra more difficult to assign because of their characteristic bands which may overlap with those of ethylene glycol groups. In the IR spectra, the bands in the $2800\text{--}3000\text{ cm}^{-1}$ region correspond to the CH stretching vibrations of the methylene groups of crown ethers. The CH stretching frequency of the methylene groups observed at 2895 cm^{-1} in 18C6 is shifted to higher frequency due to the perturbation of the methylene groups. Interaction of the O atoms of the crown with the protons of the imidazolium ring via hydrogen H-bonds are responsible for the perturbation. $1200\text{--}1300\text{ cm}^{-1}$ of the IR spectra of DB18C6 and its complex, there are two bands assignable to anisole $\nu_{\text{s}}(\text{Ph-O-C})$ and $\nu_{\text{as}}(\text{Ph-O-C})$ vibrations [33]. These anisole oxygens are involved in H-bond formation in the complex 2, as indicated by the shifts of the $\nu_{\text{as}}(\text{Ph-O-C})$ and $\nu_{\text{s}}(\text{Ph-O-C})$ bands from 1216 and 1253 cm^{-1} to 1198 and 1237 cm^{-1} , respectively. Selected IR data for the free compounds and their complexes and corresponding changes in frequencies are listed in **Table IX.3**.

Table IX.3: Comparison between the Frequencies change (cm^{-1}) of different functional group of free compound and their complexes

Functional Group	Wavenumber (cm^{-1})		Changes (cm^{-1})
	18C6	Complex 1	
$\nu(\text{C}-\text{O}-\text{C})_{\text{aliph.}}$	1102	1082	20
	DB18C6	Complex 2	
$\nu(\text{C}-\text{O}-\text{C})_{\text{arom}}$	1126	1108	18
$\nu_{\text{as}}(\text{Ph-O-C})$	1216	1198	18
$\nu_{\text{s}}(\text{Ph-O-C})$	1253	1237	16
$\nu(\text{C}-\text{H})$	IL	Complex 1	16, 25
	3082, 2930	3066, 2905	
$\nu(\text{C}-\text{H})$	IL	Complex 2	13, 9
	3082, 2930	3069, 2921	

IR spectroscopy has extensively been used to analyze the interaction present in the ILs. The shifts in C-H stretching frequencies in imidazolium-based ILs provide the information about the existence of the H-bonding in the complex. The imidazolium based IL shows the presence of C-H stretching vibrations in the region 3000-3100 cm^{-1} which is the characteristic region for the ready identification of C-H stretching vibrations [34,35]. According to Grondin et. al. [36] the IR band at $3160 \pm 15 \text{ cm}^{-1}$ are assigned to the more or less symmetric and anti-symmetric combination of the C(4)-H and C(5)-H stretching vibration of the imidazolium ring. The feature around $3120 \pm 15 \text{ cm}^{-1}$ consists of two bands and results from the C(2)-H stretching mode and Fermi resonances of the C-H stretching vibrations with overtones of in-plane ring deformations. In our investigation, the C-H vibrations have been found at 3082 and 2930 cm^{-1} in the FTIR spectrum are shifted to 3066 and 2905 cm^{-1} in complex 1 (**Figure IX.4**) and 3069 and 2921 cm^{-1} in complex 2 (**Figure IX.5**). In the IR spectra the region between 2800 cm^{-1} and 3000 cm^{-1} referred to the CH_2 and CH_3 stretching vibrations of the alkyl groups at the nitrogen atoms of the imidazolium ring.

IX.3.4 NMR Study

The complexation of imidazolium salt with crown ethers were investigated by ^1H NMR spectroscopy in CD_3CN at 298.15 K. The ^1H NMR spectra of IL (imidazolium ion) was recorded in absence and the presence of 18C6 (**Figure IX.6**) and DB18C6 (**Figure IX.7**) in CD_3CN .

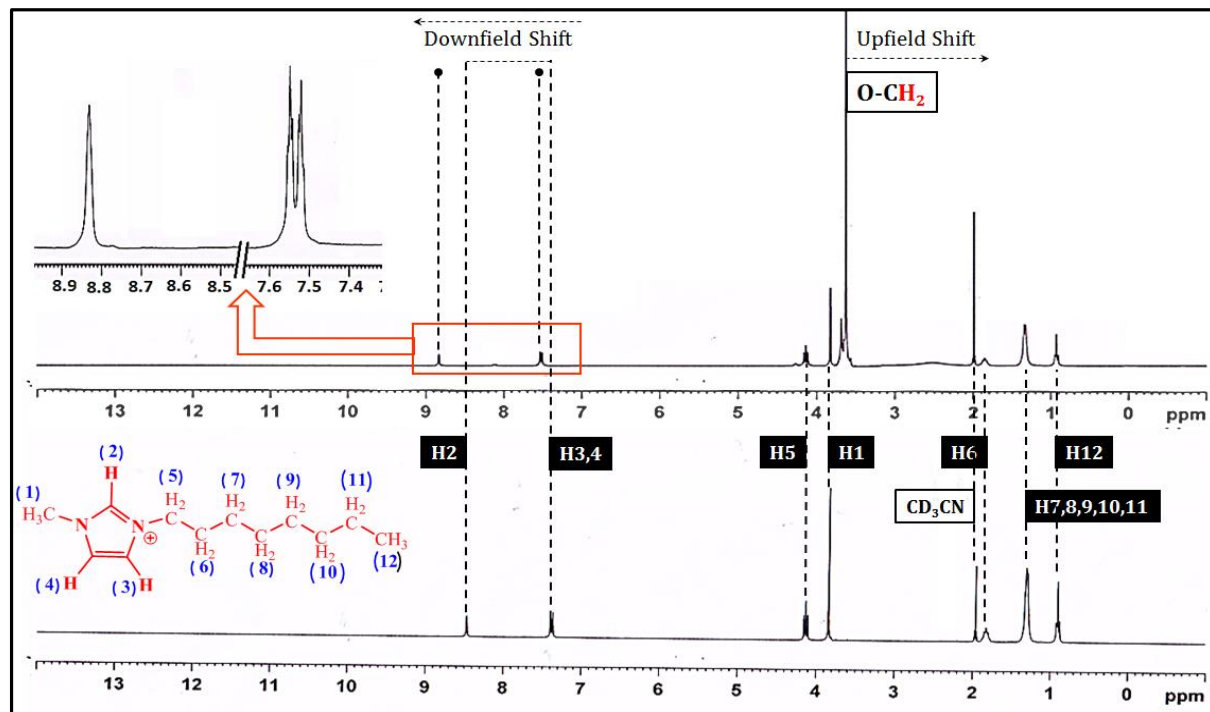


Figure IX.6: The ^1H NMR spectra of complex 1 (18C6.IL) (upper) and uncomplexed imidazolium cation (lower) recorded at 300 MHz in CD_3CN at 298.15 K.

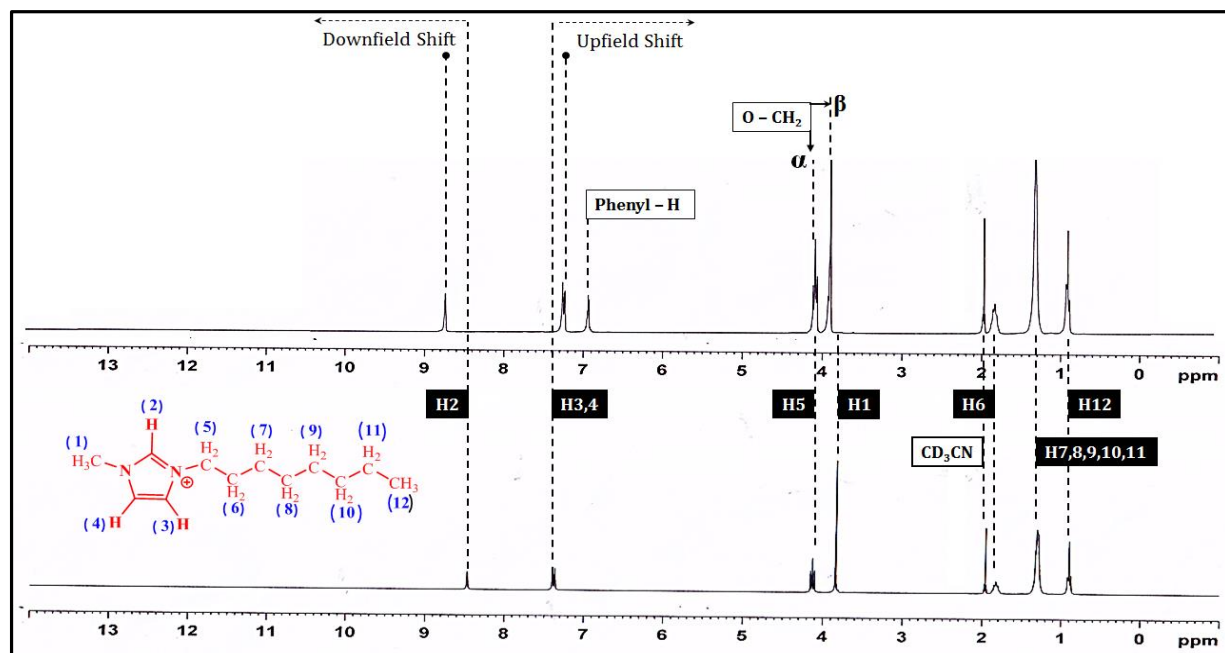


Figure IX.7: The ^1H NMR spectra of complex 2 (DB18C6.IL) (upper) and uncomplexed imidazolium cation (lower) recorded at 300 MHz in CD_3CN at 298.15 K.

A comparison of the ^1H NMR spectra for complex 1 (**Figure IX.6**) with free IL revealed that the signals for hydrogen atoms of the imidazolium ion (H2, H3 and H4) were downfield shifted. Downfield shifts of imidazolium protons supports the complex formation through H-bond formation involving for $[(\text{C}-\text{H})_{\text{Imidazolium}} \cdots \text{O}_{\text{Crown}}]$ -interaction. Signals for the $-\text{OCH}_2$ protons of crown ether were found to be little downfield shifted relative to those signals for the free individual component (**Figure IX.6**).

In case of complex 2 (**Figure IX.7**) i.e. complex of DB18C6, downfield shift for the signal of H2 was observed, while small upfield shift for the other two imidazolium protons (H3, H4) was observed [12,37]. This possibly suggest an orientation for the imidazolium ring that allows H-bond formation of H2 and a weak π - π interaction involving H3, H4. Two opposing influences namely H-bonding and π - π interaction were responsible for small upfield shifts for H3 and H4 [37]. The changes in chemical shifts suggest that host-guest complexation between crown ethers and imidazolium salt exists in both the complexes [38,39].

Based on different associated modes of interactions and ^1H NMR chemical shifts data for the two complexes, complex 1 and complex 2, a plausible interaction scheme have been proposed and schematic representation of such interaction is shown in **Scheme IX.2**. DB18C6 is a bowl-like host with two possible sites for interactions with the guest : the minor site formed by the $\text{O}-\text{CH}_2-\text{CH}_2-\text{O}$ chains and the major site located between the phenyl rings. The minor site may interact with the guest molecules only via hydrogen bonds while the major site can complex both via H-bonding and π -interactions (**Scheme IX.2**). The inclusion of a guest capable of interacting with both sites (imidazolium cation) leads to an interesting structure [11,12].

^1H NMR studies revealed apparent perpendicular orientation of the imidazolium moiety of IL in the crown cavity of complex 2; while this seemed to be different for complex 1. The possibility of such an orientation for the imidazolium ion was confirmed by Rissianen and Pursiainen for analogous inclusion complex formation between imidazolium ion and dibenzo-18-crown-6 [11]. The ^1H NMR results also suggested that the electron-deficient imidazolium ion may be wrapped by benzene-substituted crown

ethers and imidazolium ions are oriented face-to-face, such that the phenyl ring(s) and the substituents in the 1,3 position point away from the cavity of the crown ethers. In 1,3-disubstituted imidazolium salts both 1,3 positions are substituted by alkyl group which are electron donating groups relative to a hydrogen atom. Thus the substituents decrease the positive charge on the imidazolium ring and reduce the π - π stacking between dibenzo crown host and imidazolium guest in complex 2. In the complex 1 imidazolium ring can penetrate into the hollow circular based cavity of the macrocycle 18C6 and form strong H-bonding but the substituents in the 1,3 position point away from the cavity of the crown ethers.

Thus detailed ^1H NMR spectral studies indicate that hydrogen bonding interactions $[(\text{C}-\text{H})_{\text{Imidazolium}} \cdots \text{O}_{\text{Crown}}]$ apart from the weaker π - π /arene-arene donor-acceptor interactions resulted in moderately strong inclusion complex formation i.e the result of ^1H NMR spectral studies support the results obtained from conductivity and IR measurements.

Selected ^1H NMR data

1-meyhyl-3-octylimidazolium tetrafluoroborate (IL): ^1H NMR (CD_3CN , 298.15 K): δ 8.47 (s, N-CH-N, 2H), 7.40-7.36 (d, N-(CH) $_2$ -N, 2H), 3.84-3.81 (s, NCH $_3$, 3H), 4.15-4.10 (t, CH $_2$, 2H), 1.31 (m, C $_5$ H $_{10}$, 10H), 0.92-0.88 (t, oct-CH $_3$, 3H).

18-crown-6: ^1H NMR (CD_3CN , 298.15 K): δ 3.59-3.52 (s, OCH $_2$, 24H).

Dibenzo 18-crown-6: ^1H NMR (CD_3CN , 298.15 K): δ 6.96-6.89 (s, aryl, 8H), 4.13-4.10 (m, OCH $_2$, 8H), 3.88-3.85 (m, OCH $_2$, 8H),

18C6-1-meyhyl-3-octylimidazolium tetrafluoroborate (complex 1): 3.64(m, OCH $_2$) ^1H NMR (CD_3CN , 298.15 K): δ 8.83 (s, N-CH-N, 1H), 7.53-7.50 (s, N-(CH) $_2$ -N, 2H), 3.64-3.58 (m, OCH $_2$, 24H).

DB18C6-1-meyhyl-3-octylimidazolium tetrafluoroborate (complex 2): ^1H NMR (CD_3CN , 298.15 K): δ 8.75 (s, N-CH-N, 1H), 7.27-7.24 (d, N-(CH) $_2$ -N, 2H), 6.95-6.90 (s, aryl, 8H), 4.09-4.05 (m, OCH $_2$, 8H), 3.89-3.86 (m, OCH $_2$, 8H).

3.5 Typical Features of Specific Interactions involved in the Complexation

Inclusion complex formation of crown ethers with imidazolium ion involved three possible modes of interaction. The most prominent one is the hydrogen bonding interaction between oxygen atom of crown ethers (O_{Crown}) and acidic C–H protons of imidazolium ion $[(\text{C–H})_{\text{Imidazolium}}]$ for $[(\text{C–H})_{\text{Imidazolium}} \cdots O_{\text{Crown}}]$ -interaction. π - π stacking interactions between the electron poor imidazolium ring and aryl groups of the crown ether-based host (DB18C6) is the second one which is expected to contribute to the stability of the adduct formation. The possibility of such an interaction for an analogous system was reported earlier [11,14]. Apart from H-bonding and π - π stacking interactions, induced dipole-dipole interaction between imidazolium ion and O_{Crown} having $-\delta$ charge could also contribute to the overall stability of the adduct formation; such a proposition was made independently by Schmitzer *et al.* and Pursiainen *et al.* [11-14, 40-42]. However, this induced dipole-dipole interaction is expected to be weaker as compared to two previous modes of interaction discussed.

In the complex 2 (**Scheme IX.2**), hydrogen bonding seems to play a secondary role. Obviously, the π - π interaction is dominant in this complex (**Scheme IX.2**), because the benzene rings of the DB18C6 decrease the negative charge of the oxygen atoms and hence their ability to undergo hydrogen bonding, but under favorable conditions hydrogen bonds can enhance the stability of crown ether complexes. Also the electrostatic interaction between the aromatic ring of the crown and positive charge of the imidazolium ring play an important role to stabilize the complex. The negative charge on the benzene rings of the crown ether skeleton is enhanced by the ether oxygen atoms and this negative face of the aromatic ring interacts with the positive charge of the imidazolium ring. The unsubstituted crown ether imidazolium complex [complex 1] is likely stabilized by hydrogen bonds formed between acidic protons of imidazolium ring and ether oxygen atoms (C–H \cdots O interactions) [43].

The stability constants ($\log K_f$) for 1:1 complexation were measured in ACN solution by conductance study and are presented in **Table IX.2**. In both the complexes [complex 1 and complex 2], H-bonding to the ether oxygen atoms is obviously responsible for complexation. This can be shown by the suitable plausible mechanism

(Scheme 2). Complexation is mainly caused by H-bonding but either π -stacking or charge-transfer interactions (**Scheme IX.2**) also seem to have a minor contribution towards complexation and there may be possibility of ion-dipole interactions between positive N atom of imidazolium cation and ether oxygen atom. The stability constants for complex 2 is slightly lower than the corresponding value of complex 1 (**Table IX.2**). The aromatic rings of the crown ether decrease the electron density of the adjacent oxygen atoms, and this seems to decrease the strength of any H-bonding in complex of complex 2 explaining the lower stability constants. Although complex 2 has the potential for π -stacking or charge transfer interactions which is absent in the complex 1 indicates that H-bonding is dominant here for the complex formation.

IX.4. CONCLUSION

The conductometric titration data support the different types of interactions responsible for complex formation of crown ethers with IL molecule and are consistent with the IR and NMR spectra. The stability of complexes between planar, five-membered imidazolium cations and crown ethers were established by the different types of non-covalent interactions. We have found that the studied complexes are mainly stabilised by hydrogen bonds, and π -stacking or cation- π interactions play only a secondary role in case of complex 2. Larger formation constant value for complex 1 compared to complex 2 determined by conductivity study indicates that imidazolium cation form stable complex with 18C6 compared to DB18C6 in ACN solution. The 1:1 complexation of the imidazolium based IL by different crown ethers is driven by favourable changes in enthalpy ($\Delta H^0 < 0$) and proceeds spontaneously ($\Delta G^0 < 0$). This study also helps to get important information about the other host-guest system with crown ethers.

Here our studies of complexation of imidazolium ion, similar to complexation of pyridinium ions [40], provide further information on the nature of the complexation between positively charged organic guests and macrocyclic polyethers. This study is also significant for the understanding of the vital role of imidazolium cation in the design and construction of supramolecular host-guest materials.

CHAPTER- X

CONCLUDING REMARKS

In chapter II subjects discussed in this thesis were introduced. Some thoughts on host-guest chemistry were discussed and how this type of study offer new opportunities, were brought forward.

Due to the major advantage of CDs to act as drug delivery vehicles, it is proposed to study CD complexation of various significant mol an important constituent of numerous pharmaceutical products, by using analytical techniques at different pH values. The proposed studies employ cyclodextrins as potential drug delivery vehicles because of their ability to alter the physical, chemical and biological activities of guest molecules through formation of inclusion complexes. The principal advantages of natural cyclodextrins as drug carriers are the following: (1) well-defined chemical structure, yielding many potential sites for chemical modification or conjugation (2) availability of cyclodextrins of different cavity size (3) low toxicity and low pharmacological activity (4) certain water solubility (5) protection of included/conjugated drugs from biodegradation.

The aim of the works embodied in this thesis was to explore the assortment of interfaces of some Ionic Liquids by physicochemical approach. Here, I have studied the molecular as well as ionic interaction on ionic liquids in some solvent systems. The molecular interactions occurring in the solution systems have been studied with the help of physicochemical, thermodynamic, transport and optical properties along with spectroscopic studies.

The study reported in this thesis explains the procedures and results as well as the studies of the molecular interactions of ionic liquids in different solvent systems and somewhere ionic liquid as solvent media with other as solute. The overall goal was to look into the structure, property and interaction of ionic liquids in different solvent

media. Therefore the systematic study of these properties has great importance in gaining a better knowledge about different interactions.

The volumetric, viscometric, interferometric, conductometric refractive index studies helped us to evaluate the extent of molecular interaction in a particular solution quantitatively whereas the spectroscopic measurements gave an insight into the type of molecular interaction occurring in any solution systems. Various types of interactions exist between the ions in solutions, and of these, ion-ion and ion-solvent interactions are of current interest in all branches of chemistry. These interactions help in better understanding the nature of solute and solvent, that is, whether the solute modifies or distorts the structure of the solvent.

The consequences of my research lead to some new scientific results in host-guest chemistry, which can be served as explanations of the change of the physical properties of the guest molecules. The investigations on the host-guest inclusion complex formation processes provides explanation about the driving force present in inclusion complex and also structural arrangement. The results of this study have provided data to new research and development tendency, to the theoretical and practical basis of the host-guest chemistry.

The surface tension, conductance and NMR study gives the clear indication of 1:1 host-guest inclusion complex formation of a series of surface active ionic liquids, benzyltrialkylammonium chloride $[(C_6H_5CH_2)N(C_nH_{2n+1})_3Cl]$; where $n=1,2,4$] with aq. β -cyclodextrin reveal in Chapter IV. The study also expose that benzyl, the hydrophobic group of ionic liquids encapsulated insight into the cavity of β -cyclodextrin and form the inclusion complex. This study also demonstrated that hydrophobic interactions and hydrogen bonding contribute to the inclusion of ionic liquids in CDs. It was found that addition of β -CD causes the shifting of micellization of the ionic liquids towards the higher concentration. This indicates the inclusion complex formation between the ionic liquids and β -CD.

Considering the showing the amantadine ion can bind nicely to three of the six available oxygen atoms in the 18C6 ring to form a stable complex (scheme 2) with 1:1 stoichiometry have been studied. The N-H...O hydrogen bridges between the ammonium functionalities and the oxygen acceptor heteroatoms of the crown ethers

play a significant role in packing the host-guest complexes. The stable complex formation is established by physicochemical methods surface tension measurements, conductivity and IR study and the density data also support the interaction between amantadine ion and 18C6 systems. The inclusion complex formation has been explained qualitatively as well as quantitatively so as to make it dependable in its field of application.

The Host-guest complex formation based on the macrocyclic molecules is a facile and reversible process, which provides the feasibilities to design stimuli-responsive supramolecular systems and these macrocyclic molecules are basically friendly to the biological environment and exhibit good biocompatibilities. Crown ether-based host-guest interactions, which show good selectivity, high efficiency, and reversibility, have been structurally characterized and the underlying supramolecular chemistry has been presented in this work. Supramolecular chemistry i.e host-guest complex formation through noncovalent interactions offer the basis for novel approaches in medicine and also helps in understanding the interactions present in living systems. It was also found that host-guest complexation with crown ethers resembles an established principle i.e the hydrogen bonding acceptance as well as the donation propensity of crown ethers. Amantadine is an antiviral agent that specifically inhibits influenza A virus replication at micromolar concentration. This drug is also very effective in the treatment of human Parkinson's disease. The host-guest complex is capable of protecting the drug molecule from chemical reactions and photochemical/thermal degradation in biological environment and the encapsulated drug can also be released sustainably from the cavity of macrocyclic molecule, achieving prolonged therapeutic effect.

An extensive study was done on the ion-solvation behavioural aspect of the IL 1-butyl-3-methylimidazolium chloride in industrially-important non-aqueous polar solvents acetonitrile (CH_3CN), dichloromethane (CH_2Cl_2) and tetrahydrofuran ($\text{C}_4\text{H}_8\text{O}$) with the help of conductometric, FTIR, density and viscosity measurements has reveals in chapter VI. From the conductometric measurements it becomes clear that the IL exists as ion-pairs in acetonitrile and as triple ions in tetrahydrofuran, dichloromethane solvents. The tendency of the ion-pair and triple-ion formation of $[\text{bmim}][\text{Cl}]$ depends on the dielectric constant of the medium. The present study revealed that this type of

experimental study is being accompanied for a better understanding of the interionic interactions of ionic liquids. The evaluated values of thermodynamic functions of association suggest the spontaneity of the association process

The formation of three complexes of sulfa drug with several crown ethers in ACN have been investigated with the help of above mentioned spectroscopic and physicochemical studies. ¹H NMR data confirms the complex formation and the Job plot suggests the formation of complexes with 1:1 stoichiometry. The interaction of sulfa drug with crown ethers in the solution have been interpreted by density, viscosity, refractive index measurements. These measurements provide valuable information on ion-solvent and ion-ion interactions of the complexes in solutions. The association/formation constants are found highest for complex 2, then complex 1 and then complex 3 which indicates that SA form most stable complex with DC18C6 compared to other complexes. The probable structures of the three complexes of sulfa drug with crown ethers have been proposed by the above mentioned studies.

In this chapter VII we have found that the studied complexes are mainly stabilised by hydrogen bonds, and π -stacking play only a secondary role in case of complex 3 i.e complex of benzene substituted crown ether. The 1:1 complexation of the sulfa drug by different crown ethers proceeds spontaneously ($\Delta G^{\circ} < 0$). The roles of guest SA has been established in directing the formation of supramolecular architectures between crown ether and $-NH_2$ group of $-SO_2NH_2$ in SA by host-guest hydrogen-bonding interactions. Here the present work helps to understand the vital role of $-NH_2$ group in the design and construction of supramolecular host-guest materials. These results are also significant for other host-guest systems. However, with the knowledge acquired from the solution chemistry of SA-Crown complexes, we believe that the scope and future prospect of this type of studies with other supramolecules are also a promising preposition.

In chapter VIII the entire study reveals the fact of formation Host-Guest inclusion complex with 1:1 stoichiometry. The density and viscosity study confirms the formation of inclusion complexes between the drug and β -CD molecule. The single break point at the concentration near to 5mM of CD obtained from the surface tension study and Conductometric study indicates the formation of the inclusion complexes with 1:1

stoichiometry. From the UV-VIS spectroscopic data binding constant was calculated using Job's plot, which clearly explains that the drug molecule MP forms more effective inclusion complex. Taking all the parameters and results in account the plausible mechanism of the inclusion was depicted.

The conductometric titration data support the different types of interactions responsible for complex formation of crown ethers with IL molecule and are consistent with the IR and NMR spectra. The stability of complexes between planar, five-membered imidazolium cations and crown ethers were established by the different types of non-covalent interactions. We have found that the studied complexes are mainly stabilised by hydrogen bonds, and π -stacking or cation- π interactions play only a secondary role in case of complex 2. Larger formation constant value for complex 1 compared to complex 2 determined by conductivity study indicates that imidazolium cation form stable complex with 18C6 compared to DB18C6 in ACN solution. The 1:1 complexation of the imidazolium based IL by different crown ethers is driven by favourable changes in enthalpy ($\Delta H^0 < 0$) and proceeds spontaneously ($\Delta G^0 < 0$). This study also helps to get important information about the other host-guest system with crown ethers have been discussed in chapter IX.

The broad studies of the different physicochemical, thermodynamic, transport and spectral properties of the ionic liquids in different solvents will be of sufficient in understanding the nature of the ion-solvent interactions and the role of solvents in different chemical processes. Here in this research work I have also tried to explore the formation of Host-Guest inclusion complexes between ionic liquids and cyclodextrins and the formed inclusion complexes have been confirmed by Conductance, Surface tension, UV-Visible and NMR spectroscopy. Such type of ionic liquids are very important in pharmaceutical industry, cosmetic and hygiene industries, food industries, paint industries and it also increases in speed of diagnostic test reaction. So, it may be concluded that our research work has adequate significance in the different branches of Sciences and demands a far reaching effect for the augmentation of the advanced research.

BIBLIOGRAPHY

CHAPTER: I

- [1] D. V. EMM, Cyclodextrins and their uses: a review, *Process Biochem.* 39 (2004) 1033-1046.
- [2] L. Szente, J. Szejtli, *Adv. Drug Delv. Rev.*, 36 (1999) 17-28.
- [3] P. Jarho, A. Urtti, D.W. Pate, P. Suhonen, T. Järvinen, *Int. J. Pharm.* 137(1996) 209-2177.
- [4] Maffeo, L. Leondiadis, I. M. Mavridis, K. Yannakopoulou, *Org. Biomol. Chem.*, 4 (2006) 1297-1304.
- [5] T. Loftsson, *J. Incl. Phenom. Macrocycl. Chem.*, 44 (2002) 63-67.
- [6] K. Uekama, F. Hirayama, T. Irie, *Chem. Rev.* 98 (1998) 2045-2076.
- [7] E. P. Kyba, R. C. Helgeson, K. Madan, G. W. Gokel, T. L. Tarnowski, S. S. Moore, D. J. Cram, *J. Am. Chem. Soc.* 99 (1977) 2564-2571.
- [8] W. D. Curtis, D. A. Laidler, J. F. Stoddart, G. H. Jones, *J. Chem. Soc., Chem. Commun.* (1975) 833.
- [9] T. J. van Bergen, R. M. Kellogg, *J. Am. Chem. Soc.* 99 (1977) 3882-3884.
- [10] (a) J.D. Pandey, A. Yasmin, *Proc. Ind. Acad. Sci.* 109 (1997) 289-294.
(b) J.D. Pandey, Y. Akhtar, A.K. Sharma, *Ind. J. Chem.* 37A (1998) 1094-1097.
- [11] J.I. Kim, *J. Phys. Chem.* 82 (1978) 191-199.
- [12] W. Kemp, *Organic spectroscopy*, 3rd (ELBS) Ed., Macmillan Press: Hampshire: U.K., 1993.
- [13] Y. Marcus, *Ion-solvation*, Wiley: Chinchester, 1986.
- [14] R.G. Bates, *Solute –solvent Interactions*, Marcel Dekker: New York, 1969.
- [15] Meck DK. *The Chemistry of Non- Aqueous solvents*, Academic Press: New York, 1996.

CHAPTER: II

- [1] J.M. Lehn, *Angew. Chem. Int. Ed.* 50 (1978) 871-892.
- [2] J. Szejtli, *Chem. Rev.* 98 (1998) 1743-1754.
- [3] J. S. Lindsey, *New J. Chem.*, 15 (1991) 153-179.
- [4] G. M. Whitesides, J. P. Mathias, C. T. Seto, *Science*, 254 (1991)1312-1319.
- [5] D. Philp and J. F. Stoddart, *Angew. Chem. Int. Ed. Engl.*, 35 (1996) 1154-1196.
- [6] S. R. Batten and R. Robson, *Angew. Chem. Int. Ed. Engl.*, 37 (1998) 1460-1494.
- [7] D. N. Reinhoudt, J. F. Stoddart and R. Ungaro, *Chem. Eur. J.* 4 (1998)1349-1351.
- [8] J. de Mendoza, *Chem. Eur. J.* 4 (1998) 1373-1377.
- [9] J. Rebek, *Angew. Chem. Int. Ed. Engl.* 29 (1990) 245-255.
- [10] J. Trinh, T. M. Dodd, R. Bartolo, J. M. Lucas, *US Patent* 5(1999) 897, 855, 21.
- [11] Vögtle, *Supramolecular Chemistry*; John Wiley & Sons, New York, 1991.
- [12] D. B. Amabilino and J.F. Stoddart, *Chem. Rev.* 95 (1995)2715-2828.
- [13] M. C. T. Fyfe, J. F. Stoddart, *Acc. Chem. Res.* 30 (1997) 393-401.
- [14] A. Harada, J. Li and M. Kamachi, *Nature* 356 (1992) 325.
- [15] A. Harada, K. Li and M. Kamachi, *Nature* 370 (1994) 126-128.
- [16] Lehn, J. M. *Angew. Chem. Int. Ed. Engl.* 29 (1990) 1304-1319.
- [17] *Photochemistry in organized and constrained media*, Ed. V. Ramamurthy, VCH, New York, 1991.
- [18] Yu, G. Jie, K. Huang, *Chem. Rev.* 115 (2015) 7240-7303.
- [19] A. Villiers, *Rend Acad. Sci.* 112 (1891) 536-538.
- [20] F. Schardinger, *Wien Klin. Wochenschr.* 17 (1904) 207-209.
- [21] K. Freudenberg, R Jacobi, *Ann.* 518 (1935) 102-108.
- [22] K. Freudenberg, Meyer-Delius, *M. Ber. Dtsch. Chem. Ges.* 71 (1938) 1596-1600.
- [23] D. French; R.E. Rundle, *J. Am. Chem. Soc.* 64 (1942) 1651-1653.
- [24] M.L. Bender and Komiyama, *M. Cyclodextrin Chemistry*, Springer Verlag, Berlin (D), 1978.
- [25] J. Szejtli, *Pure Appl. Chem.*, 76 (2004) 1825-1845.
- [26] W. Saenger, *Angew. Chem. Int. Ed. Engl.* 19 (1980) 344-362.
- [27] K. A. Connors, *Chem. Rev.* 97 (1997) 1325-1357.

-
- [28] D. French. *Adv. Carbohydr. Chem.* 12 (1957) 189-260.
- [29] A. W. Coleman, I. Nicolis, N. Keller and J. P. Dalbiez, *J. Incl. Phenom. Mol. Recognit. Chem.* 13 (1992) 139-143.
- [30] J. Szejtli, *Cyclodextrin Technology*, Kluwer Academic Publishers, Dordrecht, 1988.
- [31] E. M. M. Del Valle, *Process Biochem.* 39 (2004) 1033-1046.
- [32] S. M. -Botella, B. del Castillo and M. A. Martyn, *Arsh. Pharm.* 36 (1995) 187-198.
- [33] T. Loftsson and M. E. Brewster, *J. Pharm. Sci.* 85 (1996) 1017-1025.
- [34] R. Singh, N. Bharti, J. Madan, S. N. Hiremath, *J. Pharm. Sci. Tech.* 2 (2010) 171-183.
- [35] U. Kemelbekov, Y. Luo, Z. Orynbeikova, Z. Rustembekov, R. Haag, W. Saenger, K. Pralivey, *J. Incl. Phenom. Macrocycl. Chem.* 69 (2011) 181-190.
- [36] S. H. Choi, S. Y. Kim, J. J. Ryoo, J. Y. Park, K. P. Lee, *Anal. Sci.* 17 (2001) 1785-1788.
- [37] E. Schneiderman and A.M. Stalcup, *J. Chromatogr. B.* 745 (2000) 83-102.
- [38] R. Breslow, M. F. Czarniecki, J. Emert, H. Hamaguchi, *J. Am. Chem. Soc.* 102 (1980) 762-770.
- [39] I. Sanemasa and Y. Akamine, *Bull. Chem. Soc. Jpn.* 60 (1987) 2059-2066.
- [40] G. Nelson, G. Patonay, I. M. Warner, *J. Inclusion Phenom.* 6 (1988) 277-289.
- [41] W. J. Park, H. J. Song, *J. Phys. Chem.* 93 (1989) 6454-6458.
- [42] D. L. P. A. Munoz, T. Ndou, J. B. Zung and I. M. Warner, *J. Phys. Chem.* 95 (1991) 3330-3334.
- [43] S. Hamai, *Bull. Chem. Soc. Jpn.* 55 (1982) 2721-2729.
- [44] T. Tamaki, T. Kokubu, *J. Inclusion Phenom.* 2 (1984) 815-822.
- [45] A. Ueno, F. Moriwaki and T. Osa, *Tetrahedron*, 43 (1987) 1571-1578.
- [46] S. Hamai, *J. Phys. Chem.* 94 (1990) 2595-2600.
- [47] M. Pumera, R. Matalova, I. Jelinek, J. Jindrich, J. Juza, *Molecules*, 6 (2001) 221-229.
- [48] H.A. Benesi, J.H. Hildebrand, *J. Am. Chem. Soc.* 71(1949) 2703-2707.
- [49] S. Li, W. Purdy, *Chem. Rev.* 92 (1992) 1457-1470.
- [50] R. Challa, A. Ahuja, J. Ali and R. K. Khar, *AAPS Pharm. Sci. Tech.* 6 (2005) E329-E357.
- [51] A. Rasheed, A. Kumar. C. K., Sravanthi. V. V. N. S.S., *Sci. Pharm.* 76 (2008) 567-598.
- [52] L. Szente, J. Szejtli, *Adv. Drug Delv. Rev.* 36 (1999) 17-28.
-

- [53] D. Maffeo, L. Leondiadis, I. M. Mavridis, K. Yannakopoulou, *Org. Biomol. Chem.* 4 (2006) 1297-1304.
- [54] T. Loftsson, *J. Incl. Phenom. Macrocycl. Chem.* 44 (2002) 63-67.
- [55] K. Uekama, F. Hirayama, T. Irie, *Chem. Rev.* 98 (1998) 2045-2076.
- [56] R. Breslow, S. D. Dong, *Chem. Rev.* 98 (1998) 1997-2012.
- [57] Z. Fan, C. H. Diao, H. B. Song, Z. L. Jing, M. Yu, X. Chen, M. J. Guo, *J. Org. Chem.* 71 (2006) 1244-1246.
- [58] H. Hashimoto, *J. Incl. Phenom. Macrocycl. Chem.* 44 (2002) 57-62.
- [59] J. Szejtli, *J. Mater. Chem.* 7 (1997) 575-587.
- [60] A. R. Hedges, *Chem. Rev.* 98 (1998) 2035-2044.
- [61] M. A. Mortellaro, D. G. Nocera, *J. Am. Chem. Soc.* 118 (1996) 7414-7415.
- [62] J. S. Bradshaw, R. M. Izatt, A. V. Bordunov, C. Y. Zhu, J. K. Hathaway, In *Comprehensive Supramolecular Chemistry*, edited by J. L. Atwood, J. E. D. Davies, D. D. MacNicol, F. Vögtle, J. -M. Lehn, Eds. Pergamon, Oxford, 1(1996) 36.
- [63] (a) R. M. Izatt, K. Pawlak, J. S. Bradshaw, R. L. Bruening, *Chem. Rev.* 91 (1991) 1721-2085.
(b) R. M. Izatt, J. S. Bradshaw, S. A. Nielsen, J. D. Lamb, J. J. Christensen, *Chem. Rev.* 85 (1985) 271-339.
- [64] R. M. Izatt, J. D. Lamb, N. E. Izatt, B. E. Jr Rossiter, J. J. Christensen, B. L. Haymore, *J. Am. Chem. Soc.* 101 (1979) 6273-6276.
- [65] R. Méric, J. -P. Vigneron, J. -M. Lehn, *J. Chem. Soc. Chem. Commun.* (1993) 129-131.
- [66] G. W. Gokel, D. J. Cram, *J. Chem. Soc., Chem. Commun.* (1973) 481-482.
- [67] R. M. Izatt, J. D. Lamb, B. E. Rossiter, N. E. Izatt, J. J. Christensen, *J. Chem. Soc., Chem. Commun.* (1978) 386-387.
- [68] E.P. Kyba, R.C. Helgeson, K Madan ,G.W. Gokel, T.L.Tarnowski ,S.S. Moore, D.J. Cram, *J Am Chem Soc.* 99 (1977) 2564-2571.
- [69] J. M. Lehn, P. Vierling, R. C. Hayward, *J. Chem. Soc., Chem. Commun.* (1979) 296-298.

- [70] (a) J. W. H. M. Uiterwijk, S. Harkema, J. Geevers, D. N. Reinhoudt, *J. Chem. Soc., Chem. Commun.* (1982) 200-201.
(b) J. W. H. M. Uiterwijk, C. J. van Staveren, D. N. Reinhoudt, H. Hertog, L. Kruise, S. Harkema, *J. Org. Chem.* 51 (1986) 1575-1587.
- [71] C. J. Van Staveren, H. J. Hertog, D. N. Reinhoudt, J. W. H. M. Uiterwijk, L. Kruise, S. Harkema (1984) 1409-1411.
- [72] M. Lämsä, K. Raitamaa, J. Pursiainen, *J. Phys. Org. Chem.* 12 (1999) 557-563.
- [73] M. Lämsä, J. Pursiainen, K. Rissanen, J. Huuskonen, *Acta. Chem. Scand.* 52 (1998) 563-570.
- [74] M. Lämsä, T. Suorsa, J. Pursiainen, J. Huuskonen, K. Rissanen, *Chem. Commun.* (1996) 1443-1444.
- [75] M. Lämsä, J. Huuskonen, K. Rissanen, J. Pursiainen, *Chem. Eur. J.* 4 (1998) 84-92.
- [76] F. N. Magill, Ed. *Nobel Prize Winners: Chemistry*, Salem Press: Pasadena, California, 3 (1990) 1165-1198.
- [77] C. J. Pedersen, *J. Am. Chem. Soc.* 89 (1967) 7017-7036.
- [78] M. Hiraoka, *New York*, 1 (1982).
- [79] R. M. Izatt, J. S. Bradshaw, S. A. Nielsen, J. D. Lamb, J. J. Christensen, D. Sen, *Chem. Rev.* 85 (1985) 271-339.
- [80] F. P. Schmidtchen, M. Berger, *Chem. Rev.* 97 (1997) 1609-1646.
- [81] F. Vögtle, H. Sieger, W. M. Müller, *Top. Curr. Chem.* 98 (1981) 107-161.
- [82] X. X. Zhang, R. M. Izatt, J. S. Bradshaw, K. E. Krakowiak, *Coord. Chem. Rev.* 174 (1988) 179-189.
- [83] D. J. Cram, *Angew. Chem., Int. Ed. Engl.* 27 (1988) 1009-1020.
- [84] T. Wang, J. S. Bradshaw, M. Izatt, *J. Heterocyclic Chem.* 31 (1994) 1097-1114.
- [85] A. K. Mandal, M. Suresh, A. Das, *Org. Biomol. Chem.* 9 (2011) 4811-4817.
- [86] L. J. Yang, S. X. Ma, S. Y. Zhou, W. Chen, M. W. Yuan, Y. Q. X. D. Yang, *Carbohydrate Polymers* 98 (2013) 861-869.
- [87] A. Fernandes, G. Ivanova, N. F. Bras, N. Mateusa, M. J. Ramos, M. Rangel, V. D. Freitas, *Carbohydrate Polymers* 102 (2014) 269-277.

- [88] C. F. Xiao, K. Li, R. Huang, G. J. Hea, J. Q. Zhang, L. Zhu, Q. Y. Yang, K. M. Jiang, Y. Jin, Y. J. Lin, *Carbohydrate Polymers* 102 (2014) 297-305.
- [89] T. Wang, M. D. Wang, C. Ding, J. Fu, *Chem. Commun.* 50 (2014) 12469-12472.
- [90] (a) P. V. Demarco, A. L. Thakkar, *J. Chem. Soc. Chem. Commun.* (1970) 2-4.
(b) A. L. Thakkar, P. V. Demarco, *J. Pharm. Sci.* 60 (1971) 652-653.
- [91] Y. Inoue, *Annu. Rep. NMR Spectrosc.* 27 (1993) 59-101.
- [92] H. J. Schneider, F. Hacket, V. Rudiger, H. Ikeda, *Chem. Rev.* 98 (1998) 1755-1786.
- [93] Z. Zhou, X. Yan, T. R. Cook, M. L. Saha, P. J. Stang, *J. Am. Chem. Soc.* 138 (2016) 806-809.
- [94] X. Yan, T. R. Cook, J. B. Pollock, P. Wei, Y. Zhang, Y. Yu, F. Huang, P. J. Stang, *J. Am. Chem. Soc.* 136 (2014) 4460-4463.
- [95] J. S. Negi, S. Singh, *Carbohydrate Polymers* 92 (2013) 1835-1843.
- [96] C. Schalley, *Analytical Methods in Supramolecular Chemistry*, Wiley-VCH Verlag GmbH, Weinheim, (2007) 817-854.
- [97] K. Sivakumar, T. R. Ragi, D. Prema, T. Stalin, *Journal of Molecular Liquids* 218 (2016) 538-548.
- [98] W. Zhang, X. Gong, Y. Cai, C. Zhang, X. Yu, J. Fan, G. Diao, *Carbohydrate Polymers* 95 (2013) 366-370.
- [99] J. S. You, X. Q. Yu, G. L. Zhang, Q. X. Xiang, J. B. Lan, R. G. Xie, *Chem. Commun.* 18 (2001) 1816-1817.
- [100] J. Polster, H. Lachman, *Spectrometric Titrations*, VCH, Wienheim, 1989.
- [101] K. A. Connors, *Binding Constants. The Measurement of Molecular Complex.* Wiley, New York, 1987.
- [102] F. Cramer, W. Saenger, H.C. Spatz: *J. Am. Chem. Soc.* 89 (1967) 14-20.
- [103] J. Szejtli, A. Kiado, Budapest, 1982.
- [104] S. Prabu, M. Swaminathan, K. Sivakumar, R. Rajamohan, *Journal of Molecular Structure.* 1099 (2015) 616-624.
- [105] Q. Zhang, Z. Jiang, Y. Guo, R. Li, *Spectrochim. Acta. Part A*, 69 (2008) 65-70.
- [106] M. Zhang, J. Li, W. Jia, J. Chao, L. Zhang, *Supramolecular Chemistry*, 21 (2009) 597-602.

-
- [107] C. N. Sanrame, R. H. Rossi, G. A. Arguello, *J. Phys. Chem.*, 100 (1996) 8151-8156.
- [108] A. Orstan, J. B. Rossi, *J. Phys. Chem.* 91 (1987) 2739-2745.
- [109] S. Scypinski, J. M. Drake, *J. Phys. Chem.*, 89 (1985) 2432-2335.
- [110] Y. Gao, Z. Li, J. Du, B. Han, G. Li, W. Hou, D. Shen, L. Zheng, G. Zhang, *Chem.-Eur. J.*, 11 (2005) 5875-5880.
- [111] A. Pineiro, X. Banquy, S. P. Casas, E. Tovar, A. Garcia, A. Villa, A. Amigo, A. E. Mark, M. Costas, *J. Phys. Chem. B*, 111 (2007) 4383-4392.
- [112] Y. Gao, X. Zhao, B. Dong, L. Zheng, N. Li and S. Zhang, *J. Phys. Chem. B*, 110 (2006) 8576-8581.
- [113] A. Apelblat, E. Manzurola, Z. Orekhova, *J. Solution Chem.*, 36 (2007) 891-900.
- [114] T. Qian, C. Yu, S. Wu, J. Shen, *Colloids Surf. B*, 112 (2013) 310-314.
- [115] H. Kubinyi, *J. Recept. Signal Transduct. Res.* 19 (1999) 15-39.
- [116] L. M. Mayr, D. Bojanic, *Current Opinion in Pharmacology*, 9 (2009) 580-588.
- [117] P. Wasserscheid, T. Welton, *Ionic Liquids in Synthesis*, 2nd Ed., Wiley VCH: 2008.
- [118] J. D. Holbrey, *Chimica. Oggi.* 22 (6) (2004) 35-37.
- [119] N. V. Plechkova, K. R. Seddon, *Chemical Society Reviews*, 37 (2008) 123-150.
- [120] F. Franks, *Water, A Comprehensive Treatise*. New York: Plenum Press; 1973.
- [121] J. F. Coetzee, C. D. Ritchie, D. Marcel, *Solute-solvent Interactions*, New York: 1973.
- [122] Strehlow, J.J. *Logo ski, The chemistry of non-aqueous solvents*. New York: Academic Press; 1978.
- [123] G. J. Janz, R. P. T. Tomkins, *Non-aqueous Electrolytes Handbook*. New York: Academic Press, 1973.
- [124] B. E. Conway, *Ionic hydration in Chemistry and Biophysics*. Amsterdam: Elsevier; 1981.
- [125] Y. Marcus, *Ion Solvation*. Chichester: Wiley Interscience; 1985.
- [126] R. M. Fuoss, F. Accascina, *Electrolytic conductance*. New York: Inter science Pub Inc; 1959.
- [127] R. A. Robinson, R.H. Stokes, *Electrolyte Solution*. London: Butter Worth's; 1968.
- [128] H. S. Harned, B. B. Owen, *Physical Chemistry of Electrolyte Solutions*. New York: Reinhold; 1958.

- [129] R. A. Horne, *Water and Aqueous solutions*. New York: Wiley Interscience; 1972.
- [130] B. E. Conway, J. O. M Bockris, *Modern Aspects of Electrochemistry*. Plenum Press: New York; 1969.
- [131] M. Kaminski, *Dis Far Soc.* 274 (1937) 171-179.
- [132] K. G. Lawrence, F. David, W. E. Waghorne, *J. Chem. Soc, Faraday Trans.* 8 (1986) 563-568.
- [133] J. B. Hasted, D. M. Ritson, C. H. Collie, *J. Chem. Phys.* 16 (1) (1948) 1-21.
- [134] V. F. Sargeeva, *Russ Chem Rev.* 34 (1965) 309-318.
- [135] A. K. Covington, T. Dickenson, *Physical chemistry of Organic Solvent Systems*. London: Plenum Press; 1973.
- [136] C. N. Rao, S. Singh, V. P. Senthilnathan, *Chem. Soc. Rev.* 5 (1976) 297-316.
- [137] N. C. R Symons, *Electron-solvent and anion- solvent interactions*. Amsterdam: Elsevier; (1976) 311.
- [138] H. G. Hertz, H. Manfred, W. Hermann, *J. Chem. Soc., Faraday Trans.* 73 (1976) 72-81.
- [139] D. R. Brown, M. C. Symons, *Journal of the Chemical Society, Faraday Transactions* 1: 73 (1977) 1490-1498.
- [140] J. W. Arthur, A. D. Haymet, *Fluid phase equilibria.* 15 (1998) 91-96.
- [141] D. W. James, R. E. Mayes, *J. Phys. Chem.* 88 (3) (1984) 637-642.
- [142] M. J. Blandamer, *Introduction to chemical ultrasonics*. New York: Academic Press; 1973.
- [143] T. C. Chang, D. E. Irish, *Canadian. J. Chem.* 51 (1) (1973) 118-125.
- [144] T. D. Alger, *J. Am. Chem. Soc.* 91 (9) (1969) 2220-2224.
- [145] A. K. Covington, P. Jones (1968: University of Newcastle upon Tyne) Taylor & Francis.
- [146] K. Gekko, *J. biochem.* 90 (6) (1981) 1643-1652.
- [147] R. Sinha, K. K. Kundu, *J. mol. liq.* 111 (1) (2004) 151-159.
- [148] R. Sinha, S. K. Bhattacharya, K. K. Kundu, *J. mol. liq.* 122 (1) (2005) 95-103.
- [149] M. N. Islam, R. K. Wadi, *Phys. Chemi. Liq.* 39 (1) (2001) 77-84.

-
- [150] R. R. Dogonadze, E. Kalman, A. A. Kornyshev, J. Ulstrup, *The Chemical Physics of Solvation, Part B, Spectroscopy Solvation*, Elsevier, Amsterdam, 1986.
- [151] M. H. Abraham, E. J. Matteoli, *J. Chem. Soc, Faraday Trans 76* (1980) 869.
- [152] D. T. Richens, Wiley: New York, 1997.
- [153] K. Ibuki, M. Nakahara, *J. Phys. Chem.* 94 (1990) 8370-8373.
- [154] A. Henni, J. H. Jonathan, T. Paitoon, C. Amit, *J. Chem. Eng. Data.* 48 (2003) 1062-1067- .
- [155] J. Burgess, *Metal Ions in Solutions*; Ellis Horwood: New York, 1978.
- [156] H. S. Harned, B. B. Owen, *The Physical Chemistry of Electrolytic Solutions*, Reinhold Publishing Corporation: New York, 1958.
- [157] J. J. Lagowski, *The Chemistry of Non-Aqueous Solvents*, Academic, New York, 1966.
- [158] B. E. Conway, R. G. Barradas, *Chemical Physics of Ionic Solutions*, Wiley: New York, 1966.
- [159] J. S. Muishead-Gould, K. J. Laidler, *Chemical Physics of Ionic Solutions*, Wiley: New York, 1966.
- [160] J. F. Coetzee, C. D. Ritchie, *Solute-Solvent Interactions*, Marcel Dekker: New York, 1969.
- [161] R. G. Bates, *Journal of Electroanalytical Chemistry and Interfacial Electrochemistry*, 29 (1971) 1-19.
- [162] G. S. Kell, C. M. Daries, J. Jarynski, *Water and Aqueous Solutions, Structure, Thermodynamics and Transport process*, Wiley: New York, 1972.
- [163] E. S. Amis, J. F. Hinton, *Solvent effects on Chemical Phenomena*, Academic: New York, 1973.
- [164] A. K. Covington, T. Dickinson, *Physical Chemistry of Organic Solvent Systems*, Plenum Press: New York, 1973.
- [165] J. E. Gordon, *The Organic Chemistry of Electrolyte Solutions*, Wiley- Interscience: New York, 1975.
- [166] F. Franks, *Physico-Chemical processes in Mixed Aqueous Solvents*, Heinemann: London, 1967.

- [167] F. Franks, Water—A Comprehensive Treatise, Plenum Press: New York, 1973.
- [168] V. Gutmann, *Electrochim. Acta.* 21 (1967) 661-670.
- [169] U. Mayer, V. Gutmann, *Adv. Inorg. Chem. Radiochem.* 17 (1975) 189-230.
- [170] R. G. Pearson, *Hard and Soft Acids and Bases*, Strondsburgh: 1973.
- [171] H. S. Harned, B. B. Owen, *The Physical Chemistry of Electrolyte Solutions*, Reinhold Publishing Corporation: New York, 1943.
- [172] C. Tanford, *Hydrophobic Effect: Formation of Micelles and Biological Membranes*, Wiley-Interscience: New York, 1980.
- [173] E. Vikingstad, *Aggregation Process in Solutions*, Elsevier: Amsterdam, 1983.
- [174] J. E. Desnoyers, M. Arel, H. Perron, C. Jolicoenn, *J. Phys. Chem.* 73(1969) 3346-3351.
- [175] A. K. Covington, T. Dickinso, *Physical Chemistry of Organic Solvent Systems*, Plenum Press: New York, 1973.
- [176] D. K. Hazra, B. Das, *J. Chem. Eng. Data* 36 (1991) 403-405.
- [177] D. O. Masson, *Phil. Mag.* 8 (1929) 218-224.
- [178] O. Redlich, D. M. Meyer, *Chem. Rev.* 64 (1964) 221-227.
- [179] B. B. Owen, S. R. Brinkley, *J. Ann. N. Y. Acad. Sci.* 51 (1949) 753-764.
- [180] K. S. Pitzer, G. Mayora, *J. Phys. Chem.*, 77 (1973) 2300-2308.
- [181] F. J. Millero, *Water and Aqueous Solutions: Structure, Thermodynamics and Transport Processes*, Wiley-Interscience: New York, 1972.
- [182] R. Gopal, M. A. Siddiqi, *J. Phys. Chem.* 73 (1969) 3390-3394.
- [183] J. Padova, I. Abrahamer, *J. Phys. Chem.* 71 (1967) 2112-2116.
- [184] R. Gopal, D. K. Agarwal, R. Kumar, *Bull. Chem. Soc. Jpn.* 46 (1973) 1973-1976.
- [185] R. Gopal, P. P. Rastogi, *Z. Phys. Chem. (N.F.)* 69 (1970) 1-10.
- [186] B. Das, D. K. Hazra, *J. Chem. Eng. Data* 36 (1991) 403-405.
- [187] L.G. Hepler, *Can. J. Chem.* 47 (1969) 4613-4617.
- [188] B. E. Conway, R. E. Verral, J. E. Desnoyers, *Trans. Faraday Soc.* 62 (1966) 2738-2749.
- [189] K. Uosaki, Y. Koudo, N. Tokura, *Bull. Chem. Soc. Jpn.* 45 (1972) 871-874.
- [190] A. W. Quin, D. F. Hoffmann, P. J. Munk, *Chem. Eng. Data* 37 (1992) 55-61.

-
- [191] Z. Atik, J. Sol. Chem. 33 (2004) 1447-1457.
- [192] Gruneisen, Wiss, Abhaudl, Physik-tech. Reich-austatt. 4 (1905) 239.
- [193] G. Jones, M. Dole, J. Am. Chem. Soc. 51 (1929) 2950-2964.
- [194] P. Debye, E. Z. Hückel, Phys. Chem. 24 (1923) 185-206.
- [195] H. Falkenhagen, M. Dole, Phys. Z. 30 (1929) 611-622.
- [196] H. Falkenhagen, E. L. Vernon, Phys. Z. 33 (1932) 140.
- [197] H. Falkenhagen, E. L. Vernon, Phil. Mag. 14 (1932) 537-565.
- [198] M. D.V. Jahagirdar, B. R. Arbad, S. R. Mirgane, M. K. Lande, A. G. Shankarwar, Journal of Molecular Liquids. 75 (1998) 33-43.
- [199] D. Feakins, D. J. Freemantle, K.G. Lawrence, J. Chem. Soc. Faraday Trans. I, 70 (1974) 795-806.
- [200] J. Crudden, G. M. Delancy, D. Feakins, P. J. O'Relly, W. E. Waghorne, K. G. Lawrence, J. Chem. Soc. Faraday Trans I. 82 (1986) 2195.
- [201] A. K. Covington, T Dickinson, Physical Chemistry of Organic Solvent Systems, Plenum Press: New York, 1973.
- [202] H. S. Harned, B. B. Owen, The Physical Chemistry of Electrolytic Solutions, Reinhold Publishing Corporation: New York, 1958.
- [203] M. Kaminsky, Z. Phys. Chem. 12 (1957) 206-231.
- [204] J. Desnoyers, G. Perron, J. Solution Chem., 1 (1972) 199-212.
- [205] R. J. M. Bicknell, K. G. Lawrence, D. Feakins, J. Chem. Soc. Faraday I, 76(1980) 637-647.
- [206] R. L. Kay, T. Vituccio, C. Zawoyski, D. F. Evans, J. Phys. Chem., 70 (1966) 2336-2341.
- [207] N. P. Yao, D. N. Bennion, J. Phys. Chem. 75 (1971) 1727-1734.
- [208] M. Kaminsky, Z. Naturforsch. 1957, 12a, 424-433.
- [209] D. Feakins, K. Lawrence, J. Chem. Soc. A, (1966) 212-219.
- [210] V. Vand, J. Phys. Chem. 52 (1948) 277-299.
- [211] D. G. Thomas, J. Colloid Sci. 20 (1965) 267-277.
- [212] MD. A. Hasan, John M. Shaw, Energy Fuels, 24 (2010) 6417-6427.
- [213] D. England, G. Pilling, J. Phys. Chem. 76 (1972) 1902-1906.

- [214] D. E. Goldsack, R. C. Franchetto, *Can. J. Chem.*, 55 (1977) 1062-1072.
- [215] D. E. Goldsack, R. C. Franchetto, *Can. J. Chem.* 56 (1978) 1442-1450.
- [216] C. A. Angell, *J. Phys. Chem.* 70 (1966) 2793-2803.
- [217] C. A. Angell, *J. Chem. Phys.* 46 (1967) 4673-4677.
- [218] P. P. Rastogi, *Bull. Chem. Soc. Japan*, 43 (1970) 2442-2444.
- [219] F. J. Millero, *Chemical Reviews*, 71 (1971) 147-176.
- [220] C. M. Criss, M. J. Mastroianni, *J. Phys. Chem.* 75 (1971) 2532-2534.
- [221] K. Tamaski, Y. Ohara, Y. Isomura, *Bull. Chem. Soc. Japan*, 46 (1973) 951.
- [222] P. P. Deluca, T. V. Rabagay, *J. Phys. Chem.* 79 (1975) 2493-2496.
- [223] B. N. Prasad, N. P. Singh, M. N. M. Singh, *Ind. J. Chem.* 14 (A) (1976) 322.
- [224] B. N. Prasad, M. M. Agarwal, *Ind. J. Chem.* 14 (A) 1976, 343.
- [225] R. T. M Bicknell, K. G. Lawrence, M. A. Scelay, D. Feakins, L. Werblan, *J. Chem. Soc. Faraday I.* 72 (1976) 307-313.
- [226] J. M. Mcdowall, N Martinus, C.A. Vincent, *J. Chem. Soc. Faraday I*, 72 (1976) 654-660.
- [227] A. Sacco, G. Petrella, M. Castagnola, *J. Phys. Chem.*, 80 (1976) 749-752.
- [228] R. L. Blokhra, Y. P. Segal, *Ind. J. Chem.*, 15(A) (1977) 36.
- [229] N. C. Das, P. B. Das, *Ind. J. Chem.*, 15(A) (1977) 826.
- [230] A. Sacco, G. Petrella, M. D. Monica, M. Castagnola, *J. Chem. Soc. Faraday I.* 73 (1977) 1936-1942.
- [231] P. K. Mandal, B. K. Seal, A. S. Basu, *Z. Phys. Chem.* 87 (1974) 295-307.
- [232] J. I. Kim, *J. Phys. Chem.* 82 (1978) 191-199.
- [233] S. K. Vijaylakshamna, *Indian J. Chem.* 17(A) (1979) 511.
- [234] A. Sacco, G. Petrella, M. D. Monica, *J. Chem. Soc. Faraday I*, 75 (1979) 2325-2331.
- [235] P. T. Thomson, M. Durbana, J. L. Turner, R. H. Wood, *J. Sol. Chem.* 9 (1980) 955-976.
- [236] K. Kurotaki, S. Kawamura, *J. Chem. Soc. Faraday I*, 77 (1981) 217-226.
- [237] N. Martinus, C. A. Vincent, *J. Chem. Soc. Faraday Trans I*, 77 (1981) 141-156.
- [238] A. Sacco, A. D. Giglio, A. D. Atti, *J. Chem. Soc. Faraday I*, 77 (1981) 2693-2699.
- [239] D. S. Gill, A.N. Sharma, *J. Chem. Soc. Faraday I*, 78 (1982) 475-484.

- [240] A. Sacco, G. Petrella, A. D. Atti, M. Castagnolo, J. Chem. Soc. Faraday I, 78 (1982) 1507-1514.
- [241] A. Sacco, A. D. Giglio, A. D. Atti, M. Castagnolo, J. Chem. Soc. Faraday I, 79 (1983) 431-438.
- [242] K. G. Lawrence, A. Sacco, J. Chem. Soc. Faraday I, 79 (1983) 615-624.
- [243] K. Miyajima, M. Sawada, M. Nakagaki, Bull. Chem. Soc. Japan 56 (1983) 827-830.
- [244] J. Doenech, S. Rivera, J. Chem. Soc. Faraday I, 80 (1984) 1249-1255.
- [245] D. Dasgupta, S. Das, D. K. Hazra, Bull. Chem. Soc. Japan, 62 (1989) 1246-1249.
- [246] S. Taniewska-Osinska, M. Jozwaik, J. Chem. Soc. Faraday Trans I, 85 (1989) 2141-2147.
- [247] D. Nandi, D. K. Hazra, J. Chem. Soc. Faraday Trans I, 85 (1989) 4227-4235.
- [248] I. Ibulci, M. Nakahara, J. Phys. Chem. 94 (1990) 8370-8373.
- [249] W. M. Cox, J. H. Wolfenden, Proc. Roy. Soc. London, 145A (1934) 475-488.
- [250] R. W. Gurney, Ionic Processes in Solution, Mc Graw Hill: New York, 1953.
- [251] E. R. Jr Nightingale, J. Phys. Chem. 63 (1959) 1381-1387.
- [252] A. Einstein, Ann. Phys. 19 (1906) 289-306.
- [253] G. S. Benson, A. R. Gordon, J. Chem. Phys. 13 (1945) 473-480.
- [254] D. F. T. Tuan, R. M. Fuoss, J. Phys. Chem. 67(1963) 1343-1347.
- [255] C. H. Springer, J. F. Coetzee, R. L. Key, J. Phys. Chem.,73 (1969) 471-476.
- [256] S. Glasstone, K. J. Laidler, H. Eyring, The Theory of Rate Process, McGraw Hill: New York, 1941.
- [257] E. R. Nightingale, R. F. Benck, J. Phys. Chem.,63 (1959)1777-1780.
- [258] D. Feakins, D. J. Freemantle, K. G. Lawrence, J. Chem. Soc. Faraday I, 70 (1974) 795-806.
- [259] R. Sinha, J. Phys. Chem. 44 (1940) 25-44.
- [260] V. Vand, J. Phys. Chem. 52 (1948) 277-299.
- [261] D. G. Thomas, J. Colloid Science, 20 (1965) 267-277.
- [262] S. P. Moulik, J. Phys. Chem. 72 (1968) 4682-4684.
- [263] S. P. Moulik, Electrochim. Acta. 17 (1972) 1491-1497.
- [264] S. P. Moulik, J. Indian Chem. Soc. 49 (1972) 483.

- [265] S. Glasstone, K. J. Laidler, H. Eyring, *The Theory of Rate Process*, McGraw Hill: New York, 1941.
- [266] D. S. Gill, T. S. Kaur, H. Kaur, I. M. Joshi, J. Singh, *J. Chem. Soc. Faraday Trans.*, 89 (1993) 1737-1740.
- [267] L. Onsager, *Z. Phys. Chem.*, 28 (1927) 277-298.
- [268] R. M. Fuoss, *Rev. Pure Appl. Chem.*, 18 (1968) 125-136.
- [269] E. Pitts, *Proc. Roy. Soc. 217A* (1953) 43-70.
- [270] R. M. Fuoss, L. Onsager, *J. Phys. Chem.*, 61 (1957) 668-682.
- [271] R. M. Fuoss, *Chemical Physics of Ionic Solutions*, Wiley: New York, 1966.
- [272] E. Pitts, R. E. Tabor, J. Daly, *Trans. Faraday Soc.*, 65 (1969) 849-862.
- [273] R. M. Fuoss, K. L. Hsia, *Proc. Natl. Acad. Sci.* 57 (1967) 1550-1555.
- [274] R. M. Fuoss, K. L. Hsia, *J. Am. Chem. Soc.*, 90 (1968) 3055-3060.
- [275] R. Fernández-Prini, J. E. Prue. "A Comparison of Conductance Equations for Unassociated Electrolytes" *Zeitschrift für Physikalische Chemie*, 2280.1 (2017) 373-379.
- [276] D. F. Evans, R. L. Kay, *J. Phys. Chem.*, 70 (1966) 366-374.
- [277] D. F. Arrington, E. Griswold, *J. Phys. Chem.* 74 (1970) 123-128.
- [278] R. M. Fuoss, C. A. Kraus, *J. Am. Chem. Soc.* 55 (1933) 476-488.
- [279] T. Shedlovsky, *J. Franklin, Instt.* 225 (1938) 739-743.
- [280] (a) J. C. Justice, *J. Chem. Phys.*, 65(1968) 353.
(b) J. C. Justice, R. Bury, C. Treiner, *J. Chem. Phys.*, 65 (1968) 1708.
- [281] R. M. Fuoss, F. Accascina, *Electrolytic Conductance*, Wiley: New York, 1959.
- [282] N. K. Bjerrum, *D. V. Selek. Mat.Fys.Medd*, 7 (1926) 9.
- [283] Fernandez-Prini R, *Trans. Faraday Soc.* 62 (1966) 1257-1264.
- [284] (a) R. M. Fuoss, L. Onsager, *J. Phys. Chem.* 66 (1962) 1722-1726.
(b) R. M. Fuoss, L. Onsager, *J. Phys. Chem.*, 67(1963) 621-628.
- [285] R. M. Fuoss, *J. Phys. Chem.* 79 (1975) 525-540.
- [286] P. C. Carman, D. P. Laurie, *J. Sol. Chem.*, 5(1976) 457-468.
- [287] R.M. Fuoss, *J. Phys. Chem.*, 81(1977) 1829-1833.
- [288] R.M. Fuoss, *Proc. Nat. Acad. Sci.* 75 (1978) 16-21.

- [289] R. M. Fuoss, J. Phys. Chem. 82 (1978) 2427-2440.
- [290] (a) W. H. Lee, R. J. Wheaton, J. Chem. Soc. Faraday II, 74 (1978) 743-766.
(b) W. H. Lee, R. J. Wheaton, J. Chem. Soc. Faraday Trans .II, 74 (1978) 1456-1482.
- [291] W. H. Lee, R. J. Wheaton, J. Chem. Soc. Faraday Trans. I, 75 (1979) 1128-1145.
- [292] W. H. Lee, R. J. Wheaton, J. Chem. Soc. Faraday Trans .II, 74 (1978) 1456-1482.
- [293] A. D. Pethybridge, S. S. Taba, J. Chem. Soc. Faraday I, 76 (1980) 368-376.
- [294] M. Bester-Rogac, R. Neueder, J. Barthel, J. Solution Chem. 28 (1999) 1071-1086.
- [295] H. S. Harned, B. B. Owen, The Physical Chemistry of Electrolytic Solutions, Reinhold Publishing Corporation: New York, 1964.
- [296] E. Balaguruswami, Numerical Methods, Tata McGraw-Hill Publishing Company: New Delhi, 2007.
- [297] M. N. Roy, B. Sinha, V. K. Dakua, Pak. J. Sci. Ind. Res. 49 (2006) 153.
- [298] (a) B. S. Krumgalz, J. Chem. Soc. Faraday I, 79 (1983) 571-587.
(b) B. S. Krumgalz, J. Chem. Soc. Faraday I, 81 (1985) 241-243.
- [299] P. Walden, H. Ulich, D. Bush, Z. Phys. Chem., 123 (1926) 429.
- [300] R. M. Fuoss, E. Hirsch, J. Am. Chem. Soc. 82 (1960) 1018-1022.
- [301] S. Takezawa, Y. Kondo, N. Tokura, J. Phys. Chem., 77 (1973) 2133-2137.
- [302] (a) D. S. Gill, J. Chem. Soc. Faraday I, 77(1981) 751-758.
(b) D. S. Gill, N. Kumari, M. S. Chauhan, J. Chem. Soc. Farada Trans I, 81 (1985) 687-693.
- [303] R. H. Stokes, R. A. Robinson, Trans. Faraday Soc. 53 (1957) 301-304.
- [304] M. Born, Z. Phys. Chem. 1 (1920) 221-249.
- [305] R. H. Boyd, J. Chem. Phys., 35 (1961) 1281-1286.
- [306] R. Zwanzig, J. Chem. Phys., 38 (1963) 1603-1605.
- [307] E. J. Passeron, J. Phys. Chem., 68 (1964) 2728-2730.
- [308] (a) P. Walden, Z. Phys. Chem., 55 (1906) 207-249.
(b) P. Walden, Z. Phys. Chem., 78(1912) 257
- [309] R. A. Robinson, R. H. Stokes, Electrolyte Solutions, Butterworths: London, 1959.
- [310] R. Gopal, M. M. Hussain, J. Ind. Chem. Soc. 40 (1963) 981.

- [311] L. G. Longworth, *J. Phys. Chem.*, 67 (1963) 689-693.
- [312] M. D. Monica, U. Lamauna, L. Seutatore, *J. Phys. Chem.* 72 (1968) 2124-2126.
- [313] S. Stokes' Broersma and Einstein's law for non-uniform viscosity, *J. Chem. Phys.* 28 (1958) 1158-1161.
- [314] D. G. Miller, *J. Phys. Chem.* 64 (1960) 1598-1599.
- [315] G. J. Hills, *Chemical Physics of Ionic Solutions*, Wiley: New York, 1966.
- [316] R. H. Stokes, I. A. Weeks, *Australian J. Chem.* 17 (1964) 304-309.
- [317] R. H. Stokes, *The Structure of Electrolytic Solutions*, Wiley: New York, 1959.
- [318] R. Zwanzig, *J. Chem. Phys.*, 52 (1970) 3625-3628.
- [319] H. S. Franks, *Chemical Physics of Ionic Solutions*, Wiley; New York, 1966.
- [320] G. Atkinson, S. K. Kor, *J. Phys. Chem.* 69(1965) 128-133.
- [321] R. L. Kay, G. P. Cunningham, D. F. Evans, *Hydrogen bonded Solvent Systems*, Taylor and Francis: London, 1968.
- [322] R. L. Kay, B. J. Hales, G. P. Cunningham, *J. Phys. Chem.*, 71 (1967) 3925-3930.
- [323] R. L. Kay, C. Zawoyski, D. F. Evans, *J. Phys. Chem.*, 69 (1965) 4208-4215.
- [324] D. F. Evans, J. L. Broadwater, *J. Phys. Chem.* 72 (1968) 1037-1041.
- [325] Kablukov, *Z. physik. Chem.*, 4 (1889) 430.
- [326] (a) Plotnikov, *Z. physik. Chem.* 67 (1906) 502.
(b) Ussanowitsch, *ibid.*, 124 (1926) 427.
- [327] P. Walden, *Bull. Acad. Imp. Sci. Sf. Pet.* 7 (1913) 934; Walden, *Z. physik. Chem.*, 147 (1930) 1.
- [328] R. M. Fuoss, F. Accascina, *Electrolytic Conductance*, Interscience: New York, 1959.
- [329] R. M. Fuoss, C. A. Kraus, *J. Am. Chem. Soc.* 55 (1933) 2387-2399.
- [330] R. M. Fuoss, *J. Am. Chem. Soc.* 82 (1960) 1013-1017.
- [331] A. Sinha, M. N. Roy, *Phys. Chem. Liq.* 45 (2007) 67-77.
- [332] M. Delsignore, H. Farber, S. Petrucci, *J. Phys. Chem.* 89 (1985) 4968-4973.
- [333] C. J. Cramer, D. G. Truhlar, *J. Am. Chem. Soc.* 113 (1991) 8305-8311.
- [334] D. J. Giesen, J.W. Stores, C. J. Cramer, D. G. Truhlar, *J. Am. Chem. Soc.* 117 (1995) 1057-1068.
- [335] (a) C. J. Cramer, D. G. Truhlar, *J. Org. Chem.* 61 (1996) 8720-8721.

- (b) C. J. Cramer, D. G. Truhlar, *Erratum*. 101 (1999) 309.
- [336] G. D. Hawkins, C. J. Cramer, D. G. Truhlar, *J. Phys. Chem. B*, 101 (1997) 7147-7157.
- [337] G. D. Hawkins, C. J. Cramer, D. G. Truhlar, *J. Phys. Chem. B*, 102 (1998) 3257-3271.
- [338] A. Gil-Villegas, A. Galindo, P. J. Whitehead, S.J. Mills, G. Jackson, A. N. Burgess, *J. Chem. Phys.*, 106 (1997) 4168-4170.
- [339] A. Galindo, L. A. Davies, A. Gil-Villegas, G. Jackson, *Mol. Phys.* 93 (1998) 241-252.
- [340] M. Roses, C. Rafols, J. Ortega, E. Bosch, *J. Chem. Soc. Perkin Trans. 2*, (1995) 1607-1616.
- [341] Y. Y. Fialkov, G. N. Fenerly, *Russ. Inorg. Chem.* 9 (1964) 1205-1213.
- [342] Y. Y. Fialkov, *Russ. J. Phys. Chem*, 41 (1967), 398.
- [343] A. Ali, M. Tariq, *Chem. Eng. Comm.*, 195 (2007) 43-56,
- [344] S.C. Bhatia, R. Bhatia, *J. Mol. Liqs.* 145 (2009) 88-102.
- [345] S. L. Oswal, P. P. Palsanwala, *Acoust. Lett.* 13 (1989) 66-73.
- [346] J. D. Pandey, P. Jain, V. Vyas, *Can. J. Chem.* 72 (1994) 2486-2492.
- [347] W. Heller, *J. Phys. Chem.* 69 (1965) 1123-1129.
- [348] V. Minkin, O. Osipov, Y. Zhdanov., *Dipole Moments in Organic Chemistry*, Plenum Press: New York, 1970.
- [349] O. Redlich, A. Kister, *Ind. Eng. Chem.* 40 (1948) 345-348.

Chapter-III

- [1] N. Saha, B. Das, *J. Chem. Eng. Data.* 42 (1997) 227-229.
- [2] M.G. Prolongo, R.M. Masegosa, I.H. Fuentes, A. Horta. *J. Phys. Chem.* 88(1984) 2163-2167.
- [3] M.N. Roy, D. Nandi, D.K. Hazra, *J. Indian Chem. Soc.* 70 (1993) 123-126.
- [4] M.N. Roy, R. Dey, A. Jha, *J. Chem. Eng. Data.* 46 (2001) 1327-1329.
- [5] Sinha A, Roy MN. *Phys. Chem. Liq.* 44 (2006) 303-314.
- [6] D.D. Perrin, W.L.F. Armarego. *Purification of Laboratory Chemicals*, 3rd Ed., Pergamon Press: Oxford, England, 1988.
- [7] J.E. Lind, J.J. Zwolenik, R.M. Fuoss, *J. Am. Chem. Soc.* 81(1959) 1557-1559.

- [8] M.N. Roy, A. Banerjee, R.K. Das, J. Chem. Thermodyn., 41 (2009) 1187-1192
- [9] B. Das, N. Saha J. Chem. Eng. Data. 45(2000) 145-145.
- [10] I. M. Abdulagatov, N.D. Azizov, Fluid Phase Equilibria, 240 (2006) 204-219.
- [11] Refractometry: Theory, Electronic document, www2.ups.edu/faculty/hanson/labtechniques/.../theory.htm. Accessed January 21, 2010.
- [12] UV-VIS Spectrophotometer, Electronic document, <http://bouman.chem.georgetown.edu/S00/handout/spectrophotometer.htm>. Spectrophotometer, accessed September, 2015.

CHAPTER: IV

- [1] H. Jiao, S.H. Goh, S. Valiyaveetil, Macromolecules 35 (2002) 3997-4002.
- [2] J. Szejtli, Chem. Rev. 98 (1998) 1743-1753.
- [3] M.L. Bender, M. Komiyama, Cyclodextrin Chemistry, Springer-Verlag, Berlin, 1978.
- [4] J. Szejtli, The Cyclodextrins and Their Inclusion Complexes, Akademiai Kiado, Budapest, 1982.
- [5] W. Saenger, Inclusion Compounds, Academic Press, London, 1984.
- [6] R.J. Clarke, J.H. Coates, S.F. Lincoln, Adv. Carbohydr. Chem. Biochem. 46 (1988) 205-210.
- [7] X. Zhao, Y. Shang, J. Hu, H. Liu, Y. Hu, Biophys. Chem 138 (2008) 144-149.
- [8] Y. Lin, Y. Zhang, Y. Qiao, J. Huang, B. Xu, J. Coll. Interf. Sci. 362 (2011) 430-438.
- [9] S. Chavda, P. Bahadur, J. Mol. Liq. 161 (2011) 72-77.
- [10] K.T. Naidu, N.P. Prabhu, J. Phys. Chem. B 115 (2011) 14760-14767.
- [11] S.K. Verma, K.K. Ghosh, J. Surfact, Detergents 14 (2011) 347-352.
- [12] M. Ikonen, L. Murtomaki, K. Kontturi, Coll. Surf., B 66 (2008) 77-83.
- [13] A.E. Kaifer, Acc. Chem. Res. 32 (1999) 62-71.
- [14] N.S. Krishnaveni, K. Surendra, M.A. Reddy, Y.V.D. Nageswar, K.R. Rao, J. Org. Chem. 68 (2003) 2018-2019.
- [15] D. Ekka, M.N. Roy, J. Phys. Chem. B 116 (2012) 11687-11694.
- [16] M.J. Rosen, Surfactant and Interfacial Phenomena, John & Wiley, New York, 1978.
- [17] C. Galant, V. Wintgens, C. Amiel, Macromolecules 38 (2005) 5243-5253.

-
- [18] M.N. Roy, D. Ekka, S. Saha, M.C. Roy, RSC Adv. 4 (2014) 42383–42390.
- [19] M.N. Roy, M.C. Roy, K. Roy, RSC Adv. 5 (2015) 56717–56723.
- [20] M.N. Roy, A. Roy, S. Saha, Carbohydr. Polym. (2016) R. Lu, J. Hao, H. Wang, L. Tong, J. Coll. Interf. Sci. 192 (1997) 37–42.
- [21] T. Liska, J. Richardson, R. Palepu, in: A.R. Hedges (Ed.), Minutes of the Sixth International Symposium on Cyclodextrins, Editions de Sante, Paris, 1992, p. 253.
- [22] R. Palepu, V.C. Reinsborough, Can. J. Chem. 66 (1988) 325–328.
- [23] K.P. Sambasevam, S. Mohamad, N.M.A. Sarih, Int. J. Mol. Sci. 14 (2013) 3671– 3682.
- [24] S. Saha, T. Ray, S. Basak, M.N. Roy, New J. Chem. 40 (2016) 651–661.
- [25] T. Wang, M.D. Wang, C.D. Ding, J. Fu, Chem. Commun. 50 (2014) 12469–12472.
- [26] N. Rajendiran, G. Venkatesh, Supramol. Chem. 26 (2014) 783–795.
- [27] M.N. Roy, S. Saha, M. Kundu, B.C. Saha, S. Barman, Chem. Phys. Lett. 655–656 (2016) 43–50.
- [28] M. Chen, G. Diao, E. Zhang, Chemosphere 63 (2006) 522–529.
- [29] J. Wang, Y. Cao, B. Sun, C. Wang, Food Chem. 127 (2011) 1680–1685.
- [30] B.W. Berry, G.F.G. Russell, J. Coll. Interf. Sci. 40 (1972) 174–194.
- [31] G. Gunnarsson, J. Jönsson, H. Wennerström, J. Phys. Chem. 84 (1980) 3114– 3121.
- [32] M.J. Jaycock, G.D. Parfitt, Chemistry of Interfaces, John Wiley and Sons, New York, USA, 1981.

CHAPTER: V

- [1] E. P. Kyba, R. C. Helgeson, K. Madan, G. W. Gokel, T. L. Tarnowski, S. S. Moore, D. J. Cram, J. Am. Chem. Soc. 99 (1977) 2564-2571.
- [2] W. D. Curtis, D. A. Laidler, J. F. Stoddart, G. H. Jones, J. Chem. Soc., Chem. Commun. (1975) 833-835.
- [3] T. J. van Bergen, R. M. Kellogg, J. Am. Chem. Soc. 99 (1977) 3882-3884.
- [4] R. M. Izatt, J. D. Lamb, R. E. Asay, G. E. Maas, J. S. Bradshaw, J. J. Christensen, S. S. Moore, J. Am. Chem. Soc. 99 (1977) 6134-6136.
- [5] Y. Chao, D. J. Cram, J. Am. Chem. Soc. 99 (1976) 1015-1017.

- [6] C. J. Pedersen, *J. Am. Chem. Soc.* 89 (1967) 7017-7036.
- [7] R. M. Izatt, N. E. Izatt, B. E. Rossiter, J. J. Christensen, *Science* 199 (1978) 994-996.
- [8] A. Metzger, K. Gloe, H. Stephan, F. P. Schmidtchen, *J. Org. Chem.* 61(1996) 2051-2055.
- [9] V. Thanabal, V. Krishnan, *J. Am. Chem. Soc.* 104 (1982) 3643-3650.
- [10] P. D. Beer, P. A. Gale, *Angew. Chem., Int. Ed.* 40 (2001) 486-516.
- [11] P. R. Ashton, I. W. Parsons, F. M. Raymo, J. F. Stoddart, A. J. P. White, D. J. Williams, R. Wolf, *Angew. Chem., Int. Ed.* 37(1998) 1913-1916.
- [12] H. W. Gibson, N. Yamaguchi, L. Hamilton, J. W. Jones, *J. Am. Chem. Soc.* 124 (2002) 4653-4665.
- [13] T. Akutagawa, T. Hasegawa, T. Nakamura, T. Inabe, *J. Am. Chem. Soc.* 124(2002) 8903-8911.
- [14] T. Akutagawa, A. Hashimoto, S. Nishihara, T. Hasegawa, T. J. Nakamura, *Phys. Chem. B* 107 (2003) 66-74.
- [15] H. Sharghi, M. A. Nasser, K. Niknam, *J. Org. Chem.* 66 (2001) 7287-7293.
- [16] R. M. Izatt, K. Pawlak, J. S. Bradshaw, R. L. Bruening, *Chem. Rev.* 91 (1991) 1721-2085.
- [17] G. W. Gokel, D. M. Goli, C. Minganti, L. M. Echegoyen, *J. Am. Chem. Soc.* 105 (1983) 6786-6788.
- [18] H. J. Buschmann, L. Mutihac, K. Jansen, *J. Inclusion Phenom. Macrocycl. Chem.* 39 (2001) 1-11.
- [19] K. M. Doxsee, J. Francis, T. J. R. Weakley, *Tetrahedron* 56 (2000) 6683-6691.
- [20] B. F. G. Johnson, C. M. G. Judkins, J. M. Matters, D. S. Shephard, S. Parsons, *Chem. Commun.* 16 (2000) 1549-1550.
- [21] D. V. Dearden, I.H. Chu, *J. Incl. Phenom.* 29 (1997) 269-282.
- [22] M. Rudolph, R.A. Kamei, K.J. Overby, *Rudolph's Fundamentals of Pediatrics*, 3rd edn, McGraw-Hill (2002) p. 308.
- [23] Y. Kawaoka, *Influenza Virology*, Caister Academic Press, Madison (2006) p. 169-177.

-
- [24] C. J. Pederson, *J. Am. Chem. Soc.* 89 (1967) 7017-7036.
- [25] B. Dietrich, J.M. Lehn, J.P. Sauvage, *Tetrahedron Lett.* 10 (1969) 2885-2970.
- [26] C. J. Pederson, *Fed. Proc. Fed. Am. Soc. Exp. Biol.* 27(1968) 1305-1309.
- [27] D. J. Cram, In: Jones, J. B. (ed.) *Applications of Biochemical Systems in Organic Chemistry*. Wiley, New York (1976).
- [28] R. A. Schultz, E. Schlegel, D.M. Dishong, G. W. Gokel, *J. Chem. Soc. Chem. Comm.* (1982) 242-243.
- [29] M. Hasani, M. Shamsipur, *J. Solution Chem.* 23 (1994) 721-725.
- [30] O.P. Kryatova, I.V. Korendovych, E.V. Rybak-Akimova, *Tetrahedron.* 60 (2004) 4579-4588.
- [31] G. Gokel, W. leevy, M. Weber, *Chemical Reviews*, 104 (2004) 2723-2750.
- [32] H. Nakamura, H. Nishida, M. Takagi, K. Ueno, *Analytica. Chimica. Acta.* 139 (1982) 219-227.
- [33] M. Shamsipur and M. Ganjali: *J. Incl. Phenom.* 28 (1997) 315-323.
- [34] M. R. Ganjali, A. Rouhollahi, A. Mardan, and M. Shamsipur, *J. Chem. Soc., Faraday Trans.* 94 (1998) 1959-1962.
- [35] F. Jalali, A. Ashrafi, M. Shamsipur, *J. Incl. Phenom. Macrocycl. Chem.* 61 (2008) 77-82.
- [36] D. P. Shoemaker, C. W. Garland, *Experiments in Physical Chemistry*. McGraw-Hill: New York, 1967, p 131.
- [37] D. Ekka, M. N. Roy, *J. Phys. Chem. B*, 116 (2012) 11687-11694.
- [38] A. Sinha, A. Bhattacharjee, M. N. Roy, *J. Dispersion Sci. Technol.* 30 (2009) 1003-1007.
- [39] M. Shamsipur, G. Khayatian, *J. Incl. Phenom.* 39 (2001) 109-113.
- [40] G. Khayatian, F. S. Karoonian, *J. Chinese chem. Soc.* 55 (2008) 377-384.
- [41] G. Khayatian, S. Shariati, M. Shamsipur, *J. Incl. Phenom.* 45 (2003) 117-121.
- [42] P. Debye and Hückel: *Phys. Z.* 24 (1928) 305-324.
- [43] Y. Gao, X. Zhao, B. Dong, L. Zheng, N. Li, S. Zhang, *J. Phys. Chem. B.* 110 (2006) 8576-8581.

- [44] M. N. Roy, D. Ekka, S. Saha, M. C. Roy, RSC Adv. 4 (2014) 42383-42390.
- [45] M. N. Roy, M. C. Roy, K. Roy, RSC Adv. 5 (2015) 56717-56723.
- [46] P. D. Harvey, D. F. R. Gilson, I. S. Butler, J Phys. Chem. 91 (1987) 1267-1270.
- [47] K. Nakamoto, Infrared and Raman Spectra of Inorganic and Coordination Compounds. 5 Edn, (John Wiley and Sons, New York) 1997.
- [48] D. O. Masson, Philos. Mag. 8 (1929) 218-235.
- [49] D. Ekka, M. N. Roy, Amino. Acids. 45 (2013) 755-777.
- [50] R. K. Wadi, P. Ramasami, J. Chem. Soc. Faraday Trans. 93 (1997) 243-247.
- [51] T. S. Banipal, D. Kaur, P. K. Banipal, J. Chem. Eng. Data 49 (2004) 1236-1246.
- [52] F. J. Millero, Wiley Interscience, New York, 1972, p 519-595.

CHAPTER: VI

- [1] (a) T. Welton, Chem Rev 99 (1999) 2071-2084; (b) R. A. Sheldon, R. M. Lau, M. J. Sorgedragar, F. V. Rantwijk, K. R. Seddon, Green Chem. 4 (2002) 147-151; (c) J. Dupont, R. F. de Souza, PAZ Suarez, Chem. Rev. 102 (2002) 3667-3692; (d) J.S. Wilkes, J. Mol. Catal A: Chem 214 (2004) 11-17.
- [2] H. Niedermeyer, J. P. Hallett, I. J. Villar-Garcia, P. A. Hunt, T. Welton, Chem. Soc. Rev. 41 (2012) 7780-7802.
- [3] N. V. Plechkova, K. R. Seddon, Chem. Soc. Rev. 37 (2008) 123-150.
- [4] S. A. Forsyth, J. M. Pringle, D. R. MacFarlane, Aust. J. Chem. 57 (2004) 113-119.
- [5] C. M. Jin, C. F. Ye, B. S. Phillips, J. S. Zabinski, X. Q. Liu, W. M. Liu, J. M. Shreeve, J. Mater. Chem. 16 (2006) 1529-1535.
- [6] Z. Zeng, B. S. Phillips, J. C. Xiao, J. M. Shreeve, Chem. Mater. 20 (2008) 2719-2726
- [7] J. H. Shin, W. A. Henderson, S. Passerini, Electrochem. Commun. 5 (2003) 1016-1020.
- [8] B. Garcia, S. Lavalley, G. Perron, C. Michot, M. Armand, Electrochim. Acta. 49 (2004) 4583-4588.
- [9] M. Galinski, A. Lewandowski, I. Stepniak, Electrochim. Acta. 51 (2006) 5567-5580
- [10] J. Vatamanu, O. Borodin, G. D. Smith, J. Am. Chem. Soc. 132 (2010) 14825-14833.
- [11] A. A. Kornyshev, J. Phys. Chem. B 111 (2007) 5545-5557.

-
- [12] Y. Zhu , S. Murali , M. D. Stoller , K. J. Ganesh , W. Cai , P. J. Ferreira, A. Pirkle , R. M. Wallace , K. A. Cychosz , M. Thommes, D. Su, E. A. Stach, R. S. Ruoff 332, *Science*, (2011) 1537–1541.
- [13] J. Ding, D. Zhou, G. Spinks, G. Wallace, S. Forsyth, M. Forsyth, D. MacFarlane, *Chem. Mater.* 15 (2003) 2392–2398.
- [14] M. S. Cho, H. J. Seo, J. D. Nam, H. R. Choi, J. C. Koo , K. G. Song , Y. Lee, Y. Sens, *Actuators B* 119 (2006) 621–624.
- [15] W. L. Hough, R. D. Rogers, *Bull. Chem. Soc. Jpn.* 80 (2007) 2262–2269.
- [16] D. Das, B. Das, D. K. Hazra, *J. Solution. Chem.* 31 (2002) 425–431.
- [17] C. Guha, J. M. Chakraborty, S. Karanjai, B. Das, *J Phys Chem B* 107 (2003) 12814–12819.
- [18] D. Das, B. Das, D. K. Hazra, *J. Solution Chem.* 32 (2003) 77–83.
- [19] M. N. Roy, D. Nandi , D. K. Hazra, *J Indian Chem Soc* 70 (1993) 121–124.
- [20] O. Popvych, R. P. T. Tomkins, Wiley-Interscience, New York Chapter 4 (1981).
- [21] A. J. Matheson, Wiley-Interscience, London, *Molecular Acoustics* (1971).
- [22] D. D Perrin , W. L. F Armarego, Pergamon Press, Oxford, third ed (1988).
- [23] N. Saha, B. Das, *J. Chem. Eng. Data.* 42 (1997) 227–229.
- [24] M. G. Prolongo, R. M. Masegosa, I. H. Fuentes, A. Horta, *J Phys. Chem.* 88 (1984) 2163–2167.
- [25] J. E. Lind Jr, J. J. Zwolenik, R. M. Fuoss, *J. Am. Chem. Soc.* 81 (1959) 1557–1559.
- [26] D. Ekka, M. N. Roy, *RSC Adv.* 4 (2014) 19831-19845.
- [27] R. M. Fuoss, *J Phys. Chem.* 82 (1978) 2427–2440.
- [28] FI El-Dossoki, *J Mol. Liq.* 151 (2010) 1–8.
- [29] D. Ekka, M.N. Roy, *J Phys. Chem. B* 116 (2012) 11687-11694
- [30] D. S. Gill, M. S. Chauhan, *Z Phys. Chem. NF* 140 (1984) 139–148.
- [31] R. M. Fuoss, F. Accascina, Interscience (1959) New York.
- [32] R. Dewan, M. N. Roy, *J. Chem. Thermodyn.* 54 (2012) 28–34.
- [33] J. M. Chakraborty, B. Das, *Z. Phys. Chem.* 218 (2004) 219–230.
- [34] R. M. Fuoss , E. Hirsch, *J. Am. Chem. Soc.* 82 (1960) 1013–1017.
- [35] R. M. Fuoss, C. A. Kraus, *J Am. Chem. Soc.* 55 (1933) 2387– 2399.
-

- [36] Y. Harada, M. Salamon, S. Petrucci, J. Phys. Chem. 89 (1985) 2006–2010.
- [37] B. S. Krungalz, J Chem. Soc., Faraday Trans 79 (1983) 571–587.
- [38] M. Delsignore, H. Farber, S. Petrucci, J Phys. Chem. 89 (1985) 4968–4973.
- [39] M. N. Roy, D. Nandi, D. K. Hazra, J Indian. Chem. Soc. 70 (1993A) 305-310.
- [40] A. Sinha, M. N. Roy, Phys. Chem. Liq. 45 (2007) 67–77.
- [41] D Nandi, S Das, D. K. Hazra, Ind. J Chem. A, 27 (1988) 574–580.
- [42] M. N. Roy, D. Ekka, S. Saha, M. C. Roy, RSC Adv. 4 (2014) 42383-42390.
- [43] D. Ekka, M. N. Roy, Amino Acids, 45 (2013) 755-777.
- [44] D. O. Masson, Philosophical Magazine, 8 (1929) 218-235.
- [45] T. S. Banipal, P Kapoor J Indian Chem. Soc. 76 (1999) 431-437.
- [46] F. Franks, ED Series; Plenum Press: New York, Ed. Vol. 4 (1975).
- [47] C. M. Romero, F. Negrete, Phys. Chem. Liq. 42 (2004) 261-267.
- [48] L. G. Hepler, Can. J. Chem. 47 (1969) 4613-4616
- [49] Y. J. Zhang, P. S. Cremer, Curr. Opin. Chem. Biol. 10 (2006) 658-663.
- [50] G. Jones, D. Dole, J Am. Chem. Soc. 51 (1929) 2950-2964.
- [51] Q. Zhao, Z. J. Sun, Q. Zhang, S. K. Xing, M. Liu, D. Z. Sun, W. L. WL, Thermochim. Acta. 487 (2009) 1–7.
- [52] R. Yandagni, P. Kebarle, J. Am. Chem. Soc. 94 (1972) 2940–2943.

CHAPTER: VII

- [1] J. W. Steed, J.L. Atwood, Supramolecular Chemistry John Wiley & Sons Ltd, Chichester, England; 2000.
- [2] H. J. Schneider, A. Yatsimirsky, Principles and methods in Supramolecular Chemistry John Wiley & Sons Ltd, Chichester, England; 2000.
- [3] C. J. Pedersen, Cyclic polyethers and their complexes with metal salts, J. Am. Chem. Soc. 89 (1967) 7017-7036.
- [4] G. W. Gokel, Crown Ethers and Cryptands, Royal Society of Chemistry, Cambridge, UK, 1991.
- [5] M. Dobler, Ionophores and their Structures, Wiley-Inter science, New York, USA, 1981.

-
- [6] L. Tavano, R. Muzzalupo, S. Trombino, I. Nicotera, C.O. Rossi, C.L. Mesa, *Colloids Surf. B* 61 (2008) 30-38.
- [7] F. A. Christy, P.S. Shrivastav, *Critical Rev. Anal. Chem.* 41 (2011) 236-269.
- [8] F. Lindoy, *The Chemistry of Macrocyclic Ligand Complexes*; Cambridge University Press: Cambridge 1989.
- [9] A. I. Popov, J.-M. Lehn, In *Coordination Chemistry of Macrocyclic Compounds*; Melson, G. A., Ed.; Plenum: New York 1979.
- [10] N.S. El-Sayed, E.R. El-Bendary, S.M. El-Ashry, M.M. El-Kerdawy, *Eur. J. Med. Chem.* 46 (2011) 3714-3720.
- [11] M. Remko, C.W. von der Lieth, *Bioorg. Med. Chem.*, 12 (2004) 5395-5403.
- [12] A. Sinha, A. Bhattacharjee, M.N. Roy, *J. Dispersion Sci. Technol.*, 30 (2009) 1003-1007.
- [13] D. P. Shoemaker, C.W. Garland, *Experiments in physical chemistry*, McGraw-Hill: New York. 1967; 131.
- [14] K. Hirose, *J. Inclusion Phenom. Macrocycl. Chem.* 39 (2001) 193-209.
- [15] P. Job, *Ann. Chim.*, 9 (1928) 113-203.
- [16] J. S. Renny, L. L. Tomasevich, E. H. Tallmadge, D. B. Collum, *Angew. Chem. Int. Ed.*, 52 (2013) 11998-12013.
- [17] J.V. Caso, L. Russo, M. Palmieri, G. Malgieri, S. Galdiero, A. Falanga, C. Isernia, R. Iacovino, *Amino Acids*, 47 (2015) 2215-2227.
- [18] C. Topacli, A. Topacli, *J. Mol. Struct.*, 644 (2003) 145-150.
- [19] H.T. Varghese, C.Y. Panicker, D. Philip, *Spectrochim. Acta A*, 65 (2006) 155-158.
- [20] A. Yu. Tsivadze, A. Yu. Varnek, V. E. Khutorskoi, *Koordinatsionnye soedineniya metallov s kraunligandami* Moscow: Nauka, 1991.
- [21] T. Wang, J.S. Bradshaw, M. Izatt, *Heterocyclic Chem.*, 31 (1994) 1097-1114.
- [22] A.K. Mandal, M. Suresh, A. Das, *Org. Biomol. Chem.*, 9 (2011) 4811-4817.
- [23] Z. Zhou, X. Yan, T.R. Cook, M.L. Saha, P.J. Stang, *J. Am. Chem. Soc.*, 13 (2016) 806-809.
- [24] X. Yan, T.R. Cook, J.B. Pollock, P. Wei, Y. Zhang, Y. Yu, F. Huang, P.J. Stang, *J. Am. Chem. Soc.*, 136 (2014) 4460-4463.
- [25] S. Barman, M.N. Roy, *RSC Adv.*, 6 (2016) 76381-76389.
-

- [26] M. N. Roy, D. Ekka, S. Saha, M. C. Roy, RSC Adv., 4 (2014) 42383-42390.
- [27] D. Ekka, M.N. Roy, Amino Acids, 45 (2013) 755-777.
- [28] D. O. Masson, Philosophical Magazine, 8 (1929) 218-235.
- [29] T. S. Banipal, P. Kapoor, J. Indian Chem. Soc. 76 (1999) 431-437.
- [30] F. Franks, Vol. 4; Franks, F., Series Ed.; Plenum Press: New York, 1975.
- [31] H. Shekaari, M.T. Zafarani-Moattar, S.N. Mirheydari, J. Chem. Eng. Data, 60 (2015) 1572-1583.
- [32] C. M. Romero, F. Negrete, Phys. Chem. Liq., 42 (2004) 261-267.
- [33] L. G. Hepler, Can. J. Chem., 47 (1969) 4613-4616.
- [34] Y. J. Zhang, P.S. Cremer Curr. Opin. Chem. Biol., 10 (2006) 658-663.
- [35] G. Jones, M. Dole J Am Chem Soc., 51 (1929) 2950-2964.
- [36] M. J. Iqbal, M.A. Chaudhry, J. Chem. Eng. Data, 54 (2009) 2772-2776.
- [37] N. L. Volkova, E.V. Parfenyuk, Thermochimica Acta 435 (2005) 108-112.
- [38] I. B. Malham, M. Turmine, J. Chem. Thermodyn., 40 (2008) 718-723.
- [39] M. Tjahjono, M. Garland, J. Solution Chem., 36 (2007) 221-236.
- [40] R. H. Robinson, R.H. Stokes, London, 125 (1955).
- [41] S. Kiviniemi, A. Sillanpaa, M. Nissinen, K. Rissanen, M.T. Lamsa, J. Pursiainen, Chem. Commun., 10 (1999) 897-898.
- [42] N. Noujeim, L. Leclercq, A.R. Schmitzer, J. Org. Chem., 73 (2008) 3784-3790.
- [43] M. L'ams'a, J. Huuskonen, K. Rissanen, J. Pursiainen, Chem.-Eur. J., 4 (1998) 84-92.
- [44] J. S. You, X.Q. Yu, G.L. Zhang, Q.X. Xiang, J.B. Lan, R.G. Xie, Chem. Commun. 18 (2001) 1816-1817.
- [45] (a) J. Polster, H. Lachman, VCH, Weinheim, 1989. (b) K.A. Connors Wiley, New York, 1987. (c) H.A. Benesi, J.H. Hildebrand, J. Am. Chem. Soc. 71(1949) 2703-2707. (d) F. Cramer, W. Saenger, H.C. Spatz, J. Am. Chem. Soc. 89 (1967) 14-20.
- [46] K. Srinivasana, T. Stalina, K. Sivakumarb, Spectrochimica Acta Part A, 94 (2012) 89-100.
- [47] H. Y. Wanga, J. Hana, X.G. Fenga, Y.L. Pangb, spectrochimica Acta Part A, 65 (2006) 100.

CHAPTER: VIII

- [1] J. Szejtli, Pure Appl. Chem., 76 (2004) 1825–1845.
- [2] W. Saenger, Angew. Chem. Int. Ed Engl. 19 (1980) 344–362.
- [3] S. Hamai, J. Phys. Chem. 94 (1990) 2595–2600.
- [4] M. L. Bender, M. Komiyama, Cyclodextrin Chemistry, Springer-Verlag, Berlin, 1978.
- [5] D. W. Armstrong, G.Y. Stine, J. Am. Chem. Soc. 105 (1983) 2962–2964.
- [6] W. Saenger, Angew. Chem. Int. Ed. Engl. 19 (1980) 344-362.
- [7] K. A. Connors, Chem. Rev. 97 (1997) 1325–1357.
- [8] J. Szejtli, Chem. Rev. 98 (1998) 1743–1753.
- [9] A. Undas, K. E. Brummel-Ziedins, K.G. Mann, J Vasc. Surg. 45 (2007)1142.
- [10] E. V. Kompantseva, M.V. Gavrillin, L.S. Ushakova, Pharm. Chem. J. 30 (1996) 258–262.
- [11] F. Van de Mannakker, T. Vermonden, C.F. van Nostrum, W.E. Hennik, Biomacromolecules 10 (2009) 3157–3175.
- [12] C. O. Mellet, J.M. Fernandez, J.M. Benito, Chem. Soc. Rev. 40 (2011) 1586–1608.
- [13] A. A. Rasheed, C.K. Kumar, V.V.N.S.S. Sravanthi, Sci. Pharm. 76 (2008) 567–598.
- [14] C. Yanez, M. Araya, S. Bollo, J Incl. Phenom Macrocycl. Chem., 68 (2010) 237–241.
- [15] H. J. Schmann, E. Schollmeyer, Cosmet. Sci., 53 (2002) 85-191.
- [16] D. Monti, S. Tampucci, P. Chetoni, S. Burgalassi, V.Saino, M. Centini, L. Staltari, C. Anselmi, AAPS Pharm Sci. Tech., 12 (2011) 514–520.
- [17] S. H. Kim, H. Y. Kim and H. S. Kwak, Asian-Aust. J. Anim. Sci., 20 (2007) 1468 – 1472.
- [18] A. Bozkiri, Z.F. Denli and B. Basaran, Acta Poloniae Pharmaceutica ñ Drug Research, 69 (2012) 719-724.
- [19] M. Zan, J. Li, S. Luo, Z. Ge, Chem. Commun. 50 (2014) 7824–7827.
- [20] T. Wang, M. D. Wang, C. D. Ding, J. J Fu, Chem. Commun. 50 (2014) 12469–12472.
- [21] J. Ding, L. Chen, C. Xiao, L. Chen, X. Zhuang, X. Chen, Chem. Commun. 50 (2014) 11274–11290.
- [22] T. A. Reineccius, G.A. Reineccius, T.L. Peppard, J Food Sci., 69 (2008) 1365- 2621.
- [23] I. Pishtiyski, Scientific papers, 35 (2007) 5-20.

- [24] A. M. Grigoriu, C. Luca, A. Grigoriu, *Cellulose Chem. Technol.*, 42(1-3) (2008)103-112.
- [25] R. A. Harrington, C.W. Hamilton, R.N. Brogden, J.A. Linkewich, J.A. Romankiewicz, R. C. Heel, *Drugs*. 25 (1983) 451-494.
- [26] P. Job, *Ann. Chim.* 9 (1928) 113-203.
- [27] J. S. Renny, L. L. Tomasevich, E. H. Tallmadge, D. B. Collum, *Angew. Chem. Int. Ed.* 52 (2013) 11998 – 12013.
- [28] J. V. Caso, L. Russo, M. Palmieri, G. Malgieri, S. Galdiero, A. Falanga, C. Isernia, R. Iacovino, *Amino Acids* 47 (2015) 2215-2227.
- [29] K. Hirose: *J. Inclusion Phenom. Macrocycl. chem.*, 39 (2001) 193-209.
- [30] S. Saha, A. Roy, K. Roy, M. N. Roy, *Sci. Rep.* 6(2016).
- [31] Y. Gao, X. Zhao, B. Dong, L. Zheng, N. Li, S. Zhang, *J. Phys. Chem. B* 110 (2006) 8576-8581.
- [32] A. Pineiro, X. Banquy, S. P. Casas, E. Tovar, A. Garcia, A. Villa, A. Amigo, A. E. Mark, M. Costas, *J. Phys. Chem. B* 111 (2007) 4383-4392.
- [33] A. Roy, S. Saha, M. N. Roy, *Fluid Phase Equilibria* 425 (2016) 252-258.
- [34] M. N. Roy, S. Saha, M. Kundu, B. C. Saha, S. Barman, *Chemical Physics Letters* 655-656 (2016) 43–50.
- [35] A. Roy, S. Saha, B. Datta, M. N. Roy, *RSC Adv.* 6 (2016) 100016–100027.
- [36] M. N. Roy, S. Saha, S. Barman, D. Ekka, *RSC Adv.* 6 (2016) 8881–8891.
- [37] M. N. Roy, D. Ekka, S. Saha, M. C. Roy, *RSC Adv.* 4(2014) , 42383–42390.
- [38] Y. Gao, Z. Li, J. Du, B. Han, G. Li, W. Hou, D. Shen, L. Zheng, G. Zhang, *Chem. Eur. J.* 11 (2005) 5875 – 5880.
- [39] M. N. Roy, A. Roy, S. Saha, *Carbohydrate Polymers* 151 (2016) 458–466.
- [40] S. Saha, T. Ray, S. Basak, M. N. Roy, *New J. Chem.* 40 (2016) 651-661.
- [41] S. Barman, D. Ekka, S. Saha, M. N. Roy, *Chemical Physics Letters* 658 (2016) 43–50.
- [42] J.S. You, X.Q. Yu, G.L. Zhang, Q.X. Xiang, J.B. Lan, R.G. Xie, *Chem. Commun.* 18 (2001) 1816-1817.
- [43] J. Polster, H. Lachman: *Spectrometric Titrations*, VCH, Wienheim, 1989.

-
- [44] K.A. Connors: Binding Constants. The Measurement of Molecular Complex. Wiley, New York, 1987.
- [45] F. Cramer, W. Saenger, H.C. Spatz, J. Am. Chem. Soc. 89 (1967) 14-20.
- [46] H.A. Benesi, J.H. Hildebrand, J. Am. Chem. Soc. 71 (1949) 2703-2707.
- [47] S Prabu, M Swaminathan, K Sivakumar, R Rajamohan, Journal of Molecular Structure 1099 (2015) 616-624.
- [48] C. N. Sanrame, R. H. Rossi, G. A. Arguello, J. Phys. Chem., 100 (1996) 8151-8156.
- [49] A. Orstan, J. B. Rossi, J. Phys. Chem., 91 (1987) 2739-2745.
- [50] Q. Zhang, Z. Jiang, Y. Guo, R. Li, Spectrochim. Acta Part A 69 (2008) 65-70.
- [51] M. Zhang, J. Li, W Jia, J. Chao, L. Zhang, Supramolecular Chemistry, 21 (2009) 597-602.
- [52] A. Fernandes, G. Ivanova, N. F. Bras, N. Mateusa, M. J. Ramos, M. Rangel, V. D. Freitas, Carbohydrate Polymers 102 (2014) 269-277.
- [53] V. Sindelar, M.A. Cejas, F.M. Raymo, W. Chen, S.E. Parker, A.E. Kaifer, Chem. Eur. J. 11 (2005) 7054-7059.
- [54] L. J. Yang, S. X. Ma, S. Y. Zhou, W. Chen, M. W. Yuan, Y. Q. Yin, X. D. Yang, Carbohydrate Polymers 98 (2013) 861-869.
- [55] J. S. Negi, S. Singh, Carbohydrate Polymers 92 (2013) 1835- 1843.
- [56] C. F. Xiao, K. Li, R. Huanga, G. J. Hea, J. Q. Zhang, L. Zhu, Q. Y. Yang, K. M. Jiang, Y. Jin, J. Lin, Carbohydrate Polymers 102 (2014) 297-305.
- [57] K. Sivakumar, T. R. Ragi, D. Prema, T. Stalin, Journal of Molecular Liquids , 218 (2016) 538-548.
- [58] W. Zhang, X. Gong, Y. Cai, C. Zhang, X. Yu, J. Fan, G. Diao, Carbohydrate Polymers 95 (2013) 366-370.
- [59] G. Socrates (2001) In Infrared and Raman Characteristic Group Frequencies-Tables and Charts 3rd ed. (Chichester: John Wiley).
- [60] G. Subhapriya, S Kalyanaraman, S Gandhimathi, N Surumbarkuzhali, V Krishnakumar, J. Chem. Sci. 129 (2017) 259-269.
- [61] H. Shekaari, F. Jebali, Phys. Chem. Liq. 49 (2011) 572-587

CHAPTER: IX

- [1] C. J. Pedersen, J. Am. Chem. Soc. 89 (1967) 7017-7036.
- [2] C. J. Pedersen, J. Am. Chem. Soc. 89 (1967) 2495-2496.
- [3] G. W. Gokel, Royal Society of Chemistry, Cambridge, UK, 1991.
- [4] M. Dobler, Wiley-Inter science, New York, USA, 1981.
- [5] A. M. Stuart, J. A. Vidal, J. Org. Chem. 72 (2007) 3735-3740.
- [6] N. Jose, S. Sengupta, J. K. Basu, J. Mol. Catal. A: Chem. 309 (2009) 153-158.
- [7] J. Malval, I. Gosse, J. Morand, R. Lapouyade, J. Am. Chem. Soc. 124 (2002) 904-905.
- [8] L. Tavano, R. Muzzalupo, S. Trombino, I. Nicotera, C. O. Rossi, C. L. Mesa, Colloids Surf. B, 61 (2008) 30-38.
- [9] F. A. Christy, P. S. Shrivastav, 41 (2011) 236-269.
- [10] T. B. Stolwijk, E. J. R. Sudhohler, D. N. Reinhoudt, S. Harkema, J. Org. Chem. 54 (1989) 1000-1004.
- [11] S. Kiviniemi, A. Sillanpaa, M. Nissinen, K. Rissanen, M. T. Lamsa, J. Pursiainen, Chem. Commun. 10 (1999) 897-898.
- [12] S. Kiviniemi, M. Nissinen, M. T. Lamsa, J. Jalonen, K. Rissanen, J. Pursiainen, New J. Chem. 24 (2000) 47-52.
- [13] M. Lee, Z. Niu, D. V. Schoonover, C. Slebodnick, H. W. Gibson, Tetrahedron, 66 (2010) 7077-7082.
- [14] N. Noujeim, L. Leclercq, A. R. Schmitzer, J. Org. Chem. 73 (2008) 3784-3790.
- [15] E. Ennis, S. T. Handy, Curr. Org. Synth. 4 (2007) 381-389.
- [16] D. Tapu, C. Owens, D. VanDerveer, K. Gwaltney, Organometallics, 28 (2009) 270-276.
- [17] J. C. Walton, M. M. Brahmī, L. Fensterbank, E. Lacôte, M. Malacria, Q. Chu, S. H. Ueng, A. Solov'yev, D. P. Curran, J. Am. Chem. Soc. 132 (2010) 2350-2358.
- [18] T. Welton, Chem. Rev. 99 (1999) 2071-2083.
- [19] W. Xu, E. I. Cooper, C. A. Angell, J. Phys. Chem. B, 107 (2003) 6170-6178.
- [20] S. G. Lee, Chem. Commun. 10 (2006) 1049-1063.
- [21] J. E. Bara, D. E. Camper, D. L. Gin, R. D. Noble, Acc. Chem. Res. 43 (2010) 152-159.
- [22] D. Ekka, M. N. Roy, J. Phys. Chem. B 116 (2012) 11687-11694.

-
- [23] A. Sinha, A. Bhattacharjee, M. N. Roy, J. Dispersion Sci. Technol. 30 (2009) 1003-1007.
- [24] Y. Takeda, T. Kimura, J. Incl. Phenom. Mol. Recognit. Chem. 11 (1991) 159-170.
- [25] M. Shamsipur, G. Khayatian, J. Incl. Phenom. 39 (2001) 109-113.
- [26] G. Khayatian, F. S. Karoonian, J. Chinese chem. Soc. 55 (2008) 377-384.
- [27] D. F. Evans, S. L. Wellington, J. A. Nadi, E. R. Cussler, J. Solution Chem. 1 (1972) 499-506.
- [28] G. Khayatian, S. Shariati, M. Shamsipur, J. Incl. Phenom. 45 (2003) 117-121.
- [29] P. Debye, Hückel: Phys. Z. 24 (1928) 305-307.
- [30] A. F. Danil de Namor, M. C. Ritt, M. J. Schwing-Weill, F. Arnaud-Neu, D. F. Lewis, J. Chem.Soc., Faraday Trans. 87 (1991) 3231-3239.
- [31] H. J. Buschman, E. Schollmeyer, L. Mutihae, J. Incl. Phenom. 30 (1998) 21-28.
- [32] M. Czekalla, K. Geo, B. Haberman, T. Kruger, H. Stephan, F. P. Schmidtchen, R. Trultzschn, Poster PB 37, XXI International Symposium on Macrocyclic Chemistry, Montecatini Terme, Italy(1996).
- [33] A. Yu. Tsivadze, A. Yu. Varnek, V.E. Khutorskoi, Koordinatsionnye soedineniya metallov s kraunligandami ,Moscow: Nauka, 1991.
- [34] H. G. Silver, J. L. Wood, Trans. Faraday Soc. 60 (1964) 5-9.
- [35] R. Ramasamy, Journal of Applied Spectroscopy, 80 (2013) 506-512.
- [36] J.-C. Lassègues, J. Gronding, D. Cavagnat, P. Johansson, J. Phys. Chem. A, 113 (2009) 6419-6421.
- [37] A. K. Mandal, M. Suresh, A. Das, Org. Biomol. Chem. 9 (2011) 4811-4817.
- [38] Z. Zhou, X. Yan, T. R. Cook, M. L. Saha, P. J. Stang, J. Am. Chem. Soc. 138 (2016) 806-809.
- [39] X. Yan, T. R. Cook, J. B. Pollock, P. Wei, Y. Zhang, Y. Yu, F. Huang, P. J. Stang, J. Am. Chem. Soc. 136 (2014) 4460-4463.

- [40] M. Lämsä, J. Huuskonen, K. Rissanen, J. Pursiainen, Chem.Eur. J. 4 (1998) 84-92.
- [41] M. Lämsä, T. Suorsa, J. Pursiainen, J.Huuskonen and K. Rissanen, Chem. Commun. (1996) 1443-1444.
- [42] M. Lämsä, J. Pursiainen, K. Rissanen and J. Huuskonen, Acta Chem. Scand. 52 (1998) 563-570.
- [43] T. Steiner, Chem. Commun. (1997) 727-734.

INDEX

Subject	Page No.
A	
Acetonitrile	74, 172, 198, 256
Amantadine hydrochloride	108, 155
Apparent molar volume	66, 164, 186, 209
Association constant	81, 150, 158, 177, 225, 262
B	
Beer-Lambert Law	130
Benzyltrimethylammonium chloride	105, 139
Benzyltriethylammonium chloride	105, 139
Benzyltributylammonium chloride	106, 139
1-butyl-3-methylimidazolium chloride	107, 172
C	
Crown ether	43, 112, 153, 197, 255
Conductance	49, 138, 156, 173
Complexation	57, 155, 198, 255
Cyclodextrin	37, 110, 137, 229
D	
Density	46, 62, 155

E

Enthalpy change	40
Entropy change	94

F

Fluorescence Spectroscopy	48, 132, 243
FTIR Spectroscopy	102
Fuoss Conductance equation	86, 172
Fuoss-Kraus equation	81, 183

G

Gibbs free energy	57, 180
-------------------	---------

H

Hydrogen bonding	36, 154, 217, 250, 270
Host-Guest Chemistry	35
Host-Guest Inclusion complex	48, 152, 229
Hydrophobic Interaction	152, 229

I

Ionic association	81
Ionic interaction	93, 120
Ion-ion interaction	61
Ionic Liquids	50, 137, 171
Ion-pair formation	67, 72

Ion-solvent interaction	44, 48, 60
Ionic Walden product	91, 180
J	
Jones-Dole equation	71, 193
L	
limiting apparent molar expansibilities	67, 192, 215
Limiting molar conductance	177
M	
1-methyl-3-octylimidazolium	107, 167
tetrafluoroborate	
Masson equation	164, 189
Methanol	89, 117, 153
Molar refractivity	101
N	
NMR	47, 128, 147, 206, 246, 267
Non-aqueous	56, 171
O	
Organic solvent	38
Optical properties	60

P

Partial molar volumes	62
Physicochemical properties	40

R

Refractive index	126, 219
Relative Viscosity	75, 193, 217

S

Spectroscopy	102, 131
Specific conductance	232
Stoke's radii	76
Structure breaker	67
Structure maker	67
Solute – solute interactions	58
Solute – solvent interactions	58
Solvation behaviour	55
Solvent – solvent interactions	58
Surface Tension	49

T

Tetrahydrofuran	116, 172
Thermodynamic properties	73
Thermodynamic equilibrium	40
Transport properties	60
Triple ion	57
	97, 172

U

UV-Visible Spectroscopy	48, 225, 233
-------------------------	--------------

V

Viscosity	43, 171, 217
Viscosity B-coefficient	56

W

Water	38, 112
Walden Product	91, 178



Research paper

NMR, surface tension and conductance study to investigate host–guest inclusion complexes of three sequential ionic liquids with β -cyclodextrin in aqueous media



Siti Barman, Deepak Ekka, Subhadeep Saha, Mahendra Nath Roy*

Department of Chemistry, University of North Bengal, Darjeeling 734013, India

ARTICLE INFO

Article history:

Received 20 May 2016

In final form 6 June 2016

Available online 7 June 2016

Chemical compounds studied in this article:

 β -Cyclodextrin (PubChem CID: 444041)

Benzyltrimethylammonium chloride

(PubChem CID: 5963)

Benzyltriethylammonium chloride

(PubChem CID: 66133)

Benzyltributylammonium chloride

(PubChem CID: 159952)

Keywords:

Inclusion complex

Benzyltrialkylammonium chloride

 β -Cyclodextrin

CMC

Surface tension

Conductance

NMR

Association constant

ABSTRACT

Host–guest inclusion complexes of three sequential cationic room temperature surface active ionic liquids, benzyltrialkylammonium chloride $[(C_6H_5CH_2)N(C_nH_{2n+1})_3Cl]$; where $n = 1, 2, 4$] with β -cyclodextrin in aqueous media have been studied using surface tension, conductance and NMR spectroscopy. All the studies have suggested that the hydrophobic benzyl group of ionic liquids is encapsulated inside into the cavity of β -cyclodextrin and played a crucial role in supporting the formation of inclusion complexes. The variation of the thermodynamic parameters with guest size, shape is used to draw inferences about contributions to the overall binding by means of the driving forces, viz., hydrophobic effect, steric hindrance, van der Waal force, and electrostatic force.

© 2016 Elsevier B.V. All rights reserved.

1. Introduction

Supramolecular assembly is the association of guest molecules into the inner cavity of a host molecule by noncovalent bonds under equilibrium conditions [1]. Cyclodextrin seems to be the most promising host molecule to form inclusion complexes [2]. β -Cyclodextrin (β -CD) is a cyclic oligosaccharide (consists of seven α -D-glucopyranose units, linked by glycosidic bonds α -1,4 obtained as the main product from the enzymatic conversion of the starch [3–6]. Due to lack of free rotation about the glycosidic bond, β -CD (as the α - and γ -CDs) has a unique spatial configuration, showing a cylindrical hollow truncated cone shape; cavity with 6.0 Å of width and 7.9 Å of height, has a hydrophobic character,

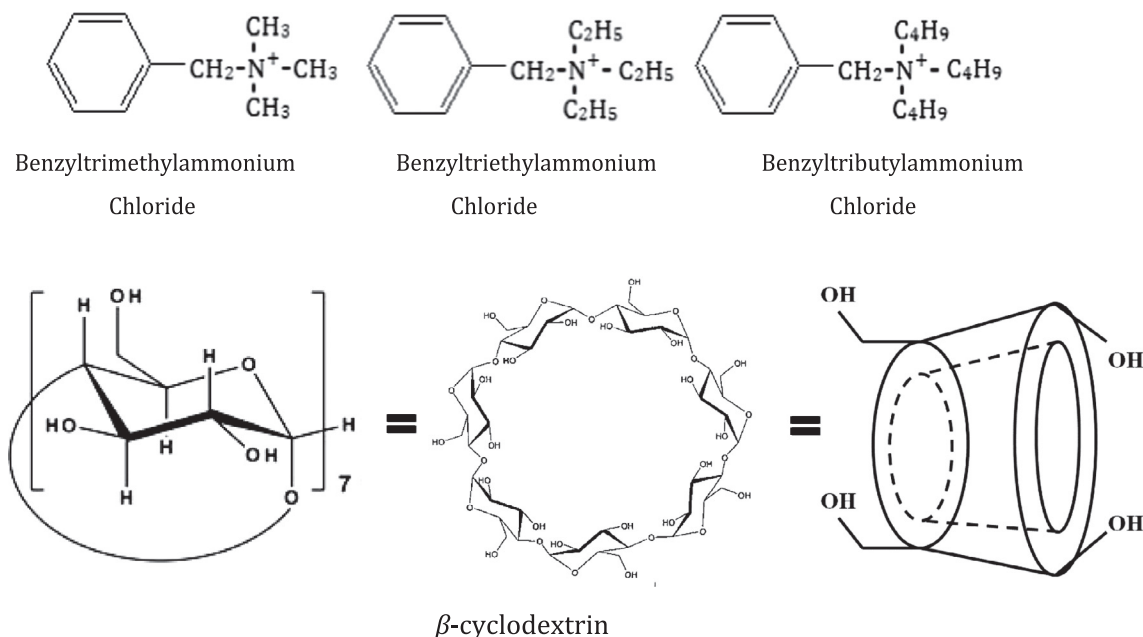
while the rims are hydrophilic: the wider one, with fourteen primary hydroxyl groups ($-OH$), and a narrower one with, the seven secondary OH groups ($-CH_2OH$) (Scheme 1). These structural features give all the fitting and encapsulating properties to β -CD, for forming inclusion complexes with molecules that fit into the hydrophobic cavity.

Cationic ionic liquids are the prominent surface active agents with positively charged hydrophilic head group and a hydrophobic tail group, have attracted immense interest in the development of methods for separation, purification, extraction of DNA; and also been tested for gene delivery and gene transfection that involve in current clinical trials based on gene therapy [7,8].

The driving force of inclusion complex formation is the displacement of water molecules by more hydrophobic guest molecules present in the solution to attain an apolar-apolar association [2]. The surface active ionic liquids are form inclusion complex with β -CD; may be applied in industries, agriculture,

* Corresponding author.

E-mail address: mahendraroy2002@yahoo.co.in (M.N. Roy).



Scheme 1. Molecular structure of cationic surfactant and β -cyclodextrin.

textile, detergent, food, cosmetics and the drug or pharmaceutical [9,10], as antibacterial, antistatic, corrosion inhibitory, dispersants, emulsifying, wetting and solubilizing agent's etc [9,11,12]. In addition to these industrial applications, CDs are related to many interesting topics, such as molecular recognition and self-assembly, molecular encapsulation, chemical stabilization, and intermolecular interactions [13,14].

However, to the best of our knowledge, no work has yet been done in as our chosen system. In this paper, size, shape, structural effect of ionic liquids in the formation of the inclusion complexes have been studied quantitatively and qualitatively to find the nature of ionic host-guest inclusion complexes of sequential cationic room temperature surface active ionic liquids, benzyltrialkylammonium chloride $[(C_6H_5CH_2)N(C_nH_{2n+1})_3]Cl$; where $n = 1, 2, 4$] (Scheme 1) with β -cyclodextrin in aqueous media using surface tension, conductance and NMR study.

2. Result and discussion

2.1. Critical micellization concentration (CMC)

The micelle forming concentration of the three cationic room temperature ionic liquids was measured by surface tension, (γ) and molar conductivity (Λ) in aqueous media.

In Fig. 1 the surface tension (γ) values obtained for the cationic based ionic liquid solution is plotted as a function of the ionic liquid concentration at 298 K. Surface tension decreases with the increase of ionic liquid concentration, reach a minima (called critical micellization concentration, CMC) and the slight increase or taken as almost constant variation with further addition of ionic liquids, have disclosed no effective variation in the surface tension as expected very seriously [15]. The break point in Fig. 1 demonstrates that the micelle starts to form at the critical micellization concentration (CMC) of 3.0×10^{-3} , 2.6×10^{-3} , and 2.0×10^{-3} M (Table 1) for $[(C_6H_5CH_2)N(CH_3)_3]Cl$, $[(C_6H_5CH_2)N(C_2H_5)_3]Cl$ and $[(C_6H_5CH_2)N(C_4H_9)_3]Cl$ respectively.

The conductance values (Λ) obtained for the cationic ionic liquid solution is also plotted as a function of the ionic liquid concentration. Conductivity increases monotonically with the increase of

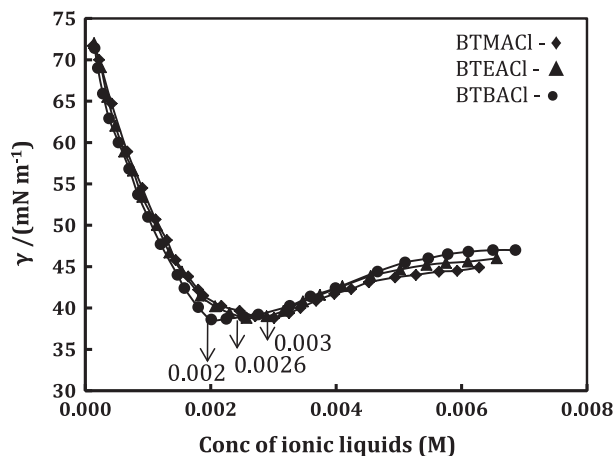


Fig. 1. Plot of surface tension (γ) with corresponding conc. (M) of ionic liquids.

the ionic liquid concentration, but after a certain point (called break point) the conductance data have not vary effectively even further addition of ionic liquid. The break point (Fig. 2) at the concentration of 3.1×10^{-3} , 2.9×10^{-3} , and 1.9×10^{-3} M for $[(C_6H_5CH_2)N(CH_3)_3]Cl$, $[(C_6H_5CH_2)N(C_2H_5)_3]Cl$ and $[(C_6H_5CH_2)N(C_4H_9)_3]Cl$ respectively (Table 1), demonstrates the critical micellization concentration (CMC), where, the micelles starts to form. The point is confirmed by conductance result in Fig. 2 where break point is also seen in good agreement with surface tension (Fig. 1).

2.2. Surface tension

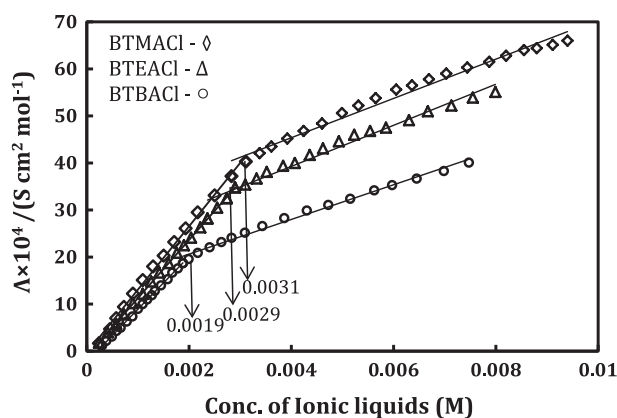
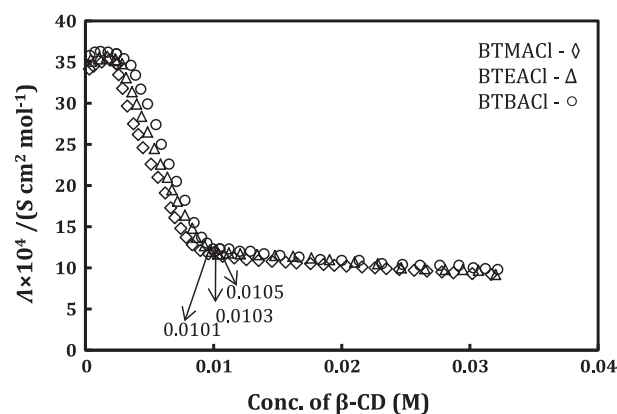
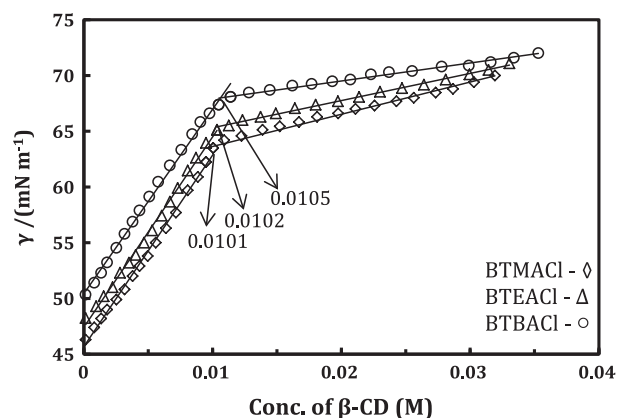
Surface tension (γ) measurement gives significant indication about the formation of inclusion complex as well as stoichiometry of the host-guest assembly [16–19]. Fig. 3 illustrates the variations of surface tension (γ) of 0.01 M chosen three aforesaid ionic liquids with β -CD concentration at 298 K.

The surface tension curves vary linearly with an addition of β -CD concentration to a maximum, and after then surface tension data not vary effectively with further adding of β -CD into the

Table 1

Molar conductance (Λ) and surface tension (γ) values with corresponding concentration at the CMC and saturation point of inclusion; and concentration ratio (ratio of inclusion IL: β -CD) at the break point of the surfactants solution (0.01 M) in aqueous β -CD.

Ionic liquids	CMC (M)	Λ_{CMC} ($\text{S cm}^2 \text{ mol}^{-1}$)	Conc. (M)	Λ ($\text{S cm}^2 \text{ mol}^{-1}$) at break point	Conc. ratio (IL: β -CD)
$[(\text{C}_6\text{H}_5\text{CH}_2)\text{N}(\text{CH}_3)_3\text{Cl}]$	0.0031	40.31	0.0101	11.90	1: 1.01
$[(\text{C}_6\text{H}_5\text{CH}_2)\text{N}(\text{C}_2\text{H}_5)_3\text{Cl}]$	0.0029	32.50	0.0103	11.71	1: 1.03
$[(\text{C}_6\text{H}_5\text{CH}_2)\text{N}(\text{C}_4\text{H}_9)_3\text{Cl}]$	0.0019	18.72	0.0105	12.30	1: 1.05
Ionic liquids	CMC (M)	γ_{CMC} (mN m^{-1})	Conc. (M)	γ (mN m^{-1}) at break point	Conc. ratio (IL: β -CD)
$[(\text{C}_6\text{H}_5\text{CH}_2)\text{N}(\text{CH}_3)_3\text{Cl}]$	0.0030	39.1	0.0101	68.0	1: 1.01
$[(\text{C}_6\text{H}_5\text{CH}_2)\text{N}(\text{C}_2\text{H}_5)_3\text{Cl}]$	0.0026	38.9	0.0102	65.5	1: 1.02
$[(\text{C}_6\text{H}_5\text{CH}_2)\text{N}(\text{C}_4\text{H}_9)_3\text{Cl}]$	0.0020	38.6	0.0105	63.8	1: 1.05

**Fig. 2.** Plot of molar conductance (Λ) with corresponding conc. (M) of ionic liquids.**Fig. 4.** Plot of molar conductance (Λ) of ionic liquids (0.01 M) with corresponding conc. (M) of β -CD.**Fig. 3.** Plot of surface tension (γ) of ionic liquids (0.01 M) with corresponding conc. (M) of β -CD.

solutions. The linear rising surface tension data demonstrates the decreasing tendency of the surface activity of the surface active ionic liquids. This is due to the fact that ionic liquids are encapsulated insight into the cavity of the β -CD and form the inclusion complexes (ICs) and loss their surface activity. The constant variation of surface tension after saturation point, make clear that the rest surface tension is only for the aqueous solutions of β -CD or pure water; because the inclusion complexes and aqueous solution of β -CD do not possess any surface activity [20]. The stoichiometry of the inclusion complexes has been obtained from concentration ratio of the ionic liquid and β -CD (IL: β -CD) at the break point or the saturation point of the inclusion. From Table 1 it has been seen that the concentration ratio of IL: β -CD is 1:1.01, 1:1.02, and 1:1.05

for $[(\text{C}_6\text{H}_5\text{CH}_2)\text{N}(\text{CH}_3)_3\text{Cl}]$, $[(\text{C}_6\text{H}_5\text{CH}_2)\text{N}(\text{C}_2\text{H}_5)_3]$ and $[(\text{C}_6\text{H}_5\text{CH}_2)\text{N}(\text{C}_4\text{H}_9)_3\text{Cl}]$ respectively. From Fig. 4 it is found that the surface tension curves of the three selected ionic liquids in the presence of fixed amount (0.005 M) of β -CD are higher than those in the absence of β -CD.

The concentration at which surface tension of ionic liquids (for fixed 0.005 M β -CD) is almost constant is called as apparent critical micelle concentrations (CMC^*). The CMC^* 0.00499, 0.00503, and 0.00505 for $[(\text{C}_6\text{H}_5\text{CH}_2)\text{N}(\text{CH}_3)_3\text{Cl}]$, $[(\text{C}_6\text{H}_5\text{CH}_2)\text{N}(\text{C}_2\text{H}_5)_3\text{Cl}]$ and $[(\text{C}_6\text{H}_5\text{CH}_2)\text{N}(\text{C}_4\text{H}_9)_3\text{Cl}]$ respectively, also suggested the 1:1 stoichiometric ratio of inclusion. Higher the CMC^* values caused by the presence of β -CD indicates that the formation of β -CD-ionic liquid inclusion complexes decreases the micelle formation ability of the ionic liquids. The surface tension values of each ionic liquid after the CMC in the presence of β -CD remain constant as that of the absence of β -CD. This also indicates that the inclusion complexes have no surface activity and that there is little interaction between the inclusion complexes and the micelles or the free surfactants.

2.3. Conductance

The shape of the curve (Fig. 5) is quite similar to those generally obtained for an aqueous mixtures of ionic liquids and monomers of β -CD [21] as the concentration in β -CD cavities rises, the conductance of the mixture slightly increases, passes through a maximum, then decreases gradually, reach a minima, up to the saturation point (existence of a break in the curve) and then the change is constant even further addition of β -CD into the solution systems. Such a behaviour denotes the formation of inclusion complexes between the ionic liquid molecules with the β -CD cavities.

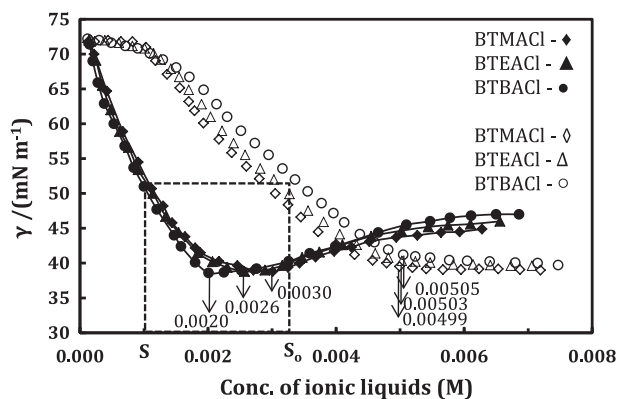
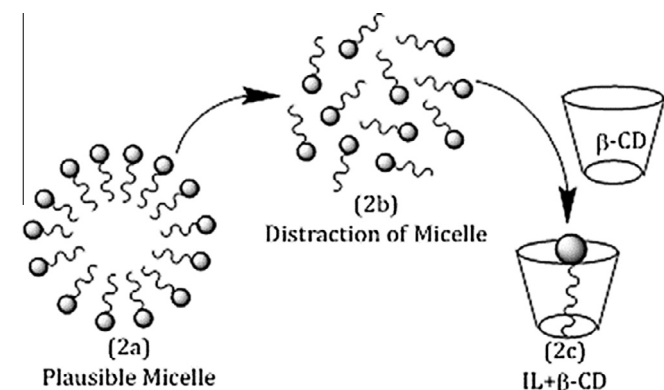


Fig. 5. Plot of surface tension (γ) with corresponding conc. of ionic liquids in absence (solid fill) and in presence (no fill) of β -CD.

The initial increase of conductance at very low conc. of β -CD is ascribed to the progressive destruction of the micelles (Scheme 2a) of ionic liquids by inclusion of the benzyl group of ionic liquid into the β -CD cavities (i.e., the β -CD-ionic liquid interactions are stronger than those of the ionic liquid-ionic liquid interactions [22]). The destruction of the micelles is accompanied by a release of surfactant monomers and a release of counter ions initially linked to the surface of the micelles, which increases the conductance values.

At the maximum of the conductance, micelles are supposed to have completely disappeared (Scheme 2b) and an excess of β -CD cavities reduces the quantity of free ionic liquids by formation of inclusion complexes (Scheme 2c), leading to a decrease of the con-



Scheme 2. Schematic illustration of plausible micelle (2a), distraction of micelle (2b) and plausible inclusion formation (2c).

ductance values. When most of the ionic liquid molecules are incorporated insight into the cyclodextrin cavities, a plateau of conductance is observed and its value is ascribed only to the charged inclusion complexes and to the counter ion Cl^- .

From output of Fig. 5 and Table 1, the ratio of the β -CD concentration to the ionic liquid concentration at the saturation point or break point is equal to the 1.01, 1.03, and 1.05 for $[(\text{C}_6\text{H}_5\text{CH}_2)\text{N}(\text{CH}_3)_3]\text{Cl}$, $[(\text{C}_6\text{H}_5\text{CH}_2)\text{N}(\text{C}_2\text{H}_5)_3]\text{Cl}$ and $[(\text{C}_6\text{H}_5\text{CH}_2)\text{N}(\text{C}_4\text{H}_9)_3]\text{Cl}$ respectively, has showed that β -CD-ionic liquid complexes are mainly formed with a 1:1 stoichiometry, i.e., only one molecule of ionic liquid encapsulated per β -CD cavity (Scheme 3).

In the surface tension (γ) study for the aforesaid three ionic liquids with β -CD shows single break point (Fig. 3) in each γ vs. conc. curve, which clearly indicates β -CD can form 1:1 inclusion complexes with the hydrophobic benzyl moiety. The hydrophilic ammonium moiety or positive charge on the nitrogen atom remains hydrated at the outside of the cyclodextrin cavity and stabilized with oxygen atom of the $-\text{OH}$ group present in the rim of cyclodextrin (only in case of benzyltrimethylammonium chloride) (Scheme 4).

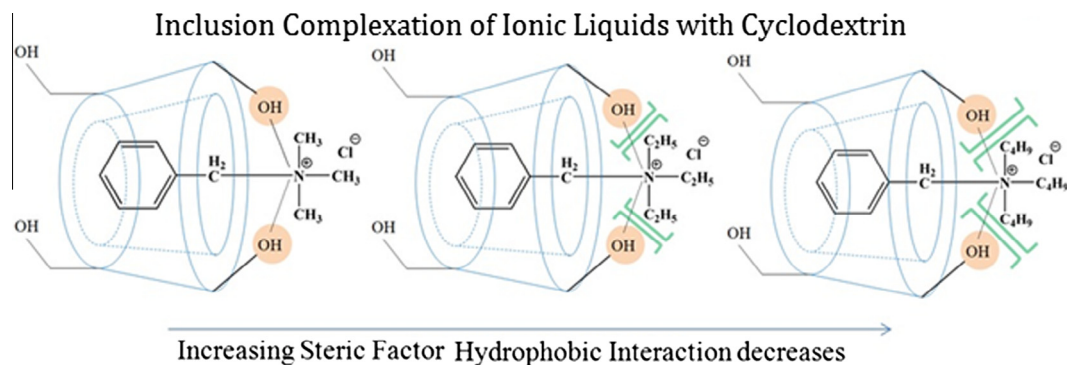
2.4. ^1H NMR

Inclusion of a guest molecule into the cavity of β -cyclodextrin has been studied by the upfield chemical shift of the protons of cyclodextrin molecule in ^1H NMR spectra. According to the ^1H NMR study in the molecular structure of β -cyclodextrin the H3 and H5 hydrogen's are situated inside the conical cavity, mainly, the H3 are placed near the wider rim whereas H5 are placed near the narrower rim, the other H1, H2 and H4 hydrogens are situated at the exterior of the cyclodextrin molecule (Fig. 6). Since the H3 is located near the wider rim of CD, through which the guest enters, the shift is higher for it than the H5 proton [23].

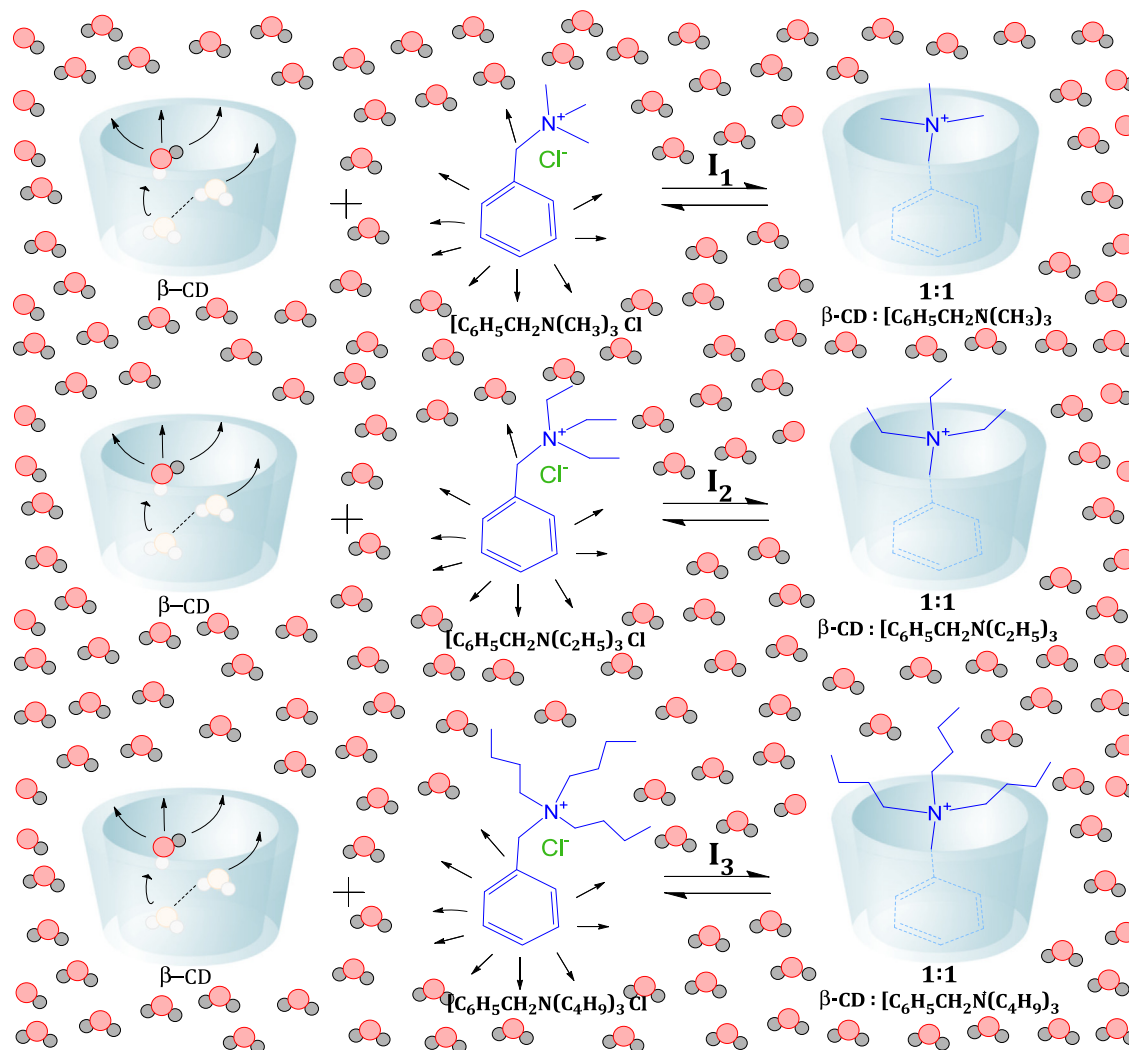
The other H1, H2 and H4 hydrogen's also show reasonable upfield chemical shift, but it is less compared to that of the interior protons [24–26]. Here, the inclusion phenomenon of chosen benzyltrialkylammonium chloride $[(\text{C}_6\text{H}_5\text{CH}_2)\text{N}(\text{C}_n\text{H}_{2n+1})_3]\text{Cl}$; where $n = 1, 2, 4$ with β -CD have been studied by ^1H NMR spectra by taking 1:1 M ratio in D_2O (Fig. 7–9). It has been found that there are considerable upfield shifts of interior H3 and H5 protons, as well as that of the interacting protons i.e., aromatic and methylene protons of the benzyl group of benzyltrialkylammonium cations [27]. This establishes that inclusion phenomenon has occurred between the chosen ionic liquid with cavity of the β -CD molecule [28,29].

2.5. Association constant and other thermodynamic properties

The association constants for 1:1 inclusion complexes of β -CD and ionic liquid was determined from the surface tension measure-



Scheme 3. Schematic representation of mechanism of formation of inclusion complexes of cationic ionic liquids with β -cyclodextrin.



Scheme 4. Schematic representation of inclusion complexes of cationic ionic liquids with β -cyclodextrin.

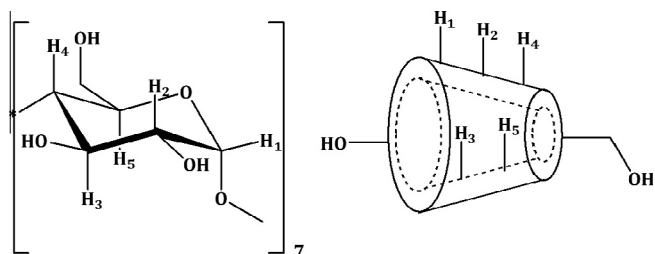


Fig. 6. (a) Stereo-chemical configuration, (b) truncated conical structure of β -cyclodextrin with interior and exterior protons.

ments by using the numerical method developed by Lu et al. [20]. We have used two surface tension curves in Fig. 5 (with and without β -CD) to determine the value of association constant, which allows justification of the assumption made. The plot of $S_0 - [S]$ vs $(\frac{S_0}{S} - 1)$ shown in Fig. 10 gives the slope $(-\frac{1}{K_a})$, and thus the association constants (K_a) for the inclusion complexes of β -CD-ionic liquids [16] and free energy change (ΔG) are determined, and listed in Table 2.

Free energy of micellization (ΔG_{mic}), degree of micellization (θ) and degree of counterion binding (ϕ) evaluated from the conduc-

tance; association constant (K_a), free energy of change (ΔG), Γ_{max} , and A_{min} obtained from surface tension of the solution (β -CD + ionic liquid) at 25 °C respectively (Table 2). The degree of micelle ionization (θ) was calculated by taking the ratio between the slopes of the linear portions above and below the break point in the conductivity profiles. The larger value of θ for the complex micelles is indication of an increased degree of ionic dissociation (Table 2) as a result of the interaction of ionic liquids with β -CD. The free energy of micellization (ΔG_{mic}) can be calculated using the equation of [30]

$$\Delta G_{mic} = RT(2 - \theta) \ln CMC$$

The negative ΔG_{mic} values (Table 2) indicates that the presence of β -CD makes the process feasible and can be explained on the basis that more β -CD will be able to encapsulate more monomers and the amount of ionic liquids needed to form the micelle will obviously disappeared. The degree of counter ions binding (ϕ) onto the self-aggregated assemblies was obtained from the slopes of the Δ vs $[(C_6H_5CH_2)N(C_nH_{2n+1})_3]Cl$ isotherm in the pre-micellar region (S_1) and the post-micellar region (S_2) using the following relationship:

$$\phi = 1 - \frac{S_2}{S_1}$$

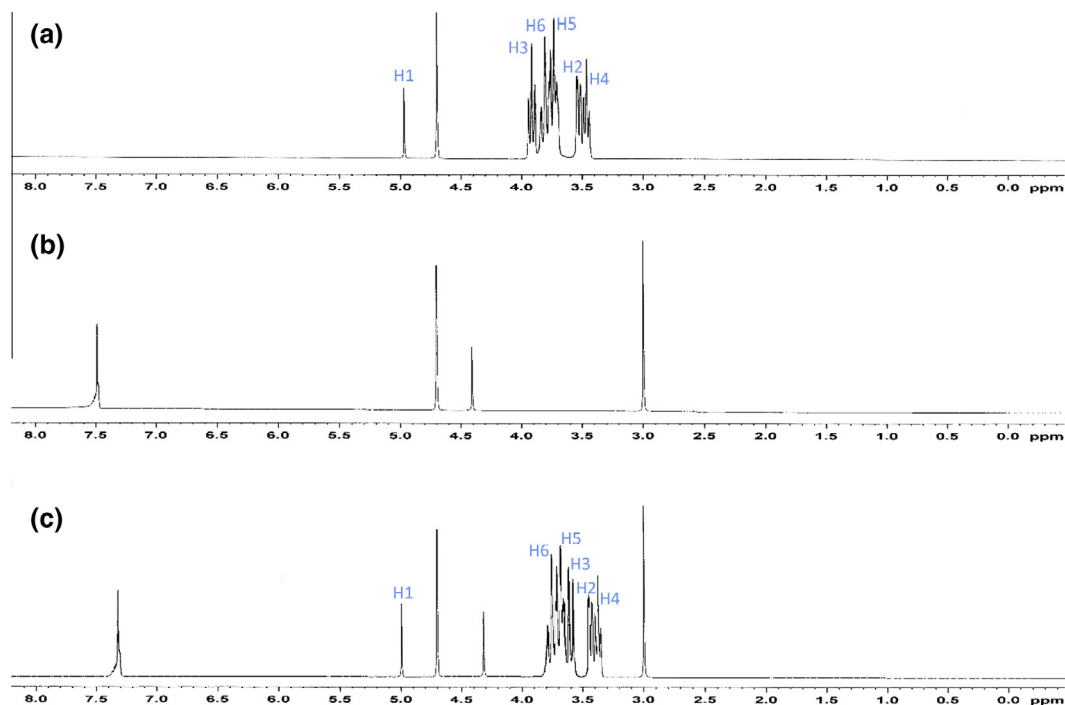


Fig. 7. ^1H NMR spectra of (a) β -CD, (b) $[(\text{C}_6\text{H}_5\text{CH}_2)\text{N}(\text{CH}_3)_3]\text{Cl}$, and (c) inclusion complex.

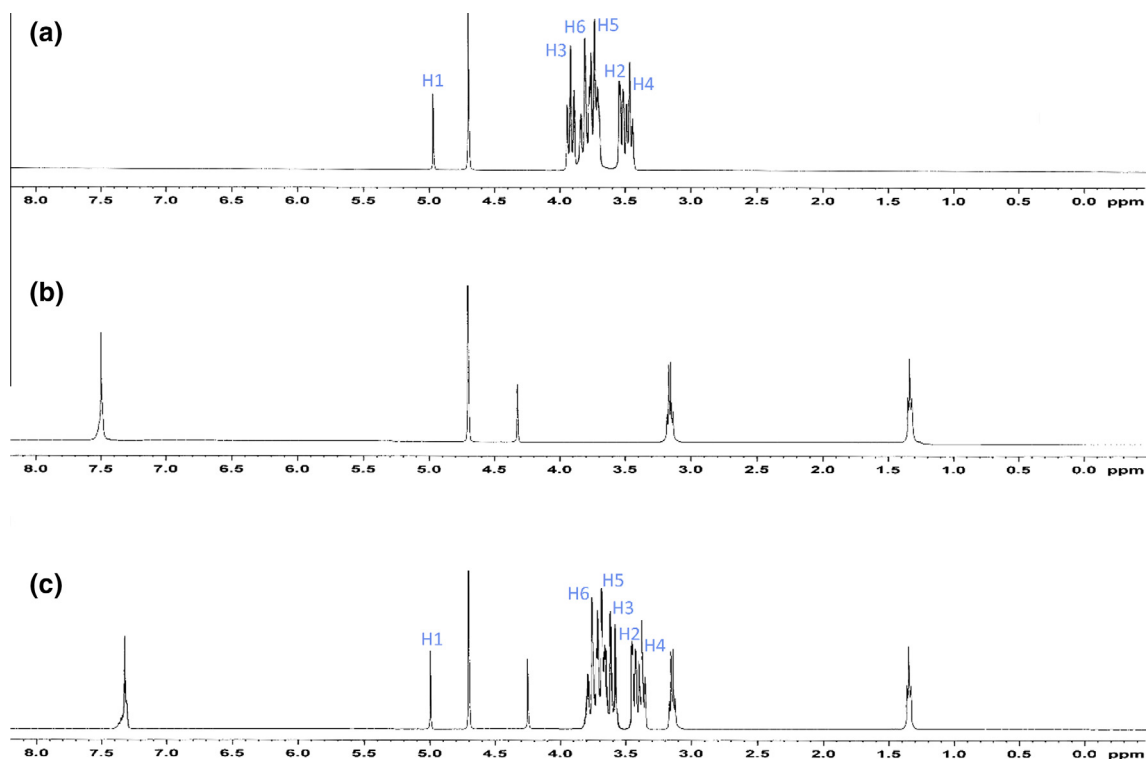


Fig. 8. ^1H NMR spectra of (a) β -CD, (b) $[(\text{C}_6\text{H}_5\text{CH}_2)\text{N}(\text{C}_2\text{H}_5)_3]\text{Cl}$, and (c) inclusion complex.

The ϕ factor includes the fraction of free energy required to condense the counter ions on the aggregate to reduce the repulsion between the adjacent monomer head groups [31].

From the perusal of Table 2 it is clear that the association constants (K_a) for benzyltrimethylammonium chloride is higher com-

pared to the other two ionic liquids; is obviously due to the fact of steric factor of the side chain group of cationic part of the chosen ionic liquids. The higher the side chain group increases the steric hindrance effect, i.e., butyl group in $[(\text{C}_6\text{H}_5\text{CH}_2)\text{N}(\text{C}_4\text{H}_9)_3]\text{Cl}$ is more steric effect than ethyl group in $[(\text{C}_6\text{H}_5\text{CH}_2)\text{N}(\text{C}_2\text{H}_5)_3]\text{Cl}$, which is in

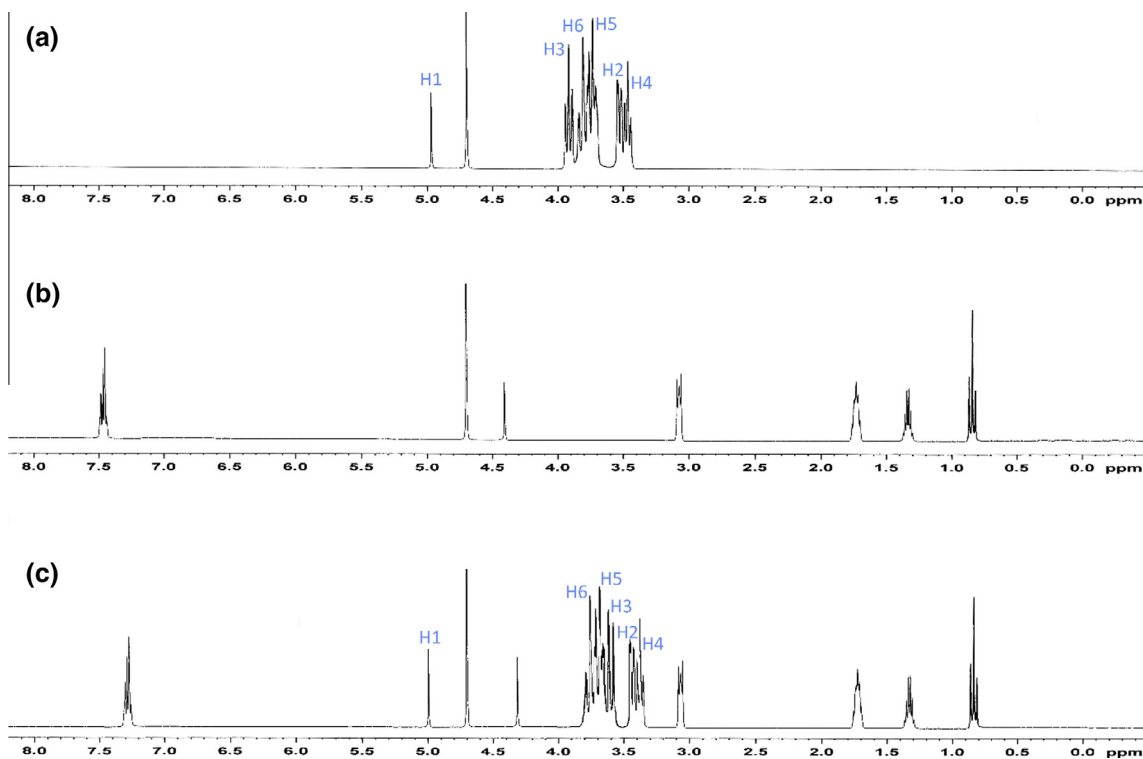


Fig. 9. ^1H NMR spectra of (a) β -CD, (b) $[(\text{C}_6\text{H}_5\text{CH}_2)\text{N}(\text{C}_4\text{H}_9)_3]\text{Cl}$, and (c) inclusion complex.

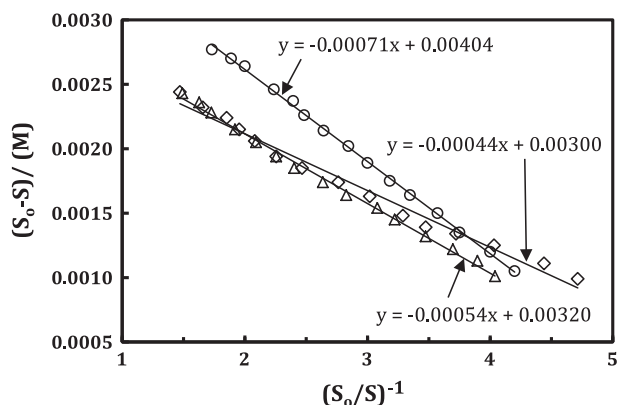


Fig. 10. Relationship between $(S_0 - S)/(M)$ and $(S_0/S) - 1$ for solution of ionic liquids along and mixed with β -CD.

turn more than methyl group in $[(\text{C}_6\text{H}_5\text{CH}_2)\text{N}(\text{CH}_3)_3]\text{Cl}$ (Scheme 4); which clearly state the benzyl group of benzyltrimethylammonium cationic part of the ionic liquid is more associated/encapsulated with β -CD (Scheme 4). On other hand more negative ΔG for $[(\text{C}_6\text{H}_5\text{CH}_2)\text{N}(\text{CH}_3)_3]\text{Cl}$ than the rest two is also undoubtedly speak out that benzyltrimethylammonium charge or cationic part of the ionic liquid is more feasibly associated.

Table 2

Free energy of micellization (ΔG_{mic}) and free energy of change (ΔG) obtained from degree of micelle ionization (α) and association constant (K_a) of the solution (β -CD + ionic liquid) at 25 °C evaluated from the conductance and surface tension measurement respectively.

Salt	α	ΔG_{mic} (kJ/mol)	K_a	ΔG (kJ/mol)	β	$10^6 \Gamma_{\text{max}}$ (mol m $^{-2}$)	A_{min} (\AA^2)
$[(\text{C}_6\text{H}_5\text{CH}_2)\text{N}(\text{CH}_3)_3]\text{Cl}$	0.57	-16.29	2252.25 ± 19	-19.14	0.43	2.37	70.19
$[(\text{C}_6\text{H}_5\text{CH}_2)\text{N}(\text{C}_2\text{H}_5)_3]\text{Cl}$	0.54	-16.56	1524.39 ± 22	-18.17	0.46	2.28	72.67
$[(\text{C}_6\text{H}_5\text{CH}_2)\text{N}(\text{C}_4\text{H}_9)_3]\text{Cl}$	0.51	-16.83	1136.36 ± 13	-17.44	0.49	2.13	77.88

The maximum surface excess concentration (Γ_{max}), and the minimum area of exclusion per molecule at the air-solution interface (A_{min}) were estimated for the three surface active ionic liquids to the slope of the tensiometric profile near the CMC, is quantified by applying the Gibbs adsorption isotherm [32]. The values of Γ_{max} and A_{min} are also listed in Table 2. The increase in the A_{min} values with temperature may be ascribed to the greater kinetic motion of the monomers populating the air-solution interface. It was noticed from Table 2 that the values of Γ_{max} decrease and those of A_{min} increase, with the increase of alkyl chain length; which means the ionic liquid molecules with the short alkyl chain (i.e., trimethyl group) can make packing more closely or arrange more tightly than longer one.

3. Conclusion

The surface tension, conductance and NMR study gives the clear indication of 1:1 host-guest inclusion complex formation of a series of surface active ionic liquids, benzyltrialkylammonium chloride $[(\text{C}_6\text{H}_5\text{CH}_2)\text{N}(\text{C}_n\text{H}_{2n+1})_3]\text{Cl}$; where $n = 1, 2, 4$] with aq. β -cyclodextrin. The study also expose that benzyl, the hydrophobic group of ionic liquids encapsulated insight into the cavity of β -cyclodextrin and form the inclusion complex. This study also demonstrated that hydrophobic interactions and hydrogen bonding contribute to the inclusion of ionic liquids in CDs. It was found

that addition of β -CD causes the shifting of micellization of the ionic liquids towards the higher concentration. This indicates the inclusion complex formation between the ionic liquids and β -CD.

4. Experimental section

4.1. Reagents

The cationic surfactants benzyltrimethylammonium chloride (97%), benzyltriethylammonium chloride (99%), benzyltributylammonium chloride (98%) and β -cyclodextrin (97%) were bought from Sigma–Aldrich, Germany and used as purchased.

4.2. Instrumentations

Prior to the start of the experimental work solubility of the chosen cyclodextrins in triply distilled and degassed water (with a specific conductance of $1 \times 10^{-6} \text{ S cm}^{-1}$) and title compounds viz., cationic surfactant in aqueous β -cyclodextrin have been precisely checked and it was observed that the selected cationic surfactant freely soluble in all proportion of aq. β -cyclodextrins. All the stock solutions of the cationic surfactant were prepared by mass (weighed by Mettler Toledo AG-285 with uncertainty 0.0003 g), and then the working solutions were obtained by mass dilution at 298.15 K.

The surface tension experiments were done by platinum ring detachment method using a Tensiometer (K9, KRÜSS; Germany) at 298.15 K. The accuracy of the measurement was within $\pm 0.1 \text{ mN m}^{-1}$. Temperature of the system has been maintained by circulating auto-thermostated water through a double-wall glass vessel containing the solution.

The conductance measurements were carried out in a Systronics-308 conductivity bridge of accuracy $\pm 0.01\%$, using a dip-type immersion conductivity cell, CD-10 having a cell constant of approximately $(0.1 \pm 0.001) \text{ cm}^{-1}$ [33]. The measurements were made in an auto-thermostated water bath maintaining the temperature at 298.15 K and using the HPLC grade water with specific conductance of $6.0 \mu\text{S m}^{-1}$. The cell was calibrated using a 0.01 M aqueous KCl solution. The uncertainty in temperature was 0.01 K.

NMR spectra were recorded in D_2O unless otherwise stated. ^1H NMR spectra were recorded at 400 MHz using Bruker ADVANCE 400 MHz instrument at 298.15 K. Signals are quoted as δ values in ppm using residual protonated solvent signals as internal standard (D_2O : δ 4.79 ppm). Data are reported as chemical shift.

Conflict of interest

No potential conflict of interest was reported by the authors.

Acknowledgements

The authors are grateful to the Special Assistance Scheme, Department of Chemistry, NBU under the University Grants Commission, New Delhi (No. 540/27/DRS/2007, SAP-1) for financial sustenance and instrumental conveniences in order to carry on this research work. Prof. M.N. Roy is also highly obliged to University Grants Commission, New Delhi, Government of India for being awarded one time Grant under Basic Scientific Research via the Grant-in-Aid No. F.4-10/2010 (BSR) concerning his dynamic service for augmenting of research facilities to expedite the advance research work.

References

- [1] H. Jiao, S.H. Goh, S. Valiyaveetil, *Macromolecules* 35 (2002) 3997–4002.
- [2] J. Szejtli, *Chem. Rev.* 98 (1998) 1743–1753.
- [3] M.L. Bender, M. Komiyama, *Cyclodextrin Chemistry*, Springer-Verlag, Berlin, 1978.
- [4] J. Szejtli, *The Cyclodextrins and Their Inclusion Complexes*, Akademiai Kiado, Budapest, 1982.
- [5] W. Saenger, *Inclusion Compounds*, Academic Press, London, 1984.
- [6] R.J. Clarke, J.H. Coates, S.F. Lincoln, *Adv. Carbohydr. Chem. Bwchem.* 46 (1988) 205–210.
- [7] X. Zhao, Y. Shang, J. Hu, H. Liu, Y. Hu, *Biophys. Chem* 138 (2008) 144–149.
- [8] Y. Lin, Y. Zhang, Y. Qiao, J. Huang, B. Xu, *J. Coll. Interf. Sci.* 362 (2011) 430–438.
- [9] S. Chavda, P. Bahadur, *J. Mol. Liq.* 161 (2011) 72–77.
- [10] K.T. Naidu, N.P. Prabhu, *J. Phys. Chem. B* 115 (2011) 14760–14767.
- [11] S.K. Verma, K.K. Ghosh, *J. Surfact, Detergents* 14 (2011) 347–352.
- [12] M. Ikonen, L. Murtomaki, K. Kontturi, *Coll. Surf., B* 66 (2008) 77–83.
- [13] A.E. Kaifer, *Acc. Chem. Res.* 32 (1999) 62–71.
- [14] N.S. Krishnaveni, K. Surendra, M.A. Reddy, Y.V.D. Nageswar, K.R. Rao, *J. Org. Chem.* 68 (2003) 2018–2019.
- [15] M.J. Rosen, *Surfactant and Interfacial Phenomena*, John & Wiley, New York, 1978.
- [16] C. Galant, V. Wintgens, C. Amiel, *Macromolecules* 38 (2005) 5243–5253.
- [17] M.N. Roy, D. Ekka, S. Saha, M.C. Roy, *RSC Adv.* 4 (2014) 42383–42390.
- [18] M.N. Roy, M.C. Roy, K. Roy, *RSC Adv.* 5 (2015) 56717–56723.
- [19] M.N. Roy, A. Roy, S. Saha, *Carbohydr. Polym.* (2016), <http://dx.doi.org/10.1016/j.carbpol.2016.05.100>.
- [20] R. Lu, J. Hao, H. Wang, L. Tong, *J. Coll. Interf. Sci.* 192 (1997) 37–42.
- [21] T. Liska, J. Richardson, R. Palepu, in: A.R. Hedges (Ed.), *Minutes of the Sixth International Symposium on Cyclodextrins*, Editions de Sante, Paris, 1992, p. 253.
- [22] R. Palepu, V.C. Reinsborough, *Can. J. Chem.* 66 (1988) 325–328.
- [23] K.P. Sambasevam, S. Mohamad, N.M.A. Sarih, *Int. J. Mol. Sci.* 14 (2013) 3671–3682.
- [24] S. Saha, T. Ray, S. Basak, M.N. Roy, *New J. Chem.* 40 (2016) 651–661.
- [25] T. Wang, M.D. Wang, C.D. Ding, J. Fu, *Chem. Commun.* 50 (2014) 12469–12472.
- [26] N. Rajendiran, G. Venkatesh, *Supramol. Chem.* 26 (2014) 783–795.
- [27] M.N. Roy, S. Saha, M. Kundu, B.C. Saha, S. Barman, *Chem. Phys. Lett.* 655–656 (2016) 43–50.
- [28] M. Chen, G. Diao, E. Zhang, *Chemosphere* 63 (2006) 522–529.
- [29] J. Wang, Y. Cao, B. Sun, C. Wang, *Food Chem.* 127 (2011) 1680–1685.
- [30] B.W. Berry, G.F.G. Russell, *J. Coll. Interf. Sci.* 40 (1972) 174–194.
- [31] G. Gunnarsson, J. Jönsson, H. Wennerström, *J. Phys. Chem.* 84 (1980) 3114–3121.
- [32] M.J. Jaycock, G.D. Parfitt, *Chemistry of Interfaces*, John Wiley and Sons, New York, USA, 1981.
- [33] D. Ekka, M.N. Roy, *J. Phys. Chem. B* 116 (2012) 11687–11694.

Mahendra Nath Roy*, Siti Barman and Subhadeep Saha
**Probing Inclusion Complex Formation of
Amantadine Hydrochloride with 18-Crown-6
in Methanol by Physicochemical Approach**

DOI 10.1515/zpch-2016-0804

Received May 24, 2016; accepted October 22, 2016

Abstract: The complex formation of amantadine hydrochloride with 18-crown-6 was studied in methanol solution by surface tension, conductivity and IR study. The limiting apparent molar volume data have been used to characterize the interaction between drug molecule (amantadine hydrochloride) and 18-crown-6 in the experimental ternary solution systems. A conductance study concerning the interaction between cationic organic ammonium ions amantadine with 18-crown-6 in methanol solution has been carried out at different temperatures. The formation constant ($\log K_f$) of the resulting 1:1 complex at various temperatures was determined from the conductivity study. The enthalpy (ΔH°) entropy (ΔS°) and free energy change (ΔG°) of the complexation reaction was determined from the temperature dependence of the formation constant.

Keywords: 18-crown-6; amantadine; complexation; formation constant; thermodynamic parameter.

1 Introduction

Host–guest interaction has been termed ‘a complementary stereo-electronic arrangement of binding sites in host and guest’ [1]. In the chemical sense the host is usually an organic molecule containing specific receptor sites while the guest is normally a metal or organic cation. Host–guest interactions have recognized importance in many biological processes, including enzyme catalysis and

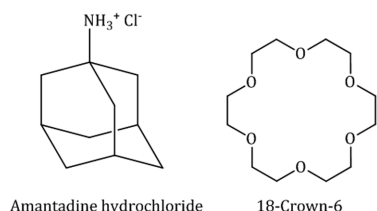
*Corresponding author: **Mahendra Nath Roy**, Department of Chemistry, University of North Bengal, Dargeeling-734013, India, Tel.: +91 353 2776381, Fax: +91 353 2699001, E-mail: mahendraroy2002@yahoo.co.in

Siti Barman and Subhadeep Saha: Department of Chemistry, University of North Bengal, Dargeeling-734013, India

inhibition, antibody-antigen interactions, and membrane transport. A particularly fruitful field of organic synthesis during the past several years has been the design and preparation of macrocyclic molecules of the cyclic polyether type with the intent to mimic certain biological host-guest interactions [1-4]. Several workers have reported the attachment of organic ammonium [5] groups to hosts which are analogues of 18-crown-6 with the subsequent enhancement of a reaction between host and guest components away from the site of primary binding.

The crown ethers were of a great interest since their discovery had been reported by Pedersen in 1967 [6]. The ability of these macrocycles to form non-covalent, H-bonding complexes with ammonium cations has been actively investigated with an eye toward biological applications [7, 8], molecular recognition [9, 10], self-assembly [11, 12], crystal engineering [13, 14], and catalysis [15]. The stoichiometry and stability of these host-guest complexes depend both on the size of the crown ether and on the nature of the ammonium cation (NH_4^+ , RNH_3^+ etc.) [16, 17]. The numerous studies of 18-crown-6 (18C6) and its derivatives, which have the highest affinity for ammonium cations, invariably showed a 1:1 stoichiometry with both NH_4^+ and RNH_3^+ cations in solution [18] and in the solid state [19, 20].

Crown ether-ammonium complexes are of fundamental interest as prototypical systems involving multiple hydrogen bonds. Study of these simple multiply-bound complexes is a promising means of gaining insight into much more complex macromolecular systems, such as those involved in protein folding or in the pairing of nucleobases in polymeric nucleus acids [21]. Host parameters of importance in binding both metals and organic ammonium cations include cavity size, donor atom number and type, ring number and type, ring substituents, and ring conformation. Guest parameters for organic ammonium cations differ from those of metal cations because of the different binding mechanisms involved for the two types of guest. Metal cations are sequestered within the macrocyclic ring, whereas ammonium cations hydrogen bond to the ring donor



Scheme 1: Molecular structure of amantadine hydrochloride and 18C6.

atoms. Thus, guest parameters significant to organic ammonium cation binding include number of hydrogen atoms available for hydrogen bonding.

Amantadine (Scheme 1) is tricyclic aminohydrocarbons with antiviral activity directed uniquely against influenza A virus. The compounds have a potential to inhibit the early phases of viral replication by preventing uncoating of the viral genome and virus-mediated membrane fusion. The drug is used in the prevention and treatment of influenza A infections [22, 23].

On the other hand, macrocyclic [24] and macrobicyclic polyethers [25] have been extensively used as interesting model compounds for the study of molecular effect on membrane permeability [26, 27], due to their many similarities to cyclic antibiotics and biological transport agents. Considerable attention has been focused on the interactions between different protonated amines and macrocyclic ligands in order to study the molecular effect on membrane permeability [28–30].

One interesting property of crown ethers is that the electron pairs present in the ring heteroatoms provide the molecule with the ability to complex a wide range of cations in the empty cavity present in the center of the ring [31]. A space filling model of 18-crown-6 is shown in Figure 1 illustrating the central cavity in

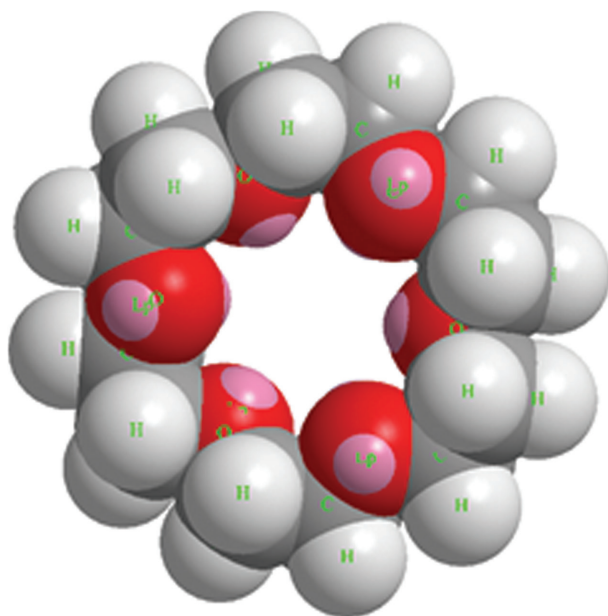


Fig. 1: A space filling model of 18-crown-6 showing the open space at the center of the crown and electron pairs present on the exposed oxygen atoms (in pink).

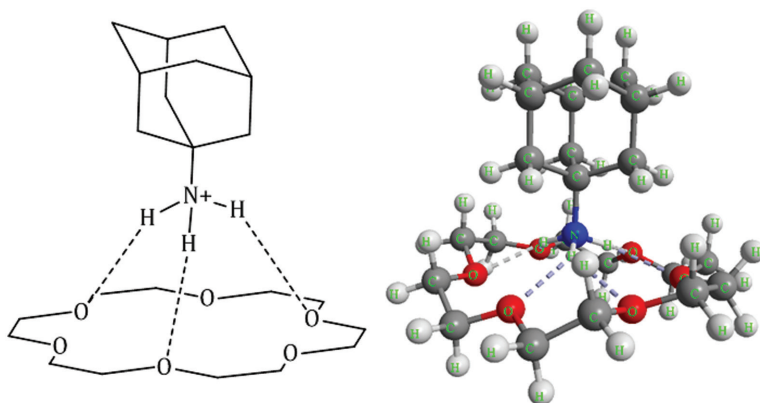
which K^+ ions bind by coordinating to the six surrounding ether oxygen atoms. In the case of 18-crown-6, the diameter of the interior hole is about 4.0 \AA [31]. That structural feature allows for crown ethers to form a number of complexes with cationic species [32].

Conductance measurements as a sensitive and powerful technique to study the complexation of macrocyclic ligands with different cations in a variety of nonaqueous and mixed solvents [33, 34]. The thermodynamics of complexation of amantadine ion with different crown ethers and cryptands in acetonitrile solvents have been reported in the literature [35]. In this paper, a conductance study, a surface tension study and a density study of the complex formed between amantadine hydrochloride (ADH) and 18-crown-6 (18C6) (Scheme 2) in methanol solution was reported and the influence of several structural and medium parameters on the complexation reaction were discussed. The structure of the crown ether is shown in Scheme 1.

2 Experimental

2.1 Materials

The amantadine hydrochloride (ADH) and 18-crown-6 (18C6) of puriss grade were bought from Sigma-Aldrich, Germany and used as purchased. The mass fraction purity of ADH and 18C6 were ≥ 0.99 and 0.98 , respectively.



Scheme 2: Schematic presentation of complexation between amantadine ion and 18C6 and corresponding energy minimized structure of the complex.

2.2 Apparatus and procedure

Prior to the start of the experimental work solubility of the chosen crown ether in methanol and ADH in methanolic solution of 18C6 have been precisely checked and observed that the drug molecule ADH freely soluble in all proportion of methanolic 18C6 solution. All the stock solutions of the drug molecule were prepared by mass (weighed by Mettler Toledo AG-285 with uncertainty 0.0003 g), and then the working solutions were obtained by mass dilution at 298.15 K. The conversions of molarity into molality have been done [36] using density values. Adequate precautions were made to reduce evaporation losses during mixing.

The surface tension experiments were done by platinum ring detachment method using a Tensiometer (K9, KRÜSS; Germany) at the experimental temperature. The accuracy of the measurement was within $\pm 0.1 \text{ mN}\cdot\text{m}^{-1}$. Temperature of the system was maintained at 298.15 K by using Omniset thermostat having uncertainty in temperature $\pm 0.01 \text{ K}$.

The conductance measurements were carried out in a Systronics-308 conductivity bridge of accuracy $\pm 0.01 \%$, using a dip-type immersion conductivity cell, CD-10 having a cell constant of approximately $(0.1 \pm 0.001) \text{ cm}^{-1}$ [37]. The study was carried out using Brookfield TC-550 water bath with thermostat maintaining at the experimental temperatures having uncertainty of $\pm 0.01 \text{ K}$.

The densities (ρ) of the solvents were measured by means of vibrating *U*-tube Anton Paar digital density meter (DMA 4500 M) with a precision of $\pm 0.00005 \text{ g cm}^{-3}$ maintained at $\pm 0.01 \text{ K}$ of the desired temperature. It was calibrated by passing triply distilled, degassed water and dry air.

Infrared spectra were recorded in 8300 FT-IR spectrometer (Shimadzu, Japan). The details of the instrument have formerly been described [38].

3 Result and discussion

3.1 Conductance

The molar conductance (Λ) of ADH ($5 \times 10^{-4} \text{ M}$) in methanol solution was monitored as a function of crown ether to amantadine ion mole ratio at various temperatures (Table S1). The resulting molar conductance vs. crown/cation mole ratio plots at 298.15, 303.15, and 308.15 K are shown in Figure 2. In every case, there is a gradual decrease in the molar conductance with an increase in the crown ether concentration. This behavior indicates that the complexed amantadine ion is less mobile than the corresponding amantadine ion in methanol. As can be seen from

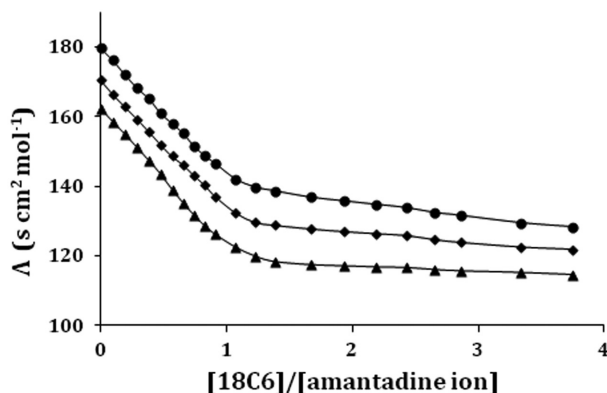


Fig. 2: Molar conductance vs. [18C6]/[amantadine ion] at 298.15 K (▲), 303.15 K (◆), 308.15 K (●).

Figure 2, the complexation of amantadine ion with 18C6, addition of the crown solution to the amantadine solution causes a continuous decrease in the molar conductance, which begins to level off at a mole ratio greater than one, indicating the formation of a stable 1 : 1 complex [39, 40]. By comparison of the molar conductance-mole ratio plot for amantadine ion – 18C6 systems obtained at different temperatures (Figure 2), it can be observed, that the corresponding molar conductance increased rapidly with temperature, due to the decreased viscosity of the solvent and, consequently, the enhanced mobility of the charged species present.

3.2 Association constant and thermodynamic parameter

The 1 : 1 complexation of amantadine ion with 18C6 crown ether can be expressed by the following equilibrium



The corresponding equilibrium constant, K_f is given by

$$K_f = \frac{[MC^+]}{[M^+][C]} \times \frac{f(MC^+)}{f(M^+)f(C)} \quad (2)$$

where $[MC^+]$, $[M^+]$, $[C]$ and f represent the equilibrium molar concentrations of the complex, free cation, free ligand and the activity coefficients of the species

indicated, respectively. Under the dilute conditions used, the activity coefficient of uncharged macrocycle, $f(C)$, can be reasonably assumed as unity [41]. The use of the Debye–Hückel limiting law [42], leads to the conclusion that $f(M^+) \sim f(MC^+)$, so the activity coefficients in Equation (2) cancel. The complex formation constant in terms of the molar conductances, Λ , can be expressed as [39, 41].

$$K_f = \frac{[MC^+]}{[M^+][C]} = \frac{(\Lambda_M - \Lambda_{\text{obs}})}{(\Lambda_{\text{obs}} - \Lambda_{MC})[C]} \quad (3)$$

where

$$[C] = C_c - \frac{C_M(\Lambda_M - \Lambda_{\text{obs}})}{(\Lambda_M - \Lambda_{MC})} \quad (4)$$

here, Λ_M is the molar conductance of the metal ion before addition of ligand, Λ_{MC} the molar conductance of the complexed ion, Λ_{obs} the molar conductance of the solution during titration, C_c the analytical concentration of the macrocycle added and C_M the analytical concentration of the salt. The complex formation constant, K_f , and the molar conductance of the complex, Λ_{MC} , were evaluated by using Equations (3) and (4).

In order to have a better understanding of the thermodynamics of the complexation reactions of amantadine ion with the 18C6 crown ether it is useful to consider the enthalpic and entropic contributions to these reactions. The ΔH^0 and ΔS^0 values for the complexation reactions were evaluated from the corresponding $\log K_f$ and temperature data by applying a linear least-squares analysis according to the equation:

$$2.303 \log K_f = -\frac{\Delta H^0}{RT} + \frac{\Delta S^0}{R} \quad (5)$$

Plots of $\log K_f$ vs. $\frac{1}{T}$ for amantadine – 18C6 complex is linear (Figure 3).

The enthalpy (ΔH^0) and entropy (ΔS^0) of complexation were determined in the usual manner from the slopes and intercepts of the plots and the results are also included in Table 1. Both of these two parameters have negative values. The negative values of enthalpy confirm that when ADH interact with the crown ether molecules the overall energy of the system is decreased, i.e. there is some stabilization interaction in the system, whereas negative values of entropy factor indicate that there is an ordered arrangement, i.e. complex formation takes place between the ADH and the 18C6 molecule. The negative value of entropy is unfavourable for the spontaneity of the complex formation, but this effect is overcome by higher negative value of ΔH^0 . The values of ΔG^0 (Table 1) for the complex

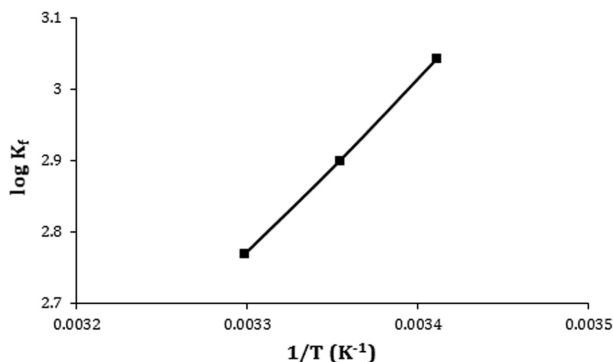


Fig. 3: The linear relationship of $\log K_f$ vs. $1/T$ for the interaction between amantadine hydrochloride with 18C6.

Tab. 1: Values of formation constant, enthalpy, entropy and free energy change of amantadine-18C6 complex in methanol solution.

Cation	Crown	Log K_f			ΔH^0 (kJ mol ⁻¹)	ΔS^0 (J mol ⁻¹ K ⁻¹)	ΔG^0 (kJ mol ⁻¹)
		298.15 K	303.15 K	308.15 K			
Amantadine	18C6	3.04	2.90	2.77	-46.56	-100.58	-16.57

formation was found negative suggesting that the complex formation process proceeds spontaneously.

The data shown in table indicates that formation constant $\log K_f$ for amantadine ion with 18C6 is highest at 298.15 K and decreases with increase in temperature i.e. amantadine ion form stable complex with 18C6 at 298.15 K.

3.3 Surface tension

Surface tension (γ) measurement provides significant indication about formation of inclusion complex as well as stoichiometry of the host-guest assembly [43–45]. The values of surface tension at different concentration of 18C6 are listed in Table S2. In the present work ADH have a hydrophobic group and a terminal $-\text{NH}_3^+$ group (Scheme 1) due to which ADH shows surfactant like activities, thus γ of the ADH solution shows decreasing trend. In this work when 18C6 was added in ADH solution the proton of the $-\text{NH}_3^+$ group binds to the alternate three oxygen atom of the crown ether and the formation of three H-bonds occurs. As a result charged portion of the amantadine ion form complex with 18C6 and due to the

formation of complex effect of hydrophobic portion increases i.e. surface tension of the solution again decreases slowly. At a certain conc. of ADH and crown ether, a single break was observed in the surface tension curve (Figure 4).

The break point in surface tension curve not only indicates the formation of complex between amantadine ion and 18C6 but also about its stoichiometry, i.e. appearance of single break point in the plot indicates 1:1 stoichiometry of the complex. The value of γ at the break point and corresponding concentration of crown ether have been listed in Table 2. Hence the plausibility of formation of complex can be predicted from surface tension study.

3.4 IR Study

FTIR spectra of the complex, 18C6 and that of pure ADH were obtained in the region $400\text{--}4000\text{ cm}^{-1}$. If the FTIR spectrum of 18C6 was compared with that

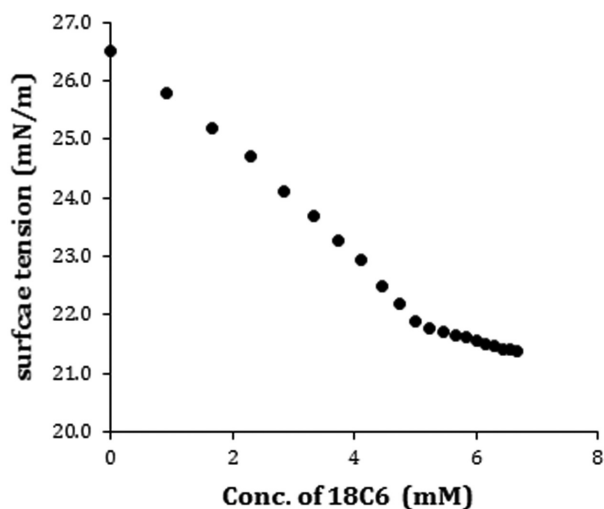


Fig. 4: Variation of surface tension of amantadine with increasing concentration of 18C6 at 298.15 K.

Tab. 2: Values of surface tension (γ) at the break point with corresponding to concentration of 18C6 in methanolic solution at 298.15 K.

Conc. (mM)	γ (mN·m ⁻¹)
5.07	21.99

of complex, it was noticed that the peaks observed in pure 18C6 (Figure 5) at 1120 cm^{-1} correspond to COC group shift to 1106 cm^{-1} in the complex (Figure 5). The frequency of the C–O–C asymmetric stretching vibrations of a polyether, ν_{as} (COC), decreases upon interaction of the O atoms with the protons of the ammonium group via hydrogen H bonds. The N–H stretching band of the ammonium group expected for amantadine ion in the region $2961\text{ to }3087\text{ cm}^{-1}$ by Pierre D. Harvey [46] was observed in pure ADH at 3047 cm^{-1} . This peak shifts to 3027 cm^{-1} revealed that the N–H bonds were involved in the complex formation. The characteristic peak of ADH at 2927 cm^{-1} was shifted to 2909 cm^{-1} in the complex. The peak at 1086 cm^{-1} corresponding to C–N bend of the C–N bond of ADH shifts to higher frequencies [47]. Thus it may be concluded that amantadine was strongly bound to 18C6 through H-bonds of the ammonium group.

3.5 Apparent molar volume

The characteristic behavior of interaction present in complex of solute has also been obtained from apparent molar volume. The apparent molar volume is the measure of the sum of the geometric volume of the central solute molecule and changes in the solvent volume due to its interaction with the solute around the co-sphere. The physical properties of binary mixtures in different mass fractions ($w_1 = 0.001, 0.004, 0.007$) of methanolic 18C6 solutions at 298.15, 303.15, 308.15 K

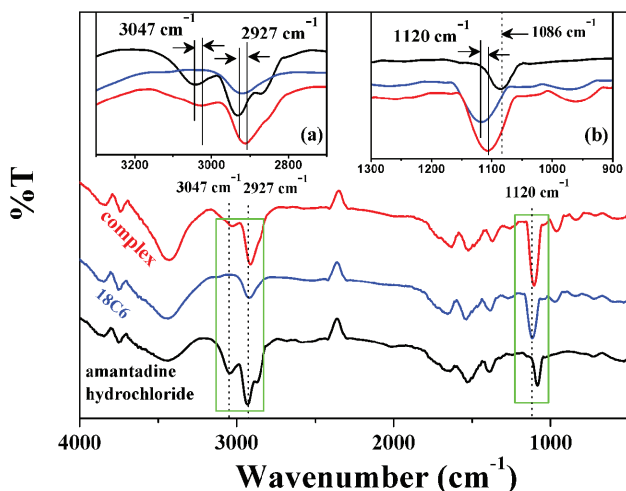


Fig. 5: FTIR spectra of pure amantadine hydrochloride (black), 18-crown-6 (blue) and complex (red).

are reported in Table S3. Here ϕ_v has been determined from the measured density of the solutions at 298.15 K, 303.15 K, 308.15 K (Table S4) and by using the suitable equation. ϕ_v varies linearly with the square root of molal concentration and is fitted to the Masson equation, from where the limiting apparent molar volume (ϕ_v^0) has been determined (Table 3) [48]. The limiting molar volume (ϕ_v^0) signify the solute–solvent interactions in the amantadine + 18C6 ternary solution systems. The magnitude of which is found to be positive for all the systems under study, indicating strong solute–solvent interactions [44, 49].

The plot of ϕ_v^0 values against different temperature at different mass fractions are represented in Figure 6, which suggests that ϕ_v^0 values increases with increase of mass fraction at same temperature and decreases with increasing the temperature. The values of ϕ_v^0 increases with the increase of mass fractions of 18C6 in methanol indicating that the ion-hydrophilic group interactions are stronger than the ion-hydrophobic group interactions. In the present ternary system interactions are taking place between the positive charge of ammonium groups and the alternative oxygen atom of the crown ether. The decreasing trend with increasing temperature suggests that the interactions between the drug molecule and crown molecules are decreased with increasing temperature. The facts support the data and the results observed from surface tension and conductivity study discussed earlier also support the facts.

The parameter S_v^* is the volumetric virial coefficient, and it characterizes the pair wise interaction of solute species in solution [50, 51]. S_v^* is found to be negative under investigations, which suggest that the pair wise interaction is

Tab. 3: Limiting apparent molar volume (ϕ_v^0) and experimental slope (S_v^*) in different mass fractions of methanolic solution of 18-crown-6.

Temp. (K)	$\phi_v^0 \times 10^6 \text{ (m}^3 \cdot \text{mol}^{-1}\text{)}$	$S_v^* \times 10^6 \text{ (m}^3 \cdot \text{mol}^{-3/2} \cdot \text{kg}^{1/2}\text{)}$
$w_1 = 0.001$		
298.15	156.91	– 174.98
303.15	152.32	– 162.19
308.15	148.11	– 139.57
$w_1 = 0.004$		
298.15	174.48	– 280.76
303.15	164.06	– 254.20
308.15	153.75	226.20
$w_1 = 0.007$		
298.15	181.95	– 311.69
303.15	175.74	– 294.20
308.15	163.04	– 284.41

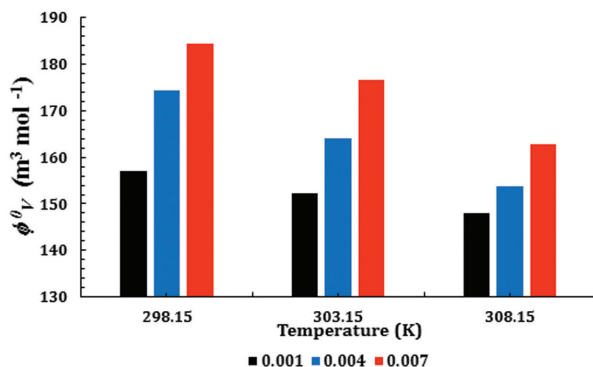


Fig. 6: Plot of limiting apparent molar volume ϕ_v^0 of amantadine against different temperature (298.15 K, 303.15 K, 308.15 K) in mass fractions $w_1 = 0.001$ (■), $w_1 = 0.004$ (■), $w_1 = 0.007$ (■) mass fractions of 18C6 in methanol solution.

restricted by the interaction of the charged functional group of ADH with crown. From Table 3, a quantitative comparison between ϕ_v^0 and S_v^* values show that, the magnitude of ϕ_v^0 values is higher than S_v^* , suggesting that the solute–solvent interactions dominate over the solute–solute interactions in all solutions at the investigated temperatures.

3.6 Temperature dependent limiting apparent molar volume:

The variation of ϕ_v^0 with the temperature of the ADH in methanolic solution of 18C6 can be expressed by the general polynomial equation as follows,

$$\phi_v^0 = a_0 + a_1T + a_2T^2 \quad (6)$$

where a_0 , a_1 , a_2 are the empirical coefficients depending on the solute, mass fraction (w_1) of the co-solute crown, and T is the temperature range under study in Kelvin.

The limiting apparent molar expansibilities, ϕ_E^0 , can be obtained by the following equation,

$$\phi_E^0 = (\delta\phi_v^0 / \delta T)_p = a_1 + 2a_2T \quad (7)$$

The limiting apparent molar expansibilities, ϕ_E^0 , change in magnitude of limiting apparent molar volume with the change of temperature. The values of ϕ_E^0 for different solutions of the studied ADH at 298.15, 303.15, and 308.15 K are

Tab. 4: Limiting apparent molar expansibilities (ϕ_E^0) for amantadine hydrochloride in different mass fraction of 18C6 in methanol solution (w_1) at 298.15 K–308.15 K, respectively.

Solvent mixture	$\phi_E^0 \cdot 10^6 \text{ (m}^3 \cdot \text{mol}^{-1} \cdot \text{K}^{-1}\text{)}$		
	Amandine+ 18C6		
	298.15 K	303.15 K	308.15 K
$w_1 = 0.001$	– 0.956	– 0.880	– 0.804
$w_1 = 0.004$	– 2.095	– 2.073	– 2.051
$w_1 = 0.007$	– 1.034	– 2.170	– 2.906

reported in Table 4. The table reveals that ϕ_E^0 is small negative in all studied temperature. This fact can ascribed to the presence of small caging or packing effect [52] for ADH in solutions.

4 Conclusion

The present study shows that amantadine ion can bind nicely to three of the six available oxygen atoms in the 18C6 ring to form a stable complex (Scheme 2) with 1 : 1 stoichiometry. The N–H...O hydrogen bridges between the ammonium functionalities and the oxygen acceptor heteroatoms of the crown ethers play a significant role in packing the host–guest complexes. The stable complex formation is established by physicochemical methods surface tension measurements, conductivity and IR study and the density data also support the interaction between amantadine ion and 18C6 systems. The inclusion complex formation has been explained qualitatively as well as quantitatively so as to make it dependable in its field of application.

The host–guest complex formation based on the macrocyclic molecules is a facile and reversible process, which provides the feasibilities to design stimuli-responsive supramolecular systems and these macrocyclic molecules are basically friendly to the biological environment and exhibit good biocompatibilities. Crown ether-based host–guest interactions, which show good selectivity, high efficiency, and reversibility, have been structurally characterized and the underlying supramolecular chemistry has been presented in this work. Supramolecular chemistry i.e. host–guest complex formation through noncovalent interactions offer the basis for novel approaches in medicine and also helps in understanding the interactions present in living systems. It was also found that host–guest complexation with crown ethers resembles an established

principle i.e. the hydrogen bonding acceptance as well as the donation propensity of crown ethers.

Amantadine is an antiviral agent that specifically inhibits influenza A virus replication at micromolar concentration. This drug is also very effective in the treatment of human Parkinson's disease. The host-guest complex is capable of protecting the drug molecule from chemical reactions and photochemical/thermal degradation in biological environment and the encapsulated drug can also be released sustainably from the cavity of macrocyclic molecule, achieving prolonged therapeutic effect.

5 Supporting information

Electronic supplementary information (ESI) available.

Acknowledgement: The authors are grateful to the Special Assistance Scheme, Department of Chemistry, NBU under the University Grants Commission, New Delhi (No. 540/27/DRS/2007, SAP-1) for financial sustenance and instrumental conveniences in order to carry on this research work. Prof. M. N. Roy is also highly obliged to University Grants Commission, New Delhi, Government of India for being awarded one time Grant under Basic Scientific Research via the Grant-in-Aid No. F.4-10/2010 (BSR) concerning his dynamic service for augmenting of research facilities to expedite the advance research work.

References

1. E. P. Kyba, R. C. Helgeson, K. Madan, G. W. Gokel, T. L. Tarnowski, S. S. Moore, D. J. Cram, *J. Am. Chem. Soc.* **99** (1977) 2564.
2. W. D. Curtis, D. A. Laidler, J. F. Stoddart, G. H. Jones, *J. Chem. Soc., Chem. Commun.* (1975) 833. DOI: 10.1039/C39750000833
3. T. J. van Bergen, R. M. Kellogg, *J. Am. Chem. Soc.* **99** (1977) 3882.
4. R. M. Izatt, J. D. Lamb, R. E. Asay, G. E. Maas, J. S. Bradshaw, J. J. Christensen, S. S. Moore, *J. Am. Chem. Soc.* **99** (1977) 6134.
5. Y. Chao, D. J. Cram, *J. Am. Chem. Soc.* **99** (1976) 1015.
6. C. J. Pedersen, *J. Am. Chem. Soc.* **89** (1967) 7017.
7. R. M. Izatt, N. E. Izatt, B. E. Rossiter, J. J. Christensen, *Science* **199** (1978) 994.
8. A. Metzger, K. Gloe, H. Stephan, F. P. Schmidtchen, *J. Org. Chem.* **61** (1996) 2051.
9. V. Thanabal, V. Krishnan, *J. Am. Chem. Soc.* **104** (1982) 3643.
10. P. D. Beer, P. A. Gale, *Angew. Chem., Int. Ed.* **40** (2001) 486.

11. P. R. Ashton, I. W. Parsons, F. M. Raymo, J. F. Stoddart, A. J. P. White, D. J. Williams, R. Wolf, *Angew. Chem., Int. Ed.* **37** (1998) 1913.
12. H. W. Gibson, N. Yamaguchi, L. Hamilton, J. W. Jones, *J. Am. Chem. Soc.* **124** (2002) 4653.
13. T. Akutagawa, T. Hasegawa, T. Nakamura, T. Inabe, *J. Am. Chem. Soc.* **124** (2002) 8903.
14. T. Akutagawa, A. Hashimoto, S. Nishihara, T. Hasegawa, T. J. Nakamura, *Phys. Chem. B* **107** (2003) 66.
15. H. Sharghi, M. A. Nasser, K. Niknam, *J. Org. Chem.* **66** (2001) 7287.
16. R. M. Izatt, K. Pawlak, J. S. Bradshaw, R. L. Bruening, *Chem. Rev.* **91** (1991) 1721.
17. G. W. Gokel, D. M. Goli, C. Minganti, L. M. Echegoyen, *J. Am. Chem. Soc.* **105** (1983) 6786.
18. H. J. Buschmann, L. Mutihac, K. Jansen, *J. Inclusion Phenom. Macrocycl. Chem.* **39** (2001) 1.
19. K. M. Doxsee, J. Francis, T. J. R. Weakley, *Tetrahedron* **56** (2000) 6683.
20. B. F. G. Johnson, C. M. G. Judkins, J. M. Matters, D. S. Shephard, S. Parsons, *Chem. Commun.* **16** (2000) 1549.
21. D. V. Dearden, I. H. Chu, *J. Incl. Phenom.* **29** (1997) 269.
22. M. Rudolph, R. A. Kamei, K. J. Overby, *Rudolph's Fundamentals of Pediatrics*, 3rd edn, McGraw-Hill, USA, (2002), P. 308.
23. Y. Kawaoka, *Influenza Virology*, Caister Academic Press, Madison (2006), P. 169.
24. C. J. Pederson, *J. Am. Chem. Soc.* **89** (1967) 7017.
25. B. Dietrich, J. M. Lehn, J. P. Sauvage, *Tetrahedron Lett.* **10** (1969) 2885.
26. C. J. Pederson, *Fed. Proc. Fed. Am. Soc. Exp. Biol.* **27** (1968) 1305.
27. D. J. Cram, In: Jones, J. B. (ed.) *Applications of Biochemical Systems in Organic Chemistry*. Wiley, New York (1976), P. 731.
28. R. A. Schultz, E. Schlegel, D. M. Dishong, G. W. Gokel, *J. Chem. Soc. Chem. Comm.* (1982) 242. DOI: 10.1039/C39820000242
29. M. Hasani, M. Shamsipur, *J. Solution Chem.* **23** (1994) 721.
30. O. P. Kryatova, I. V. Korendovych, E. V. Rybak-Akimova, *Tetrahedron* **60** (2004) 4579.
31. G. Gokel, W. leevy, M. Weber, *Chemical Reviews*, **104** (2004) 2723.
32. H. Nakamura, H. Nishida, M. Takagi, K. Ueno, *Analytica Chimica Acta.* **139** (1982) 219.
33. M. Shamsipur, M. Ganjali, *J. Incl. Phenom.* **28** (1997) 315.
34. M. R. Ganjali, A. Rouhollahi, A. Mardan, M. Shamsipur, *J. Chem. Soc., Faraday Trans.* **94** (1998) 1959.
35. F. Jalali, A. Ashrafi, M. Shamsipur, *J. Incl. Phenom. Macrocycl. Chem.* **61** (2008) 77.
36. D. P. Shoemaker, C. W. Garland, *Experiments in Physical Chemistry*. McGraw-Hill, New York, 1967, P. 131.
37. D. Ekka, M. N. Roy, *J. Phys. Chem. B*, **116** (2012) 11687.
38. A. Sinha, A. Bhattacharjee, M. N. Roy, *J. Dispersion Sci. Technol.* **30** (2009) 1003.
39. M. Shamsipur, G. Khayatian, *J. Incl. Phenom.* **39** (2001) 109.
40. G. Khayatian, F. S. Karoonian, *J. Chinese chem. Soc.* **55** (2008) 377.
41. G. Khayatian, S. Shariati, M. Shamsipur, *J. Incl. Phenom.* **45** (2003) 117.
42. P. Debye-Hückel, *Phys. Z.* **24** (1928) 305.
43. Y. Gao, X. Zhao, B. Dong, L. Zheng, N. Li, S. Zhang, *J. Phys. Chem. B.* **110** (2006) 8576.
44. M. N. Roy, D. Ekka, S. Saha, M. C. Roy, *RSC Adv.* **4** (2014) 42383.
45. M. N. Roy, M. C. Roy, K. Roy, *RSC Adv.* **5** (2015) 56717.
46. P. D. Harvey, D. F. R. Gilson, I. S. Butler, *J. Phys. Chem.* **91** (1987) 1267.
47. K. Nakamoto, *Infrared and Raman Spectra of Inorganic and Coordination Compounds*. 5 Edn, John Wiley and Sons, New York (1997).

48. D. O. Masson, *Philos. Mag.* **8** (1929) 218.
49. D. Ekka, M. N. Roy, *Amino Acids* **45** (2013) 755.
50. R. K. Wadi, P. Ramasami, *J. Chem. Soc. Faraday Trans.* **93** (1997) 243.
51. T. S. Banipal, D. Kaur, P. K. Banipal, *J. Chem. Eng. Data* **49** (2004) 1236.
52. F. J. Millero, *Water and Aqueous Solutions*, Wiley Interscience, New York (1972), P. 519.

Supplemental Material: The online version of this article (DOI: 10.1515/zpch-2016-0804) offers supplementary material, available to authorized users.



Investigation on Solvation Behavior of an Ionic Liquid (1-butyl-3-methylimidazolium Chloride) with the Manifestation of Ion Association Prevailing in Different Pure Solvent Systems

Siti Barman, Biswajit Datta, Mahendra Nath Roy*

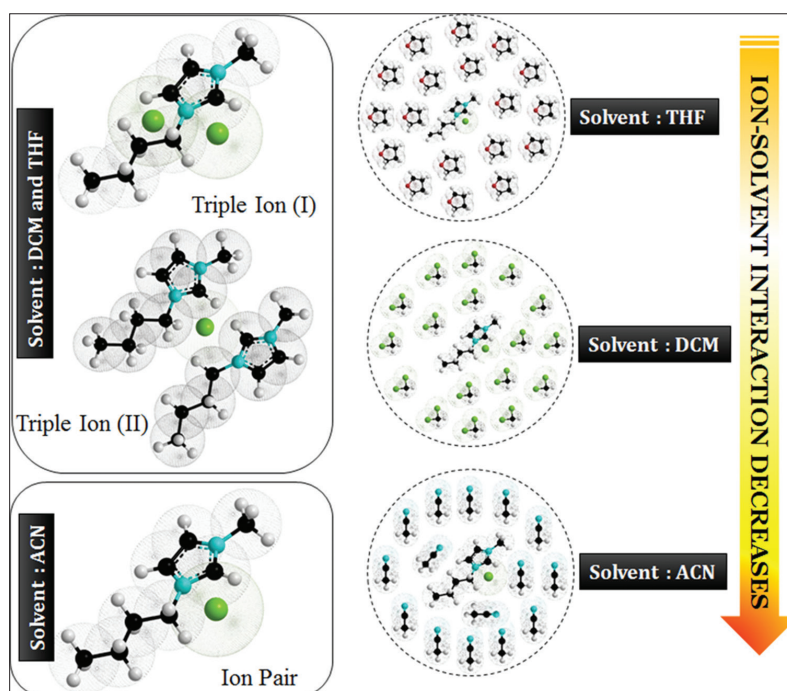
Department of Chemistry, University of North Bengal, Darjeeling - 734 013, West Bengal, India.

Received ???; Revised ??? Accepted ???

ABSTRACT

The ion-pair formation constant (K_P) and triple-ion formation constant (K_T) of 1-butyl-3-methylimidazolium chloride ($[bmim][Cl]$) have been determined conductometrically in different solvent media in the temperature range from 298.15 to 318.15 K. The Fuoss conductance equation (1978) for ion-formation and Fuoss–Kraus theory for triple-ion formations have been used for analyzing the conductance data. The Walden product is obtained and discussed. However, the deviation of the conductometric curves (Λ vs. \sqrt{m}) from linearity for the electrolyte in tetrahydrofuran and dichloromethane indicated/indicates triple-ion formation. Ion-solvent interactions have been studied with the help of density, viscosity, and Fourier transform infrared spectroscopic measurements. Apparent molar volume and viscosity B -coefficient have been calculated from experimental density and viscosity data, respectively. The limiting ionic conductances (λ_0^\pm) have been estimated from the appropriate division of the limiting molar conductance of tetrabutylammonium tetraphenylborate as “reference electrolyte” method.

Graphical abstract



Keywords: Ionic liquid, Ion-pair and triple-ion formation, Ion-solvent interaction, Thermodynamic parameters, Walden product.

1. INTRODUCTION

Ionic liquids (IL) or molten salts at room temperature presently experience significant attention in many areas of chemistry. There is competition to find a proper niche for these materials, and also more insight is needed. The most attractive property is the “tunability” of the physical and chemical properties of ILs by varying structure. There are several reviews available on different aspects of ILs [1]. ILs have attracted significant attention over the past two decades, as many of them have a negligible vapor pressure, exceptional thermal and electrochemical stability, favorable dissolution properties with many organic/inorganic compounds, and low flammability [2,3]. ILs, which may consist of a diverse variety of cations and anions, have been widely investigated for a variety of applications including biphasic systems for separation, solvents for synthetic and catalytic applications [4], lubricants [5,6], lithium batteries [7-9], supercapacitors [10-12], actuators [13,14], reaction media [15] replacement of conventional solvents [3], and active pharmaceutical ingredients [15]. Importantly, IL properties can be tailored for specific chemical or electrochemical applications by tuning the combination of cations and anions to achieve the desired thermodynamic, solvating, and transport properties, as well as safety. In the modern technology, the application of the IL is well understood by studying the ionic solvation or ion association. Ionic association of electrolytes in solution depends on the mode of solvation of its ions [16-19] which in turn depends on the solvent properties such as viscosity and the relative permittivity. These properties help in determining the extent of ion association and the solvent-solvent interactions. The nonaqueous arrangement has been of enormous prominence [20,21] to the technologist and theoretician as numerous chemical processes ensue in these systems.

In this study, we have investigated on conductometric properties of the IL 1-butyl-3-methylimidazolium chloride [bmim][Cl] in polar aprotic solvents acetonitrile (ACN), tetrahydrofuran (THF), dichloromethane (DCM) at different temperatures 298.15 K, 303.15 K and 308.15 K. The experimental data were analyzed using Fuoss conductance equation and Fuoss-Kraus theory to calculate the ion-pair formation constant K_p and triple-ion formation constants K_T . The main purpose of this study is to obtain experimental and quantitative information for the interactions between the ions. Here, the ion-pair formation constants are expected to reflect strongly the direct interactions between the ions. The structure of the IL and solvents is presented in Scheme 1.

2. EXPERIMENTAL

2.1. Materials

The IL [bmim][Cl] (purity $\geq 98\%$) was obtained from Sigma-Aldrich, Germany, and the IL was preserved in vacuum desiccator containing anhydrous P_2O_5 and

any water content of the solvents was removed using molecular sieves.

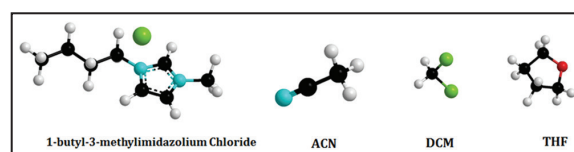
The solvents ACN, THF, and DCM were procured from Merck, India. The solvents were further purified by standard methods [22]. The purity of the solvents was checked by measuring its density and viscosity which were in good agreement with the literature values [23,24] as shown in Table 1. The purities of the solvents were $\geq 99.5\%$.

2.2. Apparatus and Procedure

All the stock solutions of the IL in considered solvents were prepared by mass (weighed by Mettler Toledo AG-285 with uncertainty 0.0003 g). In case of conductometric study, the working solutions were achieved by mass dilution of the stock solutions.

Temperature of the solution was maintained to within ± 0.01 K using Brookfield Digital TC-500 temperature thermostat bath. The viscosities were measured with an accuracy of $\pm 1\%$. Each measurement reported herein is an average of triplicate reading with a precision of 0.3%.

The conductance measurements were carried out in a Systronics-308 conductivity bridge of accuracy $\pm 0.01\%$, using a dip-type immersion conductivity



Scheme 1: Molecular structures of the ionic liquids and the solvents.

Table 1: Density (ρ), viscosity (η) and relative permittivity (ϵ) of the different solvents acetonitrile, tetrahydrofuran, and dichloromethane.

Temp./K	$\rho^a 10^{-3}/\text{kg m}^{-3}$	$\eta^b/\text{mPa s}$	ϵ
Acetonitrile			
298.15	0.78597	0.36	35.94
303.15	0.78278	0.35	35.01
308.15	0.77996	0.34	34.30
Tetrahydrofuran			
298.15	0.88599	0.48	7.58
303.15	0.88591	0.45	7.24
308.15	0.88586	0.41	7.09
Dichloromethane			
298.15	1.32571	0.43	8.93
303.15	1.31852	0.41	8.84
308.15	1.30955	0.39	8.73

^aUncertainty in the density values: $\pm 0.00001 \text{ g cm}^{-3}$.

^bUncertainty in the viscosity values: $\pm 0.03 \text{ mPa s}$

cell, CD-10 having a cell constant of approximately $(0.1 \pm 0.001) \text{ cm}^{-1}$. Measurements were made in a thermostat water bath maintained at $T = (298.15 \pm 0.01) \text{ K}$. The cell was calibrated by the method proposed by Lind *et al.* [25], and cell constant was calculated based on 0.01 (M) aqueous KCl solution. During the conductance measurements, cell constant was maintained within the range $1.10\text{-}1.12 \text{ cm}^{-1}$.

The conductance data were reported at a frequency of 1 kHz, and the accuracy was $\pm 0.3\%$. During all the measurements, uncertainty of temperatures was $\pm 0.01 \text{ K}$.

The density values of the solvents and experimental solutions (ρ) were measured using vibrating u-tube Anton Paar digital density meter (DMA 4500M) with

Table 2: The concentration (m) and molar conductance (Λ) of [bmim][Cl] in acetonitrile, dichloromethane and tetrahydrofuran at 298.15 K, 303.15 K and 308.15 K respectively.

$m \cdot 10^4 / \text{mol} \cdot \text{dm}^{-3}$	$\Lambda \cdot 10^4 / \text{S} \cdot \text{m}^2 \cdot \text{mol}^{-1}$	$m \cdot 10^4 / \text{mol} \cdot \text{dm}^{-3}$	$\Lambda \cdot 10^4 / \text{S} \cdot \text{m}^2 \cdot \text{mol}^{-1}$	$m \cdot 10^4 / \text{mol} \cdot \text{dm}^{-3}$	$\Lambda \cdot 10^4 / \text{S} \cdot \text{m}^2 \cdot \text{mol}^{-1}$
Acetonitrile		Dichloromethane		Tetrahydrofuran	
298.15 K					
0.87	176.54	8.97	41.77	0.95	40.11
11.58	166.42	10.74	39.95	1.60	38.48
24.95	160.14	13.06	37.68	2.83	37.13
35.44	155.66	15.15	36.2	4.07	36.10
57.00	149.3	17.64	34.67	6.22	34.76
70.02	146.04	19.85	33.29	7.79	33.96
84.63	142.6	22.85	31.8	10.19	32.86
105.80	138.81	25.01	30.88	13.55	31.66
129.30	134.62	27.70	29.91	15.79	31.36
156.12	130.7	33.74	27.98	17.81	30.76
177.99	127.9	39.25	26.79	20.05	30.36
206.72	123.23	46.61	26.17	22.80	30.36
233.73	120.68	53.92	26.99	25.68	30.16
266.02	116.52	60.72	28.57	29.66	31.06
306.52	112.13	66.97	31.18	34.29	33.87
303.15 K					
1.10	181.36	4.63	50.59	1.06	43.96
12.40	171.07	6.28	48.32	2.18	41.26
26.14	165.28	8.13	46.13	3.59	39.46
36.86	160.46	10.43	44.22	4.97	38.06
58.79	153.67	13.22	42.31	7.33	36.41
72.00	150.37	15.94	41.03	9.03	35.51
86.81	147.06	19.51	39.12	11.59	34.77
108.23	143.67	22.45	37.61	14.19	33.89
131.99	139.38	26.01	36.52	17.04	33.3
159.07	135.36	29.35	35.72	19.66	32.66
181.15	132.99	32.26	35.03	22.00	32.52
210.12	128.42	34.70	33.99	25.05	32.2
237.34	124.58	42.13	34.22	27.89	33.06
269.87	121.16	46.64	35.91	30.55	34.96
310.65	116.36	53.03	38.92	33.42	36.46
308.15 K					
1.34	188.20	9.09	52.14	1.43	49.66
13.18	176.91	11.09	50.22	2.70	47.56

(Contd...)

Table 2: (Continued).

$m \cdot 10^4 / \text{mol} \cdot \text{dm}^{-3}$	$\Lambda \cdot 10^4 / \text{S} \cdot \text{m}^2 \cdot \text{mol}^{-1}$	$m \cdot 10^4 / \text{mol} \cdot \text{dm}^{-3}$	$\Lambda \cdot 10^4 / \text{S} \cdot \text{m}^2 \cdot \text{mol}^{-1}$	$m \cdot 10^4 / \text{mol} \cdot \text{dm}^{-3}$	$\Lambda \cdot 10^4 / \text{S} \cdot \text{m}^2 \cdot \text{mol}^{-1}$
Acetonitrile		Dichloromethane		Tetrahydrofuran	
27.27	169.90	13.94	48.54	4.25	45.86
38.20	166.20	17.04	46.62	6.34	44.06
60.49	159.61	21.29	44.93	8.26	42.67
73.87	156.51	23.94	43.84	10.06	41.69
88.87	152.51	28.20	42.53	12.75	40.61
110.53	148.64	31.74	41.37	16.49	39.38
134.52	144.42	35.92	40.73	18.95	38.4
161.85	139.90	39.74	40.06	22.09	37.96
184.12	136.73	45.02	39.26	23.59	37.56
213.32	132.26	47.84	38.88	25.72	37.66
240.74	128.82	54.21	38.56	29.68	37.96
273.49	125.10	60.05	39.74	32.43	39.46
314.53	120.82	64.25	42.32	35.37	41.36

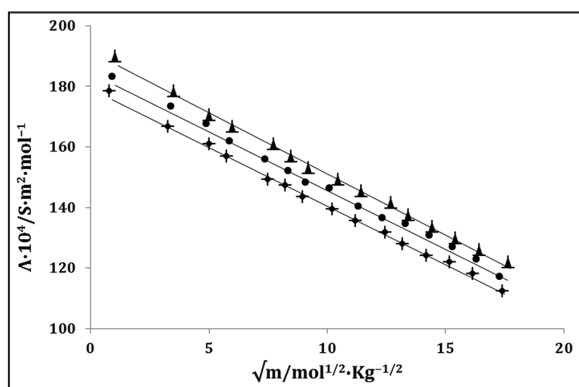


Figure 1: Plot of molar conductance (Λ) versus \sqrt{m} of [bmim][Cl] in acetonitrile at 298.15 K (\blacklozenge), 303.15 K (\bullet) and 308.15 K (\blacktriangle).

a precision of $\pm 0.00005 \text{ g cm}^{-3}$ maintained at $\pm 0.01 \text{ K}$ of the desired temperature. It was calibrated by triply-distilled water and passing dry air.

The viscosity values were measured using a Brookfield DV-III Ultra Programmable Rheometer with fitted spindle size-42 fitted to a Brookfield digital bath TC-500. The viscosities were obtained using the following equation:

$$\eta = (100/\text{RPM}) \times \text{TK} \times \text{torque} \times \text{SMC}$$

Where RPM, TK (0.09373), and SMC (0.327) are the speed, viscometer torque constant and spindle multiplier constant, respectively. The instrument was calibrated against the standard viscosity samples supplied with the instrument, water and aqueous CaCl_2 solutions [26]. The viscosities were measured with an accuracy of $\pm 1\%$.

Fourier transform infrared spectra (FT-IR) were recorded in a Perkin Elmer FT-IR spectrometer. The spectra were acquired in the frequency range 4000-400/cm at a resolution of 4/cm with a total of 10 scans. The concentration of the studied solutions used in the IR study was 0.05 M.

3. RESULTS AND DISCUSSION

3.1. Electrical Conductance

3.1.1. Ion-pair formation

The formation of ion-pair in ACN has been explored from the conductivity studies of [bmim][Cl] using the Fuoss conductance equation [27]. The physical properties solvent are given in Table 1. The molar conductance (Λ) for all studied system was calculated using suitable equation [28]. The plot of molar conductivity, Λ , versus the square root of the molar concentration, \sqrt{m} , gives a linear conductance curves for the solvent with higher to moderate relative permittivity ($\epsilon_r=35.95-14.47$), shown in Figure 1, and the values are listed in Table 2. Extrapolation of $\sqrt{m}=0$ evaluated the starting limiting molar conductances for the electrolyte [29].

The limiting molar conductance (Λ_0), the association constant (K_A), and the distance of closest approach of ions (R) these three adaptable parameters are derived from the following set of equations (Fuoss equation) using a given set of conductivity values ($c_j, \Lambda_j, j=1, \dots, n$):

$$\Lambda = P\Lambda_0[(1+R\chi)+E_L] \tag{1}$$

$$P = 1 - \alpha(1 - \gamma) \tag{2}$$

$$\gamma = 1 - K_A m \gamma^2 f^2 \tag{3}$$

$$-\ln f = \beta k / 2(1 + kR) \quad (4)$$

$$\beta = e^2 / (\epsilon_r k_B T) \quad (5)$$

$$K_A = K_R / (1 - \alpha) = K_R / (1 + K_S) \quad (6)$$

Where R_X is the relaxation field effect, E_L is the electrophoretic counter current, α is the fraction of contact pairs, γ is the fraction of solute present as unpaired ion, K_A is the overall pairing constant, f is the activity coefficient, m is the molality of the solution, β is twice the Bjerrum distance, κ is the radius of the ion atmosphere, e is the electron charge, ϵ_r is the relative permittivity of the solvent mixture, k_B is the Boltzmann constant, T is the absolute temperature, K_R is the association constant of the solvent-separated pairs, and K_S is the association constant of the contact pairs.

The computations were performed using a program suggested by Fuoss [27]. The initial A_0 values for the iteration procedure were obtained from Shedlovsky extrapolation of the data [30]. Input for the program is the set ($m_j, A_j, j=1, \dots, n$), n, ϵ, η, T , initial A_0 value, and an instruction to cover a preselected range of R values. The best values of a parameter are the one when equations are best fitted to the experimental data corresponding to minimum standard deviation δ for a sequence of predetermined R values, and standard deviation δ was calculated by the following equation:

$$\delta^2 = \sum [\Lambda_j(cal) - \Lambda_j(obs)]^2 / (n - m) \quad (7)$$

Where n is the number of experimental points and m is the number of fitting parameters. The conductance data were examined by fixing the distance of closest approach (R) of ions with two fitting parameters ($m=2$). No significant minima were detected in the δ versus R curves, whereas the R values were arbitrarily preset at the center to center distance of solvent-separated ion-pair [26,29]. Thus, R values are assumed to be $R = (a + d)$; where $a=(r_+ + r_-)$ is the sum of the crystallographic radii of the cation (r_+) and anion (r_-) and d is the average distance corresponding to the side of a cell occupied by a solvent molecule. The distance, d is given by Fuoss and Accascina [31].

$$d (\text{\AA}) = 1.183 (M/\rho)^{1/3} \quad (8)$$

Where M is the molar mass of the solvent and ρ is its density. The values of A_0, K_A and R obtained by using Fuoss conductance equation for [bmim][Cl] in ACN at 298.15 K, 303.15 K, and 308.15 K are represented in Table 3. The values in Table 3 shows that the limiting molar conductances (A_0) of [bmim][Cl] is highest in ACN (Table 3) and lowest in case of THF (Table 4). Thus, the observed trend of the A_0 values is ACN > DCM > THF. The observed trend of solvent A_0 is found to be the opposite of the viscosity trend. As

expected, limiting molar conductance values decrease when the viscosity of the solvents increases because ionic mobility is diminished in viscous media.

Ion-solvation can also be explained with the help of another characteristic property called the Walden product ($A_0\eta$) (Table 5) [32]. A_0 increases for the IL in ACN with increasing temperature, and the $A_0\eta$ also increases even though the viscosity of the solvent decreases. This fact indicates the prevalence of A_0 over η .

To investigate the role of the individual IL ions in ion-solvation, we have to split the limiting molar conductance values into their ionic contributions. The ionic conductances λ_0^\pm for the [bmim]⁺ cation and Cl⁻ anion in different solvents were calculated using tetrabutylammonium tetraphenylborate (Bu₄NBPh₄) as a “reference electrolyte” by the method of Das *et al.* [33]. The ionic limiting molar conductances λ_0^\pm values for [bmim]⁺ cation and [Cl]⁻ anion has been determined in ACN solvents by interpolating conductance data from the literature [34] using cubic spline fitting, and the values are given in Table 6. It is observed from Table 6 that a smaller limiting molar conductivity value of the [bmim]⁺ than Cl⁻ in

Table 3: Limiting molar conductance (A_0), association constant (K_A), cosphere diameter (R) and standard deviations of experimental A (δ) obtained from Fuoss conductance equation of [bmim][Cl] in Acetonitrile at 298.15 K, 303.15 K and 308.15 K respectively.

Temp./K	$A_0 \cdot 10^4 / S \cdot m^2 \cdot mol^{-1}$	$K_A / dm^3 \cdot mol^{-1}$	$R / \text{\AA}$	δ
298.15	178.45	725.21	8.98	3.43
303.15	191.43	641.23	8.82	3.54
308.15	199.56	571.34	8.73	3.92

Table 4: Thermodynamic parameters for [bmim][Cl] in ACN.

$\Delta G_a^0 / kJ \cdot mol^{-1}$	$\Delta H_a^0 / kJ \cdot mol^{-1}$	$\Delta S_a^0 / JK^{-1} mol^{-1}$	$E_d / kJ \cdot mol^{-1}$
-16.33	-18.22	-6.35	8.55

ACN: Acetonitrile

Table 5: Walden product ($A_0 \cdot \eta$) and Gibb's energy change (ΔG^0) of [bmim][Cl] in acetonitrile at 298.15 K, 303.15 K, and 308.15 K, respectively.

Temp./K	$A_0 \cdot \eta \cdot 10^4 / S \cdot m^2 \cdot mol^{-1} mPa$	$\Delta G^0 / kJ \cdot mol^{-1}$
298.15	64.24	-16.33
303.15	67.00	-16.29
308.15	67.85	-16.26

Table 6: Limiting ionic conductance (λ_0^\pm), ionic Walden product ($\lambda_0^\pm\eta$), Stokes' Radii (r_s), and crystallographic Radii (r_c) of [bmim][Cl] in acetonitrile at 298.15 K, 303.15 K, and 308.15 K, respectively.

Temp./K	Ion	$\lambda_0^\pm/\text{S}\cdot\text{m}^2\cdot\text{mol}^{-1}$	$\lambda_0^\pm\eta/\text{S}\cdot\text{m}^2\cdot\text{mol}^{-1}\text{ mPa}$	$r_s/\text{\AA}$	$r_c/\text{\AA}$
298.15	Bmim ⁺	87.41	31.47	3.15	2.25
	Cl ⁻	99.42	35.78	2.19	1.95
303.15	Bmim ⁺	89.42	31.28	3.14	2.27
	Cl ⁻	103.31	36.15	2.16	1.98
308.15	Bmim ⁺	93.24	31.70	3.12	2.28
	Cl ⁻	105.84	35.99	2.12	2.03

a solvent suggests enhanced solvation of the cation in that specific medium, i.e., the [bmim]⁺ cation is responsible for a greater portion of ionic association with the solvents. Estimation of the ionic contributions to conductance is based mostly on Stokes' law, which provides valuable insight for the limiting ionic Walden product. The law states that the limiting ionic Walden product ($\lambda_0^\pm\eta$); the product of the limiting ionic conductance and solvent viscosity) for any singly charged, spherical ion is a function of the ionic radius (crystallographic radius), and thus, is a constant under normal conditions. The values of ionic conductance λ_0^\pm and the product of ionic conductance and viscosity of the solvent named ionic Walden product ($\lambda_0^\pm\eta$) along with Stokes' radii (r_s) and crystallographic radii (r_c) of [bmim][Cl] in ACN at different temperatures are given in Table 5.

3.1.2. Thermodynamic parameters

The Gibbs free energy change ΔG^0 is given by the following relationship [35] and is given in Table 5.

$$\Delta G^0 = -RT \ln K_a \quad (9)$$

The negative values of ΔG^0 can be explained by considering the participation of specific covalent interaction in the ion-association process.

The variation of conductance of an ion with temperature can be treated as similar to the variation of the rate constant with temperature which is given by the Arrhenius equation [27]:

$$\Lambda_0 = A e^{E_a/RT} \quad (10)$$

$$\log \Lambda_0 = \log A - \frac{E_a}{2.303RT} \quad (11)$$

Where A is an Arrhenius constant, E_a is the activation energy of the rate process which determines the rate of movement of ions in solution. The slope of the linear plot of $\log \Lambda_0$ versus $1/T$ gives the value of E_a (Table 4).

To have a better understanding of the thermodynamics of the ion-association process, it is beneficial to consider the contributions obtained from the

thermodynamic parameters. The ΔH_a^0 and ΔS_a^0 values for the ion-association process were evaluated by applying the linear least-squares analysis according to the equation:

$$\ln K_a = -\frac{\Delta H_a^0}{RT} + \frac{\Delta S_a^0}{R} \quad (12)$$

From the slopes and intercepts of linear plots of $\ln K_a$ vs. $\frac{1}{T}$ (Figure 2), the values of enthalpy (ΔH_a^0)

and entropy (ΔS_a^0) of ion association process were determined and the results are also included in Table 6. Both of these two parameters have negative values. The negative values of enthalpy confirm that when ion association occurs the overall energy of the system is decreased, i.e., there is some stabilization interaction in the system, whereas negative values of entropy factor indicate that there is an ordered arrangement, i.e., ion-pair formation takes place. The negative value of entropy is unfavorable for the spontaneity of the system, but this effect is overcome by higher negative value of ΔH^0 . The value of ΔG_a^0 was calculated using equation $\Delta G_a^0 = \Delta H_a^0 - T \Delta S_a^0$. The negative values of ΔG_a^0 (Table 4) suggest that the ion-pair formation process proceeds spontaneously.

3.1.3. Triple-ion formation

Figure 3 shows the deviations in the conductance curves from linearity which indicates the triple-ion formation. The curves show a decrease in conductance values with increasing concentration, reaches a minimum and then increases.

The conductance data for the IL in THF and DCM have been analyzed by the classical Fuoss-Kraus theory of triple-ion formation in the form [31,35]:

$$\Lambda g(c)\sqrt{c} = \frac{\Lambda_0}{\sqrt{K_p}} + \frac{\Lambda_0^T K_T}{\sqrt{K_p}} \left(1 - \frac{\Lambda}{\Lambda_0}\right) c \quad (13)$$

Where $g(c)$ is a factor that lumps together all the intrinsic interaction terms and is defined by:

$$g(c) = \frac{\exp\{-2.303\beta'(c\Lambda)^{0.5}/\Lambda_0^{0.5}\}}{\{1 - S(c\Lambda)^{0.5}/\Lambda_0^{1.5}\}(1 - \Lambda/\Lambda_0)^{0.5}} \quad (14)$$

$$\beta' = 1.8247 \times 10^6 / (\epsilon T)^{1.5} \quad (15)$$

$$S = \alpha \Lambda_0 + \beta = \frac{0.8204 \times 10^6}{(\epsilon T)^{1.5}} \Lambda_0 + \frac{82.501}{\eta(\epsilon T)^{0.5}} \quad (16)$$

In the above equations, Λ_0 is the sum of the molar conductance of the simple ions at infinite dilution, Λ_0^T is the sum of the conductance value of the two triple-ions $[\text{bmim}^+]_2\text{Cl}^-$ and $\text{bmim}^+[\text{Cl}^-]_2$. $K_P \approx K_A$ and K_T are the ion-pair and triple-ion formation constants, respectively, and S is the limiting Onsager coefficient. To make equation (13) applicable, the symmetrical approximation of the two possible formation constants of triple-ions, $K_{T1} = \frac{[\text{bmim}^+]_2[\text{Cl}^-]}{[\text{bmim}^+][\text{bmim}][\text{Cl}^-]}$ and $K_{T2} = \frac{[\text{bmim}][\text{Cl}^-]_2}{[\text{Cl}^-][\text{bmim}][\text{Cl}^-]}$ equal to each other has been adopted, i.e., $K_{T1} = K_{T2} = K_T$ [36] and Λ_0 values for the studied electrolyte have been calculated following the scheme as suggested by Krungalz [37]. Λ_0^T has been calculated by setting the triple-ion conductance equal to $2/3 \Lambda_0$ [38].

Thus, the ratio Λ_0^T / Λ_0 was set equal to 0.667 during linear regression analysis of equation (13). The linear regression analysis of equation (13) for the electrolytes with an average regression constant, $R^2 = 0.9436$, gives intercepts and slopes. The calculated limiting molar conductance of simple ion (Λ_0), limiting molar conductance of triple-ion (Λ_0^T), slope and intercept of

Equation (13) for $[\text{bmim}][\text{Cl}]$ in DCM, THF at different temperature are given in Table 7. We obtain K_P and K_T by applying the Fuoss–Kraus equation; the values are presented in Table 5. These values permit the calculation of other derived parameters such as K_P and K_T listed in Table 8. The values of K_P and K_T predict that a major portion of the electrolytes exists as ion-pairs with a minor portion as triple ions. The tendency of triple ion formation can be judged from

Table 7: The calculated limiting molar conductance of ion-pair (Λ_0), limiting molar conductances of triple ion Λ_0^T , experimental slope and intercept obtained from Fuoss–Kraus Equation for $[\text{bmim}][\text{Cl}]$ in DCM and THF at 298.15 K, 303.15 K and 308.15 K respectively.

Solvents	$\Lambda_0 \cdot 10^4 / \text{S} \cdot \text{m}^2 \cdot \text{mol}^{-1}$	$\Lambda_0^T \cdot 10^4 / \text{S} \cdot \text{m}^2 \cdot \text{mol}^{-1}$	Slope $\times 10^{-2}$	Intercept $\times 10^{-2}$
298.15 K				
DCM	42.71	28.83	0.19	-5.21
THF	35.59	23.61	0.14	-6.83
303.15 K				
DCM	47.53	31.35	0.34	-5.27
THF	39.33	25.15	0.27	-6.91
308.15 K				
DCM	52.43	35.59	0.46	-5.53
THF	43.93	27.98	0.47	-7.83

THF: Tetrahydrofuran, DCM: Dichloromethane

the K_T/K_P ratios and $\log(K_T/K_P)$, which are highest in THF. These ratios suggest that strong association between the ions is due to the Coulombic interactions as well as covalent forces present in the solution. These results are in good agreement with those of Hazra et al. [39]. At very low permittivity of the

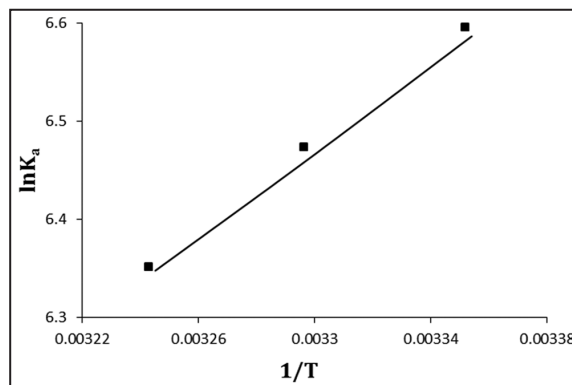


Figure 2: The linear relationships of $\ln K_a$ versus $1/T$ for the ion-pair formation in acetonitrile.

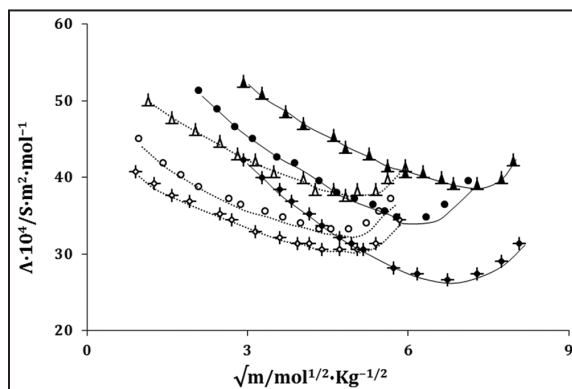


Figure 3: Plot of molar conductance (Λ) versus \sqrt{m} for $[\text{bmim}][\text{Cl}]$ in dichloromethane at 298.15 K (\blacklozenge), 303.15 K (\bullet) and 308.15 K (\blacktriangle) and in tetrahydrofuran at 298.15 K (\diamond), 303.15 K (\circ) and 308.15 K (\triangle).

solvent, i.e., $\epsilon < 10$, electrostatic ionic interactions are very large. Hence, the ion-pairs attract the free cations (+ve) or anions (-ve) present in the solution medium as the distance of the closest approach of the ions becomes minimum resulting in the formation of triple-ions, which acquires the charge of the respective ions, attracted from the solution bulk [34,35], i.e.,



where M^+ is $[bmim^+]$ and A^- is $[Cl^-]$. The effect of ternary association [40] thus removes some nonconducting species, MA, from solution, and replaces them with triple-ions which increase the conductance manifested by non-linearity observed in

conductance curves for the electrolyte in DCM, THF (Figure 3). The pictorial representation of triple-ion formation for the selected IL ($[bmim^+][Cl^-]$) in DCM and THF solvents is depicted in Scheme 2.

The ion-pair and triple-ion concentrations, C_P and C_T , respectively, of the IL in DCM, THF have also been calculated using the following set of equations [41]:

$$\alpha = 1 / (K_P^{1/2} \cdot C^{1/2}) \quad (20)$$

$$\alpha_T = (K_T / K_P^{1/2}) C^{1/2} \quad (21)$$

$$C_P = C(1 - \alpha - 3\alpha_T) \quad (22)$$

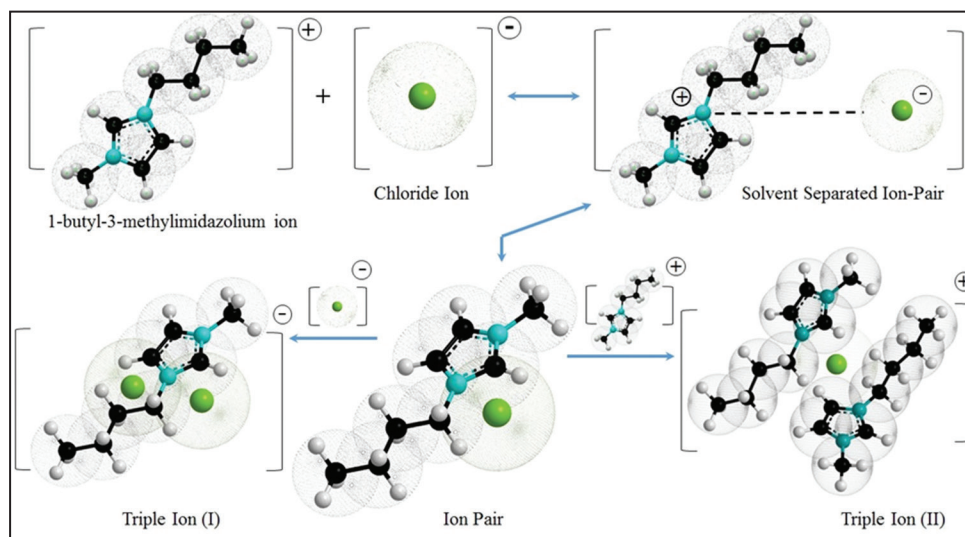
$$C_T = (K_T / K_P^{1/2}) C^{3/2} \quad (23)$$

The fraction of ion-pairs (α) and triple-ions (α_T) present in the salt solutions are given in Table 8. The

Table 8: Salt concentration at the minimum conductivity (C_{min}) along with the ion-pair formation constant (K_P), triple-ion formation constant (K_T) for $[bmim][Cl]$ in DCM and THF at 298.15 K, 303.15 K, and 308.15 K, respectively.

Solvents	$c_{min} \cdot 10^4 / \text{mol} \cdot \text{dm}^{-3}$	$\log c_{min}$	$K_P \cdot 10^2 / (\text{mol} \cdot \text{dm}^{-3})^{-1}$	$K_T \cdot 10^3 / (\text{mol} \cdot \text{dm}^{-3})^{-1}$	$K_T / K_P \cdot 10^5$	$\log K_T / K_P$
298.15 K						
DCM	5.31	0.7298	5.62	57.63	10.25	1.011
THF	5.25	0.7158	5.25	62.54	11.91	1.076
303.15 K						
DCM	6.36	0.8655	5.18	64.21	12.39	1.093
THF	5.38	0.7291	5.03	67.59	13.44	1.128
308.15 K						
DCM	7.12	0.8675	5.03	66.97	13.31	1.124
THF	5.51	0.7381	4.98	69.95	14.05	1.148

THF: Tetrahydrofuran, DCN: Dichloromethane



Scheme 2: Pictorial representation of ion-pair and triple-ion formation for the electrolyte in diverse solvent systems.

calculated values of C_P and C_T are also presented in Table 9. Comparison of the C_P and C_T values shows that the C_P is higher than C_T , indicating that the major portion of ions are present as ion-pairs even at high concentrations, and a small fraction exists as triple-ions. The conductance value decreases with increasing concentration and reach a minimum called A_{min} . The concentration at which the conductance value reaches a minimum is termed C_{min} (Table 9); after that, the fraction of triple-ions in the solution increases with the increasing concentration in the studied solution medium.

3.2. Volumetric Properties

The apparent molal volume (ϕ_V) and limiting apparent molal volume (ϕ_V^0) provide information regarding the solute-solvent interactions present in our systems. [42]. The apparent molal volume of the IL can be considered to be the sum of the geometric volume of the solute molecule [bmim][Cl] and changes in the solvent volume due to its interaction with the solute [43]. The values of ϕ_V of the IL (Table 10) at different concentrations were calculated using density data (Table 11) through the following equation:

$$\phi_V = M/\rho - Mp - \rho_0/m\rho_0\rho \quad (24)$$

Where M is the molar mass of the solute, m is the molality of the solution, ρ and ρ_0 are the densities of the solution and solvent, respectively. The values of the apparent molar volume at infinite dilution (ϕ_V^0) and the experimental slopes (S_V^*) were determined using least squares fitting of the linear plots of ϕ_V against the square root of the molar concentrations ($m^{1/2}$) using the Masson equation [44].

$$\phi_V = \phi_V^0 + S_V^* \cdot \sqrt{m} \quad (25)$$

The calculated values of ϕ_V^0 and S_V^* are reported in Table 12. The plot of ϕ_V^0 values for the studied IL in

Table 9: Salt concentration at the minimum conductivity (c_{min}), the ion-pair fraction (α), triple-ion fraction (α_T), ion-pair concentration (c_P) and triple-ion concentration (c_T) for [bmim][Cl] in DCM and THF at 298.15 K, 303.15 K, and 308.15 K, respectively.

Solvents	$c_{min} \cdot 10^4 / \text{mol} \cdot \text{dm}^{-3}$	$\alpha \cdot 10^{-2}$	$\alpha_T \cdot 10^2$	$c_P \cdot 10^{-3} / \text{mol} \cdot \text{dm}^{-3}$	$c_T \cdot 10^{-2} / \text{mol} \cdot \text{dm}^{-3}$
298.15 K					
DCM	6.89	14.98	57.34	0.96	3.43
THF	5.19	17.67	59.23	0.94	3.12
303.15 K					
DCM	6.86	15.21	65.24	1.56	5.45
THF	5.11	16.14	67.81	1.04	3.46
308.15 K					
DCM	6.84	18.34	71.26	1.61	5.97
THF	5.04	15.93	68.92	1.21	3.62

THF: Tetrahydrofuran, DCN: Dichloromethane

different solvent systems at different temperatures has shown in Figure 4. The values of ϕ_V^0 are positive for all the systems and is highest in THF, suggesting the presence of strong solute-solvent interactions in case of THF than in DCM than in ACN shown in Scheme 3. The values of ϕ_V^0 increases with an increase in temperature which indicates that stronger interaction occurs between the IL and solvent at higher temperatures [45,46]. Because of the release of some of the solvent molecules from loose solvation layers during the solute-solvent interactions, the value of ϕ_V^0 increases with the increase in temperature. The highest values of ϕ_V^0 in THF leads to lower conductance of [bmim][Cl] than in DCM and ACN as discussed in above section. The S_V^* values designate the extent of ion-ion interaction, and the small values indicate the presence of less ion-ion interaction in the medium. The degree of ion-ion interactions are highest in case of ACN and are lowest in THF. A quantitative comparison shows that the magnitude of ϕ_V^0 values is much greater than the magnitude of S_V^* values suggests that the ion-solvent interactions dominant over ion-ion interactions.

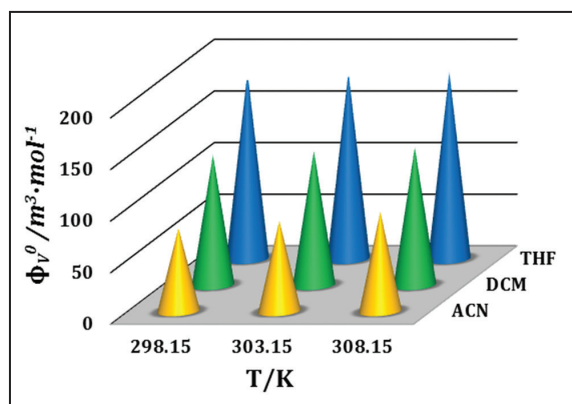
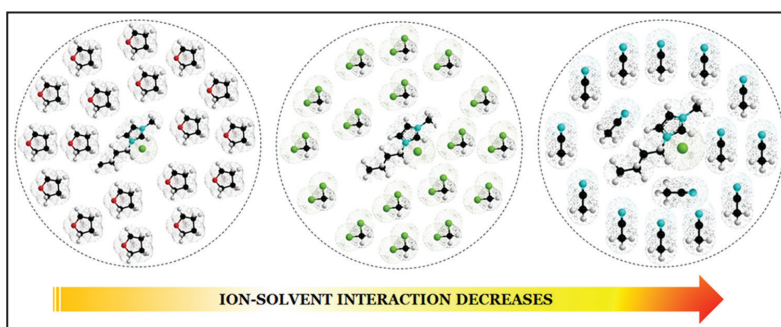


Figure 4: Plot of limiting apparent molal volume (ϕ_V^0) versus temperature for [bmim][Cl] in acetonitrile (yellow), dichloromethane (green) and tetrahydrofuran (blue).

Table 10: Apparent molal volume (ϕ_V) and $\frac{(\eta_r - 1)}{\sqrt{m}}$ for 1-butyl-3-methylimidazolium chloride ([bmim][Cl]) in different mass fraction of ACN, DCM and THF at different temperatures.

Molality/ mol·kg ⁻¹	$\phi_V \cdot 10^6 / \text{m}^3 \cdot \text{mol}^{-1}$	$\frac{(\eta_r - 1)}{\sqrt{m}}$	Molality/ mol·kg ⁻¹	$\phi_V \cdot 10^6 / \text{m}^3 \cdot \text{mol}^{-1}$	$\frac{(\eta_r - 1)}{\sqrt{m}}$	Molality/ mol·kg ⁻¹	$\phi_V \cdot 10^6 / \text{m}^3 \cdot \text{mol}^{-1}$	$\frac{(\eta_r - 1)}{\sqrt{m}}$
ACN			303.15 K			308.15 K		
0.0127	74.66	0.556	0.0128	81.35	0.286	0.0128	89.34	0.235
0.0319	71.61	0.703	0.0320	77.52	0.488	0.0321	85.49	0.409
0.0510	69.25	0.778	0.0513	74.96	0.571	0.0515	82.61	0.529
0.0702	67.26	0.829	0.0705	72.87	0.658	0.0708	80.13	0.627
0.0895	65.39	0.924	0.0899	70.95	0.756	0.0902	78.17	0.700
0.1087	63.73	0.953	0.1092	69.10	0.804	0.1097	76.29	0.807
DCM			303.15 K			308.15 K		
0.0076	120.45	0.465	0.0076	124.14	0.244	0.0076	127.28	0.256
0.0189	117.58	0.588	0.0190	120.95	0.463	0.0192	124.23	0.487
0.0303	115.36	0.698	0.0305	118.83	0.610	0.0307	121.74	0.641
0.0417	113.52	0.793	0.0420	116.90	0.666	0.0423	119.51	0.754
0.0532	111.83	0.879	0.0535	115.15	0.737	0.0539	117.68	0.804
0.0647	110.20	0.957	0.0651	113.65	0.837	0.0655	115.86	0.879
THF			303.15 K			308.15 K		
0.0113	165.55	0.208	0.0113	168.96	0.444	0.0113	173.48	0.244
0.0283	162.39	0.395	0.0283	165.12	0.675	0.0283	169.19	0.463
0.0454	159.35	0.521	0.0454	162.18	0.811	0.0455	165.86	0.610
0.0626	156.73	0.622	0.0626	159.62	0.919	0.0627	163.53	0.728
0.0799	154.43	0.709	0.0799	157.18	1.016	0.0799	161.06	0.830
0.0972	152.67	0.786	0.0972	155.21	1.075	0.0973	158.94	0.934

ACN: Acetonitrile, THF: Tetrahydrofuran, DCN: Dichloromethane



Scheme 3: Extent of ion-solvent interaction of ionic liquid in various solvent systems.

3.3. Temperature Dependent Limiting Apparent Molal volume

The variation of ϕ_V^0 values with temperature can be expressed by the general polynomial equation as follows:

$$\phi_V^0 = a_0 + a_1T + a_2T^2 \quad (26)$$

Where T is the temperature in degree Kelvin and a_0 , a_1 , a_2 are the empirical coefficients and the values of these coefficients have been calculated by the least-

squares fitting of apparent molar volume at different temperatures (Table 13).

The limiting apparent molar expansibilities, ϕ_E^0 can be obtained by the following equation:

$$\phi_E^0 = \left(\delta \phi_V^0 / \delta T \right)_P = a_1 + 2a_2T \quad (27)$$

Differentiation of Equation 26 with respect to temperature gives the values of the limiting apparent

Table 11: Density (ρ) and viscosity (η) of 1-butyl-3-methylimidazolium chloride in different mass fraction of ACN, DCM, and THF at different temperatures.

Molality/mol·kg ⁻¹	ρ 10 ⁻³ /kg m ⁻³	η /mPa s
ACN		
298.15 K		
0.0127	0.78713	0.38
0.0319	0.78893	0.40
0.0510	0.79078	0.42
0.0702	0.79267	0.43
0.0895	0.79460	0.45
0.1087	0.79656	0.46
303.15 K		
0.0128	0.78389	0.36
0.0320	0.78563	0.38
0.0513	0.78742	0.39
0.0705	0.78925	0.40
0.0899	0.79112	0.42
0.1092	0.79303	0.43
308.15 K		
0.0128	0.78101	0.35
0.0321	0.78266	0.36
0.0515	0.78437	0.38
0.0708	0.78613	0.39
0.0902	0.78792	0.40
0.1097	0.78975	0.42
DCM		
298.15 K		
0.0076	1.32586	0.45
0.0189	1.32618	0.47
0.0303	1.32658	0.49
0.0417	1.32704	0.51
0.0532	1.32756	0.53
0.0647	1.32814	0.55
303.15 K		
0.0076	1.31863	0.42
0.0190	1.31890	0.44
0.0305	1.31924	0.46
0.0420	1.31965	0.47
0.0535	1.32012	0.49
0.0651	1.32074	0.51
308.15 K		
0.0076	1.30963	0.40
0.0192	1.30985	0.42
0.0307	1.31016	0.44

(Contd...)

Table 11: (Continued).

Molality/mol·kg ⁻¹	ρ 10 ⁻³ /kg m ⁻³	η /mPa s
0.0423	1.31055	0.46
0.0539	1.31099	0.47
0.0655	1.31158	0.49
THF		
298.15 K		
0.0113	0.88627	0.49
0.0283	0.88676	0.51
0.0454	0.88733	0.53
0.0626	0.88796	0.55
0.0799	0.88864	0.57
0.0972	0.88934	0.59
303.15 K		
0.0113	0.88616	0.47
0.0283	0.88662	0.50
0.0454	0.88715	0.52
0.0626	0.88774	0.55
0.0799	0.88839	0.57
0.0972	0.88907	0.59
308.15 K		
0.0113	0.88607	0.42
0.0283	0.88648	0.44
0.0455	0.88697	0.46
0.0627	0.88750	0.48
0.0799	0.88810	0.50
0.0973	0.88874	0.53

ACN: Acetonitrile, THF: Tetrahydrofuran, DCM: Dichloromethane

molar expansibilities (ϕ_E^0) (Table 14). These values are also employed in interpreting of the structure-making or breaking properties of various solutes. Positive expansivity, i.e., increasing volume with increasing temperature is a characteristic property of nonaqueous solutions of hydrophobic solvation [47].

Hepler [48] developed a technique of examining the sign of $(\delta\phi_E^0/\delta T)_p$ for the solute in terms of long-range structure-making and -breaking capacity of the solute in the solution using the general thermodynamic expression:

$$(\delta\phi_E^0/\delta T)_p = (\delta^2\phi_V^0/\delta T^2)_p = 2a_2 \quad (28)$$

If the sign of the second derivatives of the limiting apparent molal volume with respect to the temperature $(\delta\phi_E^0/\delta T)_p$ is positive or a small negative, the molecule is a structure maker; otherwise, it is a

Table 12: Limiting apparent molar volume (ϕ_V^0), experimental slope (S_V^*), viscosity *B*- and viscosity *A*-coefficient for [bmim][Cl] in ACN, DCM and THF at T=(298.15-308.15) K respectively.

Solvents	$\phi_V^0 \cdot 10^6 / \text{m}^3 \cdot \text{mol}^{-1}$	$S_V^* \cdot 10^6 / \text{m}^3 \cdot \text{mol}^{-3/2} \cdot \text{kg}^{1/2}$	$B / \text{kg}^{1/2} \cdot \text{mol}^{-1/2}$	$A / \text{kg}^{-1/2} \cdot \text{mol}^{-1/2}$
298.15 K				
ACN	80.511	-50.44	2.0710	+0.3593
DCM	125.89	-61.04	2.5905	+0.1910
THF	172.77	-64.16	3.0063	-0.0855
303.15 K				
ACN	87.607	-55.78	2.6746	+0.0371
DCM	129.6	-62.31	2.9687	-0.0252
THF	176.32	-67.25	3.3026	+0.1360
308.15 K				
ACN	96.189	-60.06	2.9162	-0.0555
DCM	133.46	-67.99	3.2438	-0.0381
THF	181.02	-70.56	3.5642	-0.1072

ACN: Acetonitrile, THF: Tetrahydrofuran, DCN: Dichloromethane

Table 13: Values of empirical coefficients (a_0 , a_1 , and a_2) of Equation 26 of the [bmim][Cl] in ACN, DCM and THF.

Solvents	$a_0 \cdot 10^6 / \text{m}^3 \cdot \text{mol}^{-1}$	$a_1 \cdot 10^6 / \text{m}^3 \cdot \text{mol}^{-1} \cdot \text{K}^{-1}$	$a_2 \cdot 10^6 / \text{m}^3 \cdot \text{mol}^{-1} \cdot \text{K}^{-2}$
ACN	2343.6	-16.451	0.0297
DCM	175.82	-1.062	0.0030
THF	2039.9	-13.12	0.0230

ACN: Acetonitrile, THF: Tetrahydrofuran, DCN: Dichloromethane

Table 14: Limiting apparent molar expansibilities (ϕ_E^0) of [bmim][Cl] in ACN, DCM and THF at T=(298.15-308.15) K.

T/K ^a	$\frac{\phi_E^0}{10^6} / \text{m}^3 \cdot \text{mol}^{-1} \cdot \text{K}^{-1}$	$(\partial \phi_E^0 / \partial T)_P \cdot 10^6 / \text{m}^3 \cdot \text{mol}^{-1} \cdot \text{K}^{-2}$
[bmim][Cl]+ACN		
298.15	0.595	
303.15	0.825	0.046
308.15	1.055	
[bmim][Cl]+DCM		
298.15	0.727	
303.15	0.757	0.006
308.15	0.787	
[bmim][Cl]+THF		
298.15	1.259	
303.15	1.556	0.059
308.15	1.853	

^aStandard uncertainties in temperature (T)=±0.01 K. ACN: Acetonitrile, THF: Tetrahydrofuran, DCN: Dichloromethane

structure breaker [49]. It is evident from Table 14 that the values for all the complexes are positive, i.e., [bmim][Cl] is predominantly structure makers in all the solvent systems studied here.

3.4. Viscosity *B* Coefficients

The experimental values of viscosity (η) measured at different temperatures for the studied systems under investigation are listed in Table 11. The relative viscosity (η_r) has been analyzed applying the Jones-Dole equation [50]:

$$(\eta/\eta_o - 1)/\sqrt{m} = (\eta_r - 1)/\sqrt{m} = A + B\sqrt{m} \quad (29)$$

Where relative viscosity $\eta_r = \eta/\eta_o$, η_o and η are the viscosities of the solvent and solution, respectively, and m is the molality of the IL in the solutions. A and B are experimental constants known as viscosity *A*- and *B*-coefficients, which are specific to ion-ion and ion-solvent interactions, respectively. The values of A and B -coefficients are obtained from the slope of linear plot of $(\frac{\eta}{\eta_o} - 1)/\sqrt{m}$ against \sqrt{m} by least-squares method and reported in Table 10.

The viscosity *B* coefficient is a measure of the effective solvodynamic volume of solvated

species and depends on shape, size, and ion-ion interactions [51].

Positive values of the B -coefficient indicate the presence of strong ion-solvent interaction of the IL in the studied solvent system. This type of ion-solvent interaction arises mainly due to the hydrogen bonding of the solvent with the IL molecule and resulting in an increase in viscosity of the solution due to the large size of the moving molecules. The higher values of the B -coefficient are due to the solvated solutes molecule associated with the solvent molecules all round to the formation of associated molecule by ion-solvent interaction, would present greater resistance, and this type of interactions are strengthened with a rise in temperature and follow the trend $\text{THF} > \text{DCM} > \text{ACN}$ (Figure 5). These observations are in excellent agreement with the conclusions drawn from the analysis of apparent molal volume, ϕ_V^0 discussed earlier.

Thus, the volumetric and viscometric properties of the sulfa drug in the present work provide useful information in medicinal and pharmaceutical chemistry for the prediction of absorption and permeability of drug through membranes.

3.5. Infrared Spectroscopy

Solvation is caused by specific interactions of functional groups. The FT-IR spectroscopy provides the supportive evidence for such type of ion-solvent interactions present in the studied solvent system. The IR spectra of the pure solvents as well as the solutions of $\{[\text{bmim}][\text{Cl}]+\text{solvents}\}$ were investigated in the wave number range $400\text{--}4000\text{ cm}^{-1}$, and the stretching frequencies of the functional groups are given in Table 15. The $\nu(\text{C}\equiv\text{N})$ stretching vibrations of ACN are observed at 2253.66 cm^{-1} , and this peak is shifted to 2290.64 cm^{-1} when the IL is added to ACN solvent. The shifts of the IR spectra occur due to the disruption of the dipole-dipole interaction of ACN [52] leading to the formation of ion-dipole interaction between the $[\text{bmim}]^+$ ions and $\text{C}\equiv\text{N}$ bond. A sharp peak for C-O is obtained at 1069.30 cm^{-1} in case of THF and a peak for C-Cl is obtained at 746.54 cm^{-1} in DCM. After addition of IL to THF and DCM solvent, these peaks are shifted to 1086 cm^{-1} and 736 cm^{-1} , respectively. The observed shifts in the bands are due to the disruption of weak H-bonding interaction between the solvent molecules and formation of ion-dipole interaction between IL and solvent molecules [26].

4. CONCLUSIONS

An extensive study was done on the ion-solvation behavioral aspect of the IL 1-butyl-3-methylimidazolium chloride in industrially-important nonaqueous polar solvents ACN

Table 15: Stretching frequencies of the functional groups present in the pure solvent and change of frequency after addition of $[\text{bmim}][\text{Cl}]$ in the solvents.

Solvents	Functional group	Stretching frequencies (cm^{-1})	
		Pure solvents	Solvent+ $[\text{bmim}][\text{Cl}]$
ACN	$\text{C}\equiv\text{N}$	2253.66	2290.64
DCM	C-Cl	746.54	736.00
THF	C-O	1069.30	1086.00

ACN: Acetonitrile, THF: Tetrahydrofuran, DCM: Dichloromethane

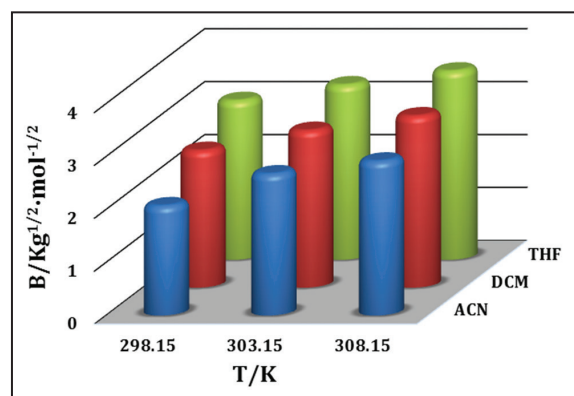


Figure 5: Plot of viscosity B -coefficient versus temperature for $[\text{bmim}][\text{Cl}]$ in acetonitrile (blue), dichloromethane (red), and tetrahydrofuran (green).

(CH_3CN), DCM (CH_2Cl_2) and THF ($\text{C}_4\text{H}_8\text{O}$) with the help of conductometric, FT-IR, density and viscosity measurements. From the conductometric measurements, it becomes clear that the IL exists as ion-pairs in ACN and as triple ions in THF, DCM solvents. The tendency of the ion-pair and triple-ion formation of $[\text{bmim}][\text{Cl}]$ depends on the dielectric constant of the medium. This study revealed that this type of experimental study is being accompanied for a better understanding of the interionic interactions of ILs. The evaluated values of thermodynamic functions of association suggest the spontaneity of the association process.

5. ACKNOWLEDGMENTS

The authors are thankful to the Departmental Special Assistance Scheme under the University Grants Commission, New Delhi (No.540/6/DRS/2007, SAP-1), India, and Department of Chemistry, University of North Bengal for financial support and instrumental facilities to continue this research work.

6. REFERENCES

- (a) T. Welton, (1999) Room-temperature ionic liquids. Solvents for synthesis and catalysis,

- 1 *Chemical Review*, **99**: 2071-2084; (b)
 2 R. A. Sheldon, R. M. Lau, M. J. Sorgedraeger,
 3 F. V. Rantwijk, K. R. Seddon, (2002) Biocatalysis
 4 in ionic liquids, *Green Chemistry*, **4**: 147-151.
 5 2. H. Niedermeyer, J. P. Hallett, I. J. Villar-
 6 Garcia, P. A. Hunt, T. Welton, (2012) Mixtures
 7 of ionic liquids, *Chemical Society Reviews*, **41**:
 8 7780-7802.
 9 3. N. V. Plechkova, K. R. Seddon, (2008)
 10 Applications of ionic liquids in the chemical
 11 industry, *Chemical Society Reviews*, **37**: 123-
 12 150.
 13 4. S. A. Forsyth, J. M. Pringle, D. R. MacFarlane,
 14 (2004) Ionic liquids-an overview, *Australian*
 15 *Journal of Chemistry*, **57**: 113-119.
 16 5. C. M. Jin, C. F. Ye, B. S. Phillips,
 17 J. S. Zabinski, X. Q. Liu, W. M. Liu,
 18 J. M. Shreeve, (2006) Polyethylene glycol
 19 functionalized dicationic ionic liquids with
 20 alkyl or polyfluoroalkyl substituents as high
 21 temperature lubricants, *Journal of Materials*
 22 *Chemistry*, **16**: 1529-1535.
 23 6. Z. Zeng, B. S. Phillips, J. C. Xiao, J. M. Shreeve,
 24 (2008) Polyfluoroalkyl, polyethylene glycol,
 25 1,4-bismethylenebenzene or 1,4-bismethylene-
 26 2,3,5,6-tetrafluorobenzene bridged functionalized
 27 dicationic ionic liquids: Synthesis and properties
 28 as high temperature lubricants, *Chemistry of*
 29 *Materials*, **20**: 2719-2726.
 30 7. J. H. Shin, W. A. Henderson, S. Passerini, (2003)
 31 Ionic liquids to the rescue? Overcoming the ionic
 32 conductivity limitations of polymer electrolytes,
 33 *Electrochemistry Communications*, **5**: 1016-
 34 1020.
 35 8. B. Garcia, S. Lavalley, G. Perron, C. Michot, M.
 36 Armand, (2004) Room temperature molten salts
 37 as lithium battery electrolyte, *Electrochimica*
 38 *Acta*, **49**: 4583-4588.
 39 9. M. Galinski, A. Lewandowski, I. Stepniak, (2006)
 40 Ionic liquids as electrolytes, *Electrochimica Acta*,
 41 **51**: 5567-5580.
 42 10. J. Vatamanu, O. Borodin, G. D. Smith, (2010)
 43 Molecular insights into the potential and
 44 temperature dependences of the differential
 45 capacitance of a room-temperature ionic liquid
 46 at graphite electrodes, *Journal of the American*
 47 *Chemical Society*, **132**: 14825-14833.
 48 11. A. A. Kornyshev, (2007) Double-layer in ionic
 49 liquids: Paradigm change? *Journal of Physical*
 50 *Chemistry B*, **111**: 5545-5557.
 51 12. Y. Zhu, S. Murali, M. D. Stoller, K. J. Ganesh,
 52 W. Cai, P. J. Ferreira, A. Pirkle, R. M. Wallace,
 53 K. A. Cychoz, M. Thommes, D. Su, E. A. Stach,
 54 R. S. Ruoff, (2011) Carbon-based supercapacitors
 55 produced by activation of graphene, *Science*,
 56 **332**: 1537-1541.
 actuator systems based on inherently conducting
 polymers, *Chemistry of Materials*, **15**: 2392-
 2398.
 14. M. S. Cho, H. J. Seo, J. D. Nam, H. R. Choi, J. C.
 Koo, K. G. Song, Y. Lee, (2006) A solid state
 actuator based on the PEDOT/NBR System,
Sensors and Actuators B: Chemical,
119: 621-624.
 15. W. L. Hough, R. D. Rogers, (2007) Ionic liquids
 then and now: From solvents to materials to
 active pharmaceutical ingredients, *Bulletin of the*
Chemical Society of Japan, **80**: 2262-2269.
 16. D. Das, B. Das, D. K. Hazra, (2002) Conductance
 of some 1:1 electrolytes in N,N-dimethylacetamide
 at 25°C, *Journal of Solution Chemistry*, **31**: 425-
 431.
 17. C. Guha, J. M. Chakraborty, S. Karanjai, B.
 Das, (2003) The structure and thermodynamics
 of ion association and solvation of some
 thiocyanates and nitrates in 2-methoxyethanol
 studied by conductometry and FTIR
 spectroscopy, *Journal of Physical Chemistry*
B, **107**: 12814-12819.
 18. D. Das, B. Das, D. K. Hazra, (2003)
 Electrical conductance of some symmetrical
 tetraalkylammonium and alkali salts in N,N-
 dimethylacetamide at 25°C, *Journal of Solution*
Chemistry, **32**: 77-83.
 19. M. N. Roy, D. Nandi, D. K. Hazra, (1993)
 Conductance studies of alkali metal chlorides
 and bromides in aqueous binary mixtures of
 tetrahydrofuran at 25°C, *Journals of Indian*
Chemical Society, **70**: 121-124.
 20. O. Popvyh, R. P. T. Tomkins, (1981) *Nonaqueous*
Solution Chemistry, Ch. 4. New York: Wiley-
 Interscience.
 21. A. J. Matheson, (1971) *Molecular Acoustics*,
 London: Wiley-Interscience.
 22. D. D. Perrin, W. L. F. Armarego, (1988)
Purification of Laboratory Chemicals, 3rd ed.
 Oxford: Pergamon Press.
 23. N. Saha, B. Das, (1997) Apparent molar volumes
 of some symmetrical tetraalkylammonium
 bromides in acetonitrile at (298.15, 308.15, and
 318.15)K, *Journal of Chemical and Engineering*
Data, **42**: 227-229.
 24. M. G. Prolongo, R. M. Masegosa, I. H. Fuentes,
 A. Horta, (1984) Viscosities and excess volumes
 of binary mixtures formed by the liquids
 acetonitrile, pentyl acetate, 1-chlorobutane, and
 carbon tetrachloride at 25.degree.C, *Journal of*
Physical Chemistry B, **88**: 2163-2167.
 25. J. E. Jr. Lind, J. J. Zwolenik, R. M. Fuoss,
 (1959) Calibration of conductance cells at 25°
 with aqueous solutions of potassium chloride,
Journal of the American Chemical Society, **81**:
 1557-1559.
 26. D. Ekka, M. N. Roy, (2014) Quantitative
 and qualitative analysis of ionic solvation of

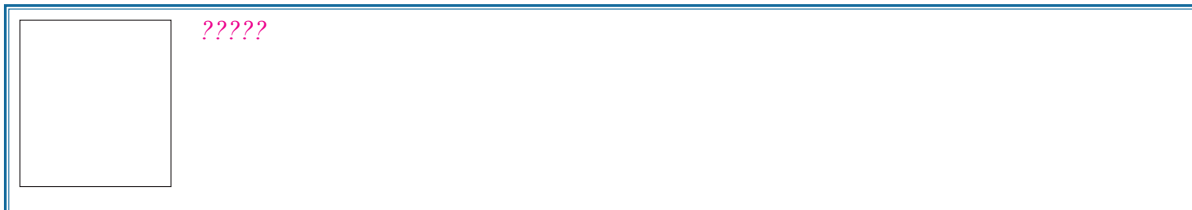
- individual ions of imidazolium based ionic liquids in significant solution systems by conductance and FT-IR spectroscopy, *RSC Advances*, **4**: 19831-19845.
27. R. M. Fuoss, (1978) Conductance-concentration function for the paired ion model, *Journal of Physical Chemistry*, **82**: 2427-2440.
28. F. I. El-Dossoki, (2010) Effect of hydrogen bond, relative permittivity and temperature on the transport properties and the association behaviour of some 1:1 electrolytes in some binary mixed solvents, *Journal of Molecular Liquids*, **151**: 1-8.
29. D. Ekka, M. N. Roy, (2012) Conductance, a contrivance to explore ion association and solvation behaviour of an ionic liquid (tetrabutylphosphonium tetrafluoroborate) in acetonitrile, tetrahydrofuran, 1,3-dioxolane, and their binaries, *Journal of Physical Chemistry B*, **116**: 11687-11694.
30. D. S. Gill, M. S. Chauhan, (1984) Preferential solvation of ions in mixed solvents, *Zeitschrift für Physikalische Chemie NF*, **140**: 139-148.
31. R. M. Fuoss, F. Accascina, (1959) *Electrolytic Conductance*, New York: Interscience.
32. R. Dewan, M. N. Roy, (2012) Physico-chemical studies of sodium tetraphenylborate and tetrabutylammonium tetraphenylborate in pure nitrobenzene and nitromethane and their binaries probed by conductometry, refractometry and FT-IR spectroscopy, *The Journal of Chemical Thermodynamics*, **54**: 28-34.
33. J. M. Chakraborty, B. Das, (2004) Electrical conductances and viscosities of tetrabutylammonium thiocyanate in acetonitrile in the temperature range 25-45°C, *Zeitschrift für Physikalische*, **218**: 219-230.
34. R. M. Fuoss, E. Hirsch, (1960) Single ion conductances in non-aqueous solvents, *Journal of the American Chemical Society*, **82**: 1013-1017.
35. R. M. Fuoss, C. A. Kraus, (1933) Properties of electrolytic solutions. IV. The conductance minimum and the formation of triple ions due to the action of coulomb forces, *Journal of the American Chemical Society*, **55**: 2387-2399.
36. Y. Harada, M. Salamon, S. Petrucci, (1985) Molecular dynamics and ionic associations of lithium hexafluoroarsenate (LiAsF₆) in 4-butyrolactone mixtures with 2-methyltetrahydrofuran, *Journal of Physical Chemistry B*, **89**: 2006-2010.
37. B. S. Krumgalz, (1983) Separation of limiting equivalent conductances into ionic contributions in non-aqueous solutions by indirect methods, *Journal of the Chemical Society, Faraday Transactions*, **179**: 571-587.
38. M. Delsignore, H. Farber, S. Petrucci, (1985) Ionic conductivity and microwave dielectric relaxation of lithium hexafluoroarsenate (LiAsF₆) and lithium perchlorate (LiClO₄) in dimethyl carbonate, *Journal of Physical Chemistry*, **89**: 4968-4973.
39. M. N. Roy, D. Nandi, D. K. Hazra, (1993A) Electrical conductances for tetraalkylammonium bromides, LiBF₄ and LiAsF₆ in THF at 25°C, *Journal of Indian Chemical Society*, **70**: 305-310.
40. A. Sinha, M. N. Roy, (2007) Conductivity studies of sodium iodide in pure tetrahydrofuran and aqueous binary mixtures of tetrahydrofuran and 1, 4-dioxane at 298.15 K, *Physics and Chemistry of Liquids*, **45**: 67-77.
41. D. Nandi, S. Das, D. K. Hazra, (1988) Conductances of tetraalkylammonium bromides in 1, 2-dimethoxyethane at 25-degrees-c-analysis of data by fuoss-kraus, *Indian Journal of Chemistry*, **A27**: 574-580.
42. M. N. Roy, D. Ekka, S. Saha, M. C. Roy, (2014) Host-guest inclusion complexes of α and β -cyclodextrins with α -amino acids, *RSC Advances*, **4**: 42383-42390.
43. D. Ekka, M. N. Roy, (2013) Molecular interactions of α -amino acids insight into aqueous β -cyclodextrin systems, *Amino Acids*, **45**: 755-777.
44. D. O. Masson, (1929) Solute molecular volumes in relation to solvation and ionization, *Philosophical Magazine*, **8**: 218-235.
45. T. S. Banipal, P. Kapoor, (1999) Partial molal volumes and expansibilities of some amino acids in aqueous solutions, *Journals of Indian Chemical Society*, **76**: 431-437.
46. F. Franks, (Ed.), (1975) *Aqueous Solutions of Amphiphiles and Macromolecules; Water, a Comprehensive Treatise*, Vol. 4. New York: Plenum Press.
47. C. M. Romero, F. Negrete, (2004) Effect of temperature on partial molar volumes and viscosities of aqueous solutions of α -dl-Aminobutyric acid, dl-norvaline and dl-norleucine, *Physics and Chemistry of Liquids*, **42**: 261-267.
48. L. G. Hepler, (1969) Thermal expansion and structure in water aqueous solutions, *Canadian Journal of Chemistry*, **47**: 4613-4616.
49. Y. J. Zhang, P. S. Cremer, (2006) Interactions between macromolecules and ions: The hofmeister series, *Current Opinion in Chemical Biology*, **10**: 658-663.
50. G. Jones, D. Dole, (1929) The viscosity of aqueous solutions of strong electrolytes with special reference to barium chloride, *Journal of the American Chemical Society*, **51**: 2950-2964.
51. Q. Zhao, Z. J. Sun, Q. Zhang, S. K. Xing, M. Liu, D. Z. Sun, L. W. Li, (2009) Densities and apparent molar volumes of myoinositol in

1 aqueous solutions of alkaline earth metal salts
2 at different temperatures, *Thermochimica Acta*,
3 **487**: 1-7.
4 52. R. Yandagni, P. Kebarle, (1972) Solvation of

negative ions by protic and aprotic solvents. Gas-
phase solvation of halide ions by acetonitrile
and water molecules, *Journal of the American*
Chemical Society, **94**: 2940-2943.

6 ***Bibliographical Sketch**

7
8
9 **AQ2**



16 Author Queries???

17 AQ1: Kindly provide history details

18 AQ2: Kindly provide text par


 CrossMark
click for updates

 Cite this: *RSC Adv.*, 2016, 6, 76381

Hollow circular compound-based inclusion complexes of an ionic liquid

Siti Barman and Mahendra Nath Roy*

Inclusion complex formation between hollow circular compounds, e.g. crown ethers, and an ionic liquid, 1-methyl-3-octylimidazolium tetrafluoroborate, in acetonitrile solvent is studied by means of conductivity measurements, IR spectra and NMR spectra. The results reveal the formation of 1 : 1 complexes between the crown ethers and ionic liquid molecules in acetonitrile. Crown ether complexes with electron-deficient imidazolium cations are formed by H-bond formation between the acidic protons of the imidazolium ring of the ionic liquid and the lone pair of electrons of the crown oxygen atom. In the case of dibenzo-18-crown-6, complexation is caused by H-bonding; however, π -stacking or charge-transfer interactions also appear to have minor contributions to the complex formation. Thus, hydrogen bonding is mainly responsible for the complexation, and ion-dipole interactions also may be responsible for complex formation between ionic liquid molecules and the crown ethers. The interactions in the complexation are analyzed and discussed.

 Received 31st May 2016
Accepted 27th July 2016

DOI: 10.1039/c6ra14138b

www.rsc.org/advances

1. Introduction

The crown ether (CE) family of macrocyclic compounds has attracted an enormous amount of interest since their discovery in 1967,^{1,2} especially in the fields of host-guest and coordination chemistry. CEs can form complexes with a variety of guest species, such as metal cations, protonated species and neutral molecules, in their cavities *via* different types of interactions with multiple oxygen atoms.^{3,4} Studies of applications of CEs, such as phase transfer catalysts,^{5,6} photo-switching devices,⁷ and drug carriers,⁸ are in progress on the basis of this inclusion ability. Crown ethers have proved to be unique cyclic molecules for molecular recognition of suitable substrates by hydrogen bonds, ionic interactions and hydrophobic interactions. The study of the interactions involved in the complexation of different cations with crown ethers in mixtures of solvents is important to improve our understanding of the mechanisms of biological transport, molecular recognition, and other analytical applications.⁹

It is already known that imidazolium cations can form inclusion complexes with large crown-ether-type hosts *via* H-bonding.¹⁰ 1,3-Disubstituted imidazolium salts are known to form inclusion complexes with DB24C8 or its derivatives through intermolecular hydrogen-bond formation, as demonstrated by different research groups.¹¹⁻¹⁴ In 1,3-disubstituted imidazolium salts, all protons on the imidazolium ring are quite acidic, as the positive charge is delocalized over the entire imidazolium ring.¹⁵ Acidic protons are attractive in

supramolecular chemistry because the acidic protons participate in stronger hydrogen-bond formation with the lone pair of electrons of the oxygen; this accounts for the stability of the adduct formed. Biologically important heterocyclic bases, such as imidazole, form planar cations and act as effective structural units at the active sites of various proteins and nucleic acids. However, during enzymatic reactions, imidazole can also exist as a protonated cation and may thus interact with the substrate by direct electrostatic or π - π interactions. Imidazolium salts have been and will be significant not only in organometallic chemistry as precursors of N-heterocyclic carbenes,^{16,17} but also in organic chemistry and material science areas as ionic liquids due to their unique chemical, physical, and electrical properties.¹⁸⁻²¹

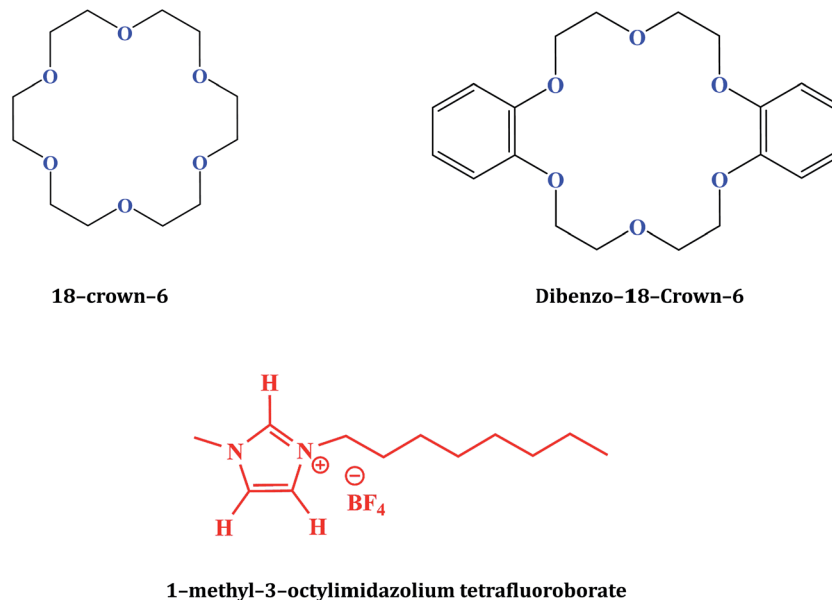
In this work, we have studied the inclusion complex formation of an ionic liquid (IL), 1-methyl-3-octylimidazolium tetrafluoroborate, with hollow circular hosts, 18-crown-6 (18C6) [complex 1] and dibenzo-18-crown-6 (DB18C6) [complex 2], in acetonitrile (ACN). The complexes were characterised by conductance, IR and NMR studies. The formation constants and thermodynamic parameters of the above-specified interactions in solution are discussed here. The structures of the IL, 1-methyl-3-octylimidazolium tetrafluoroborate, and both crown ethers are shown in Scheme 1.

2. Experimental section

2.1 Reagents

The ionic liquid (97%) and crown ethers [18C6 (99%), DB18C6 (98%)] were bought from Sigma-Aldrich, Germany and were used as purchased.

Department of Chemistry, University of North Bengal, Darjeeling-734013, India.
E-mail: mahendraroy2002@yahoo.co.in; Fax: +91 353 2699001; Tel: +91 353 2776381



Scheme 1 Molecular structures of the crown ethers and the Ionic Liquid.

2.2 Instrumentation

Prior to the start of the experimental work, the solubility of the chosen CEs and IL in ACN were precisely checked; it was observed that the selected IL salt was freely soluble in all proportions of the CE solutions.

The conductance measurements were carried out in a Systronics-308 conductivity bridge with an accuracy of $\pm 0.01\%$ using a dip-type immersion conductivity cell, CD-10, with a cell constant of approximately $(0.1 \pm 0.001) \text{ cm}^{-1}$.²² The measurements were performed in an auto-thermostated water bath while maintaining the experimental temperature. The cell was calibrated using 0.01 M aqueous KCl solution. The uncertainty in temperature was 0.01 K.

Infrared spectra were recorded on an 8300 FT-IR spectrometer (Shimadzu, Japan). The details of the instrument have been described previously.²³

¹H NMR spectra were recorded in CD₃CN at 300 MHz using a Bruker AVANCE 300 MHz instrument. Signals are quoted as δ values in ppm using residual protonated solvent signals as the internal standard (CD₃CN: δ 1.98 ppm). Data are reported as chemical shifts.

3. Results and discussion

3.1 Conductance

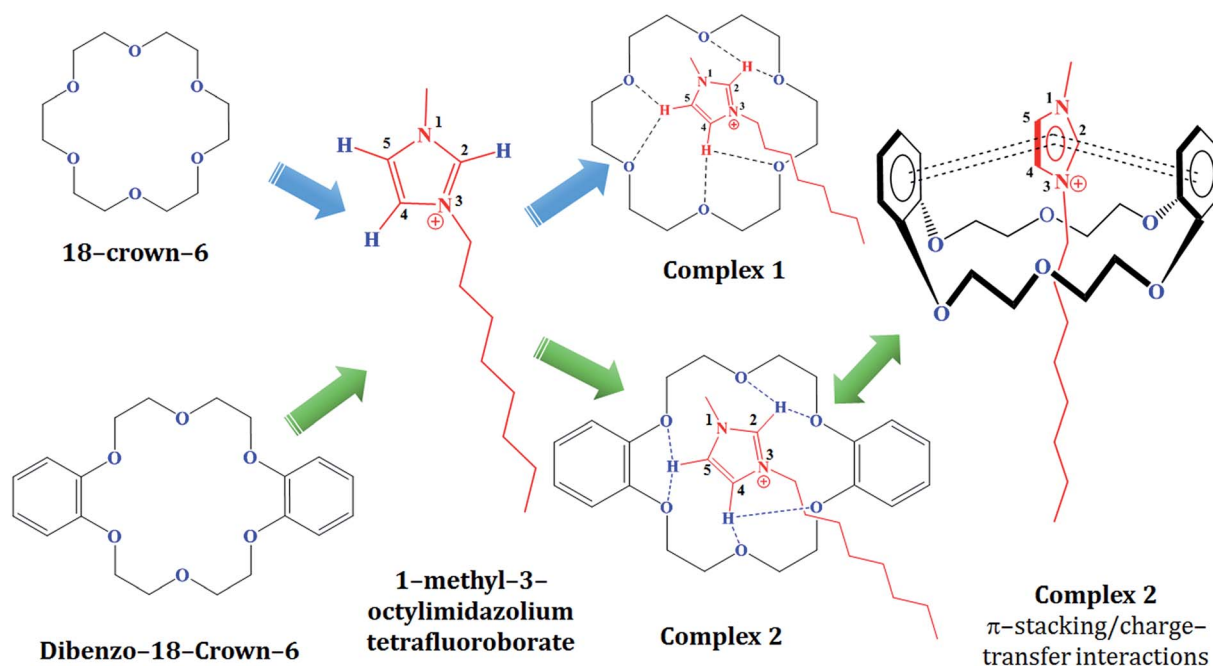
The advantage of conductometry is that measurements can be carried out with high precision at very low concentrations in solution systems. Conductance measurements of a solution of IL in the presence of a crown ether provide information about the stability and transport phenomena of the cation-crown ether complex in solution. Also, conductometry is one of the most reliable methods for obtaining the formation constants of cation-macrocyclic complexes (Takeda *et al.*, 1991).²⁴

Conductance studies of the interactions between the imidazolium cation of the IL and 18C6 and DB18C6 in ACN solution were conducted at different temperatures, and the values are presented in Table 1. The stability of these complexes depends mainly on the strength of the bonds between the acidic protons of the imidazolium ring and the oxygen atoms of the crown ethers (Scheme 2). The formation constants ($\log K_f$) of the 1 : 1 complexes at different temperatures varied in the order 18C6 > DB18C6 for the IL. The formation constants determined by the conductivity studies and the thermodynamic values for complex formation between the crown ethers and the imidazolium cation in acetonitrile solution are summarized in Table 2.

The molar conductance (Λ) of the imidazolium salt (5×10^{-4} M) in ACN solution was monitored as a function of the crown ether to imidazolium cation mole ratio at various temperatures. The resulting molar conductance *vs.* crown/cation mole ratio plots at 298.15, 303.15, and 308.15 K are shown in Fig. 1 and 2. In both cases, there is a gradual decrease in the molar conductance with increasing crown ether concentration. This behavior indicates that the complexed imidazolium cation is less mobile than the corresponding free imidazolium cation in ACN; because the imidazolium salt is a strong electrolyte in acetonitrile, the changes are not due to ion pairing, unless the complexation of the cation causes the imidazolium salt to associate. Both Fig. 1 and 2 show that in the complexation of imidazolium cation with both crown ethers, addition of the crown solution to the imidazolium salt solution causes a continuous decrease in the molar conductance, which begins to level off at a mole ratio greater than one, indicating the formation of a stable 1 : 1 complex.^{25,26} By comparison of the molar conductance-mole ratio plot for imidazolium cation-crown ether systems obtained at different temperatures (Fig. 1 and 2), it can be observed that the corresponding molar conductance increased rapidly with temperature due to the

Table 1 Values of observed molar conductivities, Λ , at various mole ratios for the IL-18C6 (complex 1) and IL-DB186 (complex 2) systems at different temperatures

Mole ratio	Λ (S cm ² mol ⁻¹)					
	DB18C6			18C6		
	293.15 K	298.15 K	303.15 K	293.15 K	298.15 K	303.15 K
0	135.80	143.72	152.21	154.00	162.58	168.36
0.099	132.10	138.34	147.60	149.10	156.50	163.84
0.196	128.50	133.80	143.12	144.60	151.68	159.56
0.291	125.07	130.60	139.72	140.76	147.20	154.72
0.385	121.61	127.82	135.80	137.88	143.12	150.50
0.476	117.82	124.92	132.24	134.10	138.34	145.42
0.566	114.24	121.52	128.56	130.18	134.80	141.64
0.654	110.12	117.92	125.14	126.84	130.60	137.68
0.740	107.30	115.60	122.46	123.18	127.82	134.54
0.825	105.20	112.32	119.32	120.24	124.50	131.50
0.909	102.30	109.50	116.22	117.46	121.92	128.96
1.071	100.14	106.44	113.6	113.38	118.06	124.58
1.228	99.06	105.46	111.52	112.14	116.82	121.80
1.379	98.90	104.14	110.72	111.70	116.22	120.62
1.667	98.20	103.56	109.28	111.22	115.54	120.04
1.935	97.70	102.12	108.14	110.82	114.92	119.38
2.187	96.80	101.30	107.58	110.34	114.34	118.92
2.424	95.50	100.28	107.02	109.68	113.62	118.46
2.647	95.00	99.88	106.66	109.06	113.02	117.70
2.857	94.40	99.08	106.16	108.52	112.44	117.32
3.333	94.02	98.52	104.08	108.24	112.06	116.84
3.750	93.36	97.44	103.42	108.58	111.42	115.46

**Scheme 2** Plausible schematic of complex formation between the imidazolium cation and the crown ethers.

decreased viscosity of the solvent and, consequently, the enhanced mobility of the charged species present.

The stability of these complexes depends mainly on the strength of the bonds between the acidic protons of the

imidazolium ring and the crown ether oxygen atoms (Scheme 2). The formation constants ($\log K_f$) of the 1 : 1 complexes at different temperatures varied in the order 18C6 > DB18C6 for the IL. Thus, a decrease in the net charge on the oxygen atoms

Table 2 Formation constant, enthalpy, entropy and free energy change values of the crown ether complexes in ACN solution

Crown	log K_f (M^{-1})			ΔH° ($kJ\ mol^{-1}$)	ΔS° ($J\ mol^{-1}\ K^{-1}$)	ΔG° ($kJ\ mol^{-1}$)
	298.15 K	303.15 K	308.15 K			
18C6	3.35	3.14	2.97	-65.02	-157.67	-18.01
DB18C6	3.05	2.96	2.87	-29.90	-43.57	-16.91

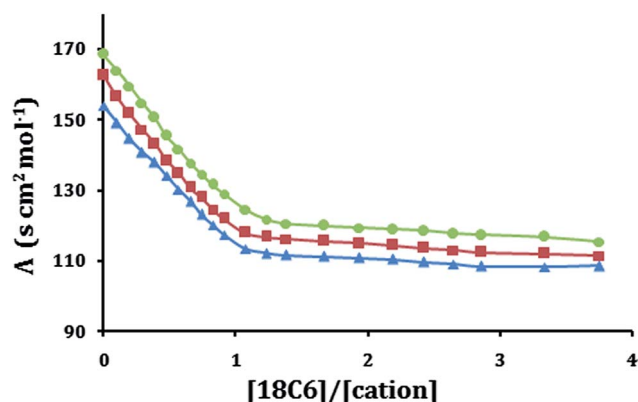


Fig. 1 Molar conductance vs. [18C6]/[cation] at 298.15 K (▲), 303.15 K (■), and 308.15 K (●).

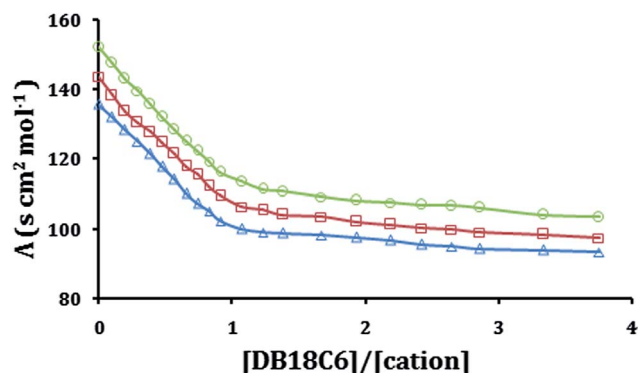


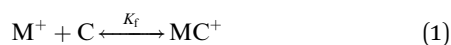
Fig. 2 Molar conductance vs. [DB18C6]/[cation] at 298.15 K (▲), 303.15 K (■), and 308.15 K (●).

during the introduction of two benzo groups into the macrocycle destabilizes the obtained complex.

3.2 Association constants and thermodynamic parameters

The following mathematical treatment to calculate the formation constant is based on Evans *et al.* (1972).²⁷

The 1 : 1 complexation of IL with 18C6 crown ether can be expressed by the following equilibrium:



The corresponding equilibrium constant, K_f is given by

$$K_f = \frac{[MC^+]}{[M^+][C]} \times \frac{f(MC^+)}{f(M^+)f(C)} \quad (2)$$

where $[MC^+]$, $[M^+]$, $[C]$ and f represent the equilibrium molar concentrations of the complex, free cation, and free ligand (crown ether) and the activity coefficients of the species indicated, respectively. Under the dilute conditions used, the activity coefficient of the uncharged macrocycle, $f(C)$, can be reasonably assumed as unity.²⁸ The use of the Debye-Hückel limiting law²⁹ leads to the conclusion that $f(M^+) \sim f(MC^+)$; therefore, the activity coefficients in eqn (2) cancel. The complex formation constant in terms of the molar conductances, Λ , can be expressed as:^{25,28}

$$K_f = \frac{[MC^+]}{[M^+][C]} = \frac{(\Lambda_M - \Lambda_{obs})}{(\Lambda_{obs} - \Lambda_{MC})[C]} \quad (3)$$

where

$$[C] = C_C - \frac{C_M(\Lambda_M - \Lambda_{obs})}{(\Lambda_M - \Lambda_{MC})} \quad (4)$$

here, Λ_M is the molar conductance of the metal ion before the addition of ligand, Λ_{MC} is the molar conductance of the complexed ion, Λ_{obs} is the molar conductance of the solution during titration, C_C is the analytical concentration of the macrocycle added and C_M is the analytical concentration of the salt. The complex formation constant, K_f , and the molar conductance of the complex, Λ_{MC} , were evaluated using eqn (3) and (4).

Complexation enthalpy changes are mainly related to (i) cation-crown interactions, (ii) solvation energies of the species in solvent systems involved in the complexation reactions, (iii) repulsion between neighboring donor atoms, (iv) steric deformation of the crown, and (v) the number of H-bonds present for H-bonding. Entropy changes are linked to (i) changes in the number of particles involved in the complexation process and (ii) conformational changes of the crown ether accompanying the complexation.

In order to better understand the thermodynamics of the complexation reactions of imidazolium cation with crown ethers, it is useful to consider the enthalpic and entropic contributions to these reactions. The ΔH° and ΔS° values for the complexation reactions were evaluated from the corresponding $\log K_f$ and temperature data by applying linear least-squares analysis according to the equation:

$$2.303 \log K_f = -\frac{\Delta H^\circ}{RT} + \frac{\Delta S^\circ}{R} \quad (5)$$

The plots of $\log K_f$ vs. $\frac{1}{T}$ for both complexes (complex 1 and complex 2) are linear (Fig. 3 and 4).

The enthalpy (ΔH°) and entropy (ΔS°) of complexation were determined from the slopes and intercepts of the plots, and the results are also listed in Table 2. Both of these parameters have negative values. True molecular recognition and physical attraction between host and guest should result in a favorable enthalpy change (ΔH) on complexation. The negative values of enthalpy confirm that when the imidazolium cation interacts with the crown ether molecules, the overall energy of the system is decreased, *i.e.*, there is some stabilizing interaction in the system, whereas negative values of the entropy factor indicate that there is an ordered arrangement, *i.e.*, complex formation takes place between the imidazolium and the crown molecules. Other investigators^{30–32} established that the binding of free amino acids with 18C6 has negative enthalpy and negative entropy, which indicates that the process is driven by a favorable enthalpy change only.

The two fundamental equations $\Delta G = -RT \ln K$ and $\Delta G = \Delta H - T\Delta S$ are useful in comparing the contributions of

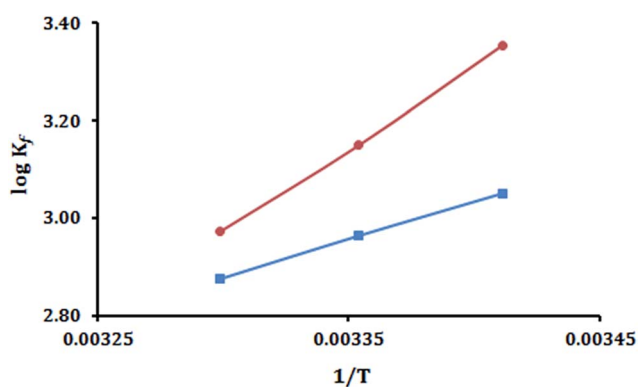


Fig. 3 The linear relationships of $\log K_f$ vs. $1/T$ for the interaction of IL with 18C6 (●) and DB18C6 (■).

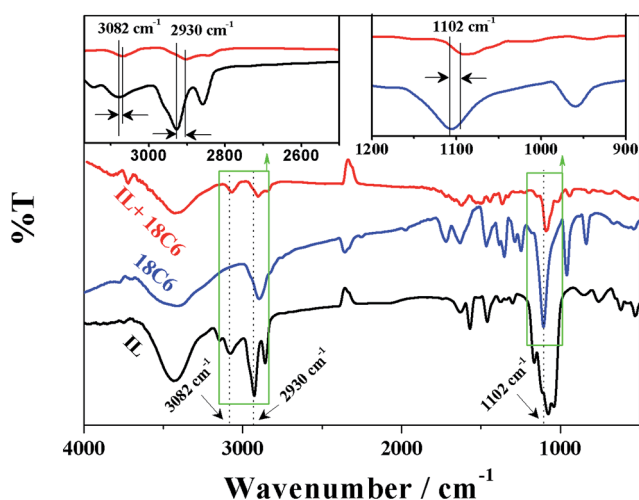


Fig. 4 FTIR spectra of free IL (black), 18-crown-6 (blue) and their complex (red).

enthalpy and entropy to the stabilities of different complexes. A negative value of entropy is unfavourable for spontaneous complex formation; however, this effect is overcome by higher negative values of ΔH° . The values of ΔG° (Table 2) for complex formation were found to be negative, suggesting that the complex formation process proceeds spontaneously.

The data shown in Table 2 indicate that the formation constant $\log K_f$ for imidazolium cation with both crowns is highest at 298.15 K and decreases with increasing temperature, *i.e.* imidazolium cation forms stable complexes with the crowns at 298.15 K.

3.3 IR studies

The IR spectra of 18C6, IL and complex 1 are shown in Fig. 4 and the spectra of DB18C6, IL and complex 2 are shown in Fig. 5 in the 4000 to 500 cm^{-1} region. The shift of the IR spectra of the crown ethers in ACN solution indicates that the specific interactions observed in the crown ether complexes are in fact typical hydrogen bonds of the imidazolium ring with the donor atoms of the crown ether. Compared with the spectra of the free crown ethers, most of these bands are shifted to lower energies, presumably due to less restriction on the coupling of some vibrational modes caused by bonding of the oxygen atoms of the polyether ring with the C–H protons of the imidazolium ring in both complexes. In the case of 18C6, a very strong and sharp IR band centered at 1102 cm^{-1} is assigned to the characteristic absorption due to the C–O–C asymmetric stretching vibrational motion [$\nu(\text{C–O–C})_{\text{aliph}}$]. This sharp peak is shifted to a lower frequency of 1082 cm^{-1} in complex 1 (Fig. 4). The $\nu(\text{C–O–C})_{\text{arom}}$ stretching vibrations of DB18C6 are observed at 1126 cm^{-1} ; this peak is also shifted to a lower frequency, 1108 cm^{-1} , in complex 2 (Fig. 5). The presence of benzene rings in DB18C6 make the IR spectra more difficult to assign because their characteristic bands may overlap with those of the ethylene glycol groups. In the IR spectra, the bands in the 2800 to 3000 cm^{-1} region correspond to the CH stretching vibrations of the methylene

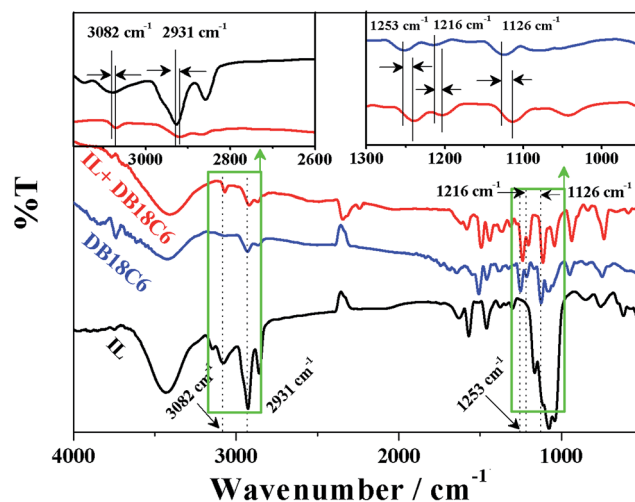


Fig. 5 FTIR spectra of free IL (black), dibenzo-18-crown-6 (blue) and their complex (red).

groups of crown ethers. The CH stretching frequency of the methylene groups observed at 2895 cm^{-1} in 18C6 is shifted to a higher frequency due to the perturbation of the methylene groups. Interaction of the O atoms of the crown with the protons of the imidazolium ring *via* hydrogen H-bonds are responsible for the perturbation. In the 1200 to 1300 cm^{-1} range of the IR spectra of DB18C6 and its complex, there are two bands assignable to anisole $\nu_s(\text{Ph-O-C})$ and $\nu_{as}(\text{Ph-O-C})$ vibrations.³³ These anisole oxygens are involved in H-bond formation in complex 2, as indicated by the shifts of the $\nu_{as}(\text{Ph-O-C})$ and $\nu_s(\text{Ph-O-C})$ bands from 1216 and 1253 cm^{-1} to 1198 and 1237 cm^{-1} , respectively. Selected IR data for the free compounds and their complexes and the corresponding changes in frequencies are listed in Table 3.

IR spectroscopy has been extensively used to analyse the interactions present in ILs. Shifts in the C–H stretching frequencies in imidazolium-based ILs provide information about the existence of H-bonding in complexes. The imidazolium based IL shows the presence of C–H stretching vibrations in the region of 3000 to 3100 cm^{-1} , which is the characteristic region for the ready identification of C–H stretching vibrations.^{34,35} According to Grondin *et al.*,³⁶ the IR bands at $3160 \pm 15\text{ cm}^{-1}$ can be assigned to the more or less symmetric and anti-symmetric combination of the C(4)–H and C(5)–H stretching vibrations of the imidazolium ring. The two bands around $3120 \pm 15\text{ cm}^{-1}$ result from the C(2)–H stretching mode and Fermi resonances of the C–H stretching vibrations with overtones of in-plane ring deformations. In our investigation, the C–H vibrations at 3082 and 2930 cm^{-1} in the FTIR spectrum are shifted to 3066 and 2905 cm^{-1} in complex 1 (Fig. 4) and to 3069

and 2921 cm^{-1} in complex 2, respectively (Fig. 5). In the IR spectra, the region between 2800 cm^{-1} and 3000 cm^{-1} shows the CH_2 and CH_3 stretching vibrations of the alkyl groups at the nitrogen atoms of the imidazolium ring.

3.4 NMR studies

The complexations of the imidazolium salt with the crown ethers were investigated by ^1H NMR spectroscopy in CD_3CN at 298.15 K . The ^1H NMR spectra of IL (imidazolium ion) was recorded in the absence and the presence of 18C6 (Fig. 6) and DB18C6 (Fig. 7) in CD_3CN . A comparison of the ^1H NMR spectra for complex 1 (Fig. 6) with free IL revealed that the signals for the hydrogen atoms of the imidazolium ion (H2, H3 and H4) were shifted downfield. This downfield shift of the imidazolium protons supports the formation of the complex through H-bond formation involving $[(\text{C-H})_{\text{Imidazolium}} \cdots \text{O}_{\text{Crown}}]^-$ interactions. Signals for the $-\text{OCH}_2$ protons of the crown ethers were found to be shifted slightly downfield relative to those signals for the free individual components (Fig. 6).

In the case of complex 2 (Fig. 7), *i.e.* the complex of DB18C6, a downfield shift for the H2 signal was observed, while small upfield shifts for the other two imidazolium protons (H3, H4) were observed.^{12,37} This suggests an orientation for the imidazolium ring that allows H-bond formation of H2 and a weak π – π interaction involving H3 and H4. Two opposing influences, namely H-bonding and π – π interactions, are responsible for the small upfield shifts for H3 and H4.³⁷ The changes in the chemical shifts suggest that host–guest complexation between the crown ether and the imidazolium salt exists in both complexes.^{38,39}

Based on the different associated modes of interaction and the ^1H NMR chemical shift data for the two complexes, complex 1 and complex 2, a plausible interaction scheme has been proposed; a schematic representation of this interaction is shown in Scheme 2. DB18C6 is a bowl-like host with two possible sites for interaction with the guest: the minor site formed by the $\text{O-CH}_2\text{-CH}_2\text{-O}$ chains and the major site located between the phenyl rings. The minor site may interact with the guest molecules only *via* hydrogen bonds, while the major site can complex both *via* H-bonding and π -interactions (Scheme 2). The inclusion of a guest capable of interacting with both sites (imidazolium cation) leads to an interesting structure.^{11,12}

^1H NMR studies revealed an apparent perpendicular orientation of the imidazolium moiety of IL in the crown cavity of complex 2; however, this seemed to be different for complex 1. The possibility of such an orientation for the imidazolium ion was confirmed by Rissanen and Pursiainen for analogous inclusion complex formation between imidazolium ion and dibenzo-18-crown-6.¹¹ The ^1H NMR results also suggested that the electron-deficient imidazolium ion may be wrapped by benzene-substituted crown ethers and that the imidazolium ions are oriented face-to-face, such that the phenyl ring(s) and the substituents in the 1,3 position point away from the cavities of the crown ethers. In the 1,3-disubstituted imidazolium salt, both the 1 and 3 positions are substituted by alkyl groups,

Table 3 Comparison between the frequency changes (cm^{-1}) of different functional groups of the free compounds and their complexes

Functional group	Wavenumber (cm^{-1})		Change (cm^{-1})
	18C6	Complex 1	$\Delta\delta$
$\nu(\text{C-O-C})_{\text{aliph}}$	1102	1082	20
Functional group	Wavenumber (cm^{-1})		Change (cm^{-1})
	DB18C6	Complex 2	$\Delta\delta$
$\nu(\text{C-O-C})_{\text{arom}}$	1126	1108	18
$\nu_{as}(\text{Ph-O-C})$	1216	1198	18
$\nu_s(\text{Ph-O-C})$	1253	1237	16
Functional group	Wavenumber (cm^{-1})		Change (cm^{-1})
	IL	Complex 1	$\Delta\delta$
$\nu(\text{C-H})$	3082, 2930	3066, 2905	16, 25
Functional group	Wavenumber (cm^{-1})		Change (cm^{-1})
	IL	Complex 2	$\Delta\delta$
$\nu(\text{C-H})$	3082, 2930	3069, 2921	13, 9

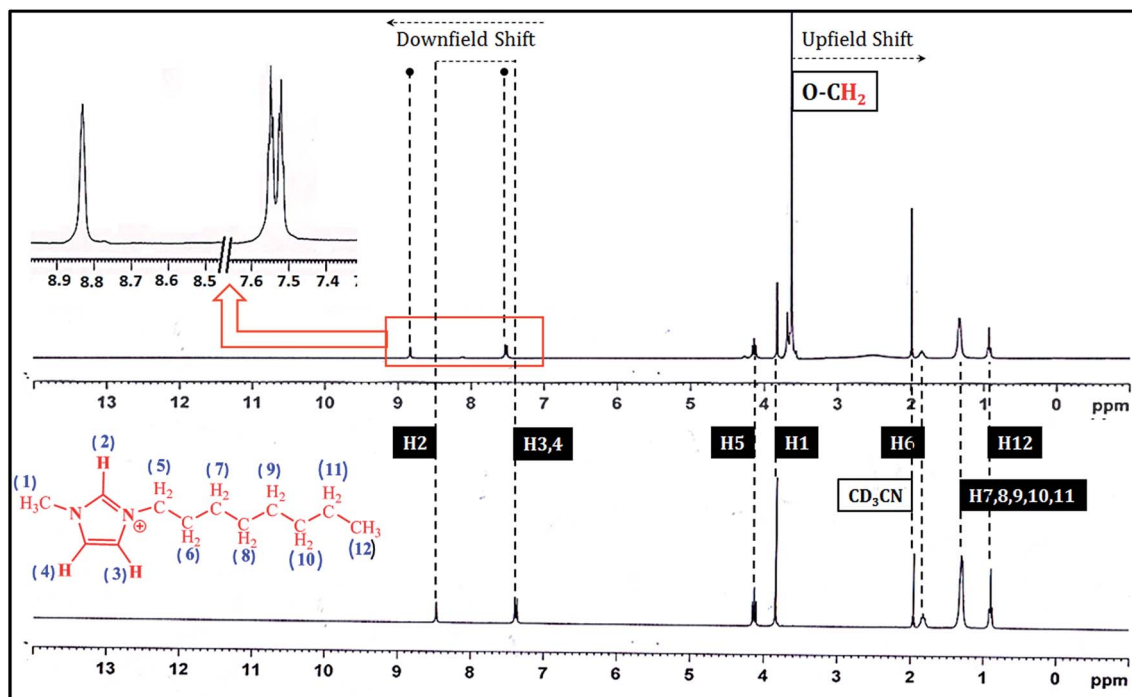


Fig. 6 ^1H NMR spectra of complex 1 (18C6.IL) (above) and the uncomplexed imidazolium cation (below) recorded at 300 MHz in CD_3CN at 298.15 K.

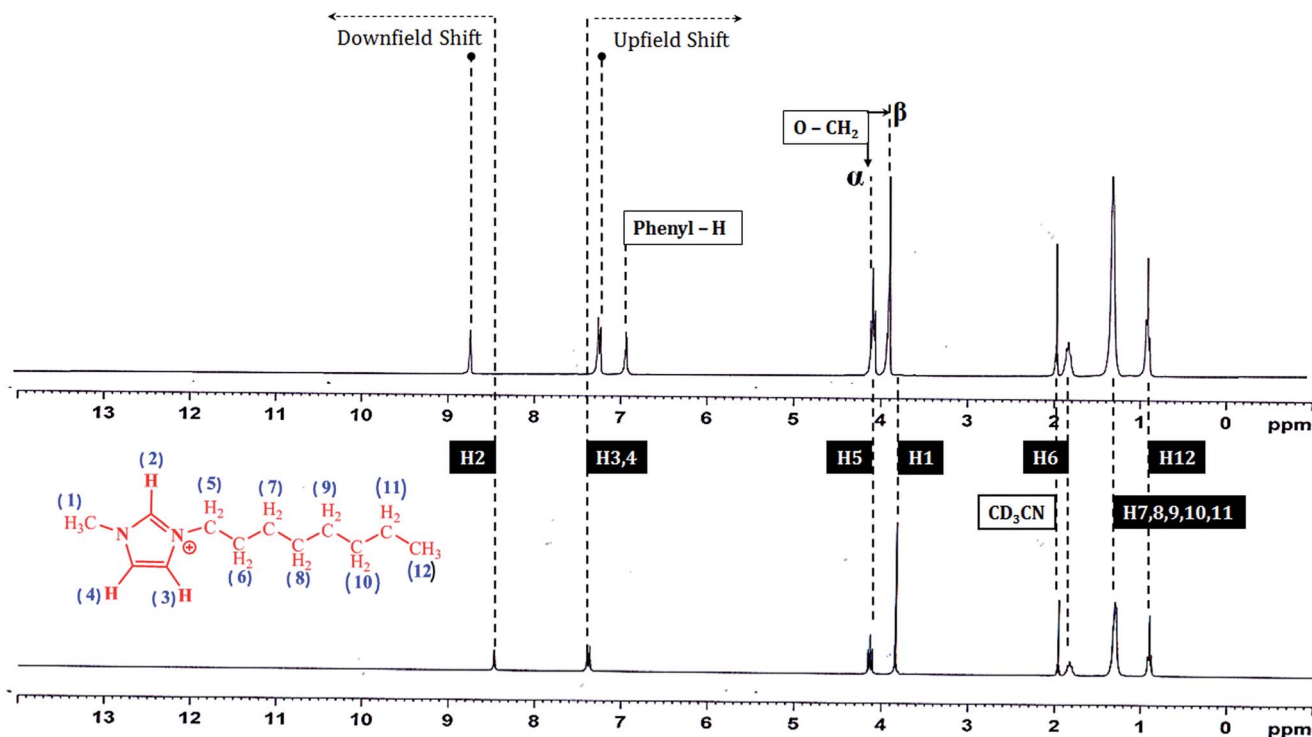


Fig. 7 ^1H NMR spectra of complex 2 (DB18C6.IL) (above) and the uncomplexed imidazolium cation (below) recorded at 300 MHz in CD_3CN at 298.15 K.

which are electron donating groups relative to hydrogen atoms. Thus, the substituents decrease the positive charge on the imidazolium ring and reduce the π - π stacking between the

dibenzo crown host and the imidazolium guest in complex 2. In complex 1, the imidazolium ring can penetrate into the hollow circular based cavity of the macrocycle 18C6 and form strong H-

bonds; however, the substituents in the 1,3 position point away from the cavities of the crown ethers.

Thus, detailed ^1H NMR spectral studies indicate that hydrogen bonding interactions $[(\text{C}-\text{H})_{\text{Imidazolium}} \cdots \text{O}_{\text{Crown}}]$ in addition to weaker π - π /arene-arene donor-acceptor interactions resulted in moderately strong inclusion complex formation, *i.e.* the results of the ^1H NMR spectral studies support the results obtained from the conductivity and IR measurements.

3.5 Selected ^1H NMR data

1-Methyl-3-octylimidazolium tetrafluoroborate (IL). ^1H NMR (CD_3CN , 298.15 K): δ 8.47 (s, N-CH-N, 2H), 7.40–7.36 (d, N-(CH) $_2$ -N, 2H), 3.84–3.81 (s, NCH $_3$, 3H), 4.15–4.10 (t, CH $_2$, 2H), 1.31 (m, C $_5$ H $_{10}$, 10H), 0.92–0.88 (t, oct-CH $_3$, 3H).

18-Crown-6. ^1H NMR (CD_3CN , 298.15 K): δ 3.59–3.52 (s, OCH $_2$, 24H).

Dibenzo 18-crown-6. ^1H NMR (CD_3CN , 298.15 K): δ 6.96–6.89 (s, aryl, 8H), 4.13–4.10 (m, OCH $_2$, 8H), 3.88–3.85 (m, OCH $_2$, 8H).

18C6-1-methyl-3-octylimidazolium tetrafluoroborate (complex 1). 3.64 (m, OCH $_2$) ^1H NMR (CD_3CN , 298.15 K): δ 8.83 (s, N-CH-N, 1H), 7.53–7.50 (s, N-(CH) $_2$ -N, 2H), 3.64–3.58 (m, OCH $_2$, 24H).

DB18C6-1-methyl-3-octylimidazolium tetrafluoroborate (complex 2). ^1H NMR (CD_3CN , 298.15 K): δ 8.75 (s, N-CH-N, 1H), 7.27–7.24 (d, N-(CH) $_2$ -N, 2H), 6.95–6.90 (s, aryl, 8H), 4.09–4.05 (m, OCH $_2$, 8H), 3.89–3.86 (m, OCH $_2$, 8H).

3.6 Typical features of specific interactions involved in the complexation

The formation of inclusion complexes of crown ethers with the imidazolium ion involved three possible modes of interaction. The most prominent mode is the hydrogen bonding interaction between the oxygen atoms of the crown ethers (O_{Crown}) and the acidic C-H protons of the imidazolium ion $[(\text{C}-\text{H})_{\text{Imidazolium}}]$ for $[(\text{C}-\text{H})_{\text{Imidazolium}} \cdots \text{O}_{\text{Crown}}]$ interaction. π - π stacking interactions between the electron poor imidazolium ring and the aryl groups of the crown ether-based host (DB18C6) is the second mode which is expected to contribute to the stability of the adduct formation. The possibility of such an interaction for an analogous system was reported earlier.^{11,14} In addition to H-bonding and π - π stacking interactions, induced dipole-dipole interactions between the imidazolium ion and O_{Crown} , having $-\delta$ charges, could also contribute to the overall stability of the adduct formation; this proposition was made independently by Schmitzer *et al.* and Pursiainen *et al.*^{11–14,40–42} However, this induced dipole-dipole interaction is expected to be weaker compared to the two previous modes of interaction discussed.

In complex 2 (Scheme 2), hydrogen bonding seems to play a secondary role. Obviously, the π - π interaction is dominant in this complex (Scheme 2) because the benzene rings of DB18C6 decrease the negative charge of the oxygen atoms and hence decrease their ability to undergo hydrogen bonding; however, under favourable conditions, hydrogen bonds can enhance the stability of crown ether complexes. Also, the electrostatic interactions between the aromatic ring of the crown and the positive charge of the imidazolium ring play an important role to stabilise the complex. The negative charge on the benzene rings of the

crown ether skeleton is enhanced by the ether oxygen atoms, and this negative face of the aromatic ring interacts with the positive charge of the imidazolium ring. The unsubstituted crown ether imidazolium complex [complex 1] is likely stabilized by hydrogen bonds formed between the acidic protons of the imidazolium ring and the ether oxygen atoms (C-H \cdots O interactions).⁴³

The stability constants ($\log K_f$) for 1 : 1 complexation were measured in ACN solution by conductance studies and are presented in Table 2. In both complexes [complex 1 and complex 2], H-bonding with the ether oxygen atoms is obviously responsible for the complexation. This can be shown by a suitable plausible mechanism (Scheme 2). Complexation is mainly caused by H-bonding; however, either π -stacking or charge-transfer interactions (Scheme 2) also seem to make minor contributions towards complexation, with the possibility of ion-dipole interactions between the positive N atom of the imidazolium cation and ether oxygen atoms. The stability constant for complex 2 is slightly lower than the corresponding value for complex 1 (Table 2). The aromatic rings of the crown ether decrease the electron density of the adjacent oxygen atoms, and this seems to decrease the strength of the H-bonding in complex 2, explaining the lower stability constant. Although complex 2 has potential π -stacking or charge transfer interactions which are absent in complex 1, these results indicate that H-bonding is dominant for the formation of these complexes.

4. Conclusion

Conductometric titration data support the different types of interactions responsible for the complex formation of crown ethers with IL molecules and are consistent with the IR and NMR spectra. The stabilities of complexes between planar, five-membered imidazolium cations and crown ethers were established by different types of non-covalent interactions. We have found that the studied complexes are mainly stabilised by hydrogen bonds, and π -stacking or cation- π interactions play only a secondary role in the case of complex 2. The larger formation constant value for complex 1 compared to complex 2 determined by conductivity studies indicates that the imidazolium cation forms a more stable complex with 18C6 than with DB18C6 in ACN solution. The 1 : 1 complexation of the imidazolium-based IL by different crown ethers is driven by favourable changes in enthalpy ($\Delta H^\circ < 0$) and proceeds spontaneously ($\Delta G^\circ < 0$). This study may also help to provide important information about other host-guest systems with crown ethers.

Here, our studies of the complexation of an imidazolium ion, similar to the complexation of pyridinium ions,⁴⁰ provide further information on the nature of the complexation between positively charged organic guests and macrocyclic polyethers. This study is also significant for understanding the vital role of imidazolium cations in the design and construction of supramolecular host-guest materials.

Acknowledgements

The authors are grateful to the Special Assistance Scheme, Department of Chemistry, NBU under the University Grants

Commission, New Delhi (No. 540/27/DRS/2007, SAP-1) for financial sustenance and instrumental conveniences in order to carry out this research. Prof. M. N. Roy is also highly obliged to the University Grants Commission, New Delhi, Government of India for being awarded a one-time grant under Basic Scientific Research *via* Grant-in-Aid No. F.4-10/2010 (BSR) in recognition of his dynamic service for the augmenting of research facilities to expedite and advance research.

References

- 1 C. J. Pedersen, *J. Am. Chem. Soc.*, 1967, **89**, 7017–7036.
- 2 C. J. Pedersen, *J. Am. Chem. Soc.*, 1967, **89**, 2495–2496.
- 3 G. W. Gokel, *Crown Ethers and Cryptands*, Royal Society of Chemistry, Cambridge, UK, 1991.
- 4 M. Dobler, *Ionophores and their Structures*, Wiley-Interscience, New York, USA, 1981.
- 5 A. M. Stuart and J. A. Vidal, *J. Org. Chem.*, 2007, **72**, 3735–3740.
- 6 N. Jose, S. Sengupta and J. K. Basu, *J. Mol. Catal. A: Chem.*, 2009, **309**, 153–158.
- 7 J. Malval, I. Gosse, J. Morand and R. Lapouyade, *J. Am. Chem. Soc.*, 2002, **124**, 904–905.
- 8 L. Tavano, R. Muzzalupo, S. Trombino, I. Nicotera, C. O. Rossi and C. L. Mesa, *Colloids Surf., B*, 2008, **61**, 30–38.
- 9 F. A. Christy and P. S. Shrivastav, *Crit. Rev. Anal. Chem.*, 2011, **41**, 236–269.
- 10 T. B. Stolwijk, E. J. R. Sudhölter, D. N. Reinhoudt and S. Harkema, *J. Org. Chem.*, 1989, **54**, 1000–1004.
- 11 S. Kiviniemi, A. Sillanpää, M. Nissinen, K. Rissanen, M. T. Lamsa and J. Pursiainen, *Chem. Commun.*, 1999, **10**, 897–898.
- 12 S. Kiviniemi, M. Nissinen, M. T. Lamsa, J. Jalonen, K. Rissanen and J. Pursiainen, *New J. Chem.*, 2000, **24**, 47–52.
- 13 M. Lee, Z. Niu, D. V. Schoonover, C. Slebodnick and H. W. Gibson, *Tetrahedron*, 2010, **66**, 7077–7082.
- 14 N. Noujeim, L. Leclercq and A. R. Schmitzer, *J. Org. Chem.*, 2008, **73**, 3784–3790.
- 15 E. Ennis and S. T. Handy, *Curr. Org. Synth.*, 2007, **4**, 381–389.
- 16 D. Tapu, C. Owens, D. VanDerveer and K. Gwaltney, *Organometallics*, 2009, **28**, 270–276.
- 17 J. C. Walton, M. M. Brahmi, L. Fensterbank, E. Lacôte, M. Malacria, Q. Chu, S. H. Ueng, A. Solov'ev and D. P. Curran, *J. Am. Chem. Soc.*, 2010, **132**, 2350–2358.
- 18 T. Welton, *Chem. Rev.*, 1999, **99**, 2071–2083.
- 19 W. Xu, E. I. Cooper and C. A. Angell, *J. Phys. Chem. B*, 2003, **107**, 6170–6178.
- 20 S. G. Lee, *Chem. Commun.*, 2006, **10**, 1049–1063.
- 21 J. E. Bara, D. E. Camper, D. L. Gin and R. D. Noble, *Acc. Chem. Res.*, 2010, **43**, 152–159.
- 22 D. Ekka and M. N. Roy, *J. Phys. Chem. B*, 2012, **116**, 11687–11694.
- 23 A. Sinha, A. Bhattacharjee and M. N. Roy, *J. Dispersion Sci. Technol.*, 2009, **30**, 1003.
- 24 Y. Takeda and T. Kimura, *J. Inclusion Phenom. Mol. Recognit. Chem.*, 1991, **11**, 159–170.
- 25 M. Shamsipur and G. Khayatian, *J. Inclusion Phenom.*, 2001, **39**, 109–113.
- 26 G. Khayatian and F. S. Karoonian, *J. Chin. Chem. Soc.*, 2008, **55**, 377–384.
- 27 D. F. Evans, S. L. Wellington, J. A. Nadi and E. R. Cussler, *J. Solution Chem.*, 1972, **1**, 499–506.
- 28 G. Khayatian, S. Shariati and M. Shamsipur, *J. Inclusion Phenom.*, 2003, **45**, 117–121.
- 29 P. Debye and H. Hückel, *Phys. Z.*, 1928, **24**, 305–307.
- 30 A. F. Danil de Namor, M. C. Ritt, M. J. Schwing-Weill, F. Arnaud-Neu and D. F. Lewis, *J. Chem. Soc., Faraday Trans.*, 1991, **87**, 3231–3239.
- 31 H. J. Buschman, E. Schollmeyer and L. Mutihae, *J. Inclusion Phenom.*, 1998, **30**, 21–28.
- 32 M. Czekalla, K. Geo, B. Haberman, T. Kruger, H. Stephan, F. P. Schmidtchen and R. Trultsch, *Poster PB 37, XXI International Symposium on Macrocyclic Chemistry*, Montecatini Terme, Italy, 1996.
- 33 A. Yu. Tsivadze, A. Yu. Varnek and V. E. Khutorskoi, *Koordinatsionnye soedineniya metallov s kraunligandami (Coordination Compounds of Metals with Crown Ligands)*, Nauka, Moscow, 1991.
- 34 H. G. Silver and J. L. Wood, *Trans. Faraday Soc.*, 1964, **60**, 5–9.
- 35 R. Ramasamy, *J. Appl. Spectrosc.*, 2013, **80**, 506–512.
- 36 J.-C. Lassègues, J. Grondin, D. Cavagnat and P. Johansson, *J. Phys. Chem. A*, 2009, **113**, 6419–6421.
- 37 A. K. Mandal, M. Suresh and A. Das, *Org. Biomol. Chem.*, 2011, **9**, 4811–4817.
- 38 Z. Zhou, X. Yan, T. R. Cook, M. L. Saha and P. J. Stang, *J. Am. Chem. Soc.*, 2016, **138**, 806–809.
- 39 X. Yan, T. R. Cook, J. B. Pollock, P. Wei, Y. Zhang, Y. Yu, F. Huang and P. J. Stang, *J. Am. Chem. Soc.*, 2014, **136**, 4460–4463.
- 40 M. Lämsä, J. Huuskonen, K. Rissanen and J. Pursiainen, *Chem.–Eur. J.*, 1998, **4**, 84–92.
- 41 M. Lämsä, T. Suorsa, J. Pursiainen, J. Huuskonen and K. Rissanen, *Chem. Commun.*, 1996, 1443–1444.
- 42 M. Lämsä, J. Pursiainen, K. Rissanen and J. Huuskonen, *Acta Chem. Scand.*, 1998, **52**, 563–570.
- 43 T. Steiner, *Chem. Commun.*, 1997, 727–734.